Josep Francesc Abril Ferrando

# Comparative Analysis of Eukaryotic Gene Sequence Features

## Anàlisi Comparativa d'Elements de Seqüència dels Gens Eucariotes

PhD Thesis

Barcelona, May 2005

# Comparative Analysis of Eukaryotic Gene Sequence Features

**Anàlisi Comparativa d'Elements de Seqüència dels Gens Eucariotes**

**Josep Francesc Abril Ferrando**

PhD Thesis

Barcelona, May 2005

**First Edition**, April 2005.

**Printed at:**

COPISTERIA MIRACLE
Rector Ubach, 6–10 (Aribau corner)
08021 — Barcelona
Phone: +034 93 200 85 44
Fax: +034 93 209 17 82
Email: `miracle at miraclepro.com`

**Cover Figure:**

An artistic representation of how Bioinformatics helped to decode the human genome. Metaphasic chromosomes are lying on top of a changing background where the DNA nucleic acids—A, C, G, and T, the language of life—, are converted into a binary code—0's and 1's, the language of computers—. A montage by J.F. Abril made with the `Gimp` (`http://www.gimp.org/`).

UNIVERSITAT POMPEU FABRA
*Departament de Ciències Experimentals i de la Salut*

# Comparative Analysis of Eukaryotic Gene Sequence Features

**Anàlisi Comparativa d'Elements de Seqüència dels Gens Eucariotes**

**Josep Francesc Abril Ferrando**

Memòria presentada per optar al grau de Doctor
en Biologia per la Universitat Pompeu Fabra.

Aquesta Tesi Doctoral ha estat realitzada sota la direcció del
Dr. *Roderic Guigó i Serra* al Departament de Ciències Experimentals
i de la Salut de la Universitat Pompeu Fabra.

**Roderic Guigó i Serra** **Josep Francesc Abril Ferrando**

Barcelona, May 2005

The research in this thesis has been carried out at the Genome BioInformatics Lab (GBIL) within the Grup de Recerca en Informàtica Biomèdica (GRIB) at the Parc de Recerca Biomèdica de Barcelona (PRBB), a consortium of the Institut Municipal d'Investigació Mèdica (IMIM), the Universitat Pompeu Fabra (UPF) and the Centre de Regulació Genòmica (CRG).

The research carried out in this thesis has been supported by predoctoral fellowships from Instituto de Salut Carlos III (Beca de Formación de personal Investigador, BEFI, 1999-2003) and from Fundació IMIM (2003-2004) to J. F. Abril, and grants from Ministerio de Ciencia y Tecnología to R. Guigó.

To my wife Marta,
for her ever lasting patience
with me and computers...

To my daughter Ruth,
for taking all those dark clouds
away with her smiles...

# Preface

During the last century biologists have been accumulating an overwhelming amount of information, but it has been during the last decade when we have experienced an explosion of data acquisition. At all levels, living beings have become more and more complex than the reductionists would ever have expected. Never before it was possible to assert, as nowadays, that life is not only the sum of the constituent molecules, acting as the gears of a clock, but also the raising network of interactions between them. Biology, starting as a descriptive subject, has evolved into an information-driven subject, taking biologists from the wet lab to the computer screens. Currently, quoting Lincoln Stein from his foreword to Tisdall [2003], "if you can't do Bioinformatics, you can't do Biology".

We, as humans, are prone to define sets, clustering elements with similar features into groups, to face the complexity. Within this landscape, a bunch of "omics" terms have been coined. We will focus on the analysis of genomic sequences, more precisely, the computational approach to genome annotation. As it has been pointed by Stein [2001]: annotation is bridging the gap from sequence to the biology of the organism. All the steps required to improve the understanding of biological processes can be grouped into three categories to answer three complementary questions: where we can find the relevant information encoded in the sequence (the gene-level annotation); what roles the products of the gene expression play (the function-level annotation); and, how the genes and their products are integrated into a network of interactions (the process-level annotation).

In the late eighties, obtaining the genome sequence of a single eukaryotic organism, the human genome of course, was seen as a giant enterprise, that could only be tackled by an international consortium of research centers in a coordinated long term project. Although initially scheduled over fifteen years, as sequencing technology improved, faraway deadlines became closer, specially because of process automation. But it was the introduction of shotgun methodology what really spurred the production of huge eukaryotic genomes. The method heavily relies on the computational assembly of a myriad of sequenced fragments. It was first applied to produce bacterial genomes after which the team at Celera Genomics demonstrated its scalability to larger genomes by obtaining, in about a year, the genome sequence of *Drosophila melanogaster* [Adams *et al.*, 2000]. The competition between Celera and the Public Consortium yielded early results with the publication of the first draft version of the human genome in 2001 [Venter *et al.*, 2001; Lander *et al.*, 2001]. Nowadays, several large eukaryotic genome projects are undergoing, with a rate of one per year being published. The future will bring better sequences for more individuals and in less time. Examples of current developments for those forthcoming technologies were described by Kling [2003].

On the other hand, computational power has increased along with the availability of novel algorithms to analyze data. Traditional hypothesis testing is being more than complemented with the acquisition of large-scale data sets to which pattern recognition and data mining techniques are applied. The patterns arising from such analyses suggest novel hypotheses to test, while hypotheses can be tested directly using databases. Another milestone that must be taken into account is the development of the internet technologies during the last decade. The widespread use of the web to share data, software to analyze it and knowledge, has caused a revolution in science, among other subjects of our lives. It has also changed the way collaborative projects among groups all around the world can tackle larger and deeper analyses.

I have been part of this incessant flow of knowledge, of this never-ending endeavour, in which the analysis of genomes has become a key element. Writing this dissertation was like a stop in the road. Not only a break to rest, but also a time to think over, in order to gain an insight of what has been done, what is going on around and what can be done in the near future, before jumping again into the fast rivers of Genomics. In other words, I have tried to summarize my contribution to this field, grouping topics by their relationship rather than chronologically.

It is amazing how the availability of each new species genome can enhance our knowledge, not only of our own species, but also of life on Earth. I hope this grain of sand from the shores of Genomics will satisfy your scientific interest.

*Josep Francesc Abril Ferrando*
Barcelona, May 2005

# Contents

# Appendices

# List of Tables

# List of Figures

# Acknowledgements

Gratitude is born in hearts that take time to count up past mercies.

—Charles E. Jefferson

I am grateful to my wife Marta for her constant support to continue the unpredictable endeavour that scientific research is. Since we met, she has been helping me more than she probably will imagine. I hope she will ever forgive me for my dedication to work and computers if I ever failed to give her attention. To her not only my deepest love but also my most grateful acknowledgements. Thank you for bringing into this world the cutest and most precious little girl I have ever met, my daughter Ruth. She also helped her father in her own way, just by being herself, making me happy, raising my spirit and, of course, encouraging me to keep going on those days you feel truly blue or stressed-out. Many thanks to my parents, for encouraging me to study when I was young, for sharing in the distance all our achievements, for their enthusiasm. Thanks also to my parents-in-law for all their support, for adopting me as a son, for the relaxing family Sunday dinners.

After several years working at a research institute it is not difficult to have met lots of interesting people, many of them really impressive. Therefore, I must first apologize for anybody who will think he or she has been left out. Those who know me, are already aware that it is easier for me to remember a face than a name. So that, I have tried to make up my mind and walk along my memories. I have to mention the long list of friends made in the Research Group in Biomedical Informatics (RGBI, or GRIB in Catalan). Not only for encouraging and helpful discussions; for the funny chitchats at coffee breaks; for sharing knowledge, code, data, and sometimes efforts too; for enjoying my jokes—although I have to admit that those were quite often uncomprehensible to the point that they were suffering rather than enjoying them—; for all the parties—and my apologies for attending less of them that I wanted to, thanks for understanding that I am a family man—.

I will begin with the old timers, they were already in the Research Group in Biomedical Informatics, when I started. They introduced me to *nix, to networks, to free software, to Bioinformatics. They also showed me what scientific research looks like. Juanjo Lozano, Moisès Burset and Jordi Rodrigo, I have to admit that it was a pleasure to meet you three, the most hilarious triplet I have ever seen. When I began, Roderic's team was only him and Moisès, and few undergraduate students—me, Jesus Feliu and David Alarcón—. I already met Jesus and David at the School of Biological Sciences of Universitat de Barcelona. We were part of a gang of computer maniacs that were regularly meeting to share tips and tricks, journals and programs. From the triplet, I was the only one who kept up doing

research; so that it was a pleasing surprise when David Alarcón joined Baldo Oliva's group recently. Specially thanks to Juanjo and Moisès for struggling to install Linux in a machine despite the mistrust and arguments against such a system from the informatics support team of the center at that time.

I would like to thank Genís Parra, Sergi Castellano, Enrique Blanco, Charles Chapple, Nicolás Bellora, Francisco Câmara, Juan Antonio de los Cobos, Hugo Gutiérrez de Terán, Josep Pareja, Montserrat Barbany, Cristina Dezi, Fabien Fontaine, Elisabeth Gregori, Ramón Aragüés, Julio Bonis, Joan Planas, Adrián López, Alfons Nonell, Ruth Garriga, Jorge Naranjo, Lulla Opatowski, Cristina Herraiz, Pilar Noguerón, Claudio Silveira and Nuria Boada. Many, many thanks to Robert Castelo, Jan-Jaap Wesselink, Mar Albà, Eduardo Eyras, Jordi Villà, Baldomero Oliva, Nuria Centeno, Manolo Pastor, Jordi Mestres. Further thanks to Miguel Pignatelli, Alberto Roverato, Juan Valcárcel, Lluis Armengol, Mónica Bayés, Xavier Estivill, Marta Soldevila, Aida Andrés, Jordi Clarimón, Jaume Bertranpetit, Viviana Belalcázar and Marta Tomàs. I do not also forget those who visited us, Noura Dabbouseh, Marcos Rodrígues, Rachid Kara, Vanessa Adaui, David González, Juan Carlos Sánchez and Diego Miranda.

Of course, I have a special mention to our system administrators, Alfons González, Xavier Fustero and Òscar González. Not only because of friendship, but also because our work depends in great manner on their task and they are always patient with our endless requirements. Thanks for their helpful hints for solving this or that installation problem, sometimes related to my computer at home.

My deepest gratitude to those people from our group who helped me to review and proof-read this document. I would like here to point out and acknowledge the time spent, the comments, the corrections and suggestions made by Jan-Jaap Wesselink, Enrique Blanco, Charles Chapple, Òscar González and my wife, Marta, to this dissertation. Thanks again to Jan-Jaap for his commitment and his exhaustive proof-reading of this work. Further thanks to Robert Castelo for providing us the LaTeX files from his PhD thesis and for introducing us to `PDFlatex`. His templates were extended by Sergi Castellano and Genís Parra for their theses. The templates on which this document was built upon were derived from them.

To the secretaries that have been working for the group or for the IMIM along the time I have been there. Esther Román, Maite Cebrián, Yolanda Losada, Raquel Furió, Esther Callizo, Mireia Gusi, Nathalie Villahoz, and the veteran, Mercedes Fuertes. Thanks for their affection, for the chit-chats about our families, specially about our kids. To Eva Molero and Carlos Díaz. Further thanks to Alba Valls, Cristina García and Teresa Duran for their assistance in all the issues related with the PhD courses and, of course, the proceedings to submit and defend this thesis.

Thanks to the users of our software, especially those contributing with bug reports and/or patches to fix them, that interaction made those tools more useful. We appreciate their patience when the responsibilities of our own research took precedence over improving and maintaining the software. To those people who motivated and encouraged us to develop `gff2ps`, specially to Elena Casacuberta and Ampar Monfort. To Martin Reese, Sussana Lewis and Michael Ashburner, for allowing us to contribute to the GASP tutorial at ISMB99 meeting. The three-panel poster summarizing the results of the gene-prediction assessment were the first big dataset in which we tested `gff2ps`. Further thanks to Thomas Wiehe for initial suggestions for developing `gff2aplot` and latter involvement in its im-

plementation; to Steffi Gebauer-Jung for providing parsers for alignment tools other than BLAST. To those people who motivated and encouraged us to continue improving it, specially to Matthias Plattzer; to those who gave valuable comments regarding this tool, as Web Miller.

I would like to thank Jim Fickett, for inviting Roderic and me, to SmithKline-Beecham (now Glaxo-Smithkline) research center in Philadelphia. It was my first trip to the States. There we met Pankaj Agarwal and I was able to see how a big pharmaceutical company looks like. To the people at Institut für Molekulare Biotechnologie (IMB), Jena; specially thanks to Matthias Plattzer, Gernot Glöckner, Karol Szafranski, Rüdiger Lehmann and Cornelia Baumgart. I wish to thank Thomas Wiehe and Steffi Gebauer-Jung for their friendliness and all the warm scientific collaborations with them, also for their hospitality when visiting them in Germany.

To the people at Celera Genomics at Rockville, Maryland, who got in contact with us to collaborate with the visualization of the fruit fly, the human and the mosquito genomes. Those collaborations allowed us to jump into the genomics field, moving from single gene sequences to work with whole genomes, from individual work to big collaborative efforts to solve one of the most complex problems to date. On the personal side, the warm welcome and all their attention, the opportunity to become part of such team of great minds, will be always in my heart. Thanks to Jennifer R. Wortman, Mark D. Adams, Patrick Dunn, Mark Yandell, William Majoros, Richard J. Mural, Robert A. Holt, George L. Gabor Miklos, Catherine Nelson, Gangadharan Subramanian (Mani), and J. Craig Venter. Thanks also to the *Drosophila melanogaster* jamboree people, specially to Gerald M. Rubin and Nomi L. Harris.

To the people at the international consortia for the sequencing and analysis of the mouse, rat and chicken genomes. For sharing preliminary data and knowledge, for the willingness in solving problems, for the endless conference calls, and so on. The list of people involved in such large projects is too big, but few people stand out by their exceptional organizational effort, such as Kim Worley, Victoria Hagigi and Ladeana Hillier. To Ewan Birney and Jim Kent, for ENSEMBL and GOLDEN PATH respectively, for replying to a mail as soon as it was sent, and for "wise" and funny discussions too. Further thanks to Web Miller, Peer Bork, Ivica Letunic, Chris Pontig, Donna Karolchik, Adam Siepel, David Haussler, Robert Baertsch, Ian Korf, Michael R. Brent, Chris Burge, Lior Pachter, Arian Smith, Emmanouil T. Dermitzakis, Alexandre Reymond, and Stylianos Antonarakis among others.

The publication of the first draft of the human genome had a tremendous impact on the media. We already had a small contact with journalists because of our participation in the fruit fly genome, reported just one year before. For the human genome that was not the case. Despite our small contribution, our group was the only Spanish partner directly involved in this huge project—unfortunately, boosting science in Spain was not one of the government priorities for a long time—. We were overwhelmed by interviews for newspapers and for radio and television programs. Elvira López and Maite Cebrián helped us to cope with them and to organize the appointments agenda for those "mad" weeks. This was when we met Marc Permanyer, from the Press department of Universitat Pompeu Fabra. The experience served, at least, to get more organized in advance, preparing press releases and concentrating interviews into press conferences. Thanks again to Elvira López, Marta Calsina and Marc Permanyer for organizing the press for the mouse, rat and chicken genomes. Further thanks to our group secretaries, for buffering all the incoming

visits and telephone calls. Having cameras, photographers and journalists interfered with the work of many other members of our lab. Their patience and sense of humor must be acknowledged too. I would like to stress from this lines the contribution to the divulgation of scientific discovery in general, of our contributions in particular, made by many journalists. Among them, I would like to acknowledge Josep Corbella ("La Vanguardia"), Joaquim Elcacho ("Diari Avui"), Xavier Pujol Gebellí ("El Pais"), Antonio Madridejos ("El Periodico") and Javier López Rejas ("El Mundo").

To those great speakers that demonstrate their love for what they are doing, Roderic Guigó, Alfonso Valencia, Antonio Marín, Modesto Orozco and so on...I specially recall, not without fear but also with laughter, the de-construction of Bioinformatics lecture by Alfonso Valencia. On the other hand, I wish to thank all those who invited me to give talks about our work. To the Departmento de Biología y Geología of the Instituto de Enseñanza Secundaria Sanje at Alcantarilla, Murcia, for their warm welcome and for the interest demonstrated by students and teachers; specially thanks to Eva Palacios and Ángel Martínez. To Lola Andrade at the public library of Masnou, Barcelona, and the town council of Sant Carles de la Ràpita, Tarragona, particularly to Elvira Franquet i Tudó, Miguel Alonso Herrera and Josep Pere Geira, for inviting me to talk about the human genome too. I wish to thank also the organization committee of the meeting of the Sociedad Española de Genética, specially to José L. Oliver, for inviting me to present our research in their annual meeting held in El Escorial in 2003. I would like to thank the people of Fundació "La Caixa" for inviting us to organize the workshops on "Computational Analysis of DNA Sequences", held in Barcelona and Madrid; specially to Sílvia Maldonado, Sílvia Godó and Gloria Trías. Further thanks to Residència d'Investigadors for inviting us to the great première of *Verbum* ("Genoma in musica"), a piece for piano composed by Joan Guinjoan.

I also have many things to be thankful for to Ferran Sanz; for starting up the Research Group in Biomedical Informatics, which we have been part of; for his constant search of the excellence in science; for his wisdom and willingness to help, not only at scientific and academic levels; for his capacity to take new projects; for the Viladrau group retreats.

I am grateful to my PhD advisor, Roderic Guigó, for pushing us far beyond and at the same time for his patience when any analysis took longer than expected—and for his famous sentence, "that would take just five minutes, wouldn't it?"—; for his insights in the field and his dedication to science—I agree that science is not just a job but a way of life, although one needs to make a living too—; for introducing me to `gawk`, POSTSCRIPT and LaTeX. For his efforts to get funds for the research, as we all know how much it takes to fill in all the bureaucracy related to a project—and how this interferes with the "field" work. For introducing us to outstanding people in the field. For his deadline last minute questions. For a scholarship in 1998/1999, that permitted to devote myself full-time to research. For a scholarship in 2003/2004, mainly because that allowed me to finalize my PhD thesis and write this dissertation.

I acknowledge the support from the Instituto de Salud Carlos III (ISCIII) for the Beca de Formación de personal Investigador (BEFI, a PhD studentship) for the 1999/2003 four years period. Thanks to the ISMB'99 organizing committee for a travel scholarship to attend to the 1999 meeting held in Heidelberg (Germany). To a joint grant from the German Academic Exchange Service (DAAD) to Thomas Wiehe and the Ministerio de Educación y Ciencia (Spain) to Roderic Guigó, which made possible, among other things, our scientific stays in the Institut für Molekulare Biotechnologie (IMB) at Jena (Germany). I would also mention all the people that, from the Federación de Jóvenes Investigadores and the Precar-

ios association, are trying to improve the labor situation of research scholarships. Thanks to their efforts current and future generations of PhD students will have hopefully better work conditions than us. Special thanks to Sergi Castellano for getting so involved with Precarios and getting us up to date with their activities and achievements.

Finally, I would like to thank Linus Torwalds (for developing the Linux kernel), the GNU Free-Software Foundation (for `bash`, `gawk`, `make` and a myriad of other useful *NIX tools, but also for the advocacy of free software), Larry Wall *et al* (for the `perl` programming language, its dynamic community and the useful modules from CPAN), Richard M. Stallman *et al* (for the arguably best programming text editor, `emacs`, and my apologies to `vi` advocators), Norman Ramsey (for the `noweb` literate programming tool), Donald Knuth and Lesslie Lamport (for the TEX and LATEX typesetting systems, respectively—and thanks to all the developers of a whole bunch of useful packages, such as `PStricks`, `PDFLaTeX`, `natbib`, `makeidx`, `hyperref`, and so on—), Sergie Brin and Larry Page (for devising the page rank technology behind `Google`). To the efforts of all the people that have demonstrated that sharing will hopefully provide a better future. All the advances of humankind are the result of the accumulation of knowledge. All their contributions provided us with the tools with which we have performed our analyses and developed our software.

*To all of you, many, many thanks from the heart...*

# Abstract

The constantly increasing amount of available genome sequences, along with an increasing number of experimental techniques, will help to produce the complete catalog of cellular functions for different organisms, including humans. Such a catalog will define the base from which we will better understand how organisms work at the molecular level. At the same time it will shed light on which changes are associated with disease. Therefore, the raw sequence from genome sequencing projects is worthless without the complete analysis and further annotation of the genomic features that define those functions. This dissertation presents our contribution to three related aspects of gene annotation on eukaryotic genomes.

First, a comparison at sequence level of human and mouse genomes was performed by developing a semi-automatic analysis pipeline. The SGP2 gene-finding tool was developed from procedures used in this pipeline. The concept behind SGP2 is that similarity regions obtained by TBLASTX are used to increase the score of exons predicted by geneid, in order to produce a more accurate set of gene structures. SGP2 provides a specificity that is high enough for its predictions to be experimentally verified by RT-PCR. The RT-PCR validation of predicted splice junctions also serves as example of how combined computational and experimental approaches will yield the best results.

Then, we performed a descriptive analysis at sequence level of the splice site signals from a reliable set of orthologous genes for human, mouse, rat and chicken. We have explored the differences at nucleotide sequence level between U2 and U12 for the set of orthologous introns derived from those genes. We found that orthologous splice signals between human and rodents and within rodents are more conserved than unrelated splice sites. However, additional conservation can be explained mostly by background intron conservation. Additional conservation over background is detectable in orthologous mammalian and chicken splice sites. Our results also indicate that the U2 and U12 intron classes have evolved independently since the split of mammals and birds. We found neither convincing case of interconversion between these two classes in our sets of orthologous introns, nor any single case of switching between AT-AC and GT-AG subtypes within U12 introns. In contrast, switching between GT-AG and GC-AG U2 subtypes does not appear to be unusual.

Finally, we implemented visualization tools to integrate annotation features for gene-finding and comparative analyses. One of those tools, gff2ps, was used to draw the whole genome maps for human, fruitfly and mosquito. gff2aplot and the accompanying parsers facilitate the task of integrating sequence annotations with the output of homology-based tools, like BLAST. We have also adapted the concept of pictograms to the comparative analysis of orthologous splice sites, by developing compi.

# Resum

L'incessant augment del nombre de seqüències genòmiques, juntament amb l'increment del nombre de tècniques experimentals de les que es disposa, permetrà obtenir el catàleg complet de les funcions cel·lulars de diferents organismes, incloent-hi la nostra espècie. Aquest catàleg definirà els fonaments sobre els que es podrà entendre millor com els organismes funcionen a nivell molecular. Al mateix temps es tindran més pistes sobre els canvis que estan associats amb les malalties. Per tant, la seqüència en brut, tal i com s'obté dels projectes de seqüenciació de genomes, no té cap valor sense les anàlisis i la subsegüent anotació de les característiques que defineixen aquestes funcions. Aquesta tesi presenta la nostra contribució en tres aspectes relacionats de l'anotació dels gens en genomes eucariotes.

Primer, la comparació a nivell de seqüència entre els genomes humà i de ratolí es va dur a terme mitjançant un protocol semi-automàtic. El programa de predicció de gens SGP2 es va desenvolupar a partir d'elements d'aquest protocol. El concepte al darrera de l'SGP2 és que les regions de similaritat obtingudes amb el programa TBLASTX, es fan servir per augmentar la puntuació dels exons predits pel programa geneid, amb el que s'obtenen conjunts d'anotacions més acurats d'estructures gèniques. SGP2 té una especificitat que és prou gran com per que es puguin validar experimentalment via RT-PCR. La validació de llocs d'*splicing* emprant la tècnica de la RT-PCR és un bon exemple de com la combinació d'aproximacions computacionals i experimentals produeix millors resultats que per separat.

S'ha dut a terme l'anàlisi descriptiva a nivell de seqüència dels llocs d'*splicing* obtinguts sobre un conjunt fiable de gens ortòlegs per humà, ratolí, rata i pollastre. S'han explorat les diferències a nivell de nucleòtid entre llocs U2 i U12, pel conjunt d'introns ortòlegs que se'n deriva d'aquests gens. S'ha trobat que els senyals d'*splicing* ortòlegs entre humà i rossegadors, així com entre rossegadors, estan més conservats que els llocs no relacionats. Aquesta conservació addicional pot ser explicada però a nivell de conservació basal dels introns. D'altra banda, s'ha detectat més conservació de l'esperada entre llocs d'*splicing* ortòlegs entre mamífers i pollastre. Els resultats obtinguts també indiquen que les classes intròniques U2 i U12 han evolucionat independentment des de l'ancestre comú dels mamífers i les aus. Tampoc s'ha trobat cap cas convincent d'interconversió entre aquestes dues classes en el conjunt d'introns ortòlegs generat, ni cap cas de substitució entre els subtipus AT-AC i GT-AG d'introns U12. Al contrari, el pas de GT-AG a GC-AG, i viceversa, en introns U2 no sembla ser inusual.

Finalment, s'han implementat una sèrie d'eines de visualització per integrar anotacions obtingudes pels programes de predicció de gens i per les anàlisis comparatives sobre genomes. Una d'aquestes eines, el gff2ps, s'ha emprat en la cartografia dels genomes humà, de la mosca del vinagre i del mosquit de la malària, entre d'altres. El programa gff2aplot i els filtres associats, han facilitat la tasca d'integrar anotacions de seqüència amb els resultats d'eines per la cerca d'homologia, com ara el BLAST. S'ha adaptat també el concepte de pictograma a l'anàlisi comparativa de llocs d'*splicing* ortòlegs, amb el desenvolupament del programa compi.

# Resumen

El aumento incesante del número de secuencias genómicas, junto con el incremento del número de técnicas experimentales de las que se dispone, permitirá la obtención del catálogo completo de las funciones celulares de los diferentes organismos, incluida nuestra especie. Este catálogo definirá las bases sobre las que se pueda entender mejor el funcionamiento de los organismos a nivel molecular. Al mismo tiempo, se obtendrán más pistas sobre los cambios asociados a enfermedades. Por tanto, la secuencia en bruto, tal y como se obtiene en los proyectos de secuenciación masiva, no tiene ningún valor sin los análisis y la posterior anotación de las características que definen estas funciones. Esta tesis presenta nuestra contribución a tres aspectos relacionados de la anotación de los genes en genomas eucariotas.

Primero, la comparación a nivel de secuencia entre el genoma humano y el de ratón se llevó a cabo mediante un protocolo semi-automático. El programa de predicción de genes `SGP2` se desarrolló a partir de elementos de dicho protocolo. El concepto sobre el que se fundamenta el `SGP2` es que las regiones de similaridad obtenidas con el programa `TBLASTX`, se utilizan para aumentar la puntuación de los exones predichos por el programa `geneid`, con lo que se obtienen conjuntos más precisos de anotaciones de estructuras génicas. `SGP2` tiene una especificidad suficiente como para validar esas anotaciones experimentalmente vía RT-PCR. La validación de los sitios de *splicing* mediante el uso de la técnica de la RT-PCR es un buen ejemplo de cómo la combinación de aproximaciones computacionales y experimentales produce mejores resultados que por separado.

Se ha llevado a cabo el análisis descriptivo a nivel de secuencia de los sitios de *splicing* obtenidos sobre un conjunto fiable de genes ortólogos para humano, ratón, rata y pollo. Se han explorado las diferencias a nivel de nucleótido entre sitios U2 y U12 para el conjunto de intrones ortólogos derivado de esos genes. Se ha visto que las señales de *splicing* ortólogas entre humanos y roedores, así como entre roedores, están más conservadas que las no ortólogas. Esta conservación puede ser explicada en parte a nivel de conservación basal de los intrones. Por otro lado, se ha detectado mayor conservación de la esperada entre sitios de *splicing* ortólogos entre mamíferos y pollo. Los resultados obtenidos indican también que las clases intrónicas U2 y U12 han evolucionado independientemente desde el ancestro común de mamíferos y aves. Tampoco se ha hallado ningún caso convincente de interconversión entre estas dos clases en el conjunto de intrones ortólogos generado, ni ningún caso de substitución entre los subtipos AT-AC y GT-AG en intrones U12. Por el contrario, el paso de GT-AG a GC-AG, y viceversa, en intrones U2 no parece ser inusual.

Finalmente, se han implementado una serie de herramientas de visualización para integrar anotaciones obtenidas por los programas de predicción de genes y por los análisis comparativos sobre genomas. Una de estas herramientas, `gff2ps`, se ha utilizado para cartografiar los genomas humano, de la mosca del vinagre y del mosquito de la malaria. El programa `gff2aplot` y los filtros asociados, han facilitado la tarea de integrar anotaciones a nivel de secuencia con los resultados obtenidos por herramientas de búsqueda de homología, como `BLAST`. Se ha adaptado también el concepto de pictograma al análisis comparativo de los sitios de *splicing* ortólogos, con el desarrollo del programa `compi`.

# Chapter 1

# Introduction

> All our progress is an unfolding, like vegetable bud. You have first an instinct, then an opinion, then a knowledge
> —Ralph Waldo Emerson, "*Essays*"

Genes encode all the information necessary for the cell to carry out all its functions. Although protein sequences are continuous[1], the sequence of the genes defining them in the eukaryotic organisms appears in the DNA sequence interspersed in a sea of non-coding regions. Furthermore, evolution has made the problem of finding those genes in anonymous DNA sequences harder. Not only because of the intrinsic mutational changes of the DNA sequences, which makes homology finding more difficult; but also due to the variation accumulated in the gene catalog of each species, which has been expanded—by duplications, for instance— or reduced—i.e., by deletions and lose of function (pseudogenes). In addition to that, genes have been reordered, some of them have lost their function, becoming useless, and so on. On the other hand, to search for genes means that we have to look for the features that characterize them, examining the raw DNA sequences for the signals that delineate them. Therefore, obtaining the genome sequence of an organism does not grant that we will be able to find all the genes easily, as the real ones will be hidden in a forest of false signals and real non-coding regions. The fact that in the human genome, made up of three billions[2] of nucleic acids distributed in 23 chromosomes (the haploid set of course), there is only about 2% of sequence in coding regions, helps us to understand the magnitude of the problem of finding the genes encoded in it [Guigó *et al.*, 2000; Venter *et al.*, 2001; Lander *et al.*, 2001].

At the moment of transcription, the sequence containing a gene is copied from the DNA to RNA, the so called primary transcript. This undergoes a series of modifications before being transported from the nucleus to the cytoplasm. Once there, the sequence of the RNA, known at this step as messenger RNA (mRNA), serves as a template to produce the corresponding protein, the translation process. The pathway from DNA to protein synthesis became the central dogma of Biology. One of the most important changes performed on

[1] Genes that do not translate into proteins can still have a function, such as the transfer RNA (tRNA) genes and other non-coding RNAs (ncRNA). Whatever they are still coding for a cellular function, the term coding will be used along this document as protein-coding, as for protein-coding genes.

[2] US notation: $3 \times 10^9$, more intuitively 3,000,000,000 bp.

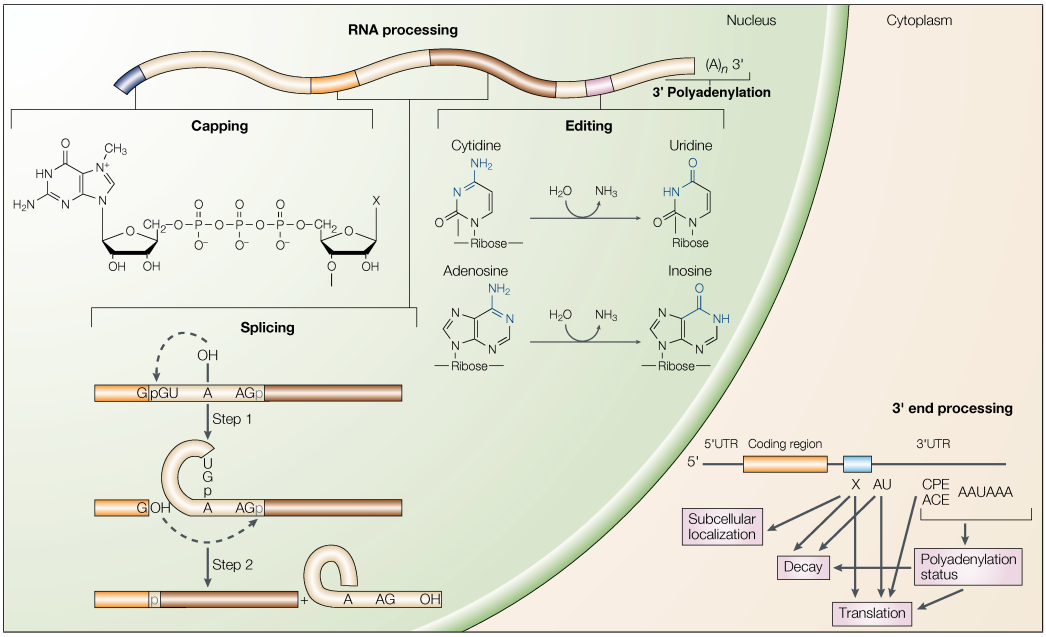


Figure 1.1: **The processing of RNA in the cell.** Immediately after the RNA is transcribed in the nucleus, capping, splicing, editing and 3′ polyadenylation of the pre-mRNA occur. In mammals, RNA editing can be of two types, either the conversion of cytidine to uridine or the conversion of adenosine to inosine. Once the mRNA is transported into the cytoplasm, additional processing of the polyA tail can occur. The elements required for this and for subcellular localization, stability and translation are present in the untranslated regions (UTRs). Adapted from Keegan *et al.* [2001].

the primary transcript is the elimination of the fragments not coding for proteins, the so called introns, by means of a set of biochemical reactions in the cell nucleus, known as the splicing process. The final product of splicing is a molecule of mRNA in which the gene's exons have been concatenated to get a continuous gene sequence. Figure 1.1 illustrates the modifications that the primary transcript undergoes. Capping of the 5′ terminus, splicing of the exonic segments and polyadenylation are the major events leading to the mature mRNA molecule. All those steps can be coupled in the cell as has been suggested in recent publications [Proudfoot *et al.*, 2002; Zorio and Bentley, 2004].

The next challenge is how to delineate the exonic structures that define a gene product. Unlike prokaryotic organisms, for which genes are formed by a single exon—and the intergenic sequences, if present, are very short—, the eukaryotic genes can have more than one, up to hundreds in some cases. In the human genome, for example, approximately a 10% of the 33,000 genes annotated in the last human genome version[3] are single exon genes, and all the rest are multi-exonic gene structures. The following big problem, yet to be solved, is to find all the alternative exonic structures encoded in a given gene region, what is also known as alternative splicing . Recent estimates suggest that more than 60% of human

[3]Calculated from ENSEMBL genes found in the GOLDEN PATH HG16 version (July, 2003), obtained from: `http://hgdownload.cse.ucsc.edu/goldenPath/hg16/database/ensGene.txt.gz`

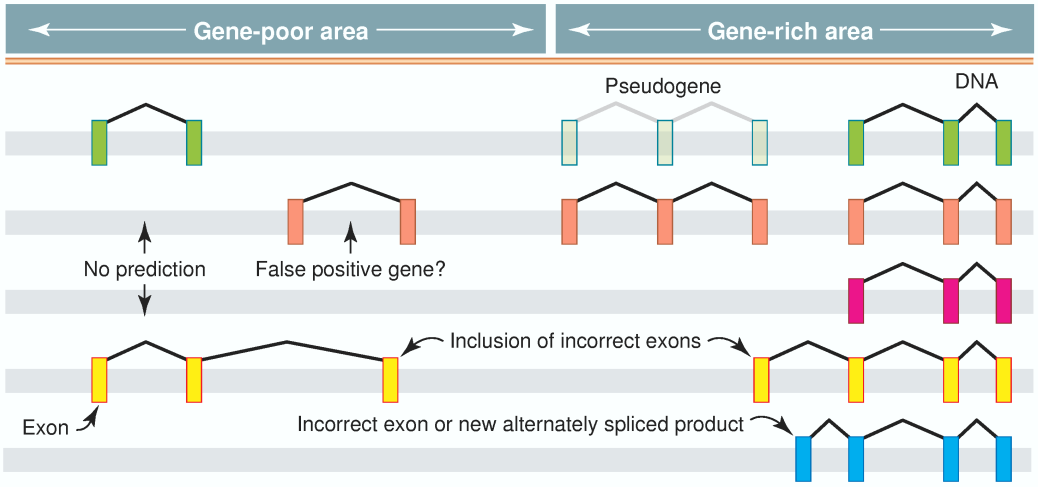


Figure 1.2: **Common pitfalls among gene-finding approaches.** No program is yet able to find all genes in anonymous genomic sequences correctly. Some overpredict and report genes where there are none; some misspredict genes; in other cases they are not able to properly group exons belonging to one or more genes, joining or splitting the corresponding gene structures. The upper track shows a putative set of real genes, the other tracks simulate the output of four different gene-finding tools. Adapted from Pennisi [2003].

genes show this phenomenon [Lander *et al.*, 2001; Modrek *et al.*, 2001]. Landscape becomes more complex if one wants to take into account the regulation of gene expression [Zhang, 2002] and the rules of the alternative splicing control [Woodley and Valcárcel, 2002].

## 1.1 Finding Genes in the Genomes

In the early eighties, DNA sequences under analysis were long enough to find initially open reading frames (ORFs), then exons. The first computational approaches focused then on the search for coding regions—see, for example, the pioneering works of Pustell and Kafatos [1982], Staden [`ANALYSEQ` and the `Staden` package, 1984b; 1986 respectively], Devereux *et al.* [`GCG` suite, 1984], Keller *et al.* [1984], or Blattner and Schroeder [1984]. It was not until the nineties that programs able to assemble those exons into a complete gene were developed [Uberbacher and Mural, 1991; Guigó *et al.*, 1992; Burge and Karlin, 1997]. Although sequencing technology was improving, most of the available sequences contained a single gene, often incomplete. By that time, the number of sequences stored in databases was relatively small. Whole genome sequencing projects changed that scenario. Databases started to grow exponentially and new problems had to be faced by the sequence analysis algorithms. Speed was one of the main requirements of the new era, not only to look for genes but also for the search of homologies between sequences of different species, mapping repetitive sequences, and so on. Novel algorithms for homology search, less sensitive but faster, were developed to screen an ever growing set of sequences. Models underlying the gene-finding software were developed from different approaches—for instance, neural

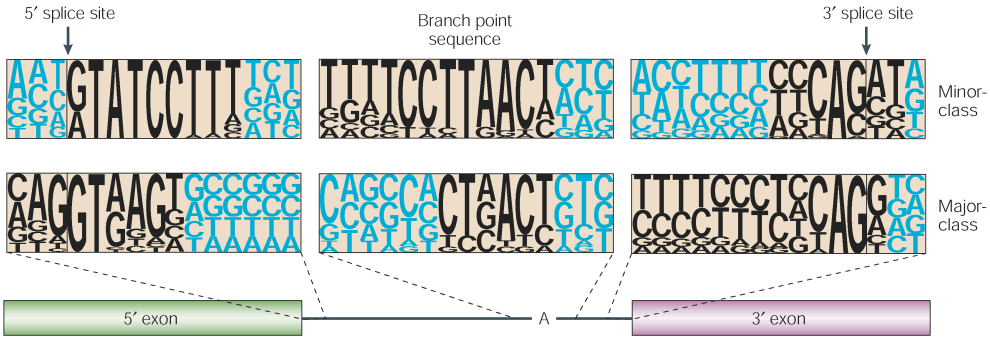


Figure 1.3: **Consensus sequences of U2 and U12 splicing signals.** The consensus sequences of the 5′ splice site, branch site and 3′ splice site are shown from left to right for minor-class introns (upper row) and for major-class introns (lower row). The letter heights at each position represent the frequency of occurrence of the corresponding nucleotides at that position. The positions that are thought to be involved in intron recognition are shown in black; other positions are shown in blue. Adapted from Patel and Steitz [2003].

networks and hidden Markov models (HMMs). However, as the length of the sequences increased, it was evident that gene distribution along them and their structural complexity became a hard problem to solve. The reliability of the results obtained by computational gene prediction tools has not improved so fast [Burset and Guigó, 1996; Guigó *et al.*, 2000; Reese *et al.*, 2000].

Gene prediction has changed substantially in the past few years. The sequencing of an increasing number of eukaryotic genomes, and the distribution through centralized genome browsers,—such as those at the University of California Santa Cruz (UCSC), the National Center for Biotechnology Information (NCBI) and the European Bioinformatics Institute (EBI)—of precomputed genome-wide annotations may often make it unnecessary for scientists to run gene prediction programs themselves. Gene prediction, however, is still useful in these genomes, because researchers may want, for instance, to investigate in detail the pattern of alternative splicing of a given gene. On the other hand, gene prediction is still essential to analyze sequences from the many genomes that have not been completely characterized yet. The obvious conclusion is that gene prediction is still an open problem. Figure 1.2 highlights some of the common failings that the current tools have yet to overcome.

Chapter 3 presents a brief overview of gene finding, both classical and comparative approaches, and the evaluation of the predictions, as well as a description of the semi-automatic protocols used for large genome-sized data sets.

## 1.2 Eukaryotic Gene Structure

The precise removal of pre-mRNA introns is a critical aspect of gene expression. The splicing machinery must recognize and remove introns to make the correct message for protein

production, but also, for many genes, alternative splicing mechanisms must be in place to generate functionally diverse protein isoforms in a spatially and temporally regulated manner [Hastings and Krainer, 2001]. Paradoxically, in higher eukaryotes, the requirement for accurate splicing is accompanied by exon-intron junctions that are defined, in most cases, by weakly conserved intronic *cis*-elements, the splice sites and the branch point [Cartegni *et al.*, 2002]. These elements are necessary but by no means sufficient to define exon-intron boundaries. Sequences that match the consensus splice site signals as well as, or better than, natural splice sites are very common in introns. They define a set of pseudo-exons that greatly outnumber genuine exons and greatly complicate the task of assembling real gene structures by the computational gene-finding approaches.

The splicing reaction is mediated by two distinct yet analogous pools of small nuclear ribonucleoprotein particles. The RNA component of such particles takes part in the recognition of sequence motifs at both ends of the introns, the 5′ and 3′ splice sites, and a region within the intron known as the branch point [Patel and Steitz, 2003]. The works of Hall and Padgett [1994] revealed a minor class of introns having unusual consensus splice site sequences. Figure 1.3 shows, side by side, the sequence patterns for both the major and minor intron classes and illustrates the fact that the minor-class sequence motifs are far more conserved than those for the major-class [Sharp and Burge, 1997].

After a detailed description of the splicing biochemistry, we will focus on the sequence features that define the boundaries between exons and introns in chapter 4. Our contribution to understanding the biological characteristics of such features, based on the comparative analysis of introns from orthologous genes of several vertebrate genomes, is also described.

## 1.3 Visualizing Genomic Features

Despite substantial progress in computational gene finding, currently available methods are not yet able to automatically provide accurate enough descriptions of the gene content of eukaryotic genomes and a substantial amount of manual curation is required. This is a task in which visualization and integration tools play an essential role.

Any result in Bioinformatics, whether it is a sequence alignment, a structure prediction, or an analysis of gene expression patterns, should answer a biological question. For this reason, it is up to the researchers to interpret their results in the context of such a question. This interpretation is the most important part of the scientific process and a number of programs are used to visualize the sort of data arising from Bioinformatics research. These programs range from general-purpose plotting and statistical packages for the analysis of numerical data to programs dedicated to presenting sequence annotations in an integrated, intuitive and comprehensive fashion, such as the ENSEMBL genome browser examples from Figure 1.4. Visualization tools exploit the abilities of the eye and brain to find patterns that may be interesting. After that, statistical and data mining tools restrict those searches to the patterns that can be quantitatively and repeatedly shown to be significant [Gybas and Jambeck, 2003].

In chapter 5, we provide an overview of visualization tools that have been applied to the analysis of genome annotations and the inter-specific comparative analyses. Furthermore, we show a set of tools we have developed to visualize genomic annotations.

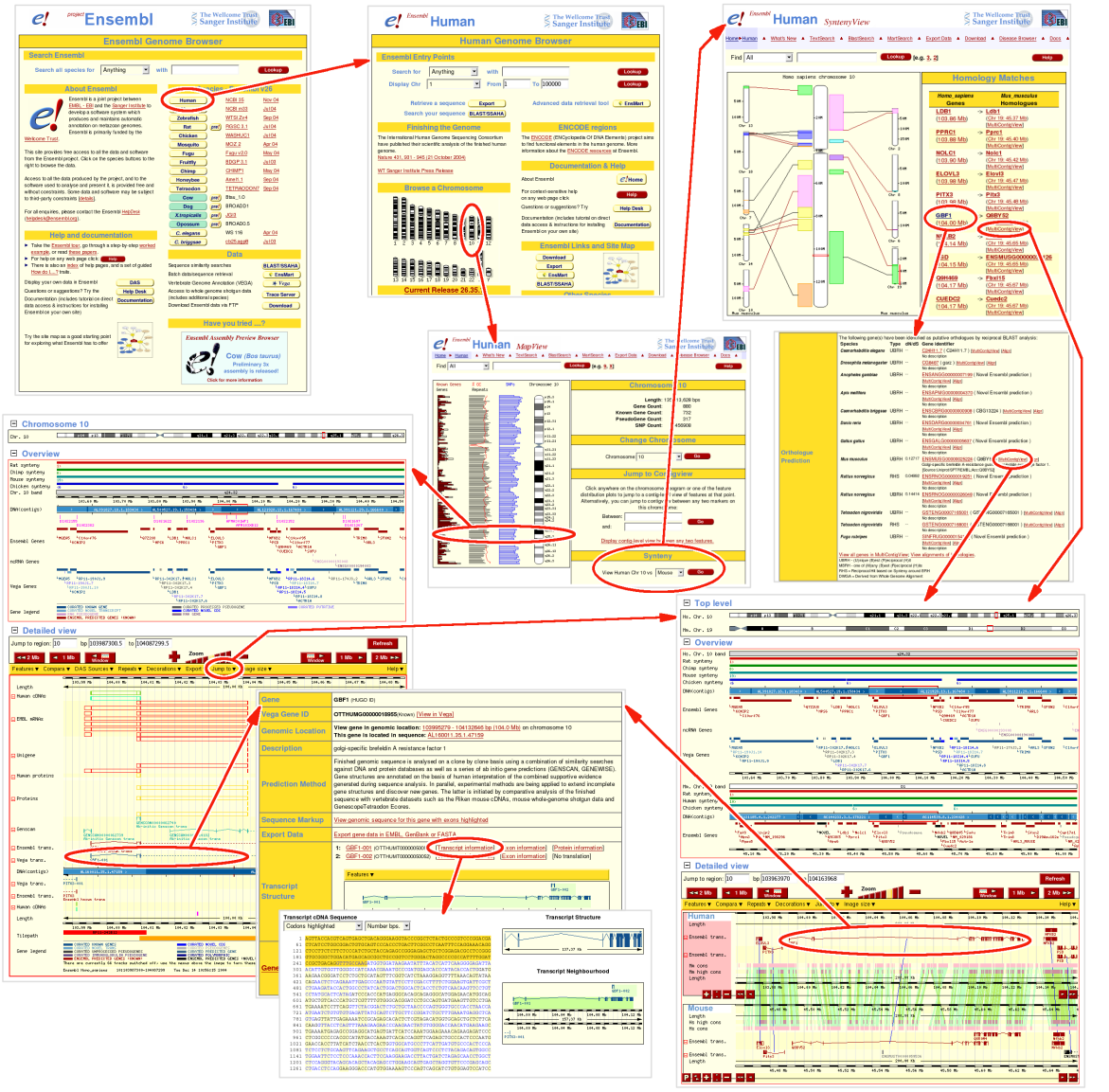


Figure 1.4: **Browsing through genome annotations.** A quick tour through the ENSEMBL genome browser pinpoints the different information levels we can access via its web interface. From their home page located in the upper left corner, a researcher can jump into the desired genome, the human genome in this example. Specific queries can be performed by using the text forms, but a very intuitive interface allows the user to zoom from the chromosome level (the Map View window placed in the center of this figure), to the sequence level (the Contig Viewer on the lower left panel), and to the gene or transcript reports (middle lower panels). Integration with other species-specific genome databases is also possible by using the Synteny panels (upper right panel). Comparative analyses at the genomic sequence level are shown in the Multi-Contig View (lower right panel). Red arrows indicate only few of the possible paths a researcher can follow through this browser.

## 1.4 About This Thesis

None of the articles composing this thesis were collected in an appendix or as separate chapters. They appear as sections where links to the journal web references and supplementary material are provided, followed by the article itself. Presenting the publications this way may break the storyline but it puts related subjects together which seems to be more appropriate. In those papers in which we were part of an international consortium, the article is reproduced in part due to its size but also because we have atempted to focus on our specific contribution. This should not be a problem, since the link to retrieve the whole article is provided as was already mentioned. Several figures and tables are referred to along the text via hyperlinks pointing directly to the page of the corresponding embedded article. Absolute page numbers relative to this document were used in all of these hyperlinks and in the list of figures or tables. Nevertheless, the reader can find easily the original paper page numbers just by following the hyperlinks.

The electronic version of this document has hyperlinks for the table of contents, for the bibliographic references, but most important of all, also for the web addresses on the Internet—from now on, their Uniform Resource Locator (URL). This means that you can visit the corresponding web page by clicking your pointer on them, in case that you have your PDF viewer properly customized. Many of the URLs presented in this book have been collected in a web links reference index available on page 213. URLs within paragraphs have been moved into that web glossary in order to avoid unbalanced line breaks and for a more pleasant reading. A reference to the corresponding page in the web reference index is provided instead. That does not include those URLs refering to the supplementary materials of the attached articles, which are put together in the corresponding article section (see Section 3.2.1 in page 20 for an example).

An attempt has been made to keep software names as provided by their authors. Those names appear in a `monospaced serif font`. Database names are typeset in a SMALL-CAPS SANS-SERIF FONT. A *slanted sans-serif font* was used for gene names, while a upright sans-serif font was chosen for protein names.

The first time an acronym appears in the document, the full name will be provided and the acronym itself will be shown in parentheses. From then on, the short form will be used. In order to help the reader, a list of abbreviations can be found on page 203. A glossary of terms is also available on page 207.

# Chapter 2

# Objectives

Don't bite my finger, look where it's pointing.
—Warren S. McCulloch

The research in this *PhD thesis* was initially targeted, in late 1998, to the goals enumerated below. In what follows, they are described and an account of their achievement status given.

1. To analyze through bioinformatic means the exonic structures of homologous genes, in order to determine the extent of conservation at gene structure level.
2. To describe possible evolutive patterns for those exonic structures within mammals and vertebrates.
3. To compare the conservation of the signals that delineate exons between different species. Both, acceptor and donor, splice sites are the main players in the definition of the exonic structure of eukaryotic genes.
4. To investigate the relationship between the conservation of exonic structures and alternative splicing patterns.
5. To develop visualization tools focusing specifically on the annotation of genomic sequences (including output from gene finding tools) and the comparative analysis of exonic structures.
6. To provide and distribute the results of our analyses and the bioinformatic tools to the research community.

These objectives were established based on data and knowledge of that time. They were intended to explore very basic questions about the exonic structure of eukaryotic genes and the evolutionary fates of introns. These goals have been accomplished to different degrees as related further down. Therefore, several of these points should be considered as ongoing work and yet many questions, both old and new, remain unanswered.

Some of the work presented in this dissertation has been done in collaboration with international genome sequencing consortia. These collaborations gave me the opportunity

to meet and work with specialists from all over the world, and made our work very relevant. However, those collaborations put a lot of pressure on us and a lot of effort has been invested in such genome annotation projects. On the other hand, participating in the annotation of recently sequenced genomes has proven fruitful, as we have had to develop methodologies to analyze large amounts of data from different sources for each species. This means that we had to implement specific software to solve new problems, as well as to establish protocols to handle large sequence and annotation data sets. Such an effort was detrimental to some of the initial objectives and it made that this thesis took more time than expected.

The protocols and software we developed for finding genes by the comparison of the human and mouse genomes [Parra *et al.*, 2003; Waterston *et al.*, 2002], have been adapted to produce gene annotations in a semi-automatic pipeline for each novel assembly version of eukaryotic genomes. Annotations for several species, including human, chimpanzee, mouse, rat, chicken and the fruitfly, are available through a web repository (see page 214, on Web Glossary).

Despite the fact that we were able to undertake the analysis of the orthologous splice sites for four vertebrate species, we have not been able to investigate the conservation of exonic structures of alternatively spliced isoforms of orthologous genes. We could not tackle the evolutionary analysis of exonic gene structure either. However, during the last year, our group has joined the Alternative Splicing Database Project [Thanaraj *et al.*, 2004], and has been also chosen as a partner of the ENCODE project [ENCODE Project Consortium, 2004]. ASD aims to analyze the mechanism of splicing on a genome-wide scale by creating both, human-curated and computer-generated databases containing alternatively spliced exons from human and other model species. The main aims of the ENCODE project are both to validate known genes and to confirm reliable computational predictions experimentally. However, also to identify previously unknown genes and the characterization of a number of splice variants of the genes found in the corresponding target regions. In both projects, there are people in our laboratory that will continue this promising research line.

For the last objective, all the programs and data sets have been made available through our group's web server. Most of our published papers have their own web page with supplementary materials, as can be seen in the corresponding sections. Regarding the visualization software developed, `gff2ps` and `gff2aplot`, both have several tutorials and a user's reference manual. Furthermore, these tools are distributed under the GNU General Public License (GNU-GPL). The GNU-GPL is intended to guarantee the freedom to share and change free software–to make sure the software is free for all its users. If our research is publicly funded, the fruits of our work should be made publicly available. Both, the GNU-GPL and the Internet, are in our honest opinion most forthright approach to accomplish that responsibility with the society. As stated in Jamison [2003], software security measures which don't allow for examination of original code or for reasonable mechanisms of validity testing are in contrast with the open communication needed to do science properly.

# Chapter 3

# Comparative Gene Finding

> When this circuit learns your job,
> what are you going to do ?
>
> —Herbert Marshall McLuhan

Life processes, from the information flow from DNA to proteins to biochemical or regulatory pathways, have an intrinsic algorithmic nature. An algorithm can be defined as a detailed sequence of actions to perform to accomplish some task. The cells of living beings steadily perform step-by-step chemical reactions. Interactions between molecules modulate the flow of energy or information across the cell. The analogy works the other way around, as we attempt to emulate such biological processes by computational methods. The organization of a gene, as any other biological structure, is determined by functional and evolutionary constraints. All computational methods are therefore based on our experimental understanding of such constraints.

In this chapter we explore the computational modeling of protein-coding gene structures. After that, we describe our contribution to the gene-finding using comparative genomics approaches.

## 3.1 Computational Gene Prediction

After the genome of an organism is sequenced and assembled, comprehensive and accurate initial gene prediction and annotation by computational analysis have become the necessary first step towards understanding the functional content of the genome [Guigó and Zhang, 2004]. Despite the fact that, in practice, there are tools that can be classified in more than one of them, we can split the computational approaches to find genes in DNA sequences into three main categories.

- "*Ab initio*" methods are based on a search for those signals that specify the boundaries of coding regions, as in the analysis of coding biases and regularities of the protein-coding versus non-coding regions [Guigó, 1999]. The main handicap of such approaches is that the molecular mechanisms used by eukaryotic cells to define the signals that determine the gene structure are not completely well understood.

- Homology-based methods use information related to the similarity of the query coding region with respect to a set of known sequences from databases. The major drawback here is the bias towards known genes or proteins. Therefore novel families that are under-represented or not found in the databases, will still be hard to retrieve [Guigó *et al.*, 2000].

- The whole-genome sequencing projects allowed to extend the previous approach. Instead of searching for sequences of known genes, the entire genomes of two or more species are compared. The idea behind this is that evolution tends to retain those regions that are important because they have a function, whatever it encodes: a protein or structural or regulatory elements. When comparing genomes of closely related species, a set of genes emerges that is characteristic for the taxonomic group to which they belong. A good example of this has been the comparison between the human [Lander *et al.*, 2001] and mouse [Waterston *et al.*, 2002] genomes, during which approximately 9,000 novel mouse and 1,000 novel human genes have been annotated [Guigó *et al.*, 2003; Flicek *et al.*, 2003; Parra *et al.*, 2003]. However, comparative genomics approaches are not only a useful tool to find novel genes, but they are also a tool to improve the annotations of known genes [Reichwald *et al.*, 2000] and to hypothesize about their functions [Wiehe *et al.*, 2000].

### 3.1.1 "*Ab initio*" developments

Computational gene finding is not a brand new field and a large body of literature has accumulated during the last 25 years. Early studies by Shepherd [1981], Fickett [1982] and Staden and McLachlan [1982] showed that statistical measures related to biases in amino acid and codon usage could be used to approximately identify protein coding regions in genomic sequences. Based on these differences, the first generation of gene predictions programs, designed to identify approximate locations of coding regions in genomic DNA, was developed. The most widely known of this kind of programs were probably `testcode` (based on Fickett [1982]) and `grail` [Uberbacher and Mural, 1991]. These programs were able to identify coding regions of sufficient length (100-200 bp) with fairly high reliability, but did not accurately predict exon locations.

In order to predict exon boundaries, a new generation of algorithms was developed. A second generation of programs, such as `sorfind` [Hutchinson and Hayden, 1992], `grailII` [Xu *et al.*, 1994b,a] and `xpound` [Thomas and Skolnick, 1994], uses a combination of splice signal and coding region identification techniques to predict potential sets of exons (spliceable open reading frames), but does not attempt to assemble predicted exons into complete genes. A third generation of programs attempts the more difficult task of predicting complete gene structures: sets of exons which can be assembled into translatable coding sequences. The earliest examples of such integrated gene finding algorithms were probably the `genemodeler` program [Fields and Soderlund, 1990] for prediction of genes in *Caenorhabditis elegans* and the method of Gelfand [1990] for mammalian sequences. Subsequently, there has been a mini-boom of interest in development of such methods and a wide variety of programs have appeared, including: `geneid` [Guigó *et al.*, 1992], which used a hierarchical rule-based structure; `geneparser` [Snyder and Stormo, 1993], which scored all subintervals in a sequence for content statistics and splice site signals, then weighted

them by a neural network and it chained the resulting features by dynamic programing; `genemark` [Borodovsky and McIninch, 1993] which combined the specific Markov models of coding and non-coding region together with Bayes' decision making function; `genlang` [Dong and Searls, 1994], which treated the problem by linguistic methods describing a grammar and parser for eukaryotic protein-encoding genes; and `fgenes` [Solovyev *et al.*, 1994] which used a discriminant analysis for identification of splice sites, exons and promoter elements.

At the end of the last decade, the introduction of the Generalized Hidden Markov Models (GHMMs) produced a new generation of gene prediction programs. GHMMs have some advantages over the previous approaches. The main advantage is that all the parameters of the model are probabilities and that, given a set of curated sequences and defined states, the Viterbi algorithm can be used to compute the set of optimal parameters. A great variety of programs appeared simultaneously exploring the capabilities of GHMMs: `genie` [Kulp *et al.*, 1996], `hmmgene` [Krogh, 1997], `veil` [Henderson *et al.*, 1997], `genscan` [Burge and Karlin, 1997] and the GHMMs version of `genemark` (`genemark.hmm`, Lukashin and Borodovsky [1998]) and `fgenes` (`fgenesh`, Salamov and Solovyev [2000]).

Other gene prediction approaches have been appeared in the same period of time, for instance: `mzef` [Zhang, 1997], which identified internal coding exons by quadratic discriminant analysis; `morgan` [Salzberg *et al.*, 1998], which was an integrated system for finding genes in vertebrate DNA sequences by combining different methods with a decision tree classifier; and `Augustus` [Stanke and Waack, 2003], which incorporated an intron model to an underlying HMM. However, `genscan` is still considered the standard gene prediction program (at least for human) and it is used in most of the genome annotation pipelines like ENSEMBL and the NCBI genome resources.

### 3.1.2 Homology based gene-finding

The backbone of similarity-aided or homology-based gene structure determination is constituted by those methods that rely on comparison f the query sequence with protein or cDNA sequences. Database search software, such as `BLAST` [Altschul *et al.*, 1990, 1997] and related tools, is not capable of automatically identifying start and stop codons or splice sites. Therefore, additional tools are required to define the exonic structures on the potential targets found by the database search programs. Several tools, though, have been developed to calculate spliced alignments, where large gaps—likely to correspond to introns—are only allowed at legal splice junctions, between the query sequence and the to database matches. Among those one can cite `SIM4` [Florea *et al.*, 1998], `EST_genome` [Mott, 1997], `Spidey` [Wheelan *et al.*, 2001] and `exonerate` [Slater and Birney, 2005].

`Procrustes` [Gelfand *et al.*, 1996] and `genewise` [Birney and Durbin, 1997; Birney *et al.*, 2004b], both predict genes based on a comparison of a genomic query with protein targets. `GeneSeqer` [Usuka and Brendel, 2000] is a similar spliced alignment program for plant genomes. `Projector` [Meyer and Durbin, 2004] makes explicit use of the conservation of the exon-intron structure between related genes, which outperforms other tools when the conservation at the amino acid level is weak. Other tools increase the score of candidate exons as a function of the similarity between these exons and known coding sequences resulting of a database search. Examples of this approach are `genomescan` [Yeh

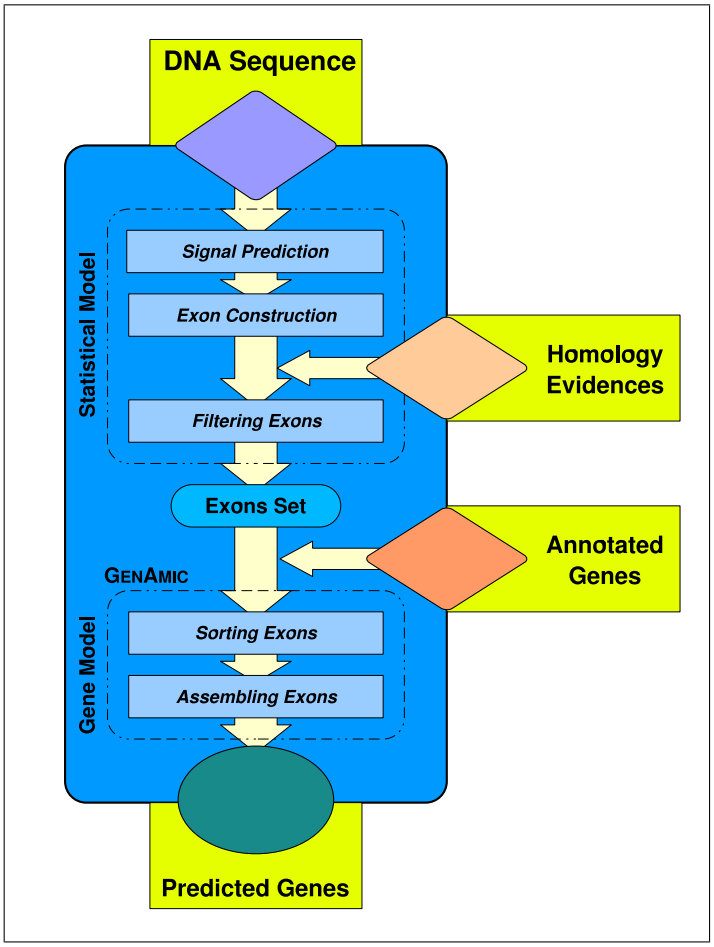


Figure 3.1:
**Overall flowchart of `geneid`.** DNA sequences are scanned to find signals which are then used to build exons. Homology evidences can modify the weights of exons in conserved regions before such exons get filtered to retrieve the high scoring ones. This feature is extensively exploited on `SGP2` implementation [Parra *et al.*, 2003]. Those exons are assembled into gene structures by `GenAmic`, a dynamic programming algorithm with linear asymptotic cost [Guigo, 1998], under a user-defined gene model. At this point, already annotated features can be integrated in the pool of predicted exons. Redrawn from `geneid` manual figure kindly provided by Enrique Blanco.

*et al.*, 2001], `grailexp` [Xu *et al.*, 1997] and `crasa` [Chuang *et al.*, 2003]; the first incorporates similarity to known proteins, the later two use ESTs instead.

### 3.1.3 Comparative genomics approach

With the availability of many genomes from different species, a number of strategies have been developed to use genome comparisons to predict genes. The rationale behind comparative genomic methods is that functional regions, protein coding regions among them, are more conserved than non-coding ones between genome sequences from different organisms. See, for instance, Figure 3.3 on page 22 (Parra *et al.* 2003, page 109, figure 1) and Figure 5.2 on page 153. This characteristic conservation can be used to identify protein coding exons in the sequences. The approach taken by different programs to exploit this idea differ notably.

In one such approach [Blayo *et al.*, 2002; Pedersen and Scharl, 2002], the problem is

stated as a generalization of pairwise sequence alignment: given two genomic sequences coding for homologous genes, the goal is to obtain the predicted exonic structure in each sequence maximizing the score of the alignment of the resulting amino acid sequences. Both Blayo *et al.* [2002] and Pedersen and Scharl [2002] solve the problem through a complex extension of the classical dynamic programming algorithm for sequence alignment. Although very appropriate for short sequences, in practice, the time and memory requirements of this algorithm limit its usefulness for very large genomic sequences. Although the approach theoretically guarantees to produce the optimal amino acid sequence alignment, the fact that sequence conservation may also occur in regions other than protein coding, could lead to overprediction of coding regions, in particular when comparing large genomic sequences from homologous genes from closely related species.

To overcome this limitation, the programs `doublescan` [Meyer and Durbin, 2002] and `SLAM` [Alexandersson *et al.*, 2003] rely on more sophisticated models of coding and noncoding DNA and splice signals, in addition to sequence similarity. Since sequence alignment can be solved with Pair Hidden Markov Models [PHMMs, Durbin *et al.*, 1998] and GHMMs have proven to be very useful to model the characteristics of eukaryotic genes [Burge and Karlin, 1997], `SLAM` and `doublescan` are built upon the so-called Generalized Pair HMMs. In these, gene prediction is not the result of the sequence alignment, as in the programs above, but both gene prediction and sequence alignment are obtained simultaneously.

A third class of programs adopts a more heuristic approach, and separates gene prediction from sequence alignment. The programs `rosetta`[Batzoglou *et al.*, 2000], `SGP1` [from Syntenic Gene Prediction, Wiehe *et al.*, 2001], and `cem` [from the Conserved Exon Method, Bafna and Huson, 2000] are representative of this approach. All these programs start by aligning two syntenic regions (specifically human and mouse in `rosetta`, and `cem`; less species specific in `SGP1`), using some alignment tool (the `glass` program, specifically developed in the case of `rosetta`, or generic ones, such as `TBLASTX`, or `sim96` in the case of `cem` and `SGP1` respectively) and then predict gene structures in which the exons are compatible with the alignment. This compatibility often requires conservation of exonic structure of the homologous genes encoded in the anonymous syntenic regions. Although conservation of exonic structure is an almost universal feature of orthologous human/mouse genes [Waterston *et al.*, 2002], it does not necessarily occur when comparing genomic sequences of homologous genes from other species.

The programs described so far rely on the comparison of fully assembled (and when from different organisms, syntenic) genomic regions. This limits their utility when analyzing complete large eukaryotic genomes and in particular when the informant genome is in non-assembled shotgun form. To overcome this limitation, the programs `Twinscan` [Korf *et al.*, 2001] and `SGP2` [Parra *et al.*, 2003] take a still different approach. The approach in these programs is reminiscent of that used in `genomescan` [Yeh *et al.*, 2001] to incorporate similarity to known proteins to modify the `genscan` scoring schema. Essentially, the query sequence from the target genome is compared against a collection of sequences from the informant genome (which can be a single homologous sequence to the query sequence, a whole assembled genome, or a collection of shotgun reads) and the results of the comparison are used to modify the scores of the exons produced by "*ab initio*" gene prediction programs. In `Twinscan`, the genome sequences are compared using `BLASTN` and the results serve to modify the underlying probability of the potential exons predicted by `genscan`. In `SGP2`, the genome sequences are compared using `TBLASTX`, and the results

used to modify the scores of the potential scores predicted by `geneid`; see methods section and Figure 3.4 on page 24 (page 110 and Figure 2 on page 111 of Parra *et al*. 2003).

As the number of available genome sequences of species at different evolutionary distances increases, methods to predict genes based on the comparative analysis of multiple genomes (and not only of two species) look promising. For instance, Dewey *et al*. [2004] combine pairwise predictions from `SLAM` in the human, mouse and rat genomes to simultaneously predict genes with conserved exonic structure in all three species. In the so-called Phylogenetic Hidden Markov Models (phylo-HMMs) or Evolutionary Hidden Markov Models (EHMMs), a gene prediction Hidden Markov Model is combined with a set of evolutionary models, based on phylogenetic trees. Phylo-HMMs take into account that the rate (and type) of evolutionary events differ in protein-coding and non-coding regions. Recently, phylo-HMMs have been applied to gene prediction with encouraging results [Pedersen and Hein, 2003; Siepel and Haussler, 2004].

Phylo-HMMs also have been used in the context of phylogenetic shadowing [Boffelli *et al*., 2003]. Phylogenetic shadowing examines sequences of closely related species and takes into account the phylogenetic relationship of the set of species analyzed. This approach enables the localization of regions of collective variation and complementary regions of conservation, facilitating the identification of coding as well as non-coding functional regions. The likelihood ratio under a fast (versus slow) mutation regime can be computed for each aligned nucleotide site across all the sequences being analyzed. This ratio represents the relative likelihood that any given nucleotide site was subjected to a faster or slower rate of accumulation of variation and is related to functional constraints imposed on each site. Exon containing sequences will display the least amount of cross species variation, in agreement with the constraint imposed by their function. Regions from different parts of the genome, in which functional non-coding sequences appear, may evolve at different rates [Ebersberger *et al*., 2002], reflected by differences in their absolute likelihoods. Despite that, functional non-coding regions can be retrieved from stretches of sequence having minimal variation similar to exonic ones.

### 3.1.4 Analysis pipelines to automatize sequence annotation

Gene prediction software is often integrated into analysis pipelines in order to produce annotations on sets of genomic sequences, for instance a set of chromosome assemblies for a given species or even a bunch of shotgun sequence reads. Here we will shift the focus towards the management of data on which the programs are run and the flow of annotation outputs among different tools. Systems developed to summarize and visualize annotations, that can be incorporated as another step of the annotation process, are extensively described in Chapter 5.

Human annotators use their intuition and experience to synthesize the often contradictory evidence into a single gene structure. Pipelines generally use rules based on the intuition and experience of their designers [Brent and Guigó, 2004]. Human interpretation of the results of these raw analysis by manual curators gives the highest-quality data and most accurate gene structures. However, this process is slow by nature, and annotators may produce conflicting interpretations of the analysis. Fully automated prediction of gene structures has the advantage of being fast, does not require a team of trained annotators, and will process the raw analysis results consistenly. Its major drawback, though, is that

it can underpredict both the number of genes and the number of alternative transcripts [Potter *et al.*, 2004].

`Pise` [Letondal, 2001], a web interface generator for molecular biology software, can combine related programs in order to perform more complex analyses. The macros generated by `Pise` constitute a procedure that will redo the same processing as that already performed, with another initial input. `SEALS` [Walker and Koonin, 1997] provides a suite of programs designed to facilitate analysis projects involving large amounts of data. The system is designed to provide modular elements which can be combined, modified and integrated with other methods. `Pise` can be understood as a web interface to analysis programs, while `SEALS` can be seen as a Unix command-line tool set. However, the first is not meant for automated large-scale analysis, and the latter requires too much manual interaction to be considered a true analysis pipeline.

The ENSEMBL gene-building system [Curwen *et al.*, 2004] enables fast automated annotation of eukaryotic genomes. It annotates genes based on evidence derived from known protein, cDNA and EST sequences. The initial stage of computation is known as the 'raw compute' and comprises various stand-alone analyses, including homology searches using `BLAST` [Altschul *et al.*, 1997]. Then, ENSEMBL takes these types of analyses one step further and provides a set of gene annotations based on them, to which extra biological information such as gene family, expression data and gene ontologies are linked. Similar systems have been developed for other databases: FLYBASE uses `BOP` [Mungall *et al.*, 2002], NCBI has its own pipeline [Kitts, 2002] as does the UCSC group [Kent *et al.*, 2002]. The ENSEMBL analysis pipeline [Potter *et al.*, 2004] is split into two parts. The first deals solely with the running of the individual analyses and parsing the output. The second part deals with the automated running, in the correct order, of the many analyses that constitute the pipeline. It keeps track of those that have run succesfully, while also coping with problems such as job failures. In order to scale up the process for the analysis of whole genomes, the pipeline only uses flat files locally on the execution nodes; input data are retrieved directly from a database, and the output data are written back the same way.

Large software systems usually consist of many independently developed parts, and there is a need for data exchange mechanisms to move information among the components. Data integration is a related problem, but with the focus on combining information in scientifically valid ways. Workflow management is the software technology used for keeping track of tasks to be done in generating large datasets or in the automated analysis of such datasets [Goodman, 2002]. A classification of tasks in Bioinformatics emphasizes that most bioinformatics requirements may be described in terms of filters, transformers, transformer-filters, forks and collections of data [Stevens *et al.*, 2001]. Two themes are consistent in these requirements: the need for running analyses in a serial rule-dependent fashion (workflow) and the ability to run these tasks in parallel where possible (highthroughput).

`Biopipe` [Hoon *et al.*, 2003] is a generic system for large-scale bioinformatics analysis, that has been influenced by the ENSEMBL pipeline. Smaller pipeline systems also exist for annotation of ESTs or individual clones. These systems include `Genescript` [Hudek *et al.*, 2003] and `ASAP` [Glasner *et al.*, 2003]. `PLAN` [Chagoyen *et al.*, 2004] is a simple `XML`-based language for the definition of executable workflows that simplifies data search and analysis by providing a uniform `XML` view on both data sources and analytical applications.

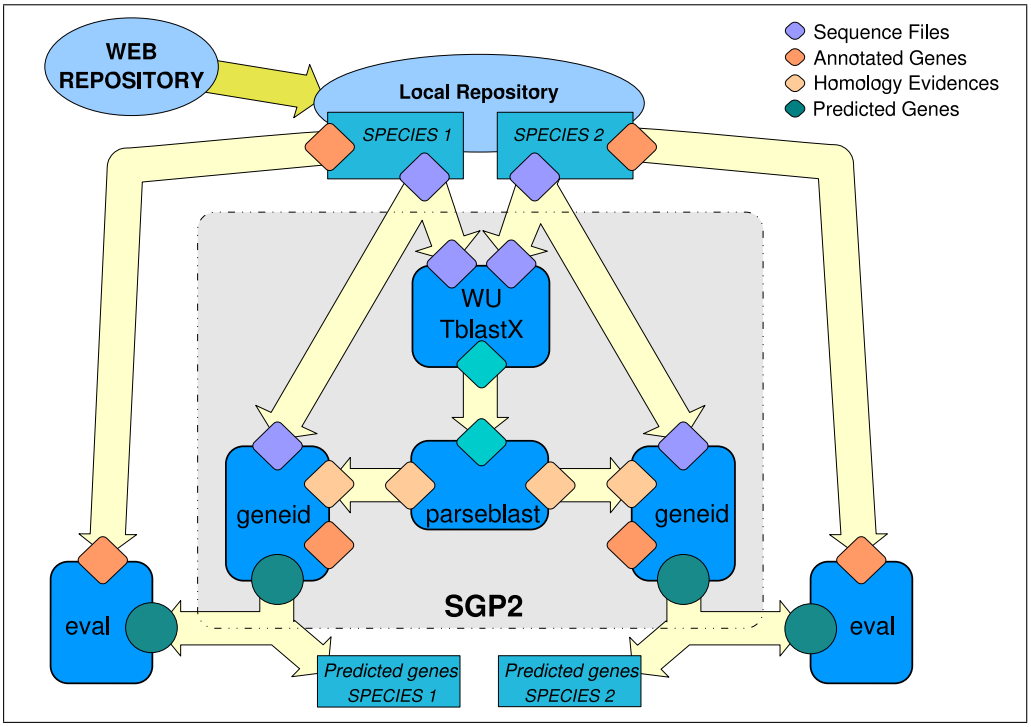


Figure 3.2: **SGP2-based analysis pipeline for pair-wise genome comparisons.** Data is retrieved from a remote server and it is reformatted in the local repository to suit the input for the programs involved in the pipeline. Annotations of known features can be used to train program parameters and to evaluate the outputs for the whole process. In such a scenario, visualizing tools, like `gff2ps` and `gff2aplot` (see sections 5.2 and 5.3.1, respectively), can be integrated in the pipeline to summarize predicted genes and homology features.

## 3.2 SGP2: Syntenic Gene Prediction Tool

The computational approach to incorporate information from the comparison of two genomes to `geneid` is described in the research article attached in the following subsection (see Section 3.2.1 on page 20), and it was briefly discussed on page 15 of Section 3.1.3. Here, we would like to discuss `SGP2` in the context of the genomic comparison between human and mouse, which is reflected in Section 3.2.2, page 31. The results for those analyses are summarized in Section "*De novo* gene prediction" on page 38 (page 539 of Waterston *et al.* 2002).

Figure 3.2 on page 18 displays a general analysis protocol to produce a set of gene predictions in a set of sequences for different species. `SGP2` can be seen there as a procedure based on `TBLASTX` and `geneid`. It also requires some programs to filter the similarity regions found by `TBLASTX`. In the figure, only the `parseblast` filter was drawn for the sake of simplicity, but there are a few other programs involved in the `SGP2` processing of similarity data. The algorithms and the parameter settings for the software are detailed in methods section and Figure 3.4 on page 24 (page 110 and Figure 2 on page 111 of Parra *et al.*

2003)

A whole analysis pipeline was developed for the human and mouse genome comparisons. It included preprocessing of the genome sequences and annotations from the UCSC FTP server; the search for homology between the sequences of the two genomes; the computational gene prediction approaches, both the "*ab initio*" (`geneid` and `genscan`) and the comparative genomics approach (`SGP2`). Results from other groups were also integrated in the pipeline in order to perform the evaluation of the gene predictions against different reference annotation sets (including RefSeq and Ensembl genes). At that time there were updates of sequence sets for each genome version that was assembled for the human and mouse genomes. This required to run again the whole protocol on those new genomic sequences. Another issue was the growing number of elements to be included in the analysis pipeline. To face both problems, we developed a simple task manager in `perl` to control the processes to be run on a given set of sequences, and to distribute the task among different machines of our lab. The `perl` program was provided with a set of unix shell scripts to be run in a given order and with a set of sequences. It scheduled all the jobs to be run for each sequence by using a simple execution queue. The task manager sent each job script to be executed on a sequence to a machine in the list of available computers of our lab. This was achieved with `rsh` remote shell calls, while the sequence files and the results were shared among all the computers involved in the analysis via the Network File System (`NFS`). The task scheduler also kept a record of the execution status of each submitted job, reporting those cases in which the remote execution failed, without resubmitting them.

The major drawback of this simple approach was the bottleneck of using flat files throught the `NFS` on multiple computers when programs required intensive input/output flow to the file system. This has been already stated in Potter *et al.* [2004], and was the reason for the development of the Ensembl analysis pipeline with a relational database system. However, the modular design of the shell scripts defining each job warranted that many of the components of the semi-automated analysis pipeline described in this section were recycled. They have been used to obtain predictions for new versions of the human and mouse genomes, but also for other genomes of species such as rat and chicken. The results have been collected in a web repository (see the "Gene Predictions on Genomes" entry in the *Web Glossary*, on page 214).

### 3.2.1 Parra *et al*, *Genome Research*, 13(1):108–117, 2003

**PubMed Accession:**

http://www.ncbi.nlm.nih.gov/entrez/query.fcgi?cmd=Retrieve&db=PubMed&list_uids=12529313&dopt=Abstract

**Journal Abstract:**

http://www.genome.org/cgi/content/abstract/13/1/108

**Supplementary Materials:**

http://genome.imim.es/datasets/sgp2002/

**Program Home Page:**

http://genome.imim.es/software/sgp2/

**Methods**

# Comparative Gene Prediction in Human and Mouse

Genís Parra,[1] Pankaj Agarwal,[2] Josep F. Abril,[1] Thomas Wiehe,[3] James W. Fickett,[4] and Roderic Guigó[1,5]

*[1]Grup de Recerca en Informàtica Biomèdica. Institut Municipal d'Investigació Medica / Universitat Pompeu Fabra / Centre de Regulació Genòmica 08003 Barcelona, Catalonia, Spain; [2]GlaxoSmithKline, King of Prussia, Pennsylvania 19406, USA; [3]Freie Universität Berlin and Berlin Center for Genome Based Bioinformatics (BCB), 14195 Berlin, Germany; [4]AstraZeneca R&D Boston, Waltham, Massachusetts 02451, USA*

**The completion of the sequencing of the mouse genome promises to help predict human genes with greater accuracy. While current ab initio gene prediction programs are remarkably sensitive (i.e., they predict at least a fragment of most genes), their specificity is often low, predicting a large number of false-positive genes in the human genome. Sequence conservation at the protein level with the mouse genome can help eliminate some of those false positives. Here we describe SGP2, a gene prediction program that combines ab initio gene prediction with TBLASTX searches between two genome sequences to provide both sensitive and specific gene predictions. The accuracy of SGP2 when used to predict genes by comparing the human and mouse genomes is assessed on a number of data sets, including single-gene data sets, the highly curated human chromosome 22 predictions, and entire genome predictions from ENSEMBL. Results indicate that SGP2 outperforms purely ab initio gene prediction methods. Results also indicate that SGP2 works about as well with 3x shotgun data as it does with fully assembled genomes. SGP2 provides a high enough specificity that its predictions can be experimentally verified at a reasonable cost. SGP2 was used to generate a complete set of gene predictions on both the human and mouse by comparing the genomes of these two species. Our results suggest that another few thousand human and mouse genes currently not in ENSEMBL are worth verifying experimentally.**

After the genome sequence of an organism has been obtained, the very first next step is to compile a complete and accurate catalog of the genes encoded in this sequence. For higher eukaryotic organisms, however, the accuracy of currently available gene prediction methods to perform such a task is limited (Guigó et al. 2000; Rogic et al. 2001; Guigó and Wiehe 2003). The increasing availability of genome sequences from different organisms, however, has lead to the development of new computational gene finding methods that use sequence conservation to help identifying coding exons, and improve the accuracy of the predictions (Fig. 1; Crollius et al. 2000; Wiehe et al. 2000; Miller 2001; Rinner and Morgenstern 2002). Indeed, three such comparative gene prediction programs, SLAM (Pachter et al. 2002), SGP2, and TWINSCAN (Korf et al. 2001) have been used for the comparative analysis of the human and mouse genomes. These analyses lead to more accurate gene predictions, and to the verification of previously unconfirmed genes. In this paper, we describe the program SGP2. Typical computational ab initio gene prediction methods rely on the identification of suitable splicing sites, start and stop codons along the query sequence, and the computation of some measure of coding likelihood to predict and score candidate exons, and delineate gene structures (see Claverie 1997; Burge and Karlin 1998; Haussler 1998; Zhang 2002 and references therein for reviews on computational gene finding).

Similarity between the query sequence and known coding sequences (amino acid or cDNA) can also be used to infer gene structures. When the query sequence encodes a protein for which a close homolog exists, a special type of alignment can be used between the DNA sequence and the target protein/cDNA sequence, in which gaps in the target sequence corresponding to introns in the query sequence must be compatible with potential splicing signals. This is the approach in GENEWISE (Birney and Durbin 1997) and PROCRUSTES (Gelfand et al. 1996). Alternatively, the results of searching the query sequence against a database of known coding sequences, using for instance BLASTX (Altschul et al. 1990, 1997; Gish and States 1993), can be incorporated more or less ad hoc into the scoring schema of an ab initio gene prediction method. The program GENOMESCAN (Yeh et al. 2001), which incorporates BLASTX search results into the predictions by the GENSCAN program (Burge and Karlin 1997), is an example of a recent development in that direction.

Recently developed comparative gene prediction programs further exploit sequence similarity. Instead of comparing anonymous genomic sequences to known coding sequences, anonymous genomic sequences are compared to anonymous genomic sequences from the same or different organisms, under the assumption that regions conserved in the sequence will tend to correspond to coding exons from homologous genes. The approach taken by the different programs to exploit this idea differs notably.

In one such approach (Blayo et al. 2002; Pedersen and Scharl 2002), the problem is stated as a generalization of pairwise sequence alignment: Given two genomic sequences coding for homologous genes, the goal is to obtain the predicted exonic structure in each sequence maximizing the score of the

**[5]Corresponding author.**
**E-MAIL rguigo@imim.es; FAX 34 93 224-0875.**
Article and publication are at http://www.genome.org/cgi/doi/10.1101/gr.871403.


13:108–117 ©2003 by Cold Spring Harbor Laboratory Press ISSN 1088-9051/03 $5.00; www.genome.org

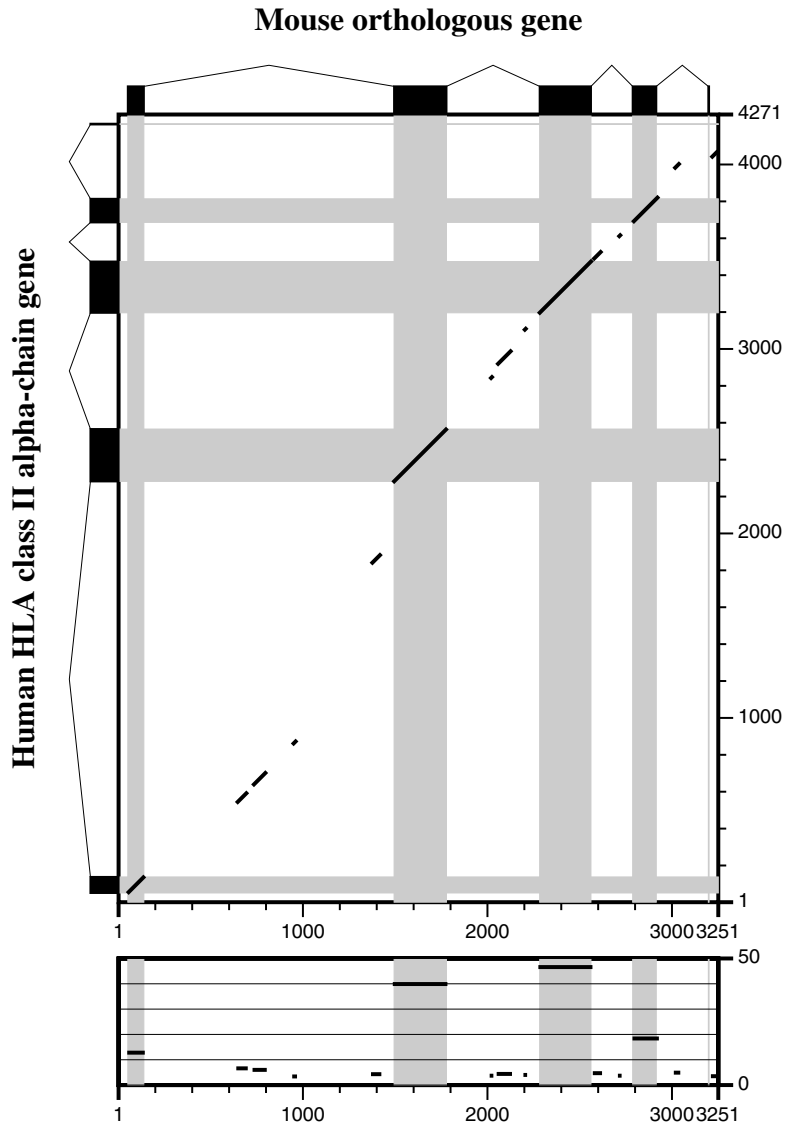


**Figure 1** Pairwise comparison using TBLASTX of the human and mouse genomic sequences coding for the HLA class II alpha chain. Black boxes indicate the coding exons, while black diagonals indicate the conserved alignments. The score of the conserved alignments (divided by 10) is given in the lower panels. Although conserved regions between the human and mouse genomic sequences coding for these genes fully include the coding exons, a substantial fraction of intronic regions is also conserved. The TBLASTX outptut was post-processed to show a continuous non-overlapping alignment.

alignment of the resulting amino acid sequences. Both Blayo et al. (2002) and Pedersen and Scharl (2002) solve the problem through a complex extension of the classical dynamic programming algorithm for sequence alignment.

In a different approach, the programs SLAM (Pachter et al. 2002) and DOUBLESCAN (Meyer and Durbin 2002) combine sequence alignment pair hidden Markov Models (HMMs; Durbin et al. 1998) with gene prediction generalized HMMs (GHMMs; Burge and Karlin 1997) into the so-called generalized pair HMMs. In these, gene prediction is not the result of the sequence alignment, as in the programs above; gene prediction and sequence alignment are obtained simultaneously.

A third class of programs adopt a more heuristic approach, and separate clearly gene prediction from sequence alignment. The programs ROSSETA (Batzoglou et al. 2000), SGP1 (from 'syntenic gene prediction'; Wiehe et al. 2001), and CEM (from 'conserved exon method'; Bafna and Huson 2000) are representative of this approach. All these programs start by aligning two syntenic sequences and then predict gene structures in which the exons are compatible with the alignment. The programs described thus far rely on the comparison of fully assembled (and when from different organisms, syntenic) genomic regions. This limits their utility when analyzing complete large eukaryotic genomes, and in particular when the informant genome is in nonassembled shotgun form. To overcome this limitation, the programs TWINSCAN (Korf et al. 2001) and SGP2 take still a different approach. The approach is reminiscent of that used in GENOMESCAN (Yeh et al. 2001) to incorporate similarity to known proteins to modify the GENSCAN scoring schema. Essentially, the query sequence from the target genome is compared against a collection of sequences from the informant genome (which can be a single homologous sequence to the query sequence, a whole assembled genome, or a collection of shotgun reads), and the results of the comparison are used to modify the scores of the exons produced by ab initio gene prediction programs. In TWINSCAN, the genome sequences are compared using BLASTN, and the results serve to modify the underlying probability of the potential exons predicted by GENSCAN. In SGP2, the genome sequences are compared using TBLASTX (W. Gish, 1996–2002, http://blast.wustl.edu), and the results are used to modify the scores of the potential scores predicted by GENEID. TWINSCAN and SGP2 have been successfully applied to the annotation of the mouse genome

(Mouse Genome Sequencing Consortium 2002), and have helped to identify previously unconfirmed genes (Guigó et al. 2003).

In the next section, we describe the algorithmic details of SGP2, and its implementation. We also describe the sequence sets used to benchmark SGP2 accuracy. Results based on these data sets indicate that SGP2 is an improvement over pure ab initio gene prediction programs, even when the informant genome is only in shotgun form. We have found that 3x coverage will generally suffice to achieve maximum accuracy. Finally, we describe the application of SGP2 to the comparative analysis of the human and mouse genomes.

## METHODS

### SGP2

SGP2 is a method to predict genes in a *target* genome sequence using the sequence of a second *informant* or *reference* genome. Essentially, SGP2 is a framework to integrate the ab initio gene prediction program GENEID (Guigó et al. 1992; Parra et al. 2000) with the sequence similarity search program TBLASTX. The approach is conceptually similar to that used in TWINSCAN to incorporate BLASTN searches into GENSCAN.

GENEID is a genefinder that predicts and scores all potential coding exons along a query sequence. Scores of exons are computed as log-likelihood ratios, which are a function of the splice sites defining the exon, and of the coding bias in composition of the exon sequence as measured by a Markov Model of order five (Borodovsky and McIninch 1993). From the set of predicted exons, GENEID assembles the gene structure (eventually multiple genes in both strands), maximizing the sum of the scores of the assembled exons, using a dynamic programming chaining algorithm (Guigó 1998).

When using an informant genome sequence to predict genes in a target genome sequence, ideally we would like to incorporate into the scores of the candidate exons predicted along the target sequence, the score of the optimal alignment at the amino acid level between the target exon sequence and the counterpart homologous exon in the informant genome sequence. If a substitution matrix, for instance from the BLOSUM family, is used to score the alignment, the resulting score can also be assumed to be a log-likelihood ratio: informally, the ratio between the likelihood of the alignment when the amino acid sequences code for functionally related proteins, and the likelihood of the alignment, otherwise. In principle, this score could be added to the GENEID score for the exon. TBLASTX provides an appropriate shortcut to often find a good enough approximation to such an optimal alignment, and infer the corresponding score: The optimal alignment can be assumed to correspond to the maximal scoring high-scoring segment pairs (HSP) overlapping the exon. However, when dealing in particular with the informant genome sequence in fragmentary shotgun form, often different regions of a candidate exon sequence will align optimally to different informant genome sequences. Thus, in the approach used here, we identify the optimal HSPs covering each fraction of the exon, and compute separately the contribution of each HSP into the score of the exon. In the next section, we describe in detail how this computation is performed.

#### *Scoring of Candidate Exons*

Let $e$ be one of the candidate exons predicted by GENEID along the query DNA sequence $S$. In SGP2, the final score of $e$, $s(e)$, is computed as

$$s(e) = s_g(e) + w s_t(e)$$

where $s_g(e)$ is the score given by GENEID to the exon $e$, and $s_t(e)$ is the score derived from the HSPs found by a TBLASTX search overlapping the exon $e$. Both scores are log-likelihood ratios (and we compute both base two). Assuming that both components are independent, they can be summed up into a single score. However, the assumption of independence is not realistic, $s_g(e)$ depends on the probability of the sequence of $e$, assuming that $e$ codes for a protein, while $s_t(e)$ depends on the probability of the optimal alignment of $e$ with a sequence fragment of the mouse genome, assuming that both sequences code for related proteins. Obviously, these two probabilities are not independent. Their joint distribution could only be investigated—at least empirically—if the Markov Model of coding DNA used in GENEID, and the substitution matrix used by TBLASTX were inferred from the very same set of coding sequences. Since this is quite difficult, if not unfeasible, we use an "ad hoc" coefficient, $w$, to weight the contribution of TBLASTX search, $s_t(e)$ into the final exon score.

We compute $s_t(e)$ in the following way. Let $h_1 \cdots h_q$ be the set of HSPs found by TBLASTX after comparing the query sequence $S$ against a database of DNA sequences (Fig. 2A).

First, we find the *maximum scoring projection* of the HSPs onto the query sequence. We simply register the maximum score among the scores of all HSPs covering each position, and then partition the query sequence in equally maximally scoring segments (bounded by dotted lines in Fig. 2A) $x_1 \cdots x_r$, with scores $s_p(x_1) \cdots s_p(x_r)$ (Fig. 2B).

Then, for each predicted exon $e$ (Fig. 2C), we find $X_e$, the set of maximally scoring segments overlapping $e$

$$X_e = \{x_i : x_i \cap e \neq \emptyset\}$$

where $a \cap b$ denotes the overlap between sequence segments $a$ and $b$, and $\emptyset$ means no overlap. We compute $s_t(e)$in the following way:

$$s_t(e) = \sum_{x \in X_e} s_p(x) \frac{|x \cap e|}{|x|}$$

where $|a|$ denotes the length of sequence segment $a$.

That is, each exon gets the score of the maximally scoring HSPs along the exon sequence proportional to the fraction of the HSP covering the exon. In other words, $s_t(e)$ is the integral of the maximum scoring projection function within the exon interval.

Once the scores $s$ have been computed for all predicted exons in the sequence $S$, gene prediction proceeds as usual in GENEID: The gene structure is assembled maximizing the sum of scores of the assembled exons.

#### *Running SGP2*

In practice, we run SGP2 in the following way. Given a DNA query sequence and a collection of DNA sequences, we compare the query sequence against the collection using TBLASTX 2.0MP-WashU [23-Sep-2001]. The query sequence can be a genomic fragment of any size, including complete eukaryotic chromosomes, whereas the collection of sequences may be almost anything from just a homologous region or a partial collection of genomic sequences from the same or another species to the whole genome sequence of a second species, either completely assembled or in shotgun form at any degree of coverage. In particular, two different regions of the same genome coding for homologous genes can be used within SGP2; in this case the same genome acts as target and informant.

In all the analyses reported here, we used BLOSUM62 as the amino acid substitution matrix, but changed the penalty for aligning any residue to a stop codon to $-500$. This helps to get rid of a large fraction of HSPs in noncoding regions. Because of TBLASTX limitations, large query sequences may need to be split in fragments before the search, and the results reconstructed afterwards. Results of TBLASTX search are then

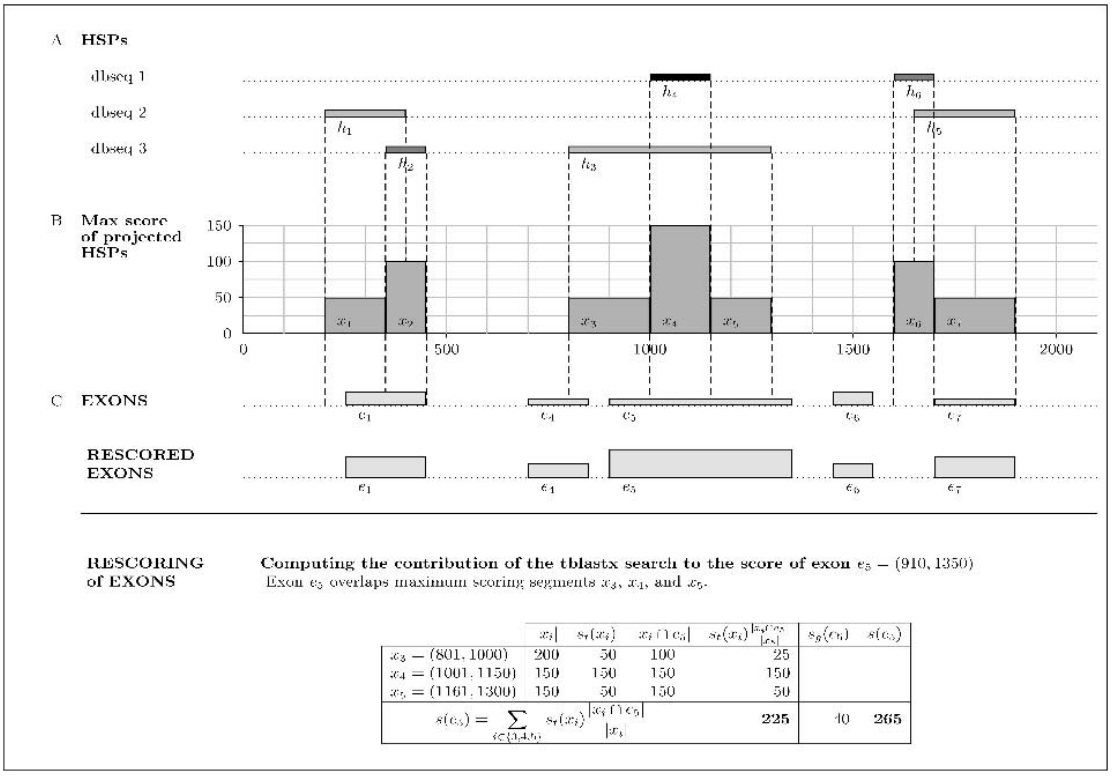


| | $\|x_i\|$ | $s_t(x_i)$ | $\|x_i \cap e_5\|$ | $s_t(x_i)^{\frac{\|x_i \cap e_5\|}{\|x_i\|}}$ | $s_g(e_5)$ | $s(e_5)$ |
|---|---|---|---|---|---|---|
| $x_3 = (801, 1000)$ | 200 | 50 | 100 | 25 | | |
| $x_4 = (1001, 1150)$ | 150 | 150 | 150 | 150 | | |
| $x_5 = (1161, 1300)$ | 150 | 50 | 150 | 50 | | |
| $s(e_5) = \sum_{i \in \{3,4,5\}} s_t(x_i)^{\frac{\|x_i \cap e_5\|}{\|x_i\|}}$ | | | | **225** | 40 | **265** |

**Figure 2** Rescoring of the exons predicted by GENEID according to the results of a TBLASTX search. See the "SGP2" section for a detailed explanation of the figure.

parsed to obtain the *maximum scoring projection* of the HSPs onto the query sequence. The parsing includes discarding all HSPs below a given bit score cutoff, subtracting this value from the score of the remaining HSPs, weighting the resulting score by *w* (see above), and collapsing the HSPs in to the maximum scoring projections. In all analyses described here, the bit score cutoff was set to 50, and *w* to 0.20. These values were chosen to optimize the gene predictions in sequence sets of known homologous human and mouse genomic sequences (see the Results section).

The *maximum scoring projection* is given to GENEID in general feature format (GFF; R. Durbin and D. Haussler, http://www.sanger.ac.uk/Software/GFF/). GENEID uses it to rescore the exons predicted along the query sequence as explained, and assembles the corresponding optimal gene structure. GENEID was already designed to incorporate external information into the gene predictions, and no changes were required in the program to accommodate it into the SGP2 context, only a small adjustment in the parameter file to cope with the change in scale of the exon scores.

We have written a simple PERL script which, given a query DNA sequence and the results of the TBLASTX search, performs all the components of the SGP2 analysis transparently: the parsing of the TBLASTX search results, and the GENEID predictions. In the case wherein both the query and the informant sequence are single genomic fragments, the gene predictions can be obtained in both sequences (without the need for a second TBLASTX search). The script, as well as the individual components, can be found at http://www1.imim.es/software/sgp2/.

GENEID has essentially no limits to the length of the input sequence, and deals well with chromosome size sequences. Limits to the length of the input query sequence that can be analyzed by SGP2 are, thus, those imposed by TBLASTX. GENEID is quite fast; given the parsed TBLASTX results, it takes 6 h to reannotate the whole human genome in a MOSIX cluster containing four PCs (PentiumIII Dual 500 Mhz processors).

### *Accelerating TBLASTX Searches*

TBLASTX searches, although efficient, are much slower. Its default usage may become computationally prohibitive when comparing complete eukaryotic genomes. In the context of SGP2, however, a number of TBLASTX options can be changed to speed up the search, without significant loss of sensitivity in the predictions (see the Results section). Thus, results in human chromosome 22 and whole-genome comparisons have been performed using the following set of parameters: W = 5, -nogap, -hspmax = 150,000, B = 200, V = 200, E = 0.01, E2 = 0.01, Z = 30,000,000, -filter = xnu + seg, and S2 = 80. In these cases, the query sequences have been broken up in 5 MB fragments, and the database sequences in 10 MB fragments. In all cases, stop codons are heavily penalized ($-500$) in the alignments. After the search is completed, locations of the resulting HSPs are recomputed in chromosomal coordinates. Results in the single-gene sequence benchmark data sets were obtained with default TBLASTX parameters.

## Sequence Data Sets

### *Benchmark Sequence Sets*

To optimize some of the parameters in SGP2 and to test its performance, we used a set of known pairs of genomic sequences coding for homologous human and rodent genes. The set is built after the set constructed by Jareborg et al. (1999). This is a set of 77 orthologous mouse and human gene pairs. We considered only the 33 pairs of sequences in this set

coding for single complete genes. In addition, we discarded six additional pairs, when we suspected that one of the members could be wrongly annotated. Orthology in the Jareborg et al. (1999) data set is based on sequence conservation. This could bias the set towards the more highly conserved human/mouse orthologous genes. To compensate for this bias, we obtained an additional set of pairs of human/rodent orthologous genes through an approach which does not involve sequence conservation: We obtained the set of pairs of human/mouse sequences from the SWISSPROT database sharing the prefix (indicating the gene) in their locus names. We kept only those pairs for which it was possible to find the corresponding annotated genomic sequence—including the mapping of the transcript, and not only of the coding regions—in the EMBL database. Fifteen additional genes were found this way. Three of them were discarded because we suspected wrong annotation in at least one of the members of the pair. We believe that orthology in the remaining cases is highly likely because of the absolute conservation of the exonic structure (number and length of exons, and intron phases) that we observed. We will call the resulting concatenated set of 39 pairs of human/mouse homologous genes the SCIMOG dataset (from Sanger Center IMim Orthologous Genes). The data set and the detailed protocol used to obtain it can be accessed at http://www1.imim.es/datasets/sgp2002/.

To test the accuracy of SGP2, we used the data set constructed by Batzoglou et al. (2000) of 117 orthologous human and mouse genes. We discarded those pairs in which in at least one of the sequences contained multiple genes, and those in which the coding region started in position 1 in one of the sequences of the pair. This resulted in 110 genes. We will call this set the MIT data set. There is some overlap between the SCIMOG and MIT data sets, and thus the latter cannot properly be called a test set. However, we decided not to eliminate the redundant entries, so that the results could be compared to those published for the ROSSETA program (Batzoglou et al. 2000).

Finally, we tested SGP2 in the complete sequence of human chromosome 22 (Dunham et al. 1999). The masked sequence was obtained from http://genome.cse.ucsc.edu/goldenPath/22dec2001/. Chromosome 22 is probably the best annotated human chromosome. We used the gene annotations at http://www.cs.columbia.edu/~vic/sanger2gbd/. The CDS set contains 554 genes. This is a conservative set that only contains the coding region of genes and does not include pseudogenes. This may lead to an underestimation of the specificity of the predictions.

#### *Mouse and Human Genome Sequences*

We used versions MGSCv3 of the mouse genome (2,726,995,854 bp, http://genome.cse.ucsc.edu/goldenPath/mmFeb2002/) and NCBI28 of the human genome (3,220,912,202 bp, http://genome.cse.ucsc.edu/goldenPath/22dec2001/). Both masked and unmasked sequences were obtained from these locations. ENSEMBL gene annotations for these genomes were obtained from http://genome.cse.ucsc.edu/goldenPath/22dec2001/database/ensGene.txt.gz for the human genome, and from http://genome.cse.ucsc.edu/goldenPath/mmFeb2002/database/ensGene.txt.gz for the mouse genome. ENSEMBL predicts 23,005 and 22,076 nonoverlapping transcripts genes on the human and mouse genome, respectively.

### Evaluating Accuracy

The measures of accuracy used here are extensively discussed in Burset and Guigó (1996). We will restate them briefly. Accuracy is measured at three different levels: nucleotide, exon, and gene. At the nucleotide and exon levels, we compute essentially the proportion of actual coding nucleotides/exons that have been correctly predicted—which we call *sensitivity*—and the proportion of predicted coding nucleotides/exons that are actually coding nucleotides/exons—which we call *specificity*. To compute these measures at the exon level, we will assume that an exon has been correctly predicted only when both its boundaries have been correctly predicted. To summarize both *sensitivity* and *specificity*, we compute the *correlation coefficient* at the nucleotide level, and the average of *sensitivity* and *specificity* at the exon level. At the exon level, we also compute the *missing exons*, the proportion of actual exons that overlap no predicted exon, and the *wrong exons*, the proportion of predicted exons that overlap no real exons.

At the gene level, a gene is correctly predicted if all of the coding exons are identified, every intron–exon boundary is correct, and all of the exons are included in the proper gene. In addition, we compute the missed genes (MGs), real genes for which none of its exons are overlapped by a predicted gene, and the wrong genes (WGs), predictions for which none of the exons are overlapped by a real gene. In general, gene finders predict the initial and terminal exons very poorly. This often leads to so-called chimeric predictions—one predicted gene encompassing more than one real gene—or to split predictions—one real gene split in multiple predicted genes. Reese et al. (2000) developed two measures, split genes (SG) and joined genes (JG), to account for these tendencies. SG is the total number of predicted genes overlapping real genes divided by the number of genes that were split. Similarly, JG is the total number of real genes that overlap predicted genes divided by the number of predicted genes that were joined.

## RESULTS

### Benchmarking SGP2

We evaluated the accuracy of SGP2 using a number of different data sets. The lack of a gold standard of gene prediction makes it difficult to get accurate assessments from any single data set. We primarily used three data sets as described earlier.

To benchmark SGP2, we constructed BLAST databases from the mouse and human sections of SCIMOG and MIT, and each mouse/human sequence to the entire human/mouse database, respectively. This enabled us to predict genes in both the mouse and human databases. The results from

**Table 1.** Gene Prediction in the SCIMOG Data Set

| | Nucleotide | | | Exon | | | | |
|---|---|---|---|---|---|---|---|---|
| Program | Sn | Sp | CC | Sn | Sp | (Sn+Sp)/2 | ME | WE |
| GENSCAN | 0.98 | 0.86 | 0.92 | 0.84 | 0.75 | 0.79 | 0.04 | 0.14 |
| TBLASTX default | 0.89 | 0.76 | 0.81 | 0.81 | — | — | 0.19 | 0.11 |
| SGP2 (single complete genes) | 0.97 | 0.98 | 0.97 | 0.89 | 0.89 | 0.89 | 0.03 | 0.03 |
| SGP2 (multiple genes) | 0.94 | 0.97 | 0.95 | 0.80 | 0.87 | 0.83 | 0.10 | 0.02 |

**Table 2.** Gene Prediction Accuracy in the MIT Data Set

| | Nucleotide | | | Exon | | | | |
|---|---|---|---|---|---|---|---|---|
| Program | Sn | Sp | CC | Sn | Sp | (Sn+Sp)/2 | ME | WE |
| GENSCAN | 0.98 | 0.89 | 0.93 | 0.82 | 0.75 | 0.78 | 0.06 | 0.13 |
| ROSSETA | 0.95 | 0.97 | — | — | — | — | 0.02 | 0.03 |
| TBLASTX default | 0.94 | 0.79 | 0.85 | — | — | — | 0.13 | 0.13 |
| SGP2 (single complete genes) | 0.97 | 0.98 | 0.97 | 0.84 | 0.85 | 0.84 | 0.05 | 0.03 |
| SGP2 (multiple genes) | 0.96 | 0.97 | 0.96 | 0.71 | 0.79 | 0.75 | 0.12 | 0.03 |

comparing SGP2, GENSCAN, and ROSSETA accuracy values in this case are taken from Batzoglou et al. (2000), and the results of a simple TBLASTX search on the MIT data set are in Table 2 (below). For the TBLASTX searches, the *maximum scoring projection* of the HSPs (see the above section titled "SGP2") was assumed to be the gene prediction. The score cutoff for the HSPs was chosen to maximize the correlation coefficient (CC) between the projected HSPs and the coding exons. In Table 1,2, we report the accuracy of GENSCAN, SGP2, and TBLASTX on the SCIMOG dataset. The accuracy values for SGP2 are reported under two scenarios: assuming a single complete gene and assuming multiple genes. Both GENEID and SGP2 allow the external specification of a *gene model* (i.e., a small number of rules specifying the legal assemblies of exons into gene structures). These rules can be used to force SGP2 to predict a single complete gene to make the results comparable to those of ROSSETA. Without such a restriction (i.e., making no assumptions about the number and completeness of the genes potentially encoded in the query sequence), the results are more directly comparable to those of GENSCAN (although GENSCAN also has a tendency to start a prediction in any sequence with an initial exon, and to terminate it with a terminal exon).

The accuracy of SGP2 is comparable to that of ROSSETA, and is significantly higher than that of GENSCAN. SGP2 also improves substantially over a simple TBLASTX search. The relative low specificity of the TBLASTX search—even after the large penalties for stop codons—reflects the fact that a substantial fraction of the conservation between the human and mouse genomes extends into the noncoding regions (Mouse Genome Sequencing Consortium 2002). At the nucleotide level, SGP2 accuracy is almost equal in the MIT data set and the SCIMOG data set (even though the SGP2 was trained on SCIMOG). The accuracy at the exact exon level, however, decreases, in particular when prediction of multiple genes is allowed. This is a problem inherited from GENEID, which tends to replace short initial and terminal exons with longer internal exons.

### *Accuracy of SGP2 as a Function of the Coverage of the Mouse Genome*

To investigate the utility of partial shotgun data as informant sequence in our approach based on TBLASTX, we simulated shotgun mouse sequence data at different levels of coverage (1.5x, 3x, and 6x) from the mouse genes in the SCIMOG data set, and used them to compare the human sequences in SCIMOG using TBLASTX. The mouse genomic sequences was shredded with uniformly distributed length between 500 and 600 bp with random starting points. No sequencing errors were introduced. At each coverage, we measured the CC between the TBLASTX hits projected along the human genome sequence, and the coding exons (choosing the TBLASTX score cutoff resulting in the optimal CC). With 1.5x coverage, a substantial fraction of the human coding region is not identified by TBLASTX, whereas with 3x, the results are quite similar to those obtained with 6x, which are identical to those obtained with the fully assembled syntenic regions (Table 3). This indicates that even with 3x coverage of the informant genome, our method will produce results nearly identical to those obtained with fully assembled regions. Assembled genomes, however, result in faster TBLASTX searches.

### *Accuracy of SGP2 in Human Chromosome 22*

Human chromosome 22 was the first human chromosome fully sequenced (Dunham et al. 1999), and it is quite the best annotated thus far, due to a number of experimental followups (Das et al. 2001; Shoemaker et al. 2001). Therefore, it provides an excellent data set to validate any gene prediction technology. Human chromosome 22 was searched using TBLASTX against the masked whole-genome assembly from the mouse genome (MGSCv3). The HSPs in chromosomal coordinates resulting from the TBLASTX search were used in GENEID to perform SGP2 gene prediction. Although the HSPs had been computed on the masked sequence, in this case the SGP2 predictions were obtained on the unmasked one. SGP2 predicted 729 genes on human chromosome 22. Table 4 shows the comparative accuracy of the SGP2, GENSCAN, GENOMESCAN, and pure ab initio GENEID predictions (without TBLASTX data). GENSCAN predictions on the masked sequence were taken from the USCS genome browser http://genome.cse.ucsc.edu/. GENOMESCAN predictions were obtained from ftp://ftp.ncbi.nih.gov/genomes/H_sapiens/build28_chr_genomescan.gtf.gz. Pure ab initio GENEID predictions were obtained on the masked sequence, and can also be downloaded from http://www1.imim.es/genepredictions/.

Although SGP2 is not more sensitive than GENSCAN, it appears to be more specific (as it utilizes the mouse genome).

**Table 3.** Accuracy of TBLASTX Predictions as a Function of the Degree of Coverage in the SCIMOG Data Set

| | Nucleotide | | | Exon | |
|---|---|---|---|---|---|
| Coverage | Sn | Sp | CC | ME | WE |
| Simulated 1.5x | 0.79 | 0.78 | 0.77 | 0.25 | 0.10 |
| Simulated 3x | 0.86 | 0.76 | 0.80 | 0.21 | 0.11 |
| Simulated 6x | 0.89 | 0.76 | 0.81 | 0.19 | 0.11 |
| Fully assembled | 0.89 | 0.76 | 0.81 | 0.19 | 0.11 |

**Table 4.** Accuracy of Gene-finding Programs on Human Chromosome 22

| | Nucleotide | | | Exon | | | | | Gene | | | | | | |
|---|---|---|---|---|---|---|---|---|---|---|---|---|---|---|---|
| Program | Sn | Sp | CC | Sn | Sp | (Sn+Sp)/2 | ME | WE | Sn | Sp | (Sn+Sp)/2 | MG | WG | JG | SG |
| GENSCAN | 0.86 | 0.50 | 0.64 | 0.70 | 0.40 | 0.55 | 0.13 | 0.50 | 0.06 | 0.04 | 0.05 | 0.11 | 0.45 | 1.24 | 1.07 |
| GENOMESCAN | 0.87 | 0.44 | 0.59 | 0.72 | 0.36 | 0.54 | 0.10 | 0.55 | 0.11 | 0.06 | 0.08 | 0.12 | 0.52 | 1.07 | 1.14 |
| GENEID | 0.80 | 0.63 | 0.69 | 0.66 | 0.53 | 0.59 | 0.19 | 0.35 | 0.09 | 0.07 | 0.08 | 0.14 | 0.39 | 1.20 | 1.08 |
| TBLASTX | 0.84 | 0.39 | 0.54 | — | — | — | 0.12 | 0.74 | — | — | — | 0.11 | — | — | — |
| SGP2 | 0.83 | 0.67 | 0.73 | 0.68 | 0.56 | 0.62 | 0.16 | 0.31 | 0.13 | 0.10 | 0.11 | 0.14 | 0.36 | 1.14 | 1.13 |

Fifty percent of the GENSCAN-predicted exons do not overlap annotated chromosome 22 exons; this number is only 31% for SGP2. Overall, SGP2 appears to be more accurate than GENSCAN in human chromosome 22: GENSCAN's CC at the nucleotide level is 0.64, whereas that of SGP2 is 0.73. Although accuracy decreases for both programs when going from single-gene sequences (Tables 1, 2) to an entire chromosome, SGP2 retains more accuracy. GENSCAN overall shows higher sensitivity than SGP2, but there were 45 real genes not predicted by GENSCAN on human chromosome 22, and SGP2 was able to predict, at least partially, 15 of them. This suggests that SGP2 and GENSCAN may play complementary roles. GENOMESCAN, on the other hand, did not appear to be superior to GENSCAN in human chromosome 22.

Mouse matches (TBLASTX HSPs) covered 11% of the human chromosome 22. Though they covered 85% of the coding nucleotides, 74% of the HSPs fell outside annotated coding regions. This illustrates the difficulties of using genome sequence conservation even at the protein level between human and mouse genomes to infer coding genes.

## Prediction of Genes in the Human and Mouse Genomes

We used SGP2 to predict the entire complement of human (NCBI28) and mouse (MGSCv3) genes. The masked sequences of these two genomes were compared using TBLASTX. The TBLASTX HSPs were used within SGP2. SGP2 predicted 44,242 genes in the human genome, and 44,777 genes in the mouse genome. Obviously, it is difficult to accurately assess these predictions. We used ENSEMBL genes as the set of reference annotations and compared both GENSCAN and SGP2 predictions to it. Figure 3 shows summaries of the accuracy of SGP2 at the chromosome level in the human and mouse genomes. When compared against ENSEMBL, SGP2 is more accurate than GENSCAN.GENSCAN. It is more specific at the nucleotide level: the average SGP2 specificity is 0.60 for human and 0.61 for mouse, whereas these values for GENSCAN are 0.43 and 0.44. SGP2 is also equally sensitive at the nucleotide level: The average SGP2 sensitivity is 0.82 for human and 0.85 for mouse; these values for GENSCAN are 0.82 and 0.84. Overall, the average SGP2 CCs are 0.70 for human and 0.72 for mouse, and for GENSCAN, the respective averages are 0.59 and 0.61. The accuracy of the SGP2 predictions, moreover, appears to be more consistent across chromosomes than that of the GENSCAN predictions. Interestingly, human chromosome Y is an outlier, with genes in this chromosome being poorly predicted. Genes in chromosome Y appear to be more difficult to predict than genes in other chromosomes for pure ab initio gene prediction programs, because chromosome Y is also an outlier for GENSCAN. SGP2 suffers, in addition, on human chromosome Y because the mouse chromosome Y has yet to be sequenced, and thus there was no comparative information available.

Overall, 23,913 of the human predictions and 24,203 of the mouse predictions overlapped ENSEMBL genes, whereas 95% of the mouse and 93% of the human ENSEMBL genes were among the genes predicted by SGP2. Of the remaining putative novel 20,570 mouse SGP2 genes and 20,193 human SGP2 genes, 10,456 mouse and 9,006 human predictions were found to be similar at $P < 10^{-6}$ to a prediction in the counterpart genome. Of these, 5,960 and 4,909 have multiple exons and are longer than 300 bp. A significant fraction of these putative homologous predictions are likely to correspond to real genes (Guigó et al. 2003). The predictions are interactively accessible through the USCS genome browser (http://genome.cse.ucsc.edu/) and through the DAS server at ENSEMBL (http://www.ensembl.org, under "DAS sources"). The complete set of prediction files is available at http://www1.imim.es/genepredictions/.

### *Speeding Up TBLASTX Searches*

Using TBLASTX to compare human and mouse whole-genome sequences, even in masked form, is quite expensive computationally because of the 6-frame translation on both query and target. To substantially reduce the search time, we used a word size of 5 and sacrificed some sensitivity (see the section above titled "Accelerating TBLASTX Searches" for details). We also penalized stop codons heavily and did not permit gaps. The computation took an estimated 500 CPU days on a farm of Compaq Alphas.

Accuracy in Tables 1 and 2 was computed using default TBLASTX parameters. Table 5 shows the comparative accuracy of TBLASTX and SGP2 predictions, under the default and the speed-up configuration of TBLASTX parameters on the SCIMOG data set. The sensitivity of speed-up TBLASTX searches drops from 0.89 to 0.72, but specificity increases slightly. SGP2 is more robust, and it compensates for some of the sensitivity lost in the TBLASTX search. Overall accuracy for SGP2, as measured by the CC, drops only from 0.95 to 0.93.

Predictions on human chromosome 22 and the whole human and mouse genomes have been obtained with this speed-up configuration of parameters.

## DISCUSSION

We have described the program SGP2 for comparative gene finding, and presented the results of its application to the human and mouse genome sequences. Results in controlled benchmark sequence data sets indicate that, by including in-

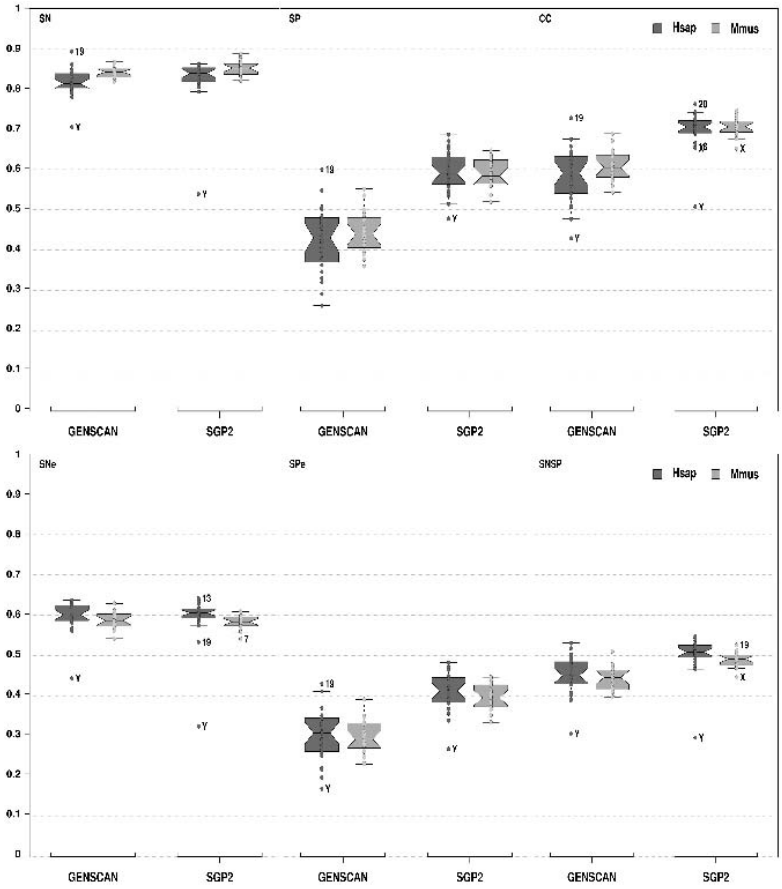


**Figure 3** Accuracy of the human and mouse SGP2 and GENSCAN predictions. The accuracy was measured in the entire chromosome sequences using the standard accuracy measures: SN, (sensitivity); SP, (specificity); CC, (correlation coefficient); SNe, (exon sensitivity); SPe, (exon specificity); and SNSP, (average of sensitivity and specificity at exon level). Predictions from both programs were compared against the human and mouse ENSEMBL annotations. Each dot corresponds to the accuracy measure of one chromosome. Chromosome labels are shown for outlier values. The boxplots (Tukey 1977) were obtained using the R-package (http://cran.r-project.org/).

formation from genome sequence conservation, predictions by SGP2 appear to be more accurate than those obtained by pure ab initio programs, exemplified here by GENSCAN and GENEID. Although there is not a significant gain in sensitivity, the specificity of the predictions appears to increase substantially, and a smaller number of false positive exons are predicted.

Indeed, one the major obstacles towards the completion of the catalog of human (mammalian) genes is our inability to assess the reliability of the large number of computational gene predictions that have not been verified experimentally. Whereas the ENSEMBL pipeline produces about 25,000 human and mouse genes, the NCBI annotation pipeline predicts almost 50,000 genes in mouse, and the program GENOMESCAN predicts close to 55,000 genes in this species. Although a large fraction of the ENSEMBL genes correspond to computational predictions without experimental verification, the method is quite conservative, and recent experiments suggest that essentially all ENSEMBL genes are indeed real (Guigó et al. 2003). The problem remains with the tens of thousands of additional computational predictions that are not included in ENSEMBL. A fraction of them are likely to be real, but the question is how large this fraction is. The results obtained here in human chromosome 22 seem to indicate that it may not be very large. Although the existence of hundreds of unidentified genes in this chromosome cannot be completely ruled out, the results strongly suggest that a substantial fraction of these additional computational gene predictions are false positives.

In this regard, the results presented here demonstrate that through the comparison of the human and mouse genomes using SGP2 (or another available comparative gene prediction tool), the false-positive rate can be reduced significantly, and the catalog of mammalian genes better defined. SGP2 predicts a few thousand candidate genes not in ENSEMBL that we believe are worth verifying experimentally. Indeed, the experimental verification of a subset of these provides evidence of at least 1000 previously nonconfirmed genes (Guigó et al. 2003).

The predictions by SGP2 obtained here are, of course, still far from definitively setting this catalog. For one thing, the mouse may be too close a species to human: A large fraction of the sequence has been conserved between the genomes of these two species. Indeed, most sequence conservation between human and mouse does not correspond to coding exons (Mouse Genome Sequencing Consortium 2002), compounding gene prediction. This suggests that the genome of another vertebrate species evolutionarily located between fish and mammals could be of great utility towards closing in the vertebrate (and mammalian) gene catalog.

SGP2 is flexible enough so that it can be easily accommodated to analyze species other than human and mouse. The fact that it can deal with shotgun data at any level of coverage means that as the sequence of a new genome starts becoming available, it can be used to improve the annotation of other already existing genomes. Particularly relevant in this context is a feature of SGP2 (and GENEID) that we have not explored here. SGP2 can produce predictions on top of preexisting annotations. For instance, we could have given to SGP2 the location and exonic coordinates (in GFF format) of known REFSEQ genes (or ENSEMBL), and SGP2 would have predicted genes only outside the boundaries of these genes of

**Table 5.** Accuracy of TBLASTX and SGP2 Predictions Using "Default" versus Speed-Up Parameters

| | | Nucleotide | | | Exon | | | | |
|---|---|---|---|---|---|---|---|---|---|
| | | Sn | Sp | CC | Sn | Sp | (Sn+Sp)/2 | ME | WE |
| Default | TBLASTX | 0.89 | 0.76 | 0.81 | — | — | — | 0.19 | 0.11 |
| | SGP2 | 0.94 | 0.97 | 0.95 | 0.80 | 0.87 | 0.83 | 0.10 | 0.02 |
| Speed-up | TBLASTX | 0.72 | 0.80 | 0.75 | — | — | — | 0.22 | 0.10 |
| | SGP2 | 0.88 | 0.98 | 0.93 | 0.77 | 0.85 | 0.81 | 0.12 | 0.02 |

already well known exonic structure. Preliminary results indicate that this approach improves gene prediction outside of the preassumed genes, and reduces the rate of chimeric predictions (i.e., predictions encompassing multiple genes). Moreover, we believe that SGP2 can be substantially improved. The flexibility of the SGP2/GENEID framework makes it quite easy to integrate additional information that can contribute to the accuracy of the predictions: synonymous versus nonsynonymous substitution rates in the alignments by TBLASTX, conservation of the splice signals in the informant genome, amino acid substitution matrices specific to the phylogenetic distance between the species compared, etc.

In this regard, the reasons to use the default BLOSUM62 matrix are not obvious. Given the expected sequence similarity between mouse–human orthologs, BLOSUM80 appears to be a better choice. However, we intended to also detect divergent families. Towards that end, the superiority of BLOSUM80 is less clear. We have compared TBLASTX search results on human chromosome 22 against the whole mouse genome. Whereas the HSPs resulting from the BLOSUM62 search cover 84% of the chromosome 22 coding nucleotides, BLOSUM80 HSPs cover 88% of them. However, BLOSUM80 is much less specific than BLOSUM62: 60% of the nucleotides in the BLOSUM62 HSPs fall outside coding regions, compared to 88% for BLOSUM80. It is thus clear that the optimal matrix or combination of matrices for comparative gene-finding using TBLASTX requires further investigation.

Although a large fraction of the human genome sequence has been known for more than a year, the exact number of human genes and their precise definition remain unknown. Gene specification in higher eukaryotic sequences is the result of the complex interplay of sequence signals encoded in the primary DNA sequence, which is only partially understood. Without an exhaustive catalog of human genes, however, the promises of genome research in medicine and technology cannot be completely fulfilled. The work presented here, in which it is shown that human–mouse comparisons can contribute to the completion of the mammalian (human) gene catalog, underscores the importance of the comparisons of the genomes of different organisms to fully understand the phenomenon of life, and in particular to deciphering the mechanism, central to life, by means of which the genome DNA sequence specifies the amino acid sequence of the proteins.

## ACKNOWLEDGMENTS

We thank the Mouse Genome Sequencing Consortium for providing the mouse genome sequence as well as support throughout the analysis process. We especially thank Francisco Câmara for arranging the data listed in the gene-prediction page on our group Web site, and for setting up and taking care of our DAS server. We also thank Ian Korf for inspiring discussions regarding the parameters to use in the TBLASTX search. We thank Enrique Blanco, Sergi Castellano, and Moisés Burset for helpful discussions and constant encouragement. This work was supported by a grant from Plan Nacional de I+D (BIO2000-1358-C02-02), Ministerio de Ciencia y Tecnologia (Spain), and from a fellowship to J.F.A. from the Instituto de Salud Carlos III (99/9345).

The publication costs of this article were defrayed in part by payment of page charges. This article must therefore be hereby marked "advertisement" in accordance with 18 USC section 1734 solely to indicate this fact.

## REFERENCES

Altschul, S.F., Gish, W., Miller, W., Myers, E.W., and Lipman, D. 1990. Basic local alignment search tool. *J. Mol. Biol.* **215:** 403–410.

Altschul, S.F., Madden, T., Schaffer, A., Zhang, J., Zhang, Z., Miller, W., and Lipman, D. 1997. Gapped BLAST and PSI-BLAST: A new generation of protein database search programs. *Nucleic Acids Res.* **25:** 3389–3402.

Bafna, V. and Huson, D.H. 2000. The conserved exon method. *Proc. Int. Conf. Intell. Syst. Mol. Biol.* **8:** 3–12.

Batzoglou, S., Pachter, L., Mesirov, J.P., Berger, B., and Lander, E.S. 2000. Human and mouse gene structure: Comparative analysis and application to exon prediction. *Genome Res.* **10:** 950–958.

Birney, E. and Durbin, R. 1997. Dynamite: A flexible code generating language for dynamic programming methods used in sequence comparison. *Proc. Int. Conf. Intell. Syst. Mol. Biol.* **5:** 56–64.

Blayo, P., Rouzé, P., and Sagot, M.-F. 2002. Orphan gene finding—An exon assembly approach. *Theoretical Computer Science* (in press).

Borodovsky, M. and McIninch, J. 1993. GenMark: Parallel gene recognition for both DNA strands. *Comput. Chem.* **17:** 123–134.

Burge, C.B. and Karlin, S. 1997. Prediction of complete gene structures in human genomic DNA. *J. Mol. Biol.* **268:** 78–94.

Burge, C.B. and Karlin, S. 1998. Finding the genes in genomic DNA. *Curr. Opin. Struct. Biol.* **8:** 346–354.

Burset, M. and Guigó, R. 1996. Evaluation of gene structure prediction programs. *Genomics* **34:** 353–357.

Claverie, J.-M. 1997. Computational methods for the identification of genes in vertebrate genomic sequences. *Hum. Mol. Genet.* **6:** 1735–1744.

Crollius, H.R., Jaillon, O., Bernot, A., Dasilva, C., Bouneau, L., Fischer, C., Fizames, C., Wincker, P., Brottier, P., Quetier, F., et al. 2000. Estimate of human gene number provided by genome-wide analysis using *Tetraodon nigroviridis* DNA sequence. *Nat. Genet.* **25:** 235–238.

Das, M., Burge, C.B., Park, E., Colinas, J., and Pelletier, J. 2001. Assessment of the total number of human transcription units. *Genomics* **77:** 71–78.

Dunham, I., Hunt, A.R., Collins, J.E., Bruskiewich, R., Beare, D.M., Clamp, M., Smink, L.J., Ainscough, R., Almeida, J.P., Babbage, A., et al. 1999. The DNA sequence of human chromosome 22. *Nature* **402:** 489–495.

Durbin, R., Eddy, S., Crogh, A., and Mitchison, G. 1998. *Biological sequence analysis: Probabilistic models of protein and nucleic acids.* Cambridge University Press, Cambridge.

Gelfand, M.S., Mironov, A.A., and Pevzner, P.A. 1996. Gene recognition via spliced alignment. *Proc. Natl. Acad. Sci.* **93:** 9061–9066.

Gish, W. and States, D. 1993. Identification of protein coding regions by database similarity search. *Nat. Genet.* **3:** 266–272.

Guigó, R. 1998. Assembling genes from predicted exons in linear time with dynamic programming. *J. Comp. Biol.* **5:** 681–702.
Guigó, R. and Wiehe, T. 2003. Gene prediction accuracy in large DNA sequences. In *Frontiers in computational genomic* (eds. M.Y. Galperin and E.V. Koonin), Caister Academic Press, Norfolk, UK.
Guigó, R., Knudsen, S., Drake, N., and Smith, T.F. 1992. Prediction of gene structure. *J. Mol. Biol.* **226:** 141–157.
Guigó, R., Agarwal, P., Abril, J.F., Burset, M., and Fickett, J.W. 2000. Gene prediction accuracy in large DNA sequences. *Genome Res.* **10:** 1631–1642.
Guigó, R., Dermitzakis, E.T., Agarwal, P., Pontig, C.P., Parra, G., Reymond, A., Abril, J.F., Keibler, E., Lyle, R., Ucla, C., et al. 2003. Comparison of mouse and human genomes followed by experimental verification yields an estimated 1,019 additional genes. *Proc. Natl. Acad. Sci.* (in press).
Haussler, D. 1998. Computational genefinding. *Trends in biochemical sciences, supplementary guide to bioinformatics*, pages 12–15.
Jareborg, N., Birney, E., and Durbin, R. 1999. Comparative analysis of noncoding regions of 77 orthologous mouse and human gene pairs. *Genome Res.* **9:** 815–824.
Korf, I., Flicek, P., Duan, D., and Brent, M.R. 2001. Integrating genomic homology into gene structure prediction. *Bioinformatics* **17 Suppl 1:** 140–148.
Meyer, I.M. and Durbin, R. 2002. Comparative ab initio prediction of gene structures using pair HMMs. *Bioinformatics* **18:** 1309–1318.
Miller, W. 2001. Comparison of genomic DNA sequences: Solved and unsolved problems. *Bioinformatics* **17:** 391–397.
Mouse Genome Sequencing Consortium 2002. Initial sequencing and comparative analysis of the mouse genome. *Nature* **420:** 520–562.
Pachter, L., Alexandersson, M., and Cawley, S. 2002. Applications of generalized pair hidden Markov models to alignment and gene finding problems. *J. Comp. Biol.* **9:** 389–400.
Parra, G., Blanco, E., and Guigó, R. 2000. Geneid in *Drosophila*. *Genome Res.* **10:** 511–515.
Pedersen, C. and Scharl, T. 2002. Comparative methods for gene structure prediction in homologous sequences. In *Algorithms in Bioinformatics* (eds. R. Guigó, and D. Gusfield), Springer-Verlag, Berlin, Germany.
Reese, M.G., Hartzell, G., Harris, N.L., Ohler, U., Abril, J.F., and Lewis, S.E. 2000. Genome annotation assessment in *Drosophila melanogaster*. *Genome Res.* **10:** 483–501.
Rinner, O. and Morgenstern, B. 2002. Agenda: Gene prediction by comparative sequence analysis. *In Silico Biol.* **2:** 0018.
Rogic, S., Mackworth, A.K., and Ouellette, F. 2001. Evaluation of gene-finding programs on mammalian sequences. *Genome Res.* **11:** 817–832.
Shoemaker, D.D., Schadt, E.E., Armour, C.D., He, Y.D., Garrett-Engele, P., McDonagh, P.D., Loerch, P.M., Leonardson, A., Lum, P.Y., Cavet, G., et al. 2001. Experimental annotation of the human genome using microarray technology. *Nature* **409:** 922–927.
Tukey, J.W. 1977. *Exploratory data analysis*. pp. 39–41. Addison-Wesley, Boston, MA.
Wiehe, T., Guigó, R., and Miller, W. 2000. Genome sequence comparisons: Hurdles in the fast lane to functional genomics. *Brief. Bioinform.* **1:** 381–388.
Wiehe, T., Gebauer-Jung, S., Mitchell-Olds, T., and Guigó, R. 2001. SGP-1: Prediction and validation of homologous genes based on sequence alignments. *Genome Res.* **11:** 1574–1583.
Yeh, R., Lim, L., and Burge, C. 2001. Computational inference of homologous gene structures in the human genome. *Genome Res.* **11:** 803–816.
Zhang, M.Q. 2002. Computational prediction of eukaryotic protein-coding genes. *Nat. Rev. Genet.* **3:** 698–709.

## WEB SITE REFERENCES

http://www.sanger.ac.uk/Software/formats/GFF/; GFF format description page.
http://genome.cse.ucsc.edu/goldenPath/22dec2001/; Human genome sequence goldenpath from Dec. 22, 2001 (hg10) equivalent to NCBI28 build.
http://genome.cse.ucsc.edu/goldenPath/mmFeb2002/; Mouse genome sequence goldenpath from Feb. 2002 (mm2) equivalent to MGSCv3.
http://www.cs.columbia.edu/~vic/sanger2gbd; Victoria Haghighi, Human chromosome 22 curated annotations.
ftp://ftp.ncbi.nih.gov/genomes/H_sapiens/build28_chr_genomescan.gtf.gz; Genomescan predictions from NCBI.
http://genome.cse.ucsc.edu/goldenPath/mmFeb2002/database/ensGene.txt.gz; Mouse ENSEMBL annotations file.
http://blast.wustl.edu; Washington University BLAST Archives
http://genome.cse.ucsc.edu/goldenPath/22dec2001/database/ensGene.txt.gz; Human ENSEMBL annotations file.
http://genome.cse.ucsc.edu; UCSC genome browser.
http://www.ensembl.org; ENSEMBL genome browser.
http://www1.imim.es/genepredictions/; GENEID and SGP2 full data predictions.
http://www1.imim.es/software/sgp2/; SGP2 home page.
http://www1.imim.es/datasets/sgp2002/; SGP2 training data sets page.

*Received November 4, 2002; accepted in revised form November 15, 2002.*

### 3.2.2 IMGSC, *Nature*, 420(6915):520–562, 2002

**PubMed Accession:**

http://www.ncbi.nlm.nih.gov/entrez/query.fcgi?cmd=Retrieve&db=PubMed&list_uids=12466850&dopt=Abstract

**Journal Abstract:**

http://www.nature.com/cgi-taf/DynaPage.taf?file=/nature/journal/v420/n6915/abs/nature01262_fs.html

**Supplementary Materials:**

http://www.nature.com/nature/journal/v420/n6915/suppinfo/nature01262.html
http://genome.imim.es/datasets/mouse2002/

articles

# Initial sequencing and comparative analysis of the mouse genome

**Mouse Genome Sequencing Consortium***

**A list of authors and their affiliations appears at the end of the paper*

**The sequence of the mouse genome is a key informational tool for understanding the contents of the human genome and a key experimental tool for biomedical research. Here, we report the results of an international collaboration to produce a high-quality draft sequence of the mouse genome. We also present an initial comparative analysis of the mouse and human genomes, describing some of the insights that can be gleaned from the two sequences. We discuss topics including the analysis of the evolutionary forces shaping the size, structure and sequence of the genomes; the conservation of large-scale synteny across most of the genomes; the much lower extent of sequence orthology covering less than half of the genomes; the proportions of the genomes under selection; the number of protein-coding genes; the expansion of gene families related to reproduction and immunity; the evolution of proteins; and the identification of intraspecies polymorphism.**

With the complete sequence of the human genome nearly in hand[1,2], the next challenge is to extract the extraordinary trove of information encoded within its roughly 3 billion nucleotides. This information includes the blueprints for all RNAs and proteins, the regulatory elements that ensure proper expression of all genes, the structural elements that govern chromosome function, and the records of our evolutionary history. Some of these features can be recognized easily in the human sequence, but many are subtle and difficult to discern. One of the most powerful general approaches for unlocking the secrets of the human genome is comparative genomics, and one of the most powerful starting points for comparison is the laboratory mouse, *Mus musculus*.

Metaphorically, comparative genomics allows one to read evolution's laboratory notebook. In the roughly 75 million years since the divergence of the human and mouse lineages, the process of evolution has altered their genome sequences and caused them to diverge by nearly one substitution for every two nucleotides (see below) as well as by deletion and insertion. The divergence rate is low enough that one can still align orthologous sequences, but high enough so that one can recognize many functionally important elements by their greater degree of conservation. Studies of small genomic regions have demonstrated the power of such cross-species conservation to identify putative genes or regulatory elements[3–12]. Genome-wide analysis of sequence conservation holds the prospect of systematically revealing such information for all genes. Genome-wide comparisons among organisms can also highlight key differences in the forces shaping their genomes, including differences in mutational and selective pressures[13,14].

Literally, comparative genomics allows one to link laboratory notebooks of clinical and basic researchers. With knowledge of both genomes, biomedical studies of human genes can be complemented by experimental manipulations of corresponding mouse genes to accelerate functional understanding. In this respect, the mouse is unsurpassed as a model system for probing mammalian biology and human disease[15,16]. Its unique advantages include a century of genetic studies, scores of inbred strains, hundreds of spontaneous mutations, practical techniques for random mutagenesis, and, importantly, directed engineering of the genome through transgenic, knockout and knockin techniques[17–22].

For these and other reasons, the Human Genome Project (HGP) recognized from its outset that the sequencing of the human genome needed to be followed as rapidly as possible by the sequencing of the mouse genome. In early 2001, the International Human Genome Sequencing Consortium reported a draft sequence covering about 90% of the euchromatic human genome, with about 35% in finished form[1]. Since then, progress towards a complete human sequence has proceeded swiftly, with approximately 98% of the genome now available in draft form and about 95% in finished form.

Here, we report the results of an international collaboration involving centres in the United States and the United Kingdom to produce a high-quality draft sequence of the mouse genome and a broad scientific network to analyse the data. The draft sequence was generated by assembling about sevenfold sequence coverage from female mice of the C57BL/6J strain (referred to below as B6). The assembly contains about 96% of the sequence of the euchromatic genome (excluding chromosome Y) in sequence contigs linked together into large units, usually larger than 50 megabases (Mb).

With the availability of a draft sequence of the mouse genome, we have undertaken an initial comparative analysis to examine the similarities and differences between the human and mouse genomes. Some of the important points are listed below.

- The mouse genome is about 14% smaller than the human genome (2.5 Gb compared with 2.9 Gb). The difference probably reflects a higher rate of deletion in the mouse lineage.
- Over 90% of the mouse and human genomes can be partitioned into corresponding regions of conserved synteny, reflecting segments in which the gene order in the most recent common ancestor has been conserved in both species.
- At the nucleotide level, approximately 40% of the human genome can be aligned to the mouse genome. These sequences seem to represent most of the orthologous sequences that remain in both lineages from the common ancestor, with the rest likely to have been deleted in one or both genomes.
- The neutral substitution rate has been roughly half a nucleotide substitution per site since the divergence of the species, with about twice as many of these substitutions having occurred in the mouse compared with the human lineage.
- By comparing the extent of genome-wide sequence conservation to the neutral rate, the proportion of small (50–100 bp) segments in the mammalian genome that is under (purifying) selection can be estimated to be about 5%. This proportion is much higher than can be explained by protein-coding sequences alone, implying that the genome contains many additional features (such as untranslated regions, regulatory elements, non-protein-coding genes, and chromosomal structural elements) under selection for biological function.
- The mammalian genome is evolving in a non-uniform manner,

  

with various measures of divergence showing substantial variation across the genome.

- The mouse and human genomes each seem to contain about 30,000 protein-coding genes. These refined estimates have been derived from both new evidence-based analyses that produce larger and more complete sets of gene predictions, and new *de novo* gene predictions that do not rely on previous evidence of transcription or homology. The proportion of mouse genes with a single identifiable orthologue in the human genome seems to be approximately 80%. The proportion of mouse genes without any homologue currently detectable in the human genome (and vice versa) seems to be less than 1%.
- Dozens of local gene family expansions have occurred in the mouse lineage. Most of these seem to involve genes related to reproduction, immunity and olfaction, suggesting that these physiological systems have been the focus of extensive lineage-specific innovation in rodents.
- Mouse–human sequence comparisons allow an estimate of the rate of protein evolution in mammals. Certain classes of secreted proteins implicated in reproduction, host defence and immune response seem to be under positive selection, which drives rapid evolution.
- Despite marked differences in the activity of transposable elements between mouse and human, similar types of repeat sequences have accumulated in the corresponding genomic regions in both species. The correlation is stronger than can be explained simply by local (G+C) content and points to additional factors influencing how the genome is moulded by transposons.
- By additional sequencing in other mouse strains, we have identified about 80,000 single nucleotide polymorphisms (SNPs). The distribution of SNPs reveals that genetic variation among mouse strains occurs in large blocks, mostly reflecting contributions of the two subspecies *Mus musculus domesticus* and *Mus musculus musculus* to current laboratory strains.

The mouse genome sequence is freely available in public databases (GenBank accession number CAAA01000000) and is accessible through various genome browsers (http://www.ensembl.org/Mus_musculus/, http://genome.ucsc.edu/ and http://www.ncbi.nlm.nih.gov/genome/guide/mouse/).

In this paper, we begin with information about the generation, assembly and evaluation of the draft genome sequence, the conservation of synteny between the mouse and human genomes, and the landscape of the mouse genome. We then explore the repeat sequences, genes and proteome of the mouse, emphasizing comparisons with the human. This is followed by evolutionary analysis of selection and mutation in the mouse and human lineages, as well as polymorphism among current mouse strains. A full and detailed description of the methods underlying these studies is provided as Supplementary Information. In many respects, the current paper is a companion to the recent paper on the human genome sequence[1]. Extensive background information about many of the topics discussed below is provided there.

## Background to the mouse genome sequencing project

### Origins of the mouse

The precise origin of the mouse and human lineages has been the subject of recent debate. Palaeontological evidence has long indicated a great radiation of placental (eutherian) mammals about 65 million years ago (Myr) that filled the ecological space left by the extinction of the dinosaurs, and that gave rise to most of the eutherian orders[23]. Molecular phylogenetic analyses indicate earlier divergence times of many of the mammalian clades. Some of these studies have suggested a very early date for the divergence of mouse from other mammals (100–130 Myr[23–25]) but these estimates partially originate from the fast molecular clock in rodents (see below). Recent molecular studies that are less sensitive to the differences in evolutionary rates have suggested that the eutherian mammalian radiation took place throughout the Late Cretaceous period (65–100 Myr), but that rodents and primates actually represent relatively late-branching lineages[26,27]. In the analyses below, we use a divergence time for the human and mouse lineages of 75 Myr for the purpose of calculating evolutionary rates, although it is possible that the actual time may be as recent as 65 Myr.

### Origins of mouse genetics

The origin of the mouse as the leading model system for biomedical research traces back to the start of human civilization, when mice became commensal with human settlements. Humans noticed spontaneously arising coat-colour mutants and recorded their observations for millennia (including ancient Chinese references to dominant-spotting, waltzing, albino and yellow mice). By the 1700s, mouse fanciers in Japan and China had domesticated many varieties as pets, and Europeans subsequently imported favourites and bred them to local mice (thereby creating progenitors of modern laboratory mice as hybrids among *M. m. domesticus*, *M. m. musculus* and other subspecies). In Victorian England, 'fancy' mice were prized and traded, and a National Mouse Club was founded in 1895 (refs 28, 29).

With the rediscovery of Mendel's laws of inheritance in 1900, pioneers of the new science of genetics (such as Cuenot, Castle and Little) were quick to recognize that the discontinuous variation of fancy mice was analogous to that of Mendel's peas, and they set out to test the new theories of inheritance in mice. Mating programmes were soon established to create inbred strains, resulting in many of the modern, well-known strains (including C57BL/6J)[30].

Genetic mapping in the mouse began with Haldane's report[31] in 1915 of linkage between the pink-eye dilution and albino loci on the linkage group that was eventually assigned to mouse chromosome 7, just 2 years after the first report of genetic linkage in *Drosophila*. The genetic map grew slowly over the next 50 years as new loci and linkage groups were added—chromosome 7 grew to three loci by 1935 and eight by 1954. The accumulation of serological and enzyme polymorphisms from the 1960s to the early 1980s began to fill out the genome, with the map of chromosome 7 harbouring 45 loci by 1982 (refs 29, 31).

The real explosion, however, came with the development of recombinant DNA technology and the advent of DNA-sequence-based polymorphisms. Initially, this involved the detection of restriction-fragment length polymorphisms (RFLPs)[32]; later, the emphasis shifted to the use of simple sequence length polymorphisms (SSLPs; also called microsatellites), which could be assayed easily by polymerase chain reaction (PCR)[33–36] and readily revealed polymorphisms between inbred laboratory strains.

### Origins of mouse genomics

When the Human Genome Project (HGP) was launched in 1990, it included the mouse as one of its five central model organisms, and targeted the creation of genetic, physical and eventually sequence maps of the mouse genome.

By 1996, a dense genetic map with nearly 6,600 highly polymorphic SSLP markers ordered in a common cross had been developed[34], providing the standard tool for mouse genetics. Subsequent efforts filled out the map to over 12,000 polymorphic markers, although not all of these loci have been positioned precisely relative to one another. With these and other loci, Haldane's original two-marker linkage group on chromosome 7 had now swelled to about 2,250 loci.

Physical maps of the mouse genome also proceeded apace, using sequence-tagged sites (STS) together with radiation-hybrid panels[37,38] and yeast artificial chromosome (YAC) libraries to construct dense landmark maps[39]. Together, the genetic and physical maps provide thousands of anchor points that can be used to tie

  

clones or DNA sequences to specific locations in the mouse genome.

Other resources included large collections of expressed-sequence tags (EST)[40], a growing number of full-length complementary DNAs[41,42] and excellent bacterial artificial chromosome (BAC) libraries[43]. The latter have been used for deriving large sets of BAC-end sequences[37] and, as part of this collaboration, to generate a fingerprint-based physical map[44]. Furthermore, key mouse genome databases were developed at the Jackson (http://www.informatics. jax.org/), Harwell (http://www.har.mrc.ac.uk/) and RIKEN (http://genome.rtc.riken.go.jp/) laboratories to provide the community with access to this information.

With these resources, it became straightforward (but not always easy) to perform positional cloning of classic single-gene mutations for visible, behavioural, immunological and other phenotypes. Many of these mutations provide important models of human disease, sometimes recapitulating human phenotypes with uncanny accuracy. It also became possible for the first time to begin dissecting polygenic traits by genetic mapping of quantitative trait loci (QTL) for such traits.

Continuing advances fuelled a growing desire for a complete sequence of the mouse genome. The development of improved random mutagenesis protocols led to the establishment of large-scale screens to identify interesting new mutants, increasing the need for more rapid positional cloning strategies. QTL mapping experiments succeeded in localizing more than 1,000 loci affecting physiological traits, creating demand for efficient techniques capable of trawling through large genomic regions to find the underlying genes. Furthermore, the ability to perform directed mutagenesis of the mouse germ line through homologous recombination made it possible to manipulate any gene given its DNA sequence, placing an increasing premium on sequence information. In all of these cases, it was clear that genome sequence information could markedly accelerate progress.

#### Origin of the Mouse Genome Sequencing Consortium

With the sequencing of the human genome well underway by 1999, a concerted effort to sequence the entire mouse genome was organized by a Mouse Genome Sequencing Consortium (MGSC). The MGSC originally consisted of three large sequencing centres—the Whitehead/Massachusetts Institute of Technology (MIT) Center for Genome Research, the Washington University Genome Sequencing Center, and the Wellcome Trust Sanger Institute—together with an international database, Ensembl, a joint project between the European Bioinformatics Institute and the Sanger Institute.

In addition to the genome-wide efforts of the MGSC, other publicly funded groups have been contributing to the sequencing of the mouse genome in specific regions of biological interest. Together, the MGSC and these programmes have so far yielded clone-based draft sequence consisting of 1,859 Mb (74%, although there is redundancy) and finished sequence of 477 Mb (19%) of the mouse genome. Furthermore, Mural and colleagues[45] recently reported a draft sequence of mouse chromosome 16 containing 87 Mb (3.5%).

To analyse the data reported here, the MGSC was expanded to include the other publicly funded sequencing groups and a Mouse Genome Analysis Group consisting of scientists from 27 institutions in 6 countries.

### Generating the draft genome sequence

#### Sequencing strategy

Sanger and co-workers developed the strategy of random shotgun sequencing in the early 1980s, and it has remained the mainstay of genome sequencing over the ensuing two decades. The approach involves producing random sequence 'reads', generating a preliminary assembly on the basis of sequence overlaps, and then performing directed sequencing to obtain a 'finished' sequence with gaps closed and ambiguities resolved[46]. Ansorge and colleagues[47] extended the technique by the use of 'paired-end sequencing', in which sequencing is performed from both ends of a cloned insert to obtain linking information, which is then used in sequence assembly. More recently, Myers and co-workers[48], and others, have developed efficient algorithms for exploiting such linking information.

A principal issue in the sequencing of large, complex genomes has been whether to perform shotgun sequencing on the entire genome at once (whole-genome shotgun, WGS) or to first break the genome into overlapping large-insert clones and to perform shotgun sequencing on these intermediates (hierarchical shotgun)[46]. The WGS technique has the advantage of simplicity and rapid early coverage; it readily works for simple genomes with few repeats, but there can be difficulties encountered with genomes that contain highly repetitive sequences (such as the human genome, which has near-perfect repeats spanning hundreds of kilobases). Hierarchical shotgun sequencing overcomes such difficulties by using local assembly, thus decreasing the number of repeat copies in each assembly and allowing comparison of large regions of overlaps between clones. Consequently, efforts to produce finished sequences of complex genomes have relied on either pure hierarchical shotgun sequencing (including those of *Caenorhabditis elegans*[49], *Arabidopsis thaliana*[49] and human[1]) or a combination of WGS and hierarchical shotgun sequencing (including those of *Drosophila melanogaster*[50], human[2] and rice[51]).

The ultimate aim of the MGSC is to produce a finished, richly annotated sequence of the mouse genome to serve as a permanent reference for mammalian biology. In addition, we wished to produce a draft sequence as rapidly as possible to aid in the interpretation of the human genome sequence and to provide a useful intermediate resource to the research community. Accordingly, we adopted a hybrid strategy for sequencing the mouse genome. The strategy has four components: (1) production of a BAC-based physical map of the mouse genome by fingerprinting and sequencing the ends of clones of a BAC library[44]; (2) WGS sequencing to approximately sevenfold coverage and assembly to generate an initial draft genome sequence; (3) hierarchical shotgun sequencing of BAC clones covering the mouse genome combined with the WGS data to create a hybrid WGS-BAC assembly; and (4) production of a finished sequence by using the BAC clones as a template for directed finishing. This mixed strategy was designed to exploit the simpler organizational aspects of WGS assemblies in the initial phase, while still culminating in the complete high-quality sequence afforded by clone-based maps.

We chose to sequence DNA from a single mouse strain, rather than from a mixture of strains[45], to generate a solid reference foundation, reasoning that polymorphic variation in other strains could be added subsequently (see below). After extensive consultation with the scientific community[52], the B6 strain was selected because of its principal role in mouse genetics, including its well-characterized phenotype and role as the background strain on which many important mutations arose. We elected to sequence a female mouse to obtain equal coverage of chromosome X and autosomes. Chromosome Y was thus omitted, but this chromosome is highly repetitive (the human chromosome Y has multiple duplicated regions exceeding 100 kb in size with 99.9% sequence identity[53]) and seemed an unwise target for the WGS approach. Instead, mouse chromosome Y is being sequenced by a purely clone-based (hierarchical shotgun) approach.

#### Sequencing and assembly

The genome assembly was based on a total of 41.4 million sequence reads derived from both ends of inserts (paired-end reads) of various clone types prepared from B6 female DNA. The inserts ranged in size from 2 to 200 kb (Table 1). The three large MGSC

  

Overall, mouse has 2.25–3.25-fold more short SSRs (1–5 bp unit) than human (Table 8); the precise ratio depends on the percentage identity required in defining a tandem repeat. The mouse seems to represent an exception among mammals on the basis of comparison with the small amount of genomic sequence available from dog (4 Mb) and pig (5 Mb), both of which show proportions closer to human[136] (E. Green, unpublished data; Table 8).

The analysis can be refined, however, by excluding transposable elements that contain SSRs at their 3′ ends. For example, 90% of A-rich SSRs in human are provided by or spawned from poly(A) tails of Alu and L1 elements, and 15% of $(CA)_n$-like SSRs in mouse are contained in B2 element tails. When these sources are eliminated, the contrast between mouse and human grows to roughly fourfold.

The reason for the greater density of SSRs in mouse is unknown. Table 9 shows that SSRs of >20 bp are not only more frequent, but are generally also longer in the mouse than in the human genome, suggesting that this difference is due to extension rather than to initiation. The equilibrium distribution of SSR length has been proposed[137] to be determined by slippage between exact copies of the repeat during meiotic recombination[138]. The shorter lengths of SSRs in human may result from the higher rate of point substitutions per generation (see above), which disrupts the exactness of the repeats.

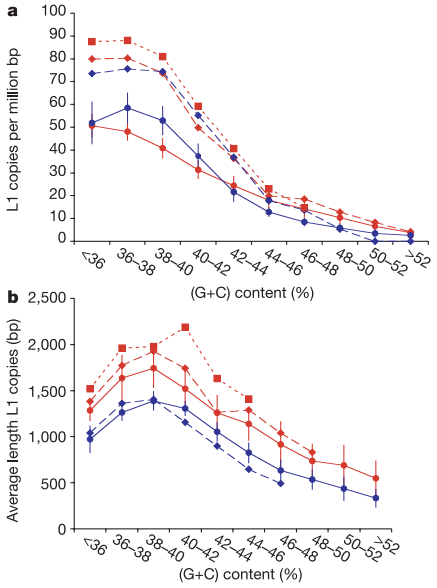


**Figure 15** Comparison of L1 characteristics of autosomes and sex chromosomes as a function of (G+C) content in mouse (blue) and human (red). Error bars depict standard deviation over all autosomes (circles). Diamonds, X chromosomes; squares, human Y chromosome. The mouse Y chromosome is not represented in the whole-genome assembly, and too little clone-based information is available to be included. **a**, The number of lineage-specific L1 copies per megabase declines 13- to 20-fold from lowest to highest (G+C) content. This relationship is stronger in mouse and on the sex chromosomes. Note that, for the same (G+C) content, L1 density is 1.5- to twofold higher on the sex chromosomes. **b**, The average length of lineage-specific L1 copies peaks at around the 39% (G+C) level, where it is three- (human) to fourfold (mouse) higher than in the (G+C)-richest regions. The average length in mouse is underestimated owing to the bias against full-length young elements in the shotgun assembly. On average, L1 copies are longer on human Y than on either X chromosome or the autosomes.

Apart from the absolute number of SSRs, there are also some marked differences in the frequency of certain SSR classes (Table 9)[136]. The most extreme is the tetramer $(ACAG)n$, which is 20-fold more common in mouse than human (even after eliminating copies associated with B2 and B4 SINEs); the sequence does not occur in large clusters, but rather is distributed throughout the genome. In general, SSRs in which one strand is a polypurine tract and the other a polypyrimidine tract are much more common and extended in mouse than human. For the six such di-, tri- and tetramer SSRs (AG, AAG, AGG, AAAG, AAGG, AGGG), copies with at least 20 bp and 95% identity are 1.6-fold longer and tenfold more common in mouse than human.

Analysis of the distribution of SSRs across chromosomes also reveals an interesting feature common to both organisms (see Supplementary Information). In both human and mouse, there is a nearly twofold increase in density of SSRs near the distal ends of chromosome arms. Because mouse chromosomes are acrocentric, they show the effect only at one end. The increased density of SSRs in telomeric regions may reflect the tendency towards higher recombination rates in subtelomeric regions[1].

## Mouse genes

Genes comprise only a small portion of the mammalian genome, but they are understandably the focus of greatest interest. One of the most notable findings of the initial sequencing and analysis of the human genome[1] was that the number of protein-coding genes was only in the range of 30,000–40,000, far less than the widely cited textbook figure of 100,000, but in accord with more recent, rigorous estimates[55,139–141]. The lower gene count was based on the observed and predicted gene counts, statistically adjusted for systematic under- and overcounting.

Our goal here is to produce an improved catalogue of mammalian protein-coding genes and to revisit the gene count. Genome analysis has been enhanced by a number of recent developments. These include burgeoning mammalian EST and cDNA collections, knowledge of the genomes and proteomes of a growing number of organisms, increasingly complete coverage of the mouse and human genomes in high-quality sequence assemblies, and the ability to use *de novo* gene prediction methodologies that exploit information from two mammalian genomes to avoid potential biases inherent in using known transcripts or homology to known genes.

We focus here on protein-coding genes, because the ability to recognize new RNA genes remains rudimentary. As used below, the terms 'gene catalogue' and 'gene count' refer to protein-coding genes only. We briefly discuss RNA genes at the end of the section.

### Evidence-based gene prediction

We constructed catalogues of human and mouse gene predictions on the basis of available experimental evidence. The main computational tool was the Ensembl gene prediction pipeline[142] augmented with the Genie gene prediction pipeline[143]. Briefly, the Ensembl

Table 8 **Density of short SSRs in mouse compared with other mammals**

| Cutoff (%) | All 1–5-bp unit SSRs including those in IRs | | | | | Excluding SSRs within IRs and IR tails | | |
|---|---|---|---|---|---|---|---|---|
| | Mouse (%) | Human (%) | Ratio* | Dog (%) | Pig (%) | Mouse (%) | Human (%) | Ratio* |
| 5 | 0.82 | 0.25 | 3.24 | 0.38 | 0.25 | 0.64 | 0.15 | 4.41 |
| 10 | 1.35 | 0.46 | 2.91 | 0.72 | 0.50 | 1.03 | 0.25 | 4.19 |
| 15 | 1.86 | 0.68 | 2.73 | 1.14 | 0.72 | 1.38 | 0.37 | 3.77 |
| None | 2.67 | 1.19 | 2.24 | 1.90 | 1.27 | 1.99 | 0.64 | 3.10 |

The cutoff indicates the maximum level of imperfect copies allowed, with 'none' indicating that all SSRs are recognized by RepeatMasker. To determine which SSRs were spawned from within IRs or IR tails, the locations of SSRs were overlapped with the RepeatMasker output. We excluded those SSRs overlapped by IRs and those resembling unmasked tails; that is, occurring more than one-third of the time adjacent to the same type of IR. IR, interspersed repeat; SSR, simple sequence repeat.
*Ratio was determined by dividing mouse percentage by human percentage.

  

Table 9 **Frequency of different SSRs in mouse and human**

| Simple sequence repeat (SSR) | Including SSRs in IRs | | | | | Excluding SSRs from SINE and LINE tails and within IRs | |
|---|---|---|---|---|---|---|---|
| | Fraction of mouse genome (bp Mb$^{-1}$) | Average no. units per SSR (mouse) | Average no. units per SSR (human) | Frequency (number SSRs per Mb) | Frequency ratio (mouse/human) | Frequency (number per Mb) | Frequency ratio (mouse/human) |
| A | 555 | 26.7 | 25.0 | 20.8 | 0.4 | 10.4 | 1.6 |
| C | 11 | 22.7 | 25.2 | 0.5 | 6.2 | 0.2 | 4.6 |
| AC | 3070 | 20.8 | 18.1 | 73.8 | 3.5 | 62.1 | 3.2 |
| AG | 1365 | 24.3 | 15.7 | 28.1 | 6.9 | 26.7 | 7.5 |
| AT | 370 | 21.2 | 17.8 | 8.7 | 1.9 | 8.6 | 2.2 |
| CG | 4 | 11.6 | 11.2 | 0.2 | 10.5 | 0.1 | 11.1 |
| AAC | 148 | 9.5 | 8.6 | 5.2 | 1.7 | 3.9 | 2.8 |
| AAG | 152 | 29.1 | 15.9 | 1.7 | 11.7 | 1.6 | 14.5 |
| AAT | 147 | 12.2 | 9.7 | 4.0 | 0.9 | 2.9 | 1.9 |
| ACC | 53 | 11.2 | 9.6 | 1.6 | 6.2 | 1.3 | 6.4 |
| AGC | 30 | 11.3 | 8.8 | 0.9 | 3.0 | 0.8 | 3.3 |
| AGG | 46 | 12.2 | 8.9 | 1.3 | 5.1 | 1.1 | 6.4 |
| AAAC | 465 | 6.7 | 6.2 | 17.5 | 2.2 | 10.3 | 4.5 |
| AAAG | 203 | 16.2 | 10.2 | 3.1 | 2.8 | 2.3 | 5.6 |
| AAAT | 346 | 8.2 | 7.1 | 10.5 | 0.8 | 5.8 | 2.0 |
| AACC | 36 | 8.8 | 7.2 | 1.0 | 8.3 | 0.6 | 6.1 |
| AAGG | 122 | 13.5 | 12.3 | 2.3 | 4.9 | 2.0 | 6.7 |
| AATG | 41 | 7.8 | 6.7 | 1.3 | 1.1 | 1.0 | 1.6 |
| ACAG | 70 | 7.4 | 6.5 | 2.4 | 21.1 | 1.8 | 21.2 |
| ACAT | 85 | 10.3 | 8.4 | 2.1 | 6.0 | 1.7 | 8.6 |
| AGAT | 282 | 16.2 | 12.8 | 4.4 | 4.0 | 3.7 | 4.0 |
| AGGG | 39 | 8.2 | 6.6 | 1.2 | 6.2 | 1.1 | 8.8 |
| AAAAC | 369 | 5.9 | 5.0 | 12.4 | 1.5 | 7.2 | 2.9 |

Frequency and density of monomeric and dimeric SSRs and the most common trimeric and tetrameric SSRs. The numbers are for >20-bp-long SSRs containing <10% substitutions and indels. The two right columns show the density of each repeat, excluding those SSRs spawned from the tails of SINEs and LINEs or inherently part of other IRs. For this, SSRs were counted in a default (-m −s) RepeatMasker run.

system uses three tiers of input. First, known protein-coding cDNAs are mapped onto the genome. Second, additional protein-coding genes are predicted on the basis of similarity to proteins in any organism using the GeneWise program[144]. Third, *de novo* gene predictions from the GENSCAN program[145] that are supported by experimental evidence (such as ESTs) are considered. These three strands of evidence are reconciled into a single gene catalogue by using heuristics to merge overlapping predictions, detect pseudogenes and discard misassemblies. These results are then augmented by using conservative predictions from the Genie system, which predicts gene structures in the genomic regions delimited by paired 5′ and 3′ ESTs on the basis of cDNA and EST information from the region.

We also examined predictions from a variety of other computational systems (see Supplementary Information). These methods tended to have significant overlap with the above-generated gene catalogues, but each tended to introduce significant numbers of predictions that were unsupported by other methods and that appeared to be false positives. Accordingly, we did not add these predictions to our gene catalogues; however, we did use them to fill in missing exons in existing predictions (see Supplementary Information).

The computational pipeline produces predicted transcripts, which may represent fragmentary products or alternative products of a gene. They may also represent pseudogenes, which can be difficult in some cases to distinguish from real genes. The predicted transcripts are then aggregated into predicted genes on the basis of sequence overlaps (see Supplementary Information). The computational pipeline remains imperfect and the predictions are tentative.

### Initial and current human gene catalogue

The initial human gene catalogue[1] contained about 45,000 predicted transcripts, which were aggregated into about 32,000 predicted genes containing a total of approximately 170,000 distinct exons (Table 10). Many of the predicted transcripts clearly represented only gene fragments, because the overall set contained considerably fewer exons per gene (mean 4.3, median 3) than known full-length human genes (mean 10.2, median 8).

This initial gene catalogue was used to estimate the number of human protein-coding genes, on the basis of estimates of the fragmentation rate, false positive rate and false negative rate for true human genes. Such corrections were particularly important, because a typical human gene was represented in the predictions by about half of its coding sequence or was significantly fragmented. The analysis suggested that the roughly 32,000 predicted genes represented about 24,500 actual human genes (on the basis of fragmentation and false positive rates) out of the best-estimate total of approximately 31,000 human protein-coding genes on the basis of estimated false negatives[1]. We suggested a range of 30,000–40,000 to allow for additional genes.

Several papers have re-analysed the initial gene catalogue and argued for a substantially larger human gene count[146,147]. Most of these analyses, however, did not account for the incomplete nature of the catalogoue[148], the complexities arising from alternative splicing, and the difficulty of interpreting evidence from fragmentary messenger RNAs (such as ESTs and serial analysis of gene expression (SAGE) tags) that may not represent protein-coding genes[149].

Since the initial paper[1], the human gene catalogue has been refined as sequence becomes more complete and methods are

Table 10 **Gene count in human and mouse genomes**

| Genome feature | Human | | Mouse | |
|---|---|---|---|---|
| | Initial (Feb. 2001) | Current (Sept. 2002) | Initial* (this paper) | Extended† (this paper) |
| Predicted transcripts | 44,860 | 27,048 | 28,097 | 29,201 |
| Predicted genes | 31,778 | 22,808 | 22,444 | 22,011 |
| Known cDNAs | 14,882 | 17,152 | 13,591 | 12,226 |
| New predictions | 16,896 | 5,656 | 8,853 | 9,785 |
| Mean exons/transcript‡ | 4.2 (3) | 8.7 (6) | 8.2 (6) | 8.4 (6) |
| Total predicted exons | 170,211 | 198,889 | 191,290 | 213,562 |

*Without RIKEN cDNA set.
†With RIKEN cDNA set.
‡Median values are in parentheses.

revised. The current catalogue (Ensembl build 29) contains 27,049 predicted transcripts aggregated into 22,808 predicted genes containing about 199,000 distinct exons (Table 10). The predicted transcripts are larger, with the mean number of exons roughly doubling (to 8.7), and the catalogue has increased in completeness, with the total number of exons increasing by nearly 20%. We return below to the issue of estimating the mammalian gene count.

### Mouse gene catalogue

We sought to create a mouse gene catalogue using the same methodology as that used for the human gene catalogue (Table 10). An initial catalogue was created by using the same evidence set as for the human analysis, including cDNAs and proteins from various organisms. This set included a previously published collection of mouse cDNAs produced at the RIKEN Genome Center[41].

We also created an extended mouse gene catalogue by including a much larger set of about 32,000 mouse cDNAs with significant ORFs (see Supplementary Information) that were sequenced by RIKEN (see ref. 150). These additional mouse cDNAs improved the catalogue by increasing the average transcript length through the addition of exons (raising the total from about 191,000 to about 213,000, including many from untranslated regions) and by joining fragmented transcripts. The set contributed roughly 1,200 new predicted genes. The total number of predicted genes did not change significantly, however, because the increase was offset by a decrease due to mergers of predicted genes. These mouse cDNAs have not yet been used to extend the human gene catalogue. Accordingly, comparisons of the mouse and human gene catalogues below use the initial mouse gene catalogue.

The extended mouse gene catalogue contains 29,201 predicted transcripts, corresponding to 22,011 predicted genes that contain about 213,500 distinct exons. These include 12,226 transcripts corresponding to cDNAs in the public databases, with 7,481 of these in the well-curated RefSeq collection[151]. There are 9,785 predicted transcripts that do not correspond to known cDNAs, but these are built on the basis of similarity to known proteins.

The new mouse and human gene catalogues contain many new genes not previously identified in either genome. These include new paralogues for genes responsible for at least five diseases: *RFX5*, responsible for a type of severe combined immunodeficiency resulting from lack of expression of human leukocyte antigen (HLA) antigens on certain haematopoietic cells[152]; bestrophin, responsible for a form of muscular degeneration[153]; otoferlin, responsible for a non-syndromic prelingual deafness[154]; *Crumbs1*, mutated in two inherited eye disorders[155,156]; and adiponectin, a deficiency of which leads to diet-induced insulin resistance in mice[157]. The *RFX5* case is interesting, because disruption of the known mouse homologue alone does not reproduce the human disease, but may do so in conjunction with disruption of the newly identified paralogue[158].

Recently, Mural and colleagues[45] analysed the sequence of mouse chromosome 16 and reported 731 gene predictions (compared with 756 gene predictions in our set for chromosome 16). Our gene catalogue contains 656 of these gene predictions, indicating extensive agreement between these two independent analyses. Most of the remaining 75 genes reported by ref. 45 seem to be systematic errors (common to all such programs), such as relatively short gene predictions arising from protein matches to low-complexity regions.

It should be emphasized that the human and mouse gene catalogues, although increasingly complete, remain imperfect. Both genome sequences are still incomplete. Some authentic genes are missing, fragmented or otherwise incorrectly described, and some predicted genes are pseudogenes or are otherwise spurious. We describe below further analysis of these challenges.

### Pseudogenes

An important issue in annotating mammalian genomes is distinguishing real genes from pseudogenes, that is, inactive gene copies. Processed pseudogenes arise through retrotransposition of spliced or partially spliced mRNA into the genome; they are often recognized by the loss of some or all introns relative to other copies of the gene. Unprocessed pseudogenes arise from duplication of genomic regions or from the degeneration of an extant gene that has been released from selection. They sometimes contain all exons, but often have suffered deletions and rearrangements that may make it difficult to recognize their precise parentage. Over time, pseudogenes of either class tend to accumulate mutations that clearly reveal them to be inactive, such as multiple frameshifts or stop codons. More generally, they acquire a larger ratio of non-synonymous to synonymous substitutions ($K_A/K_S$ ratio; see section on proteins below) than functional genes. These features can sometimes be used to recognize pseudogenes, although relatively recent pseudogenes may escape such filters.

The well-studied *Gapdh* gene and its pseudogenes illustrate the challenges[159]. The mouse genome contains only a single functional *Gapdh* gene (on chromosome 7), but we find evidence for at least 400 pseudogenes distributed across 19 of the mouse chromosomes. Some of these are readily identified as pseudogenes, but 118 have retained enough genic structure that they appear as predicted genes in our gene catalogue. They were identified as pseudogenes only after manual inspection. The *Gapdh* pseudogenes typically have no orthologous human gene in the corresponding region of conserved synteny.

To assess the impact of pseudogenes on gene prediction, we focused on two classes of gene predictions: (1) those that lack a corresponding gene prediction in the region of conserved synteny in the human genome (2,705); and (2) those that are members of apparent local gene clusters and that lack a reciprocal best match in the human genome (5,143). A random sample of 100 such predicted genes was selected, and the predictions were manually reviewed. We estimate that about 76% of the first class and about 30% of the second class correspond to pseudogenes. Overall, this would correspond to roughly 4,000 of the predicted genes in mouse. (A similar proportion of gene predictions on chromosome 16 by Mural and colleagues[45] seem, by the same criteria, to be pseudogenes.) These two classes contain relatively few exons (average 3), and thus comprise only about 12,000 exons of the 213,562 in the mouse gene catalogue. Pseudogenes similarly arise among human gene predictions and are greatly enriched in the two classes above. This analysis shows the benefit of comparative genome analysis and suggests ways to improve gene prediction.

We also sought to identify the many additional pseudogenes that had been correctly excluded during the gene prediction process. To do so, we searched the genomic regions lying outside the predicted genes in the current catalogue for sequence with significant similarity to known proteins. We identified about 14,000 intergenic regions containing such putative pseudogenes. Most (>95%) appear to be clear pseudogenes (on the basis of such tests as ratio of non-synonymous to synonymous substitutions; see Supplementary Information and the section on proteins below), with more than half being processed pseudogenes. This is surely an underestimate of the total number of pseudogenes, owing to the limited sensitivity of the search.

### Further refinement

We analysed the mouse gene predictions further, focusing on those whose best human match fell outside the region of conserved synteny and those without clear orthologues in the human genome. Two suspicious classes were identified. The first (0.4%) consists of 63 predicted genes that seem to encode Gag/Pol proteins from mouse-specific retrovirus elements. The second (about 2.5%) consists of 591 predicted genes for which the only supporting evidence

  

comes from a single collection of mouse cDNAs (the initial RIKEN cDNAs[41]). These cDNAs are very short on average, with few exons (median 2) and small ORFs (average length of 85 amino acids); whereas some of these may be true genes, most seem unlikely to reflect true protein-coding genes, although they may correspond to RNA genes or other kinds of transcripts. Both groups were omitted in the comparative analysis below.

#### Comparison of mouse and human gene sets

We then sought to assess the extent of correspondence between the mouse and human gene sets. Approximately 99% of mouse genes have a homologue in the human genome. For 96% the homologue lies within a similar conserved syntenic interval in the human genome. For 80% of mouse genes, the best match in the human genome in turn has its best match against that same mouse gene in the conserved syntenic interval. These latter cases probably represent genes that have descended from the same common ancestral gene, termed here 1:1 orthologues.

Comprehensive identification of all orthologous gene relationships, however, is challenging. If a single ancestral gene gives rise to a gene family subsequent to the divergence of the species, the family members in each species are all orthologous to the corresponding gene or genes in the other species. Accordingly, orthology need not be a 1:1 relationship and can sometimes be difficult to discern from paralogy (see protein section below concerning lineage-specific gene family expansion).

There was no homologous predicted gene in human for less than 1% (118) of the predicted genes in mouse. In all these cases, the mouse gene prediction was supported by clear protein similarity in other organisms, but a corresponding homologue was not found in the human genome. The homologous genes may have been deleted in the human genome for these few cases, or they could represent the creation of new lineage-specific genes in the rodent lineage—this seems unlikely, because they show protein similarity to genes in other organisms. There are, however, several other possible reasons why this small set of mouse genes lack a human homologue. The gene predictions themselves or the evidence on which they are based may be incorrect. Genes that seem to be mouse-specific may correspond to human genes that are still missing owing to the incompleteness of the available human genome sequence. Alternatively, there may be true human homologues present in the available sequence, but the genes could be evolving rapidly in one or both lineages and thus be difficult to recognize. The answers should become clear as the human genome sequence is completed and other mammalian genomes are sequenced. In any case, the small number of possible mouse-specific genes demonstrates that *de novo* gene addition in the mouse lineage and gene deletion in the human lineage have not significantly altered the gene repertoire.

#### Mammalian gene count

To re-estimate the number of mammalian protein-coding genes, we studied the extent to which exons in the new set of mouse cDNAs sequenced by RIKEN[132] were already represented in the set of exons contained in our initial mouse gene catalogue, which did not use this set as evidence in gene prediction. This cDNA collection is a much broader and deeper survey of mammalian cDNAs than previously available, on the basis of sampling of diverse embryonic and adult tissues[150]. If the RIKEN cDNAs are assumed to represent a random sampling of mouse genes, the completeness of our exon catalogue can be estimated from the overlap with the RIKEN cDNAs. We recognize this assumption is not strictly valid but nonetheless is a reasonable starting point.

The initial mouse gene catalogue of 191,290 predicted exons included 79% of the exons revealed by the RIKEN set. This is an upper bound of sensitivity as some RIKEN cDNAs are probably less than full length and many tissues remain to be sampled. On the basis of the fraction of mouse exons with human counterparts, the percentage of true exons among all predicted exons or the specificity of the initial mouse gene catalogue is estimated to be 93%. Together, these estimates suggest a count of about 225,189 exons in protein-coding genes in mouse ($191{,}290 \times 0.93/0.79$).

To estimate the number of genes in the genome, we used an exon-level analysis because it is less sensitive to artefacts such as fragmentation and pseudogenes among the gene predictions. One can estimate the number of genes by dividing the estimated number of exons by a good estimate of the average number of exons per gene. A typical mouse RefSeq transcript contains 8.3 coding exons per gene, and alternative splicing adds a small number of exons per gene. The estimated gene count would then be about 27,000 with 8.3 exons per gene or about 25,000 with 9 exons per gene. If the sensitivity is only 70% (rather than 79%), the exon count rises to 254,142, yielding a range of 28,000–30,500.

In the next section, we show that gene predictions that avoid many of the biases of evidence-based gene prediction result in only a modest increase in the predicted gene count (in the range of about 1,000 genes). Together, these estimates suggest that the mammalian gene count may fall at the lower end of (or perhaps below) our previous prediction of 30,000–40,000 based on the human draft sequence[1]. Although small, single-exon genes may add further to the count, the total seems unlikely to greatly exceed 30,000. This lower estimate for the mammalian gene number is consistent with other recent extrapolations[141]. However, there are important caveats. It is possible that the genome contains many additional small, single-exon genes expressed at relatively low levels. Such genes would be hard to detect by our various techniques and would also decrease the average number of exons per gene used in the analysis above.

#### *De novo* gene prediction

The gene predictions above have the strength of being based on experimental evidence but the weakness of being unable to detect new exons without support from known transcripts or homology to known cDNAs or ESTs in some organism. In particular, genes that are expressed at very low levels or that are evolving very rapidly are less likely to be present in the catalogue (R. Guigó, unpublished data).

Ideally, one would like to perform *de novo* gene prediction directly from genomic sequence by recognizing statistical properties of coding regions, splice sites, introns and other gene features. Although this approach works relatively well for small genomes with a high proportion of coding sequence, it has much lower specificity when applied to mammalian genomes in which coding sequences are sparser. Even the best *de novo* gene prediction programs (such as GENSCAN[145]) predict many apparently false-positive exons.

In principle, *de novo* gene prediction can be improved by analysing aligned sequences from two related genomes to increase the signal-to-noise ratio[135]. Gene features (such as splice sites) that are conserved in both species can be given special credence, and partial gene models (such as pairs of adjacent exons) that fail to have counterparts in both species can be filtered out. Together, these techniques can increase sensitivity and specificity.

We developed three new computer programs for dual-genome *de novo* gene prediction: TWINSCAN[160,325], SGP2 (refs 161, 326) and SLAM[162]. We describe here results from the first two programs. The results of the SLAM analysis can be viewed at http://bio.math.berkeley.edu/slam/mouse/. To predict genes in the mouse genome, these two programs first find the highest-scoring local mouse–human alignment (if any) in the human genome. They then search for potential exonic features, modifying the probability scores for the features according to the presence and quality of these human alignments. We filtered the initial predictions of these programs, retaining only multi-exon gene predictions for which there were corresponding consecutive exons with an intron in an aligned position in both species[327].

After enrichment based on the presence of introns in aligned

  

locations, TWINSCAN identified 145,734 exons as being part of 17,271 multi-exon genes. Most of the gene predictions (about 94%) were present in the above evidence-based gene catalogue. Conversely, about 78% of the predicted genes and about 81% of the exons in this catalogue were at least partially represented by TWINSCAN predictions. TWINSCAN predicted an extra 4,558 (3%) new exons not predicted by the evidence-based methods. SGP2 produced qualitatively similar results. The total number of predicted exons was 168,492 contained in 18,056 multi-exon genes, with 86% of the predicted genes in the evidence-based gene catalogue at least partially represented. Approximately 83% of the exons in the catalogue were detected by SGP2, which predicted an additional 9,808 (6%) new exons. There is considerable overlap between the two sets of new predicted exons, with the TWINSCAN predictions largely being a subset of the SGP2 predictions; the union of the two sets contains 11,966 new exons.

We attempted to validate a sample of 214 of the new predictions by performing PCR with reverse transcription (RT) between consecutive exons using RNA from 12 adult mouse tissues[163] and verifying resulting PCR products by direct DNA sequencing. Our sampling involved selecting gene predictions without nearby evidence-based predictions on the same strand and with an intron of at least 1 kb. The validation rate was approximately 83% for TWINSCAN and about 44% for SGP2 (which had about twice as many new exons; see above). Extrapolating from these success rates, we estimate that the entire collection would yield about 788 validated gene predictions that do not overlap with the evidence-based catalogue.

The second step of filtering *de novo* gene predictions (by requiring the presence of adjacent exons in both species) turns out to greatly increase prediction specificity. Predicted genes that were removed by this criterion had a very low validation rate. In a sample of 101 predictions that failed to meet the criteria, the validation rate was 11% for genes with strong homology to human sequence and 3% for those without. The filtering process thus removed 24-fold more apparent false positives than true positives. Extrapolating from these results, testing the entire set of such predicted genes (that is, those that fail the test of having adjacent homologous exons in the two species) would be expected to yield only about 231 additional validated predictions.

Overall, we expect that about 1,000 (788+231) of the new gene predictions would be validated by RT–PCR. This probably corresponds to a smaller number of actual new genes, because some of these may belong to the same transcription unit as an adjacent *de novo* or evidence-based prediction. Conversely, some true genes may fail to have been detected by RT–PCR owing to lack of sensitivity or tissue, or developmental stage selection[327].

An example of a new gene prediction, validated by RT–PCR, is a homologue of dystrophin (Fig. 16). Dystrophin is encoded by the *DMD* gene, which is mutated in individuals with Duchenne muscular dystrophy[164]. A gene prediction was found on mouse chromosome 1 and human chromosome 2, showing 38% amino acid identity over 36% of the dystrophin protein (the carboxy terminal portion, which interacts with the transmembrane protein β-dystroglycan). Other new gene predictions include homologues of aquaporin. These gene predictions were missed by the evidence-based methods because they were below various thresholds. These and other examples are described in a companion paper[327].

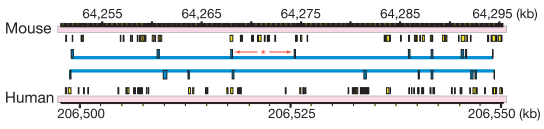


**Figure 16** Structure of a new homologue of dystrophin as predicted on mouse chromosome 1 and human chromosome 2. Mouse and human gene structures are shown in blue on the chromosomes (pink). The mouse intron marked with an asterisk was verified by RT–PCR from primers complementary to the flanking exons followed by direct product sequencing[327]. Regions of high-scoring alignment to the entire other genome (computed before gene predictions and identification of predicted orthologues) are shown in yellow. Note the weak correspondence between predicted exons and blocks of high-scoring whole-genome alignment. Nonetheless, the predicted proteins considered in isolation show good alignment across several splice sites.

The overall results of the *de novo* gene prediction are encouraging in two respects. First, the results show that *de novo* gene prediction on the basis of two genome sequences can identify (at least partly) most predicted genes in the current mammalian gene catalogues with remarkably high specificity and without any information about cDNAs, ESTs or protein homologies from other organisms. It can also identify some additional genes not detected in the evidence-based analysis. Second, the results suggest that methods that avoid some of the inherent biases of evidence-based gene prediction do not identify more than a few thousand additional predicted exons or genes. These results are thus consistent with an estimate in the vicinity of 30,000 genes, subject to the uncertainties noted above.

### RNA genes

The genome also encodes many RNAs that do not encode proteins, including abundant RNAs involved in mRNA processing and translation (such as ribosomal RNAs and tRNAs), and more recently discovered RNAs involved in the regulation of gene expression and other functions (such as micro RNAs)[165,166]. There are probably many new RNAs not yet discovered, but their computational identification has been difficult because they contain few hallmarks. Genomic comparisons have the potential to significantly increase the power of such predictions by using conservation to reveal relatively weak signals, such as those arising from RNA secondary structure[167]. We illustrate this by showing how comparative genomics can improve the recognition of even an extremely well understood gene family, the tRNA genes.

In our initial analysis of the human genome[1], the program tRNAscan-SE[168] predicted 518 tRNA genes and 118 pseudogenes. A small number (about 25 of the total) were filtered out by the RepeatMasker program as being fossils of the MIR transposon, a long-dead SINE element that was derived from a tRNA[169,170].

The analysis of the mouse genome is much more challenging because the mouse contains an active SINE (B2) that is derived from a tRNA and thus vastly complicates the task of identifying true tRNA genes. The tRNAscan-SE program predicted 2,764 tRNA genes and 22,314 pseudogenes in mouse, but the RepeatMasker program classified 2,266 of the 'genes' and 22,136 of the 'pseudogenes' as SINEs. After eliminating these, the remaining set contained 498 putative tRNA genes. Close analysis of this set suggested that it was still contaminated with a substantial number of pseudogenes. Specifically, 19 of the putative tRNA genes violated the wobble rules that specify that only 45 distinct anticodons are expected to decode the 61 standard sense codons, plus a selenocysteine tRNA species complementary to the UGA stop codon[171]. In contrast, the initial analysis of the human genome identified only three putative tRNA genes that violated the wobble rules[172,173].

To improve discrimination of functional tRNA genes, we exploited comparative genomic analysis of mouse and human. True functional tRNA genes would be expected to be highly conserved. Indeed, the 498 putative mouse tRNA genes differ on average by less than 5% (four differences in about 75 bp) from their nearest human match, and nearly half are identical. In contrast, non-genic tRNA-related sequences (those labelled as pseudogenes by tRNAscan-SE or as SINEs by RepeatMasker) differ by an average of 38% and none is within 5% divergence. Notably, the 19 suspect predictions that violate the wobble rules show an average of 26%

  

divergence from their nearest human homologue, and none is within 5% divergence.

On the basis of these observations, we identified the set of tRNA genes having cross-species homologues with <5% sequence divergence. The set contained 335 tRNA genes in mouse and 345 in human. In both cases, the set represents all 46 expected anti-codons and exactly satisfies the expected wobble rules. The sets probably more closely represent the true complement of functional tRNA genes.

Although the excluded putative genes (163 in mouse and 167 in human) may include some true genes, it seems likely that our earlier estimate of approximately 500 tRNA genes in human is an overestimate. The actual count in mouse and human is probably closer to 350.

We also analysed the mouse genome for other known classes of non-coding RNAs. Because many of these classes also seem to have given rise to many pseudogenes, we conservatively considered only those loci that are identical or that are highly similar to RNAs that have been published as 'true' genes. We identified a total of 446 non-coding RNA genes, which includes 121 small nucleolar RNAs, 78 micro RNAs, and 247 other non-coding RNA genes, including rRNAs, spliceosomal RNAs, and telomerase RNA. We also classified 2,030 other loci with significant similarities to known RNA genes as probable pseudogenes.

## Mouse proteome

Eukaryotic protein invention appears to have occurred largely through two important mechanisms. The first is the combination of protein domains into new architectures. (Domains are compact structures serving as evolutionarily conserved functional building blocks that are often assembled in various arrangements (architectures) in different proteins[174].) The second is lineage-specific expansions of gene families that often accompany the emergence of lineage-specific functions and physiologies[175] (for example, expansions of the vertebrate immunoglobulin superfamily reflecting the invention of the immune system[1], receptor-like kinases in *A. thaliana* associated with plant-specific self-incompatibility and disease-resistance functions[49], and the trypsin-like serine protease homologues in *D. melanogaster* associated with dorsal–ventral patterning and innate immune response[176,177]).

The availability of the human and mouse genome sequences provides an opportunity to explore issues of protein evolution that are best addressed through the study of more closely related genomes. The great similarity of the two proteomes allows extensive comparison of orthologous proteins (those that descended by speciation from a single gene in the common ancestor rather than by intragenome duplication), permitting an assessment of the evolutionary pressures exerted on different classes of proteins. The differences between the mouse and human proteomes, primarily in gene family expansions, might reveal how physiological, anatomical and behavioural differences are reflected at the genome level.

### Overall proteome comparison

We compared the largest transcript for each gene in the mouse gene catalogue to the National Center for Biotechnology Information

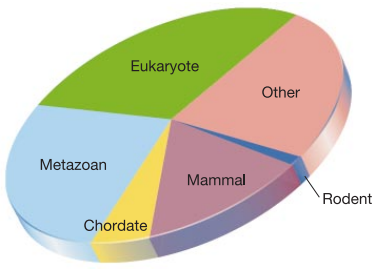


**Figure 17** Taxonomic breakdown of homologues of mouse proteins according to taxonomic range. Note that only a small fraction of genes are possibly rodent-specific (<1%) as compared with those shared with other mammals (14%, not rodent-specific); shared with chordates (6%, not mammalian-specific); shared with metazoans (27%, not chordate-specific); shared with eukaryotes (29%, not metazoan-specific); and shared with prokaryotes and other organisms (23%, not eukaryotic-specific).

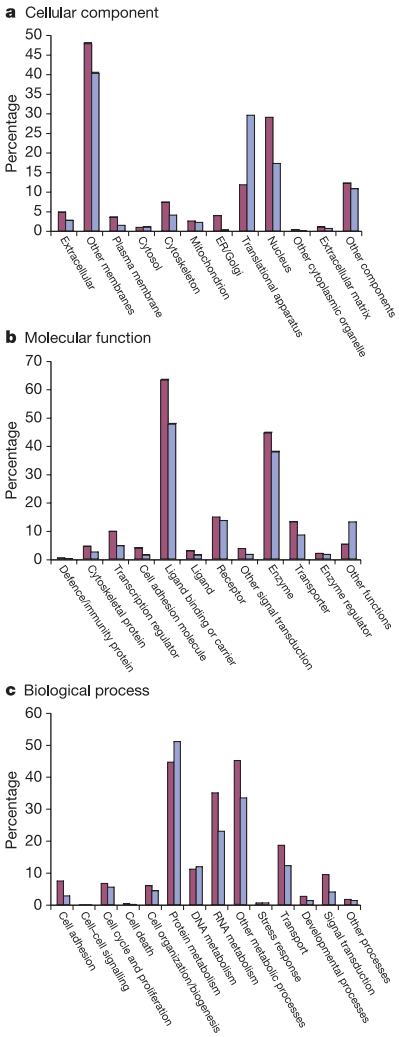


**Figure 18** Gene ontology (GO) annotations for mouse and human proteins. The GO terms assigned to mouse (blue) and human (red) proteins based on sequence matches to InterPro domains are grouped into approximately a dozen categories. These categories fell within each of the larger ontologies of cellular component (**a**) molecular function (**b**) and biological process (**c**) (D. Hill, personal communication). In general, mouse has a similar percentage of proteins compared with human in most categories. The apparently significant difference between the number of mouse and human proteins in the translational apparatus category of the cellular component ontology may be due to ribosomal protein pseudogenes incorrectly assigned as genes in mouse.

RepeatMasker program to allow for incomplete sensitivity in the more rapidly changing mouse genome. This would imply roughly 1,300 Mb of deletions, corresponding to the deletion of about 45% (1,330 out of 2,900) and retention of 55% of the ancestral genome.

If there was no correlation in the fixation of deletions in the two lineages, the expected proportion of the ancestral genome retained in both lineages would be about 42% (76% × 55%). Complete independence is unlikely because deletions of functional sequences would have been selectively disadvantageous. However, deletions of modest size may largely be neutral given the relatively low proportion of functional sequence in the genome.

The estimates can be adjusted (see Supplementary Information) to account for nucleotide-level insertions and deletions and lineage-specific duplications (the expectation remains roughly the same), or to allow for different assumptions about ancestral genome size (the expectation increases by 3–4% for an intermediate size of about 2.7 Gb). This simple analysis suggests that the observed proportion of alignable genome (about 40%) is not surprising, but rather it probably reflects the actual proportion of orthologous genome remaining after the deletion in the two lineages.

In a preliminary test of this hypothesis, we identified ancestral repeats in the mouse that lay in intervals defined by orthologous landmarks. Examination of the corresponding interval in the human genome showed a rate of loss of these elements, broadly consistent with the 24% deletion rate in the human lineage assumed above (see Supplementary Information).

Such a deletion rate in the human lineage over about 75 million years is also roughly compatible with the observation that roughly 6% has been deleted over about 22 million years since the divergence from baboon, an estimate derived from the sequencing of specific regions in human and baboon (E. Green, unpublished data). Although we do not have a corresponding direct estimate of large-scale deletions in the mouse lineage, the predicted rate of about 45% is roughly twice as high as for the human lineage, which is similar to the ratio seen for nucleotide substitutions.

#### Rate of neutral substitution

The genome-wide alignments can be used to measure divergence rates for different types of sequence. The neutral substitution rate, for example, can be estimated from the alignment of non-functional DNA. We believe that the best representative of this class is ancestral repeat sequence, representing transposable elements inserted and fixed before the mouse–human divergence. Such ancestral repeats are more likely than any other sequence in the genome to have been under no functional constraint.

The human–mouse alignment catalogue contains approximately 165 Mb of ancestral repeat sequences, with most being clearly orthologous by alignment of adjacent non-repetitive DNA. These alignments show 66.7% sequence identity. The observed base changes can be used to infer the underlying substitution rate, which includes back mutations, by using various continuous-time Markov models[230]. Applying the REV model[231] to the ancestral repeat sites, we estimate that neutral divergence has led to between 0.46 and 0.47 substitutions per site (see Supplementary Information). Similar results are obtained for any of the other published continuous-time Markov models that distinguish between transitions and transversions (D. Haussler, unpublished data). Although the model does not assign substitutions separately to the mouse and human lineages, as discussed above in the repeat section, the roughly twofold higher mutation rate in mouse (see above) implies that the substitutions distribute as 0.31 per site (about $4 \times 10^{-9}$ per year) in the mouse lineage and 0.16 (about $2 \times 10^{-9}$ per year) in the human lineage.

Having established the neutral substitution rate by examining aligned ancestral repeats, we then investigated a second class of potentially neutral sites: fourfold degenerate sites in codons of genes. Fourfold degenerate sites are subject to selection in invertebrates, such as *Drosophila*, but the situation is unclear for mammals. We examined alignments between fourfold degenerate codons in orthologous genes. The fourfold degenerate codons were defined as GCX (Ala), CCX (Pro), TCX (Ser), ACX (Thr), CGX (Arg), GGX (Gly), CTX (Leu) and GTX (Val). Thus for Leu, Ser and Arg, we used four of their six codons. Only fourfold degenerate codons in which the first two positions were identical in both species were considered, so that the encoded amino acid was identical. Slightly fewer than 2 million such sites were studied, defined in the human genome from about 9,600 human RefSeq cDNAs and aligned to their mouse orthologues. The observed sequence identity in fourfold degenerate sites was 67%, and the estimated number of substitutions per site, between 0.46 and 0.47, was similar to that in the ancestral repeat sites (see Supplementary Information).

#### Conservation in gene-related features

We used the genome-wide alignments to examine the extent of conservation in gene-related features, including coding regions, introns, untranslated regions, upstream regions and CpG islands.

For each type of feature, we characterized the nature of sequence conservation (including typical percentage identity, inferred substitution rates and insertion/deletion rate). We also defined a conservation score $S$ that measures the extent to which a given window (typically 50 or 100 bp, in applications below) shows higher conservation than expected by chance. The conservation score $S$ for an aligned region $R$ is the normalized fraction of aligned bases that are identical (obtained by subtracting the mean and dividing by the standard deviation) and is given by:

$$S = S(R) = \frac{(p - \mu)}{\sqrt{\mu(1 - \mu)/n}}$$

where $n$ is the number of sites within the window that are aligned, $p$ is the fraction of aligned sites that are identical in the two genomes, and $\mu$ is the average fraction of sites that are identical in aligned ancestral repeats in the surrounding region ($\mu = 0.667$ as a genome-wide average, but, as discussed below, fluctuates locally). When the conservation score $S$ is calculated for the set of all ancestral repeats, it has a mean of 0 (by definition) and a standard deviation of 1.19 and 1.23 for windows of 50 and 100 bp, respectively (Fig. 23). This defines the typical fluctuation in conservation score in neutral sequences. The properties of the alignments are shown in Table 16 and the distribution of conservation scores relative to neutral substitution is shown in Fig. 24.

Coding regions are distinctive in many ways. They show the highest degree of conservation (85% sequence identity or 0.165 substitutions per nucleotide site). Alignment gaps are tenfold less common than in non-coding regions. In addition, 52% of coding regions have highly significant alignments to more than one genomic region (typically, paralogues and pseudogenes), whereas only 3.3% of the genome shows such multiple alignments.

Introns are very similar, in most respects, to the genome as a whole in terms of percentage identity, gaps and multiple alignment statistics.

Conservation levels in 5′ and 3′ UTRs are similar to one another and intermediate between levels in coding regions and introns. The sequence identity of 75–76% is well above the intronic level of 69%. Note that our estimate of sequence identity is higher than the 70–71% reported previously[181], in large part because that study used a global rather than a local alignment programme. The insertion and deletion characteristics of the UTRs are very similar to those of introns. Overall, 5′ UTRs are slightly better conserved than 3′ UTRs; however, significantly more of 3′-UTR sequence is covered by multiple alignments than 5′-UTR sequence (21% compared with 16%). This may reflect the fact that pseudogene insertion tends to proceed from the 3′ end and often terminates before completion.

Promoter regions are of considerable interest. We analysed the regions located 200 bp upstream of transcription start because they

  

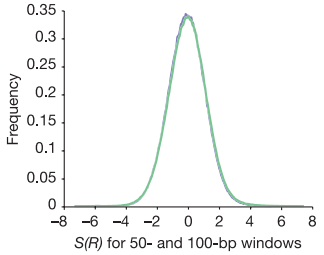


**Figure 23** Distribution of the conservation score $S(R)$. The empirical distribution of $S(R)$ for all 1.9 million non-overlapping 50-bp windows (blue) containing at least 45 aligned ancestral repeat sites (standard deviation 1.19) and 1.7 million non-overlapping 100-bp windows (green) containing at least 50 aligned ancestral repeat sites (standard deviation 1.23). Both curves are bell-shaped, with a mean of zero, but the standard deviations are higher than would be expected if the sites in each window were independent and conserved with (locally estimated) probability $\mu$. In that case the distribution of $S$ would be approximately normal with a standard deviation of 1. Thus, these data show that there is some dependency between the substitutions within the window.

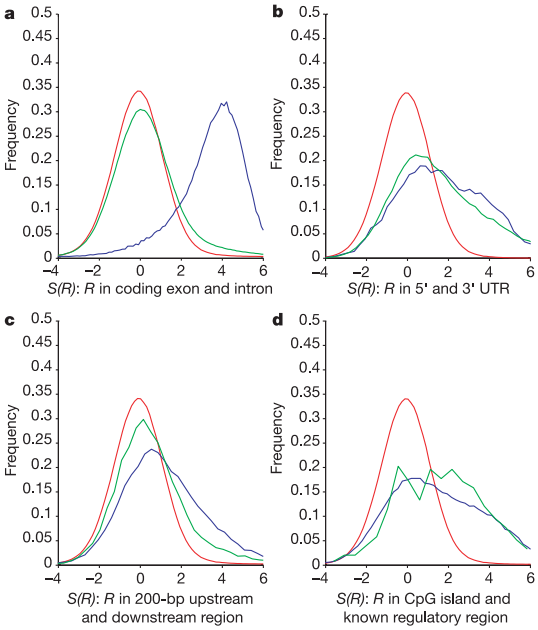


**Figure 24** Comparison of histograms for conservation scores for 100-bp windows in ancient transposons (red) with 100-bp windows in other kinds of regions (blue and green). We required that at least 50 bp be aligned in each window. **a**–**d**, Comparisons with coding exons (blue) and introns (green) (**a**), 5′ UTR (blue) and 3′ UTR (green) (**b**), 200-bp upstream of transcription start (blue) and 200 bp downstream of transcription end (green) (**c**), and CpG islands (blue) and known regulatory regions (green) (**d**) are shown. The RefSeq database was used to define gene features. CpG islands were determined as discussed in the text, and known regulatory regions were collected as discussed in the text.

were likely to contain important promoter and regulatory signals. However, such analysis is necessarily limited by the fact that transcriptional start sites remain poorly defined for many genes. With this caveat, the upstream regions share many characteristics of 5′ UTRs but have a lower percentage identity, a significantly lower proportion covered by multiple alignments, and a higher (G+C) content.

CpG islands show a conservation level similar to those of promoter and UTR regions (Fig. 24).

We also observed that levels of conservation were not uniform across these features (coding regions, introns, UTRs, upstream regions and CpG islands)[232]. Figure 25 shows how conservation levels vary regionally within the features of a 'typical' gene. Sequence identity rises gradually from a background level to 78% near the approximate transcription start site, where the level reaches a plateau. It is possible that sharper definitions of transcriptional start sites would allow the footprint of the TATA box and other common structures near the transcription start site to emerge. Conversely, many human promoters lack a TATA box, and transcription start at such promoters is not typically sharply defined[233]. Sequence identity falls slowly across the 5′ UTR, and then starts to rise again near the start codon. As expected, conservation levels rise sharply at the translation start site[234], remain high throughout the coding regions, and have sharp peaks at splice sites. After the stop codon, the per cent identity is relatively low for most of the 3′ UTR, but then begins to increase about 200 bases before the polyadenylation site. The

Table 16 **Alignment statistics for various known features in human**

| Feature | Coding (%) | 5′ UTR (%) | 3′ UTR (%) | Upstream 200 bp (%) | Downstream 200 bp (%) | Intron (%) | Known regulatory regions* (%) | Ancient repeats† (%) | Genome‡ (%) |
|---|---|---|---|---|---|---|---|---|---|
| Identity (%)§ | 84.7 | 75.9 | 74.7 | 73.9 | 70.9 | 68.6 | 75.4 | 66.7 | 69.1 |
| Gap initiations‖ | | | | | | | | | |
| Human | 0.1 | 0.9 | 1 | 1.1 | 1.2 | 1.1 | 1.2 | 1.1 | 1.1 |
| Mouse | 0.1 | 1.5 | 1.9 | 1.7 | 2.1 | 2 | 1.6 | 2 | 1.8 |
| Gap extensions¶ | | | | | | | | | |
| Human | 0.8 | 4 | 4.6 | 5.3 | 5.8 | 6.5 | 5.5 | 6.4 | 6.2 |
| Mouse | 0.9 | 7.8 | 9.3 | 9.1 | 11.2 | 11.2 | 7 | 10.9 | 9.9 |
| Alignment# | | | | | | | | | |
| X1 | 98.2 | 86.1 | 85.9 | 85.2 | 75 | 47.8 | 93.4 | 33.5 | 39.9 |
| X2 | 52.4 | 16.2 | 20.8 | 11 | 11.4 | 3.5 | 9.7 | 1.2 | 3.3 |
| X10 | 8.2 | 1.2 | 1.7 | 1 | 0.6 | 0.3 | 0 | 0 | 0.4 |
| X100 | 1.5 | 0.3 | 0.4 | 0.1 | 0.2 | 0.04 | 0 | 0 | 0.1 |
| (G+C) (%)☆ | 52.3 | 58.4 | 43.9 | 60.1 | 43.7 | 41.5 | 56.7 | 37.2 | 40.9 |

The coding, intron and UTR regions are defined by 14,729 alignments of human mRNA from the RefSeq database against the genome. Upstream 200 bp and downstream 200 bp indicate the regions 200-bp upstream and downstream of these alignments.
*From the collection of the 95 known regulatory regions described in the text.
†The ancient repeats are a collection of 2.1 million transposon relics that predate the mouse–human split, as discussed in the text.
‡The figures for the genome as a whole.
§The percentage of aligned bases in these regions that are identical.
‖The number of gap initiations in the human and mouse sequences, respectively, as a percentage of the human bases in the alignments.
¶The number of gap extensions as a percentage of the human bases in the alignments.
#The percentage of human bases covered by at least 1, 2, 10 and 100 significant alignments, respectively. These numbers are taken before the last step in the construction of the alignment, when all but the best alignments for each human region are discarded.
☆The percentage of (G+C) in the human sequence.

  

main polyadenylation signal is AATAAA or ATTAAA positioned 10–30 bases upstream of polyadenylation[235]. The region of increased conservation is considerably longer than can be explained by the polyadenylation signal alone, suggesting that other 3′-UTR regulatory signals, such as those that affect mRNA stability and localization, may frequently occur near the end of the mRNA. After the polyadenylation site, there is a 30-base plateau of moderate conservation, corresponding to the weaker (T)-rich or (G+T)-rich downstream region following the polyadenylation signal.

### Conservation of gene structure

We also examined the conservation of exon structure and splice signals in more detail using 1,506 pairs of human–mouse RefSeq genes confidently assigned to be orthologous (http://www.ncbi.nlm.nih.gov/HomoloGene/). As previously reported using smaller data sets[236], overall gene structures are highly conserved between orthologous pairs: 86% of the cases (1,289 out of 1,506) have the identical number of coding exons, and 46% (692 out of 1,506) have the identical coding sequence length. When we consider all exons rather than just coding exons, we find that 941 pairs (62%) have the same number of exons. The true concordance of gene structure between the two species is probably higher, because differences will be exaggerated by differential representation of alternative splice forms between the two data sets, difficulties in mapping the cDNA sequences back to the genome, and the absence of true 5′ and 3′ ends.

The set of 1,289 genes with an identical number of coding exons contains 10,061 pairs of orthologous exons (plus 124 intronless genes). Exon length between orthologous exons is highly conserved: 9,131 (91%) of these human–mouse exon pairs have identical exon length. When exon pairs do have different lengths, the differences are predominantly multiples of three (858 out of the 930 with different lengths), as expected from coding-frame constraints. Nearly all orthologous exons conserve phase (10,015 or 99.5%). In contrast, only 90 out of 8,896 orthologous introns (1%) have identical length, although there is strong correlation between the lengths of orthologous introns. Consistent with the smaller size of the mouse genome overall, orthologous mouse introns tend to be shorter. Excluding outliers, the average human intron in this data set is 4,661 bp, whereas the average mouse intron is 3,888 bp.

Within the set of 1,506 orthologous human–mouse gene pairs, there are 22 cases in which the overall coding length is identical between the gene pairs, but they differ in the number of exons. Most of these cases can be explained by a single intron insertion/deletion (Fig. 26)[237], demonstrating the dynamic (but slow) evolution of gene structure.

We also found several non-canonical splice sites in the set of 8,896 orthologous introns, including RTATCCTY 5′ splice signals characteristic of U12 introns, which are singularly conserved (see ref. 238 for review). We found this 5′ splice signal in 20 human and 22 mouse introns from the set of 8,896, and 19 of these cases correspond to orthologous introns, indicating high levels of conservation of this distinct splicing mechanism. Also conserved are the non-canonical GC-AG introns (mechanistically identical to the GT-AG canonical introns): in the set there are 23 non-canonical GC-AG introns in human and 23 in mouse, including 19 orthologous pairs.

### Conservation in known regulatory regions

We similarly sought to study the extent of conservation in regulatory control regions of genes[232,239,240]. So far, relatively few regulatory elements have been studied extensively. We compiled a list of 95 well-characterized regulatory regions, including some liver-specific[241], muscle-specific[242] and general regulatory regions[243]. The sequences were carefully checked against the primary publications and trimmed to contain the smallest reported functional unit. The distribution of the elements was: 10% in introns, 85% in the immediate vicinity (<2 kb) of promoters, and 5% more distal from promoters. About 19% overlapped a CpG island.

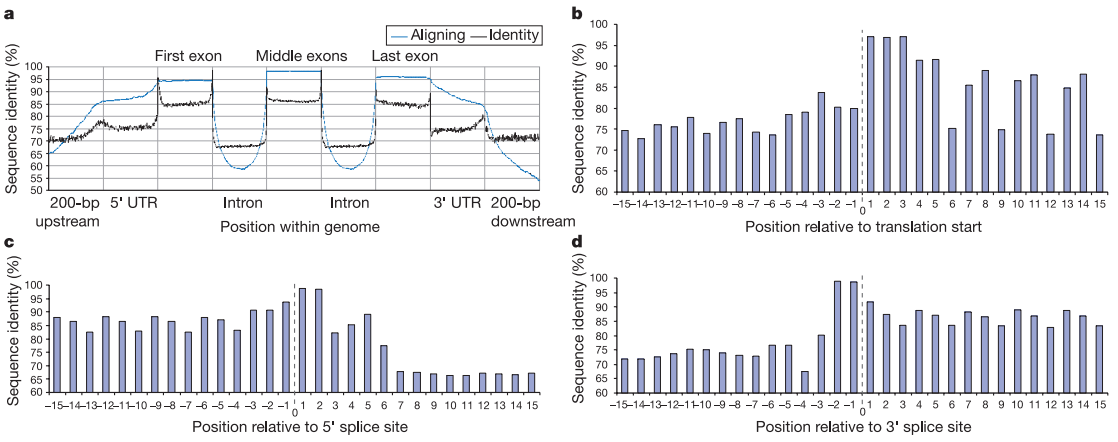


**Figure 25** Variation in conservation across a gene. **a**, Conservation across a generic gene, on the basis of 3,165 human RefSeq mRNAs with known position in the genome. We sampled 200 evenly spaced bases across each of the variable-length regions labelled, resampling completely from regions shorter than 200 bp. The graph shows the average percentage of bases aligning and the average base identity when there is an alignment over each sample. There are peaks of conservation at the transition from one region to another. Here, in contrast to Table 16, only reviewed RefSeq mRNAs were used, and only those having at least 40 bases of annotated 5′ and 3′ UTRs. The resulting picture, however, is nearly indistinguishable from that obtained by using all RefSeq genes with at least 40 base UTRs. **b**, Conservation near translation start site using the same data set as in **a**. The bars show per cent identity of the 15 bases to either side of translation start. Note the extreme conservation of the first codon. After this, there is substantially less conservation at the third codon position. The peak at position −3 corresponds to a purine in the Kozak consensus sequence. **c**, Conservation near the 5′ splice site. The peak of conservation corresponds to the AG/GT consensus at this location, with the first G in the intron being nearly invariant. A G in the fifth base of the intron is also found in a large majority of 5′ splice sites. An echo of the variation in the third codon position occurs here because it is common for exons to begin and end at codon boundaries. **d**, Conservation near the 3′ splice site. Conservation in the last two bases of the intron—always AG for introns processed by the major spliceosome—is very apparent. The polypyrimidine tract beginning five bases into the intron is also visibly conserved. Once again, an echo of the variation in the third codon position can be seen.

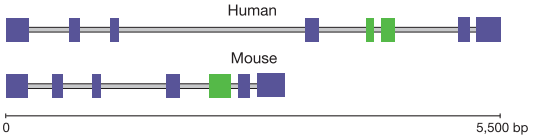


**Figure 26** The human spermidine synthase gene (*SRM*) on chromosome 1, involved in the biosynthesis of polyamines, and its mouse orthologue (*Srm*) on chromosome 4. The fifth exon in the mouse gene (green) is interrupted by an intron in the human homologue. All other exons are purple.

The extent of conservation (Fig. 24 and Table 16) was considerably lower than in coding regions, but much higher than the neutral rate in ancestral repeats or than the average rate across the genome. Overall, the known regulatory regions showed a level of conservation similar to that of 5′ UTRs. The (G+C) content is also substantially higher for the regulatory elements than for the genome as a whole, a property shared with exons and 5′ UTRs.

Although the extent of conservation in regulatory regions—as measured by the score $S(R)$—overlaps with that in neutral DNA (Fig. 24), this does not preclude the use of this measure to identify candidate regulatory elements. An example is given by the insulin-like growth factor binding protein acid-labile subunit gene (*IGFALS*), where the region surrounding a well-known transcription factor binding site[244–246] stands out as unusually conserved using this measure (Fig. 27). More sophisticated models, such as Markov models on the fine texture of the alignments (matches, transitions, transversions and gaps), may discriminate regulatory regions under selection from neutrally evolving regions with better efficiency[329].

### Proportion of genome under selection

We then set out to investigate the fraction of a mammalian genome under evolutionary selection for biological function.

To do this, we estimated the proportion of the genome that is better conserved than would be expected given the underlying neutral rate of substitution. We compared the overall distribution $S_{\text{genome}}$ of conservation scores for the genome to the neutral distribution $S_{\text{neutral}}$ of conservation scores for ancestral repeats (Fig. 23, blue curve) using a genome-wide set of 14.3 million non-overlapping 50-bp (human) windows, each containing at least 45 bp (mean 48.67 bp) of aligned sequence. The genome-wide score distribution for these windows has a prominent tail extending to the right, reflecting a substantial excess of windows with high conservation scores relative to the neutral rate (Fig. 28). The excess can be estimated by decomposing the genome-wide distribution $S_{\text{genome}}$ as a mixture of two components: $S_{\text{neutral}}$ and $S_{\text{selected}}$ (reflecting windows under selection).

The mixture coefficients indicate that at least 20.8% of the windows are under selection, with the remainder consistent with neutral substitution. Because about 25.2% of all human bases are contained in the windows, this suggests that at least 5.25% (25.2% of 20.8%) of the 50-base windows in the human genome is under selection. Repeating the analysis on more stringently filtered alignments (with non-syntenic and non-reciprocal best matches removed) requiring different numbers of aligned bases per window and with 100-bp windows, yields similar estimates, ranging mostly from 4.8% to about 6.1% of windows under selection (D. Haussler, unpublished data), as does using an alternative score function that considers flanking base context effects and uses a gap penalty[330]. Significantly smaller window sizes, for example, 30 bp, do not provide sufficient statistical separation between the neutral and genome-wide score distributions to provide useful estimates of the share under selection.

The analysis thus suggests that about 5% of small segments (50 bp) in the human genome are under evolutionary selection for biological functions common to human and mouse. This corresponds to regions totalling about 140 Mb of human genomic DNA, although not all of the nucleotides in these windows are under selection. In addition, some bases outside these windows are likely to be under selection. In a loose sense, these regions might be regarded as containing the 'functional' conserved subset of the mammalian genome. Of course, it should be noted that non-conserved sequence may have important roles, for example, as a passive spacer or providing a function specific to one lineage. Notably, protein-coding regions of genes can account for only a fraction of the genome under selection. From our analysis of the

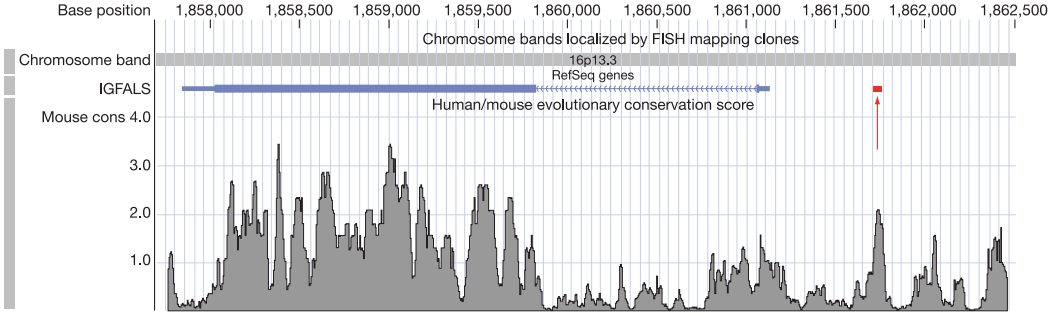


**Figure 27** Conservation scores for 50-bp windows in a 4.5-kb region containing the human insulin-like growth factor binding protein acid labile subunit (*IGFALS*) gene. In the track near the top of figure, the two coding exons of the gene are displayed as taller blue rectangles, UTRs as shorter rectangles, and the intron, which separates the coding exons, is shown as a barbed line indicating direction of transcription (the gene is on the reverse strand). Log probability scores (L-scores) for all 50-bp windows are shown below the gene. The L-score is $-\log_{10}(p)$, where $p$ is the probability under the neutral density, $S_{\text{neutral}}$, of getting a conservation score as high as is observed in the window. Many windows in the coding region get L-scores greater than 3, indicating less than a 1/1,000 chance of occurring under neutral evolution ($P_{\text{selected}}(S) > 0.94$; see Fig. 28), and some in a local peak in the upstream region of the gene on the right show L-scores greater than 2, indicating less than a 1/100 chance of occurring ($P_{\text{selected}}(S) > 0.75$). The red bar shows the location of the interferon-γ-activated sequence-like element (GLE), which is bound by transcription factors from the STAT5a and STAT5b protein family to control expression of this gene[244,245]. Additional regulatory elements may be located in the other peaks of conservation. This figure is taken with permission from the UCSC browser (http://genome.ucsc.edu).

  

the genome sequence now makes it straightforward to obtain a desired gene in a BAC for such experiments; end-sequenced BAC libraries from other strains should be available in the future. BACs also provide the ability to make mutant alleles with relative ease, by taking advantage of powerful genetic engineering techniques for custom mutagenesis in the *Escherichia coli* host.

### Applications to cancer

The mouse genome sequence also has powerful applications to the molecular characterization of the somatic mutations that result in neoplasia. High-density SNP mapping to identify loss of heterozygosity[288,289], combined with comparative genomic hybridization using cDNA or BAC arrays[290,291], can be used to identify chromosomal segments showing loss or gain of copy number in particular tumour types. The combination of such approaches with expression arrays that include all mouse genes should further enhance the ability to pinpoint the molecular lesions that result in carcinogenesis. Full sequencing of all the exons and regulatory regions of known tumour suppressors, oncogenes, and other candidate genes can now be contemplated, as has been initiated in a few centres for human tumours[292].

As a specific example of the use of the draft sequence for oncogene discovery, several groups recently used retroviral infection in mice to recover new cancer susceptibility loci. The ability to compare rapidly retrieved sequence tags to the draft genome sequence greatly accelerated the process of cancer gene discovery[293–295].

### Making better mouse models

Not all mouse models replicate the human phenotype in the expected way. The availability of the full human and mouse sequences provides an opportunity to anticipate these differences, and perhaps to compensate for them. In some instances, it may turn out that the murine mutation did not reside in the true orthologue of the human disease gene. Alternatively, in a circumstance where the human genome contains only a single gene family member, but the mouse genome contains a paralogue as well as the orthologue, one can anticipate that knockout of the orthologue alone may give a much milder phenotype (or none at all). Such was the case, for instance, with the occulocerebrorenal syndrome described by Lowe and colleagues[296]. Creating double knockout mice may then provide a closer match to the human disease phenotype.

### Understanding gene regulation

Of the approximately 5% of windows of the mammalian genome that are under selection, most do not appear to code for protein. Much of this sequence is probably involved in the regulation of gene expression. It should be possible to pinpoint these regulatory elements more precisely with the availability of additional related genomes. However, mouse is likely to provide the most powerful experimental platform for generating and testing hypotheses about their function. An example is the recent demonstration, based on mouse–human sequence alignment followed by knockout manipulation, of several long-range locus control regions that affect expression of the Il4/Il13/Il5 cluster[4].

## Conclusion

The mouse provides a unique lens through which we can view ourselves. As the leading mammalian system for genetic research over the past century, it has provided a model for human physiology and disease, leading to major discoveries in such fields as immunology and metabolism. With the availability of the mouse genome sequence, it now provides a model and informs the study of our genome as well.

Comparative genome analysis is perhaps the most powerful tool for understanding biological function. Its power lies in the fact that evolution's crucible is a far more sensitive instrument than any other available to modern experimental science: a functional alteration that diminishes a mammal's fitness by one part in $10^4$ is undetectable at the laboratory bench, but is lethal from the standpoint of evolution.

Comparative analysis of genomes should thus make it possible to discern, by virtue of evolutionary conservation, biological features that would otherwise escape our notice. In this way, it will play a crucial role in our understanding of the human genome and thereby help lay the foundation for biomedicine in the twenty-first century.

The initial sequence of the mouse genome reported here is merely a first step in this intellectual programme. The sequencing of many additional mammalian and other vertebrate genomes will be needed to extract the full information hidden within our chromosomes. Moreover, as we begin to understand the common elements shared among species, it may also become possible to approach the even harder challenge of identifying and understanding the functional differences that make each species unique. □

## Methods

### Production of sequence reads

Paired-end reads from libraries with different insert sizes were produced as previously described[1] using 384-well trays to ensure linkages.

### Availability of sequence and assembly data

Unprocessed sequence reads are available from the NCBI trace archive (ftp://ftp.ncbi.nih.gov/pub/TraceDB/mus_musculus/). Raw assembly data (before removal of contaminants, anchoring to chromosomes, and addition of finished sequence) are available from the Whitehead Institute for Biomedical Research (WIBR) (ftp://wolfram.wi.mit.edu/pub/mouse_contigs/Mar10_02/). The released assembly MGSCv3 is available from Ensembl (http://www.ensembl.org/Mus_musculus/), NCBI (ftp://ftp.ncbi.nih.gov/genomes/M_musculus/MGSCv3_Release1/), UCSC (http://genome.ucsc.edu/downloads.html) and WIBR (ftp://wolfram.wi.mit.edu/pub/mouse_contigs/MGSC_V3/). (See Supplementary Information for detailed Methods.)

Received 18 September; accepted 31 October 2002; doi:10.1038/nature01262.


1. International Human Genome Sequencing Consortium Initial sequencing and analysis of the human genome. *Nature* **409,** 860–921 (2001).
2. Venter, J. C. *et al.* The sequence of the human genome. *Science* **291,** 1304–1351 (2001).
3. O'Brien, S. J. *et al.* The promise of comparative genomics in mammals. *Science* **286,** 458–462, 479–481 (1999).
4. Loots, G. G. *et al.* Identification of a coordinate regulator of interleukins 4, 13, and 5 by cross-species sequence comparisons. *Science* **288,** 136–140 (2000).
5. Pennacchio, L. A. & Rubin, E. M. Genomic strategies to identify mammalian regulatory sequences. *Nature Rev. Genet.* **2,** 100–109 (2001).
6. Oeltjen, J. C. *et al.* Large-scale comparative sequence analysis of the human and murine Bruton's tyrosine kinase loci reveals conserved regulatory domains. *Genome Res.* **7,** 315–329 (1997).
7. Ellsworth, R. E. *et al.* Comparative genomic sequence analysis of the human and mouse cystic fibrosis transmembrane conductance regulator genes. *Proc. Natl Acad. Sci. USA* **97,** 1172–1177 (2000).
8. Mallon, A. M. *et al.* Comparative genome sequence analysis of the Bpa/Str region in mouse and man. *Genome Res.* **10,** 758–775 (2000).
9. Dehal, P. *et al.* Human chromosome 19 and related regions in mouse: conservative and lineage-specific evolution. *Science* **293,** 104–111 (2001).
10. DeSilva, U. *et al.* Generation and comparative analysis of approximately 3.3 Mb of mouse genomic sequence orthologous to the region of human chromosome 7q11.23 implicated in Williams syndrome. *Genome Res.* **12,** 3–15 (2002).
11. Toyoda, A. *et al.* Comparative genomic sequence analysis of the human chromosome 21 down syndrome critical region. *Genome Res.* **12,** 1323–1332 (2002).
12. Ansari-Lari, M. A. *et al.* Comparative sequence analysis of a gene-rich cluster at human chromosome 12p13 and its syntenic region in mouse chromosome 6. *Genome Res.* **8,** 29–40 (1998).
13. Lercher, M. J., Williams, E. J. & Hurst, L. D. Local similarity in evolutionary rates extends over whole chromosomes in human-rodent and mouse-rat comparisons: implications for understanding the mechanistic basis of the male mutation bias. *Mol. Biol. Evol.* **18,** 2032–2039 (2001).
14. Makalowski, W. & Boguski, M. S. Evolutionary parameters of the transcribed mammalian genome: an analysis of 2,820 orthologous rodent and human sequences. *Proc. Natl Acad. Sci. USA* **95,** 9407–9412 (1998).
15. Rossant, J. & McKerlie, C. Mouse-based phenogenomics for modelling human disease. *Trends Mol. Med.* **7,** 502–507 (2001).
16. Paigen, K. A miracle enough: the power of mice. *Nature Med.* **1,** 215–220 (1995).
17. Hogan, B., Beddington, R., Costantini, F. & Lacy, E. *Manipulating the Mouse Embryo: A Laboratory Manual* (Cold Spring Harbor Laboratory Press, Woodbury, New York, 1994).
18. Joyner, A. L. *Gene Targeting: A Practical Approach* (Oxford Univ. Press, New York, 1999).
19. Copeland, N. G., Jenkins, N. A. & Court, D. L. Recombineering: a powerful new tool for mouse functional genomics. *Nature Rev. Genet.* **2,** 769–779 (2001).
20. Yu, Y. & Bradley, A. Engineering chromosomal rearrangements in mice. *Nature Rev. Genet.* **2,** 780–790 (2001).
21. Bucan, M. & Abel, T. The mouse: genetics meets behaviour. *Nature Rev. Genet.* **3,** 114–123 (2002).


  

articles


22. Silver, L. M. *Mouse Genetics: Concepts and Practice* (Oxford Univ. Press, New York, 1995).
23. Bromham, L., Phillips, M. J. & Penny, D. Growing up with dinosaurs: molecular dates and the mammalian radiation. *Trends Ecol. Evol.* **14,** 113–118 (1999).
24. Nei, M., Xu, P. & Glazko, G. Estimation of divergence times from multiprotein sequences for a few mammalian species and several distantly related organisms. *Proc. Natl Acad. Sci. USA* **98,** 2497–2502 (2001).
25. Kumar, S. & Hedges, S. B. A molecular timescale for vertebrate evolution. *Nature* **392,** 917–920 (1998).
26. Madsen, O. *et al.* Parallel adaptive radiations in two major clades of placental mammals. *Nature* **409,** 610–614 (2001).
27. Murphy, W. J. *et al.* Molecular phylogenetics and the origins of placental mammals. *Nature* **409,** 614–618 (2001).
28. Keeler, C. E. *The Laboratory Mouse: Its Origin, Heredity and Culture* (Harvard Univ. Press, Cambridge, Massachusetts, 1931).
29. Morse, H. *The Mouse in Biomedical Research* (eds Foster, H. L., Small, J. D. & Fox, J. G.) 1–16 (Academic, New York, 1981).
30. Morse, H. C. *Origins of Inbred Mice* (ed. Morse, H. C.) 1–21 (Academic, New York, 1978).
31. Haldane, J. B. S., Sprunt, A. D. & Haldane, N. M. Reduplication in mice. *J. Genet.* **5,** 133–135 (1915).
32. Botstein, D., White, R. L., Skolnick, M. & Davis, R. W. Construction of a genetic linkage map in man using restriction fragment length polymorphisms. *Am. J. Hum. Genet.* **32,** 314–331 (1980).
33. Dietrich, W. *et al. Genetic Maps* (ed. O'Brien, S.) 4.110–4.142, (1992).
34. Dietrich, W. F. *et al.* A comprehensive genetic map of the mouse genome. *Nature* **380,** 149–152 (1996).
35. Love, J. M., Knight, A. M., McAleer, M. A. & Todd, J. A. Towards construction of a high resolution map of the mouse genome using PCR-analysed microsatellites. *Nucleic Acids Res.* **18,** 4123–4130 (1990).
36. Weber, J. L. & May, P. E. Abundant class of human DNA polymorphisms which can be typed using the polymerase chain reaction. *Am. J. Hum. Genet.* **44,** 388–396 (1989).
37. Hudson, T. J. *et al.* A radiation hybrid map of mouse genes. *Nature Genet.* **29,** 201–205 (2001).
38. Van Etten, W. J. *et al.* Radiation hybrid map of the mouse genome. *Nature Genet.* **22,** 384–387 (1999).
39. Nusbaum, C. *et al.* A YAC-based physical map of the mouse genome. *Nature Genet.* **22,** 388–393 (1999).
40. Marra, M. *et al.* An encyclopedia of mouse genes. *Nature Genet.* **21,** 191–194 (1999).
41. Kawai, J. *et al.* Functional annotation of a full-length mouse cDNA collection. *Nature* **409,** 685–690 (2001).
42. Strausberg, R. L., Feingold, E. A., Klausner, R. D. & Collins, F. S. The mammalian gene collection. *Science* **286,** 455–457 (1999).
43. Osoegawa, K. *et al.* Bacterial artificial chromosome libraries for mouse sequencing and functional analysis. *Genome Res.* **10,** 116–128 (2000).
44. Gregory, S. G. *et al.* A physical map of the mouse genome. *Nature* **418,** 743–750 (2002).
45. Mural, R. J. *et al.* A comparison of whole-genome shotgun-derived mouse chromosome 16 and the human genome. *Science* **296,** 1661–1671 (2002).
46. Green, E. D. Strategies for the systematic sequencing of complex genomes. *Nature Rev. Genet.* **2,** 573–583 (2001).
47. Edwards, A. *et al.* Automated DNA sequencing of the human HPRT locus. *Genomics* **6,** 593–608 (1990).
48. Huson, D. H. *et al.* Design of a compartmentalized shotgun assembler for the human genome. *Bioinformatics* **17,** S132–S139 (2001).
49. Analysis of the genome sequence of the flowering plant *Arabidopsis thaliana*. *Nature* **408,** 796–815 (2000).
50. Adams, M. D. *et al.* The genome sequence of *Drosophila melanogaster. Science* **287,** 2185–2195 (2000).
51. Yu, J. *et al.* A draft sequence of the rice genome. *Science* **296,** 79–92 (2002).
52. Battey, J., Jordan, E., Cox, D. & Dove, W. An action plan for mouse genomics. *Nature Genet.* **21,** 73–75 (1999).
53. Kuroda-Kawaguchi, T. *et al.* The AZFc region of the Y chromosome features massive palindromes and uniform recurrent deletions in infertile men. *Nature Genet.* **29,** 279–286 (2001).
54. Zhao, S. *et al.* Mouse BAC ends quality assessment and sequence analyses. *Genome Res.* **11,** 1736–1745 (2001).
55. Ewing, B. & Green, P. Analysis of expressed sequence tags indicates 35,000 human genes. *Nature Genet.* **25,** 232–234 (2000).
56. Batzoglou, S. *et al.* ARACHNE: a whole-genome shotgun assembler. *Genome Res.* **12,** 177–189 (2002).
57. Jaffe, D. B. *et al.* Whole-genome sequence assembly for mammalian genomes: Arachne 2. *Genome Res.* (in the press).
58. Mullikin, J. & Ning, Z. The Phusion Assembler. *Genome Res.* (in the press).
59. Bailey, J. A. *et al.* Recent segmental duplications in the human genome. *Science* **297,** 1003–1007 (2002).
60. Traut, W., Winking, H. & Adolph, S. An extra segment in chromosome 1 of wild *Mus musculus*: a C-band positive homogeneously staining region. *Cytogenet. Cell Genet.* **38,** 290–297 (1984).
61. Weichenhan, D. *et al.* Source and component genes of a 6-200 Mb gene cluster in the house mouse. *Mamm. Genome* **12,** 590–594 (2001).
62. Purmann, L., Plass, C., Gruneberg, M., Winking, H. & Traut, W. A long-range repeat cluster in chromosome 1 of the house mouse, *Mus musculus*, and its relation to a germline homogeneously staining region. *Genomics* **12,** 80–88 (1992).
63. Wong, A. K. & Rattner, J. B. Sequence organization and cytological localization of the minor satellite of mouse. *Nucleic Acids Res.* **16,** 11645–11661 (1988).
64. Joseph, A., Mitchell, A. R. & Miller, O. J. The organization of the mouse satellite DNA at centromeres. *Exp. Cell Res.* **183,** 494–500 (1989).
65. Davisson, M. T. & Roderick, T. H. *Genetic Variants and Strains of the Laboratory Mouse* (eds Lyon, M. F. & Searle, A. G.) 416–427 (Oxford Univ. Press, Oxford, 1989).
66. Mouse Genome Sequencing Consortium Progress in sequencing the mouse genome. *Genesis* **31,** 137–141 (2001).
67. Clark, F. H. Inheritance and linkage relations of mutant characteristics in the deermouse. *Contrib. Lab. Vert. Biol.* **7,** 1–11 (1938).
68. Castle, W. W. Observations of the occurrence of linkage in rats and mice. *Car. Inst. Wash. Pub.* **288,** 29–36 (1919).
69. Lalley, P. A., Minna, J. D. & Francke, U. Conservation of autosomal gene synteny groups in mouse and man. *Nature* **274,** 160–163 (1978).
70. Nadeau, J. H. & Taylor, B. A. Lengths of chromosomal segments conserved since divergence of man and mouse. *Proc. Natl Acad. Sci. USA* **81,** 814–818 (1984).
71. Ma, B., Tromp, J. & Li, M. PatternHunter: faster and more sensitive homology search. *Bioinformatics* **18,** 440–445 (2002).
72. Ohno, S. *Sex Chromosomes and Sex-Linked Genes* (Springer, Berlin, 1996).
73. Sturtevant, A. H. & Beadle, G. W. The relations of inversions in the X chromosome of *Drosophila melanogaster* to crossing over and disjunction. *Genetics* **21,** 554–604 (1936).
74. Ranz, J. M., Casals, F. & Ruiz, A. How malleable is the eukaryotic genome? Extreme rate of chromosomal rearrangement in the genus *Drosophila*. *Genome Res.* **11,** 230–239 (2001).
75. Nadeau, J. H. & Sankoff, D. The lengths of undiscovered conserved segments in comparative maps. *Mamm. Genome* **9,** 491–495 (1998).
76. Ferretti, V., Nadeau, J. H. & Sankoff, D. *Combinatorial Pattern Matching, 7th Annual Symposium* (eds Hirschberg, D. & Myers, G.) 159–167 (Springer, Berlin, 1996).
77. Bourque, G. & Pevzner, P. A. Genome-scale evolution: reconstructing gene orders in the ancestral species. *Genome Res.* **12,** 26–36 (2002).
78. Thiery, J. P., Macaya, G. & Bernardi, G. An analysis of eukaryotic genomes by density gradient centrifugation. *J. Mol. Biol.* **108,** 219–235 (1976).
79. Salinas, J., Zerial, M., Filipski, J. & Bernardi, G. Gene distribution and nucleotide sequence organization in the mouse genome. *Eur. J. Biochem.* **160,** 469–478 (1986).
80. Sabeur, G., Macaya, G., Kadi, F. & Bernardi, G. The isochore patterns of mammalian genomes and their phylogenetic implications. *J. Mol. Evol.* **37,** 93–108 (1993).
81. Zerial, M., Salinas, J., Filipski, J. & Bernardi, G. Gene distribution and nucleotide sequence organization in the human genome. *Eur. J. Biochem.* **160,** 479–485 (1986).
82. Mouchiroud, D., Fichant, G. & Bernardi, G. Compositional compartmentalization and gene composition in the genome of vertebrates. *J. Mol. Evol.* **26,** 198–204 (1987).
83. Mouchiroud, D., Gautier, C. & Bernardi, G. The compositional distribution of coding sequences and DNA molecules in humans and murids. *J. Mol. Evol.* **27,** 311–320 (1988).
84. Mouchiroud, D. & Gautier, C. Codon usage changes and sequence dissimilarity between human and rat. *J. Mol. Evol.* **31,** 81–91 (1990).
85. Robinson, M., Gautier, C. & Mouchiroud, D. Evolution of isochores in rodents. *Mol. Biol. Evol.* **14,** 823–828 (1997).
86. Bernardi, G. *et al.* The mosaic genome of warm-blooded vertebrates. *Science* **228,** 953–958 (1985).
87. Mouchiroud, D. *et al.* The distribution of genes in the human genome. *Gene* **100,** 181–187 (1991).
88. Zoubak, S., Clay, O. & Bernardi, G. The gene distribution of the human genome. *Gene* **174,** 95–102 (1996).
89. Saccone, S., Pavlicek, A., Federico, C., Paces, J. & Bernard, G. Genes, isochores and bands in human chromosomes 21 and 22. *Chromosome Res.* **9,** 533–539 (2001).
90. Bernardi, G. Compositional constraints and genome evolution. *J. Mol. Evol.* **24,** 1–11 (1986).
91. Bernardi, G., Mouchiroud, D. & Gautier, C. Compositional patterns in vertebrate genomes: conservation and change in evolution. *J. Mol. Evol.* **28,** 7–18 (1988).
92. Wolfe, K. H., Sharp, P. M. & Li, W. H. Mutation rates differ among regions of the mammalian genome. *Nature* **337,** 283–285 (1989).
93. Sueoka, N. Directional mutation pressure and neutral molecular evolution. *Proc. Natl Acad. Sci. USA* **85,** 2653–2657 (1988).
94. Sueoka, N. On the genetic basis of variation and heterogeneity of DNA base composition. *Proc. Natl Acad. Sci. USA* **48,** 582–592 (1962).
95. Bird, A. P. DNA methylation and the frequency of CpG in animal DNA. *Nucleic Acids Res.* **8,** 1499–1504 (1980).
96. Larsen, F., Gundersen, G., Lopez, R. & Prydz, H. CpG islands as gene markers in the human genome. *Genomics* **13,** 1095–1107 (1992).
97. Gardiner-Garden, M. & Frommer, M. CpG islands in vertebrate genomes. *J. Mol. Biol.* **196,** 261–282 (1987).
98. Antequera, F. & Bird, A. Number of CpG islands and genes in human and mouse. *Proc. Natl Acad. Sci. USA* **90,** 11995–11999 (1993).
99. Adams, R. L. & Eason, R. Increased G+C content of DNA stabilizes methyl CpG dinucleotides. *Nucleic Acids Res.* **12,** 5869–5877 (1984).
100. Smit, A. F. Interspersed repeats and other mementos of transposable elements in mammalian genomes. *Curr. Opin. Genet. Dev.* **9,** 657–663 (1999).
101. Laird, C. D., McConaughy, B. L. & McCarthy, B. J. Rate of fixation of nucleotide substitutions in evolution. *Nature* **224,** 149–154 (1969).
102. Kohne, D. E. Evolution of higher-organism DNA. *Q. Rev. Biophys.* **3,** 327–375 (1970).
103. Goodman, M., Barnabas, J., Matsuda, G. & Moore, G. W. Molecular evolution in the descent of man. *Nature* **233,** 604–613 (1971).
104. Kumar, S. & Subramanian, S. Mutation rates in mammalian genomes. *Proc. Natl Acad. Sci. USA* **99,** 803–808 (2002).
105. Easteal, S., Collet, C. & Betty, D. *The Mammalian Molecular Clock* (Landes, Austin, Texas, 1995).
106. Li, W. H., Ellsworth, D. L., Krushkal, J., Chang, B. H. & Hewett-Emmett, D. Rates of nucleotide substitution in primates and rodents and the generation-time effect hypothesis. *Mol. Phylogenet. Evol.* **5,** 182–187 (1996).
107. Martin, A. P. & Palumbi, S. R. Body size, metabolic rate, generation time, and the molecular clock. *Proc. Natl Acad. Sci. USA* **90,** 4087–4091 (1993).
108. Bromham, L. Molecular clocks in reptiles: life history influences rate of molecular evolution. *Mol. Biol. Evol.* **19,** 302–309 (2002).
109. Wu, C. I. & Li, W. H. Evidence for higher rates of nucleotide substitution in rodents than in man. *Proc. Natl Acad. Sci. USA* **82,** 1741–1745 (1985).
110. Smit, A. F., Toth, G., Riggs, A. D. & Jurka, J. Ancestral, mammalian-wide subfamilies of LINE-1 repetitive sequences. *J. Mol. Biol.* **246,** 401–417 (1995).
111. Adey, N. B. *et al.* Rodent L1 evolution has been driven by a single dominant lineage that has repeatedly acquired new transcriptional regulatory sequences. *Mol. Biol. Evol.* **11,** 778–789 (1994).


  

112. Mears, M. L. & Hutchison, C. A. III The evolution of modern lineages of mouse L1 elements. *J. Mol. Evol.* **52,** 51–62 (2001).
113. Goodier, J. L., Ostertag, E. M., Du, K. & Kazazian, H. H. Jr A novel active L1 retrotransposon subfamily in the mouse. *Genome Res.* **11,** 1677–1685 (2001).
114. Hardies, S. C. *et al.* LINE-1 (L1) lineages in the mouse. *Mol. Biol. Evol.* **17,** 616–628 (2000).
115. Ohshima, K., Hamada, M., Terai, Y. & Okada, N. The 3′ ends of tRNA-derived short interspersed repetitive elements are derived from the 3′ ends of long interspersed repetitive elements. *Mol. Cell Biol.* **16,** 3756–3764 (1996).
116. Smit, A. F. The origin of interspersed repeats in the human genome. *Curr. Opin. Genet. Dev.* **6,** 743–748 (1996).
117. Quentin, Y. A master sequence related to a free left Alu monomer (FLAM) at the origin of the B1 family in rodent genomes. *Nucleic Acids Res.* **22,** 2222–2227 (1994).
118. Kim, J. & Deininger, P. L. Recent amplification of rat ID sequences. *J. Mol. Biol.* **261,** 322–327 (1996).
119. Lee, I. Y. *et al.* Complete genomic sequence and analysis of the prion protein gene region from three mammalian species. *Genome Res.* **8,** 1022–1037 (1998).
120. Serdobova, I. M. & Kramerov, D. A. Short retroposons of the B2 superfamily: evolution and application for the study of rodent phylogeny. *J. Mol. Evol.* **46,** 202–214 (1998).
121. Coffin, J. M., Hughes, S. H. & Varmus, H. E. (eds) *Retroviruses* (Cold Spring Harbor Laboratory Press, Cold Spring Harbor, New York, 1997).
122. Smit, A. F. Identification of a new, abundant superfamily of mammalian LTR- transposons. *Nucleic Acids Res.* **21,** 1863–1872 (1993).
123. Hamilton, B. A. & Frankel, W. N. Of mice and genome sequence. *Cell* **107,** 13–16 (2001).
124. Turner, G. *et al.* Insertional polymorphisms of full-length endogenous retroviruses in humans. *Curr. Biol.* **11,** 1531–1535 (2001).
125. Kidwell, M. G. Horizontal transfer. *Curr. Opin. Genet. Dev.* **2,** 868–873 (1992).
126. Feng, Q., Moran, J. V., Kazazian, H. H. Jr & Boeke, J. D. Human L1 retrotransposon encodes a conserved endonuclease required for retrotransposition. *Cell* **87,** 905–916 (1996).
127. Jurka, J. Sequence patterns indicate an enzymatic involvement in integration of mammalian retroposons. *Proc. Natl Acad. Sci. USA* **94,** 1872–1877 (1997).
128. Bernardi, G. The isochore organization of the human genome. *Annu. Rev. Genet.* **23,** 637–661 (1989).
129. Holmquist, G. P. Chromosome bands, their chromatin flavors, and their functional features. *Am. J. Hum. Genet.* **51,** 17–37 (1992).
130. Korenberg, J. R. & Rykowski, M. C. Human genome organization: Alu, lines, and the molecular structure of metaphase chromosome bands. *Cell* **53,** 391–400 (1988).
131. Boyle, A. L., Ballard, S. G. & Ward, D. C. Differential distribution of long and short interspersed element sequences in the mouse genome: chromosome karyotyping by fluorescence *in situ* hybridization. *Proc. Natl Acad. Sci. USA* **87,** 7757–7761 (1990).
132. Lyon, M. F. X-chromosome inactivation: a repeat hypothesis. *Cytogenet. Cell Genet.* **80,** 133–137 (1998).
133. Bailey, J. A., Carrel, L., Chakravarti, A. & Eichler, E. E. Molecular evidence for a relationship between LINE-1 elements and X chromosome inactivation: the Lyon repeat hypothesis. *Proc. Natl Acad. Sci. USA* **97,** 6634–6639 (2000).
134. Boissinot, S. & Furano, A. V. Adaptive evolution in LINE-1 retrotransposons. *Mol. Biol. Evol.* **18,** 2186–2194 (2001).
135. Beckman, J. S. & Weber, J. L. Survey of human and rat microsatellites. *Genomics* **12,** 627–631 (1992).
136. Toth, G., Gaspari, Z. & Jurka, J. Microsatellites in different eukaryotic genomes: survey and analysis. *Genome Res.* **10,** 967–981 (2000).
137. Kruglyak, S., Durrett, R. T., Schug, M. D. & Aquadro, C. F. Equilibrium distributions of microsatellite repeat length resulting from a balance between slippage events and point mutations. *Proc. Natl Acad. Sci. USA* **95,** 10774–10778 (1998).
138. Santibanez-Koref, M. F., Gangeswaran, R. & Hancock, J. M. A relationship between lengths of microsatellites and nearby substitution rates in mammalian genomes. *Mol. Biol. Evol.* **18,** 2119–2123 (2001).
139. Dunham, I. *et al.* The DNA sequence of human chromosome 22. *Nature* **402,** 489–495 (1999).
140. Hattori, M. *et al.* The DNA sequence of human chromosome 21. *Nature* **405,** 311–319 (2000).
141. Roest Crollius, H. *et al.* Estimate of human gene number provided by genome-wide analysis using *Tetraodon nigroviridis* DNA sequence. *Nature Genet.* **25,** 235–238 (2000).
142. Hubbard, T. *et al.* The Ensembl genome database project. *Nucleic Acids Res.* **30,** 38–41 (2002).
143. Kulp, D., Haussler, D., Reese, M. G. & Eeckman, F. H. Integrating database homology in a probabilistic gene structure model. *Pac. Symp. Biocomput.* 232–244 (1997).
144. Birney, E. & Durbin, R. Using GeneWise in the *Drosophila* annotation experiment. *Genome Res.* **10,** 547–548 (2000).
145. Burge, C. & Karlin, S. Prediction of complete gene structures in human genomic DNA. *J. Mol. Biol.* **268,** 78–94 (1997).
146. Hogenesch, J. B. *et al.* A comparison of the Celera and Ensembl predicted gene sets reveals little overlap in novel genes. *Cell* **106,** 413–415 (2001).
147. Saha, S. *et al.* Using the transcriptome to annotate the genome. *Nature Biotechnol.* **20,** 508–512 (2002).
148. Daly, M. J. Estimating the human gene count. *Cell* **109,** 283–284 (2002).
149. Kapranov, P. *et al.* Large-scale transcriptional activity in chromosomes 21 and 22. *Science* **296,** 916–919 (2002).
150. The FANTOM Consortium and the RIKEN Genome Exploration Research Group Phase I & II Team. Analysis of the mouse transcriptome based on functional annotation of 60,770 full-length cDNAs. *Nature* **420,** 563–573 (2002).
151. Pruitt, K. D. & Maglott, D. R. RefSeq and LocusLink: NCBI gene-centered resources. *Nucleic Acids Res.* **29,** 137–140 (2001).
152. Steimle, V. *et al.* A novel DNA-binding regulatory factor is mutated in primary MHC class II deficiency (bare lymphocyte syndrome). *Genes Dev.* **9,** 1021–1032 (1995).
153. Sun, H., Tsunenari, T., Yau, K. W. & Nathans, J. The vitelliform macular dystrophy protein defines a new family of chloride channels. *Proc. Natl Acad. Sci. USA* **99,** 4008–4013 (2002).
154. Yasunaga, S. *et al.* A mutation in OTOF, encoding otoferlin, a FER-1-like protein, causes DFNB9, a nonsyndromic form of deafness. *Nature Genet.* **21,** 363–369 (1999).
155. den Hollander, A. I. *et al.* Leber congenital amaurosis and retinitis pigmentosa with Coats-like exudative vasculopathy are associated with mutations in the crumbs homologue 1 (CRB1) gene. *Am. J. Hum. Genet.* **69,** 198–203 (2001).
156. den Hollander, A. I. *et al.* Mutations in a human homologue of *Drosophila* crumbs cause retinitis pigmentosa (RP12). *Nature Genet.* **23,** 217–221 (1999).
157. Maeda, N. *et al.* Diet-induced insulin resistance in mice lacking adiponectin/ACRP30. *Nature Med.* **8,** 731–737 (2002).
158. Clausen, B. E. *et al.* Residual MHC class II expression on mature dendritic cells and activated B cells in RFX5-deficient mice. *Immunity* **8,** 143–155 (1998).
159. Garcia-Meunier, P., Etienne-Julan, M., Fort, P., Piechaczyk, M. & Bonhomme, F. Concerted evolution in the GAPDH family of retrotransposed pseudogenes. *Mamm. Genome* **4,** 695–703 (1993).
160. Korf, I., Flicek, P., Duan, D. & Brent, M. R. Integrating genomic homology into gene structure prediction. *Bioinformatics* **17,** S140–S148 (2001).
161. Wiehe, T., Gebauer-Jung, S., Mitchell-Olds, T. & Guigo, R. SGP-1: prediction and validation of homologous genes based on sequence alignments. *Genome Res.* **11,** 1574–1583 (2001).
162. Alexandersson, M., Cawley, S. & Pachter, L. SLAM—cross-species GeneFinding and alignment with a generalized pair hidden Markov model. *Genome Res.* (in the press).
163. Reymond, A. *et al.* Human chromosome 21 gene expression atlas in the mouse. *Nature* **420,** 582–586 (2002).
164. Blake, D. J., Weir, A., Newey, S. E. & Davies, K. E. Function and genetics of dystrophin-related proteins in muscle. *Physiol. Rev.* **82,** 291–329 (2002).
165. Eddy, S. R. Non-coding RNA genes and the modern RNA world. *Nature Rev. Genet.* **2,** 919–929 (2001).
166. Storz, G. An expanding universe of noncoding RNAs. *Science* **296,** 1260–1263 (2002).
167. Eddy, S. R. Computational genomics of noncoding RNA genes. *Cell* **109,** 137–140 (2002).
168. Lowe, T. M. & Eddy, S. R. tRNAscan-SE: a program for improved detection of transfer RNA genes in genomic sequence. *Nucleic Acids Res.* **25,** 955–964 (1997).
169. Daniels, G. R. & Deininger, P. L. Repeat sequence families derived from mammalian tRNA genes. *Nature* **317,** 819–822 (1985).
170. Lawrence, C., McDonnell, D. & Ramsey, W. Analysis of repetitive sequence elements containing tRNA-like sequences. *Nucleic Acids Res.* **13,** 4239–4252 (1985).
171. Baron, C. & Bock, A. *tRNA: Structure, Biosynthesis, and Function* (eds Soll, D. & RajBhandary, U. L.) 529–544 (Am. Soc. Microbiol., Washington DC, 1995).
172. Crick, F. H. Codon–anticodon pairing: the wobble hypothesis. *J. Mol. Biol.* **19,** 548–555 (1966).
173. Guthrie, C. & Abelson, J. *The Molecular Biology of the Yeast Saccharomyces: Metabolism and Gene Expression* (eds Strathern, J. N., Jones, E. W. & Broach, J. R.) 487–528 (Cold Spring Harbor Laboratory Press, Woodbury, New York, 1982).
174. Ponting, C. P. & Russell, R. R. The natural history of protein domains. *Annu. Rev. Biophys. Biomol. Struct.* **31,** 45–71 (2002).
175. Lespinet, O., Wolf, Y. I., Koonin, E. V. & Aravind, L. The role of lineage-specific gene family expansion in the evolution of eukaryotes. *Genome Res.* **12,** 1048–1059 (2002).
176. Ponting, C. P., Mott, R., Bork, P. & Copley, R. R. Novel protein domains and repeats in *Drosophila melanogaster*: insights into structure, function, and evolution. *Genome Res.* **11,** 1996–2008 (2001).
177. Rubin, G. M. *et al.* Comparative genomics of the eukaryotes. *Science* **287,** 2204–2215 (2000).
178. Altschul, S. F. *et al.* Gapped BLAST and PSI-BLAST: a new generation of protein database search programs. *Nucleic Acids Res.* **25,** 3389–3402 (1997).
179. Zdobnov, E. M. & Apweiler, R. InterProScan—an integration platform for the signature-recognition methods in InterPro. *Bioinformatics* **17,** 847–848 (2001).
180. Creating the gene ontology resource: design and implementation. *Genome Res.* **11,** 1425–1433 (2001).
181. Makalowski, W. & Boguski, M. S. Synonymous and nonsynonymous substitution distances are correlated in mouse and rat genes. *J. Mol. Evol.* **47,** 119–121 (1998).
182. Hughes, A. L. & Nei, M. Pattern of nucleotide substitution at major histocompatibility complex class I loci reveals overdominant selection. *Nature* **335,** 167–170 (1988).
183. Yang, Z. & Nielsen, R. Estimating synonymous and nonsynonymous substitution rates under realistic evolutionary models. *Mol. Biol. Evol.* **17,** 32–43 (2000).
184. Nekrutenko, A., Makova, K. D. & Li, W. H. The K(A)/K(S) ratio test for assessing the protein-coding potential of genomic regions: an empirical and simulation study. *Genome Res.* **12,** 198–202 (2002).
185. Sharp, P. M. In search of molecular darwinism. *Nature* **385,** 111–112 (1997).
186. Letunic, I. *et al.* Recent improvements to the SMART domain-based sequence annotation resource. *Nucleic Acids Res.* **30,** 242–244 (2002).
187. Mott, R., Schultz, J., Bork, P. & Ponting, C. P. Predicting protein cellular localization using a domain projection method. *Genome Res.* **12,** 1168–1174 (2002).
188. Hurst, L. D. & Smith, N. G. Do essential genes evolve slowly? *Curr. Biol.* **9,** 747–750 (1999).
189. Goodstadt, L. & Ponting, C. P. Sequence variation and disease in the wake of the draft human genome. *Hum. Mol. Genet.* **10,** 2209–2214 (2001).
190. Bairoch, A. & Apweiler, R. The SWISS-PROT protein sequence database and its supplement TrEMBL in 2000. *Nucleic Acids Res.* **28,** 45–48 (2000).
191. Polymeropoulos, M. H. *et al.* Mutation in the alpha-synuclein gene identified in families with Parkinson's disease. *Science* **276,** 2045–2047 (1997).
192. Fredman, D. *et al.* HGVbase: a human sequence variation database emphasizing data quality and a broad spectrum of data sources. *Nucleic Acids Res.* **30,** 387–391 (2002).
193. Young, J. M. *et al.* Different evolutionary processes shaped the mouse and human olfactory receptor gene families. *Hum. Mol. Genet.* **11,** 535–546 (2002).
194. Zhang, X. & Firestein, S. The olfactory receptor gene superfamily of the mouse. *Nature Neurosci.* **5,** 124–133 (2002).
195. Glusman, G., Yanai, I., Rubin, I. & Lancet, D. The complete human olfactory subgenome. *Genome Res.* **11,** 685–702 (2001).
196. Rouquier, S. *et al.* Distribution of olfactory receptor genes in the human genome. *Nature Genet.* **18,** 243–250 (1998).
197. Del Punta, K. *et al.* Deficient pheromone responses in mice lacking a cluster of vomeronasal receptor genes. *Nature* **419,** 70–74 (2002).
198. Nelson, D. R. Cytochrome P450 and the individuality of species. *Arch. Biochem. Biophys.* **369,** 1–10 (1999).

**articles**


199. Lane, R. P. *et al.* Genomic analysis of orthologous mouse and human olfactory receptor loci. *Proc. Natl Acad. Sci. USA* **98,** 7390–7395 (2001).
200. Rossant, J. & Cross, J. C. Placental development: lessons from mouse mutants. *Nature Rev. Genet.* **2,** 538–548 (2001).
201. Georgiades, P., Ferguson-Smith, A. C. & Burton, G. J. Comparative developmental anatomy of the murine and human definitive placentae. *Placenta* **23,** 3–19 (2002).
202. Deussing, J. *et al.* Identification and characterization of a dense cluster of placenta- specific cysteine peptidase genes and related genes on mouse chromosome 13. *Genomics* **79,** 225–240 (2002).
203. Afonso, S., Tovar, C., Romagnano, L. & Babiarz, B. Control and expression of cystatin C by mouse decidual cultures. *Mol. Reprod. Dev.* **61,** 155–163 (2002).
204. Sutton, K. A. & Wilkinson, M. F. The rapidly evolving Pem homeobox gene and Agtr2, Ant2, and Lamp2 are closely linked in the proximal region of the mouse X chromosome. *Genomics* **45,** 447–450 (1997).
205. Wilkinson, M. F., Kleeman, J., Richards, J. & MacLeod, C. L. A novel oncofetal gene is expressed in a stage-specific manner in murine embryonic development. *Dev. Biol.* **141,** 451–455 (1990).
206. Han, Y. J., Park, A. R., Sung, D. Y. & Chun, J. Y. Psx, a novel murine homeobox gene expressed in placenta. *Gene* **207,** 159–166 (1998).
207. Chun, J. Y., Han, Y. J. & Ahn, K. Y. Psx homeobox gene is X-linked and specifically expressed in trophoblast cells of mouse placenta. *Dev. Dyn.* **216,** 257–266 (1999).
208. Takasaki, N., McIsaac, R. & Dean, J. Gpbox (Psx2), a homeobox gene preferentially expressed in female germ cells at the onset of sexual dimorphism in mice. *Dev. Biol.* **223,** 181–193 (2000).
209. Lundwall, A. & Lazure, C. A novel gene family encoding proteins with highly differing structure because of a rapidly evolving exon. *FEBS Lett.* **374,** 53–56 (1995).
210. Simon, A. M., Veyssiere, G. & Jean, C. Structure and sequence of a mouse gene encoding an androgen-regulated protein: a new member of the seminal vesicle secretory protein family. *J. Mol. Endocrinol.* **15,** 305–316 (1995).
211. Morel, L. *et al.* Mouse seminal vesicle secretory protein of 99 amino acids (MSVSP99): characterization and hormonal and developmental regulation. *J. Androl.* **22,** 549–557 (2001).
212. Linzer, D. I. & Fisher, S. J. The placenta and the prolactin family of hormones: regulation of the physiology of pregnancy. *Mol. Endocrinol.* **13,** 837–840 (1999).
213. Huang, Y. H., Chu, S. T. & Chen, Y. H. A seminal vesicle autoantigen of mouse is able to suppress sperm capacitation-related events stimulated by serum albumin. *Biol. Reprod.* **63,** 1562–1566 (2000).
214. Yoshida, M., Kaneko, M., Kurachi, H. & Osawa, M. Identification of two rodent genes encoding homologues to seminal vesicle autoantigen: a gene family including the gene for prolactin-inducible protein. *Biochem. Biophys. Res. Commun.* **281,** 94–100 (2001).
215. Bain, P. A., Yoo, M., Clarke, T., Hammond, S. H. & Payne, A. H. Multiple forms of mouse 3 beta-hydroxysteroid dehydrogenase/delta 5-delta 4 isomerase and differential expression in gonads, adrenal glands, liver, and kidneys of both sexes. *Proc. Natl Acad. Sci. USA* **88,** 8870–8874 (1991).
216. Payne, A. H., Abbaszade, I. G., Clarke, T. R., Bain, P. A. & Park, C. H. The multiple murine 3 beta-hydroxysteroid dehydrogenase isoforms: structure, function, and tissue- and developmentally specific expression. *Steroids* **62,** 169–175 (1997).
217. Blume, N. *et al.* Characterization of Cyp2d22, a novel cytochrome P450 expressed in mouse mammary cells. *Arch. Biochem. Biophys.* **381,** 191–204 (2000).
218. Lakso, M., Masaki, R., Noshiro, M. & Negishi, M. Structures and characterization of sex-specific mouse cytochrome P-450 genes as members within a large family. Duplication boundary and evolution. *Eur. J. Biochem.* **195,** 477–486 (1991).
219. Tegoni, M. *et al.* Mammalian odorant binding proteins. *Biochim. Biophys. Acta* **1482,** 229–240 (2000).
220. Miyawaki, A., Matsushita, F., Ryo, Y. & Mikoshiba, K. Possible pheromone-carrier function of two lipocalin proteins in the vomeronasal organ. *EMBO J.* **13,** 5835–5842 (1994).
221. Karn, R. C. & Nachman, M. W. Reduced nucleotide variability at an androgen-binding protein locus (Abpa) in house mice: evidence for positive natural selection. *Mol. Biol. Evol.* **16,** 1192–1197 (1999).
222. Karn, R. C., Orth, A., Bonhomme, F. & Boursot, P. The complex history of a gene proposed to participate in a sexual isolation mechanism in house mice. *Mol. Biol. Evol.* **19,** 462–471 (2002).
223. Singer, A. G., Macrides, F., Clancy, A. N. & Agosta, W. C. Purification and analysis of a proteinaceous aphrodisiac pheromone from hamster vaginal discharge. *J. Biol. Chem.* **261,** 13323–13326 (1986).
224. Zhang, J., Dyer, K. D. & Rosenberg, H. F. Evolution of the rodent eosinophil-associated RNase gene family by rapid gene sorting and positive selection. *Proc. Natl Acad. Sci. USA* **97,** 4701–4706 (2000).
225. Natarajan, K., Dimasi, N., Wang, J., Margulies, D. H. & Mariuzza, R. A. MHC class I recognition by Ly49 natural killer cell receptors. *Mol. Immunol.* **38,** 1023–1027 (2002).
226. Natarajan, K., Dimasi, N., Wang, J., Mariuzza, R. A. & Margulies, D. H. Structure and function of natural killer cell receptors: multiple molecular solutions to self, nonself discrimination. *Annu. Rev. Immunol.* **20,** 853–885 (2002).
227. Yeager, M. & Hughes, A. L. Evolution of the mammalian MHC: natural selection, recombination, and convergent evolution. *Immunol. Rev.* **167,** 45–58 (1999).
228. Ichikawa, T., Itakura, T. & Negishi, M. Functional characterization of two cytochrome P-450s within the mouse, male-specific steroid 16 alpha-hydroxylase gene family: expression in mammalian cells and chimeric proteins. *Biochemistry* **28,** 4779–4784 (1989).
229. Miao, Y. J., Subramaniam, N. & Carlson, D. M. cDNA cloning and characterization of rat salivary glycoproteins. Novel members of the proline-rich-protein multigene families. *Eur. J. Biochem.* **228,** 343–350 (1995).
230. Whelan, S., Lio, P. & Goldman, N. Molecular phylogenetics: state-of-the-art methods for looking into the past. *Trends Genet.* **17,** 262–272 (2001).
231. Taveré, S. Some probabilistic and statistical problems on the analysis of DNA sequences. *Lec. Math. Life Sci.* **17,** 57–86 (1986).
232. Jareborg, N., Birney, E. & Durbin, R. Comparative analysis of noncoding regions of 77 orthologous mouse and human gene pairs. *Genome Res.* **9,** 815–824 (1999).
233. Suzuki, Y. *et al.* Diverse transcriptional initiation revealed by fine, large-scale mapping of mRNA start sites. *EMBO Rep.* **2,** 388–393 (2001).
234. Kozak, M. Do the 5′ untranslated domains of human cDNAs challenge the rules for initiation of translation (or is it vice versa)? *Genomics* **70,** 396–406 (2000).
235. Zhao, J., Hyman, L. & Moore, C. Formation of mRNA 3′ ends in eukaryotes: mechanism, regulation, and interrelationships with other steps in mRNA synthesis. *Microbiol. Mol. Biol. Rev.* **63,** 405–445 (1999).
236. Batzoglou, S., Pachter, L., Mesirov, J. P., Berger, B. & Lander, E. S. Human and mouse gene structure: comparative analysis and application to exon prediction. *Genome Res.* **10,** 950–958 (2000).
237. Ogata, H., Fujibuchi, W. & Kanehisa, M. The size differences among mammalian introns are due to the accumulation of small deletions. *FEBS Lett.* **390,** 99–103 (1996).
238. Burge, C. B., Padgett, R. A. & Sharp, P. A. Evolutionary fates and origins of U12-type introns. *Mol. Cell* **2,** 773–785 (1998).
239. Wasserman, W. W., Palumbo, M., Thompson, W., Fickett, J. W. & Lawrence, C. E. Human-mouse genome comparisons to locate regulatory sites. *Nature Genet.* **26,** 225–228 (2000).
240. Loots, G. G., Ovcharenko, I., Pachter, L., Dubchak, I. & Rubin, E. M. rVista for comparative sequence-based discovery of functional transcription factor binding sites. *Genome Res.* **12,** 832–839 (2002).
241. Krivan, W. & Wasserman, W. W. A predictive model for regulatory sequences directing liver-specific transcription. *Genome Res.* **11,** 1559–1566 (2001).
242. Wasserman, W. W. & Fickett, J. W. Identification of regulatory regions which confer muscle-specific gene expression. *J. Mol. Biol.* **278,** 167–181 (1998).
243. Dermitzakis, E. & Clark, A. Evolution of transcription factor binding sites in mammalian gene regulatory regions: conservation and turnover. *Mol. Biol. Evol.* **19,** 1114–1121 (2002).
244. Ooi, G. T., Hurst, K. R., Poy, M. N., Rechler, M. M. & Boisclair, Y. R. Binding of STAT5a and STAT5b to a single element resembling a gamma-interferon-activated sequence mediates the growth hormone induction of the mouse acid-labile subunit promoter in liver cells. *Mol. Endocrinol.* **12,** 675–687 (1998).
245. Suwanichkul, A., Boisclair, Y. R., Olne, R. C., Durham, S. K. & Powell, D. R. Conservation of a growth hormone-responsive promoter element in the human and mouse acid-labile subunit genes. *Endocrinology* **141,** 833–838 (2000).
246. Campbell, S. M., Rosen, J. M., Hennighausen, L. G., Strech-Jurk, U. & Sippel, A. E. Comparison of the whey acidic protein genes of the rat and mouse. *Nucleic Acids Res.* **12,** 8685–8697 (1984).
247. Dermitzakis, E. T. *et al.* Numerous potentially functional but non-genic conserved sequences on human chromosome 21. *Nature* **420,** 578–582 (2002).
248. Koop, B. F. Human and rodent DNA sequence comparisons: a mosaic model of genomic evolution. *Trends Genet.* **11,** 367–371 (1995).
249. DeBry, R. W. & Seldin, M. F. Human/mouse homology relationships. *Genomics* **33,** 337–351 (1996).
250. Gottgens, B. *et al.* Long-range comparison of human and mouse SCL loci: localized regions of sensitivity to restriction endonucleases correspond precisely with peaks of conserved noncoding sequences. *Genome Res.* **11,** 87–97 (2001).
251. Shiraishi, T. *et al.* Sequence conservation at human and mouse orthologous common fragile regions, FRA3B/FHIT and Fra14A2/Fhit. *Proc. Natl Acad. Sci. USA* **98,** 5722–5727 (2001).
252. Wilson, M. D. *et al.* Comparative analysis of the gene-dense ACHE/TFR2 region on human chromosome 7q22 with the orthologous region on mouse chromosome 5. *Nucleic Acids Res.* **29,** 1352–1365 (2001).
253. Hardison, R. C. Conserved noncoding sequences are reliable guides to regulatory elements. *Trends Genet.* **16,** 369–372 (2000).
254. Chiaromonte, F. *et al.* Association between divergence and interspersed repeats in mammalian noncoding genomic DNA. *Proc. Natl Acad. Sci. USA* **98,** 14503–14508 (2001).
255. Matassi, G., Sharp, P. M. & Gautier, C. Chromosomal location effects on gene sequence evolution in mammals. *Curr. Biol.* **9,** 786–791 (1999).
256. Williams, E. J. & Hurst, L. D. The proteins of linked genes evolve at similar rates. *Nature* **407,** 900–903 (2000).
257. Chen, F. C., Vallender, E. J., Wang, H., Tzeng, C. S. & Li, W. H. Genomic divergence between human and chimpanzee estimated from large-scale alignments of genomic sequences. *J. Hered.* **92,** 481–489 (2001).
258. Lercher, M. J. & Hurst, L. D. Human SNP variability and mutation rate are higher in regions of high recombination. *Trends Genet.* **18,** 337–340 (2002).
259. Castresana, J. Genes on human chromosome 19 show extreme divergence from the mouse orthologs and a high GC content. *Nucleic Acids Res.* **30,** 1751–1756 (2002).
260. Smith, N. G. C., Webster, M. & Ellegren, H. Deterministic mutation rate variation in the human genome. *Genome Res.* **12,** 1350–1356 (2002).
261. Hardison, R. *et al.* Co-variation in frequencies of substitution, deletion, transposition and recombination during eutherian evolution. *Genome Res.* (in the press).
262. Bernardi, G. The human genome: organization and evolutionary history. *Ann. Rev. Genet.* **23,** 637–661 (1995).
263. Hurst, L. D. & Willliams, E. J. B. Covarication of GC content and the silent site substitution rate in rodents: implications for methodology and for the evolution of isochores. *Gene* **261,** 107–114 (2000).
264. Bernardi, G. Misunderstandings about isochores. Part 1. *Gene* **276,** 3–13 (2001).
265. The SNP Consortium An SNP map of the human genome generated by reduced representation shotgun sequencing. *Nature* **407,** 513–516 (2000).
266. Perry, J. & Ashworth, A. Evolutionary rate of a gene affected by chromosomal position. *Curr. Biol.* **9,** 987–989 (1999).
267. Begun, D. J. & Aquadro, C. F. Levels of naturally occurring DNA polymorphism correlate with recombination rates in *D. melanogaster*. *Nature* **356,** 519–520 (1992).
268. Nachman, M. W. Single nucleotide polymorphisms and recombination rate in humans. *Trends Genet.* **17,** 481–485 (2001).
269. Kong, A. *et al.* A high-resolution recombination map of the human genome. *Nature Genet.* **31,** 241–247 (2002).
270. Charlesworth, B. The effect of background selection against deleterious mutations on weakly selected, linked variants. *Genet. Res.* **63,** 213–227 (1994).
271. Hudson, R. R. & Kaplan, N. L. Deleterious background selection with recombination. *Genetics* **141,** 1605–1617 (1995).
272. Maynard Smith, J. & Haigh, J. The hitch-hiking effect of a favourable gene. *Genet. Res.* **23,** 23–35 (1974).
273. Birky, C. W. & Walsh, J. B. Effects of linkage on rates of molecular evolution. *Proc. Natl Acad. Sci. USA* **85,** 6414–6418 (1988).
274. Francino, M. P. & Ochman, H. Strand asymmetries in DNA evolution. *Trends Genet.* **13,** 240–245 (1997).


  

275. Gilbert, N., Lutz-Prigge, S. & Moran, J. Genomic deletions created upon LINE-1 retrotransposition. *Cell* **110,** 315–325 (2002).
276. Symer, D. *et al.* Human l1 retrotransposition is associated with genetic instability *in vivo*. *Cell* **110,** 327–338 (2002).
277. Moran, J. *et al.* High frequency retrotransposition in cultured mammalian cells. *Cell* **87,** 917–927 (1996).
278. Hughes, J. F. & Coffin, J. M. Evidence for genomic rearrangements mediated by human endogenous retroviruses during primate evolution. *Nature Genet.* **29,** 487–489 (2001).
279. Wolfe, K. H. Mammalian DNA replication: mutation biases and the mutation rate. *J. Theor. Biol.* **149,** 441–451 (1991).
280. Gu, X. & Li, W. H. A model for the correlation of mutation rate with GC content and the origin of GC-rich isochores. *J. Mol. Evol.* **38,** 468–475 (1994).
281. Gabriel, S. B. *et al.* The structure of haplotype blocks in the human genome. *Science* **296,** 2225–2229 (2002).
282. Lindblad-Toh, K. *et al.* Large-scale discovery and genotyping of single-nucleotide polymorphisms in the mouse. *Nature Genet.* **24,** 381–386 (2000).
283. Wade, C. M. *et al.* The mosaic structure of variation in the laboratory mouse genome. *Nature* **420,** 574–578 (2002).
284. Loftus, S. K. *et al.* Mutation of melanosome protein RAB38 in chocolate mice. *Proc. Natl Acad. Sci. USA* **99,** 4471–4476 (2002).
285. Paigen, K. & Eppig, J. T. A mouse phenome project. *Mamm. Genome* **11,** 715–717 (2000).
286. Doerge, R. W. Mapping and analysis of quantitative trait loci in experimental populations. *Nature Rev. Genet.* **3,** 43–52 (2002).
287. Cormier, R. T. *et al.* The Mom1AKR intestinal tumour resistance region consists of Pla2g2a and a locus distal to D4Mit64. *Oncogene* **19,** 3182–3192 (2000).
288. Mei, R. *et al.* Genome-wide detection of allelic imbalance using human SNPs and high- density DNA arrays. *Genome Res.* **10,** 1126–1137 (2000).
289. Lindblad-Toh, K. *et al.* Loss-of-heterozygosity analysis of small-cell lung carcinomas using single-nucleotide polymorphism arrays. *Nature Biotechnol.* **18,** 1001–1005 (2000).
290. Heiskanen, M. *et al.* CGH, cDNA and tissue microarray analyses implicate FGFR2 amplification in a small subset of breast tumors. *Anal. Cell Pathol.* **22,** 229–234 (2001).
291. Cai, W. W. *et al.* Genome-wide detection of chromosomal imbalances in tumors using BAC microarrays. *Nature Biotechnol.* **20,** 393–396 (2002).
292. Davies, H. *et al.* Mutations of the *BRAF* gene in human cancer. *Nature* **417,** 949–954 (2002).
293. Mikkers, H. *et al.* High-throughput retroviral tagging to identify components of specific signaling pathways in cancer. *Nature Genet.* **32,** 153–159 (2002).
294. Hwang, H. C. *et al.* Identification of oncogenes collaborating with p27Kip1 loss by insertional mutagenesis and high-throughput insertion site analysis. *Proc. Natl Acad. Sci. USA* **99,** 11293–11298 (2002).
295. Lund, A. *et al.* Genome-wide retroviral insertional tagging of genes involved in cancer in Cdkn2a-deficient mice. *Nature Genet.* **32,** 160–165 (2002).
296. Janne, P. A. *et al.* Functional overlap between murine Inpp5b and Ocrl1 may explain why deficiency of the murine ortholog for OCRL1 does not cause Lowe syndrome in mice. *J. Clin. Invest.* **101,** 2042–2053 (1998).
297. Saitou, N. & Nei, M. The neighbour-joining method: a new method for reconstructing phylogenetic trees. *Mol. Biol. Evol.* **4,** 406–425 (1987).
298. Sokal, R. & Rohlf, F. *Biometry: The Principles and Practice of Statistics in Biological Research* (Freeman, New York, 1995).
299. Sutton, K. A. & Wilkinson, M. F. Rapid evolution of a homeodomain: evidence for positive selection. *J. Mol. Evol.* **45,** 579–588 (1997).
300. Kasper, S. & Matusik, R. J. Rat probasin: structure and function of an outlier lipocalin. *Biochim. Biophys. Acta* **1482,** 249–258 (2000).
301. Briand, L. *et al.* Odorant and pheromone binding by aphrodisin, a hamster aphrodisiac protein. *FEBS Lett.* **476,** 179–185 (2000).
302. Gow, A. *et al.* CNS myelin and sertoli cell tight junction strands are absent in Osp/claudin-11 null mice. *Cell* **99,** 649–659 (1999).
303. Kollmar, R., Nakamura, S. K., Kappler, J. A. & Hudspeth, A. J. Expression and phylogeny of claudins in vertebrate primordia. *Proc. Natl Acad. Sci. USA* **98,** 10196–10201 (2001).
304. Ashcroft, G. S. *et al.* Secretory leukocyte protease inhibitor mediates non-redundant functions necessary for normal wound healing. *Nature Med.* **6,** 1147–1153 (2000).
305. Henderson, C. J., Bammler, T. & Wolf, C. R. Deduced amino acid sequence of a murine cytochrome P-450 Cyp4a protein: developmental and hormonal regulation in liver and kidney. *Biochim. Biophys. Acta.* **1200,** 182–190 (1994).
306. Simpson, A. E. The cytochrome P450 4 (CYP4) family. *Gen. Pharmacol.* **28,** 351–359 (1997).
307. Sundseth, S. S. & Waxman, D. J. Sex-dependent expression and clofibrate inducibility of cytochrome P450 4A fatty acid omega-hydroxylases. Male specificity of liver and kidney CYP4A2 mRNA and tissue-specific regulation by growth hormone and testosterone. *J. Biol. Chem.* **267,** 3915–3921 (1992).
308. Myal, Y. *et al.* Tissue-specific androgen-inhibited gene expression of a submaxillary gland protein, a rodent homolog of the human prolactin-inducible protein/GCDFP-15 gene. *Endocrinology* **135,** 1605–1610 (1994).
309. Huang, Y. H., Chu, S. T. & Chen, Y. H. Seminal vesicle autoantigen, a novel phospholipid-binding protein secreted from luminal epithelium of mouse seminal vesicle, exhibits the ability to suppress mouse sperm motility. *Biochem. J.* **343,** 241–248 (1999).
310. Ann, D. K., Smith, M. K. & Carlson, D. M. Molecular evolution of the mouse proline-rich protein multigene family. Insertion of a long interspersed repeated DNA element. *J. Biol. Chem.* **263,** 10887–10893 (1988).
311. Rosinski-Chupin, I. & Rougeon, F. A new member of the glutamine-rich protein gene family is characterized by the absence of internal repeats and the androgen control of its expression in the submandibular gland of rats. *J. Biol. Chem.* **265,** 10709–10713 (1990).
312. Rajkovic, A., Yan, C., Yan, W., Klysik, M. & Matzuk, M. M. Obox, a family of homeobox genes preferentially expressed in germ cells. *Genomics* **79,** 711–717 (2002).
313. Talley, H. M., Laukaitis, C. M. & Karn, R. C. Female preference for male saliva: implications for sexual isolation of *Mus musculus* subspecies. *Evol. Int. J. Org. Evol.* **55,** 631–634 (2001).
314. Dlouhy, S. R., Taylor, B. A. & Karn, R. C. The genes for mouse salivary androgen-binding protein (ABP) subunits alpha and gamma are located on chromosome 7. *Genetics* **115,** 535–543 (1987).
315. Jia, H. P. *et al.* A novel murine beta-defensin expressed in tongue, esophagus, and trachea. *J. Biol. Chem.* **275,** 33314–33320 (2000).
316. Peters, J. Nonspecific esterases of *Mus musculus*. *Biochem. Genet.* **20,** 585–606 (1982).
317. Abou-Haila, A., Orgebin-Crist, M. C., Skudlarek, M. D. & Tulsiani, D. R. Identification and androgen regulation of egasyn in the mouse epididymis. *Biochim. Biophys. Acta.* **1401,** 177–186 (1998).
318. Lin, J., Toft, D. J., Bengtson, N. W. & Linzer, D. I. Placental prolactins and the physiology of pregnancy. *Recent Prog. Horm. Res.* **55,** 37–51 (2000).
319. Goffin, V., Binart, N., Touraine, P. & Kelly, P. A. Prolactin: the new biology of an old hormone. *Annu. Rev. Physiol.* **64,** 47–67 (2002).
320. Batten, D., Dyer, K. D., Domachowske, J. B. & Rosenberg, H. F. Molecular cloning of four novel murine ribonuclease genes: unusual expansion within the ribonuclease A gene family. *Nucleic Acids Res.* **25,** 4235–4239 (1997).
321. Cormier, S. A. *et al.* Mouse eosinophil-associated ribonucleases: a unique subfamily expressed during hematopoiesis. *Mamm. Genome* **12,** 352–361 (2001).
322. Tsui, F. W. *et al.* Molecular characterization and mapping of murine genes encoding three members of the stefin family of cysteine proteinase inhibitors. *Genomics* **15,** 507–514 (1993).
323. Parham, P. Virtual reality in the MHC. *Immunol. Rev.* **167,** 5–15 (1999).
324. Ning, Z., Cox, A. J. & Mullikin, J. C. SSAHA: a fast search method for large DNA databases. *Genome Res.* **11,** 1725–1729 (2001).
325. Flicek, P. *et al.* Leveraging the mouse genome for gene prediction in human: From the whole-genome shotgun reads to a global synteny map. *Genome Res.* (in the press).
326. Parra, G. *et al.* Comparative gene prediction in human and mouse. *Genome Res.* (in the press).
327. Guigó, R. *et al.* Comparison of mouse and human genomes followed by experimental verification yields an estimated 1,019 additional genes. *Proc. Natl Acad. Sci. USA* (in the press).
328. Schwartz, S. *et al.* Human-mouse alignments with Blastz. *Genome Res.* (in the press).
329. Elnitski, L. *et al.* Distinguishing regulatory DNA from neutral sites. *Genome Res.* (in the press).
330. Roskin, K. M. Score Functions for Assessing Conservation in Locally Aligned Regions of DNA from Two Species. UCSC Tech Report UCSC-CRL-02-30, School of Engineering, Univ. California (2002).


**Supplementary Information** accompanies the paper on *Nature*'s website (http://www.nature.com/nature).

**Acknowledgements** We thank J. Takahashi and M. Johnston for comments on the manuscript; the Mouse Liaison Group for strategic advice; L. Gaffney, D. Leja and K.-S. Toh for graphical help; B. Graham and G. Roberts for administrative work on sequencing of individual mouse BACs; and P. Kassos and M. McMurtry for secretarial assistance. We thank D. Hill and L. Corbani of the Mouse Genome Informatics Group for their contributions to the GO analysis for mouse and human, and the members of the Bork group at EMBL for discussions. Funding was provided by the National Institutes of Health (National Human Genome Research Institute, National Cancer Institute, National Institute of Dental and Craniofacial Research, National Institute of Diabetes and Digestive and Kidney Diseases, National Institute of General Medical Sciences, National Eye Institute, National Institute of Environmental Health Sciences, National Institute of Aging, National Institute of Arthritis and Musculoskeletal and Skin Diseases, National Institute on Deafness and Other Communication Disorders, National Institute of Mental Health, National Institute on Drug Abuse, National Center for Research Resources, the National Heart Lung and Blood Institute and The Fogarty International Center); the Wellcome Trust; the Howard Hughes Medical Institute; the United States Department of Energy; the National Science Foundation; the Medical Research Council; NSERC; BMBF (German Ministry for Research and Education); the European Molecular Biology Laboratory; Plan Nacional de I+D and Instituto Carlos III; Swiss National Science Foundation, NCCR Frontiers in Genetics, the Swiss Cancer League and the 'Childcare' and 'J. Lejeune' Foundations; and the Ministry of Education, Culture, Sports, Science and Technology of Japan. The initial threefold sequence coverage was partly supported by the Mouse Sequencing Consortium (GlaxoSmithKline, Merck and Affymetrix) through the Foundation for the National Institutes of Health. We acknowledge A. Holden for coordinating the Mouse Sequencing Consortium. We thank the Sanger Institute systems group for maintenance and provision of the computer resource. The MGSC also used Hewlett-Packard Company's BioCluster, a configuration of 27 HP AlphaServer ES40 systems with 100 CPUs and 1 terabyte of storage. The BioCluster is housed in Hewlett-Packard's IQ Solutions Center, and was accessed remotely. The computing resource greatly accelerated the analysis.

**Competing interests statement** The authors declare that they have no competing financial interests.

**Correspondence** and requests for materials should be addressed to R.H.W. (e-mail: waterston@gs.washington.edu), K.L.T. (e-mail: kersli@genome.wi.mit.edu) or E.S.L. (e-mail: lander@genome.wi.mit.edu).

**Authors' contributions** The following authors contributed to project leadership: R. H. Waterston, K. Lindblad-Toh, E. Birney, J. Rogers, M. R. Brent, F. S. Collins, R. Guigó, R. C. Hardison, D. Haussler, D. B. Jaffe, W. J. Kent, W. Miller, C. P. Ponting, A. Smit, M. C. Zody and E. S. Lander.

  

articles

**Robert H. Waterston[1]*, Kerstin Lindblad-Toh[2]*, Ewan Birney[3]*, Jane Rogers[4], Josep F. Abril[5]*, Pankaj Agarwal[6]*, Richa Agarwala[7], Rachel Ainscough[4], Marina Alexandersson[8]*, Peter An[2], Stylianos E. Antonarakis[9]*, John Attwood[4], Robert Baertsch[10]*, Jonathon Bailey[4], Karen Barlow[4], Stephan Beck[4], Eric Berry[2]*, Bruce Birren[2], Toby Bloom[2], Peer Bork[11]*, Marc Botcherby[12], Nicolas Bray[13]*, Michael R. Brent[14]*, Daniel G. Brown[2,15]*, Stephen D. Brown[12], Carol Bult[16]*, John Burton[4], Jonathan Butler[2]*, Robert D. Campbell[12], Piero Carninci[17], Simon Cawley[18]*, Francesca Chiaromonte[19]*, Asif T. Chinwalla[1]*, Deanna M. Church[7]*, Michele Clamp[4]*, Christopher Clee[4], Francis S. Collins[20]*, Lisa L. Cook[1], Richard R. Copley[21]*, Alan Coulson[4], Olivier Couronne[13]*, James Cuff[2]*, Val Curwen[4]*, Tim Cutts[4]*, Mark Daly[2]*, Robert David[2], Joy Davies[4], Kimberly D. Delehaunty[1], Justin Deri[2], Emmanouil T. Dermitzakis[9]*, Colin Dewey[22]*, Nicholas J. Dickens[23]*, Mark Diekhans[10]*, Sheila Dodge[2], Inna Dubchak[13]*, Diane M. Dunn[24], Sean R. Eddy[25]*, Laura Elnitski[26]*, Richard D. Emes[23]*, Pallavi Eswara[27]*, Eduardo Eyras[4]*, Adam Felsenfeld[20]*, Ginger A. Fewell[1], Paul Flicek[14]*, Karen Foley[2], Wayne N. Frankel[16]*, Lucinda A. Fulton[1]*, Robert S. Fulton[1], Terrence S. Furey[10]*, Diane Gage[2], Richard A. Gibbs[28], Gustavo Glusman[29]*, Sante Gnerre[2]*, Nick Goldman[3]*, Leo Goodstadt[23]*, Darren Grafham[4], Tina A. Graves[1], Eric D. Green[30]*, Simon Gregory[4]*, Roderic Guigó[5]*, Mark Guyer[20], Ross C. Hardison[31]*, David Haussler[32]*, Yoshihide Hayashizaki[17], LaDeana W. Hillier[1]*, Angela Hinrichs[10]*, Wratko Hlavina[7]*, Timothy Holzer[2], Fan Hsu[10]*, Axin Hua[33], Tim Hubbard[4]*, Adrienne Hunt[4], Ian Jackson[12], David B. Jaffe[2]*, L. Steven Johnson[25], Matthew Jones[4], Thomas A. Jones[25], Ann Joy[4], Michael Kamal[2]*, Elinor K. Karlsson[2]*, Donna Karolchik[10]*, Arkadiusz Kasprzyk[3]*, Jun Kawai[17], Evan Keibler[14]*, Cristyn Kells[2], W. James Kent[10]*, Andrew Kirby[2]*, Diana L. Kolbe[26]*, Ian Korf[14]*, Raju S. Kucherlapati[34], Edward J. Kulbokas III[2]*, David Kulp[18]*, Tom Landers[2], J. P. Leger[2], Steven Leonard[4], Ivica Letunic[11]*, Rosie Levine[2], Jia Li[35]*, Ming Li[36]*, Christine Lloyd[4], Susan Lucas[37], Bin Ma[38]*, Donna R. Maglott[7]*, Elaine R. Mardis[1], Lucy Matthews[4], Evan Mauceli[2]*, John H. Mayer[2], Megan McCarthy[2], W. Richard McCombie[39], Stuart McLaren[4], Kirsten McLay[4], John D. McPherson[1], Jim Meldrim[2], Beverley Meredith[4], Jill P. Mesirov[2]*, Webb Miller[27]*, Tracie L. Miner[1], Emmanuel Mongin[3], Kate T. Montgomery[34], Michael Morgan[40], Richard Mott[21]*, James C. Mullikin[4]*, Donna M. Muzny[28], William E. Nash[1], Joanne O. Nelson[1], Michael N. Nhan[1], Robert Nicol[2], Zemin Ning[4]*, Chad Nusbaum[2], Michael J. O'Connor[27], Yasushi Okazaki[17], Karen Oliver[4], Emma Overton-Larty[4], Lior Pachter[6]*, Genís Parra[5]*, Kymberlie H. Pepin[1], Jane Peterson[20], Pavel Pevzner[41]*, Robert Plumb[4], Craig S. Pohl[1], Alex Poliakov[13]*, Tracy C. Ponce[1], Chris P. Ponting[23]*, Simon Potter[4]*, Michael Quail[4], Alexandre Reymond[9]*, Bruce A. Roe[33], Krishna M. Roskin[10]*, Edward M. Rubin[13], Alistair G. Rust[3], Ralph Santos[2], Victor Sapojnikov[7]*, Brian Schultz[1], Jörg Schultz[42]*, Matthias S. Schwartz[10]*, Scott Schwartz[27]*, Carol Scott[4], Steven Seaman[2], Steve Searle[4]*, Ted Sharpe[2], Andrew Sheridan[2], Ratna Shownkeen[4], Sarah Sims[4], Jonathan B. Singer[2]*, Guy Slater[3]*, Arian Smit[29]*, Douglas R. Smith[43], Brian Spencer[2], Arne Stabenau[3]*, Nicole Stange-Thomann[2], Charles Sugnet[10]*, Mikita Suyama[11]*, Glenn Tesler[41]*, Johanna Thompson[1], David Torrents[11]*, Evanne Trevaskis[1], John Tromp[44]*, Catherine Ucla[5]*, Abel Ureta-Vidal[3], Jade P. Vinson[2]*, Andrew C. von Niederhausern[24], Claire M. Wade[2]*, Melanie Wall[4], Ryan J. Weber[10]*, Robert B. Weiss[24], Michael C. Wendl[1], Anthony P. West[4], Kris Wetterstrand[20], Raymond Wheeler[18]*, Simon Whelan[3]*, Jamey Wierzbowski[2], David Willey[4], Sophie Williams[4], Richard K. Wilson[1], Eitan Winter[23]*, Kim C. Worley[45]*, Dudley Wyman[2], Shan Yang[31], Shiaw-Pyng Yang[1]*, Evgeny M. Zdobnov[11]*, Michael C. Zody[2]* & Eric S. Lander[2,46]***

*Affiliations for authors: 1, Genome Sequencing Center, Washington University School of Medicine, Campus Box 8501, 4444 Forest Park Avenue, St Louis, Missouri 63108, USA; 2, Whitehead Institute/MIT Center for Genome Research, 320 Charles Street, Cambridge, Massachusetts 02141, USA; 3, European Bioinformatics Institute, Wellcome Trust Genome Campus, Hinxton, Cambridge CB10 1SD, UK; 4, Wellcome Trust Sanger Institute, Wellcome Trust Genome Campus, Hinxton, Cambridge CB10 1SA, UK; 5, Research Group in Biomedical Informatics, Institut Municipal d'Investigacio, Medica/Universitat Pompeu Fabra, Centre de Regulacio Genomica, Barcelona, Catalonia, Spain; 6, Bioinformatics, GlaxoSmithKline, UW2230, 709 Swedeland Road, King of Prussia, Pennsylvania 19406, USA; 7, National Center for Biotechnology Information, National Institutes of Health, Bethesda, Maryland 20892, USA; 8, Department of Mathematics, University of California at Berkeley, 970 Evans Hall, Berkeley, California 94720, USA; 9, Division of Medical Genetics, University of Geneva Medical School, 1 rue Michel-Servet, CH-1211 Geneva, Switzerland; 10, Center for Biomolecular Science and Engineering, University of California, Santa Cruz, California 95064, USA; 11, EMBL, Meyerhofstrasse 1, Heidelberg 69117, Germany; 12, UK MRC Mouse Sequencing Consortium, MRC Mammalian Genetics Unit, Harwell OX11 0RD, UK; 13, Lawrence Berkeley National Laboratory, 1 Cyclotron Road, Mailstop 84-171, Berkeley, California 94720, USA; 14, Department of Computer Science, Washington University, Box 1045, St Louis, Missouri 63130, USA; 15, School of Computer Science, University of Waterloo, Waterloo, Ontario N2L 3G1, Canada; 16, The Jackson Laboratory, 600 Main Street, Bar Harbor, Maine 04609, USA; 17, Laboratory for Genome Exploration, RIKEN Genomic Sciences Center, Yokohama Institute, 1-7-22 Suchiro-cho, Tsurumi-ku, Yokohama, Kanagawa 230-0045, Japan; 18, Affymetrix Inc., Emeryville, California 94608, USA; 19, Departments of Statistics and Health Evaluation Sciences, The Pennsylvania State University, University Park, Pennsylvania 16802, USA; 20, National Human Genome Research Institute, National Institutes of Health, 31 Center Drive, Room 4B09, Bethesda, Maryland 20892, USA; 21, Wellcome Trust Centre for Human Genetics, University of Oxford, Roosevelt Drive, Oxford OX3 7BN, UK; 22, Department of Electrical Engineering, University of California, Berkeley, 231 Cory Hall, Berkeley, California 94720, USA; 23, Department of Human Anatomy and Genetics, MRC Functional Genetics Unit, University of Oxford, South Parks Road, Oxford OX1 3QX, UK; 24, Department of Human Genetics, University of Utah, Salt Lake City, Utah 84112, USA; 25, Howard Hughes Medical Institute and Department of Genetics, Washington University School of Medicine, St Louis, Missouri 63110, USA; 26, Departments of Biochemistry and Molecular Biology and Computer Science and Engineering, The Pennsylvania State University, University Park, Pennsylvania 16802, USA; 27, Department of Computer Science and Engineering, The Pennsylvania State University, University Park, Pennsylvania 16802, USA; 28, Baylor College of Medicine, Human Genome Sequencing Center, One Baylor Plaza, MSC-226, Houston, Texas 77030, USA; 29, The Institute for Systems Biology, 1441 North 34th Street, Seattle, Washington 98103, USA; 30, National Human Genome Research Institute, National Institutes of Health, 50 South Drive, Building 50, Room 5523, Bethesda, Maryland 20892, USA; 31, Department of Biochemistry and Molecular Biology, The Pennsylvania State University, University Park, Pennsylvania 16802, USA; 32, Howard Hughes Medical Institute, University of California, Santa Cruz, California 95064, USA; 33, Department of Chemistry and Biochemistry, University of Oklahoma Advanced Center for Genome Technology, University of Oklahoma, 620 Parrington Oval, Room 311, Norman, Oklahoma 73019, USA; 34, Departments of Genetics and Medicine and Harvard-Partners Center for Genetics and Genomics, Harvard Medical School, Boston, Massachusetts 02115, USA; 35, Department of Statistics, The Pennsylvania State University, University Park, Pennsylvania 16802, USA; 36, Department of Computer Science, University of California, Santa Barbara, California 93106, USA; 37, US DOE Joint Genome Institute, 2800 Mitchell Drive, Walnut Creek, California 94598, USA; 38, Department of Computer Science, University of Western Ontario, London, Ontario N6A 5B7, Canada; 39, Cold Spring Harbor Laboratory, PO Box 100, 1 Bungtown Road, Cold Spring Harbor, New York 11724, USA; 40, Wellcome Trust, 183 Euston Road, London NW1 2BE, UK; 41, Department of Computer Science and Engineering, University of California, San Diego, 9500 Gilman Drive, La Jolla, California 92093-0114, USA; 42, Max Planck Institute for Molecular Genetics, Ihnestrasse 73, 14195 Berlin, Germany; 43, Genome Therapeutics Corporation, 100 Beaver Street, Waltham, Massachusetts 02453, USA; 44, Bioinformatics Solutions Inc., 145 Columbia Street W, Waterloo, Ontario N2L 3L2, Canada; 45, Department of Molecular and Human Genetics, Baylor College of Medicine, Mailstop BCM226, Room 1419.01, One Baylor Plaza, Houston, Texas 77030, USA; 46, Department of Biology, Massachusetts Institute of Technology, Cambridge, Massachusetts 02138, USA*
** Members of the Mouse Genome Analysis Group*

  

## 3.3 Validation of Results from Gene Predictors

Annotations from computational gene-finding can be seen as hypotheses about given loci in a genomic sequence encoding cellular functions. Therefore, we initially need to test one of such tools against a controlled data set of reliable annotations to determine its performance. On the other hand, evaluation of predicted genes will be part of the parameters estimation for such software. An iterative procedure may test different program settings under a fixed control set of training sequences in order to determine the parameters that give the best results.

### 3.3.1 Measures of gene prediction accuracy

To evaluate the accuracy of a gene prediction program, the gene structure predicted by the program is compared with the structure of the actual gene encoded in the problem sequence. As extensively discussed in Burset and Guigó [1996], the accuracy can be evaluated at three different levels of resolution: the nucleotide, exon, and gene levels. These levels offer complementary views of the accuracy of the program. At each level, there are two basic measures: sensitivity and specificity. Briefly, sensitivity ($Sn$) is the proportion of real elements (coding nucleotides, exons or genes) that have been correctly predicted, while specificity ($Sp$) is the proportion of predicted elements that are correct. More specifically, if true positive ($TP$) is the total number of coding elements correctly predicted; true negative ($TN$), the number of correctly predicted non-coding elements; false positive ($FP$) the number of non-coding elements predicted as coding; and false negative ($FN$) the number of coding elements predicted as non-coding. Then, in the gene finding literature, $Sn$ is defined as:

$$Sn = \frac{TP}{TP + FN} \quad ,$$

and $Sp$ as:

$$Sp = \frac{TP}{TP + FP} \quad .$$

Both $Sn$ and $Sp$ take values from 0 to 1, with perfect prediction when both measures are equal to 1. Neither $Sn$ nor $Sp$ alone constitute good measures of global accuracy, since high sensitivity can be reached with low specificity and vice versa. It is desirable to use a single measure for accuracy. In gene finding literature, the preferred such measure at the nucleotide level is the Correlation Coefficient ($CC$), which is defined as:

$$CC = \frac{(TP \times TN) - (FN \times FP)}{\sqrt{(TP + FN) \times (TN + FP) \times (TP + FP) \times (TN + FN)}} \quad ,$$

and ranges from -1 to 1, with 1 corresponding to a perfect prediction, and -1 to a prediction in which each coding nucleotide is predicted as non-coding and vice versa.

At exon level, these measures determine if predictions correspond to real exons, with the exon boundaries perfectly predicted. The prediction is considered incorrect if only a

single base does not correspond to the coordinates of the real exon. Therefore, $Sn$ at exon level measures the proportion of actual exons that have been correctly predicted, and $Sp$ measures the proportion of predicted exons that correspond to actual exons. The average exon prediction accuracy $SnSp$ is computed as:

$$SnSp = \frac{Sn + Sp}{2} \quad .$$

Apart from $Sn$, $Sp$ and $SnSp$, two extra measures are used to determine the accuracy at exon level: the missed exons ($ME$) and the wrong exons ($WE$). $ME$ measures how frequently a predictor completely failed to identify exons (no prediction overlap at all) whereas $WE$ identifies the ratio of exons that do not overlap with any exon of the training data set.

At gene level $Sn$ and $Sp$ measure if a predictor is able to correctly identify and assemble all of the exons of a gene. For a prediction to be counted as $TP$, all coding exons must be identified, every intron-exon boundary must match exactly, and all the exons must be included in the right gene. In addition, missed genes ($MG$) and wrong genes ($WG$) can also be computed in the same way as at the exon level.

The exon level scores discussed above measure how well a predictor recognizes exons and gets their boundaries exactly correct. The gene level scores measure how well a predictor can recognize exons and assemble them into complete genes. In general, gene finders predict the initial and terminal exons very poorly. This often leads to so-called chimeric predictions—one predicted gene encompassing more than one real gene—or to split predictions—where one real gene split in multiple predicted genes. Reese *et al.* [2000] developed two measures to account for these tendencies: split genes ($SG$) and joined genes ($JG$). $SG$ is the total number of predicted genes overlapping real genes divided by the number of genes that were split. Similarly, $JG$ is the total number of real genes that overlap predicted genes divided by the number of predicted genes that were joined. A score of 1 is perfect and means that each of the genes from the real genes set overlaps exactly one gene from the set of predicted genes.

### 3.3.2 Evaluating computational gene-finding results

The evaluations by Burset and Guigó [1996], Rogic *et al.* [2001], and others suffered from the same limitation: gene finders were tested in controlled data sets made of short genomic sequences encoding a single gene with a simple gene structure. These datasets are not representative of the genome sequences that are currently being produced: large sequences of low coding density, encoding several genes and/or incomplete genes, with complex gene structures. This was addressed in the acompanying research article in section 3.3.3, page 54. Table 3.2 on page 56 (Table 1 on page 1632 of Guigó *et al.* 2000) summarizes the results of different gene finding tools in a set of single gene sequences.

The Genome Annotation Assessment Project (GASP) was the first attempt to test the available gene-prediction tools with a well annotated genomic sequence. The 2.9 Mb *Adh* region from *Drosophila melanogaster* was chosen to provide both curated training datasets for the programs and a set of curated annotations to evaluate predictions with them. Table 3.4 on page 79 (Table 3 on page 494 of Reese *et al.* 2000) sums up the results of the gene-finding tools that were evaluated in this experiment.

Table 3.1 on page 27 (Table 4 on page 114 of Parra *et al*. 2003) reports the accuracy of gene-finding programs, including `geneid` and `SGP2`, on human chromosome 22. For the human and mouse comparative analysis we ended up with lots of tables taking into account results for each chromosome sequence and each program, and the evaluations were made with different reference annotation sets. The box-plots shown on Figure 3.5, page 28 (Figure 3 on page 115 of Parra *et al*. 2003), illustrate the differences between gene-finding tools better. This graphical representation provides a compact summary of the different measures being compared, but also shows the dispersion distribution of the data and the outliers. One of the most interesting outliers in the human-mouse analysis was chromosome Y, for which the comparative gene-finding approaches were yielding results similar to those of the "*ab initio*" tools. Of course, this was a result of the lack of orthologous sequences between human and mouse, because for the rodent only female DNA samples were used for sequencing.

In Guigó *et al*. [2003], a protocol for selecting computational predictions to be tested by experimental means, via RT-PCR in this case, is described. `SGP2` results from the gene prediction pipeline, detailed in section 3.2, were classified into three groups in function of the homolgy between the human and mouse predictions and the conservation of their exonic structures. Table 3.5 on page 92 (Table 1 on page 1143 of Guigó *et al*. 2003) sumarizes the RT-PCR success rate within each of those groups. Figure 3.6 on page 39 (Figure 16 on page 540 of Waterston *et al*. 2002) shows the structures, side by side, of a human and mouse predicted new homologue of *dystrophin*, for which an exon pair from the mouse gene was verified by RT-PCR. Another example, a novel homolog to *Drosophila melanogaster* brain-specific homeobox protein, can be found on Figure 3.8, page 91, for which the primers and RT-PCR results are depicted on the same page in Figure 3.9 (Figures 2 and 3 on page 1142 respectively, of Guigó *et al*. 2003). A database was built for the 476 gene structures that were tested by RT-PCR. It contains not only the sequences and coresponding annotations for those genes, but also the results yielded from each RT-PCR test done in 12 different mouse tissues. Figure 3.10 on page 95 shows the web interface we have created for that database.

All results indicate that there is room for improvement in the computational gene prediction field. Efforts to provide more accurate gene-finding tools, as well as more reliable annotations, are ongoing. The best example of such efforts is the ENCODE project [ENCODE Project Consortium, 2004]. During its pilot phase, the procedures that can be applied cost-effectively and at high-throughput to accurately and comprehensively characterize large sequences, will be evaluated.

### 3.3.3 Guigó *et al*, *Genome Research*, 10(10):1631–1642, 2000

**PubMed Accession:**

http://www.ncbi.nlm.nih.gov/entrez/query.fcgi?cmd=Retrieve&db=PubMed&list_uids=11042160&dopt=Abstract

**Journal Abstract:**

http://www.genome.org/cgi/content/abstract/10/10/1631

**Supplementary Materials:**

http://genome.imim.es/datasets/gpeval2000/

**Methods**

# An Assessment of Gene Prediction Accuracy in Large DNA Sequences

Roderic Guigó,[1,3] Pankaj Agarwal,[2] Josep F. Abril,[1] Moisés Burset,[1] and James W. Fickett[2]

*[1]Grup de Recerca en Informática Mèdica, Institut Municipal d'Investigació Mèdica, Universitat Pompeu Fabra, E-08003 Barcelona, Spain; [2]Department of Bioinformatics, SmithKline Beecham Pharmaceuticals Research and Development, King of Prussia, Pennsylvania 19406, USA*

**One of the first useful products from the human genome will be a set of predicted genes. Besides its intrinsic scientific interest, the accuracy and completeness of this data set is of considerable importance for human health and medicine. Though progress has been made on computational gene identification in terms of both methods and accuracy evaluation measures, most of the sequence sets in which the programs are tested are short genomic sequences, and there is concern that these accuracy measures may not extrapolate well to larger, more challenging data sets. Given the absence of experimentally verified large genomic data sets, we constructed a semiartificial test set comprising a number of short single-gene genomic sequences with randomly generated intergenic regions. This test set, which should still present an easier problem than real human genomic sequence, mimics the ~200kb long BACs being sequenced. In our experiments with these longer genomic sequences, the accuracy of GENSCAN, one of the most accurate ab initio gene prediction programs, dropped significantly, although its sensitivity remained high. Conversely, the accuracy of similarity-based programs, such as GENEWISE, PROCRUSTES, and BLASTX, was not affected significantly by the presence of random intergenic sequence, but depended on the strength of the similarity to the protein homolog. As expected, the accuracy dropped if the models were built using more distant homologs, and we were able to quantitatively estimate this decline. However, the specificities of these techniques are still rather good even when the similarity is weak, which is a desirable characteristic for driving expensive follow-up experiments. Our experiments suggest that though gene prediction will improve with every new protein that is discovered and through improvements in the current set of tools, we still have a long way to go before we can decipher the precise exonic structure of every gene in the human genome using purely computational methodology.**

The nucleotide genomic sequence is the primary product of the Human Genome Project, but a major short- and mid-term interest will be the amino acid sequences of the proteins encoded in the genome. Thus, methods that reliably predict the genes encoded in genomic sequence are essential, and computational gene identification continues to be an active field of research (for reviews, see Fickett 1996; Claverie 1997; Guigó 1997a; Burge and Karlin 1998; Haussler 1998). A new generation of gene prediction programs based on Hidden Markov Models (Burge and Karlin 1997) have shown significantly greater accuracy than previous programs based on other methodologies (Burset and Guigó 1996). Conversely, as the databases of known coding sequences increase in size, gene prediction methods based on sequence similarity to coding sequences, mainly proteins and ESTs, are becoming increasingly useful and are routinely used to identify putative genes in genomic sequences (The *C. elegans* Sequencing Consortium 1998). We have recently published an evaluation of sequence similarity-based gene prediction methods, in particular of EST-based gene prediction (Guigó et al. 2000). The accuracy of gene identification programs, however, has usually been estimated on controlled data sets made of short genomic sequences encoding a single and complete gene with a simple structure. Moreover, these data sets are often similar if not overlapping, to the sets of sequences on which the programs have been trained. Thus, these data sets are not representative of the sequences being produced at the genome centers, which are mostly large sequences of low coding density, encoding several genes or incomplete genes with complex gene structure. It is thus difficult to know how well the figures of accuracy estimated in the controlled benchmark data sets extrapolate to actual genomic sequences. Furthermore, programs that combine both sequence similarity and ab initio gene finding approaches, and those that predict genes by producing a splicing alignment between a genomic sequence and a candidate amino acid sequence have become recently available, such as PROCRUSTES (Gelfand et al. 1996) and GENEWISE (Birney and Durbin 1997), (http://www.sanger.ac.uk/Software/Wise2/). Programs that align genomic sequences with

**[3]Corresponding author.**
**E-MAIL rguigo@imim.es; FAX 3493-221-3237.**
Article and publication are at www.genome.org/cgi/doi/10.1101/gr.122800.

EST sequences, such as EST_GENOME (Mott 1997), could also be included in this category. These programs promise highly accurate predictions, but at the cost of greater computational time. However, this increase in accuracy has not been well-quantified on challenging data sets. The effects of the degree of similarity between the candidate homolog and the genomic sequence also deserve careful evaluation.

We believe a more realistic evaluation of the currently available gene prediction tools on challenging data sets would be useful. Ideally, one would like to benchmark the computational gene identification programs in real genomic sequences. The main problem is that most real sequences the structure of the genes has not been verified exhaustively by experimental means, and thus it is impossible to calibrate the accuracy of the predictions. Only recently, extensively annotated large genomic sequences from higher eukaryotic organisms have become available from the human genome (http://www.hgmp.mrc.ac.uk/Genesafe) and from the fly genome (http://www.fruitfly.org/GASP1/). In spite of the experimental analysis, the possibility of undetected genes in the sequence cannot be easily ruled out, which makes accuracy difficult to measure. Here, we attempt to overcome the lack of well-annotated large genomic sequences by constructing semiartificial ones. In these semiartificial sequences, known genomic sequences have been embedded in simulated intergenic DNA, and therefore, the location of all coding exons is known. Although the approach may seem unrealistic, we believe that the results obtained are instructive with regard to the accuracy of currently available gene identification tools.

We evaluate the accuracy of representatives of a wide variety of computational gene identification approaches: GENSCAN (Burge and Karlin 1997), an ab initio genefinder; BLASTX (Altschul et al. 1990; Gish and States 1993), a genefinding-oriented similarity search program; and PROCRUSTES (Gelfand et al. 1996) and GENEWISE (Birney and Durbin 1997), genefinders based on aligning a genomic DNA sequence fragment to a homologous protein sequence. We evaluate these programs on two benchmark data sets: A set of well-annotated single-gene DNA sequences, and a set of semiartificial genomic (SAG) sequences created by embedding the single-gene sequences from the first data set in simulated intergenic DNA.

## RESULTS

We investigated the accuracy of the gene prediction tools (GENSCAN, PROCRUSTES, GENEWISE, BLASTX) described in Methods on two benchmark sets. In all cases, sequences were masked previously for repeated regions using REPEATMASKER (A. Smit and P. Green, unpubl.). The gene predictions obtained using the different tools were compared with the actual gene annotations using the accuracy measures described Methods.

### Accuracy in Single Gene Sequences

Table 1 shows the accuracy of the different gene prediction tools on h178, the set of single gene sequences.

GENSCAN's accuracy is comparable to that reported earlier (Burge and Karlin 1997). On average, 90% of the coding nucleotides and 70% of the exons are predicted correctly by GENSCAN. Only 7% of the actual exons are missed completely, and only 9% of the predicted exons are wrong. We believe this is close to the maximum accuracy that can be achieved using currently available ab initio gene prediction programs.

The quality of the gene models inferred from BLASTX searches depends on the strategy used. Default usage of BLASTX produced poorer predictions than more sophisticated strategies. (Results for BLASTX default correspond to those published in Guigó et al. 2000.) Discrepancies between numbers in Table 1 and those reported in Guiqoet al. (2000) are due to the differences in the way the accuracy measures are summarized. In Guigó et al. 2000, we computed the accuracy measures on each test sequence, and averaged all of them. Here, we compute the accuracy measures globally from the total number of prediction successes and failures (at the base or exon level) on all sequences. The default BLASTX strategy produces reasonably high sensitivity (0.91) by projecting all HSPs over a given threshold along the query DNA sequence, but the sensitivity rises to an amazing 0.97, if the topcomboN fea-

**Table 1.** Accuracy of Gene Prediction Tools in the Set of Single Gene Sequences (h178)

| | | Nucleotide | | | Exon | | | | |
|---|---|---|---|---|---|---|---|---|---|
| Program | No. | Sn | Sp | CC | Sn | Sp | $\frac{Sn + Sp}{2}$ | ME | WE |
| GenScan | 177 | 0.93 | 0.90 | 0.90 | 0.78 | 0.75 | 0.76 | 0.08 | 0.10 |
| Blastx default | 175 | 0.91 | 0.79 | 0.82 | 0.04 | 0.04 | 0.04 | 0.12 | 0.05 |
| Blastx topcomboN | 174 | 0.97 | 0.80 | 0.86 | 0.04 | 0.04 | 0.04 | 0.08 | 0.05 |
| Blastx 2 stages | 175 | 0.90 | 0.92 | 0.90 | 0.10 | 0.12 | 0.11 | 0.19 | 0.02 |
| GeneWise | 177 | 0.98 | 0.98 | 0.97 | 0.88 | 0.91 | 0.89 | 0.06 | 0.02 |
| Procrustes | 177 | 0.93 | 0.95 | 0.93 | 0.76 | 0.82 | 0.79 | 0.11 | 0.04 |

ture is used. The topcomboN feature eliminates the need for low-complexity filters (seg + xnu), and for strict secondary HSP cutoff (S2 threshold). Surprisingly, its use does not appear to hurt specificity. The two-stage method (in which the top homolog with low-complexity filtering is chosen to build the BLASTX model with topcomboN in the second stage) increases specificity from 0.79 to 0.92. Using a single protein to build a model improves specificity because the noise from the less significant hits is reduced. But the two stage method does have lower sensitivity from a lack of information from the weaker secondary hits. However, this is still the best purely BLASTX-based strategy in terms of either specificity or overall accuracy, and the numbers are comparable to the accuracy of ab initio gene finders at the nucleotide level.

The proteins encoded by the sequences in h178 are mostly included in the nonredundant database of amino acid sequences (*nr*). However, BLASTX still does not produce perfect predictions. This certainly has an artefactual component: We have discovered a few annotation errors in h178. However, perfect gene predictions from BLASTX searches are intrinsically impossible because of the inability of BLASTX to predict the splice boundaries when they occur within codons (this especially affects its accuracy at the exon level, which is actually rather meaningless for BLASTX). In this regard, splicing alignment or sequence similarity-based gene prediction tools (SSBGP), such as GENEWISE and PROCRUSTES could, in principle, result in more accurate predictions. Thus, the protein sequence with the lowest *P* value after the BLASTX search was given to PROCRUSTES and GENEWISE to model their gene predictions. SSBGP tools improved the accuracy of the gene predictions inferred directly from BLASTX searches, and also slightly outperform GENSCAN in this set. GENEWISE predictions with an overall accuracy of 0.97, in particular, were close to perfect given the intrinsic inaccuracy of the database annotation considered to be the gold standard here. Of course, there is a price paid in computational time, and GENEWISE is expensive with its linear-memory dynamic programming technique.

GENSCAN accuracy, in theory, should be unaffected, whether the query sequence encodes genes for which a close homolog, remote homolog, or no homolog exists. GENEWISE and PROCRUSTES accuracy, on the other hand, should decrease as the homology becomes distant, and these programs have little utility if a homolog does not exist.

As we have already pointed out, *nr* database contains protein translations of most of the genes in our data set, which could be a significant drawback of the data set. It is difficult (if not impossible) to come up with criteria for eliminating just the translations. Mouse orthologs are often 100% identical at the protein level and variants of the same protein may be highly (98%–99%) identical. Thus, we chose to evaluate the effect of the similarity level (*P* value) of an available homolog on the accuracy of GENEWISE and PROCRUSTES by considering a variety of *P* value bins. Conceptually, identical or close to identical proteins would fall in the most significant *P* value bin, and other bins would be devoid of identical hits.

A set of Blast-probability (*P* value) thresholds was chosen to provide bins with varying levels of similarity ($10^{-120}$, $10^{-80}$, $10^{-60}$, $10^{-40}$, $10^{-30}$, $10^{-20}$, $10^{-10}$, and $10^{-5}$). For each of these *P* values ($10^{-80}$, for instance), we performed the following experiment. After running BLASTX against *nr* for the DNA sequences in h178, we discarded for each DNA sequence all HSPS corresponding to all protein sequences with a *P* value below cutoff (as if we were ignoring all known amino acid sequences over a given level of similarity to the protein encoded in the query DNA sequence). Then, the protein with the remaining top hit below the next higher *P* value threshold ($10^{-60}$, in the case of the example) was used, if it existed, as a candidate homolog for the SSBGP tools. If there was no protein hit in the bin ($10^{-80}$ to $10^{-60}$ in the example) then this gene was discarded for the evaluation of this bin.

Thus, the BLASTX gene models are based on all the protein homologs with probability higher than the threshold considered. The *P* value thresholds were chosen so as to generate roughly equal numbers of data points (sequences from h178) for each set. The minimum number of data points in any set is 73, large enough to avoid significant sampling bias.

The accuracy results as a function of *P* value of the homologs are shown in Figure 1. GENSCAN performance is expected to be constant, and was for the most part; the minor variations are because of changes in the data set. Only a fraction of the genes had homologs in each of the bins, thus the data set changed a little from bin to bin. The overall performance of SSBGP tools suffered substantially as the similarity decreased. Somewhat surprisingly, the performance of GENSCAN is superior to that of SSBGP tools even at rather high levels of similarity (*P* value between $10^{-80}$ and $10^{-60}$). When the similarity is strong, GENEWISE appears to outperform PROCRUSTES in the h178 sequence set. However, when the similarity is weak the difference in performance between the two tools at the nucleotide level is small, and for low levels of similarity PROCRUSTES seems to outperform GENEWISE, particularly at the exon level. This is not unexpected considering the design of these programs: GENEWISE is primarily a sequence alignment tool, and thus it performs very well when there is strong sequence similarity. PROCRUSTES is more of a gene prediction program; it possibly encodes a more sophisticated splice site and exon model, which allows for better exon prediction at low

levels of similarity. As shown in Figure 3, a decrease in accuracy for sequence similarity-based methods is most likely a result of the decline in sensitivity, while specificity remains high, which is a very desirable feature.

Interestingly, when the similarity is weak (*P* value > $10^{-20}$), the advantage of sophisticated SSBGP tools as opposed to direct gene modeling from database searches such as those performed by BLASTX, seems to vanish. It is not unlikely that when the similarity is weak, the query DNA sequence and the top database search homolog share only a conserved domain. In such cases, SSBGP, relying on sequence similarity only to the top homolog, are only able to detect the part of the gene exonic structure encoding these domains. Direct gene modeling from BLASTX search results builds on all potential homologs (not only the top one); thus, weak homologs that share different conserved regions with the gene encoded in the DNA sequence may allow for better recovery of the overall exonic structure of the gene. In fairness to GENEWISE and PROCRUSTES, they can be used with multiple protein homologs and complete gene models synthesized, but that is computationally expensive and analytically problematic. Figure 1 illustrates an extreme example. A possible solution (at least when using GENEWISE) is to build a profile or an HMM based on the top few homologs and then align this profile with the target genomic sequence.

Conversely, when the similarity with the top ho-

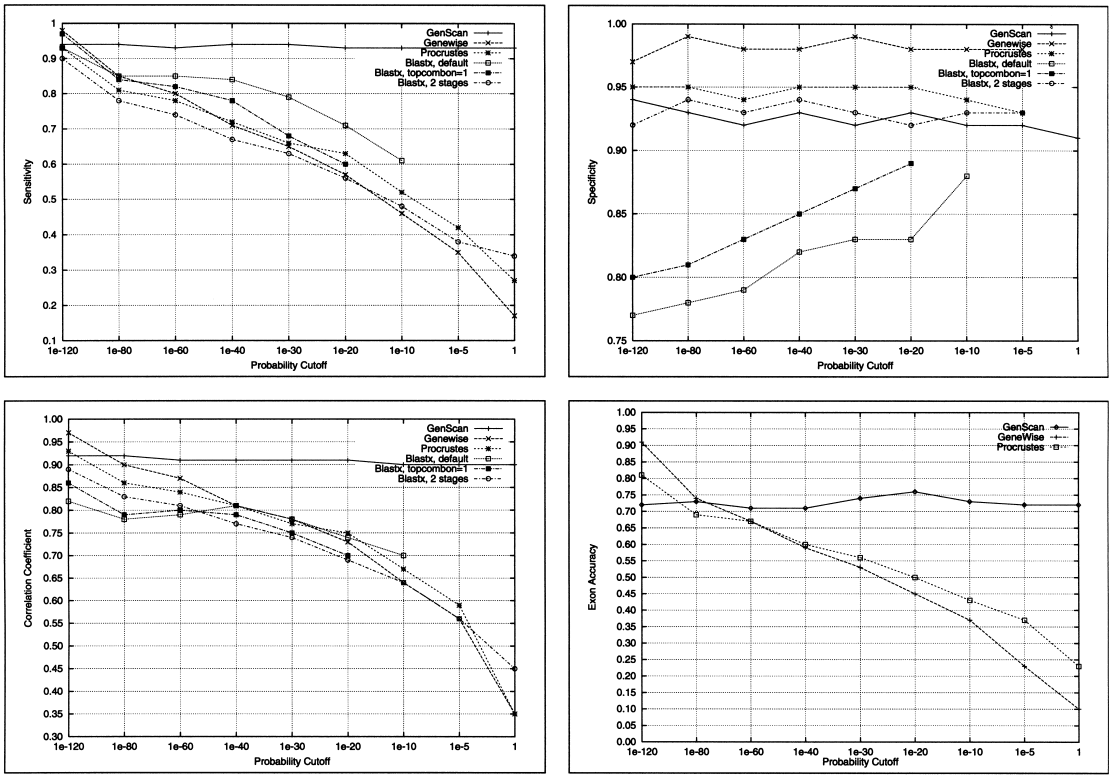


| P-value cutoff | 1e-120 | 1e-80 | 1e-60 | 1e-40 | 1e-30 | 1e-20 | 1e-10 | 1e-05 | 1 |
|---|---|---|---|---|---|---|---|---|---|
| # sequences | 73 | 99 | 100 | 116 | 102 | 108 | 109 | 96 | 119 |
| P-value log-average | 1e-206 | 1e-104 | 1e-73 | 1e-54 | 1e-37 | 1e-27 | 1e-17 | 1e-8 | 1e-3 |

**Figure 1** The accuracy of the gene prediction tools as a function of the similarity to the chosen homolog. For each *P*-value cutoff, the homolog with the lowest *P* value above the cutoff was chosen to build the gene prediction models. The table indicates the different ranges considered, the log-average of the *P* values in each range, and the number of sequences with acceptable homologs in the range. For example, there were 99 sequences in h178 for which after discarding all hits with *P* value < $10^{-120}$, the top remaining hit had a *P* value < $10^{-80}$. There were 73 sequences for which the top hit had a *P* value < $10^{-120}$, and 119 sequences for which the top hit had a *P* value > $10^{-5}$.

molog is weak, the BLASTX search picks up only the stronger regions of similarity between the homolog and the gene encoded in the query sequence, although lower levels of sequence similarity are shared in other regions between the protein and the query DNA sequences. These can be detected by the SSBGP tools (Fig. 1). Finally, in other cases, both situations occur simultaneously, and direct gene modeling from BLASTX search and SSBGP tools may complement each other to produce a more accurate overall prediction (Fig. 1).

Examining the data in Table 1 and Figure 1, one may be tempted to conclude that the gene identification problem is almost solved. When a strong homolog exists, programs like GENEWISE and PROCRUSTES are likely to pick up the correct exon structure; when such a homolog does not exist, programs like GENSCAN will still be able to recover most of this structure. This, we believe, is rather optimistic, as the sequence set in which these programs have been tested is extremely easy. Although the results obtained are instructive of the comparative performance of the tools, they cannot necessarily be extrapolated to the performance of these tools in the large genomic sequences. In the next section, we present the results obtained on evaluating the tools on a set of simulated genomic sequences, which we believe provide a more realistic estimation of the actual accuracy of the gene prediction tools in large genomic sequences.

### Accuracy in Semiartificial Genomic Sequences

A SAG data set containing known genes in random intergenic context (as described in Methods) was constructed to check if the accuracy measures from the previous section extrapolate to larger, more difficult data sets.

Because each SAG sequence contains multiple genes, the choice of the set of protein homologs to predict all the genes was no longer trivial. For ease of evaluation, we used the knowledge of the genes to pick these homologs, but there are other techniques that can be used to pick up a single candidate homolog for each gene-like region. In short, the top-scoring protein homolog from the BLASTX search for each of the genic sequences was used by GENEWISE and PROCRUSTES to predict the gene based on sequence similarity. For instance, artificial sequence AGS01 was obtained by embedding EMBL sequences HS10116, HSDNAAMHI, and HSNUCLEO in artificial intergenic DNA, with BLASTX top homologs being NCBI:gi 134635, 1136442, and 128841, respectively. The GENEWISE and PROCRUSTES predictions on the artificial sequence AGS01 were obtained by three independent executions of the programs, with each of the above top homolog proteins in turn. The programs were executed to predict genes on both strands and the model on the strand with the higher score was used to assess accuracy. This approach isolated the issue of the accuracy of these programs if the genomic sequence is large and the gene is encoded only in a small region of this sequence. There are other factors, such as the ability to choose the correct set of homologs that affect accuracy, but these factors were similar for all the programs, and other suboptimal (but perhaps more realistic) techniques would lead to lower accuracy. Thus, the accuracy numbers for the semiartificial sequences are not underestimated.

Table 2 shows the accuracy of the gene identification tools in Gen178, the set of simulated genomic sequences. As expected from theoretical considerations, SSBGP tools were mostly unaffected by the inclusion of genic sequences in the random intergenic-like DNA. PROCRUSTES appears to be less robust than GENEWISE when analyzing large genomic sequences. In particular, there is a significant decrease in specificity at the exon level (from 0.82 to 0.75), the likely result of predicting a relatively large number of small exons in otherwise noncoding DNA [wrong exons (WE) increasing from 0.04 to 0.16]. The comparatively low decrease in specificity at the nucleotide level, from 0.95 to 0.94, suggests that most of these false exons are rather short. Surprisingly, PROCRUSTES sensitivity at

**Table 2.** Accuracy of Gene Prediction Tools in the Set of Semiartificial Genomic (SAG) Sequences (Gen178)

| | | Nucleotide | | | Exon | | | | | Gene | |
|---|---|---|---|---|---|---|---|---|---|---|---|
| Program | No. | Sn | Sp | CC | Sn | Sp | $\frac{Sn+Sp}{2}$ | ME | WE | MG | WG |
| GenScan | 43 | 0.89 | 0.64 | 0.76 | 0.64 | 0.44 | 0.54 | 0.14 | 0.41 | 0.03 | 0.28 |
| | | *0.92* | *0.92* | *0.91* | *0.76* | *0.76* | *0.76* | *0.09* | *0.09* | | |
| GeneWise | 43 | 0.98 | 0.98 | 0.97 | 0.88 | 0.91 | 0.89 | 0.06 | 0.02 | | |
| | | *0.98* | *0.98* | *0.97* | *0.88* | *0.91* | *0.89* | *0.06* | *0.02* | | |
| Procrustes | 43 | 0.93 | 0.94 | 0.93 | 0.80 | 0.75 | 0.77 | 0.10 | 0.16 | | |
| | | *0.93* | *0.95* | *0.93* | *0.76* | *0.82* | *0.79* | *0.11* | *0.04* | | |

(Italics) The accuracy values in the set of single gene sequences (from Table 1).

the exon level is slightly higher in the set of artificial sequences than in the set of single gene sequences.

The accuracy of BLASTX was not affected by the intergenic context (data not shown) because no hits with a *P* value more significant than $10^{-10}$ were found in the simulated DNA.

Accuracy of ab initio gene finders suffered substantially in the set of artificial genomic sequences. Because of the tendency of gene finders to overpredict exons, one would expect that by placing the genic sequences in the simulated-intergenic context, some loss of specificity would be observed, with programs predicting perhaps a few extra exons in otherwise random DNA. On the other hand, one would expect the sensitivity to remain essentially constant as the exons predicted in the genic sequences should still be predicted when these are included in simulated-intergenic DNA. However, a significant decrease in specificity is observed (Table 2). For instance, GENSCAN specificity at the exon level drops to 0.64 from 0.92, and the proportion of WEs climbs to 41% from 9% in the single gene sequences. In addition, a significant decrease in sensitivity is also observed, with programs failing to predict exons that were correctly identified in the single gene sequences. For instance, the proportion of missing exons increases for GENSCAN from 9% to 14%. Almost 30% of the GENSCAN genes are predicted in the simulated-intergenic DNA. For ab initio gene finders, we believe these accuracy values (on SAG sequences) are more representative of their true accuracy on large genomic sequences than those obtained in the typical single gene benchmark experiments.

Figure 2 shows the predictions of the different programs in one of the artificially generated genomic sequences (~157-kb long). As mentioned, SSBGPs predict the genic structure of the artificial genomic sequence rather well. Performance of ab initio gene finders, on the other hand, degrades substantially.

Although all genes predicted by GENSCAN overlap real genes, it still predicts a large number of false positive exons. In addition, even when predicting the exons correctly, their assembly into genes is often incorrect. For instance, in the sequence in Figure 2, GENSCAN has difficulty in predicting the correct gene boundaries, and it expands the gene beyond its actual limits. In the lower portion of the Figure 2, we compare the predictions in the region between positions 23,000 and 41,000 from the SAG sequence to the predictions on just the actual genic sequence (without the random context). GENSCAN performance suffers substantially from this inclusion in pseudointergenic context. One explanation is that GENSCAN uses the wrong isochore model for this sequence: the actual isochore structure being destroyed by the usage of artificial intergenic context. In such a case, decrease in performance would be an artifact of our SAG sequences rather than a feature of GENSCAN. Experiments with gene finders other than GENSCAN (data not shown) indicate that such a decrease in performance is not specific to GENSCAN, but rather a general feature of ab initio gene finders.

As with the set of single gene sequences, the comparison of GENSCAN with SSBGP tools is not strictly fair. The SSBGPs are affected by the existence of closer homologs, while GENSCAN is not affected. To study the effects of the range of similarity on the accuracy of gene prediction in the SAG data set, we extracted two different sets of SAG sequences. In the first set, each gene in each SAG sequence has a strong homolog (BLASTX *P* value < $10^{-50}$), and in the other set, each gene in each sequence had a moderate homolog (BLASTX *P* value between $10^{-50}$ and $10^{-6}$). Some of the genes in the second set also had better homologs which were ignored for this analysis. The results are shown in Table 3. If the similarity is strong, the sequence similarity-based methods perform very well, outperforming ab initio tools (as in Table 2). However, if the average similarity between the genes encoded and the known proteins is only moderate (though perhaps, still better than expected for real genomic sequences), the performance of these tools is similar to the performance of GENSCAN. At the exon level, the overall accuracy stays at ~50%. A very similar accuracy has also been observed independently on test sets on actual genomic sequences (http://predict.sanger.ac.uk/th/brca2/; see Discussion). We believe this is still an overestimation of the actual accuracy of these tools in real genomic sequences.

## DISCUSSION

Computational genefinders produce acceptable predictions of the exonic structure of the genes when analyzing single gene sequences with very little flanking intergenic sequence, but are unable to correctly infer the exonic structure of multigene genomic sequences. In particular, ab initio genefinders predict and utilize intergenic boundaries poorly. Conversely, as our results indicate, sequence similarity searches on databases of known coding sequences are extremely helpful in deciphering the exonic structure for the genes that have known homologs. For very strong similarity, SSBGP tools appear to be the most useful. Surprisingly even for genes predicted based on homologs with a moderate degree of similarity ($10^{-50} < P$ value < $10^{-6}$), GENSCAN performs comparably to SSBGP programs. It appears that at such levels of similarity, potential splice signals and statistical biases in the sequence composition carry information comparable to sequence similarity for the purposes of identifying coding regions. It is possible that the use of SAG sequences does not provide a realistic scenario to test the accuracy of computational gene finders. Ideally, one would like to use large genomic sequences with gene structure experi-

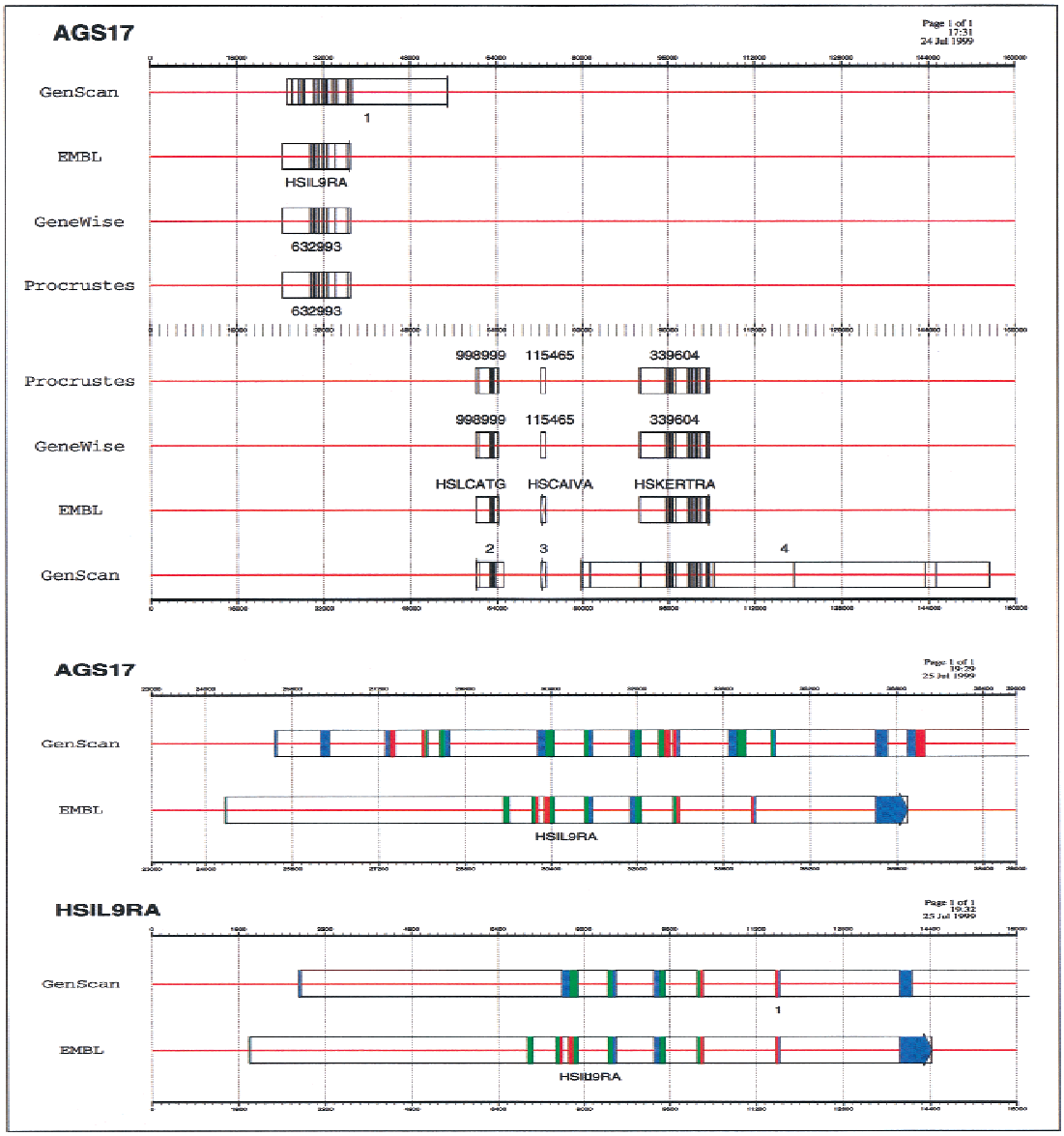


**Figure 2** (AGS17, *top*) Gene predictions in one of the artificial genomic sequences. The row EMBL indicates the coordinates of the actual genes. Exons corresponding to the same gene (or predicted to be in the same gene) are linked by a box. (AGS17, *middle*) Predictions of GENSCAN finders in the region 23,000 to 41,000 from the semiartificial genomic sequence. (HSIL9RA, *bottom*) The predictions improve if GENSCAN is provided only the 18,000-bp long genic sequence that has been inserted in this region. This figure, as well as Fig. 1, has been prepared using gff2ps. (Abril and Guigó 2000)

mentally verified. However, experimentally verifying each and every gene along with alternative splice structures in a large genomic sequence remains a difficult challenge. Techniques such as exon-trapping (Church et al. 1994) have high sensitivity but poor specificity, while RT–PCR or identifying a cDNA clone for every transcript can be fairly specific (Hochgeschwender 1992), but have less than perfect sensitivity and are dependent on finding a tissue in a developmental stage under an environmental condition in which that gene (or alternative gene product) is expressed. In particular, proving that a piece of sequence (that appears coding

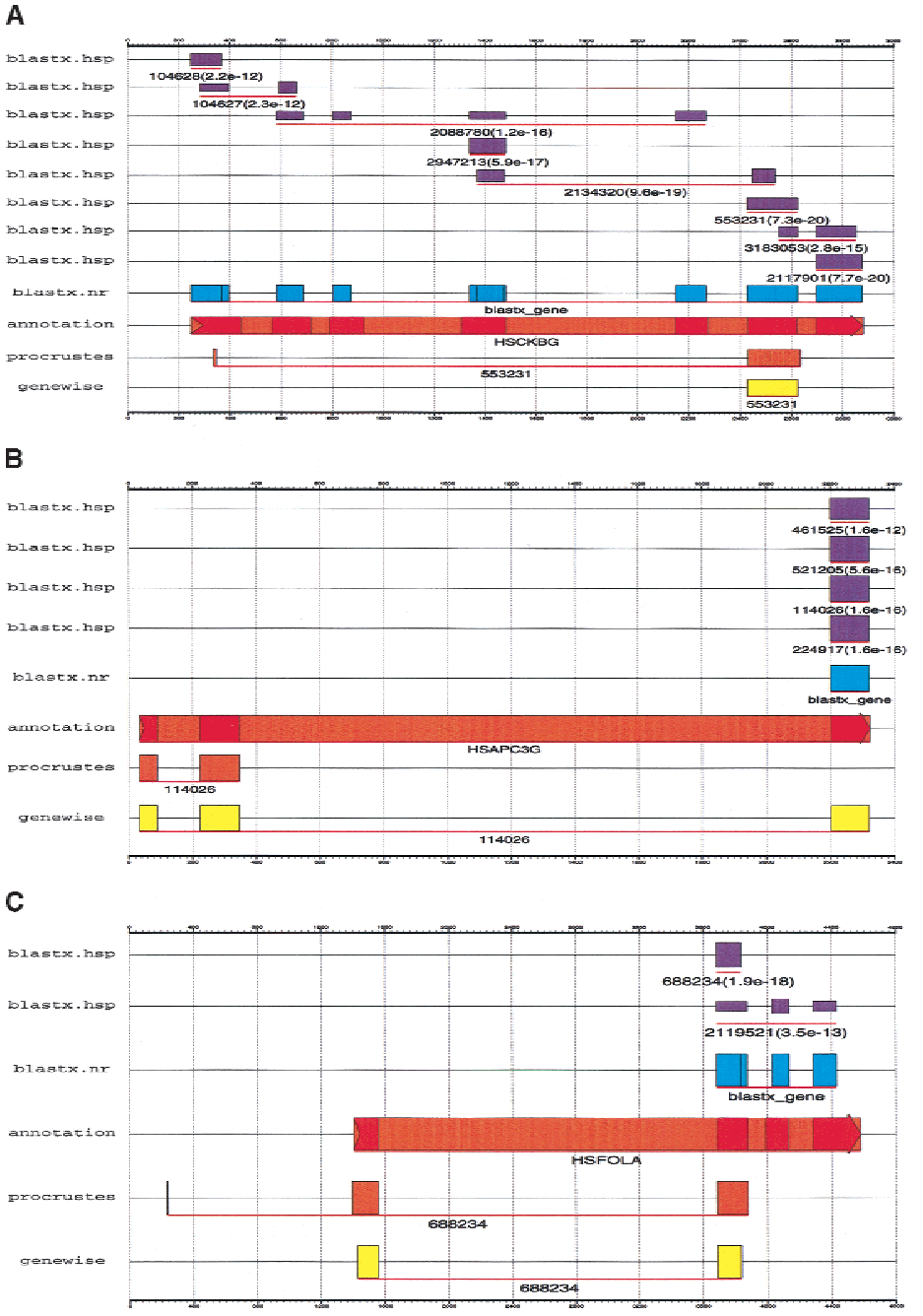


to gene-prediction programs) is not coding is extremely difficult. Thus, even though there are a number of attempts to consolidate genomic gene prediction data sets [Banbury Cross (http://igs-server.cnrs-mrs.fr/igs/banbury), GeneSafe (http://www.hgmp.mrc.ac.uk/Genesafe), GASP (http://www.fruitfly.org/GASP1/)], the number of experimentally well-annotated large genomic sequences remains small, and even in those

**Figure 3** If the candidate protein sequence is a remote homolog, direct gene modeling from BLAST-like database searches may have different predictions compared to more sophisticated SSBGP tools. (*A*) EMBL DNA sequence HSCKBG was compared with the protein sequences in the nr sequence database using BLASTX. Hits with *P* value < $10^{-20}$ were discarded, the top remaining corresponded to a fragmentary protein sequence gi:553231. Not surprisingly, only a small fraction of the actual gene was recovered using this homolog by either GENEWISE or PROCRUSTES. Other choices of homologs may have yielded different predictions but none of them by themselves appears to be perfect. Conversely, the gene model derived directly from the BLASTX search reproduces the exonic structure of the gene fairly well. Thus, even though upon discarding the close homologs, the remaining proteins individually showed only little overall similarity to the encoded protein product, as a collection they enable to walk its exonic structure. (*B*) If database protein sequences with hits below *P*-value = $10^{-20}$ are discarded, BLASTX is able to detect significant similarity between only one of the encoded exons in EMBL sequence HSPAC3G and the remaining protein sequences in the database. But with the top homolog among these, the SSBGP tools (GENEWISE in particular) are able to infer the correct exonic structure, picking up both the additional upstream exons. This is because the SSBGP tools are able to detect more distant sequence relationships than BLASTX with our choice of thresholds or because (as in this case) coding exons occur in low-complexity regions, which are usually masked when performing BLASTX searches to avoid large numbers of false positives. (*C*) In another case, direct gene modeling from BLASTX searches and SSBGP tools can complement each other to produce more accurate gene predictions. As in *A* and *B*, HSP hits below *P*-value = $10^{-20}$ were ignored after comparing EMBL sequence HSFOLA with the nonredundant protein sequence database.

cases, the reliability of the annotation is difficult to assess (Reese et al. 2000). To compensate for the lack of these verified data sets, we have built semiartificial data sets with known genes placed in the context of random intergenic sequence. This ensures that all the genes in these sequences are known. In fact, most of these genes have fairly small genomic spread (i.e., none of the introns is very large), and a number of the ab initio gene prediction programs have been trained on them. This should make this data set easy for most programs. However, our model for intergenic sequence is possibly imperfect for at least two reasons: The genes are not necessarily placed in the correct isochore context; and the apparent codon composition in the simulated intergenic DNA may be different from that of actual intergenic sequence. These imperfections may conceivably make gene prediction more difficult on this data set for ab initio programs, but we think these are more than offset at least in part by the small genes and the fact that the programs have partly trained on these genes. Overall, the sensitivity and specificity numbers are most instructive in the relative context. The sensitivity of most tools remains high even when confronted with large intergenic sequences, but the specificity of the ab initio tools drops because of large intergenic regions.

Interestingly, the accuracy reported here for GENSCAN is very similar to the accuracy found in the *BRCA2* region (Chruch et al. 1994; Couch et al. 1996); probably the best annotated human genomic region from an experimental standpoint. BRCA2 region is a large genomic tract with multiple genes, thus, a difficult data set for most gene prediction programs. At the exon level, Tim Hubbard and Richard Bruskiewich (Sanger Center, UK) report for GENSCAN in this region a sensitivity of 0.63 (termed *coverage* there) and a specificity of 0.38 (termed *accuracy* there) (http://predict.sanger.ac.uk/th/brca2/). As anticipated, these values are slightly worse than the ones we have found here in the SAG data set (0.64 and 0.44, respectively). This seems to indicate that the approach of building artificial genomic sequences is not too unrealistic, and that it could be useful both for training and testing gene prediction programs. Results in these sequences, however, should be taken as an upper bound estimate of the accuracy of the programs in real genomic sequences.

There is a growing class of gene identification programs that combine both sequence similarity and traditional coding potential measures, such as Genie (Kulp et al. 1996 1997), HMMgene (Krogh 1997), and GSA (Huang et al. 1997). Unfortunately, because of a

**Table 3. Accuracy of Gene Prediction Tools in the Set of Semiartificial Genomic Sequences, When Either Strongly or Moderately Similar Sequences are Used to Model the Genes**

| | Strong similarity *P* Value < $10^{-50}$ 17 SAG sequences | | | | | | Moderate similarity $10^{-50}$ < *P* value < $10^{-6}$ 26 SAG sequences | | | | | |
|---|---|---|---|---|---|---|---|---|---|---|---|---|
| | Nucleotide | | | Exon | | | Nucleotide | | | Exon | | |
| Program | Sn | Sp | CC | Sn | Sp | $\frac{Sn+Sp}{2}$ | Sn | Sp | CC | Sn | Sp | $\frac{Sn+Sp}{2}$ |
| GenScan | 0.91 | 0.66 | 0.77 | 0.67 | 0.46 | 0.56 | 0.91 | 0.61 | 0.74 | 0.67 | 0.43 | 0.55 |
| GeneWise | 0.99 | 0.99 | 0.99 | 0.90 | 0.93 | 0.91 | 0.68 | 0.98 | 0.81 | 0.46 | 0.63 | 0.54 |
| Procrustes | 0.92 | 0.96 | 0.94 | 0.80 | 0.75 | 0.77 | 0.66 | 0.79 | 0.72 | 0.48 | 0.32 | 0.40 |

The geometric mean of the *P* values of the strong similarity sequences was $10^{-135}$ and for the weaker similarity group it was $10^{-39}$.

lack of public availability at the time of the initiation of this study, their evaluation will have to await a future analysis.

EST similarity can also provide useful information regarding gene structure for ~85% of the common genes (Guigó et al. 2000). A set of single gene sequences in h178 was used to optimize a method for deriving exonic structures from EST matches. When using the EST sequences in the public databases, the method yielded an accuracy of $Sn = 0.72$, $Sp = 0.87$, and $CC = 0.69$ at the nucleotide level, when predicted gene structures were compared to the annotated mRNA (not the coding) exonic structure. Other secondary questions regarding EST-based gene prediction may also be important, such as the extent to which EST matches help in delineating the gene boundaries.

Though there is considerable variation in the accuracy of various gene prediction programs depending on data sets and the availability and choice of homolog, we believe that a judicious use of these programs in combination can result in highly accurate gene structures for genes with known homologs. There is, however, still considerable progress to be made on predicting alternative spliced structures and genes with no known homologs.

## METHODS

### Computational Gene Identification Tools

Gene identification tools may be categorized into ab initio tools (those not utilizing sequence similarity and relying on intrinsic gene measures such as coding potential and splice signals), and those based (at least partly) on sequence similarity.

### Ab initio Gene Identification Tools

The ab initio gene identification tools use information from both the gene signals in the genomic DNA (such as splice sites, start and stop codons, and promoter elements), and the statistical biases in DNA composition that is characteristic of coding regions. There are a number of such programs (for reveiws, see Fickett 1996; Claverie 1997; Guigó 1997a; Burge and Karlin 1998; Haussler 1998). GENSCAN (Burge and Karlin 1997) is one of the most accurate and widely used programs in this category, and we use it as a representative.

### SSBGP Tools

A number of recent programs predict genes by aligning genomic sequences with candidate homologous protein sequences. These programs may include a splice site model, coding potential, and sequence similarity to known proteins to infer gene predictions. We evaluated two of these programs, PROCRUSTES (Gelfand et al. 1996), and GENEWISE (Birney and Durbin 1997) (http://www.sanger.ac.uk/Software/Wise2/).

These programs require as input a candidate homologous protein sequence; therefore, in typical use, a sequence similarity database search with the query genomic sequence is performed a priori and the top hit is used as the candidate (or top hits are used as candidates, in the case of a query sequence encoding multiple genes). The database similarity searches were performed against the nonredundant protein sequence database from NCBI, *nr*, using BLASTX (Altschul et al. 1990; Gish and Sates 1993). BLASTX performs a translation of the query sequence into the six frames, and searches for similarities between each of these translations and the protein sequences in the database.

BLASTX was designed as a similarity-based gene prediction tool, and it is possible to model a gene directly from the database search results. BLASTX, however, does not confine its similarity to exon;, thus the similarity region is not constrained to begin or end on splice sites. Moreover, BLASTX does not explicitly predict genes in genomic sequences, and some postprocessing of its output is required to infer gene predictions from the search results. Indeed, while computational gene finders predict genes, that is pairs of positions (corresponding to exon starts and ends) along the query genomic sequence, database searches only produce lists of sequence database hits along the query sequence. Each hit above a given similarity threshold may be assumed to be a coding exon. For different database entries, however the set of hits may be different. The problem is then to infer a gene model from the set of database hits. A simple solution is to project the hits into a single axis along the genomic sequence, and to assume the union of these projections to be the coding exons.

In total, three strategies based on BLAST were tested:

(1) default — A procedure consisting of projecting the HSPs onto the genomic sequences was used (see Guigó et al. 2000). BLASTX was run with *E = 1e-10 − filter xnu + seg S2 = 60*, and all HSPs with identity <40% were discarded. The choices of S2 and percentage identity were influenced by the need to restrict false matches.

(2) topcomboN — BLASTX was used with default parameters except for *−filter xnu + seg topcomboN = 1*. HSPs with *P* value > $10^{-20}$ were discarded, and the projections along the query sequence of the remaining HSPs assumed to be the predicted coding exons. WashU-BLAST has a parameter topcomboN that limits all HSPs generated to be in one consistent group. For example, for BLASTX searches, each region of the nucleotide sequence is only aligned to a single region on the protein sequence and the ordering of these HSPs has to be consistent along both the nucleotide and protein sequences. This restricts spurious matches arising from repetitive domains with query sequences, and from low scoring hits in introns and flanking regions.

(3) two-stage — BLASTX was used in a two stage process that first identifies one or more candidate protein sequences in the presence of a low-complexity filter. In the second stage, BLASTX is used to align the candidates individually with the genomic sequence, this time without the filter and with topcomboN = 1. This two pass technique is closer to the strategy used with GENEWISE and PROCRUSTES, where a first BLASTX search pinpoints the protein homolog to be used, and a subsequent GENEWISE uses this protein homolog.

Both GENEWISE and PROCRUSTES were run with mostly standard parameters: GENEWISE v2.1.16b *-both -gff -pretty -para -cdna -genes -quiet* and PROCRUSTES was run in the local mode with *MIN_EXN 20, MIN_IVS*

*50, GAP 2, INI_GAP 10, MATRIX pam120.mtx*. GENSCAN was run with default parameters.

### Benchmark Sets

Two sets of sequences have been used to evaluate the programs discussed above. First, a typical benchmark set made of sequences from the EMBL database release 50 (1997) that included 178 human genomic sequences coding for single complete genes for which both the mRNA and the coding exons are known. The procedure used to extract the sequences is described in Burset and Guigó (1996) and Guigó (1997b). We will refer to this set here as h178. All the genes in this data set are on the forward strand. Other characteristics of h178 are provided in Table 4.

For the reasons discussed in this paper, this does not appear to be a challenging benchmark set for estimating the accuracy of gene identification programs in the larger genomic sequences. Unfortunately, very few large genomic sequences have been studied extensively to produce complete experimental determinations of the exact structure of each gene. To overcome this limitation, we generated a semiartificial set of genomic sequences in which accurate gene annotation can be guaranteed.

In essence, a set of annotated genic sequences are placed randomly in a background of random intergenic DNA. The length of the semiartificial sequence is generated randomly according to a normal distribution. Genomic fragments containing genes and random-sized segments of intergenic sequence are then concatenated until their combined lengths exceed the target. The strands are also chosen at random for each genic subsequence.

Table 4 shows the characteristics of the generated sequences when the method is applied to the sequences in h178 and the intergenic background is generated using a Markov Model of order 5 as described in Guigó and Fickett (1995) assuming an average intergenic G + C content of 38%. The 178 genic sequences were collapsed into 42 SAG sequences. Some of the resulting parameters, such as average G + C content of 40%, a gene every 43 Kb, and a coding density of 2.3% are in agreement with that for the overall human genome. This data set has flaws and is not a perfect representative of the human genome. Some of the ignored characteristics include the isochore organization of the human genome, known and unknown repeats in the intergenic regions, presence of pseudogenes and other evolutionary remnants, genes with huge introns, and tandem gene clusters. Most of the missing properties (pseudogenes, repeats, huge introns) make gene prediction much more difficult. Thus, we expect the accuracy results on Gen178 to still be an overestimate of the true accuracy.

### Evaluating Accuracy

The measures of accuracy used here are discussed extensively in Burset and Guigó (1996). We will restate them briefly. Accuracy is measured at three different levels: nucleotide, exon, and gene. At the nucleotide and exon levels, we essentially compute the proportion of actual coding nucleotides/exons that have been predicted correctly–(which we call Sensitivity) and the proportion of predicted coding nucleotides/exons that are actually coding nucleotides/exons (which we call Specificity). To compute these measures at the exon level, we will assume that an exon has been predicted correctly only when both its boundaries have been predicted correctly. To summarize both Sensitivity and Specificity, we compute the Correlation Coefficient at the nucleotide level, and the average of Sensitivity and Specificity at the exon level. At the exon and gene level, we also compute the Missing Exons/Genes (the proportion of actual exons/genes that overlap no predicted exon/gene) and the Wrong Exons/Genes (the proportion of predicted exons/genes that overlap no actual exon/gene).

The measures are computed globally from the total number of prediction successes and failures (at the base and exon level) on all sequences. Accuracy in Table 1 is computed ignoring predictions in the reverse (wrong) strand. The first column in Tables 1 and 2 indicates the number of sequences for which the progams produced predictions.

### Data Availability

Both the set of single gene sequences and the set of semiartificially generated genomic sequences will be available from http://www1.imim.es/databases/gpecal2000/.

## ACKNOWLEDGMENTS

We thank Randall F. Smith, Ewan Birney, Chris Burge, and Warren Gish, and the anonymous referees (one in particular for pointing out the topcomboN feature in WU-BLAST) for useful comments. This work was partially supported by a grant from Plan Nacional de I + D, BIO98-0443-C02-01, and from the Ministerio de Educación y Ciencia (Spain) to R.G. M.B. is supported by a Formación de Personal Investigador fellowship, FP95-38817943, from the Ministerio de Educación y Ciencia (Spain), J.F.A. is supported by a predoctoral fellowship, 99/9345, from the Instituto de Salud Carlos III (Spain).

The publication costs of this article were defrayed in part by payment of page charges. This article must therefore be

**Table 4.** Characteristics of the Benchmark Sequence Sets

| | | | Sequence length | | | Genes (average) | | | | CDS (average) | | |
|---|---|---|---|---|---|---|---|---|---|---|---|---|
| Set | No. | G + C | average | min | max | no. | length | density | | no. exons | length | density |
| h178 | 178 | 50% | 7169 | 622 | 86640 | 1 | 3657 | 53% | 7169 | 5.1 | 968 | 21% |
| Gen178 | 42 | 40% | 177160 | 70037 | 282097 | 4.1 | 15136 | 8.6% | 43000 | 21 | 4007 | 2.3% |

The columns Genes (average) and CDS (average) provide values averaged over all the sequences (178 in h178 and 42 in Gen178). Gene density provides the percentage of nucleotides that occur in genic regions (exons, introns, and UTRs), and the number of kilobases per gene. CDS no. exons is the average number of coding exons per sequence, and CDS density is the percentage of nucleotides that occur in coding regions.

hereby marked "advertisement" in accordance with 18 USC section 1734 solely to indicate this fact.

## REFERENCES

Abril, J.F. and Guigó, R. 2000. gff2ps: A tool for visualizing genomic annotations. *Bioinformatics* in press.

Altschul, S.F., Gish, W., Miller, W., Myers, E.W., and Lipman, D. 1990. Basic local alignment search tool. *J. Mol. Biol.* **215:** 403–410.

Birney, E. and Durbin, R. 1997. Dynamite: A flexible code generating language for dynamic programming methods used in sequence comparison. *Ismb* **5:** 56–64.

Burge, C.B. and Karlin, S. 1997. Prediction of complete gene structures in human genomic DNA. *J. Mol. Biol.* **268:** 78–94.

———. 1998. Finding the genes in genomic DNA. *Curr. Opin. Struc. Biol.* **8:** 346–354.

Burset, M. and Guigó, R. 1996. Evaluation of gene structure prediction programs. *Genomics* **34:** 353–357.

Church, D.M., Stotler, C.J., Rutter, J.L., Murrell, J.R., Trofatter, J.A., and Buckler, A.J. 1994. Isolation of genes from complex sources of mammalian genomic DNA using exon amplification. *Nat. Genet.* **6:** 98–105.

Claverie, J.-M. 1997. Computational methods for the identification of genes in vertebrate genomic sequences. *Hum. Mol. Genet.* **6:** 1735–1744.

Couch, F.J., Rommens, J.M., Neuhausen, S.L., Couch, E.J., Rommens, J.M., Neuhausen, S.L., Belanger, C., Dumont, M., Abel, K., Bell, R., Berry, S., Bogden, R., Cannon-Albright, L. 1996. Generation of an integrated transcription map of the BRCA2 region on chromosome 13q12-q13. *Genomics* **36:** 86–99.

Fickett, J.W. 1996. Finding genes by computer: the state of the art. *Trends Genet.* **12:** 316–320.

Gelfand, M.S., Mironov, A.A., and Pevzner, P.A. 1996. Gene recognition via spliced alignment. *PNAS* **93:** 9061–9066.

Gish, W. and States, D. 1993. Identification of protein coding regions by database similarity search. *Nat. Genet.* **3:** 266–272.

Guigó, R. 1997a. Computational gene identification. *J. Mol. Med.* **75:** 389–393.

———. 1997b. Computational gene identification: An open problem. *Comput. Chem.* **21:** 215–222.

Guigó, R. and Fickett, J.W. 1995. Distinctive sequence features in protein coding, genic non-coding, and inter-genic human DNA. *J. Mol. Biol.* **253:** 51–60.

Guigó, R., Burset, M., Agarwal, P., Abril, J.F., Smith, R.F., and Fickett, J.W. 2000. Sequence similarity based gene prediction. In *Genomics and proteomics: Functional and computational aspects* (ed. S. Suhai), pp. 95–105. Kluwer Academic / Plenum Publishing, New York, NY.

Haussler, D. 1998. Computational genefinding. In *Trends Biochem. Sci., supplementary guide to bioinformatics*, pp. 12–15.

Hochgeschwender, U. 1992. Toward a transcriptional map of the human genome. *Trends Genet.* **8:** 41–44.

Huang, X., Adams, M.D., Zhou, H., and Kerlavage, A.R. 1997. A tool for analyzing and annotating genomic sequences. *Genomics* **46:** 37–45.

Krogh, A. 1997. Two methods for improving performance of an HMM and their application for gene finding. *ISMB* **5:** 179–186.

Kulp, D., Haussler, D., Reese, M.G., and Eeckman, F.H. 1996. A generalized hidden markov model for the recognition of human genes in DNA. In *Intelligent systems for molecular biology* (eds. D.J. States, P. Agarwal, T. Gaasterland, L. Hunter, and R. Smith), pp. 134–142. AAAI Press, Menlo Park, CA.

Kulp, D., Haussler, D., Reese, M.G., and Eeckman, F.H. 1997. Integrating database homology in a probabilistic gene structure mode. In *Biocomputing: Proceedings of the 1997 Pacific Symposium* (eds. R.B. Altman, A.K. Dunke, L. Hunter, and T.E. Klein), pp. 232–244. World Scientific, New York, NY.

Mott, R. 1997. EST_GENOME: A program to align spliced DNA sequences to unspliced genomic DNA. *Comput. Appl. Biosci.* **13:** 477–478.

Reese, M.G., Hartzell, G., Harris, N.L., Ohler, U., Abril, J.F., and Lewis, S.E. 2000. Genome annotation assessment in *Drosophila melanogaster*. *Genome Res.* **10:** 483–501.

The *C. elegans* Sequencing Consortium. 1998. Genome sequence of the nematode *C. elegans*: A platform for investigating biology. *Science* **282:** 2012–2018.

*Received October 12, 1999; accepted in revised form August 11, 2000.*

### 3.3.4 Reese *et al*, *Genome Research*, 10(4):483–501, 2000

**PubMed Accession:**

http://www.ncbi.nlm.nih.gov/entrez/query.fcgi?cmd=Retrieve&db=PubMed&list_uids=10779488&dopt=Abstract

**Journal Abstract:**

http://www.genome.org/cgi/content/abstract/10/4/483

**Supplementary Materials:**

http://www.fruitfly.org/GASP1/
http://genome.imim.es/datasets/Dro_me/
http://genome.imim.es/software/gfftools/GFF2PS-ADHposter.html

**Companion Poster:**

See Figure 3.7 and the following URLs:
http://www.genome.org/content/vol10/issue4/images/data/483/DC1/GR10n4_poster.zip
http://genome.imim.es/references/genome_maps/2000_GenomeResearch_v10_i4_p483_poster_GASP.ps.gz

**Letter**

# Genome Annotation Assessment in *Drosophila melanogaster*

Martin G. Reese,[1,4] George Hartzell,[1] Nomi L. Harris,[1] Uwe Ohler,[1,2] Josep F. Abril,[3] and Suzanna E. Lewis[1]

[1]*Berkeley Drosophila Genome Project, Department of Molecular and Cell Biology, University of California, Berkeley, California 94720-3200 USA;* [2]*Chair for Pattern Recognition, University of Erlangen–Nuremberg, D-91058 Erlangen, Germany;*[3]*Institut Municipal d'Investigació Médica—Universitat Pompeu Fabra, Department of Medical Informatics (IMIM—UPF), 08003 Barcelona, Spain*

Computational methods for automated genome annotation are critical to our community's ability to make full use of the large volume of genomic sequence being generated and released. To explore the accuracy of these automated feature prediction tools in the genomes of higher organisms, we evaluated their performance on a large, well-characterized sequence contig from the *Adh* region of *Drosophila melanogaster*. This experiment, known as the Genome Annotation Assessment Project (GASP), was launched in May 1999. Twelve groups, applying state-of-the-art tools, contributed predictions for features including gene structure, protein homologies, promoter sites, and repeat elements. We evaluated these predictions using two standards, one based on previously unreleased high-quality full-length cDNA sequences and a second based on the set of annotations generated as part of an in-depth study of the region by a group of *Drosophila* experts. Although these standard sets only approximate the unknown distribution of features in this region, we believe that when taken in context the results of an evaluation based on them are meaningful. The results were presented as a tutorial at the conference on Intelligent Systems in Molecular Biology (ISMB-99) in August 1999. Over 95% of the coding nucleotides in the region were correctly identified by the majority of the gene finders, and the correct intron/exon structures were predicted for >40% of the genes. Homology-based annotation techniques recognized and associated functions with almost half of the genes in the region; the remainder were only identified by the ab initio techniques. This experiment also presents the first assessment of promoter prediction techniques for a significant number of genes in a large contiguous region. We discovered that the promoter predictors' high false-positive rates make their predictions difficult to use. Integrating gene finding and cDNA/EST alignments with promoter predictions decreases the number of false-positive classifications but discovers less than one-third of the promoters in the region. We believe that by establishing standards for evaluating genomic annotations and by assessing the performance of existing automated genome annotation tools, this experiment establishes a baseline that contributes to the value of ongoing large-scale annotation projects and should guide further research in genome informatics.

Genome annotation is a rapidly evolving field in genomics made possible by the large-scale generation of genomic sequences and driven predominantly by computational tools. The goal of the annotation process is to assign as much information as possible to the raw sequence of complete genomes with an emphasis on the location and structure of the genes. This can be accomplished by ab initio gene finding, by identifying homologies to known genes from other organisms, by the alignment of full-length or partial mRNA sequences to the genomic DNA, or through combinations of such methods. Related techniques can also be used to identify other features, such as the location of regulatory elements or repetitive sequence elements. The ultimate goal of genome annotation, the functional classification of all the identified genes, currently depends on discovering homologies to genes with known functions.

**[4]Corresponding author.**
**E-MAIL mgreese@lbl.gov; FAX (510) 486-6798.**

We are interested in an objective assessment of the state of the art in automated tools and techniques for annotating complete genomes. The Genome Annotation Assessment Project (GASP) was organized to formulate guidelines and accuracy standards for evaluating computational tools and to encourage the development of new models and the improvement of existing approaches through a careful assessment and comparison of the predictions made by current state-of-the-art programs.

The GASP experiment, the first of its kind, was similar in many ways to the CASP (Critical Assessment of techniques for protein Structure Prediction) contests for protein structure prediction (Dunbrack et al. 1997;

10:483–501 ©2000 by Cold Spring Harbor Laboratory Press ISSN 1088-9051/00 $5.00; www.genome.org

Levitt 1997; Moult et al. 1997, 1999; Sippl et al. 1999; Zemla et al. 1999), described at http://predictioncenter.llnl.gov. However, unlike the CASP contest, GASP was promoted as a collaboration to evaluate various techniques for genome annotation.

The GASP experiment consisted of the following stages: (1) Training data for the *Adh* region, including 2.9 Mb of *Drosophila melanogaster* genomic sequence, was collected by the organizers and provided to the participants; (2) a set of standards was developed to evaluate submissions while the participating groups produced and submitted their annotations for the region; and (3) the participating groups' predictions were compared with the standards, a team of independent assessors evaluated the results of the comparison, and the results were presented as a tutorial at ISMB-99(Reese et al. 1999).

Participants were given the finished sequence for the *Adh* region and some related training data, but they did not have access to the full-length cDNA sequences that were sequenced for the paper by Ashburner et al. (1999b) that describes the *Adh* region in depth. The experiment was widely announced and open to any participants. Submitters were allowed to use any available technologies and were encouraged to disclose their methods. Because we were fortunate to attract a large group of participants who provided a wide variety of annotations, we believe that our evaluation addresses the state of art in genome annotation.

Twelve groups participated in GASP, submitting annotations in one or more of six categories: ab initio gene finding, promoter recognition, EST/cDNA alignment, protein similarity, repetitive sequence identification, and gene function. Table 1 lists each participating group, the names of the programs or systems it used, and which of the six classes of annotations it submitted (see enclosed poster in this issue for a graphic overview of all the groups' results). Additional papers in this issue are written by the participants themselves and describe their methods and results in detail.

It should be noted that the lack of a standard that is absolutely correct makes evaluating predictions problematic. The expert annotations described by the *Drosophila* experts (Ashburner et al. 1999b) are our best available resource, but their accuracy will certainly improve as more data becomes available. At best, the data we had in hand is representative of the true situation, and our conclusions would be unchanged by using a more complete data set. At worst, there is a bias in the available data that makes our conclusions significantly misleading. We believe that the data is not unreasonable and that conclusions based on it are correct enough to be valuable as the basis for discussion and future development. We do not believe that the values for the various statistics introduced below are precisely what they would be using the extra information, and we emphasize that they should always be considered in the context of this particular annotated data set [for a further detailed discussion of evaluating these predictions, see Birney and Durbin (2000)].

In the next section we describe the target genomic sequence and the auxiliary data, including a critical discussion of our standard sets. Methods gives a short

**Table 1.** Participating Groups and Associated Annotation Categories

| | Program name | Gene finding | Promoter recognition | EST/c DNA alignment | Protein similarity | Repeat | Gene function |
|---|---|---|---|---|---|---|---|
| Mural et al. Oakridge, US | GRAIL | X | | X | | | X |
| Parra et al. Barcelona, ES | GeneID | X | | | | | |
| Krogh Copenhagen, DK | HMMGene | X | | | | | |
| Henikoff et al. Seattle, US | BLOCKS | | | | X | | X |
| Solovyev et al. Sanger, UK | FGenes | X | | | | | |
| Gaasterland et al. Rockefeller, US | MAGPIE | X | X | X | | X | X |
| Benson et al. Mount Sinai, US | TRF | | | | | X | |
| Werner et al. Munich, GER | CoreInspector | | X | | | | |
| Ohler et al. Nuremberg, GER | MCPromoter | | X | | | | |
| Birney Sanger, UK | GeneWise | | | | X | | X |
| Reese et al. Berkeley/Santa Cruz, US | Genie | X | X | | | | |

description of existing annotation methods that complements other papers in this issue, including a review article of existing gene-finding methods by Stormo (2000) and papers describing the methods used by the individual participants. Results assesses the individual annotation methods and the Conclusions discusses what the experiment revealed about issues involved in annotating complete genomes. An article by Ashburner (2000) provides a biological perspective on the experiment.

### Data: The Benchmark Sequence: The *Adh* Region in *D. melanogaster*

The selection of a genomic target region for assessing the accuracy of computational genome annotation methods was a difficult task for several reasons: The genomic region had to be large enough, the organism had to be well studied, and enough auxiliary data had to be available to have a good experimentally verified "correct answer," but the data should be anonymous so that a blind test would be possible. The *Adh* region of the *D. melanogaster* genome met these criteria. *D. melanogaster* is one of the most important model organisms, and although the *Adh* region had been extensively studied, the best gene annotations and cDNAs for the region were not published until after the conclusion of the GASP experiment. The 2.9 Mb *Adh* contig was large enough to be challenging, contained genes with a variety of sizes and structures, and included regions of high and low gene density. It was not a completely blind test, however, because several cDNA and genomic sequences for known genes in the region were available prior to the experiment.

#### *Genomic DNA Sequence*

The contiguous genomic sequence of the *Adh* region in the *D. melanogaster* genome spans nearly 3 Mb and has been sequenced from a series of overlapping P1 and BAC clones as a part of the Berkeley Drosophila Genome Project (BDGP; Rubin et al. 1999) and the European Drosophila Genome Project (EDGP; Ashburner et al. 1999c). This sequence is believed to be of very high quality with an estimated error rate of <1 in 10,000 bases, based on PHRAP quality scores. A detailed analysis of this region can be accessed through the BDGP Web site (http://www.fruitfly.org/publications/Adh.html) as well as in Ashburner et al. (1999b).

#### *Curated Training Sequences*

We provided several *D. melanogaster*-specific data sets to the GASP participants. This enabled participants to tune their tools for *Drosophila* and facilitated a comparison of the various approaches that was unbiased by organism-specific factors. The following curated sequence sets, extracted from Flybase and EMBL (provided by the EDGP at Cambridge and provided by the BDGP, were made available and can be found at http://www.fruitfly.org/GASP/data/data.html): (1) A set of complete coding sequences (start to stop codon), excluding transposable elements, pseudogenes, noncoding RNAs, and mitochondrial and viral sequences (2122 entries); (2) nonredundant set of repetitive sequences, not including transposable elements (96 entries); (3) transposon sequences, containing only the longest sequence of each transposon family and excluding defective transposable elements (44 entries); (4) genomic DNA data from 275 multi- and 141 single-exon nonredundant genes together with their start and stop codons and splice sites, taken from GenBank version 109; (5) a set of 256 unrelated promoter regions, taken from the Eukaryotic Promoter Database (EPD; Cavin Périer et al. 1999, 2000) and a collection made by Arkhipova (1995); and (6) an uncurated set of cDNA and EST sequences from work in progress at the BDGP. Five of the 12 participating groups reported making use of these data sets.

#### *Resources for Assessing Predictions: The "Correct" Answer*

In a comparative study, the gold standard used to evaluate solutions is the most important factor in determining the usefulness of the study's results. For the results to be meaningful, the standard must be appropriate and correct in the eyes of the study's audience. Because our goal was to evaluate tools that predict genes and gene structure in complex eukaryotic organisms, we drew our standard from a complex eukaryotic model organism, choosing to work with a 2.9-Mb sequence contig from the *Adh* region of *D. melanogaster*. Comparing predicted annotations in such a region is only consequential if the standard is believed to be correct, if that correctness has been established by techniques that are independent of the approaches being studied, and if the predictors had no prior knowledge of the standard. Ideally, it would contain the correct structure of all the genes in the region without any extraneous annotations. Unfortunately, such a set is impossible to obtain because the underlying biology is incompletely understood. We built a two-part approximation to the perfect data set, taking advantage of data from the BDGP cDNA sequencing project (http://www.fruitfly.org/EST) and a *Drosophila* community effort to build a set of curated annotations for this region (Ashburner et al. 1999b). Our first component, known as the std1 data set, used high-quality sequence from a set of 80 full-length cDNA clones from the *Adh* region to provide a standard with annotations that are very likely to be correct but certainly are not exhaustive. The second component, known as the std3 data set, was built from the annotations being developed for Ashburner et al.(1999b) to give a standard with more complete coverage of the region, although with less confidence about the accuracy and independence of the annotations. We believe that this two-part approxi-

mation allows us to draw useful conclusions about the ability to accurately predict gene structure in complex eukaryotic organisms even though the absolutely perfect data set does not exist.

Eukaryotic transcript annotations have complex structures based on the composition of fundamental features such as the TATA box and other transcription factor binding sites, the transcription start site (TSS), the start codon, 5′ and 3′ splice site boundaries, the stop codon, the polyadenylation signal, exon start and end positions, and coding exon start and end positions. Our gene prediction evaluations focused on annotations that are specific to the coding region, from the start codon through the various intron–exon boundaries to the stop codon, and on promoter annotations. Although other types of features are also biologically interesting, we were unable to devise reliable methods for evaluating their predictions. Whenever possible, we relied on unambiguous biological evidence for our evaluations; when that was not available, we combined several types of evidence curated by domain experts.

Our goal for our first standard set, called std1, was to build a set of annotations that we believed were very likely to be correct in their fine details (e.g., exact locations for splice sites), even if we were unable to include every gene in the region. We based std1 on alignments of 80 high-quality, full-length cDNA sequences from this region with the high-quality genomic sequence for the contig. The cDNA sequences are the product of a large cDNA sequencing project at the BDGP and had not been submitted to GenBank at the time of the experiment. Working from five cDNA libraries, the longest clone for each unique transcript was selected and sequenced to a high-quality level. Starting with these cDNA sequences, we generated alignments to the genomic sequence using `sim4` (Florea et al. 1998) and filtered them on several criteria. Of the 80 candidate cDNA sequences, 3 were paralogs of genes in the *Adh* region and 19 appeared to be cloning artifacts (unspliced RNA or multiple inserts into the cloning vector), leaving us with alignments for 58 cDNA clones. These alignments were further filtered based on splice site quality. We required that all of the proposed splice sites include a simple "GT"/"AG" core for the 5′ and 3′ splice sites, respectively, and that they scored highly (5′ splice sites $\geq 0.35$ threshold, which gives a 98% true positive rate, and 3′ splice sites $\geq 0.25$, which gives a 92% true positive rate) using a neural network splice site predictor trained on *D. melanogaster* data (Reese et al. 1997). This process left us with 43 sequences from the *Adh* region for which we had structures confirmed by alignments of high-quality cDNA sequence data with high-quality genomic data and by the fit of their splice sites to a *Drosophila* splice site model. Of these 43 sequences, 7 had a single coding exon and 36 had multiple coding exons. We added start codon and stop codon annotations to these structures from the corresponding records in the std3 data set.

After the experiment, we recently discovered four inconsistent genes in the std1 data set. For two genes (*DS07721.1*, *DS003192.4*), the cDNA clones (CK02594, CK01083, respectively) are likely to be untranscribed genomic DNA that was inappropriately included in the cDNA library. Two other genes from std3 (*DS00797.5* and *wb*) were incorrectly reported in std1 as three partial all incomplete EST alignments (cDNA clones: CK01017, LD33192, and CK02229). In keeping with std1's goal of highly reliable annotations, all four sequences have been removed from the std1 data set that is currently available on the GASP web site. The results reported here use the larger, less reliable, data set as presented at the ISMB-99 tutorial.

The complete set of the original 80 aligned high-quality, full-length cDNA sequences was named std2. This set was never used in the evaluation process because it did not add any further compelling information or conclusions because of the unreliable alignments.

Our goal for the second, used standard set, called std3, was to build the most complete set of annotations possible while maintaining some confidence about their correctness. Ashburner et al. (1999b) compiled an exhaustive and carefully curated set of annotations for this region of the *Drosophila* genome based on information from a number of sources, included `BLASTN`, `BLASTP` (Altschul et al. 1990), and `PFAM` alignments (Sonnhammer et al. 1997, 1998; Bateman et al. 2000), high scoring `GENSCAN` (Burge and Karlin 1997) and `Genefinder` (P. Green, unpubl.) predictions, `ORFFinder` results (E. Friese, unpubl.), full-length cDNA clone alignments (including those used in std1), and alignments with full-length genes from GenBank. This set included 222 gene structures: 39 with a single coding exon and 183 with multiple coding exons. Of these 222 gene structures, 182 are similar to a homologous protein in another organism or have a *Drosophila* EST hit. For these structures, the intron–exon boundaries were verified by partial cDNA/EST alignments using `sim4` (Florea et al. 1998), homologies were discovered using `BLASTX`, `TBLASTX`, and `PFAM` alignments, and gene structure was verified using a version of `GENSCAN` trained for finding human genes. Of the 54 remaining genes, 14 had EST or homology evidence but were not predicted by `GENSCAN` or `Genefinder`, and 40 were based entirely on strong `GENSCAN` and `Genefinder` predictions. All of this evidence was evaluated and edited by experienced *Drosophila* biolo gists, resulting in a protein coding gene data set that exhaustively covers the region with a high degree of confidence and represents their view of what should or

should not be considered an annotated gene. Their gene data set excluded the 17 found transposable elements [6 LINE-like elements (*G*, *F*, *Doc*, and *jockey*) and 11 retrotransposons with long terminal repeats (LTRs; *copia*, *roo*, *297*, *blood*, *mdg1*-like, and *yoyo*)], which almost all contain long ORFs. Some of these ORFs code for known and some others for, so far, unknown protein sequences.

Both of these data sets have shortcomings. As mentioned above, std1 only includes a subset of the genes in the region. It also includes a pair of transcripts that represent alternatively spliced products of a single gene. Although this is not incorrect, it confounds our scoring process. Because the cDNA alignments do not provide any evidence for the location of the start and stop codons, we based those annotations in std1 on information from the std3 set. Many of the gene structures in std3 are based on `GENSCAN` and `Genefinder` predictions without other supporting evidence, so it is possible that the fine details are incorrect, that the entries are not entirely independent of the techniques used by the predictors in the experiment, and that the set overestimates the number of genes in the region.

See Birney and Durbin (2000) and Henikoff and Henikoff (2000) for further discussion of the difficulties of evaluating these predictions especially in the protein homology annotation category, in which, by training, these programs will recognize protein-like sequences such as the ORFs in transposable elements as genes. They and others (see other GASP publications in this issue) have raised the issues of annotation oversights, transposons, and pseudogenes. In cases where GASP submissions suggest a missed annotation, this information has been passed onto biologists for further research, including screening cDNA libraries. We believe that it would have been biased to retroactively change the scoring scheme used at the GASP experiment based solely on missed annotations discovered by the participant's submissions. See Discussion for an example of an annotation that may be missing in the standard data sets. In the std3 data set we based our standard for what is or is not a *Drosophila* gene on the expert annotations provided by Ashburner et al. (1999b). It is clear that both transposons and pseudogenes are genuine features of the genome and that gene-finding technologies might recognize them. Because they were not included as coding genes in the expert annotations, we decided against including them in the standard set.

Building a set for the evaluation of transcription start site or, more generally, for promoter recognition proved to be even more difficult. For the genes in the *Adh* region almost no experimentally confirmed annotation for the transcription start site exists. As the 5′ UTR regions in *Drosophila* can extend up to several kilobases, we could not simply use the region directly upstream of the start codon. To obtain the best possible approximation, we took the 5′ ends of annotations from Ashburner et al. (1999b) where the upstream region relied on experimental evidence (the 5′ ends of full-length cDNAs) and for which the alignment of the cDNA to the genomic sequence included a good ORF. The resulting set contained 92 genes of the 222 annotations in the std3 set (Ashburner et al. 1999b). This number is larger than the number of cDNAs used for the construction of the std1 set described above because we included cDNAs that were already publicly available. The 5′ UTR of these 96 genes has an average length of 1860 bp, a minimum length of 0 bp (when the start codon was annotated at the beginning, due to the lack of any further cDNA alignment information; this is very likely to be only a partial 5′ UTR and therefore an annotation error), and a maximum length of 36,392 bp.

### *Data Exchange Format*

One of the challenges of a gene annotation study is finding a common format in which to express the various groups' predictions. The format must be simple enough that all of the groups involved can adapt their software to use it and still be rich enough to express the various annotations.

We found that the `General Feature Format` (`GFF`) (formerly known as the `Gene Feature Finding format`) was an excellent fit to our needs. The `GFF` format is an extension of a simple *name*, *start*, *end* record that includes some additional information about the sequence being annotated: the source of the feature; the type of feature; the location of the feature in the sequence; and a score, strand, and frame for the feature. It has an optional ninth field that can be used to group multiple predictions into single annotations. More information can be found at the `GFF` web site: http://www.sanger.ac.uk/Software/formats/GFF/. Our evaluation tools used a `GFF` parser for the `PERL` programming language that is also available at the `GFF` web site.

We found that it was necessary to specify a standard set of feature names within the `GFF` format, for instance, declaring that submitters should describe coding exons with the feature name CDS. We produced a small set of example files (accessible from the GASP web site) that we distributed to the submitters and were pleased with how easily we were able to work with their results.

## METHODS

Genome annotation is an ongoing effort to assign functional features to locations on the genomic DNA sequence. Traditionally, most of these annotations record information about an organism's genes, including protein-coding regions, RNA genes, promoters, and other gene regulatory elements, as well

as gene function. In addition to these gene features, the following general genome structure features are also commonly annotated: repetitive elements and general A, C, G, T content measures (e.g., isochores).

## Genome Annotation Classes

Although the GASP experiment invited and encouraged any class of annotations, most submissions were for gene-related features, emphasizing ab initio gene predictions and promoter predictions. In addition, two groups submitted functional protein domain annotations, and two groups submitted repeat element annotations. In the sections that follow, we categorize and discuss the submitted predictions.

### *Gene Finding*

Protein coding region identification is a major focus of computational biology. A separate article in this issue (Stormo 2000) discusses and compares current methods, whereas an early paper by Fickett and Tung (1992) and a more recent review of gene identification systems by Burge and Karlin (1998) give excellent overviews of the field. Table 2 lists the six groups that predicted protein-coding regions with the corresponding program names. It also categorizes the submissions based on the types of information used to build the model for predictions. Although all groups used statistical information for their models—predominantly coding bias, coding preference, and consensus sequences for start codon, splice sites, and stop codons—only two groups used protein similarity information or promoter information to predict gene structure. More than half of the groups incorporated sequence information from cDNA sequences. In general, state-of-the-art gene prediction systems use complex models that integrate multiple gene features into a unified model.

### *Promoter Prediction*

The complicated nature of the transcription initiation process makes computational promoter recognition a hard problem. We define promoter prediction as the identification of TSSs of protein coding genes that are transcribed by eukaryotic RNA polymerase II. A detailed description of the structure of promoter regions and existing promoter prediction systems is beyond the scope of this paper. Fickett and Hatzigeorgiou (1997) provide an excellent review of the field.

We can broadly identify three different approaches to promoter prediction, with at least one GASP submission in each category. The first class consists of "search by signal" programs, which identify single binding sites of proteins involved in transcription initiation or combinations of sites to improve the specificity. The program `CoreInspector` by Werner's group (M. Scherf, A. Klingenhoff, and T. Werner, in prep.) belongs to this category and searches for co-occurrences of two common binding sites within the core promoter (the core promoter usually denotes the region where the direct contact between the transcription machinery, the holoenzyme of the transcription complex, and the DNA takes place). The second class is often termed "search by content," as programs within this group do not rely on specific signals but take the more general approach of identifying the promoter region as a whole, frequently based on statistical measures. Sometimes the promoter is split into several regions to obtain more accurate statistics. The `MCPromoter` program (Ohler et al. 1999) is a member of this second group. In comparison with the signal-based group, the content-based systems usually are more sensitive but less specific. The third class can be described as "promoter prediction through gene finding." Simply using the start of a gene prediction as a putative TSS can be very successful if the 5′ UTR region is not too large. This approach can be improved by including similarity to EST sequences and/or a promoter module in the statistical systems used for gene prediction. The TSS predictions submitted by the participants of the `MAGPIE` and the `Genie` groups belong to this last class.

The notorious difficulty of the problem itself is exacerbated by the limited amount of existing reliably annotated training material. The experimental mapping of a TSS is a laborious process and is therefore not routinely carried out, even if the gene itself is studied extensively. So, both training the models and evaluating the results is a difficult task, and the conclusions we draw from the results must be considered with much caution.

### *Repeat Finders*

Detecting repeated elements plays a very important role in modeling the three-dimensional structure of a DNA molecule, specifically, the packing of the DNA in the cell nucleus. It is believed that the packing of the DNA around the nucleosome is correlated with the global sequence structure produced predominantly by repetitive elements. Repeats also play a major role in evolution (for review, see Jurka 1998). Two groups, Gary Benson [tandem repeats finder v. 2.02 (`TRF`; Benson 1999)] and the `MAGPIE` team using two programs `Calypso` (D. Field, unpubl.) and `REPuter` (Kurtz and Schleiermacher 1999) submitted repetitive sequence annotations. `TRF` (Benson 1999) locates approximate tandem repeats (i.e., two or more contiguous, approximate copies of a pattern of nucleotides) where the pattern size is unspecified but falls within the range from 1 to 500 bases. The `Calypso` program (D. Field, unpubl.) is an evolutionary genomics program. Its primary function is to find repetitive regions in DNA and protein sequences that have higher than average mutation rates. The `REPuter` program (Kurtz and Schleiermacher 1999) determines repeats of a fixed preselected length in complete genomes.

**Table 2.** Gene-Finding Submissions

| | Program name | Statistics | Promoter | EST/cDNA alignment | Protein similarity |
|---|---|---|---|---|---|
| Mural et al. (Oakridge, US) | `GRAIL` | X | | X | |
| Guigó et al. (Barcelona, ES) | `GeneID` | X | | | |
| Krogh (Copenhagen, DK) | `HMMGene` | X | | X | X |
| Solovyev et al. (Sanger, UK) | `FGenes` | X | | | |
| Gaasterland et al. (Rockefeller, US) | `MAGPIE` | X | X | X | |
| Reese et al. (Berkeley/Santa Cruz, US) | `Genie` | X | X | X | X |

### *Protein Homology Annotation*

Homologies to gene sequences from other organisms can often be used to identify protein-coding regions in anonymous genomic sequence. In addition to the location, it is often possible to infer the function of the predicted gene based on the function of the homologous gene in the other organism or of a known structural and functional protein element in the gene. Whereas the tools in the gene prediction category and the EST/cDNA alignment category are usually intended to determine the exact structure of a gene, the protein homology-based tools are usually optimized to find conserved parts of the sequence without worrying about the exact gene structure. Traditionally, this area of genome annotations has been dominated by the suite of local alignment search tools of BLAST (Altschul et al. 1990) and more global search tools such as FASTA (Pearson and Lipman 1988). Recent reviews in this area include Agarwal and States (1998), Marcotte et al. (1999), and Pearson (1995).

In the GASP experiment, two groups specializing in functional protein domain or motif identification in genomic DNA submitted annotations. The Henikoff group found hits to the BLOCKS+ database (http://blocks.fhcrc.org), a database consisting of conserved protein motifs (Henikoff and Henikoff 1994; Henikoff et al. 1999a). The second group in this category submitted results from the GeneWise program (Birney 1999). This program searches genomic DNA against a comprehensive hidden Markov model (HMM)-based library (PFAM; Sonnhammer et al. 1997, 1998; Bateman et al. 2000) of protein domains. Both programs look for conserved regions by searching translated DNA against a representation of multiple aligned sequences. Whereas in BLOCKS+ the multiple protein alignments consist of sets of ungapped regions, the GeneWise program searches against a gapped alignment. Both methods will turn up distantly related sequences.

### *EST/cDNA Alignment*

Computational predictions of gene location and structure go hand in hand with EST/cDNA sequencing and alignment techniques for building transcript annotations in genomic sequence. Either can be used as a discovery tool, with the other held in reserve for verification. A researcher can verify the existence and structure of predicted genes by sequencing the corresponding mRNA molecules and aligning their sequences to the original genomic sequence. Alternatively, one can start with an EST or cDNA sequence and build an alignment to the genomic sequence that has been guided and/or verified by tools from the gene prediction arsenal, for example, using likely splice site locations and checking for long ORFs and potential frame shifts.

There are many tools for aligning sequences. Although they have generally been specialized for aligning sequences that are evolutionarily related, some are designed for niche applications such as recognizing overlaps among sequencing runs. Aligning EST/cDNA sequences to the original genomic sequence also presents a unique set of tradeoffs and issues. In some cases (interspecies EST/genomic alignments), these tools must model evolutionary changes in the sequence. Sometimes (e.g., for low-quality EST sequences), they need to model errors in the sequence generated by the sequencing process. For multiexon genes, they need to model the intron regions as cost-free gaps tied to a model for recognizing splice sites. Several tools have been developed for this task: Mott (1997) and Birney and Durbin (1997) describe dynamic programming approaches that include models of splice sites and intron gaps. Florea et al. (1998) describe sim4, a heuristic tool that performs as well as the dynamic programming approaches and is efficient enough to support searching of large databases of genomic sequence.

Using cDNA clones and their sequences to build transcript annotations requires a variety of operations. The tools discussed above align the cDNA sequences to the genomic sequence, but steps must be taken to filter out clones that are merely paralogs of genes in the sequence and to recognize and handle various laboratory artifacts. If the clones represent short ESTs, then a likely annotation can be built by assembling a consistent model from their individual alignments. Longer ESTs or cDNAs might generate several similar alignments, and an automated tool must be able to select the most biologically meaningful variant. Although there are some gene prediction tools that can use information about homologies to known genes or ESTs, and most large-scale sequencing centers have some automated sanity checking for their database search results, there are not any tools that automate the production of transcript annotations from cDNA sequences.

### *Gene Function*

Gene function predictions are the most difficult annotations to produce and to evaluate. Current technologies use similarity to proteins (or protein domains) with known function to predict functional domains in genomic sequence. Although some tools use simple sequence alignments, more powerful tools have developed significantly more sensitive models.

It quickly became apparent that a consistent and correct assessment of function predictions as part of the GASP experiment was not possible because of the incomplete understanding of the protein products encoded by the 222 genes in the *Adh* region.

## Evaluating Gene Predictions

An ideal gene prediction tool would produce annotations that were exactly correct and entirely complete. The fact that no existing tool has these characteristics reflects our incomplete understanding of the underlying biology as well as the difficulty to build adequate gene models in a computer. Although no tool is perfect, each tool has particular strengths and weaknesses, and any performance evaluation should be in the context of an intended use. For example, researchers who are interested in identifying gene-rich regions of a genome for sequencing would be happy with a tool that successfully recognizes a gene's approximate location, even if it incorrectly described splice site boundaries. On the other hand, someone trying to predict protein structures is more interested in getting a gene's structure exactly right than in a tool's ability to predict every gene in the genome.

When assessing the accuracy of predictions, each prediction falls into one of four categories. A true-positive (TP) prediction is one that correctly predicts the presence of a feature. A false-positive (FP) prediction incorrectly predicts the presence of a feature. A true-negative (TN) prediction is correct in not predicting the presence of a feature when it isn't there. A false-negative (FN) prediction fails to predict the existence of a feature that actually exists. The sensitivity (Sn) of a tool is defined as TP / (TP + FN) and can be thought of as a measure of how successful the tool is at finding things that are really there. The specificity (Sp) of a tool is defined as TP / (TP + FP) and can be thought of as a measure of how careful a tool is about not predicting things that aren't really there. Burset and Guigó (1996) also use a correlation coefficient and an average

correlation coefficient. We chose not to use these measures because they depend on predictors' TN information, and we recognize that our evaluation sets were constructed in such a way that the TN information is not trustworthy. These Sn and Sp metrics are used for evaluating the submissions in the gene-finding, promoter recognition, and gene identification using protein homology categories. In the gene finding category, they are used for all three levels: base level, exon level, and gene level. In the protein homology category, they are used for base level and gene level only.

In one of the first reviews of gene prediction accuracy, Fickett and Tung (1992) developed a method that measured predictors' ability to correctly recognize coding regions in genomic sequence. They used their method to compare published techniques and concluded that in-frame hexamer counts were the most accurate measure of a region's coding potential. Burset and Guigó (1996) recognized that there are a wide variety of uses for gene predictions and developed measures—including base level, exon level, and gene level Sp and Sn—that describe a predictor's suitability for a particular task.

#### *Base Level*

The base level score measures whether a predictor is able to correctly label a base in the genomic sequence as being part of some gene. It rewards predictors that get the broad sweeps of a gene correct, even if they don't get the details such as the splice site boundaries entirely correct. It penalizes predictors that miss a significant portion of the coding sequence, even if they get the details correct for the genes they do predict. We used the Sn and Sp measures defined above as the measures of success in this category.

#### *Exon Level*

Exon level scores measure whether a predictor is able to identify exons and correctly recognize their boundaries. Being off by a single base at either end of the exon makes the prediction incorrect. Because we only considered coding exons in our assessment, the first exon is bracketed by the start codon and a 5′ splice site, the last exon is bracketed by a 3′ splice site and the stop codon, and the interior exons are bracketed by a pair of splice sites. As measures of success in this category, we used two statistics in addition to Sn and Sp. The missed exon (ME) score is a measure of how frequently a predictor completely failed to identify an exon (no prediction overlap at all), whereas the wrong exon (WE) score is a measure of how frequently a predictor identifies an exon that has no overlap with any exon in the standard sets. The ME score is the percentage of exons in the standard set for which there were no overlapping exons in the predicted set. Similarly, the WE score is the percentage of exons in the predicted set for which there were no overlapping exons in the standard set.

#### *Gene Level*

Gene level Sn and Sp measure whether a predictor is able to correctly identify and assemble all of a gene's exons. For a prediction to be counted as a TP, all of the coding exons must be identified, every intron–exon boundary must be exactly correct, and all of the exons must be included in the proper gene. This is a very strict measure that addresses a tool's ability to perfectly identify a gene. In addition to the Sn and Sp measures based on absolute accuracy, we used the missed genes (MG) score as a measure of how frequently a predictor completely missed a gene (a standard gene is considered missed if none of its exons are overlapped by a predicted coding gene) and the wrong genes (WG) score as a measure of how frequently a predictor incorrectly identified a gene (a prediction is considered wrong if none of its exons are overlapped by a gene from the standard set).

#### *Split and Joined Genes*

The exon level scores discussed above measure how well a predictor recognizes exons and gets their boundaries exactly correct. The gene level scores measure how well a predictor can recognize exons and assemble them into complete genes. Neither of these scores directly measures a predictor's tendency to incorrectly assemble a set of predicted exons into more or fewer genes than it should. We developed two new measures, split genes (SG) and joined genes (JG), which describe how frequently a predictor incorrectly splits a gene's exons into multiple genes and how frequently a predictor incorrectly assembles multiple genes' exons into a single gene. Because the coverage of the std1 data set is so incomplete, we have only included SG and JG scores from the comparison with std3. A gene from the standard set is considered split if it overlaps more than one predicted gene. Similarly, a predicted gene is considered joined if it overlaps more than one gene in the standard set. The SG measure is defined as the sum of the number of predicted genes that overlap each standard gene divided by the number of standard genes that were split. Similarly, the JG measure is the sum of the number of standard genes that overlap each predicted gene divided by the number of predicted genes that were joined. A score of 1 is perfect and means that all of the genes from one set overlap exactly one gene from the other set.

#### *Application of These Measures to Correct Answer Data Sets std1/std3*

We built the std1 data set in such a way that we believe it is correct in the details of the genes that it describes, though we know that it only includes a small portion of the genes in the region. The std3 data set, on the other hand, is as complete as was possible but does not have rigorous independent evidence for all of its annotations. For the std1 data set, we believe that the TP count (it was predicted, and it exists in the standard) and FN count (it was not predicted, but it does exist in the standard) are reliable because of the confidence that we have in the correctness of the predictions in the set. On the other hand, we do not believe that the TN count (it was not predicted, and it is not in the standard set) and FP count (it was predicted, but is not in the standard set) are reliable because they both assume that the standard correctly describes the absence of a feature and we know that there are genes missing from std1. It follows that we believe that Sn is meaningful for std1 because it only depends on TP and FN but that we are less confident about the Sp score because it depends on TP and FP. A similar logic applies to the std3 data set, where our confidence in the set's completeness but not its fine details suggests that the TP and FP scores are usable but that the TN and FN scores are not. This means that for std3, we believe that the Sp measure can be used to describe a predictor's performance but that Sn is likely to be misleading.

### Evaluation of Promoter Predictions

We adopted the measures proposed by Fickett and Hatzigeorgiou (1997). They evaluated the success of promoter predictions by giving the percentage of correctly identified TSSs versus the FP rate. A TSS is regarded as identified if a program makes one or more predictions within a certain "likely" region around the annotated site. The FP rate is defined as the

number of predictions within the "unlikely" regions outside the likely regions divided by the total number of bases contained in the unlikely set. As our annotation of the TSS is only preliminary and not experimentally confirmed, we chose a rather large region of 500 bases upstream and 50 bases downstream of the annotated TSS as the likely region. The upstream region is always taken as the likely region, even if it overlaps with a neighboring gene annotation on the same strand. The unlikely region for each gene then consists of the rest of the gene annotation, from base 51 downstream of the TSS to the end of the final exon.

### Visualization of the Annotations

Generating "good" annotations generally requires integrating multiple sources of information, such as the results of various sequence analysis tools plus supporting biological information. Visualization tools that display sequence annotations in a browsable graphical framework make this process much more efficient. In this experiment we found that visualization tools are essential to evaluate the genome annotation submissions. When annotations are displayed visually, overall trends become apparent, for example, gene-rich versus gene-poor regions, genes that were predicted by most participants versus those that were predicted by few. Additionally, as we discuss below, a visualization tool that is capable of displaying annotations at multiple levels of detail provides a way to examine individual predictions in detail.

Building genome annotation visualization tools is a daunting task. Many such tools have been developed, starting with ACeDB (Eeckman and Durbin 1995; Stein and Thierry-Mieg 1998). We were fortunate in that the BDGP has built a flexible suite of genome visualization tools (Helt et al. 1999) that could be extended to display the GASP submissions. We adapted the BDGP's annotated clone display and editing tool, `CloneCurator` (Harris et al. 1999), which is based on a genomic visualization toolkit (Helt et al. 1999), to read the annotation submissions in `GFF` format and display each team's predictions in a unique color and location.

`CloneCurator` (see Fig. 1) displays features on a sequence as colored rectangles. Features on the forward strand appear above the axis, whereas those on the reverse strand appear below the axis. The display can be zoomed and scrolled to view areas of interest in more detail. A configuration file identifies the feature types that are to be displayed and assigns colors and offsets to each one. For example, the std1 and std3 exons appear in yellow and orange close to the central axis.

## RESULTS

The results of an experiment such as GASP are only meaningful if enough groups participate. We were fortunate to have 12 diverse groups involved, and we were very grateful for the speed with which they were able to submit their predictions. We believe that these 12 groups provide a fair representation of the state of the art in annotation system technology. We collected submissions by electronic mail and evaluated them using the std1 and std3 data sets as described above. Before releasing our results at the Intelligent Systems in Molecular Biology conference in August 1999 in Heidelberg, Germany, we assembled a team of independent assessors (Ashburner et al. 1999a) to review our techniques and conclusions. As discussed in the introduction, the accuracy of the various measures discussed below depends heavily on how well our standard sets capture the true set of features in the region. These values should only be considered in the context of the standard data sets.

A detailed description of the results and the evaluation techniques we used can be accessed through the GASP homepage at http://www.fruitfly.org/GASP/.

### Gene Finding

Table 3 summarizes the performance of the gene-finding tools using the measures defined above. Three groups submitted multiple submissions. The first group, `Fgenes1`, `Fgenes2`, and `Fgenes3`, submitted three predictions at varying stringency (for details, see Salamov and Solovyev 2000). For the `GeneID` program, two submitted versions are presented, version 1 (`GeneID v1`) being the original submission and version 2 (`GeneID v2`) being a newer submission from a corrected version of the original program (for details, see Parra et al. 2000). The third group with multiple submissions used three versions of the `Genie` program: the first a pure statistical approach (`Genie`), the second including EST alignment information (`GenieEST`), and the third using protein homology information (`GenieESTHOM`) (for details, see Reese et al. 2000). For all other groups from Table 2, only one submission was evaluated. The following sections discuss the base level, exon level, and gene level performance of these submissions.

#### *Base Level Results*

Several gene prediction tools had a Sn of >0.95 at the base level. This suggests that current technology is able to correctly identify >95% of the *D. melanogaster* proteome. A few tools demonstrated a specificity of >0.90 at the base level, only infrequently labeling a noncoding base as coding. Generally, the tools have a higher Sn than Sp. Two programs, `Fgenes2` and `GeneID`, were designed to be conservative about their predictions and do not follow this trend.

#### *Exon Level Results*

There was a great deal of variability in the exon level scores. Several tools had Sn scores ~0.75, correctly identifying both exon boundaries ~75% of the time. Their Sps were generally much lower (the highest was 0.68), probably a reflection of the strict definition of exon level scores both splice sites had to be predicted correctly and possible inaccuracies in the std3 data set. The low ME scores (several <0.05) combined with the fairly high Sn suggest that several tools were successful at identifying exons but had trouble finding the correct exon boundaries. Programs that incorporate EST alignment information, such as `GenieEST` and `HMMGene`, had sensitivity scores that were up to 10% bet-

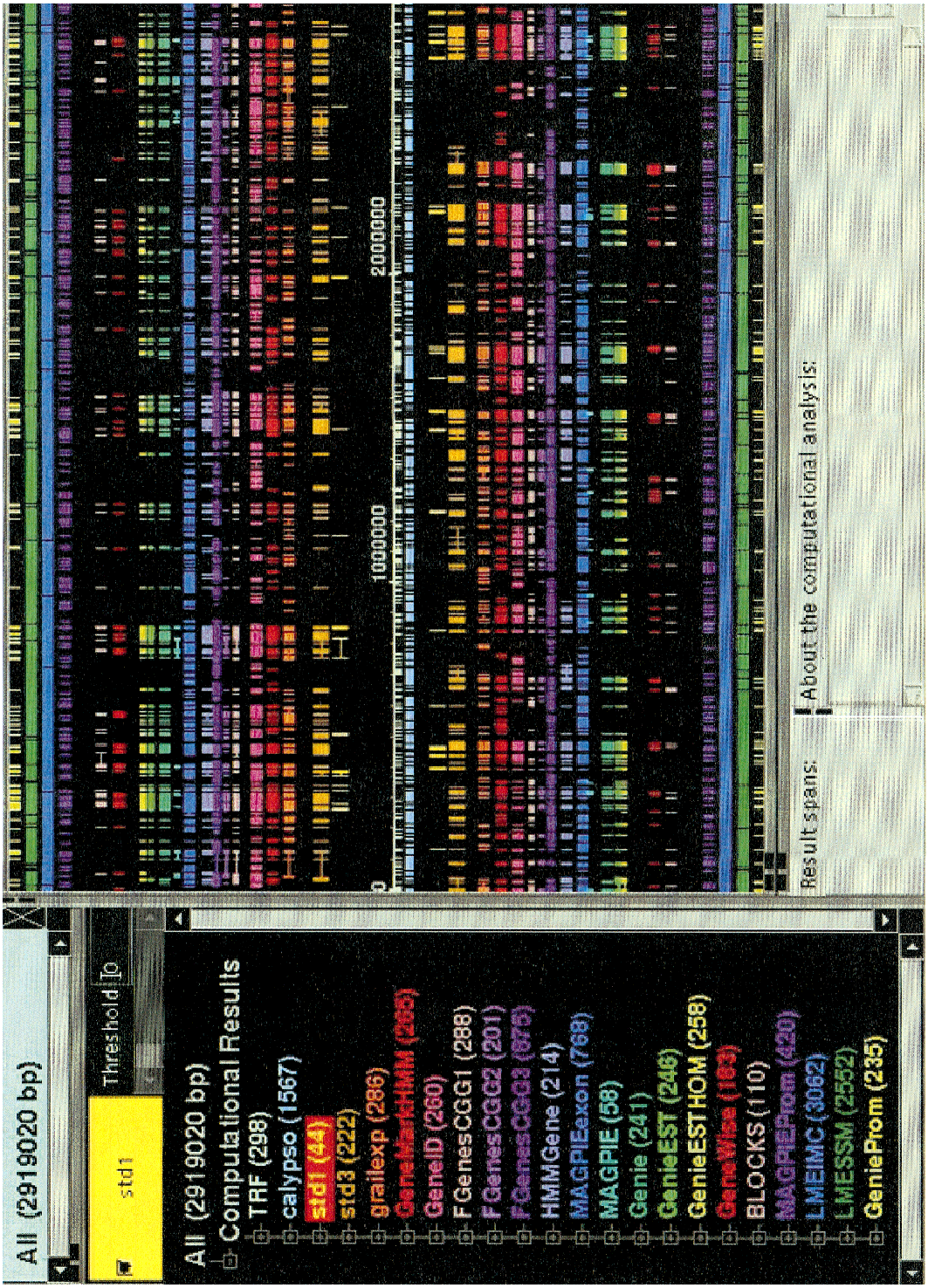


**Figure 1** (*See facing page for legend.*)

ter than the other tools. The high WE scores suggest either that the tools are overpredicting or that there are genes that are missing even from std3.

### *Gene Level Results*

All of the predictors had considerable difficulty correctly assembling complete genes. The best tools were able to achieve Sns between 0.33 and 0.44, meaning that they are incorrect over half of the time. This value seems to be very similar in *Drosophila* and human sequences, based on a recent analysis of the *BRCA2* region in human (T.J. Hubbard, pers. comm.). Even on the more complete std3 data set, the programs tended to incorrectly predict many genes. The very low MG score (as low as 4.6%) is reassuring because it suggests that several tools are able to recognize a gene, even if they have difficulty figuring out the exact details of its structure. Comparing the WG and MG measures suggests that existing tools tend to predict genes that do not exist more often than they miss genes that do exist. Because it is almost certain that there are real genes that are missing from both standard sets, this conclusion must be viewed with some skepticism. Although there were several tools with good SG or JG scores, none of them performed well in both categories.

## Promoter Prediction

Table 4 shows the performance of the promoter prediction systems, grouped by approach: search-by-signal, search-by-region, and gene prediction programs.

Gene-finding programs that include a prediction of the TSS obtained the best results. The number of false predictions made by the region-based programs is very high (giving them a low Sp), and because the signal-specific programs only identify one promoter, their Sn is very low. The high Sp of the gene finders is obviously due to the context information: All promoter predictions within gene predictions are ruled out in advance, and the location of the possible start codon provides the system with a good initial guess of where to look for a promoter. The `MAGPIE` system also uses EST alignments to obtain information on 5′ UTRs, which mirrors the way the std sets were constructed: Roughly one-third of the putative TSS assignments rely on cDNAs that were publicly available in GenBank. A closer look at the results reveals that the region-based programs have a Sn that is comparable with the gene finders and the signal based program had only a single FP, showing that both types of tools can be used for different applications.

Our data set, and the evaluation based on it, relies on the assumption that the 5′ ends of the full-length cDNAs are reasonably close to the TSS. This makes it very hard to draw strong conclusions from the pre-

**Figure 1** (*See facing page.*) Screen shot from the `CloneCurator` program (Harris et al. 1999), featuring the genome annotations of all 12 groups for the 2.9-Mb *Adh* region. The main panel shows the computational annotations on the forward (above axis) and reverse sequence strands (below axis). Genes located on the *top* half of each map are transcribed from distal to proximal (with respect to the telomere of chromosome are 2L); those on the *bottom* are transcribed from proximal to distal. Right below the axis are the two repeat finding results displayed, followed by reference sets from Ashburner et al. (1999b; std1 and std3), followed by the 12 submissions of gene-finding programs, followed by the two protein homology programs, and eventually, farthest away from the axis, the four promoter recognition programs. (*Left*) The color-coded legend for the program and the number of predictions made by the programs.

| Program identifier | Color | Reference |
|---|---|---|
| `TRF` | seafoam | Benson (1999) |
| `Calypso` | lightblue | D. Field (unpubl.) |
| `std1` | yellow | unpublished conservative alignment of cDNAs |
| `std3` | orange | Ashburner et al. (1999b) |
| `Grailexp` | red-orange | Uberbacher and Mural (1991) |
| `GeneMarkHMM` | red | Besemer and Borodovsky (1999) |
| `GeneID` | hotpink | Guigó et al. (1992) |
| `FGenesCGG1` | pink | Solovyev et al. (1995) |
| `FGenesCGG2` | magenta | Solovyev et al. (1995) |
| `FGenesCGG3` | purple | Solovyev et al. (1995) |
| `HMMGene` | cornflower | Krogh (1997) |
| `MAGPIEexon` | blue | Gaasterland and Sensen (1996) |
| `MAGPIE` | turquoise | Gaasterland and Sensen (1996) |
| `Genie` | seagreen | Reese et al. (1997) |
| `GenieEST` | green | Kupl et al. (1997) |
| `GenieESTHOM` | chartreuse | Kulp et al. (1997) |
| `GeneWise` | red | Birney (1999) |
| `BLOCKS` | pink | Henikoff et al. (1999b) |
| `MAGPIEProm` | purple | T. Gaasterland, (unpubl.) |
| `LMEIMC` | blue | Ohler et al. (1999) |
| `LMESSM` | dark green | Ohler et al. (2000) |
| `GeniePROM` | chartreuse | Reese (2000) |

**Table 3.** Evaluation of Gene-Finding Systems

| | | FGenes 1 | FGenes 2 | FGenes 3 | GeneID v1 | GeneID v2 | Genie | Genie EST | Genie ESTHOM | HMMGene | MAGPIE exon | GRAIL |
|---|---|---|---|---|---|---|---|---|---|---|---|---|
| Base level | Sn std1 | 0.89 | 0.49 | 0.93 | 0.48 | 0.86 | 0.96 | 0.97 | 0.97 | 0.97 | 0.96 | 0.81 |
| | Sp std3 | 0.77 | 0.86 | 0.60 | 0.84 | 0.83 | 0.92 | 0.91 | 0.83 | 0.91 | 0.63 | 0.86 |
| Exon level | Sn std1 | 0.65 | 0.44 | 0.75 | 0.27 | 0.58 | 0.70 | 0.77 | 0.79 | 0.68 | 0.63 | 0.42 |
| | Sp std3 | 0.49 | 0.68 | 0.24 | 0.29 | 0.34 | 0.57 | 0.55 | 0.52 | 0.53 | 0.41 | 0.41 |
| | ME (%) std1 | 10.5 | 45.5 | 5.6 | 54.4 | 21.1 | 8.1 | 4.8 | 3.2 | 4.8 | 12.1 | 24.3 |
| | WE (%) std3 | 31.6 | 17.2 | 53.3 | 47.9 | 47.4 | 17.4 | 20.1 | 22.8 | 20.2 | 50.2 | 28.7 |
| Gene level | Sn std1 | 0.30 | 0.09 | 0.37 | 0.02 | 0.26 | 0.40 | 0.44 | 0.44 | 0.35 | 0.33 | 0.14 |
| | Sp std3 | 0.27 | 0.18 | 0.10 | 0.05 | 0.10 | 0.29 | 0.28 | 0.26 | 0.30 | 0.21 | 0.12 |
| | MG (%) std1 | 9.3 | 34.8 | 9.3 | 44.1 | 13.9 | 4.6 | 4.6 | 4.6 | 6.9 | 4.6 | 16.2 |
| | WG (%) std3 | 24.3 | 24.8 | 52.3 | 22.2 | 30.5 | 10.7 | 13.0 | 15.5 | 14.9 | 55.0 | 23.7 |
| | SG | 1.10 | 1.10 | 2.11 | 1.06 | 1.06 | 1.17 | 1.15 | 1.16 | 1.04 | 1.22 | 1.23 |
| | JG | 1.06 | 1.09 | 1.08 | 1.62 | 1.11 | 1.08 | 1.09 | 1.09 | 1.12 | 1.06 | 1.08 |

The evaluation is divided into three categories: base level, exon level, and gene level. The different statistical features reported are Sn, Sp, ME, WE, MG, WG, SG, and JG. std1 and std3 indicate against which standard set the statistics are reported.

sented results. Even the most sensitive systems could identify only roughly one third of the start sites. This could of course be caused by the fact that the existing annotation is only an approximation and some of the true TSSs may be located further upstream. It also hints at the diversity of promoter regions that mirrors the possibilities for gene regulation and at the existing bias toward housekeeping genes in the current data sets used for the training of the models.

### Gene Identification Using Protein Homology

Gene-finding evaluation statistics, such as those described above, can be used to summarize the ability of a program to identify complete and accurate gene structures in genomic DNA. In Table 5 we have applied the same evaluation statistics to the homology-based search programs GeneWise and BLOCKS+. Because these programs are not optimized to deal with exact exon boundary assignments, Table 5 only shows the performance for the base level and the MG and WG.

The very low Sns at the base level are not surprising, because the programs identify only conserved protein motifs or particular domains and make no effort to predict complete genes. Sp, which should be high given that only conserved protein motifs are scored, was lower than expected. Detailed studies of these pre-

**Table 4.** Evaluation of Promoter Prediction Systems

| System name | Sensitivity | Rate of false-positive predictions in region[a] (853,180 bases) | Rate of predictions in region[b] (2,570,232 bases) |
|---|---|---|---|
| CoreInspector | 1 (1%) | 1/853,180 | 1/514,046 |
| MCPromoter v1.1 | 26 (28.2%) | 1/2,633 | 1/2,537 |
| MCPromoter v2.0 | 31 (33.6%) | 1/2,437 | 1/2,323 |
| GeniePROM | 25 (27.1%) | 1/14,710 | 1/28,879 |
| GenieESTPROM | 30 (32.6%) | 1/16,729 | 1/29,542 |
| MAGPIE | 33 (35.8%) | 1/14,968 | 1/16,370 |

We show the Sn for identified TSSs in comparison with the FP rate for non-TSS regions and general gene regions: [a]the unlikely region defined as the rest of the gene starting 51 bases downstream from its annotated TSS; [b]the general gene region, spanning from half the distance to the previous and next annotated genes including the annotated TSS (taken from the std3 annotation).

**Table 5.** Evaluation of Similarity Searching

| | | BLOCKS | GeneWise | MAGPIE cDNA | MAGPIE EST | Grail Similarity |
|---|---|---|---|---|---|---|
| Base level | Sn std1 | 0.04 | 0.12 | 0.02 | 0.31 | 0.31 |
| | Sp std3 | 0.80 | 0.82 | 0.55 | 0.32 | 0.81 |
| Gene level | MG (%) std1 | 62.7 | 69.7 | 95.3 | 27.9 | 41.8 |
| | WG (%) std3 | 12.9 | 14.1 | 0.0 | 44.3 | 7.4 |

Base and gene level statistics are shown. The base level is described using Sn and Sp, and the statistics for the gene level are given as MG and WG.

dictions (see Birney and Durbin 2000; Henikoff and Henikoff 2000) show that most of the FP predictions were hits to transposable elements or to possible genes that are missing in the standard sets. Both programs use a database of protein domains or conserved protein motifs. Both databases are large and are believed to contain at least 50% of the existing protein domains. The high number of MG, 62.7% for BLOCKS and 69.7% for GeneWise, means that these programs will miss a significant number of *Drosophila* genes when used to search genomic DNA directly. The WG scores of 12.9% BLOCKS and 14.1% for GeneWise are lower than the gene finding programs discussed in the previous section.

### Gene Identification Using EST/cDNA Alignments

It is believed that some cDNA information exists for approximately half of the genes in the *D. melanogaster* genome. This cDNA database (available as the EST data set at the GASP web site) was used as a basis for the cDNA/EST alignment category. The Sn of 31% for MAGPIEEST and GrailSimilarity (Table 5) implies that the coding portion of the available EST data currently covers one-third of the genome's coding sequence. The low Sp is very surprising and suggests that the EST/cDNA alignment problem is not a trivial one. The only program that tried to align complete cDNAs to genomic DNA, MAGPIEcDNA, could find complete cDNAs for only 2.4% of the genes. EST alignments also resulted in high numbers of missed genes, suggesting that the EST libraries are biased toward highly expressed genes. The high WG scores suggest that some genes are missing even from std3.

### Selected Gene Annotations

The summary statistics discussed above only provide a global view of the predicting programs' characteristics. A much better understanding of how the various approaches behave can be obtained by looking at individual gene annotations. Such a detailed examination can also help identify issues that are not addressed by current systems.

In the following paragraphs we will discuss a few interesting examples. Figure 1 shows the color codes of the participating groups that are used throughout this section. Genes located on the top of each map are transcribed from distal to proximal (with respect to the telomere of chromosome arm 2L); those on the bottom are transcribed from proximal to distal. std1 and std3 are the expert annotations described in Ashburner et al.(1999b). Just below the axis, you can see the annotations for the two repeat finding programs. These have no sequence orientation and are therefore only shown on one side. Farther away from the axis, after std1 and std3, we grouped all of the ab initio gene-finding programs together. Next to the gene finders are the homology-based annotations. On the bottom and the top of the figure we show the three promoter annotations, but for clarity we did not include these annotations in the subsequent figures. (On the front page and in the legend of Fig. 1, you can see the full set of annotations of all programs, which are also accessible from the GASP web site.)

Our first example is a "busy" region with 12 complete genes and 1 partial gene in a stretch of only 40 kb (Fig. 2A). This region is located at the 3′ end of the *Adh* region from base 2,735,000 to base 2,775,000. Genes exist on both strands, and it is striking that in this region the genes tend to alternate between the forward and the reverse strands. We selected this region for its gene density and because it has characteristics that are typical of the complete *Adh* region. Figure 2A vividly demonstrates that all of the gene-finding programs' predictions are highly correlated with the annotated genes from std1/std3. In the past, gene finders had often mistakenly predicted a gene on the noncoding strand opposite of a real gene, leading to FP predictions known as "shadow exons." Figure 2A makes it clear that gene finders have overcome this problem, because there are almost no shadow exon predictions for any of the genes in std3. Another characteristic, captured in the high base level sensitivity and the low missing genes statistics, is that every gene in the std3 set was predicted by at least a few groups and that most of these predictions agree with each other. Except for the second and third genes [*DS02740.5*, *I(2)35Fb*] on the forward strand (2,740,000–2,745,000), which seem to

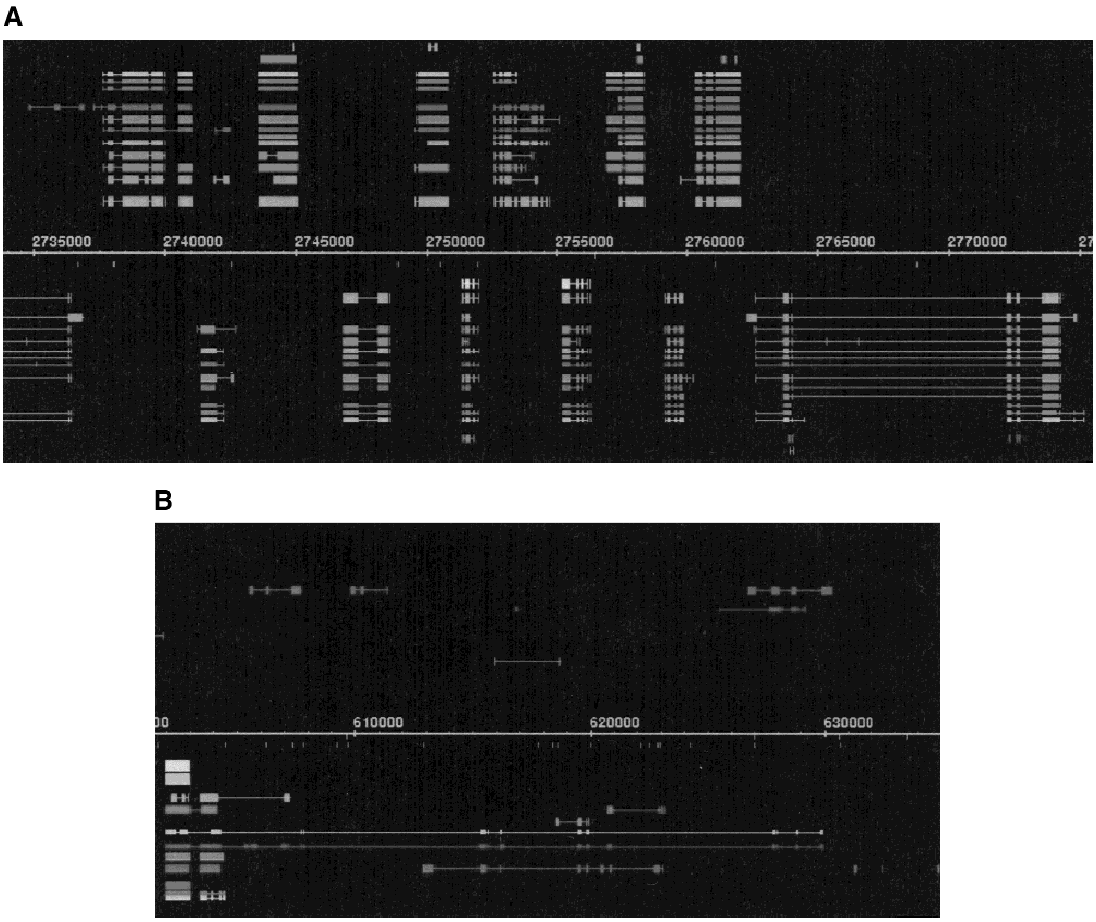


**Figure 2** (*A*) Annotations for the following known genes described in Ashburner et al. (1999b) are shown for the region from 2,735,000 to 2,775,000 (from the *left* to the *right* of the map): *crp* (partial, reverse (r)), *DS02740.4* (forward (f)), *DS02740.5* (f), *l(2)35Fb* (f), *heix* (r), *DS02740.8* (f), *DS02740.9* (r), *DS02740.10* (f), *anon-35Fa* (r), *Sed5* (f), *cni* (r), *fzy* (f), *cact* (r). (*B*) Annotations for the following known gene described in Ashburner et al. (1999b) are shown for the region from 600,000 to 635,000 (*left* to *right*): *DS01759.1* (r).

be single exon genes, all of the genes in this region are multiexon genes with between two and eight exons. The exon size varies widely. There are genes that consist of only two large exons, some that consist of a mix of large and small exons, and some that are made up exclusively of many small exons. The distribution seems to be almost random. Except for the long final intron in the last gene on the reverse strand (*cact*), the region consists exclusively of short introns.

Predictions on the reverse strand indicate a possible gene from base 2,741,000 to base 2,745,000. Most of the gene finders agree on this prediction, but neither std1 nor std3 describes a gene at this location. This could be a real gene that was missed by the expert annotation pathway described in Ashburner et al (1999b). Neither `BLOCKS+` nor `GeneWise` found any homologies in this region, but we can see from the table in the previous section that many real genes do not have any homology annotations. Interestingly, this is the only area in the region where two gene finders predicted a possible gene that likely consists of shadow exons.

The fifth gene on the forward strand (*DS02740.10*, bases 2,752,500–2,755,000) shows that long genes with multiple exons are much harder to predict than single exon genes or genes with only a few exons. In this region splitting and joining genes does not seem to be a problem. Repeats occur sparsely and mostly in noncoding regions, predominantly in introns.

In contrast to the busy region in Figure 2A, Figure

2B highlights a region of almost equal size in which only one gene (*DS01759.1*) is present in both std1 and std3. There are very few FP predictions by any group, but there is one case where the "false" predictions by different programs are located at very similar positions (on the reverse strand near base 620,000). This suggests a real gene that is missing from both standard sets.

Figure 3, A–D, depicts selected genes that illustrate some interesting challenges in gene finding. Figure 3A shows the *Adh* and the *Adhr* genes that occur as gene duplicates. The encoded proteins have a sequence identity of 33%. The positions of the two introns interrupting the coding regions are conserved and give additional evidence to tandem duplication. Both genes are under the control of the same regulatory promoter, the *Adhr* gene does not have a TSS of its own, and its transcript is always found as part of an *Adh–Adhr* dicistronic mRNA. Gene duplications occur very frequently in the *Drosophila* genome—estimates show that at least 20% of all genes occur in gene family duplications. In an additional twist, *Adh* and *Adhr* are located within an intron of another gene, *outspread* (*osp*), that is found on the opposite strand (for details, see Fig. 3B). The *Adh* gene is correctly predicted by most of the programs, although one erroneously predicts an additional first exon. Most of the programs also predict the structure of *Adhr* correctly; one program misses the initial exon and shortens the second exon. Both *Adh* and *Adhr* show hits to the protein motifs in `BLOCKS+` as well as alignments to a PFAM protein domain family through `GeneWise`. Both genes hit two different PFAM families, and the order of these two domains is conserved in the gene structure.

Figure 3B highlights the *osp* gene region. This is an example of a gene with exceptionally long (>20 kb) introns, making it hard for any gene finder to predict the entire structure correctly. In addition, there are a number of smaller genes [including the *Adh* and *Adhr* genes discussed above, *DS09219.1* (r.) and *DS07721.1* (f.)] within the introns of *osp*. No current gene finder includes overlapping gene structures in its model; as a consequence, none of the GASP gene finders were able to predict the *osp* structure without disruption. This is clearly a shortcoming of the programs because genes containing other genes are often observed in *Drosophila* (Ashburner et al. 1999b report 17 cases for the *Adh* region). However, it should be noted that most of the gene finders predict the 3′ end of *osp* correctly and therefore get most of the coding region right. The region that includes the 5′ end of *osp* shows a lot of gene prediction activity, but there is no consistency among the predictions. One program (`FGenesCCG3`) does correctly predict the *DS09219.1* gene.

Figure 3C shows the entire gene structure of the *Ca-α1D* gene. This gene is the most complex gene in the *Adh* region, with >30 exons. This is a very good example for studying gene splitting. Several predictors break the gene up into several genes, but some groups make surprisingly close predictions. This shows the complex structure that genes can exhibit and that extent to which this complexity has been captured in the state-of-the-art prediction models. It is interesting to note that most of the larger exons are predicted, whereas the shorter exons are missed. Such a large complex gene is a good candidate for alternative splicing, which can ultimately be detected only by extensive cDNA sequencing.

Figure 3D shows the triple duplication of the *idgf* gene (*idgf1*, *idgf2*, and *idgf3*) on the forward strand. Two programs mistakenly join the first two genes into a single gene; all the others correctly predict all three genes.

## DISCUSSION

The goal of the GASP experiment was to review and assess the state of the art in genome annotation tools. We believe that the noncompetitive framework and the community's enthusiastic participation helped us achieve that goal. By providing all of the participants with an unprecedented set of *D. melanogaster* training data and using unreleased information about the region as our gold standard, we were able to establish the level playing field that made it possible to compare the performance of the various techniques. The large size of the *Adh* contig and the diversity of its gene structures provided us with an opportunity to compare the capabilities of the annotation tools in a setting that models the genome-wide annotations currently being attempted. However, the lack of a completely correct standard set means that our results should only be considered in the context of the std1 and std3 data sets.

### Assessing the Results

The most difficult part of the assessment was developing a benchmark for the predicted annotations. By dividing the predictions into different classes and developing class-specific metrics that were based on the best available standards, we feel that we were able to make a meaningful evaluation of the submissions. Although most of the information that was used to evaluate the submissions was unreleased, some cDNA sequences from the region were in the public databases. As sequencing projects move forward, it will become increasingly difficult for future experiments to find similarly unexplored regions. This makes it very different from the CASP protein structure prediction contests, which can use the three-dimensional structure of a novel target protein that is unknown to the predictors.

As discussed in the introduction, the lack of an absolutely correct standard against which to evaluate the various predictions is a troubling issue. Although we believe that the standard sets sufficiently represent

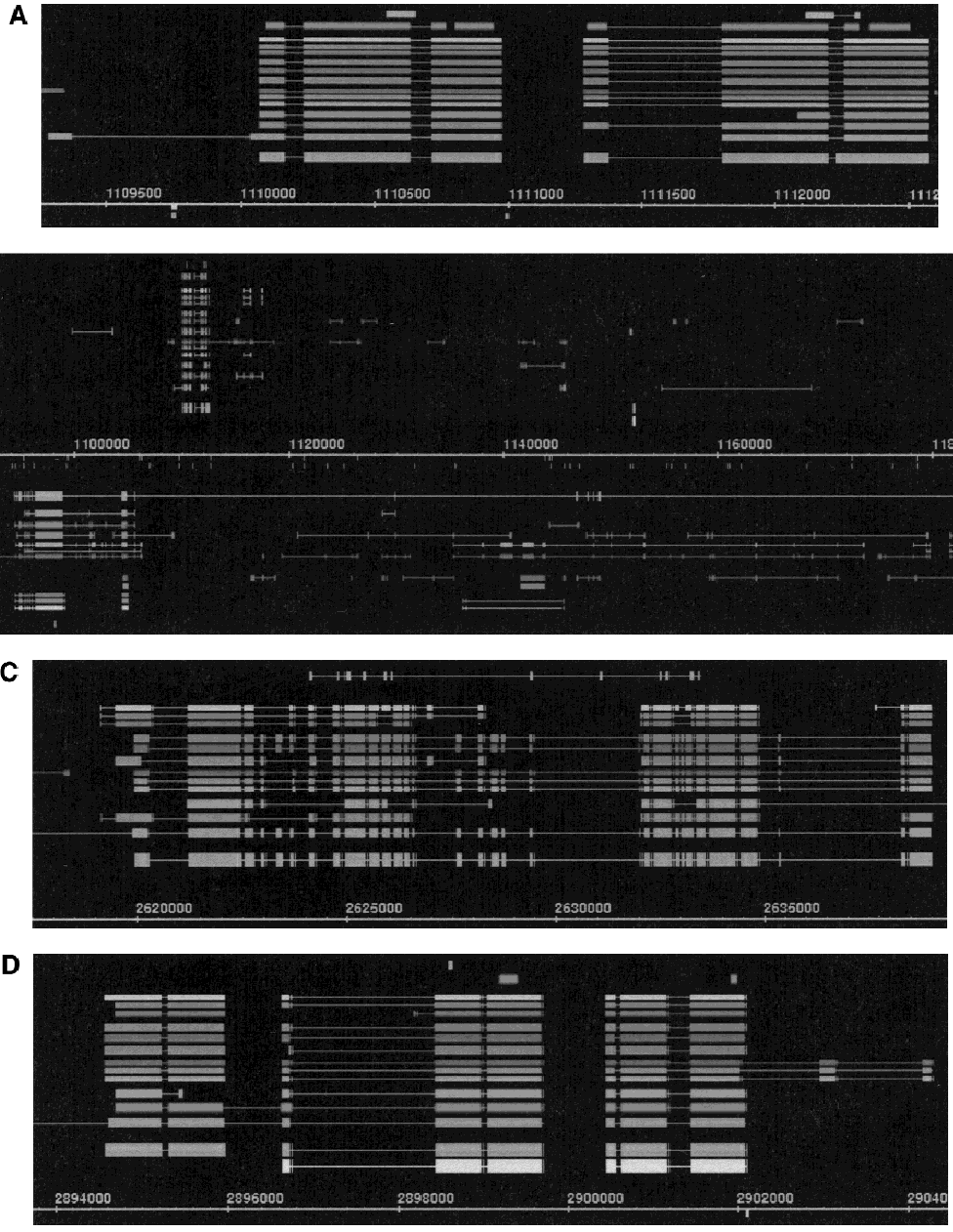


**Figure 3** (*A*) Annotations for the following known genes described in Ashburner et al. (1999b) are shown for the region from 1,109,500 to 1,112,500 (forward strand only) (*left* to *right*): *Adh*, *Adhr*. (*B*) Annotations for the following known genes described in Ashburner et al. (1999b) are shown for the region from 1,090,000 to 1,180,000 (*left* to *right*): *osp* (r), *Adh* (f), *Adhr* (f), *DS09219.1* (r), *DS07721.1* (f). (*C*) Annotations for the following known gene described in Ashburner et al. (1999b) are shown for the region from 2,617,500 to 2,640,000 (forward strand only) (*left* to *right*): *Ca-α1D*. (*D*) Annotations for the following known genes described in Ashburner et al. (1999b) are shown for the region from 2,894,000 to 2,904,000 (forward strand only) (*left* to *right*): *idgf1, idgf2, idgf3*.

the true nature of the region and that conclusions based on them are interesting, it must be remembered that the various results can only be evaluated in the context of these incomplete data sets. This also makes GASP more difficult and less clear cut than CASP, where the three-dimensional protein structure is experimentally solved at least to some degree of resolution.

It should also be noted that the gene-finding tools with the highest Sp have a great deal in common with GENSCAN, the gene prediction tool used in the development of the std3 data set. This suggests that std3's origins might have led to a bias favoring GENSCAN-like predictors. Because std1 was exclusively created using full-length cDNA alignments, this set might be biased towards highly expressed genes, because the cDNA libraries were not normalized.

### Progress in Genome-Wide Annotation

The rapid release of completed genomes, including the imminent release of the *D. melanogaster* and human genomes, has driven significant developments in genome annotation and gene-finding tools. Problems that have plagued gene-finding programs, such as predicting shadow exons, restricting predictions to a single strand, recognizing repeats, and accurately identifying splice sites, have been overcome by the current state of the art. In this section, we discuss some of the remaining issues in genome annotation that the GASP experiment highlighted.

Successful gene prediction programs use complex models that integrate information from statistical features that are driven by the three-dimensional protein–DNA/RNA interactions. They make integrated predictions on both strands and have been tuned to predict all the genes in gene-rich regions and avoid overpredicting genes in gene-poor regions (Fig. 2A,B). Although most of the programs identify almost all the existing genes (as evidenced by the Sn and MG statistics), there is significant variation in their ability to accurately predict precise gene structures (see the Sp statistics, particularly at the exon level). If any global performance conclusion can be drawn, it is that the probabilistic gene finders (mostly HMM based) seem to be more reliable. The integration of EST/cDNA sequence information into the ab initio gene finders [see HMMGene, GenieEST, and GRAIL (Fig. 2A,B and Fig. 3A–D)] significantly improves gene predictions, particularly the recognition of intron–exon boundaries. Some groups submitted multiple annotations of the *Adh* region using programs that were tuned for different tasks. The suite of Fgenes programs shows very nicely the results of such a three-part submission. The first Fgenes submission (Fgenes1) is a version adjusted to weight Sn and Sp equally. The second submission (Fgenes2) is very conservative and only annotates high-scoring genes. This results in a high Sp but a low Sn. The third submission (Fgenes3) tries to maximize Sn and to avoid missing any genes, at the cost of a loss in Sp. These differently tuned variants may be useful for different types of tasks.

A comparison (data not shown) to a gene-finding system that was trained on human data showed that it did not perform as well as the programs that were trained on *Drosophila* data.

None of the gene predictors screened for transposable elements, which have a protein-like structure. As described in Ashburner et al. (1999b), the *Adh* region has 17 transposable element sequences. Eliminating transposons from the predictions or adding them to the standard sets would have reduced the FP counts, raising the Sp and lowering the WE and WG scores. Although this accounts for a portion of the high FP scores, we believe that there may also be additional genes in this region not annotated in std3. Future biological experiments (Rubin 2000) to identify and sequence the predicted genes that were not included in std3 should improve the completeness and accuracy of the final annotations.

There were fewer submissions of homology-based annotations than those by ab initio gene finders, and their results were significantly affected by their FP rates. A significant portion of those FPs were matches to transposable elements, some appear to be matches to pseudogenes, and others are likely to be real, but as yet unannotated, genes. The homology-based approaches seem to be the most promising techniques for inferring functions for newly predicted genes.

Even using EST/cDNA alignments to predict gene structures is not as simple as expected. Paralogs, low sequence quality of mRNAs, and the difficulty of cloning infrequently expressed mRNAs make this method of gene finding more complex than believed, and it is difficult to guarantee completeness with this method. Normalized cDNA libraries and other more sophisticated technologies to purify genes with low expression levels, along with improved alignment and annotation technologies, should improve predictions based on EST/cDNA alignments.

### Lessons for the Future

To fully assess the submitted annotations, the correct answer must be improved. Only extensive full-length cDNA sequencing can accomplish this. A possible approach would be to design primers from predicted exons and/or genes in the genomic sequence and then use hybridization technologies to fish out the corresponding cDNA from cDNA libraries. For promoter predictions, another way to improve the correct answer is to make genome-to-genome alignments with the DNA of related species (e.g., *Caenorhabditis briggsae* vs. *Caenorhabditis elegans*; *D. melanogaster* vs. *D. virilis*). More detailed guidelines, including how to handle am-

biguous features such as pseudogenes and transposons, will make the results of future experiments even more useful.

A successful system to identify all genes in a genome should consist of a combination of ab initio gene finding, EST/cDNA alignments, protein homology methods, promoter recognition, and repeat finding. All of the various technologies have advantages and disadvantages, and an automated method for integrating their predictions seems ideal.

Beyond the identification of gene structure is the determination of gene functions. Most of the existing prototypes of such systems are based on sequence homologies. Although this is a good starting point, it is definitely not sufficient. The state of the art for predicting function in protein sequences uses the protein's three-dimensional structure, but the difficulty of accurately predicting three-dimensional structure from primary sequences makes applying these techniques on complete genomes problematic. The new field of structural genomics will hopefully give more answers in these areas.

Another approach to function classification is the analysis of gene expression data. Improvements in TSS annotations, along with correlation in expression profiles, should be very helpful in identifying regulatory regions.

### Conclusions

The GASP experiment succeeded in providing an objective assessment of current approaches to gene prediction. The main conclusions from this experiment are that current methods of gene predictions are tremendously improved and that they are very useful for genome scale annotations but that high-quality annotations also depend on a solid understanding of the organism in question (e.g., recognizing and handling transposons).

Experiments like GASP are essential for the continued progress of automated annotation methods. They provide benchmarks with which new technologies can be evaluated and selected.

The predictions collected in GASP showed that for most of the genes, overlapping predictions from different programs existed. Whether or not a combination of overlapping predictions would do better than the best performing individual program was not explicitly tested in this experiment. For such a test, additional experiments such as cDNA library screening and subsequent full-length cDNA sequencing in this selected *Adh* test bed region would be necessary. These experiments are currently under way, and it would be interesting to perform a second GASP experiment when more cDNAs have been sequenced.

We believe that existing automated annotation methods are scalable and that the ultimate test will occur when the complete sequence of the *D. melanogaster* genome becomes available. This experiment will set standards for the accuracy of genome-wide annotation and improve the credibility of the annotations done in other regions of the genome.

## URLs

*Gene Finding*

`HMMGene`, http://www.cbs.dtu.dk/services/HMMGene/; `GRAIL`, http://compbio/ornl.gov/droso; `Fgenes`, http://genomic/sanger.ac.uk/gf/gf.shtml; `GeneID`, http://www1/imim.es/~rguigo/AnnotationExperiment/index.html; `Genie`, http://www.neomorphic. com/genie.

*Promoter Prediction*

`MCPromoter`, http://www5.informatik.uni-erlangen.de/HTML/English/Research/Promoter; `CoreInspector`, http://www.gsf.de/biodv.

*Protein Homology*

`BLOCKS+`, http://blocks.fhcrc.org and http:/blocks.fhcrc.org/blocks-bin/getblock.sh?<block name>; `GeneWise`, http://www.sanger.ac.uk/Software/Wise2/.

*Repeat Finders*

`TRF`, http://c3.biomath.mssm.edu/trf.test.html.

## ACKNOWLEDGMENTS

We thank all of the participants who submitted their annotations, without which the project would not have been such a success, for their original contributions, their publication, and their patience with the organizers during this very intense project. We also thank the Drosophila Genome Sequencing Center at LBNL, headed by Sue Celniker, for providing such high-quality sequence; the annotation team at the Berkeley Drosophila Genome Sequencing Center and especially Sima Misra, Gerry Rubin, and Michael Ashburner; and the entire *Drosophila* community for producing such a thoroughly studied genomic region. Special thanks go to the independent assessor team, consisting of Michael Ashburner, Peer Bork, Richard Durbin, Roderic Guigó, and Tim Hubbard, who critiqued our evaluation. Thanks goes also to the organizers of ISMB-99 Heidelberg, especially Thomas Lengauer and Reinhard Schneider, for encouraging our tutorial and the tremendous support in the preparation process and during the conference. We also thank Richard Durbin, David Haussler, Tim Hubbard, and Richard Bruskiewich for developing and maintaining the `GFF` format and their associated tools. Last but not least, a big thank you goes to Gerry Rubin for making the Drosophila Genome Project such a success. This work was supported by NIH grant HG00750.

The publication costs of this article were defrayed in part by payment of page charges. This article must therefore be hereby marked "advertisement" in accordance with 18 USC section 1734 solely to indicate this fact.

## REFERENCES

Agarwal, P. and D.J. States. 1998. Comparative accuracy of methods for protein sequence similarity search. *Bioinformatics* **14:** 40–47.

Altschul, S.F., W. Gish, W. Miller, E.W. Myers and D.J. Lipman. 1990. Basic local alignment search tool. *J. Mol. Biol.* **215:** 403–410.

Arkhipova, I. R. 1995. Promoter elements in *Drosophila melanogaster* revealed by sequence analysis. *Genetics* **139:** 1359–1369.

Ashburner, M. 2000. A biologist's view of the *Drosophila* genome annotation assessment. *Genome Res.* (this issue).

Ashburner, M., P. Bork, R. Durbin, R. Guigó, and T.J. Hubbard. 1999a. *GASP1 assessment meeting, EMBL*, Heidelberg, Germany.

Ashburner, M., S. Misra, J. Roote, S.E. Lewis, R. Blazej, T. Davis, C. Doyle, R. Galle, R. George, N. Harris et al. 1999b. An exploration of the sequence of a 2.9-Mb region of the genome of drosophila melanogaster. The adh region. *Genetics* **153:** 179–219.

Ashburner, M. et al. 1999c. European *Drosophila* Genome Project (EDGP). http://edgp.ebi.ac.uk/.

Bateman, A., E. Birney, R. Durbin, S.R. Eddy, K.L. Howe, and E.L. Sonnhammer. 2000. The Pfam Protein Families Database. *Nucleic Acids Res*. **28:** 263–266.

Benson, G. 1999. Tandem repeats finder: A program to analyze DNA sequences. *Nucleic Acids Res*. **27:** 573–580.

Besemer, J. and M. Borodovsky. 1999. Heuristic approach to deriving models for gene finding. *Nucleic Acids Res*. **27:** 3911–3920.

Birney, E. 1999. Wise2. http://www.sanger.ac.uk/Software/Wise2/.

Birney, E. and R. Durbin. 1997. Dynamite: A flexible code generating language for dynamic programming methods used in sequence comparison. *Intell. Syst. Mol. Biol*. **5:** 56–64.

———. 2000. Using GeneWise in the *Drosophila* annotation experiment. *Genome Res*. (this issue).

Burge, C. and S. Karlin. 1997. Prediction of complete gene structures in human genomic DNA. *J. Mol. Biol*. **268:** 78–94.

———. 1998. Finding the genes in genomic DNA. *Curr. Opin. Struct. Biol*. **8:** 346–354.

Burset, M. and R. Guigó. 1996. Evaluation of gene structure prediction programs. *Genomics* **34:** 353–367.

Cavin Périer, R., T. Junier, C. Bonnard, and P. Bucher. 1999. The Eukaryotic Promoter Database (EPD): Recent developments. *Nucleic Acids Res*. **27:** 307–309.

Cavin Périer, R., V. Praz, T. Junier, C. Bonnard, and P. Bucher. 2000. The Eukaryotic Promoter Database (EPD). *Nucleic Acids Res*. **28:** 302–303.

Dunbrack, R.L., Jr., D.L. Gerloff, M. Bower, X. Chen, O. Lichtarge, and F.E. Cohen. 1997. Meeting review: The Second meeting on the critical assessment of techniques for protein structure prediction (CASP2), Asilomar, California, December 13–16, 1996. *Folding Design* **2:** R27–R42.

Eeckman, F.H. and R. Durbin. 1995. ACeDB and macace. *Methods Cell Biol*. **48:** 583–605.

Fickett, J.W. and C.S. Tung. 1992. Assessment of protein coding measures. *Nucleic Acids Res*. **20:** 6441–6450.

Fickett, J.W. and A.G. Hatzigeorgiou. 1997. Eukaryotic promoter recognition. *Genome Res*. **7:** 861–878.

Florea, L., G. Hartzell, Z. Zhang, G.M. Rubin, and W. Miller. 1998. A computer program for aligning a cDNA sequence with a genomic DNA sequence. *Genome Res*. **8:** 967–974.

Gaasterland, T. and C.W. Sensen. 1996. MAGPIE: Automated genome interpretation. *Trends Genet*. **12:** 76–78.

Guigó, R., S. Knudsen, N. Drake, and T. Smith. 1992. Prediction of gene structure. *J. Mol. Biol*. **226:** 141–157.

Harris, N.L., G. Helt, S. Misra, and S.E. Lewis. 1999. CloneCurator. http://www.fruitfly.org/displays/CloneCurator.html.

Helt, G., E. Blossom, J. Morris, D. Fineman, S. Cherritz, S. Shaw, and C.L. Harmon. 1999. Neomorphic Genome Software Development Toolkit (NGSDK). Neomorphic, Inc., Berkeley, CA. http://www.neomorphic.com.

Henikoff, S. and J.G. Henikoff. 1994. Protein family classification based on searching a database of blocks. *Genomics* **19:** 97–107.

———. 2000. Genomic sequence annotation based on translated searching of the Blocks+ Database. *Genome Res*. (this issue).

Henikoff, J.G., S. Henikoff, and S. Pietrokovski. 1999a. New features of the Blocks Database servers. *Nucleic Acids Res*. **27:** 226–228.

———. 1999b. Blocks+: A non-redundant database of protein alignment blocks derived from multiple compilations. *Bioinformatics* **15:** 471–479.

Jurka, J. 1998. Repeats in genomic DNA: Mining and meaning. *Curr. Opin. Struct. Biol*. **8:** 333–337.

Krogh, A. 1997. Two methods for improving performance of an HMM and their application for gene finding. *Ismb* **5:** 179–186.

Kulp, D., D. Haussler, M.G. Reese, and F.H. Eeckman. 1997. Integrating database homology in a probabilistic gene structure model. *Pac. Symp. Biocomput*. **2:** 232–244.

Kurtz, S. and C. Schleiermacher. 1999. REPuter: Fast computation of maximal repeats in complete genomes. *Bioinformatics* **15:** 426–427.

Levitt, M. 1997. Competitive assessment of protein fold recognition and alignment accuracy. *Proteins* (Suppl.) **1:** 92–104.

Marcotte, E.M., M. Pellegrini, M.J. Thompson, T.O. Yeates, and D. Eisenberg. 1999. A combined algorithm for genome-wide prediction of protein function. *Nature* **402:** 83–86.

Mott, R. 1997. EST_GENOME: A program to align spliced DNA sequences to unspliced genomic DNA. *Comp. Appl. Biosci*. **13:** 477–478.

Moult, J., T. Hubbard, S.H. Bryant, K. Fidelis, and J.T. Pedersen. 1997. Critical assessment of methods of protein structure prediction (CASP): Round II. *Proteins* (Suppl.) **1:** 2–6.

Moult, J., T. Hubbard, K. Fidelis, and J.T. Pedersen. 1999. Critical assessment of methods of protein structure prediction (CASP): Round III. *Proteins* (Suppl.) **3:** 2–6.

Ohler, U., S. Harbeck, H. Niemann, E. Noth, and M.G. Reese. 1999. Interpolated markov chains for eukaryotic promoter recognition. *Bioinformatics* **15:** 362–369.

Ohler, U., G. Stommer, and S. Harbeck. 2000. Stochastic segment models of eukaroyotic promoter regions. *Pac. Symp. Biocomput*. **5:** 377–388.

Parra, G., E. Blanco, and R. Guigó. 2000. GeneID in *Drosophila*. *Genome Res*. (this issue).

Pearson, W.R. 1995. Comparison of methods for searching protein sequence databases. *Protein Sci*. **4:** 1145–1160.

Pearson, W.R. and D.J. Lipman. 1988. Improved tools for biological sequence comparison. *Proc. Natl. Acad. Sci*. **85:** 2444–2448.

Reese, M.G. 2000. "Genome annotation in *Drosophila melanogaster*." Ph.D. thesis, University of Hohenheim, Germany.

Reese, M.G., F.H. Eeckman, D. Kulp, and D. Haussler. 1997. Improved splice site detection in Genie. *J. Comput. Biol*. **4:** 311–323.

Reese, M.G., N.L. Harris, G. Hartzell, and S.E. Lewis. 1999. *The 7th conference on Intelligent Systems in Molecular Biology (ISMB'99)*, Heidelberg, Germany, http://www.fruitfly.org/GASP.

Reese, M.G., D. Kulp, H. Tammana, and D. Haussler. 2000. Genie–Gene finding in *Drosophila melanogaster*. *Genome Res*. (this issue).

Rubin, G.M. 2000. Full-length cDNA project. http://www.fruitfly.org/EST

Rubin, G.M. et al. 1999. Berkeley Drosophia Genome Project (BDGP). http://www.fruitfly.org.

Salamov, A.A. and V.V. Solovyev. 2000. Ab initio gene finding in *Drosophila* genomic DNA. *Genome Res*. (this issue).

Sippl, M.J., P. Lackner, F.S. Domingues, and W.A. Koppensteiner. 1999. An attempt to analyse progress in fold recognition from CASP1 to CASP3. *Proteins* (Suppl.) **3:** 226–230.

Solovyev, V.V., A.A. Salamov, and C.B. Lawrence. 1995. Identification of human gene structure using linear discriminant functions and dynamic programming. *Ismb* **3:** 367–375.

Sonnhammer, E.L., S.R. Eddy, and R. Durbin. 1997. Pfam: A comprehensive database of protein domain families based on seed alignments. *Proteins* **28:** 405–420.

Sonnhammer, E.L., S.R. Eddy, E. Birney, A. Bateman, and R. Durbin. 1998. Pfam: Multiple sequence alignments and HMM-profiles of protein domains. *Nucleic Acids Res*. **26:** 320–322.

Stein, L.D. and J. Thierry-Mieg. 1998. Scriptable access to the *Caenorhabditis elegans* genome sequence and other ACEDB databases. *Genome Res*. **8:** 1308–1315.

Stormo, G.D. 2000. Gene-finding approaches for eukaryotes. *Genome Res. (this issue)*.

Uberbacher, E.C. and R.J. Mural. 1991. Locating protein-coding regions in human DNA sequences by a multiple sensor-neural network approach. *Proc. Natl. Acad. Sci*. **88:** 11261–11265.

Zemla, A., C. Venclovas, J. Moult, and K. Fidelis. 1999. Processing and analysis of CASP3 protein structure predictions. *Proteins* (Suppl.) **3:** 22–29.

*Received February 9, 2000; accepted in revised form February 29, 2000.*

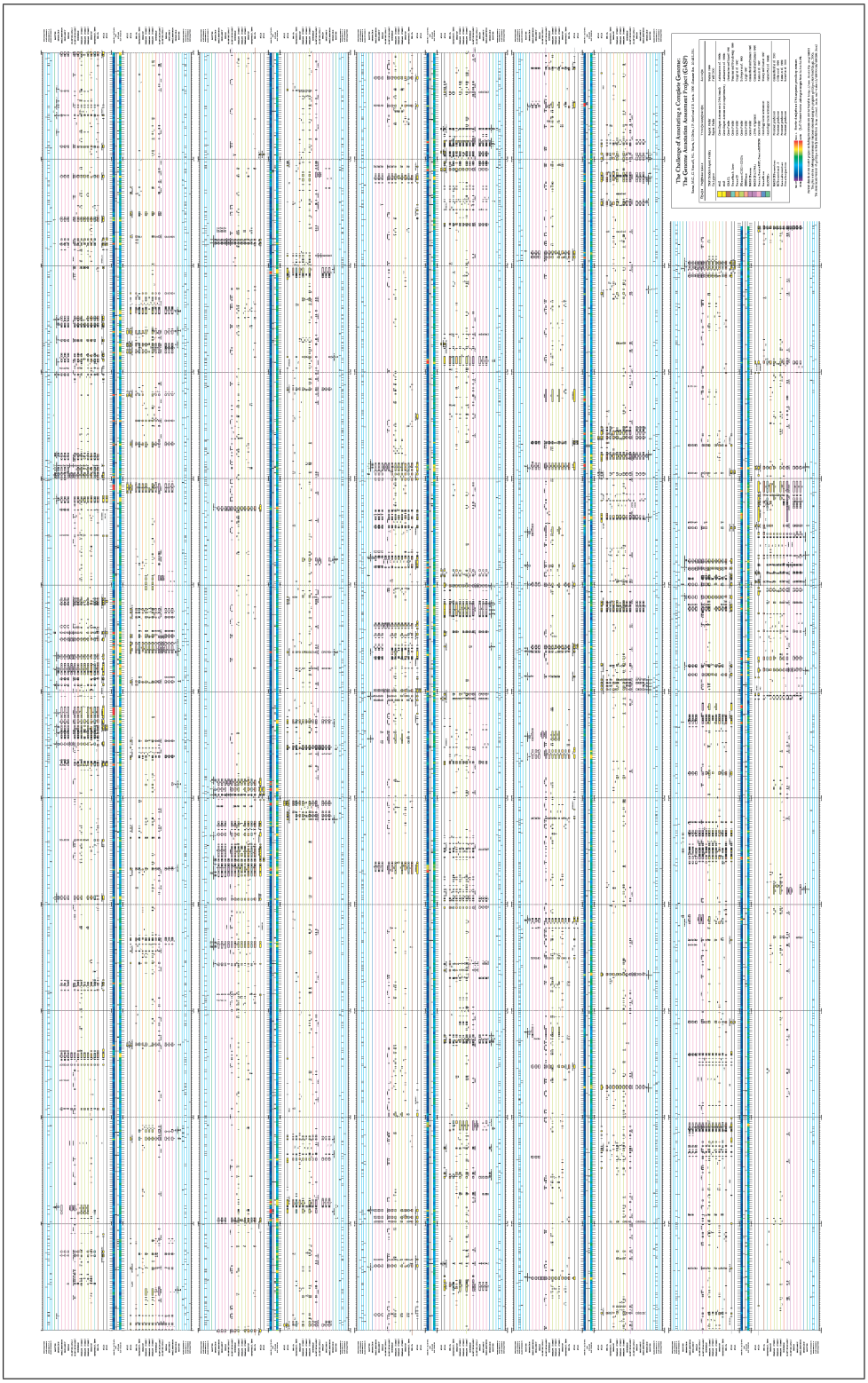

Figure 3.7: ***Drosophila* Genome Annotation Assessment Project.**

### 3.3.5 Guigó *et al*, *Proc Nat Acad Sci*,100(3):1140–1145, 2003

**PubMed Accession:**

http://www.ncbi.nlm.nih.gov/entrez/query.fcgi?cmd=Retrieve&db=PubMed&list_uids=12552088&dopt=Abstract

**Journal Abstract:**

http://www.pnas.org/cgi/content/abstract/100/3/1140

**Supplementary Materials:**

http://genome.imim.es/datasets/mouse2002/

# Comparison of mouse and human genomes followed by experimental verification yields an estimated 1,019 additional genes

**Roderic Guigó*†, Emmanouil T. Dermitzakis†‡, Pankaj Agarwal§, Chris P. Ponting¶, Genís Parra*, Alexandre Reymond‡, Josep F. Abril*, Evan Keibler‖, Robert Lyle‡, Catherine Ucla‡, Stylianos E. Antonarakis‡, and Michael R. Brent‖****

*Research Group in Biomedical Informatics, Institut Municipal d'Investigació Mèdica/Universitat Pompeu Fabra/Centre de Regulació Genòmica, E08003 Barcelona, Catalonia, Spain; ‡Division of Medical Genetics, University of Geneva Medical School and University Hospitals, 1211 Geneva, Switzerland; §GlaxoSmithKline, UW2230, 709 Swedeland Road, King of Prussia, PA 19406; ¶Medical Research Council Functional Genetics Unit, Department of Human Anatomy and Genetics, University of Oxford, South Parks Road, Oxford OX1 3QX, United Kingdom; and ‖Department of Computer Science, Washington University, One Brookings Drive, St. Louis, MO 63130

Communicated by Robert H. Waterston, Washington University School of Medicine, St. Louis, MO, December 11, 2002 (received for review October 21, 2002)

**A primary motivation for sequencing the mouse genome was to accelerate the discovery of mammalian genes by using sequence conservation between mouse and human to identify coding exons. Achieving this goal proved challenging because of the large proportion of the mouse and human genomes that is apparently conserved but apparently does not code for protein. We developed a two-stage procedure that exploits the mouse and human genome sequences to produce a set of genes with a much higher rate of experimental verification than previously reported prediction methods. RT-PCR amplification and direct sequencing applied to an initial sample of mouse predictions that do not overlap previously known genes verified the regions flanking one intron in 139 predictions, with verification rates reaching 76%. On average, the confirmed predictions show more restricted expression patterns than the mouse orthologs of known human genes, and two-thirds lack homologs in fish genomes, demonstrating the sensitivity of this dual-genome approach to hard-to-find genes. We verified 112 previously unknown homologs of known proteins, including two homeobox proteins relevant to developmental biology, an aquaporin, and a homolog of dystrophin. We estimate that transcription and splicing can be verified for >1,000 gene predictions identified by this method that do not overlap known genes. This is likely to constitute a significant fraction of the previously unknown, multiexon mammalian genes.**

Complete and precise delineation of protein coding genes in mammalian genomes remains a challenging task. To produce a preliminary gene catalog for the draft sequence of the mouse (1), the Mouse Genome Sequencing Consortium relied primarily on the ENSEMBL gene build pipeline (2). ENSEMBL works by (*i*) aligning known mouse cDNAs from REFSEQ (3), RIKEN (4, 5), and SWISSPROT (6, 7) to the genome, (*ii*) aligning known proteins from related mammalian genes to the genome, and (*iii*) using portions of GENSCAN (8) predictions that are supported by experimental evidence (such as ESTs). This conservative approach yielded ≈23,600 genes. However, ENSEMBL cannot predict genes for which there is no preexisting evidence of transcription (1). Furthermore, reliance on known transcripts may lead to a bias against predicting genes that are expressed in a restricted manner or at very low levels.

Before the production of a draft genome sequence for a second mammal, the best available methods for predicting novel mammalian genes were single-genome *de novo* gene-prediction programs, of which GENSCAN (8) is one of the most accurate and most widely used. These programs work by recognizing statistical patterns characteristic of coding sequences, splice signals, and other features in the genome to be annotated. However, they tend to predict many apparently false exons caused by the occurrence of such patterns by chance. With the availability of draft sequences for both the mouse and human genomes, it is now possible to incorporate genomic sequence conservation into *de novo* gene prediction algorithms. However, DNA alignment programs alone are not an effective means of gene prediction because a large fraction of the mouse and human genomes is conserved but does not code for protein.

We developed a procedure that greatly reduces the false-positive rate of *de novo* mammalian gene prediction by exploiting mouse–human conservation in both an initial gene-prediction stage and an enrichment stage. The first stage is to run gene-prediction programs that use genome alignment in combination with statistical patterns in the DNA sequence itself. A number of such programs have been described (9–12). For these experiments, we used SGP2 (13) and TWINSCAN (refs. 14 and 15 and http://genes.cs.wustl.edu), two such programs that we designed for efficient analysis of whole mammalian genomes. TWINSCAN is an independently developed extension of the GENSCAN probability model, whereas SGP2 is an extension of GENEID (16, 17). The probability scores these programs assign to each potential exon are modified by the presence and quality of genome alignments. TWINSCAN uses nucleotide alignment [BLASTN (18), blast.wustl.edu] and has specific models for how alignments modify the scores of coding regions, UTRs, splice sites, and translation initiation and termination signals. SGP2, in contrast, uses translated alignments [TBLASTX (18), blast.wustl.edu] to modify the scores of potential coding regions only. These programs predict many fewer exons than GENSCAN with no reduction in sensitivity to the exons of known genes (13, 14).

The second stage of our procedure is based on the observation that almost all mouse genes have a human counterpart with highly conserved exonic structure (1). We therefore compare all multiexon genes predicted in mouse in the first stage to those predicted in human. Predictions are retained only if the protein predicted in mouse aligns to a human protein predicted by the same program, with at least one predicted intron at the same location (aligned intron, Fig. 1). Predicted single-exon genes are always discarded by this procedure. Although there are many real single-exon genes, it is not currently possible to predict them reliably nor to verify them reliably in a cost-effective, high-throughput procedure.

In this article, we show that our two-stage process yields >1,400 predictions outside the standard annotation of the mouse genome. RT-PCR and direct sequencing of a single exon pair in a sample of these predictions indicates that the majority correspond to real spliced transcripts. Our results also show that this procedure is sensitive to genes that are hard to find by other methods. The combination of these computational and experimental techniques forms a powerful, cost-effective system for expanding experimentally supported genome annotation. This approach is therefore expected to bring the annotation of the mouse and human genomes nearer to closure.

## Experimental Procedures

**Genome Sequences.** The MGSCv3 assembly of the mouse genome described in ref. 1 and the December, 2001 Golden Path assembly

†R.G. and E.T.D. contributed equally to this work.

**To whom correspondence should be addressed. E-mail: brent@cse.wustl.edu.

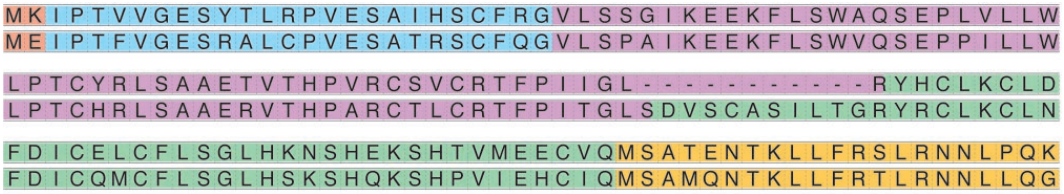


**Fig. 1.** An example of predictions with aligned introns. RT-PCR positive predicted protein 3B1 (a novel homolog of *Dystrophin*) is aligned with its predicted human ortholog (N-terminal regions shown; *Upper* of each row: mouse, *Lower* of each row: human). Each color indicates one coding exon. Three of four predicted splice boundaries (color boundaries) align perfectly. Any one of these three is sufficient for surviving the enrichment step. Gaps in the alignment (shown as dashes) may indicate mispredicted regions.

of the human genome (National Center for Biotechnology Information Build 28) were downloaded from the University of California (Santa Cruz) genome browser (http://genome.ucsc.edu).

**Genome Alignments.** TWINSCAN was run on the mouse genome by using BLASTN alignments to the human genome (WU-BLAST, http://blast.wustl.edu). Lowercase masking in the human sequence was first converted to N masking. The result was further masked with NSEG by using default parameters, all Ns were removed, and the sequence was cut into 150-kb database segments. The mouse genome sequence was divided into 1-mb query segments. BLASTN parameters were: M=1 N=−1Q=5 R=1 Z=3000000000 Y=3000000000 B=10000 V=100 W=8 X=20 S=15 S2=15 gapS2=30 lcmask wordmask=seg wordmask=dust topcomboN=3. TWINSCAN was run on the human genome by using separate BLASTN alignments to the mouse genome, which was prepared in the same way except that Ns were not removed before creating the BLAST database.

SGP2 was run on the mouse and human genomes by using a single set of alignments. The masked human genome was cut into 100-kb query segments that were compared with a database of all 100-kb segments of the mouse genome with TBLASTX (WU-BLAST, parameters: B=9000 V=9000 hspmax=500 topcomboN=100 W=5 E=0.01 E2=0.01 Z=3000000000 nogap filter=xnu+seg S2=80). The substitution matrix was BLOSUM62 modified to penalize alignments with stop codons heavily (−500).

**Initial Gene Predictions.** TWINSCAN was run on 1-mb segments of the mouse and human genomes with target genome parameters identical to the GENSCAN parameters and the 68-set-ortholog conservation parameters (available on request). Note that the TWINSCAN results described in ref. 14 are based on a subsequently developed set of target genome parameters that yields better results than those described here. SGP2 was run on unsegmented mouse and human chromosomes. The REFSEQ genes (which were not tested in the experiments reported here) were incorporated directly into the SGP2 predictions, which improved the predictions outside the REFSEQS slightly by preventing some gene fusion errors. Note that the REFSEQS were not used in generating the SGP2 results described in ref. 13.

**Novelty Criteria.** Mouse predictions were considered known if they overlapped ENSEMBL predictions or had 95% nucleotide identity to a REFSEQ mRNA or an ENSEMBL-predicted mRNA over at least 100 bp. We used the most inclusive set of ENSEMBL predictions available, based on the complete RIKEN cDNA set without further filtering (1).

**Enrichment Procedure.** The enrichment procedure was applied separately to predictions of TWINSCAN and SGP2. The protein sequences predicted by each program in human and mouse were compared by using BLASTP (19). For each predicted mouse protein, all predicted human proteins with expect values $<1\times10^{-6}$ were called homologs. A global protein alignment was produced for the best scoring homologs (up to five) by using T-COFFEE (ref. 39; http://igs-server.cnrs-mrs.fr/~cnotred/Projects_home_page/t_coffee_home_page.html) with default parameters. Exonic structure was added to the alignments by using EXSTRAL.PL (www1.imim.es/~rcastelo/exstral.html). When both members of an aligned pair contained an intron at the same coordinate with at least 50% identity over 15 aa on both sides the corresponding mouse prediction was assigned to the "enriched" pool. Predictions with homologs but no aligned intron were assigned to the "similar" pool.

**RT-PCR.** To test predictions, primers were designed in adjacent exons as described in *Results* and used in RT-PCR of total RNA from 12 normal mouse adult tissues. All procedures were as described (20), except that JumpStart REDTaq ReadyMix (Sigma) and primers from Sigma-Genosys were used.

**Additional Details.** See supplementary information at www1.imim.es/datasets/mouse2002 for additional details of these procedures.

## Results

We applied the two-stage procedure described above to the entire draft mouse and human genome sequences (see *Experimental Procedures*). TWINSCAN predicted 17,271 genes with at least one aligned intron, whereas SGP2 predicted a largely overlapping set of 18,056 genes with at least one aligned intron. These predicted gene sets contain 145,734 exons and 168,492 exons, respectively. Together the two sets overlapped 90% of multiexon ENSEMBL gene predictions.

To estimate a lower bound on the proportion of novel predictions that are transcribed and spliced, we performed a series of RT-PCR amplifications from 12 adult mouse tissues (20). We did not test genes that overlap ENSEMBL predictions nor those that are 95% identical to ENSEMBL predictions or REFSEQ mRNAs over >100 bp or more. Because ENSEMBL was the standard for annotation of the draft mouse genome, we refer to the non-ENSEMBL genes as "novel." A random sample of novel genes predicted by each program and containing at least one aligned intron was tested. Primer pairs were designed in adjacent exons separated by an aligned intron of at least 1,000 bp (Fig. 2). The exon pair to be tested was chosen on the basis of intron length (minimum 1,000 bp), primer design requirements, and *de novo* gene prediction score, with no reference to protein, EST, or cDNA databases. Amplification followed by direct sequencing of the PCR product (Fig. 3) verified the exon pair in 133 unique predicted genes of 214 tested (62%, enriched pool, see Table 1 and www1.imim.es/datasets/mouse2002). Mouse genes predicted by both programs were verified at a much higher rate than those predicted by just one program (76% vs. 27%). Extrapolating from the success rates in Table 1, testing the entire pool of 1,428 enriched predictions in this way is

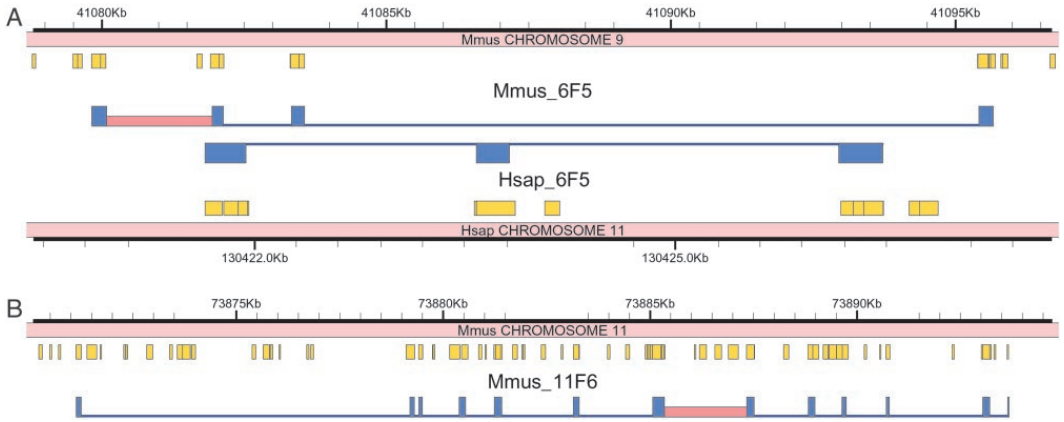


**Fig. 2.** Two examples of predicted gene structures (blue) with introns verified by RT-PCR from primers located in exons flanking the introns indicated in red. Mouse–human genomic alignments (orange) correlate with predicted exons but do not match them exactly. (*A*) Verified mouse prediction 6F5, a novel homolog of *Drosophila* brain-specific homeobox protein (bsh), with matching human prediction. (*B*) Verified mouse prediction 11F6, a homolog of rat vanilloid receptor type 1-like protein 1. No matching human gene was predicted. A cDNA (GenBank accession no. AF510316) that matches the predicted protein over four protein-coding exons was deposited in GenBank subsequent to our analysis.

expected to yield a total of 788 (±48) predictions with confirmed splices, none of which overlap ENSEMBL predictions.

Considered in isolation, genes predicted by TWINSCAN had a higher verification rate than those predicted by SGP2 (83% vs. 44%), but that difference is skewed by the fact that TWINSCAN predicted fewer exons per gene, and hence its predictions were less likely to overlap ENSEMBL predictions. We corrected for this by clustering overlapping TWINSCAN and SGP2 predictions to ensure that both were counted as positive if either was verified experimentally. For each program, the predictions belonging to a given cluster were counted only once, even if more than one was RT-PCR positive. After this correction, the confirmation rates were much closer (76% for TWINSCAN vs. 62% for SGP2). The results shown in Table 1 include the correction. The TWINSCAN verification rate is similar to the verification rate for genes predicted by both programs because the exons predicted by TWINSCAN are largely a subset of those predicted by SGP2.

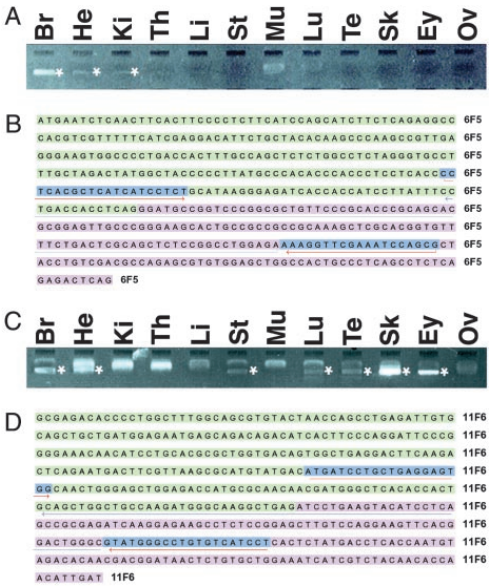


**Fig. 3.** Verification of gene predictions by RT-PCR analysis. (*A* and *B*) Test of prediction 6F5, a homolog of *Drosophila* brain-specific homeobox protein (bsh). (*C* and *D*) Test of prediction 11F6, a homolog of rat vanilloid receptor type 1-like protein. Gel analysis of amplimers (*) with the source of the cDNA pool indicated above is shown in *A* and *C*. Primers (blue) and the region to which the amplimer sequence aligned (underlining) are shown in *B* and *D*. The indicated forward primers were used to generate the amplimer sequences (brain amplimer, *B*; skin amplimer, *D*). Br, brain; Ey, eye; He, heart; Ki, kidney; Li, liver; Lu, lung; Mu, muscle; Ov, ovary; Sk, skin; St, stomach; Te, testis; Th, thymus.

Before the enrichment procedure, the combined predictions of SGP2 and TWINSCAN overlap 98% of multiexon ENSEMBL genes, as compared with 90% for the enriched pool. This finding suggests that the enrichment procedure reduces sensitivity by a small but noticeable degree. To investigate the potential loss of sensitivity further, we applied the same RT-PCR procedure to two samples of gene predictions that were excluded by the enrichment criterion and did not overlap ENSEMBL predictions. One sample had one or more regions of strong similarity to a predicted human gene but did not satisfy the aligned intron criterion (similar pool) whereas the other lacked any strong similarity to a human prediction by the same program (other pool). The verification rates for the similar and other pools were 25% and 20%, respectively, for genes predicted by both programs, and 0% and 2%, respectively, for genes predicted by only one program (Table 1 and www1.imim.es/datasets/mouse2002). This finding shows that the enrichment procedure increases specificity greatly and, consistent with the ENSEMBL overlap analysis, reduces sensitivity only slightly. If all predictions in the similar and other pools were tested the expected numbers of successes are 126 (±105) and 105 (±83), respectively, with the large standard errors resulting from the small number of successful amplifications in these pools.

As a control, we also tested 113 predictions from the enriched pool that did overlap ENSEMBL predictions. In 66 of the predictions the splice boundary we tested was predicted identically in ENSEMBL, and 64 of these tests (97%) were positive. In 47 of the predictions the splice boundary we tested was not predicted identically in ENSEMBL, and 21 of these tests (45%) were positive,

**Table 1. Predicted novel gene sets and RT-PCR verification rates**

| Pool | Programs* | No. of predictions | No. tested | No. positive | Success rate, % | Expected successes | Standard error |
|---|---|---|---|---|---|---|---|
| Enriched† | Both | 827 | 154 | 117 | 75.97 | 628 | |
| | One | 601 | 60 | 16 | 26.67 | 160 | |
| | Total | 1,428 | 214 | 133 | 62.15 | 788 | 48 |
| Similar‡ | Both | 505 | 16 | 4 | 25.00 | 126 | |
| | One | 1,620 | 22 | 0 | 0.00 | 0 | |
| | Total | 2,125 | 38 | 4 | 10.53 | 126 | 105 |
| Other§ | Both | 234 | 5 | 1 | 20.00 | 46 | |
| | One | 3,425 | 58 | 1 | 1.72 | 59 | |
| | Total | 3,659 | 63 | 2 | 3.17 | 105 | 83 |
| All | Total | 7,212 | 315 | 139 | N/A | 1,019 | |

N/A, not applicable.

*Both, Genes predicted at least partially by both TWINSCAN and SGP2 programs. One, Genes predicted by one program that are not overlapped by predictions of the other program. N/A, not applicable.

†Mouse gene predictions containing an intron whose flanking exonic regions align with flanking exonic regions predicted by the same program in human.

‡Mouse gene predictions that fail the enrichment step but show regions of strong similarity to a gene predicted by the same program in human.

§Mouse gene predictions without regions of strong similarity to any gene predicted by the same program in human.

despite the fact that ENSEMBL predictions are based on transcript evidence. This verification rate may reflect alternative splices identified by our method but not by ENSEMBL.

To determine whether tissue-restricted expression could explain the absence of the predictions we verified from the transcript-based annotation, we compared the expression patterns of our RT-PCR positive predictions to those of the complete set of mouse orthologs of genes mapping to human chromosome 21 (Hsa21). These genes were chosen for comparison because they had been previously subjected to the same protocol with the same cDNA pools in the same laboratory (20). Our verified novel gene predictions showed a significantly more restricted pattern of expression (Fig. 4*A*). The mean number of tissues for our positive predictions was 6.3, and 33% of the positive predictions showed expression in three or fewer tissues; the corresponding numbers for the mouse orthologs of human chromosome 21 genes are 8.2 tissues on average and 14% showing expression in three or fewer tissues. This difference in expression specificity was statistically significant (ANOVA, $F = 23.22$, df = 1, $P < 0.001$).

To determine whether prediction of pseudogenes by our method could explain some of the RT-PCR negatives, we computed the ratio of nonsynonymous to synonymous substitution rates ($K_A/K_S$) (21) for the subset of tested mouse predictions with unique putative human orthologs (Fig. 4*B*). The mean for PCR-positive predictions was 0.29 whereas for PCR-negative predictions it was 0.72. The difference was statistically significant (ANOVA, $F = 34.86$, df = 1, $P < 0.001$), suggesting that (*i*) some of the negative predictions may be pseudogenes, and (*ii*) $K_A/K_S$ can be efficiently incorporated in the enrichment protocol to increase specificity (22).

Among the predictions with confirmed splices, 112 had significant homology to known genes and/or domains. A few of these genes, which were not represented in databases at the beginning of our gene survey, were submitted to databases and/or published in the literature in the intervening months. For example, we correctly predicted the first four protein coding exons of *TRPV3*, a heat-sensitive TRP channel in keratinocytes (23), and both exons of *RLN3* (*preprorelaxin 3*), an insulin-like prohormone (24). The verified predictions with the most notable homologies are shown in Table 2, including a novel homolog of dystrophin that is discussed in the mouse genome paper (1). Table 2 includes two noncanonical homeobox genes, one that is most similar to fruitfly brain-specific homeobox protein (Figs. 2 and 3 *A* and *B*) (25) and another that is a Not-class homeobox, likely to be involved in notochord development (26). Four predicted genes were found to be expressed in the brain and are likely to have neuronal functions, including one paralog each of: *Nna1*, which is expressed in regenerating motor neurons (27); an *N*-acetylated-α-linked-acidic dipeptidase, which hydrolyses the neuropeptide *N*-acetyl-aspartyl-glutamate to terminate its neurotransmitter activity (28); a novel γ-aminobutyric acid type B receptor, which regulates neurotransmitter release (29); and an Ent2-like nucleoside transporter, which modulates neurotransmission by altering adenosine concentrations (30). Other verified genes are likely to be important in muscle contraction (myosin light chain kinase homolog), degradation of cell cycle proteins (fizzy/CDC20 homolog), Wnt-dependent vertebrate development (Dapper/frodo homolog), and solute and steroid transport in the liver (solute transporter β). Homologs of two further genes predicted in our studies are associated with disease. *ATP10C*, an aminophospholipid translocase, is absent from Angelman syndrome patients with imprinting mutations (31), and *otoferlin*, which is mutated in a nonsyndromic form of deafness (32).

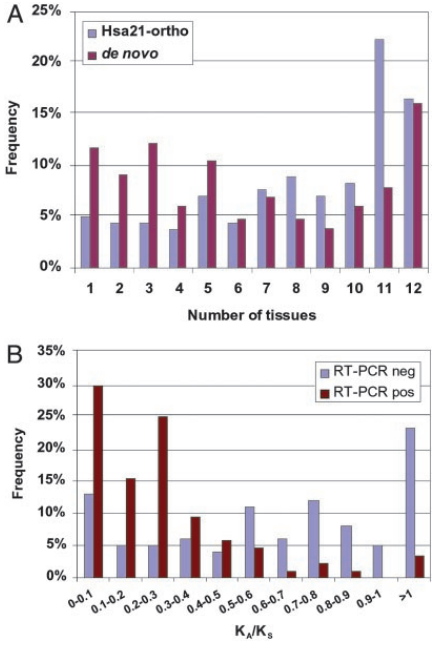


**Fig. 4.** Characteristics of verified predictions. (*A*) Expression specificity. Percentages of RT-PCR positive *de novo* predictions (red) and Hsa21 mouse orthologs (blue) expressed in 1–12 tissues, tested in the same cDNA pools. (*B*) Distributions of the ratio of nonsynonymous to synonymous substitution rate ($K_A/K_S$) in 83 RT-PCR positive (red) vs. 98 RT-PCR negative (blue) mouse predictions with reciprocal best BLAST matches among the human predictions.

**Table 2. Novel mouse genes, their tissue expression, and their homologs**

| Code | B | H | K | Y | V | S | M | L | T | K | E | O | %Id | Ln | Homology |
|---|---|---|---|---|---|---|---|---|---|---|---|---|---|---|---|
| 3B1 | | | | | | | | + | + | | | | 38 | 134 | Dystrophin-like; with ZZ domain |
| 3B3 | | | | + | | + | | + | + | + | | | 25 | 184 | Novel aquaporin; similar to *Drosophila* CG12251 |
| 3C3 | | | + | | + | | | + | + | | + | | 25 | 260 | TEP1 (telomerase associated); probable ATPase |
| 3C5 | | | | | | | | | + | | + | | 47 | 198 | Voltage-dependent calcium channel $\gamma$ subunit |
| 4B3 | | | + | | | + | | | + | | | | 34 | 74 | IFN-induced/fragilis transmembrane family |
| 4C6 | | + | | | | + | | + | + | + | | | 30 | 134 | IL-22-binding protein CRF2-10 |
| 4G4 | + | | | | | | | | + | + | + | | 64 | 109 | Nna1p, nuclear ATP/GTP-binding protein |
| 5B5 | | | | | | + | | | + | + | | | 43 | 111 | Likely aminophospholipid flippase (transporting ATPase) |
| 1E3 | + | | | + | + | | | + | | | + | | 40 | 106 | *N*-acetylated-$\alpha$-linked-acidic dipeptidase (NAALADase) |
| 6C4 | | | | | | | | + | + | | | | 42 | 117 | Not-type homeobox; poss. involved in notochord development |
| 6F5 | + | + | + | | | | | | | | | | 66 | 102 | *Drosophila* brain-specific homeobox protein (bsh) |
| 11F2 | + | | | | | + | | + | + | + | | | 29 | 216 | Human $\gamma$-aminobutyric acid type B receptor 2, neurotransmitter release regulator |
| 5A2 | | | + | | + | + | | | + | | | | 41 | 36 | Skate liver organic solute transporter $\beta$ |
| 11B6 | | | | + | | | | + | | | + | | 55 | 116 | IFN-activatable protein 203; nuclear protein |
| 12B3 | + | | | + | + | + | | + | + | + | + | | 25 | 229 | Fatty acid desaturase; maintains membrane integrity |
| 11F6 | + | + | | | | + | | + | + | + | + | | 44 | 494 | Rat vanilloid receptor type 1 like protein 1 |
| 12E3 | | | | | | | | + | + | | | | 52 | 175 | Fizzy/CDC20; modulates degradation of cell-cycle proteins |
| 12F1 | | + | | | | + | + | + | + | | | | 43 | 355 | Otoferlin (mutated in DFNB9, nonsyndromic deafness) |
| 12H1 | + | + | | | | | | | + | | | | 45 | 116 | Fruitfly additional sex combs; a Polycomb group protein |
| 12C4 | + | | | | | | | + | | | + | | 43 | 133 | *Caenorhabditis elegans* C15C8.2; single-minded-like; HLH and PAS domains |
| 12D2 | | | | | | + | | | | | | | 41 | 397 | Cytosolic phospholipase A2, group IVB |
| 12A5 | + | | | | | | | | | | | | 38 | 415 | Fruitfly GH15686p; Ent2-like nucleoside transporter |
| 12E5 | + | | | + | | | | + | | | | + | 32 | 111 | Relaxin 3 preproprotein; prohormone of the insulin family |
| 11A1 | | | + | + | + | | + | | | | | + | 89 | 75 | Mouse BET3, involved in ER to Golgi transport |
| 11A2 | + | + | | | | | | + | + | | + | + | 70 | 207 | Vacuolar ATP synthase subunit S1 |
| 11B2 | | | | | | | + | + | + | + | + | + | 54 | 271 | Myosin light chain kinase, skeletal muscle |
| 11G2 | + | | + | + | + | + | | + | + | + | + | + | 36 | 179 | Dapper/frodo (transduces Wnt signals by interacting with Dsh) |

Code, Coding name of tested gene model. B, brain; H, heart; K, kidney; Y, thymus; V, liver; S, stomach; M, muscle; L, lung; T, testis; K, skin; E, eye; O, ovary. %Id, Percentage amino acid identity. Ln, Number of amino acids in the local alignment between the prediction and the homolog.

## Discussion

We have demonstrated a remarkably efficient mammalian gene discovery system. This system exploits the draft mouse and human genome sequences in both an initial gene-prediction stage and an enrichment stage. The first stage consists of SGP2 and TWINSCAN, gene-prediction programs that use genome alignment in combination with statistical patterns in the DNA sequence. We have shown elsewhere that both programs have greater sensitivity and specificity than single-genome *de novo* predictors, such as GENSCAN (13, 14). In this article, we have demonstrated the effectiveness of the enrichment stage, in which predictions are retained only if the protein predicted in mouse aligns to a human protein predicted by the same program, with at least one predicted intron at the same location (aligned intron, Fig. 1). In our pool of predictions, the aligned intron filter is expected to eliminate 24 times more RT-PCR negatives than RT-PCR positives. This enrichment procedure can be applied to predictions from any program.

Our goal was to develop a low-cost, high-throughput system for finding and verifying coding regions that are missed by annotation systems that require existing transcript evidence. ENSEMBL was chosen as the representative of such systems because the Mouse Genome Sequencing Consortium judged it to be the most suitable tool for timely, cost-effective, reliable annotation of the mouse genome sequence. Thus, we evaluated our system by investigating genes that do not overlap ENSEMBL predictions. Our system is not designed to find genes that would be missed by expert manual annotators, who can effectively integrate information such as the predictions of GENSCAN (8) and GENOMESCAN (33), percent-identity plots (34), comparison to fish genomes (35, 36), alignment of weakly homologous proteins, and alignment of EST sequences. As a result, we did not exclude gene predictions from our evaluation based on these indicators.

Our two-stage system identified a highly reliable pool of 827 predicted genes not overlapping the standard annotation, of which we tested 154 for expression by using RT-PCR and direct sequencing. Primers designed for a single pair of adjacent exons in each predicted gene yielded a spliced PCR product whose sequence closely matched that of the predicted exons in 76% of these tests. In the only other published report of high-throughput verification of gene predictions of which we are aware, 14% of predictions not overlapping the standard annotation yielded spliced products (37). These numbers cannot be compared directly because of differences in the sampling criteria, but the magnitude of the difference suggests our method provides new levels of efficiency in experimental confirmation of genes outside the standard annotation set.

The sensitivity of our method also appears to be high. Predictions in our enriched pool overlap 90% of multiexon genes predicted by ENSEMBL. However, it has been estimated that >4,000 ENSEMBL predictions comprising 12,000 predicted exons are in fact pseudogenes (1). Although the precise number of multiexon pseudogenes in the ENSEMBL annotation is unknown, this estimate suggests that our enriched pool may overlap a much larger fraction of the functional genes identified by ENSEMBL. Further, RT-PCR tests of TWINSCAN and SGP2 predictions outside the enriched pool indicate that a relatively small number of these predictions are transcribed and spliced in the 12 tissues tested. Thus, the enrichment procedure is sensitive to both ENSEMBL predictions and verifiable predictions by TWINSCAN and SGP2.

Using our system, we confirmed one intron of 139 predicted genes that do not overlap any gene in the standard mouse genome annotation (1). Ninety-two of the RT-PCR positive introns (66%) did not align to any mouse EST, and these might have posed difficulties even for human annotators. Furthermore, seven of the RT-PCR negative introns (4%) did align to mouse ESTs and six of these were in the enriched pool, suggesting that the true percentage of transcribed and spliced predictions in this pool may be even higher than the RT-PCR positive percentage.

Among RT-PCR positive predictions, 24 had homologies to known proteins that we found particularly interesting (Table 2). The positive identification of these homologs is expected to impact numerous research programs devoted to genes of developmental and medical importance. In general, these genes were probably missed in the ENSEMBL annotation because the length and percent identity of the homologies were not sufficient to support a protein-based gene prediction (Table 2). In many cases, such as the predicted homolog of a brain-specific homeobox protein, the ex-

pression patterns we found were consistent with what would be expected from the function of the known homolog (Fig. 3 *A* and *B*).

The confirmed 139 genes also showed a relatively restricted expression pattern, on average. Because all mouse orthologs of genes on human chromosome 21 had already been tested by using the same experimental protocol and the same cDNA pools, we were able to directly compare expression patterns. To the extent that the known genes on chromosome 21 are no more tissue specific than the complete set of known genes, the results (Fig. 4) suggest that our system may be particularly sensitive to genes with tissue-restricted expression. Qualitatively similar restricted expression patterns were reported for novel GENSCAN predictions on chromosome 22 (37), lending further support to the value of *de novo* prediction for identifying genes with tissue-restricted expression.

Of the RT-PCR positive novel predictions, only 33% have identifiable homologs in the sequenced fish (*Fugu*/*Tetraodon*/zebrafish) genomes. Comparing this finding to the recent estimate that three-quarters of all human genes can be recognized in the *Fugu* genome (36) suggests that our system may be particularly sensitive to genes that are not ubiquitous in the vertebrate lineage. Genes with relatively restricted expression patterns and species distribution can be difficult to find by using transcript-based methods like GENEWISE (38) and compact-genome methods like EXOFISH (35), but they appear to be tractable for our system.

Extrapolating from the success rates in all categories, the expected total number of gene predictions that could be successfully RT-PCR amplified in the cDNA pools we tested is 1,019 (Table 1), adding ≈5% to the number of functional mouse genes identified by ENSEMBL (1). The number of distinct genes verifiable in this way may be slightly smaller, because the effect of fragmentation in ENSEMBL and in our predictions is not readily testable. However, the number of predictions that are transcribed and spliced is likely to be >1,019, because (*i*) we tested only one exon pair from each prediction and (*ii*) we used only 12 adult mouse tissues (20).

The relatively low success rate in the pools failing the enrichment step suggests that the number of real, multiexon genes whose existence has been predicted but not yet confirmed is in the range of 1,000–2,000 (including those predictions in the enriched pool that have not been confirmed). Because we have used only two prediction programs, TWINSCAN and SGP2, it is possible that other programs might yield a large additional set of predictions that pass the enrichment step. However, GENSCAN yields only 49 additional predictions that pass enrichment and novelty criteria and do not overlap the 1,428 "aligned intron" novel predictions from TWINSCAN and SGP2 (3%). These 49 are worth testing, and adding more prediction programs will yield at least a few more predictions with aligned introns. Nonetheless, the data presented here suggest that the 1,428 predictions in the enriched pool may overlap a significant fraction of the previously unannotated, multiexon mouse genes.

Using the draft sequences of the mouse and human genomes, we have developed a cost-effective, high-throughput system for predicting genes and verifying the existence of corresponding spliced transcripts. Applying this system to the entire mouse genome, we showed that an automated system can produce a large set of experimentally supported mammalian gene predictions outside the standard annotation. Further, the average cost per verified exon pair is less than two primer pairs and sequencing reactions. We expect that testing the remaining predictions in the enriched pool will locate most multiexon mouse genes that are currently unannotated, bringing us significantly closer to identification of the complete mammalian gene set.

As more mammalian genomes are sequenced, the need for experimentally validated high-throughput annotation will continue to grow, as will the data available for methods such as ours. Using the sequences of more genomes, it may be possible to extend this approach to single-exon and lineage-specific genes. In combination with methods like ENSEMBL and refinement by expert annotators, these developments may bring complete, experimentally supported genome annotation within reach.

We are grateful to the Mouse Genome Sequencing Consortium for providing the mouse genome sequence as well as support throughout the analysis process. We are particularly grateful to Eric Lander, Robert Waterston, Ewan Birney, Adam Felsenfeld, and Ross Hardison for advice and encouragement. Thanks are also due to Marc Vidal, Lior Pachter, Kerstin Lindblad-Toh, and Gwen Acton for participation in pilot experiments and Tamara Doering for helpful comments on the manuscript. Research at Institut Municipal d'Investigació Mèdica/Universitat Pompeu Fabra/Centre de Regulació Genòmica is supported by a grant from the Spanish Plan Nacional de Investigacion y Desarrollo. J.F.A. is supported by a fellowship from the Instituto de Salud Carlos III. The Division of Medical Genetics is supported by the Swiss National Science Foundation, National Centres of Competence in Research Frontiers in Genetics, and the Childcare and J. Lejeune Foundations. Research at Washington University was supported by Grant DBI-0091270 from the National Science Foundation (to M.R.B.) and Grant HG02278 from the National Institutes of Health (to M.R.B.).

1. Mouse Genome Sequencing Consortium (2002) *Nature* **420,** 520–562.
2. Hubbard, T., Barker, D., Birney, E., Cameron, G., Chen, Y., Clark, L., Cox, T., Cuff, J., Curwen, V., Down, T., *et al*. (2002) *Nucleic Acids Res.* **30,** 38–41.
3. Pruitt, K. D. & Maglott, D. R. (2001) *Nucleic Acids Res.* **29,** 137–140.
4. Kawai, J., Shinagawa, A., Shibata, K., Yoshino, M., Itoh, M., Ishii, Y., Arakawa, T., Hara, A., Fukunishi, Y., Konno, H., *et al*. (2001) *Nature* **409,** 685–690.
5. The FANTOM Consortium and The RIKEN Genome Exploration Research Group Phase II Team (2002) *Nature* **420,** 563–571.
6. Bairoch, A. & Apweiler, R. (2000) *Nucleic Acids Res.* **28,** 45–48.
7. Gasteiger, E., Jung, E. & Bairoch, A. (2001) *Curr. Issues Mol. Biol.* **3,** 47–55.
8. Burge, C. & Karlin, S. (1997) *J. Mol. Biol.* **268,** 78–94.
9. Wiehe, T., Gebauer-Jung, S., Mitchell-Olds, T. & Guigó, R. (2001) *Genome Res.* **11,** 1574–1583.
10. Pachter, L., Alexandersson, M. & Cawley, S. (2002) *J. Comput. Biol.* **9,** 389–399.
11. Batzoglou, S., Pachter, L., Mesirov, J. P., Berger, B. & Lander, E. S. (2000) *Genome Res.* **10,** 950–958.
12. Bafna, V. & Huson, D. H. (2000) *Proc. Int. Conf. Intell. Syst. Mol. Biol.* **8,** 3–12.
13. Parra, G., Agarwal, P., Abril, J. F., Wiehe, T., Fickett, J. W. & Guigó, R. (2003) *Genome Res.* **13,** 108–117.
14. Flicek, P., Keibler, E., Hu, P., Korf, I. & Brent, M. R. (2003) *Genome Res.* **13,** 46–54.
15. Korf, I., Flicek, P., Duan, D. & Brent, M. R. (2001) *Bioinformatics* **17,** Suppl. 1., S140–S148.
16. Parra, G., Blanco, E. & Guigó, R. (2000) *Genome Res.* **10,** 511–515.
17. Guigó, R., Knudsen, S., Drake, N. & Smith, T. (1992) *J. Mol. Biol.* **226,** 141–157.
18. Altschul, S. F., Gish, W., Miller, W., Myers, E. W. & Lipman, D. J. (1990) *J. Mol. Biol.* **215,** 403–410.
19. Altschul, S. F., Madden, T. L., Schaffer, A. A., Zhang, J., Zhang, Z., Miller, W. & Lipman, D. J. (1997) *Nucleic Acids Res.* **25,** 3389–3402.
20. Reymond, A., Marigo, V., Yaylaoglu, M. B., Leoni, A., Ucla, C., Scamuffa, N., Caccioppoli, C., Dermitzakis, E. T., Lyle, R., Banfi, S., *et al*. (2002) *Nature* **420,** 582–586.
21. Hughes, A. L. & Nei, M. (1988) *Nature* **335,** 167–170.
22. Nekrutenko, A., Makova, K. D. & Li, W. H. (2002) *Genome Res.* **12,** 198–202.
23. Peier, A. M., Reeve, A. J., Andersson, D. A., Moqrich, A., Earley, T. J., Hergarden, A. C., Story, G. M., Colley, S., Hogenesch, J. B., McIntyre, P., *et al*. (2002) *Science* **296,** 2046–2049.
24. Bathgate, R. A., Samuel, C. S., Burazin, T. C., Layfield, S., Claasz, A. A., Reytomas, I. G., Dawson, N. F., Zhao, C., Bond, C., Summers, R. J., *et al*. (2002) *J. Biol. Chem.* **277,** 1148–1157.
25. Jones, B. & McGinnis, W. (1993) *Development (Cambridge, U.K.)* **117,** 793–806.
26. Talbot, W. S., Trevarrow, B., Halpern, M. E., Melby, A. E., Farr, G., Postlethwait, J. H., Jowett, T., Kimmel, C. B. & Kimelman, D. (1995) *Nature* **378,** 150–157.
27. Harris, A., Morgan, J. I., Pecot, M., Soumare, A., Osborne, A. & Soares, H. D. (2000) *Mol. Cell. Neurosci.* **16,** 578–596.
28. Pangalos, M. N., Neefs, J. M., Somers, M., Verhasselt, P., Bekkers, M., van der Helm, L., Fraiponts, E., Ashton, D. & Gordon, R. D. (1999) *J. Biol. Chem.* **274,** 8470–8483.
29. Billinton, A., Ige, A. O., Bolam, J. P., White, J. H., Marshall, F. H. & Emson, P. C. (2001) *Trends Neurosci.* **24,** 277–282.
30. Crawford, C. R., Patel, D. H., Naeve, C. & Belt, J. A. (1998) *J. Biol. Chem.* **273,** 5288–5293.
31. Meguro, M., Kashiwagi, A., Mitsuya, K., Nakao, M., Kondo, I., Saitoh, S. & Oshimura, M. (2001) *Nat. Genet.* **28,** 19–20.
32. Yasunaga, S., Grati, M., Cohen-Salmon, M., El-Amraoui, A., Mustapha, M., Salem, N., El-Zir, E., Loiselet, J. & Petit, C. (1999) *Nat. Genet.* **21,** 363–369.
33. Yeh, R. F., Lim, L. P. & Burge, C. B. (2001) *Genome Res.* **11,** 803–816.
34. Schwartz, S., Zhang, Z., Frazer, K. A., Smit, A., Riemer, C., Bouck, J., Gibbs, R., Hardison, R. & Miller, W. (2000) *Genome Res.* **10,** 577–586.
35. Roest Crollius, H., Jaillon, O., Bernot, A., Dasilva, C., Bouneau, L., Fischer, C., Fizames, C., Wincker, P., Brottier, P., Quetier, F., *et al*. (2000) *Nat. Genet.* **25,** 235–238.
36. Aparicio, S., Chapman, J., Stupka, E., Putnam, N., Chia, J. M., Dehal, P., Christoffels, A., Rash, S., Hoon, S., Smit, A., *et al*. (2002) *Science* **297,** 1301–1310.
37. Das, M., Burge, C. B., Park, E., Colinas, J. & Pelletier, J. (2001) *Genomics* **77,** 71–78.
38. Birney, E. & Durbin, R. (2000) *Genome Res.* **10,** 547–548.
39. Notre dame, C., Higgins, D. G. & Heringa, J. (2000) *J. Mol. Biol.* **302,** 205–217.

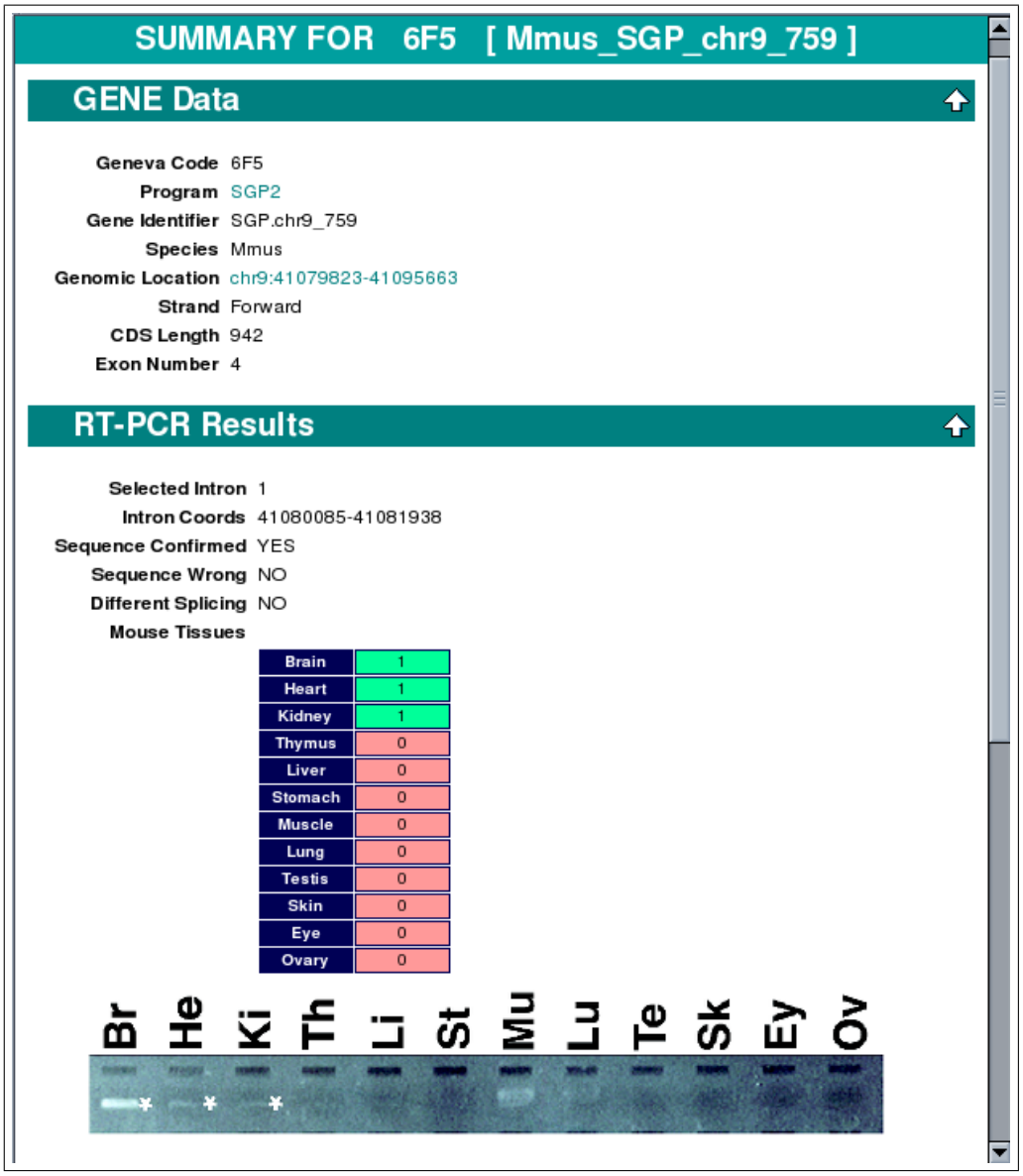


Figure 3.10: **A web server to display RT-PCR results over predicted genes.** A small database containing all the 476 genes that were submitted for the RT-PCR validation test was provided as supplementary materials for Guigó *et al.* [2003, see also page 215 on web glossary]. That pool of genes was filtered out from the gene predictions by `SGP2` and `Twinscan` on the mouse genome by exploiting conservation in mouse-human exonic structure.

# Chapter 4

# Sequence features of Eukaryotic Genes

> The human mind has first to construct forms,
> independently, before we can find them in things.
> —Albert Einstein

Most genes in higher eukaryotes are interrupted by non-coding sequences (introns) that must be precisely excised from pre-messenger RNA (pre-mRNA) molecules to yield mature, functional mRNAs. In those organisms, splicing introduces an additional level of decoding on the sequence of the primary RNA transcript, prior to translation. The genetic code is essentially deterministic. Within a given species, a given triplet in the mRNA sequence results always in the same amino acid. In contrast, the splicing code is inherently stochastic. The probability of a splicing sequence in the primary transcript to participate in the definition of an intron boundary ranges from zero to one, and is conditioned to very many different factors.

The unexpected discovery in 1977 of split genes in the adenovirus 2 (*Ad2*) mRNAs [Berget *et al.*, 1977; Chow *et al.*, 1977], started an amazing scientific endeavour. In this chapter we start with an overview of the current knowledge about the splicing process at molecular level. Then we report a comparative computational analysis of orthologous splice sites of four vertebrate genomes.

## 4.1 The Molecular Basis of Splicing

A typical mammalian gene contains nine introns and spans about 30 kb. An average intron is over 3000 bp long, while an average exon is only about 150 bp [Lander *et al.*, 2001]. It has been known for a long time that intron removal and the ligation of flanking sequences (exons) occurs through two sequential trans-esterification reactions that are carried out by a multicomponent complex that is known as the spliceosome (see Figure 4.1).

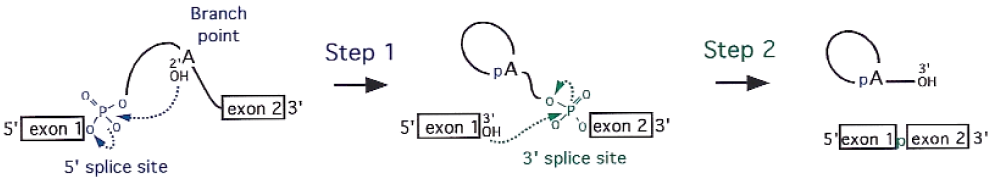


Figure 4.1: **The splicing reaction at the biochemical level.** The pre-mRNA splicing reaction consists of two phosphoryl-transfer steps. In the first step, the 5′ phosphate of the intron (at the 5′ splice site) is attacked by a 2′ hydroxyl specified within the intron (from the adenosine in the branch point). In a second step, the 3′ phosphate of the intron (at the 3′ splice site) is attacked by the 3′ hydroxyl of the cleaved 5′ exon. The final products are ligated exons and the excised intron in a branched form also known as lariat. Adapted from Collins and Guthrie [2000].

Most introns have common consensus sequences near their 5′ and 3′ ends that are recognized by spliceosomal components and are required for spliceosome formation. The assembly of a spliceosome on a pre-mRNA is an ordered process that involves five small nuclear ribonucleoprotein particles (snRNPs: U1, U2, U4, U5 and U6), as well as an array of protein factors. Catalysis of the splicing reaction proceeds by coordinated series of RNA-RNA, RNA-protein and protein-protein interactions, which lead to exon ligation and release of the intron lariat [Patel and Steitz, 2003].

### 4.1.1 U2 versus U12 splice sites

The first intron sequences ever characterized revealed highly conserved dinucleotides at the 5′ and 3′ termini (GT and AG, respectively). They were later found to be parts of longer consensus sequences at the 5′ and 3′ splice sites (such as those represented in Figure 1.3 on page 4 and those shown in Figure 4.12 on page 130 (Figure 1 on page 112 of Abril *et al.* 2005). The canonical splice site consensus sequence was first catalogued by Mount [1982] an later refined with more data by Senapathy *et al.* [1990]. The presence of non-consensus splice sites was first recognized in Jackson [1991], but it was not proposed that there was a distinct minor class of introns until the works of Hall and Padgett [1994]. They noted that four introns shared unusual consensus sequences, and predicted that their excision was mediated by a distinct spliceosome that involved low-abundance snRNPs (less than $10^4$ copies per cell), U11 and U12 [Montzka and Steitz, 1988], for which no function had been described at that time. Indeed, U11 and U12 have base-pairing potential with the 5′ splice-site and branch-site sequences, whereas their secondary structures mimic those of U1 and U2, respectively (Figure 4.2).

Because these new introns had AT and AC termini, which deviates from the nearly invariant GT-AG rule, they were initially named AT-AC introns. However, more extensive genomic database surveys revealed that AT-AC termini are not a defining feature of the minor class introns [Dietrich *et al.*, 1997; Sharp and Burge, 1997; Wu and Krainer, 1997]. In fact, most minor-class introns have canonical GT-AG termini and, very rarely, major-class introns have AT-AC termini [Sharp and Burge, 1997]. An analysis of canonical and non-canonical splice sites in mammalian genomes [Burset *et al.*, 2000] estimated the occurrence of different splice site termini: GT-AG (99.20%), CG-AG (0.62%), AT-AC (0.08%),

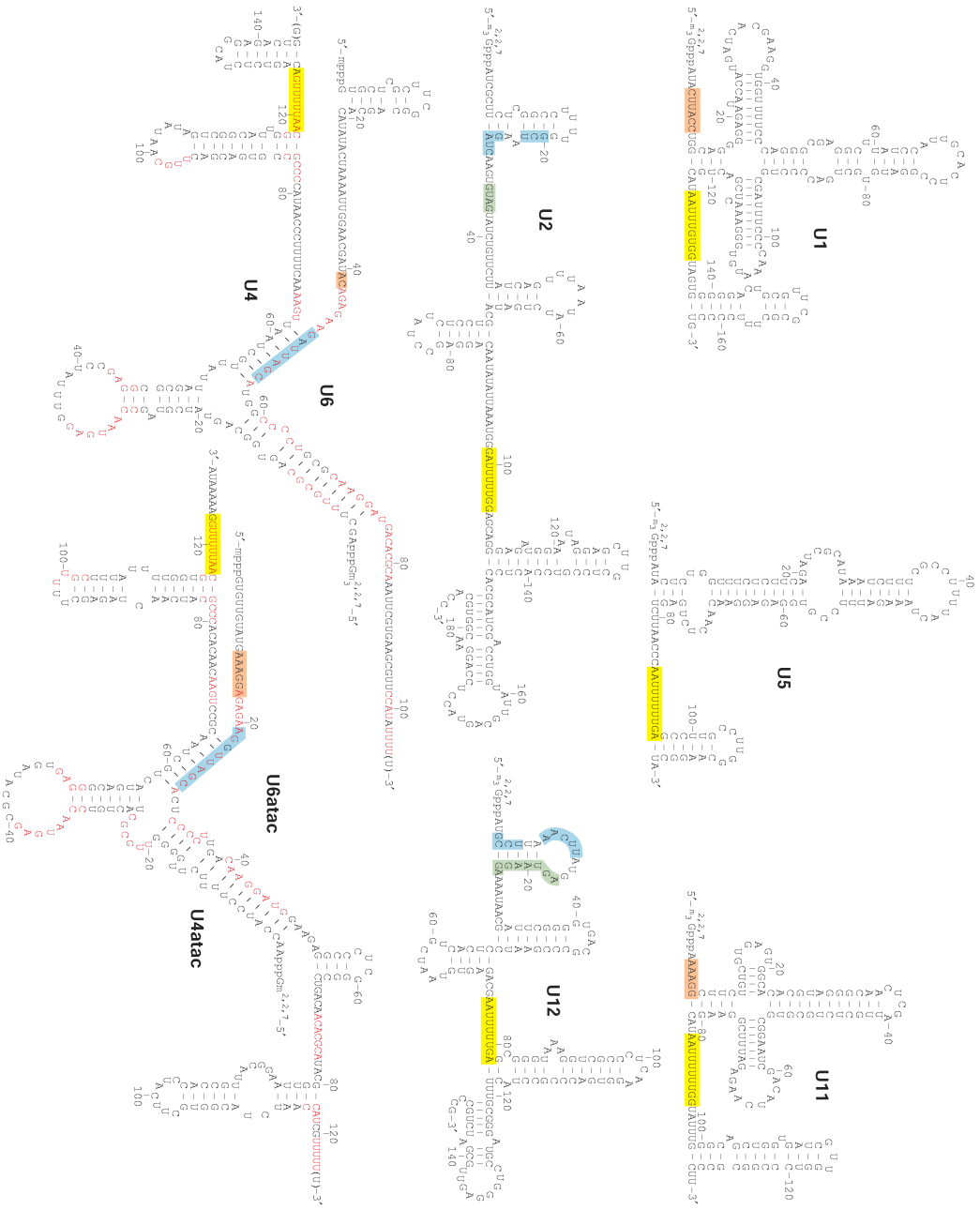


Figure 4.2: **Sequences and predicted secondary structures of the human spliceosomal snRNAs.** Similarities in secondary structure are apparent between the major- and the minor-class snRNA counterparts (U1 and U11, U2 and U12, and U4-U6 and U4ATAC-U6ATAC), despite substantial sequence divergence. The Sm-binding sites are shaded in yellow. Coloured boxes indicate sequences that are predicted to be involved in intermolecular RNA-RNA base-pairing interactions: 5′ splice site (orange), branch site (green), and U2-U6 or U12-U6ATAC helix I interactions (blue). Sequences in red represent stretches of four or more identical nucleotides between U4-U6 and U4ATAC-U6ATAC. Adapted from Patel and Steitz [2003].

other non-canonical (0.03%) and errors (0.06%). A more recent analysis of such frequencies for human, mouse and rat splice sites can be found in Table 4.3 on page 132 (Table 2 on page 114 of Abril *et al*. 2005). Biochemical studies showed that mutation of AT-AC to GT-AG termini did not interfere with splicing by the U12-dependent pathway. Instead, U12-dependent splicing is determined by the longer and more tightly constrained consensus sequences at the 5′ splice site and branch site of minor-class introns, as well as by the lack of a polypyrimidine tract upstream of the 3′ splice site [Dietrich *et al*., 1997; Sharp and Burge, 1997; Burge *et al*., 1998]. Therefore, the more suitable 'U12-type' nomenclature was adopted for this new class of introns.

### 4.1.2 The splicing process

For major-class introns, spliceosome assembly (see left pathway of Figure 4.3) is thought to begin with the association of the U1 and U2 snRNPs by base-pairing interactions with conserved sequences at the 5′ splice site (5′ss) and intron branch site, respectively [Reed, 1996]. During the spliceosome assembly, the U1 snRNP binds to the 5′ss via base base pairing between the splice site and the U1 snRNA. The 3′ splice site (3′ss) elements are bound by a special set of protein factors, SF1 (a branch-point binding protein, also called BBP in yeast), SF3, and a dimeric U2 snRNP auxiliary factor (U2AF). The 65 kDa subunit of U2AF binds to the polypyrimidine track. In at least some cases, the 35 kDa subunit of U2AF binds to the AG at the intron/exon junction. In mammalian cells, selection of the branch point is based primarily upon relative position, in the vast majority of cases the RNA branch forms 18–38 nucleotides upstream of the 3′ss. It is probable that this distance constraint reflects the requirement for the U2AF protein. The earliest defined complex in spliceosome assembly, called the commitment complex or E-complex (early), contains U1 and U2AF bound at the two intron ends [Burge *et al*., 1999]. The E-complex is joined by the U2 snRNP, whose snRNA base-pairs at the branch point, to form the A complex. The U2 branch-site duplex protrudes outwards the adenosine residue, the 2′ hydroxyl group of which participates in the first nucleophilic atack.

The tri-snRNP complex of U5 and the base-paired U4-U6 then stably joins the pre-spliceosome [Konarska and Sharp, 1987] to form the B-complex, although there is evidence to suggest that U5 interacts upstream of the 5′ss at a much earlier stage [Wyatt *et al*., 1992]. The B-complex undergoes a complicated rearrangement to form the activated spliceosome (B*-complex). This rearrangement is promoted by ATP-hydrolyzing protein factors that juxtapose the 5′ and 3′ss and form the catalytic core. U4-U6 duplexes unwind [Lamond *et al*., 1988], and the U4 and U1 snRNPs are displaced, which allows U6 to form base-pairing interactions with the 5′ss [Wassarman and Steitz, 1992] and with a region of U2 that is near the U2 branch-site duplex [Datta and Weiner, 1991; Hausner *et al*., 1990; Madhani and Guthrie, 1992; Wu and Manley, 1991]. The activated spliceosome catalyzes the first trans-esterification step of splicing and the C-complex is formed. The U5 snRNP has been shown to base-pair with sequences in both the 5′ and 3′ exons (see Figure 4.4). U5 is also believed to position the ends of the two exons for the second step of splicing [Wyatt *et al*., 1992; Wassarman and Steitz, 1992; Newman and Norman, 1991, 1992; Sontheimer and Steitz, 1993]. After the second step has been completed, the ligated exons and a lariat intron are released, and the spliceosomal components dissociate and are recycled for further rounds of splicing.

Two general properties of the spliceosome are remarkable. First, it is conserved from

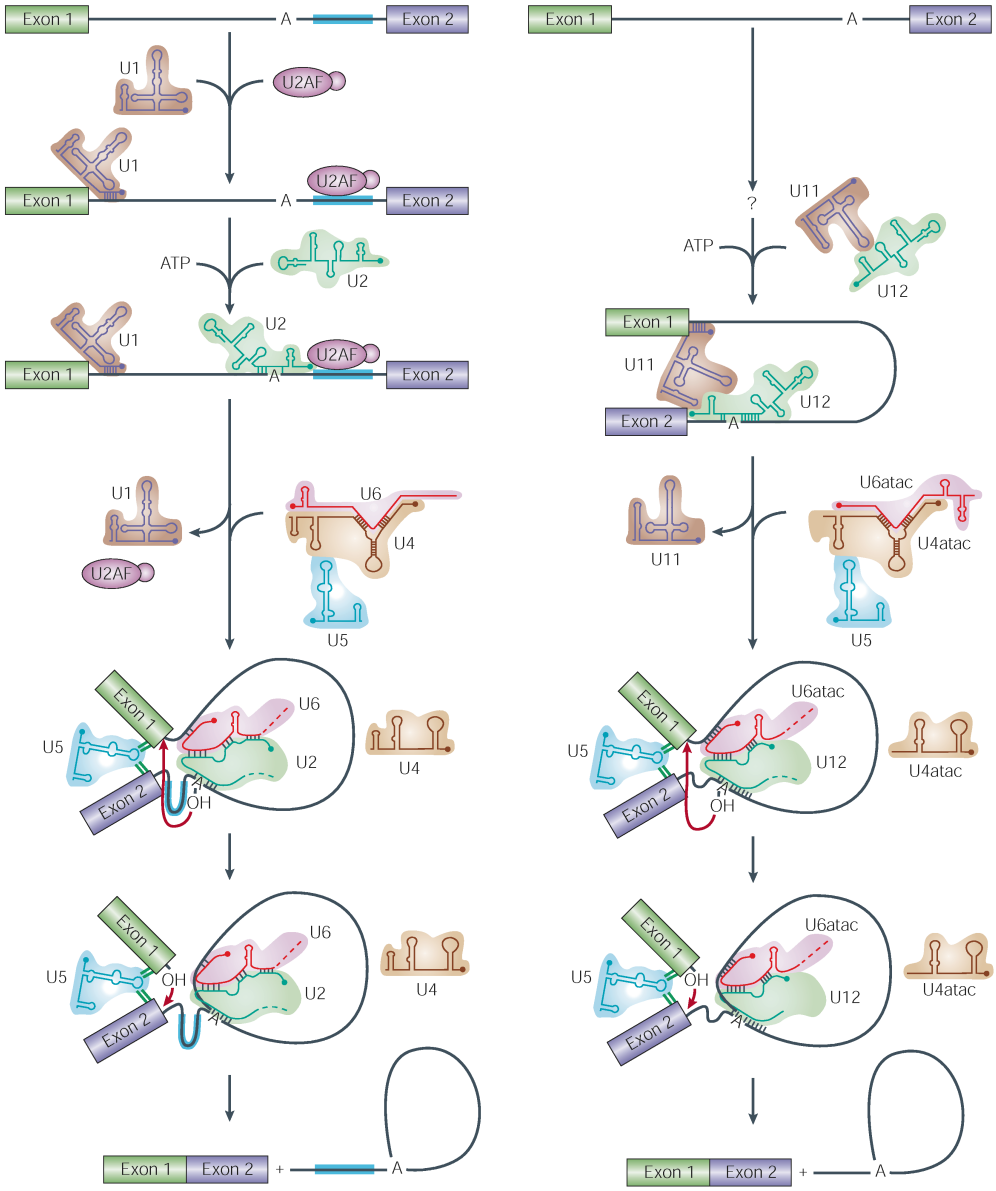


Figure 4.3: **Pathways of assembly and catalysis of U2 and U12 spliceosomes.** The major-class (*left*) and the minor-class (*right*) splicing pathways are shown side by side, highlighting their similarities and differences. The two pathways are mechanistically very similar. The primary differences occur during the early steps of spliceosome formation. The two transesterification reactions are indicated by red arrows. Each schematic snRNP is shown as a small nuclear RNA (not drawn to scale, with the 5′ terminus denoted by a dot) with the surrounding shaded area representing proteins. The polypyrimidine track of the major-class intron is shaded blue. Green bars represent interactions between the conserved loop of U5 and exon termini. Adapted from Patel and Steitz [2003].

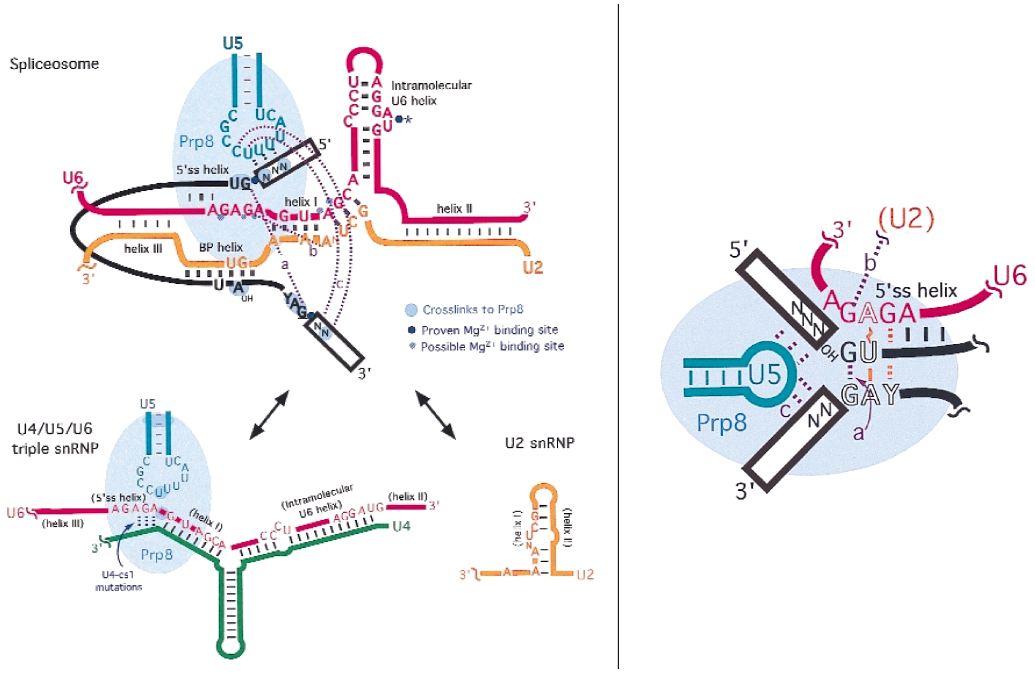


Figure 4.4: **Working model of RNA and Prp8 interactions in the catalytic core.** *Left panel*) Mutually exclusive interactions of U6 and U2 snRNAs in pre-assembled snRNPs are also shown. Large letters denote RNA sequences that are absolutely conserved in major, minor and trans spliceosomes from mammals, worms, plants, yeast and trypanosomes. Black lines denote Watson-Crick base-pairing interactions (the thinner lines denote interactions that are not absolutely conserved in all systems). Exons are drawn as rectangles, while the intron is depicted as a black line. *Right panel*) Some of the interactions of the active spliceosome are drawn for the second trans-esterification step of splicing: the 5′ splice site helix formed between U6 and the intron, and the interactions of the U5 conserved loop with exons. Purple dotted lines indicate tertiary interactions a, b, and c in both panels. Adapted from Collins and Guthrie [2000].

yeast to humans, both in its protein make-up and in its small nuclear RNAs (snRNAs), which have short, almost universally conserved sequences that are known to be juxtaposed to the reaction center during catalysis. Second, it is extraordinarily flexible, as it can excise introns of many different lengths and many different sequences. It is also subject to regulation, giving rise to alternatively spliced products in different cells or at different stages of development [Patel and Steitz, 2003].

The mechanism of U12-type splicing has been characterized *in vitro* [Tarn and Steitz, 1996]. Psoralen crosslinking studies provided evidence that U12 indeed forms a duplex with the minor-class branch site, apparently bulging the branch-point adenosine [Tarn and Steitz, 1996], which can reside at two different positions within the consensus site [McConnell *et al.*, 2002]. The minor-class splicing reaction proceeds through the same two-step pathway as the major reaction, which involves formation of a lariat intermediate [Tarn and Steitz, 1996]. Native gel electrophoresis of spliceosomal complexes allowed the initial characterization of the assembly pathway, which is shown in the right panel of Figure 4.3, and

indicated that U11, U12 and U5 were components of the minor-class spliceosome [Tarn and Steitz, 1996]. Interaction of U11 with the 5′ splice site was later confirmed by site-specific crosslinking [Yu and Steitz, 1997].

U4ATAC and U6ATAC are two low-abundance snRNPs with copy numbers similar to those of U11 and U12. Although their sequences diverge significantly from those of U4 and U6 (see Figure 4.2), they predict analogous secondary structures and interactions with the pre-mRNA and other snRNAs. Crosslinking studies confirmed the predicted interactions between U4ATAC and U6ATAC [Yu and Steitz, 1997], between U6ATAC and the minor-class 5′ss [Tarn and Steitz, 1996], and between U6ATAC and U12 [Yu and Steitz, 1997]. This showed that the two spliceosomes undergo comparable dynamic rearrangements in which the snRNAs assume equivalent architectures, as shown in Figure 4.3.

*In vivo* evidence of the requirement of U12 minor-class splicing came from genetic suppression experiments, in which the deficient splicing of a minor-class intron containing two point mutations at the branch site was rescued by co-expression of a U12 snRNA with compensatory mutations [Hall and Padgett, 1996]. Similar genetic suppression experiments provided evidence for the *in vivo* interaction between the minor-class 5′ss with U11 [Kolossova and Padgett, 1997], and U6ATAC [Incorvaia and Padgett, 1998]. Fruit-flies that are homozygous for disruptions in U12 or U6ATAC genes do not survive early development, which indicates that the minor-class spliceosome is essential for organisms that harbour U12-type introns [Otake *et al.*, 2002]. Indeed, the presence of U12-type introns within most metazoan genomes indicates that an active U12-type splicing system is indispensable for the cells of most multicellular organisms [Patel and Steitz, 2003].

Of the snRNAs employed in splicing, only U5 snRNA is shared between the two spliceosomes, whereas the vast majority of the spliceosomal proteins appear to be shared [Will *et al.*, 1999, 2001; Schneider *et al.*, 2002; Luo *et al.*, 1999]. The U5 snRNP is unique in serving as a component of both spliceosomes, which indicates that it does not base-pair with sequences that differ between the two intron types. Although its role in the major-class spliceosome can involve base-pairing [Wyatt *et al.*, 1992; Wassarman and Steitz, 1992; Newman and Norman, 1991, 1992; Sontheimer and Steitz, 1993], proteins are known to support the juxtaposition of exons for the second step of splicing. Recent evidence that the protein components of U5 undergo marked remodeling during spliceosome activation [Makarov *et al.*, 2002] indicates that U5 has a pivotal role in recruiting common protein factors to the two spliceosomes.

### 4.1.3 Integrating splicing in the protein synthesis pathway

Throughout their lifetimes mRNAs exists, *in vivo*, as mRNA-protein particles (mRNPs). The associated proteins control every aspect of mRNA metabolism, from subcellular transport to translational efficiency to their rate of decay. Exactly which proteins associate with a particular mRNA depends on its sequence, its subcellular localization and its synthetic history. Furthermore, the complement of mRNA proteins evolves as the mRNA moves to different locations and is acted on by such processes as nuclear export and translation [Reichert *et al.*, 2002].

On the other hand, many pre-mRNA processing events—including 5′ end capping, splicing exons together, and 3′ end maturation by cleavage or polyadenylation—occur while the nascent RNA chain is being synthesized by RNA polymerase II. The RNApolII

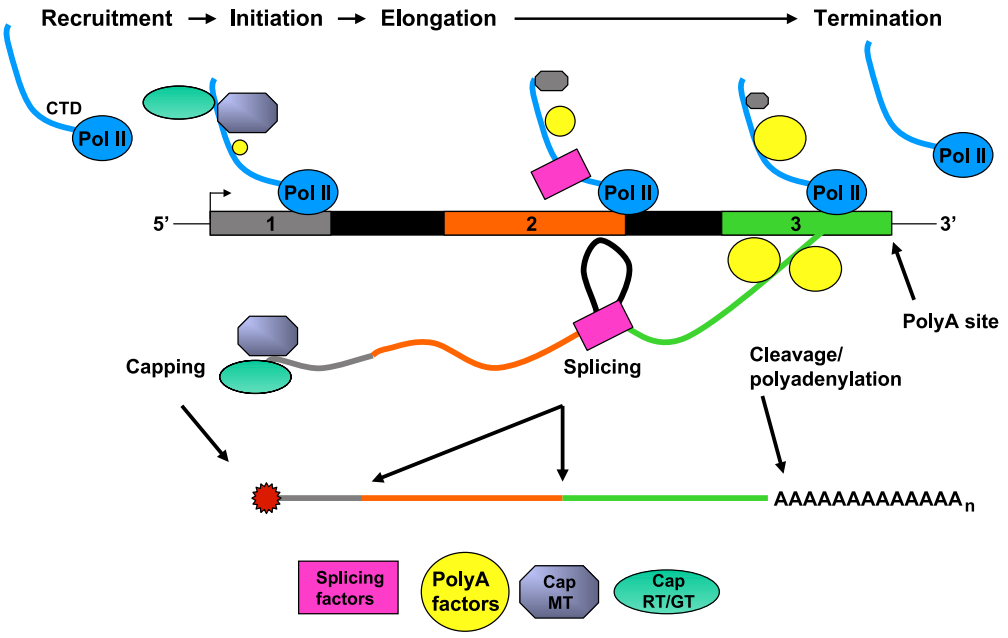


Figure 4.5: **The mRNA factory model.** Schematic representation of co-transcriptional processing. Processing factors interact with the RNApolII machinery via the carboxyl-terminal domain (CTD) of the largest subunit of RNApolII, Rpb1. The size of the symbols for processing factors corresponds to their levels of *in vivo* formaldehyde cross-linking, measured by ChIP experiments. Capping enzymes, RT, GT and MT, and 3′ end modifying factors (polyA related) are recruited at the 5′ ends of genes. As RNApolII traverses the gene, splicing factors associate with the transcription complex. Phosporylation of the $Ser_2$ and $Ser_5$ residues in the CTD heptad repeats decrease as the RNApolII advances. Exon numbers are marked in colored boxes, while introns are shown in black boxes. The red star represents the cap structure. Adapted from Zorio and Bentley [2004].

large subunit is equipped with a unique protein domain to tackle the job of directing co-transcriptional processing. This C-terminal domain (CTD) is composed of tandem repeats of the consensus heptad $Y_1S_2P_3T_4S_5P_6S_7$, which is conserved from fungi to humans [Corden and Ingles, 1992]. Deletion of the CTD in vertebrate cells reduces the overall level of transcription without necessarily affecting the accuracy of initiation. Deletion of the CTD inhibits all three major pre-mRNA processing steps in vertebrate cells: capping, splicing, and polyA site cleavage [McCracken *et al.*, 1997b,a]. The CTD functions as a landing pad for reversible interactions with RNA processing factors [Greenleaf, 1993] that serve to localize those factors close to their substrate RNAs and to act as a conduits for two-way communication with the polymerase.

As sketched in Figure 4.6, the cap binding complex (CBC) interacts with factors assembled on the 5′ss. Once the 3′ss has emerged from the elongating RNApolII, cross-intron interactions can be seen. U1 snRNP components, the U1-70K protein and Prp40/FBP11, can interact with SF1 and U2AF on the branch point, polypyrimidine track and 3′ss. Those

interactions can be facilitated by protein-protein interactions mediated by serine/arginine-rich proteins (SR), which can act as exonic splicing enhancers. After that, two scenarios are possible: a new downstream 5′ss defining an internal exon or a downstream polyadenylation signal defining a terminal exon Goldstrohm *et al.* [2001].

Several examples of intronic and exonic *cis*-acting elements that are important for correct splice-site identification and that are distinct from the classical splicing signals have been described. These elements can act by stimulating (as do enhancers) or repressing (as do silencers) splicing, and they seem to be especially relevant for regulating alternative splicing [Cartegni *et al.*, 2002]. Exonic splicing enhancers (ESEs), in particular, appear to be very prevalent, and might be present in most, if not all, exons, including constitutive ones [Liu *et al.*, 1998; Schaal and Maniatis, 1999]. The analysis of the distribution of exonic splicing silencers (ESSs) revealed that ESSs appear more frequently in skipped exons, as well as in alternative 5′ and 3′ exons, in comparison with constitutive exons [Zhang and Chasin, 2004; Wang *et al.*, 2004]. In addition to ESEs and ESSs, intronic splicing enhancers (ISEs) and silencers (ISSs) are also an important part of the regulatory program in many alternative splicing events [Black, 2003]. ISEs and ISSs may also contribute to the definition of constitutive exons. In the human genome, RNA binding proteins are almost as abundant as transcription factors and the majority of them are of unknown function. Assignment of individual ESEs and ESSs to specific mediators will be essential for deciphering regulatory networks. Together with the rules for potential co-variation of ESEs and ESSs in exons, and by integrating the information with gene expression profiles, a true splicing regulatory code might be possible [Fu, 2004].

The spliceosome is believed to undergo some level of assembly and disassembly each time an intron is removed, but exactly how spliceosome recycling is achieved between successive introns in a given transcript remains a major unanswered question. It is not known whether a spliceosome is completely released from the transcription complex after two exons are ligated or whether some components remain associated with RNApolII and reused at downstream splice sites. Because the 5′ and 3′ splice sites are often quite distant from one another, splicing is the only processing event for which the RNA recognition sites are synthesized at different times. RNApolII elongates transcripts in a highly nonuniform way, punctuated by frequent pauses but with an average rate of $1 \sim 2$ kb/min [Conaway *et al.*, 2000]. This means that the 3′ss of a 30 kb intron would therefore be synthesized $15 \sim 30$ minutes after the 5′ss, time enough for this to bind the U1 snRNP and get ready for splicing. A 5′ss may pair with the first 3′ss to appear as proposed by the "first come first served" model [Aebi *et al.*, 1987]. Slow transcription would favor a proximal 3′ss over a distal site that only appears after a significant delay. Results, from tests on yeast and mammalian cells using RNApolII mutants and an inhibitor that slows down elongation [Howe *et al.*, 2003; de la Mata *et al.*, 2003], show that polymerases shifted the balance in favor of proximal over distal alternative 3′ss thereby reducing exon skipping. These results strongly support the idea that the effect of elongation rate on the lag time between the appearances of different splice sites can modulate alternative splicing. These experiments, therefore, argue for kinetic coupling of transcription and splicing. The effect of elongation rate on alternative splicing may explain how different promoter sequences can alter alternative splice site choices [Cramer *et al.*, 1997] since transcription factors bound to a promoter can influence the efficiency of elongation [Yankulov *et al.*, 1994].

Finally, nonsense-mediated mRNA decay (NMD) is an mRNA surveillance mechanism that has been described in organisms ranging from yeast to humans and ensures mRNA

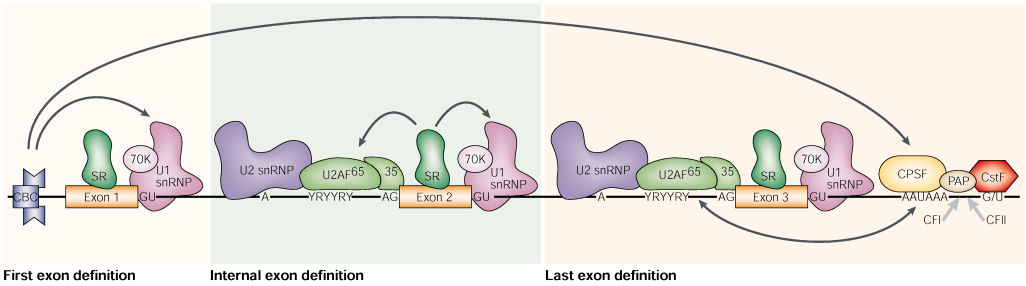


Figure 4.6: **Exon definition model in vertebrates.** Typically, exons are much shorter than introns in vertebrates. According to the exon-definition model, before introns are recognized and spliced-out, each exon is initially recognized by the protein factors that form a bridge across it. In this way, each exon, together with its flanking sequences, forms a molecular recognition module (arrows indicate molecular interactions). Adapted from Zhang [2002]. CBC, cap-binding protein; CFI/II, cleavage factor I/II; CPSF, cleavage and polyadenylation specificity factor; CstF, cleavage stimulation factor; PAP, poly(A) polymerase.

quality by selectively targeting mRNAs that harbour premature termination codons (PTCs) for rapid degradation [Hentze and Kulozik, 1999; Maquat, 1995, 2000]. PTCs that are introduced as a consequence of DNA rearrangements, frame shifts or nonsense mutations, or are caused by errors during transcription or splicing, can lead to non-functional or deleterious proteins. PTCs in higher eukaryotes are only recognized as such when they occur upstream of a boundary on the spliced mRNA that is situated approximately 55 nucleotides upstream of the last exon-exon junction [Maquat, 2000]. The prevalent view of the NMD mechanism is that the splicing process leaves a mark about 20 nucleotides upstream of each exon-exon boundary, in the form of an exon-junction complex (EJC), which in turn provides an anchor for up-frameshift suppressor proteins [Maquat, 2000; Hir *et al.*, 2000]. EJCs are formed by splicing-specific mRNP proteins, which associate with spliced mRNAs in a sequence-independent manner at a fixed distance upstream of exon-exon junctions [Hir *et al.*, 2000]. During the first round of translation, also known as pioneer round, of a normal mRNA, the stop codon is located downstream of the last mark, and all EJCs are displaced by elongating ribosomes [Ishigaki *et al.*, 2001]. During subsequent rounds of translation, the cap-binding complex is replaced by the eukaryotic initiation factor 4E (eIF4E) and the poly(A)-binding protein II (PABPII) is replaced by PABPI. New ribosomes no longer encounter EJCs and the mRNA is immune to NMD. However, when a PTC is present, ribosomes stop and fail to displace the downstream EJCs from the transcript. Then, interactions between the marking factors and components of the post-termination complex trigger mRNA decay. Moreover, intron containing genes are generally expressed at a significantly higher level in human cells than the same genes lacking introns [Buchman and Berg, 1988; Ryu and Mertz, 1989; Lu and Cullen, 2003; Nott *et al.*, 2003]. There is evidence that EJCs may be also responsible for the positive effect of splicing on gene expression [Wiegand *et al.*, 2003].

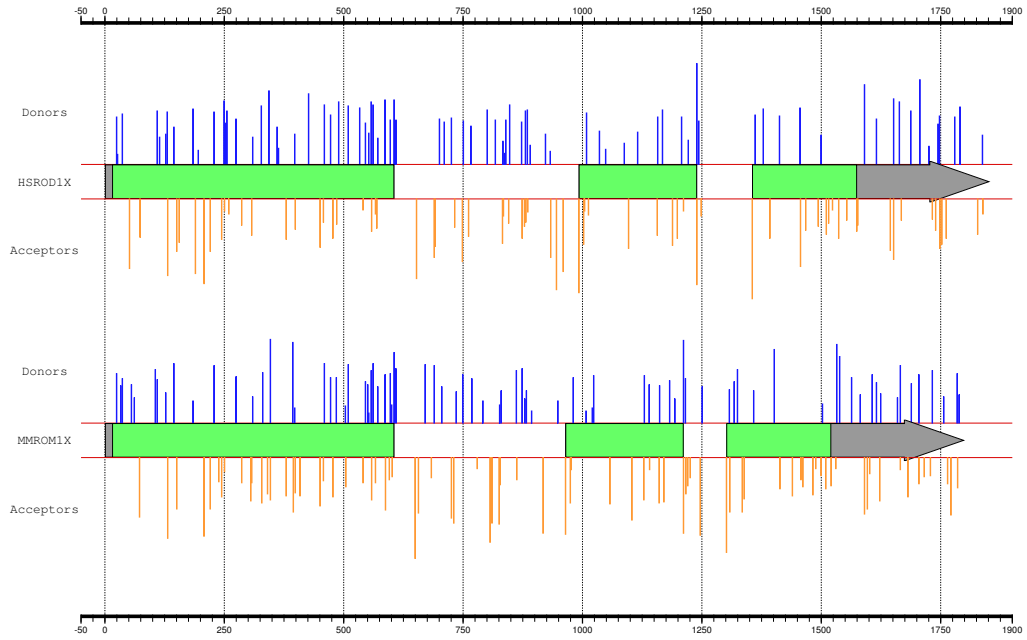


Figure 4.7: **Conservation of gene structure between human and mouse.** Human rod outer segment membrane protein 1 (Rom1, GenBank locus `HUMROD1X`) exonic structure is plotted on top, the orthologous gene structure in mouse (GenBank locus `MUSROM1X`) is shown below. Both genes have three coding exons. Exon and intron lengths are quite similar. A position-specific scoring matrix was used to calculate all potential splice sites along the sequence. Donors are shown as blue spikes and acceptors as orange ones, where the height of each spike represents the score for the corresponding site. A similar sites distribution is observed when comparing both genes. Although real splice sites have good scores, they are often not better than the surrounding predicted signals.

### 4.1.4 The conservation of exonic structure

Numerous regions that are conserved between human and mouse are found in introns [Hardison *et al.*, 1997]. Comparison of human chromosome 21 and the corresponding genomic sequences in mouse revealed that only one-third of the conserved blocks are exons, the other two-thirds being intronic and intergenic sequences [Dermitzakis *et al.*, 2002]. Hare and Palumbi [2003] describe that moderate rates of substitution rate heterogeneity, expected to result in part from mutational processes, can explain much of the conserved sequence observed in pairwise and three taxon comparisons, under a strictly neutral model of sequence evolution without indels. As a result, blocks of non-coding sequence conserved over long divergence times do not necessarily indicate selective constraints, even when observed across more than two taxa. However, they have found that half of the intron conservation observed cannot be explained by the typical levels of substitution rate heterogeneity in non-coding sequences. This strongly suggested that intronic sequences can play a larger functional role than previously realized.

After multiple complete sequences of eukaryotic genomes became available, comparative analyses revealed numerous introns that occupy the same position in orthologous genes from distant species [Fedorov *et al.*, 2002; Rogozin and Pavlov, 2003]. The great majority (>90%) of intron positions that are shared by phylogenetically distant eukaryotes—for example plants, fungi and metazoans—seem to reflect *bona fide* evolutionary conservation [Sverdlov *et al.*, 2005]. This is supported, for instance, by the observed dramatic differences between intron distributions in animal genomes. Those differences depend on non-local features of gene organization, such as the avoidance of short exons and the non-uniform distribution of introns accross the length of genes, for example preferential location of introns in the 5′ portions of genes in many species [Smith, 1988; Stoltzfus *et al.*, 1997; Mourier and Jeffares, 2003; Sverdlov *et al.*, 2004]. Therefore, it seems unlikely that those features had a substantial impact on the long-term evolution of introns [Sverdlov *et al.*, 2005].

Recent large scale comparative analyses have reported extraordinary conservation of the exonic structure between human and mouse orthologous genes [Roy, 2003]. Almost all of the protein-coding genes (99%) in human align with homologs in mouse, and over 80% are clear 1:1 orthologs. In most cases, the intron-exon structures are highly conserved [Waterston *et al.*, 2002], as can be seen, for instance, in Figure 4.7. Estimates of the proportion of 1:1 orthologs between mouse and rat lie between 86 and 94%. Surprisingly, a similar proportion, 89 to 90% of rat genes possessed a single orthologue in the human genome [Gibbs *et al.*, 2004]. About 60% of the chicken protein-coding genes have a single human orthologue [Hillier *et al.*, 2004]. Furthermore, the extent of conservation of alternative splicing between human and mouse is high. It has been suggested that patterns of alternative splicing are conserved at similar levels to genes and gene structures, with overall conservation estimates of 61% of alternative and 74% of constitutive splice junctions [Thanaraj *et al.*, 2003]. Sorek and Ast [2003] have reported that 77% of the conserved alternative spliced exons between human and mouse were flanked on both sides by long conserved intronic sequences. In comparison, only 17% of the conserved constitutively spliced exons were flanked by such conserved sequences. These results suggest that the function of many of the intronic sequence blocks that are conserved between human and mouse is the regulation of alternative splicing [Arian Smith, *pers. communic.*].

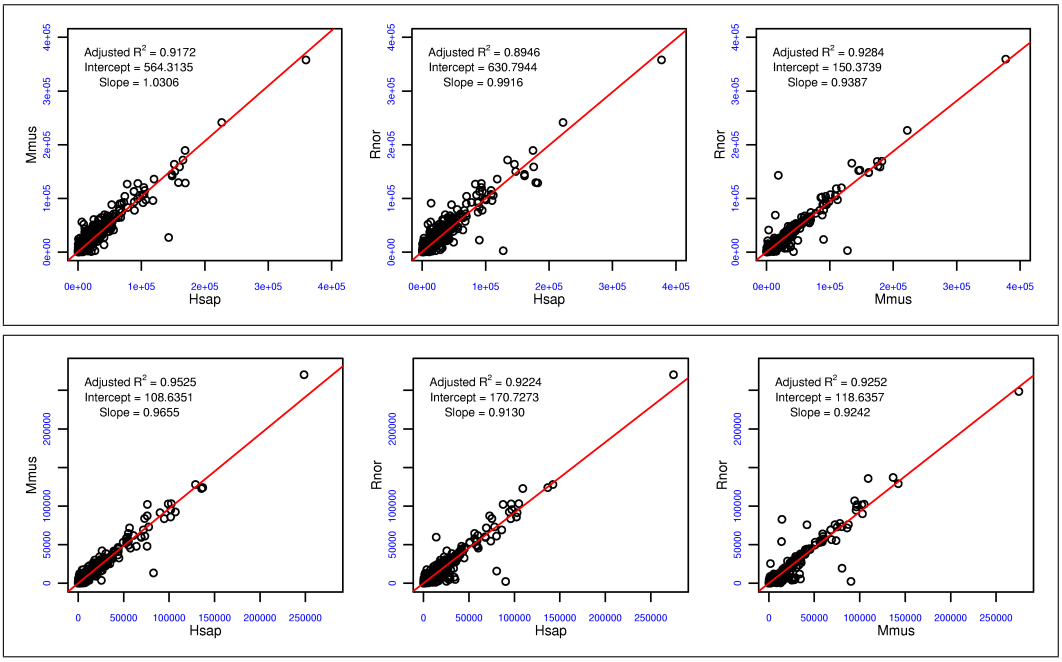


Figure 4.8: **Human/mouse/rat scatterplots for orthologous GT-AG intron lengths.** Upper panels show pair-wise comparisons of orthologous intron lengths. Repeat lengths have been removed from the corresponding total intron lengths in the pair-wise comparison in the lower panels ($N = 6,261$ orthologous introns).

## 4.2 The Comparative Analysis of Mammalian Gene Structures

Preliminary comparative analyses of the human and mouse gene structures for a set of 1,506 pais of orthologous genes are shown in the section entitled "Conservation of gene structure" on page 43 (page 551 of Waterston *et al*. 2002). In what follows, we describe our major contributions to the understanding of the exonic structures and the splice signals of the orthologous genes of human, mouse and rat.

### 4.2.1 Intron length and repeats

Of a set of 6261 human/mouse/rat orthologous introns we have computed the average intron length for each species. Results are shown in table 4.1. On average, introns are longer in human than in rodent and rat introns appear to be longer than those of mouse. Our numbers for human and mouse intron lengths are comparable to those reported in Waterston *et al*. [2002]. There is strong correlation, however, between the length of orthologous introns in different species (the correlation coefficient is about 0.90 between human and rodent, and 0.94 between mouse and rat. The correlation coefficient between length of orthologous exons is in all cases larger than 0.99).

| | Intron Length | | Percentage of Intron Length | | |
|---|---|---|---|---|---|
| **Species** | with repeats | without repeats | in all repeats | in ancient repeats | in other repeats |
| human | 4,765 | 2,747 | 42.57 | 15.70 | 26.87 |
| mouse | 3,770 | 2,558 | 32.60 | 4.72 | 27.88 |
| rat | 4,102 | 2,872 | 30.38 | 4.63 | 26.69 |

Table 4.1: **Intron length and proportion of repetitive DNA in mammalian introns.**

Differences in length between human and mouse orthologous introns are attributable to a larger fraction of repetitive DNA in human than in rodent introns: while DNA in repeats accounts for 43% of the human intron sequences, it accounts for only around 30% in rodent introns (see table 4.1). Therefore, when subtracting the number of bases masked by the program `RepeatMasker` [see page 215, on Web Glossary; Smit *et al.*, 1996–2004] differences in length between human and rodents reduce notably (see table 4.1), with rat introns having the highest proportion of non-repetitive DNA.

Since it may be argued that the orthologous intron dataset is a too small and biased sample of all introns in these organisms, we have computed intron length for all genes in the RefSeq collection [Pruitt and Maglott, 2001; Pruitt *et al.*, 2005], before applying the filtering protocol; see the corresponding methods section on page 135 (page 117 of Abril *et al.* 2005). Average intron lengths, including and excluding masked nucleotides are, respectively, 5,632 and 3,247 in human (177,931 introns), 4,423 and 2,996 in mouse (104,591 introns), and 4,933 and 3,451 in rat (37,043 introns). Therefore, even though our data set of orthologous introns appears to be biased towards shorter introns, the bias is similar in all organisms and does not affect the fraction of intronic DNA in repeats.

Interestingly, longer human introns do not appear to be the result of repeat expansion in the human lineage, but rather of the selective loss of ancient repeats in rodents. We have computed the fraction of intron sequence in repetitive DNA separately for ancient and recent repeats. As can be seen in table 4.1, the fraction of intronic DNA in recent repeats is essentially identical in the three species, suggesting that the dynamics of new repeat generation have not changed after the divergence of the lineages leading to rodent and human. However, ancient repeats are much more abundant in human introns (16% of the sequence) than in rodent introns (5% of the sequence), indicating that repeated sequences are eliminated much faster in rodents than in human. Although repeats appear to be generated slightly faster and to be lost slightly slower in the rat than in the mouse genome, repeat abundance does not account for the notable difference in intron length observed between these two rodent species. We have to take into account that due to a higher substitution level in the rodent lineage, `RepeatMasker` results can be biased to find human ancient repeats. At any rate, the youngest ancient repeats in mouse and rat have a 35–40% substitution level, which is on the border of what `RepeatMasker` can detect, while in the human genome these repeats have about 15% substitution and are reocgnized very easily [Waterston *et al.*, 2002]. `BLASTN` results from cross-matching the repeats found in all the orthologous introns against the intronic sequences of each other species, were supporting our hypothesis.

We did not continue the analyses reported in this section as a broader analysis of repeats, whole genome based, was presented for the mouse and the rat genomes [Waterston

*et al*., 2002; Gibbs *et al*., 2004]. The large scale deletion level of non-essential DNA in rodents was much larger than in the human lineage. This results further in a reduced number of ancient repeats in the current rodent genomes; for instance, approximately 50% of the ancestral junk DNA, as it was at the human-mouse split, has been lost in mouse and only about 25% in human.

### 4.2.2 Sequence conservation at orthologous splice sites

See section entitled "Conservation of intronic splice signals" on page 119 (page 505 of Gibbs *et al*. 2004).

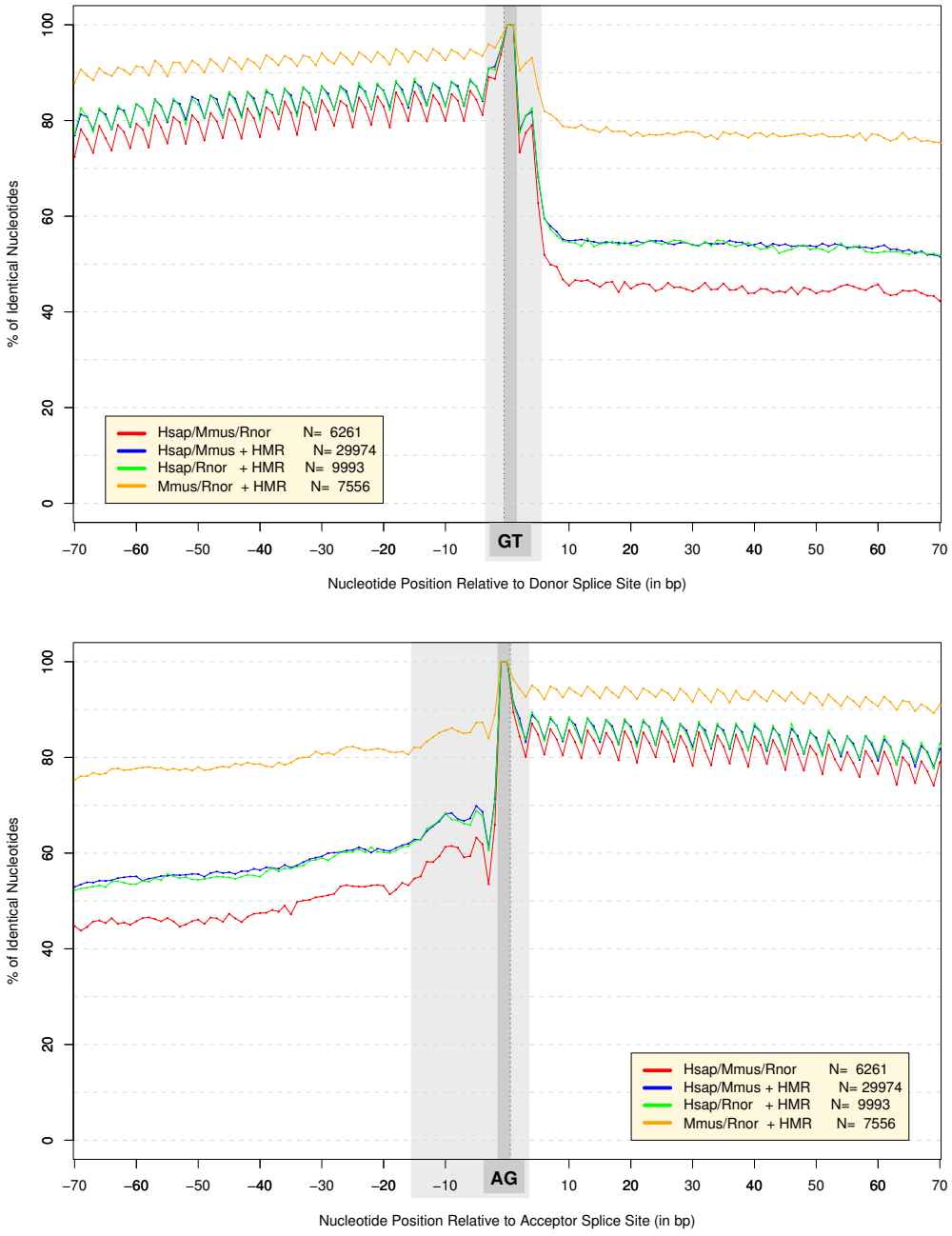


Figure 4.9: **Human/mouse/rat sequence conservation at orthologous GT-AG splice sites.** Sequence conservation for donor sites [supplementary materials Figure 8 of Gibbs *et al*. 2004] and acceptor sites [supplementary materials Figure 7 of Gibbs *et al*. 2004] are shown in upper and lower panels respectively.

### 4.2.3 RGSPC, *Nature*, 428(6982):493–521, 2004

**PubMed Accession:**

http://www.ncbi.nlm.nih.gov/entrez/query.fcgi?cmd=Retrieve&db=PubMed&list_uids=15057822&dopt=Abstract

**Journal Abstract:**

http://www.nature.com/cgi-taf/DynaPage.taf?file=/nature/journal/v428/n6982/abs/nature02426_fs.html

**Supplementary Materials:**

See Section 4.3.2 and the following URL:
http://www.nature.com/nature/journal/v428/n6982/suppinfo/nature02426.html

articles

# Genome sequence of the Brown Norway rat yields insights into mammalian evolution

**Rat Genome Sequencing Project Consortium***

**Lists of participants and affiliations appear at the end of the paper*

**The laboratory rat (*Rattus norvegicus*) is an indispensable tool in experimental medicine and drug development, having made inestimable contributions to human health. We report here the genome sequence of the Brown Norway (BN) rat strain. The sequence represents a high-quality 'draft' covering over 90% of the genome. The BN rat sequence is the third complete mammalian genome to be deciphered, and three-way comparisons with the human and mouse genomes resolve details of mammalian evolution. This first comprehensive analysis includes genes and proteins and their relation to human disease, repeated sequences, comparative genome-wide studies of mammalian orthologous chromosomal regions and rearrangement breakpoints, reconstruction of ancestral karyotypes and the events leading to existing species, rates of variation, and lineage-specific and lineage-independent evolutionary events such as expansion of gene families, orthology relations and protein evolution.**

Darwin believed that "natural selection will always act very slowly, often only at long intervals of time"[1]. The consequences of evolution over timescales of approximately 1,000 millions of years (Myr) and 75 Myr were investigated in publications comparing the human with invertebrate and mouse genomes, respectively[2,3]. Here we describe changes in mammalian genomes that occurred in a shorter time interval, approximately 12–24 Myr (refs 4, 5) since the common ancestor of rat and mouse.

The comparison of these genomes has produced a number of insights:

- The rat genome (2.75 gigabases, Gb) is smaller than the human (2.9 Gb) but appears larger than the mouse (initially 2.5 Gb (ref. 3) but given as 2.6 Gb in NCBI build 32, see http://www.ncbi.nlm.nih.gov/genome/seq/NCBIContigInfo.html).
- The rat, mouse and human genomes encode similar numbers of genes. The majority have persisted without deletion or duplication since the last common ancestor. Intronic structures are well conserved.
- Some genes found in rat, but not mouse, arose through expansion of gene families. These include genes producing pheromones, or involved in immunity, chemosensation, detoxification or proteolysis.
- Almost all human genes known to be associated with disease have orthologues in the rat genome but their rates of synonymous substitution are significantly different from the remaining genes.
- About 3% of the rat genome is in large segmental duplications, a fraction intermediate between mouse (1–2%) and human (5–6%). These occur predominantly in pericentromeric regions. Recent expansions of major gene families are due to these genomic duplications.
- The eutherian core of the rat genome—that is, bases that align orthologously to mouse and human—comprises a billion nucleotides (~40% of the euchromatic rat genome) and contains the vast majority of exons and known regulatory elements (1–2% of the genome). A portion of this core constituting 5–6% of the genome appears to be under selective constraint in rodents and primates, while the remainder appears to be evolving neutrally.
- Approximately 30% of the rat genome aligns only with mouse, a considerable portion of which is rodent-specific repeats. Of the non-aligning portion, at least half is rat-specific repeats.
- More genomic changes occurred in the rodent lineages than the primate: (1) These rodent genomic changes include approximately 250 large rearrangements between a hypothetical murid ancestor and human, approximately 50 from the murid ancestor to rat, and about the same from the murid ancestor to mouse. (2) A threefold-higher rate of base substitution in neutral DNA is found along the rodent lineage when compared with the human lineage, with the rate on the rat branch 5–10% higher than along the mouse branch. (3) Microdeletions occur at an approximately twofold-higher rate than microinsertions in both rat and mouse branches.
- A strong correlation exists between local rates of microinsertions and microdeletions, transposable element insertion, and nucleotide substitutions since divergence of rat and mouse, even though these events occurred independently in the two lineages.

## Background

### History of the rat

The rat, hated and loved at once, is both scourge and servant to mankind. The "Devil's Lapdog" is the first sign in the Chinese zodiac and traditionally carries the Hindu god Ganesh[6]. Rats are a reservoir of pathogens, known to carry over 70 diseases. They are involved in the transmission of infectious diseases to man, including cholera, bubonic plague, typhus, leptospirosis, cowpox and hantavirus infections. The rat remains a major pest, contributing to famine with other rodents by eating around one-fifth of the world's food harvest.

Paradoxically, the rat's contribution to human health cannot be overestimated, from testing new drugs, to understanding essential nutrients, to increasing knowledge of the pathobiology of human disease. In many parts of the world the rat remains a source of meat.

The laboratory rat (*R. norvegicus*) originated in central Asia and its success at spreading throughout the world can be directly attributed to its relationship with humans[7]. J. Berkenhout, in his 1769 treatise *Outline of the Natural History of Great Britain*, mistakenly took it to be from Norway and used *R. norvegicus* Berkenhout in the first formal Linnaean description of the species. Whereas the black rat (*Rattus rattus*) was part of the European landscape from at least the third century AD and is the species associated with the spread of bubonic plague, *R. norvegicus* probably originated in northern China and migrated to Europe somewhere

around the eighteenth century[8]. They may have entered Europe after an earthquake in 1727 by swimming the Volga river.

### The rat in research

*R. norvegicus* was the first mammalian species to be domesticated for scientific research, with work dating to before 1828 (ref. 9). The first recorded breeding colony for rats was established in 1856 (ref. 9). Rat genetics had a surprisingly early start. The first studies by Crampe from 1877 to 1885 focused on the inheritance of coat colour[10]. Following the rediscovery of Mendel's laws at the turn of the century, Bateson used these concepts in 1903 to demonstrate that rat coat colour is a mendelian trait[10]. The first inbred rat strain, PA, was established by King in 1909, the same year that systematic inbreeding began for the mouse[10]. Despite this, the mouse became the dominant model for mammalian geneticists, while the rat became the model of choice for physiologists, nutritionists and other biomedical researchers. Nevertheless, there are over 234 inbred strains of *R. norvegicus* developed by selective breeding, which 'fixes' natural disease alleles in particular strains or colonies[11].

Over the past century, the role of the rat in medicine has transformed from carrier of contagious diseases to indispensable tool in experimental medicine and drug development. Current examples of use of the rat in human medical research include surgery[12], transplantation[13–15], cancer[16,17], diabetes[18,19], psychiatric disorders[20] including behavioural intervention[21] and addiction[22], neural regeneration[23,24], wound[25,26] and bone healing[27], space motion sickness[28], and cardiovascular disease[29–31]. In drug development, the rat is routinely employed both to demonstrate therapeutic efficacy[15,32,33] and to assess toxicity of novel therapeutic compounds before human clinical trials[34–37].

### The Rat Genome Project

Over the past decade, investigators and funding agencies have participated in rat genomics to develop valuable resources. Before the launch of the Rat Genome Sequencing Project (RGSP), there was much debate about the overall value of the rat genome sequence and its contribution to the utility of the rat as a model organism. The debate was fuelled by the naive belief that the rat and mouse were so similar morphologically and evolutionarily that the rat sequence would be redundant. Nevertheless, an effort spearheaded by two NIH agencies (NHGRI and NHLBI) culminated in the formation of the RGSP Consortium (RGSPC).

The RGSP was to generate a draft sequence of the rat genome, and, unlike the comparable human and mouse projects, errors would not ultimately be corrected in a finished sequence[38]. Consequently, the draft quality was critical. Although it was expected to have gaps and areas of inaccuracy, the overall sequence quality had to be high enough to support detailed analyses.

The BN rat was selected as a sequencing target by the research community. An inbred animal (BN/SsNHsd) was obtained by the Medical College of Wisconsin (MCW) from Harlan Sprague Dawley. Microsatellite studies indicated heterozygosity, so over 13 generations of additional inbreeding were performed at the MCW, resulting in BN/SsNHsd/Mcwi animals. Most of the sequence data were from two females, with a small amount of whole genome shotgun (WGS) and flow-sorted Y chromosome sequencing from a male. The Y chromosome is not included in the current assembly.

A network of centres generated data and resources, led by the Baylor College of Medicine Human Genome Sequencing Center (BCM-HGSC) and including Celera Genomics, the Genome Therapeutics Corporation, the British Columbia Cancer Agency Genome Sciences Centre, The Institute for Genomic Research, the University of Utah, the Medical College of Wisconsin, The Children's Hospital of Oakland Research Institute, and the Max Delbrück Center for Molecular Medicine, Berlin. After assembly of the genome at the BCM-HGSC, analysis was performed by an international team, representing over 20 groups in six countries and relying largely on gene and protein predictions produced by Ensembl.

## Determination of the genome sequence

### *Atlas* and the 'combined' sequencing strategy

Despite progress in assembling draft sequences[2,3,39–44] the question of which method produces the highest-quality products is unresolved. A significant issue is the choice between logistically simpler WGS approaches versus more complex strategies employing bacterial artificial chromosome (BAC) clones[45–48]. In the Public Human Genome Project[2] a BAC by BAC hierarchical approach was used and provided advantages in assembling difficult parts of the genome. The draft mouse sequence was a pure WGS approach using the ARACHNE assembler[3,49,50] but underrepresented duplicated regions owing to 'collapses' in the assembly[3,51–53]. This limitation of the mouse draft sequence was tolerable owing to the planned full use of BAC clones in constructing the final finished sequence.

The RGSPC opted to develop a 'combined' approach using both WGS and BAC sequencing (Fig. 1). In the combined approach, WGS data are progressively melded with light sequence coverage of individual BACs (BAC skims) to yield intermediate products called 'enriched BACs' (eBACs). eBACs covering the whole genome are then joined into longer structures (bactigs). Bactigs are joined to form larger structures: superbactigs, then ultrabactigs. During this process other data are introduced, including BAC end sequences, DNA fingerprints and other long-range information (genetic markers, syntenic information), but the process is constrained by eBAC structures.

To execute the combined strategy we developed the *Atlas* software package[54] (Fig. 1). The *Atlas* suite includes a 'BAC-Fisher' component that performs the functions needed to generate eBACs. WGS genome coverage was generated ahead of complete BAC coverage, so a BAC-Fisher web server was established at the BCM-HGSC to enable users to access the combined BAC and WGS reads as each BAC was processed (see Methods for data access). Each eBAC is assembled with high stringency to represent the local sequence accurately, and so provide a valuable intermediate product that assists all users of the genome data. Additional *Atlas* modules joined eBACs and linked bactigs to give the complete assembly (Fig. 1). Overall, the combined approach takes advantage of the strengths of both previous methods, with few of the disadvantages.

### Sequence and genome data

Over 44 million DNA sequence reads were generated (Table 1; Methods). Following removal of low-quality reads and vector contaminants, 36 million reads were used for *Atlas* assembly, which retained 34 million reads. This was 7× sequence coverage with 60% provided by WGS and 40% from BACs. Slightly different estimates came from considering the entire 'trimmed' length of the sequence data (7.3×), or only the portion of Phred20 quality or higher (6.9×).

The sequence data were end-reads from clones either derived directly from the genome (insert sizes of $<$10 kb, 10 kb, 50 kb and $>$150 kb) or from small insert plasmids subcloned from BACs. Overall, these provided 42-fold clone coverage, with 32-fold coverage having both paired ends represented. Approximately equal contributions of clone coverage were from the different categories.

Over 21,000 BACs were used for BAC skims (1.6× coverage) with an average sequence depth of 1.8×, giving an overall 2.8× genomic sequence coverage from BACs. This was slightly more than the most efficient procedure would require ($\sim$1.2× each), because the genome size was not known at the project start.

Simultaneous with sequencing, 199,782 clones from the CHORI-230 BAC library[55] were fingerprinted by restriction enzyme

18% of the mouse genome covered by RefSeq genes; and 17% of the rat hotspots were found in the 8% of the rat genome covered by RefSeq genes. Similar numbers are observed when examining coding exon and EST regions (not shown). Half of all hotspots in the mouse genome lie totally in non-coding regions. Many hotspots are several hundred bases long, with average length 190 ± 86 bp. Future work aimed at identifying the genomic differences that contribute to phenotypic evolution may benefit from analyses such as these, which will become more powerful as the repertoire of mammalian genome sequences expands.

### Covariation of evolutionary and genomic features

To illustrate the genomic and evolutionary landscape of a single rat chromosome in depth, we characterized features for rat chromosome 10 at 1 Mb resolution (Fig. 9). This high-resolution analysis uncovered strong correlations between certain microevolutionary features[89,92,98]. Particularly strongly correlated are the local rates of microdeletion ($R^2 = 0.71$; Fig. 9a), microinsertion ($R^2 = 0.56$; Fig. 9a), and point substitution ($R^2 = 0.86$; Fig. 9b) between the two independent lineages of mouse and rat. In addition, microinsertion rates are correlated with microdeletion rates ($R^2 = 0.55$; Fig. 9a). These strong correlations are also observed in an independent genome-wide analysis, both on the original data and after factoring out the effects of G+C content (not shown, see Supplementary Information).

Perhaps surprisingly, substantially less correlation is seen between microindel and point substitution rates (compare Fig. 9a and b). The amount of correlation varies among chromosomes (not shown), but is generally weaker than the relationships mentioned above. Further studies will be required to determine whether local evolutionary pressures, which must have remained stable since the separation of the mouse and rat lineages, differentially drive microindel and point substitution rates.

We also find that the local point substitution rate in sites common to human, mouse and rat strongly correlates with that in rodent-specific sites ($R^2 = 0.57$; Fig. 9b, blue line versus red/green). These two classes of sites, while interdigitated at the level of tens to thousands of bases, constitute sites that are otherwise evolutionarily independent. This result confirms that local rate variation is not solely determined by stochastic effects and extends, at high resolution, the previously documented regional correlation in rate between 4D sites and ancestral repeat sites[3,96].

## Evolution of genes

A substantial motivation for sequencing the rat genome was to study protein-coding genes. Besides being the first step in accurately defining the rat proteome, this fundamental data set yields insights into differences between the rat and other mammalian species with a complete genome sequence. Estimation of the rat gene content is possible because of relatively mature gene-prediction programs and rodent transcript data. Mouse and human genome sequences also allow characterization of mutational events in proteins such as amino acid repeats and codon insertions and deletions. The quality of the rat sequence also allows us to distinguish between functional genes and pseudogenes.

We estimate (on the basis of a subset) that 90% of rat genes

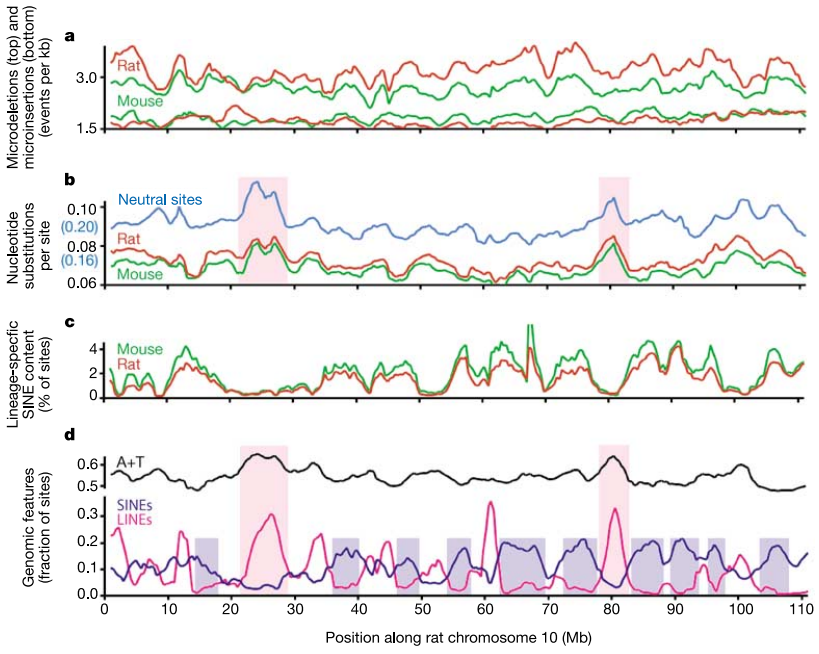


**Figure 9** Variability of several evolutionary and genomic features along rat chromosome 10. **a**, Rates of microdeletion and microinsertion events (less than 11 bp) in the mouse and rat lineages since their last common ancestor, revealing regional correlations. **b**, Rates of point substitution in the mouse and rat lineages. Red and green lines represent rates of substitution within each lineage estimated from sites common to human, mouse and rat. Blue represents the neutral distance separating the rodents, as estimated from rodent-specific sites. Note the regional correlation among all three plots, despite being estimated in different lineages (mouse and rat) and from different sites (mammalian versus rodent-specific). **c**, Density of SINEs inserted independently into the rat or mouse genomes after their last common ancestor. **d**, A+T content of the rat, and density in the rat genome of LINEs and SINEs that originated since the last common ancestor of human, mouse and rat. Pink boxes highlight regions of the chromosome in which substitution rates, A+T content and LINE density are correlated. Blue boxes highlight regions in which SINE density is high but LINE density is low.

possess strict orthologues in both mouse and human genomes. Our studies also identified genes arising from recent duplication events occurring only in rat, and not in mouse or human. These genes contribute characteristic features of rat-specific biology, including aspects of reproduction, immunity and toxin metabolism. By contrast, almost all human 'disease genes' have rat orthologues. This emphasizes the importance of the rat as a model organism in experimental science.

### Construction of gene set and determination of orthology

The Ensembl gene prediction pipeline[112] predicted 20,973 genes with 28,516 transcripts and 205,623 exons (Methods). These genes contain an average of 9.7 exons, with a median exon number of 6.0. At least 20% of the genes are alternatively spliced, with an average of 1.3 transcripts predicted per gene. Of the 17% single exon transcripts, 1,355 contain frameshifts relative to the predicted protein and 1,176 are probably processed pseudogenes. Of the 28,516 transcripts, 48% have both 5′ and 3′ untranslated regions (UTRs) predicted and 60% have at least one UTR predicted.

These gene predictions considered homology to other sequences, including 26,949 rodent proteins, 4,861 non-rodent, vertebrate proteins, 7,121 rat complementary DNAs from RefSeq and EMBL, and 31,545 mouse cDNAs from Riken, RefSeq and EMBL. The majority (61%) of transcripts are supported by rodent transcript evidence. When combined with additional private EST data, the fraction of genes supported by transcript evidence could be increased to 72%[113].

A number of other *ab initio* (GENSCAN[114], GENEID[115]), similarity-based (FGENESH++; ref. 116) and comparative (SGP[117], SLAM[118], TWINSCAN1[119–121]) gene-prediction programs were used to analyse the rat genome. The number of genes predicted by these programs ranged from 24,500 to 47,000, suggesting coding densities ranging from 1.2% to 2.2%. The coding fraction of RefSeq genes covered by these predictions ranged from 82% to 98%. Such comparative *ab initio* programs using the rat genome were successfully used to identify and experimentally verify genes missed by other methods in rat[121] and human[122]. The predictions of these programs can be accessed through the UCSC genome browser and Ensembl websites.

RefSeq genes (20,091 human, 11,342 mouse and 4,488 rat) mapped onto genome assemblies with BLAT[123] and the UCSC browser revealed that the number of coding exons per gene and average exon length were similar in the three species. Differences were observed in intron length, with an average of 5,338 bp in human, 4,212 bp in mouse and 5,002 bp in rat. These differences were also found in a smaller collection of 6,352 confidently mapped orthologous intron triads (see 'Conservation of intronic splice signals' section below): average intron lengths in this collection were 4,240 bp in human, 3,565 bp in mouse and 3,638 bp in rat.

### Properties of orthologous genes

Orthology relationships were predicted on the basis of BLASTp reciprocal best-hits between proteins of genome pairs (human–rat, rat–mouse and mouse–human)[3] (Supplementary Information). Using these methods and the ENSEMBL prediction sets, 12,440 rat genes showed clear, unambiguous 1:1 correspondence with a gene in the mouse genome. This is an underestimate, because random sampling of different classes of rat genes with less stringent criteria for comparison to mouse always identified additional gene pairs. Errors arose from pseudogene misclassification, sequence loss, duplication or fragmentation in assemblies; and missing or inappropriate gene predictions, including coding-gene predictions from non-coding RNAs. Taking these errors into account, we estimate the true proportion of 1:1 orthologues in rat and mouse genomes to lie between 86 and 94% (Methods). The remaining genes were associated with lineage-specific gene family expansions or contractions. These overall observations are consistent with a careful analysis of rat proteases showing that 93% of these genes have 1:1 orthologues in mouse[124,125].

Surprisingly, a similar proportion (89 to 90%) of rat genes possessed a single orthologue in the human genome. Because human represents an outgroup to the two rodents, it was expected that mouse and rat would share a higher fraction of orthologues. A close inspection of gene relationships indicates that these findings may suffer from incompleteness of rodent genome sequences, together with problems of misassembly and gene prediction within clusters of gene paralogues.

Further analysis of orthologous pairs considered the occurrence of nucleotide changes within protein-coding regions that reflected synonymous or non-synonymous substitutions. The majority of these studies measured evolutionary rates by determination of $K_A$ (number of non-synonymous substitutions per non-synonymous site) and $K_S$ (number of synonymous substitutions per synonymous site). $K_A/K_S$ ratios of less than 0.25 indicate purifying selection, values of 1 suggest neutral evolution, and values greater than 1 indicate positive selection[126].

Evolutionary rates were first calculated from a reduced set of orthologue pairs that are embedded in orthologous genomic segments and are related by conservative values of $K_S$ (Table 3) (Methods). A slight increase in median $K_S$ values for rat–human as compared with mouse–human, was found, indicating that the rat lineage has more neutral substitutions in gene coding regions than the mouse lineage. Sequence conservation values were similar to those previously found using smaller data sets[127,128], and the overall trend is consistent with results of other evolutionary rate analyses discussed above (Fig. 5).

Next, we investigated examples of rat genes shared with mouse, but with no counterparts in human. Such genes might be rapidly evolving so that homologues are not discernible in human, or they might have arisen from non-coding DNA, or their orthologues in the human lineage might have formed pseudogenes. Thirty-one Ensembl rat genes were collected that have no non-rodent homologues in current databases (Methods). These are twofold over-represented among genes in paralogous gene clusters, and threefold over-represented among genes whose proteins are likely to be secreted. This is consistent with observations[3] that clusters of paralogous genes, and secreted proteins, evolve relatively rapidly. Detailed examination of the 31 genes using PSI-BLAST determined that ten genes cannot be assigned homology relationships to experimentally described mammalian genes. These ten rodent-

Table 3 **One-to-one orthologous genes in human, mouse and rat genomes**

| | Human–mouse | Human–rat | Mouse–rat |
|---|---|---|---|
| 1:1 orthologue relationships | 11,084 | 10,066 | 11,503 |
| Median $K_S$ values* | 0.56 (0.39–0.80) | 0.57 (0.40–0.82) | 0.19 (0.13–0.26) |
| Median $K_A/K_S$ values* | 0.10 (0.03–0.24) | 0.09 (0.03–0.21) | 0.11 (0.03–0.28) |
| Median % amino acid identity* | 88.0% (74.4–96.3%) | 88.3% (75.9–96.4%) | 95.0%† (88.0–98.7%) |
| Median % nucleotide identity* | 85.1% (77.4–90.0%) | 85.1% (77.8–89.9%) | 93.4% (89.2–95.7%) |

Data obtained from Ensembl, *Homo sapiens* version 11.31 (24,841 genes), *Mus musculus* version 10.3 (22,345 genes), *Rattus norvegicus* version 11.2 (21,022 genes).
*Numbers in parentheses represent the 16th and 83rd percentiles.
† This value is consistent with previous findings (93.9% in ref. 130).

specific genes may have evolved particularly rapidly, or have non-coding DNA homologues, or be erroneous predictions.

The paucity of rodent-specific genes indicates that *de novo* invention of complete genes in rodents is rare. This is not unexpected, because the majority of eukaryotic protein-coding genes are modular structures containing coding and non-coding exons, splicing signals and regulatory sequences, and the chances of independent evolution and successful assembly of these elements into a functional gene are small, given the relatively short evolutionary time available since the mouse–rat split. However, individual rodent-specific exons may arise more frequently, particularly if the exon is alternatively spliced[129]. Applying a $K_A/K_S$ ratio test[130,131] to sequences that align only between rat and mouse, we identified 2,302 potential novel rodent-specific exons, with EST support, in BLASTZ alignments of rat and mouse sequences. None of these individual exons matched human transcripts, but approximately half (1,116) appear to be present in alternative splice forms found in rodents. We speculate that these exons contain the few successful lineage-specific survivors of the constant process of gene evolution, by birth and death of individual exons.

#### Indels and repeats in protein-coding sequences

In contrast to small indels occurring in the bulk of the genome (above), indels within protein-coding regions are probably lethal, or deleterious and so are rapidly removed from the population by purifying selection. Indel rates within rat coding sequences were 50-fold lower than in bulk genomic DNA[132]. The whole genome excess of deletions compared with insertions (Fig. 5b) was also evident in coding sequences. The magnitude was less, with a genome-wide deletion-to-insertion ratio of 3.1:1 reducing to 1.7:1 in the rat. In mouse this value reduced from 2.5:1 to 1.1:1 (ref. 132). These data suggest that deletions are ~16% more likely than insertions to be removed from coding sequences by selection.

Owing to the triplet nature of the genetic code, indels of multiples of three nucleotides in length ($3_n$ indels) are less likely to be deleterious. Direct comparison of $3_n$ indel rates between bulk DNA (0.77 indels per kb for mouse, 0.83 indels per kb for rat) and coding sequence (0.087 indels per kb for mouse and 0.084 indel per kb for rat) showed that $3_n$ indels were ninefold under-represented in coding sequences. At least 44% of indels were duplicative insertion or deletion of a tandemly duplicated sequence, collectively termed sequence slippage[132]. Sequence slippage contributed approximately equally to observed insertions and deletions. The overall excess of deletions could be attributed specifically to an excess of non-slippage deletion over non-slippage insertion in both mouse and rat lineages[132]. Of the slippage indels, 13% were in the context of trinucleotide repeats ($n > 2$, excluding the inserted or deleted sequence) which are known to be particularly prone to sequence slippage and encode homopolymeric amino acid tracts[133,134].

To gain better understanding of dynamic changes in the length of homopolymeric amino acid tracts on gene evolution and disease susceptibility, we searched for other characteristics of amino acid repeat variation by analysing all size-five or longer amino acid repeats in a data set of 7,039 rat, mouse and human orthologous protein sequences[135]. Most species-specific amino acid repeats (80–90%) were found in indel regions, and regions encoding species-specific repeats were more likely to contain tandem trinucleotide repeats than those encoding conserved repeats. This was consistent with the involvement of slippage in the generation of novel repeats in proteins and extended previous observations for glutamine repeats in a more limited human–mouse data set[136].

The percentage of proteins containing amino acid repeats was 13.7% in rat, 14.9% in mouse and 17.6% in human[135]. The most frequently occurring tandem amino acid repeats were glutamic acid, proline, alanine, leucine, serine, glycine, glutamine and lysine. Using the same threshold size cut-off, tandem trinucleotide repeats were significantly more abundant in human than in rodent coding sequences, in striking contrast to the frequencies observed in bulk genomic sequences (29 trinucleotide repeats per Mb in rat, 32 repeats per Mb in mouse and 13 repeats per Mb in human, see discussion of the general simple repeat structure below). The conservation of human repeats was higher in mouse (52%) than in rat (46.5%), suggesting a higher rate of repeat loss in the rat lineage than the mouse lineage.

Functional consequences of these in-frame changes in rat, mouse and human were investigated[132] through clustering of proteins based on annotation of function and cellular localization[112], and mapping indels onto protein structural and sequence features. The rate that indels accumulated in secreted ($3.9 \times 10^{-4}$ indels per amino acid) and nuclear ($4.0 \times 10^{-4}$) proteins is approximately twice that of cytoplasmic ($2.4 \times 10^{-4}$) and mitochondrial ($1.4 \times 10^{-4}$) proteins. Likewise, ligand-binding proteins acquire indels ($3.1 \times 10^{-4}$) at a higher rate than enzymes ($2.1 \times 10^{-4}$)[132]. These trends exactly mirror those observed for amino acid substitution rates[3], suggesting tight coupling of selective constraints between indels and substitutions. Transcription regulators showed the highest rate of indels ($4.3 \times 10^{-4}$), a finding that may relate to the over-representation of homopolymorphic amino acid tracts in these proteins[135].

Known protein domains exhibited 3.3-fold fewer indels than expected by chance, again paralleling nucleotide substitution rate differences between domains and non-domain sequences[3]. Of the protein-sequence and structural categories considered (transmembrane, protein domain, signal peptide, coiled coil and low complexity), the transmembrane regions were the most refractory to accumulating indels, exhibiting a sixfold reduction compared with that expected by chance. Low-complexity regions were 3.1-fold enriched, reflecting their relatively unstructured nature and enrichment in indel-prone trinucleotide repeats. Mapping of indels onto groups of known structures revealed that indels are 21% more likely to be tolerated in loop regions than the structural core of the protein[132].

We observed that indel frequency and amino acid repeat occurrence both correlated positively with the G + C coding sequence content of the local sequence environment[132,135]. This may be explained in part by the correlation of polymerase slippage-prone trinucleotide repeat sequences and G + C content[135]. There is also a positive correlation between CpG dinucleotide frequency and coding sequence insertions, but not deletions. This effect diminishes rapidly with increasing distance from the site of the insertion[132].

#### Transcription-associated substitution strand asymmetry

A recent study reported a significant strand asymmetry for neutral substitutions in transcribed regions[133]. Within introns of nine genes, the higher rate of A→G substitutions over that of T→C substitutions, together with a smaller excess of G→A over C→T substitutions, leads to an excess of G+T over C+A on the coding strand (also verified on human chromosome 22). The authors[133] hypothesized that the asymmetries are a byproduct of transcription-

Table 4 **Strand asymmetry of substitutions in introns of rat genes**

| | | |
|---|---|---|
| Base frequencies on coding strand* | Rat genome | |
| (G+T)/(C+A) | 1.060 | |
| Ratio of purine transitions to pyrimidine transitions† | Rat–mouse | Rat–human |
| Rate(A↔G)/Rate(C↔T) | 1.036 | 1.036 |
| Rate of transitions‡ | Rat | Mouse |
| Rate(A→G)/Rate(T→C) | 1.058 | 1.091 |
| Rate(G→A)/Rate(C→T) | 1.017 | 1.00 |

*Computed from the rat genome.
†Computed from pairwise alignments.
‡Computed from three-way alignments.

coupled repair in germline cells. Examining the three-way alignments of rat, mouse and human, we verified that the strand asymmetries for neutral substitutions exist in introns across the genome (Table 4).

Under the assumption of independence of sequence positions, large sample normal approximations to the binomial distribution allow us to test whether the fraction of G+T exceeds 0.5, and whether the rate at the numerator exceeds the rate at the denominator for each of the ratios in Table 4. With the large amount of data provided by pooling introns genome-wide, the tests are all highly significant ($P$ values $< 10^{-4}$), except for the rate of G→A in mouse, which does not significantly exceed that of C→T ($P$ value = 0.6369). These asymmetries are also seen if the study is limited to ancestral repeat sites, excludes ancestral repeat sites, excludes CpG dinucleotides, is limited to positions flanked by sites that are identical in the aligned sequences (in the case of observations 2 and 3 in Table 4), or considers introns of RefSeq genes for human or mouse. Thus it appears that strand asymmetry of substitution events within transcribed regions of the genome is a robust genome-wide phenomenon.

### Conservation of intronic splice signals

Using 6,352 human–mouse–rat orthologous introns from 976 genes (Methods), we examined the dynamics of evolution of consensus splice signals in mammalian genes. We found that intron class[137] is extremely well conserved: we did not observe any U2 to U12 intron conversion, or vice versa, nor within U12 introns did we find any switching between the major AT–AC and GT–AG subtypes, although such events are documented at larger evolutionary distances[137]. In contrast, conversions between canonical GT–AG and non-canonical GC–AG subtypes of U2 introns are not uncommon. Only ~70% of GC–AG introns are conserved between human and mouse/rat, and only 90% are conserved between mouse and rat. Using human as the outgroup, we detected nine GT to GC conversions after divergence of mouse and rat (from 6,282 introns that were likely to have been GT–AG before human and rodents split), and two GC to GT conversions (from 34 GC–AG introns that probably predated the human and rodent split). These results give some indication of the degree to which mutation from T to C is tolerated in donor sites. The GC donor site appears to be better tolerated in introns with very strong donor sites, because in these introns the proportion of GC donor sites is ~11%, much higher than the 0.7% overall frequency of GC donor sites in U2 introns. Although we found a variety of other non-canonical configurations in U2 introns, very few are conserved, which suggests that most correspond to transient, evolutionarily unstable states, pseudogenes, or mis-annotations.

### Gene duplications

Duplication of genomic segments represents a frequent and robust mechanism for generating new genes[138]. Because there were no compelling data showing rat-specific genes arising directly from non-coding sequences, we examined gene duplications to measure their potential contribution to rat-specific biology. A previous study showed that gene clusters in mouse without counterparts in human are subject to rapid, adaptive evolution[3,139]. We used two methods to identify recent gene duplications: methods that directly identified paralogous clusters, and methods that analysed genomic segmental duplications (see above).

Using the first approach, we found 784 rat paralogue clusters containing 3,089 genes (Methods). This was lower than in mouse (910 clusters/3,784 genes), but the difference probably reflects the larger number of gene predictions from the mouse assembly.

To investigate the timing of expansion of these individual families, we measured rates of local gene duplication and retention within clusters. BLAST is not suited to this[140,141] and so we instead calculated the number of synonymous substitutions per synonymous site ($K_S$) between all pairs of homologous genes; constructed $K_S$-derived phylogenetic trees; and predicted orthology or paralogy gene duplication events automatically from their topologies (Supplementary Information). The results showed that the neutral substitution rate varies among orthologues by approximately twofold (Fig. 10). This is similar to chromosomal variation shown previously by a study of mouse and human ancestral repeats[3]. Rates of change among ancestral gene duplications (those that predate the mouse–rat split) were relatively constant. Mouse-specific and rat-specific duplications occurred at similar rates, except for those with $K_S < 0.04$, which are reduced in mouse-specific duplications (Fig. 10). More data are required to determine whether this reduction is a biological effect, as it might be accounted for by different protocols for assembling mouse and rat genomes, which differentially collapse areas of nearly identical sequence.

The rat paralogue pairs that probably arose after the rat–mouse split (12–24 Myr ago) have $K_S$ values of ≤0.2 (Table 3). We found 649 $K_S < 0.2$ gene duplication events in rat, a lower number than is found in mouse (755). For both rodents, this represents a likelihood of a gene duplicating of between $1.3 \times 10^{-3}$ and $2.6 \times 10^{-3}$ every Myr. These are necessarily estimates, because gene deletions, conversions and pseudogene formation are not considered. Interestingly, the data are consistent with a previous estimate for *Drosophila* genes, but are an order of magnitude lower than an estimate for *Caenorhabditis elegans* genes[140].

A subset of clusters have at least three gene duplications with $K_S < 0.2$ (Table 5). These are expected to be enriched in genes whose duplications persist as a consequence of positive selection. The group is dominated by genes involved in adaptive immune response and chemosensation[87]. Inspection of the $K_S$-derived trees allowed us to infer the gene numbers in these clusters for the common ancestor of rat and mouse (that is, at $K_S = 0.2$), assuming no gene deletions or pseudogene generation (Table 5). Immunoglobulin, T-cell receptor α-chain, and $\alpha_{2u}$-globulin genes appear to be duplicating at the fastest rates in the rat genome (Table 5). Since divergence with mouse, these rat clusters have increased gene content several-fold. This recapitulates previous observations that rapidly evolving and duplicating genes are over-represented in olfaction and odorant detection, antigen recognition and reproduction[142].

An examination of duplicated genomic segments showed this enrichment for most of the same genes and also elements involved in foreign compound detoxification (cytochrome P450 and carboxylesterase genes)[87]. Together, these are exciting findings because each of these categories can easily be associated with a

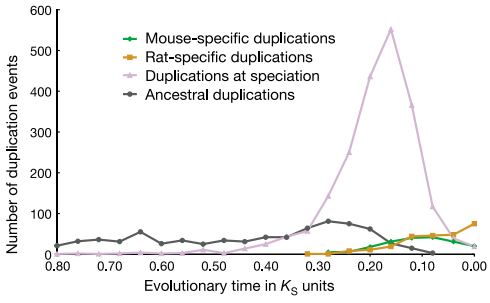


**Figure 10** Variation in the frequency of gene duplications during the evolutionary histories of the rat and mouse. The sequence of gene duplication events was inferred from phylogenetic trees determined from pairwise estimates of genetic divergence under neutral selection ($K_S$, Methods). The median $K_S$ value for mouse:rat 1:1 orthologues is 0.19. This value corresponds to the divergence time of mouse and rat lineages.

aid disease gene identification, as recently suggested for the mouse[200].

The Rnor3.1 draft sequence was generated primarily from DNA of a single inbred rat line. This maximized the likelihood of deriving an accurate sequence assembly, but reduced any likely discovery of natural variation in this phase of the project. As a consequence there has been no large-scale public SNP discovery from rat genomic sequencing. A pilot project based on coding (c)SNP discovery has been initiated, however[201], as these cSNPs represent a particularly important subset of variants that may have direct functional significance[202]. These data have illustrated both immediate applications and the long-term potential for an effort aimed at comprehensive SNP discovery.

## Conclusions

As the third mammalian genome to be sequenced, the rat genome has provided both predictable and surprising information about mammalian species. Although it was clear at the outset of this programme that ongoing rat research would benefit from the resource of a genome sequence, there was uncertainty about how many new insights would be found, especially considering the superficial similarities between the rat and the already sequenced mouse. Instead, the results of the sequencing and analysis have generated some deep insights into the evolutionary processes that have given rise to these different species. In addition, the project has been invaluable in further developing the methods for the generation and analysis of large genome sequence data sets.

The generation of the rat draft tested the new 'combined approach' for large genome sequencing. As the overall assembly is of high quality, there is no doubt that this overall strategy, and the supporting software we have developed, provides a suitable approach for this problem. Because we included a BAC 'skimming' component in the underlying data set, the assembly recovered a fraction of the genome that was expected, by analogy to the mouse project, to be difficult to assemble from pure WGS data. In addition, the BAC skimming component allowed progressive generation of high-quality local assemblies that were of use to the rat research community as the project developed. On the other hand, although the BAC component used here was far less expensive than the fully ordered and highly redundant set used in the hierarchical approach to sequencing the human genome, it nevertheless increased the overall cost of data production relative to a WGS approach.

The issue of efficacy of WGS versus other approaches to the sequencing of large genomes remains a matter of earnest scientific debate. In ongoing projects at different centres that participated in the RGSP consortium, different approaches are being used to tackle new genomes. These include pure WGS methods, the combined approach and variations on that methodology. The future application of the different procedures depends on the target genome sizes, the expected degree of heterogeneity (that is, polymorphism) in the organism to be sequenced, and the preferences of the individual centre. So far, all the genomes that have been analysed by RGSP consortium members have been of high quality and we anticipate that this will continue as the benefits and disadvantages of different approaches are further studied and analysed.

The rat genome data have improved the utility of the rat model enormously. Now that near-complete knowledge of the rat gene content is realizable, individual researchers have a data source for the rat 'parts list' that can be explored with the high degree of confidence and precision that is appropriate for biomedical research. A similar improvement has been made in the resources for physical and genetic mapping, because the relative position of individual markers is now known with high confidence and there are now computational resources to bridge the process of genetic association with gene modelling and experimental investigation. These advances have been reflected by measured increases in the use of all the rat-specific public genome data sets that can be accessed online, as well as by the informally assessed increases in overall 'genomic' research of this model.

The expected benefit of a third mammalian sequence providing an outgroup by which to discriminate the timing of events that had already been noted between mouse and human was fully realized. Using the three sequences and other partial data sets from additional organisms, it was possible to measure some of the overall faster rate of evolutionary change in the rodent lineage shared by mice and rats, as well as the peculiar acceleration of some aspects of rat-specific evolution. The observation of specific expanded gene families in the rat should provide material for targeted studies for some time.

At this time there is no plan to further upgrade or finish the rat genome sequence. This programme decision is a consequence of the high cost of converting draft sequence to finished data, and the pressing need to analyse new genomes. However, as the distant objective of very-low-cost sequencing or other advances that can improve draft sequences inexpensively are realized, it might be envisioned that a rat sequence that approaches the quality of the current human data will be produced. A finished rat genome may answer many questions, as specific clues already show that areas of the genome that are most difficult to resolve in a random sequencing project are also those areas that are most dynamic, and therefore of high potential interest in an evolutionary context.

Despite the advances represented here, we are clearly still at the beginning of the full analysis of the mammalian genome and its complex evolutionary history. Much of the additional data that are required to complete this story will be from other genomes, distantly related to rat. Nevertheless, a considerable body of data remains to be developed from this species. In addition to the distant prospect of a finished rat genome, analysis of other rat strains may yield genome-wide polymorphism data, while targeted efforts to generate cDNA clone collections will provide rat-specific reagents for routine use in research. Together with the ongoing efforts to fully develop methods to genetically manipulate whole rats and provide effective 'gene knockouts', the current and future rat genome resources will ensure a place for this organism in genomic and biomedical research for some time. □

## Methods

### DNA sequencing and data access

Paired-end reads from BAC and WGS libraries were produced as previously described[2,203]. Unprocessed sequence reads are available from the NCBI Trace Archive (ftp://ftp.ncbi.nih.gov/pub/TraceDB/rattus_norvegicus/); raw eBAC assembly data are available from the BCM-HGSC (http://www.hgsc.bcm.tmc.edu/Rat/); and the released Rnor3.1 assembly is available from the BCM-HGSC (ftp://ftp.hgsc.bcm.tmc.edu/pub/analysis/rat/), the NCBI (ftp://ftp.ncbi.nih.gov/genomes/R_norvegicus), and the UCSC (http://genome.ucsc.edu/downloads.html).

### Genome assembly

Assembly of the rat genome by the *Atlas* system is described in detail elsewhere[24]. Earlier assemblies (Rnor2.0/2.1) of the initial data set were based on 40 million total reads and 19,000 BAC skims. These assemblies spanned 2.66 Gb and comprised over 900 ultrabactigs with $N_{50}$ of over 5 Mb. They differed only in the removal of short artefactual duplications from Rnor2.0. Rnor3.1 includes another 1,100 BACs, selected to fill gaps in Rnor2.1. Because of the comprehensive coverage of the genome by Rnor2.0/2.1, it was used for the initial predictions of genes and proteins.

### BAC fingerprints

An agarose-gel-based fingerprinting methodology[204–207] was employed to generate *Hind*III fingerprints from 199,782 clones in the CHORI-230 BAC library. The contig assembly was subjected to manual review and editing to refine clone order within contigs and to make merges between contigs, using tools provided in the FPC software[208–210]. Fingerprints for 5,250 RPCI-31 PACs[211] and RPCI-32 BACs were subsequently added to allow correlation between the fingerprint map and a developing YAC map of the rat genome. BAC and PAC clones are available through BACPAC Resources at CHORI (bacpacorders@chori.org).

### BAC, PAC and YAC maps

Markers generated from BAC and PAC clones were hybridized against YAC[58] (R.D., Pmatch, unpublished software) and radiation hybrid libraries[61,212] to produce independent maps that were subsequently combined. Genetic markers from two rat

genetic maps[61] and the radiation hybrid map[59] were aligned to the Rnor3.1 assembly using BLAT[123] (when sequence was available) or electronic polymerase chain reaction (EPCR)[213].

### Finished sequence used for quality assessment of the assembly

To assess the accuracy of the *Atlas* assembly, the Rnor3.1 sequence was compared to 13 Mb of sequences that had been finished to high quality.

### Large-scale rearrangements

We compared these assemblies: Human (April 2003, NCBI build 33); Mouse (February 2003, NCBI build 30); and Rat (June 2003, Rnor3.1). Repeats were masked using RepeatMasker (A.S. & P. Green, unpublished work; see http://ftp.genome.washington.edu/RM/RepeatMasker.html) and TandemRepeatFinder[214]. Local alignments were produced using PatternHunter[70] (Supplementary Information). Repeat contamination was removed and the remaining similarities combined into two- and three-way anchors[73] and synteny blocks produced at various resolutions using GRIMM-Synteny[71].

### Genome-wide visualization of conserved synteny

Pairwise comparisons of the genomes of human, mouse and rat using MULTIZ[69,215], MLAGAN[216,217], MAVID[110], PatternHunter[70] and Pash[72] were merged into blocks of conserved synteny[69,71,72], and the 1-Mb-resolution images were displayed using the Virtual Genome Painting method (M.L.G.-G. *et al.*, unpublished work; http://www.genboree.org).

### Rat segmental duplications

Segmental duplications >5 kb were identified, extracted and aligned as described[218], and paralogous sequence relationships were assessed using PARASIGHT visualization software (J.A.B., unpublished work; Supplementary Information).

### Venn diagram

Pairwise and three-way alignments generated using BLASTZ[219] and MULTIZ[215] or HUMOR[215] were analysed to classify each nucleotide in the three genomes by the species with which it aligns: in all three species, aligning between human and rat (but not mouse), between human and mouse (but not rat), or between mouse and rat (but not human). Other nucleotides are species-specific; unassigned nucleotides occupying gaps in the genome assemblies were excluded. On the basis of output from RepeatMasker[164] and RepeatDater[89], nucleotides were assigned to categories (of non-repetitive, repetitive with a certain ancestry, or repetitive but unassigned) and counted. See Supplementary Table SI-1 for details.

### Gene prediction

ENSEMBL transcript models were built from 28,478 rodent proteins that were aligned to the genome using a combination of Pmatch (R.D., unpublished software), BLAST[220] and GeneWise[221]. Models based on 5,083 vertebrate proteins were added in regions without rodent-protein-based models. UTRs were added using 11,170 transcripts built from 8,615 different rat cDNAs aligned to the genome using BLAT, with coverage ≥90% and identity ≥95%. This procedure (as described[112] but without GENSCAN predictions), gave rise to 18,241 genes and 20,373 transcripts. This is the protein-based gene set. Rat and mouse cDNA and rat EST-based gene sets were also built. See Supplementary Information for details.

### Non-processed pseudogene identification

Human and mouse genes related by 1:1 orthology and lacking an apparent rat orthologue were considered. See Supplementary Information for details.

### High-resolution analyses of chromosome 10

These were performed predominantly on the whole genome alignments[217]. Plots in Fig. 9 were generated by sliding windows of width 2 Mb and a step size of 400 kb (total = 277 windows). See Supplementary Information for details.

Received 31 December 2003; accepted 20 February 2004; doi:10.1038/nature02426.


1. Darwin, C. *On The Origin of Species by Means of Natural Selection* 1st edn, Ch. 4, 108 (John Murray, London, 1859).
2. International Human Genome Sequencing Consortium. Initial sequencing and analysis of the human genome. *Nature* **409,** 860–921 (2001).
3. Mouse Genome Sequencing Consortium. Initial sequencing and comparative analysis of the mouse genome. *Nature* **420,** 520–562 (2002).
4. Adkins, R. M., Gelke, E. L., Rowe, D. & Honeycutt, R. L. Molecular phylogeny and divergence time estimates for major rodent groups: evidence from multiple genes. *Mol. Biol. Evol.* **18,** 777–791 (2001).
5. Springer, M. S., Murphy, W. J., Eizirik, E. & O'Brien, S. J. Placental mammal diversification and the Cretaceous-Tertiary boundary. *Proc. Natl Acad. Sci. USA* **100,** 1056–1061 (2003).
6. Canby, T. Y. The rat, lapdog of the devil. *Nat. Geogr.* July, 60–87 (1977).
7. Robinson, R. *Genetics of the Norway Rat* (Pergamon, Oxford, 1965).
8. Barnett, S. A. *The Story of Rats. Their Impact on Us, and Our Impact on Them* Ch. 2, 17–18 (Allen and Unwin, Crows Nest, Australia, 2002).
9. Hedrich, H. J. in *History, Strains, and Models in the Laboratory Rat* (ed. Krinke, G. J.) 3–16 (Academic, San Diego, 2000).
10. Lindsey, J. R. in *The Laboratory Rat* (eds Baker, H. J., Lindsey, J. R. & Weisbroth, S. H.) 1–36 (Academic, New York, 1979).
11. Greenhouse, D. D., Festing, M. F. W., Hasan, S. & Cohen, A. L. in *Genetic Monitoring of Inbred Strains of Rats* (ed. Hedrich, H. J.) 410–480 (Gustav Fischer, Stuttgart, 1990).
12. Kuntz, C. *et al.* Comparison of laparoscopic versus conventional technique in colonic and liver resection in a tumor-bearing small animal model. *Surg. Endosc.* **16,** 1175–1181 (2002).
13. Kitagawa, K., Hamada, Y., Nakai, K., Kato, Y. & Okumura, T. Comparison of one- and two-step procedures in a rat model of small bowel transplantation. *Transplant. Proc.* **34,** 1030–1032 (2002).
14. Sauve, Y., Girman, S. V., Wang, S., Keegan, D. J. & Lund, R. D. Preservation of visual responsiveness in the superior colliculus of RCS rats after retinal pigment epithelium cell transplantation. *Neuroscience* **114,** 389–401 (2002).
15. Wang, H. *et al.* Attenuation of acute xenograft rejection by short-term treatment with LF15–0195 and monoclonal antibody against CD45RB in a rat-to-mouse cardiac transplantation model. *Transplantation* **75,** 1475–1481 (2003).
16. Alves, A. *et al.* Total vascular exclusion of the liver enhances the efficacy of retroviral-mediated associated thymidine kinase and interleukin-2 genes transfer against multiple hepatic tumors in rats. *Surgery* **133,** 669–677 (2003).
17. Liu, M. Y., Poellinger, L. & Walker, C. L. Up-regulation of hypoxia-inducible factor 2α in renal cell carcinoma associated with loss of Tsc-2 tumor suppressor gene. *Cancer Res.* **63,** 2675–2680 (2003).
18. Jin, X. *et al.* Effects of leptin on endothelial function with OB-Rb gene transfer in Zucker fatty rats. *Atherosclerosis* **169,** 225–233 (2003).
19. Ravingerova, T., Neckar, J. & Kolar, F. Ischemic tolerance of rat hearts in acute and chronic phases of experimental diabetes. *Mol. Cell. Biochem.* **249,** 167–174 (2003).
20. Taylor, J. R. *et al.* An animal model of Tourette's syndrome. *Am. J. Psychiatry* **159,** 657–660 (2002).
21. Smyth, M. D., Barbaro, N. M. & Baraban, S. C. Effects of antiepileptic drugs on induced epileptiform activity in a rat model of dysplasia. *Epilepsy Res.* **50,** 251–264 (2002).
22. McBride, W. J. & Li, T. K. Animal models of alcoholism: neurobiology of high alcohol-drinking behavior in rodents. *Crit. Rev. Neurobiol.* **12,** 339–369 (1998).
23. Crisci, A. R. & Ferreira, A. L. Low-intensity pulsed ultrasound accelerates the regeneration of the sciatic nerve after neurotomy in rats. *Ultrasound Med. Biol.* **28,** 1335–1341 (2002).
24. Ozkan, O. *et al.* Reinnervation of denervated muscle in a split-nerve transfer model. *Ann. Plast. Surg.* **49,** 532–540 (2002).
25. Fray, M. J., Dickinson, R. P., Huggins, J. P. & Occleston, N. L. A potent, selective inhibitor of matrix metalloproteinase-3 for the topical treatment of chronic dermal ulcers. *J. Med. Chem.* **46,** 3514–3525 (2003).
26. Petratos, P. B. *et al.* Full-thickness human foreskin transplantation onto nude rats as an *in vivo* model of acute human wound healing. *Plast. Reconstr. Surg.* **111,** 1988–1997 (2003).
27. Hussar, P. *et al.* Bone healing models in rat tibia after different injuries. *Ann. Chir. Gynaecol.* **90,** 271–279 (2001).
28. Yang, T. D., Pei, J. S., Yang, S. L., Liu, Z. Q. & Sun, R. L. Medical prevention of space motion sickness–animal model of therapeutic effect of a new medicine on motion sickness. *Adv. Space Res.* **30,** 751–755 (2002).
29. Forte, A. *et al.* Stenosis progression after surgical injury in Milan hypertensive rat carotid arteries. *Cardiovasc. Res.* **60,** 654–663 (2003).
30. Komamura, K. *et al.* Differential gene expression in the rat skeletal and heart muscle in glucocorticoid-induced myopathy: analysis by microarray. *Cardiovasc. Drugs Ther.* **17,** 303–310 (2003).
31. McBride, M. W. *et al.* Functional genomics in rodent models of hypertension. *J. Physiol. (Lond.)* **554,** 56–63 (2004).
32. Kasteleijn-Nolst Trenite, D. G. & Hirsch, E. Levetiracetam: preliminary efficacy in generalized seizures. *Epileptic Disord.* **5,** S39–S44 (2003).
33. Malik, A. S. *et al.* A novel dehydroepiandrosterone analog improves functional recovery in a rat traumatic brain injury model. *J. Neurotrauma* **20,** 463–476 (2003).
34. Kostrubsky, V. E. *et al.* Evaluation of hepatotoxic potential of drugs by inhibition of bile acid transport in cultured primary human hepatocytes and intact rats. *Toxicol. Sci.* **76,** 220–228 (2003).
35. Lindon, J. C. *et al.* Contemporary issues in toxicology: the role of metabonomics in toxicology and its evaluation by the COMET project. *Toxicol. Appl. Pharmacol.* **187,** 137–146 (2003).
36. Tam, R. C. *et al.* The ribavirin analog ICN 17261 demonstrates reduced toxicity and antiviral effects with retention of both immunomodulatory activity and reduction of hepatitis-induced serum alanine aminotransferase levels. *Antimicrob. Agents Chemother.* **44,** 1276–1283 (2000).
37. Youssef, A. F., Turck, P. & Fort, F. L. Safety and pharmacokinetics of oral lansoprazole in preadolescent rats exposed from weaning through sexual maturity. *Reprod. Toxicol.* **17,** 109–116 (2003).
38. National Institutes of Health. *Network for Large-Scale Sequencing of the Rat Genome* (http://grants2.nih.gov/grants/guide/rfa-files/RFA-HG-00-002.html) (2000).
39. Aparicio, S. *et al.* Whole-genome shotgun assembly and analysis of the genome of *Fugu rubripes*. *Science* **297,** 1301–1310 (2002).
40. Yu, J. *et al.* A draft sequence of the rice genome (*Oryza sativa* L. ssp. *indica*). *Science* **296,** 79–92 (2002).
41. Goff, S. A. *et al.* A draft sequence of the rice genome (*Oryza sativa* L. ssp. *japonica*). *Science* **296,** 92–100 (2002).
42. Adams, M. D. *et al.* The genome sequence of *Drosophila melanogaster*. *Science* **287,** 2185–2195 (2000).
43. Dehal, P. *et al.* The draft genome of *Ciona intestinalis*: insights into chordate and vertebrate origins. *Science* **298,** 2157–2167 (2002).
44. Myers, E. W. *et al.* A whole-genome assembly of *Drosophila*. *Science* **287,** 2196–2204 (2000).
45. Myers, E. W., Sutton, G. G., Smith, H. O., Adams, M. D. & Venter, J. C. On the sequencing and assembly of the human genome. *Proc. Natl Acad. Sci. USA* **99,** 4145–4146 (2002).
46. Waterston, R. H., Lander, E. S. & Sulston, J. E. On the sequencing of the human genome. *Proc. Natl Acad. Sci. USA* **99,** 3712–3716 (2002).
47. Waterston, R. H., Lander, E. S. & Sulston, J. E. More on the sequencing of the human genome. *Proc. Natl Acad. Sci. USA* **100,** 3022–3024 (2003); author reply (**100**), 3025–3026 (2003).
48. Green, P. Whole-genome disassembly. *Proc. Natl Acad. Sci. USA* **99,** 4143–4144 (2002).
49. Batzoglou, S. *et al.* ARACHNE: a whole-genome shotgun assembler. *Genome Res.* **12,** 177–189 (2002).

50. Jaffe, D. B. *et al.* Whole-genome sequence assembly for mammalian genomes: Arachne 2. *Genome Res.* **13,** 91–96 (2003).
51. Cheung, J. *et al.* Recent segmental and gene duplications in the mouse genome. *Genome Biol.* **4,** R47 [online] (2003).
52. Eichler, E. E. Masquerading repeats: Paralogous pitfalls of the human genome. *Genome Res.* **8,** 758–762 (1998).
53. Eichler, E. E. Segmental duplications: what's missing, misassigned, and misassembled—and should we care? *Genome Res.* **11,** 653–656 (2001).
54. Havlak, P. *et al.* The *Atlas* genome assembly system. *Genome Res.* **14,** 721–732 (2004).
55. Osoegawa, K. *et al.* BAC Resources for the rat genome project. *Genome Res.* **14,** 780–785 (2004).
56. Krzywinski, M. *et al.* Integrated and sequence-ordered BAC and YAC-based physical maps for the rat genome. *Genome Res.* **14,** 766–779 (2004).
57. Chen, R., Sodergren, E., Gibbs, R. & Weinstock, G. M. Dynamic building of a BAC clone tiling path for genome sequencing project. *Genome Res.* **14,** 679–684 (2004).
58. Cai, L. *et al.* Construction and characterization of a 10-genome equivalent yeast artificial chromosome library for the laboratory rat, *Rattus norvegicus*. *Genomics* **39,** 385–392 (1997).
59. Kwitek, A. E. *et al.* High density rat radiation hybrid maps containing over 24,000 SSLPs, genes, and ESTs provide a direct link to the rat genome sequence. *Genome Res.* **14,** 750–757 (2004).
60. Felsenfeld, A., Peterson, J., Schloss, J. & Guyer, M. Assessing the quality of the DNA sequence from the Human Genome Project. *Genome Res.* **9,** 1–4 (1999).
61. Steen, R. G. *et al.* A high-density integrated genetic linkage and radiation hybrid map of the laboratory rat. *Genome Res.* **9** (insert), AP1–AP8 (1999).
62. Misra, S. *et al.* Annotation of the *Drosophila melanogaster* euchromatic genome: a systematic review. *Genome Biol.* **3,** RESEARCH0083.1-0083.22 [online] (2002).
63. Li, X. & Waterman, M. S. Estimating the repeat structure and length of DNA sequences using L-tuples. *Genome Res.* **13,** 1916–1922 (2003).
64. Riethman, H. *et al.* Mapping and initial analysis of human subtelomeric sequence assemblies. *Genome Res.* **14,** 18–28 (2004).
65. Bayona-Bafaluy, M. P. *et al.* Revisiting the mouse mitochondrial DNA sequence. *Nucleic Acids Res.* **31,** 5349–5355 (2003).
66. Kent, W. J., Baertsch, R., Hinrichs, A., Miller, W. & Haussler, D. Evolution's cauldron: duplication, deletion, and rearrangement in the mouse and human genomes. *Proc. Natl Acad. Sci. USA* **100,** 11484–11489 (2003).
67. Pevzner, P. & Tesler, G. Human and mouse genomic sequences reveal extensive breakpoint reuse in mammalian evolution. *Proc. Natl Acad. Sci. USA* **100,** 7672–7677 (2003).
68. Nadeau, J. H. & Taylor, B. A. Lengths of chromosomal segments conserved since divergence of man and mouse. *Proc. Natl Acad. Sci. USA* **81,** 814–818 (1984).
69. Schwartz, S. *et al.* Human–mouse alignments with BLASTZ. *Genome Res.* **13,** 103–107 (2003).
70. Ma, B., Tromp, J. & Li, M. PatternHunter: faster and more sensitive homology search. *Bioinformatics* **18,** 440–445 (2002).
71. Pevzner, P. & Tesler, G. Genome rearrangements in mammalian evolution: lessons from human and mouse genomes. *Genome Res.* **13,** 37–45 (2003).
72. Kalafus, K. J., Jackson, A. R. & Milosavljevic, A. Pash: Efficient genome-scale sequence anchoring by positional hashing. *Genome Res.* **14,** 672–678 (2004).
73. Bourque, G., Pevzner, P. A. & Tesler, G. Reconstructing the genomic architecture of ancestral mammals: lessons from human, mouse, and rat genomes. *Genome Res.* **14,** 507–516 (2004).
74. Graves, J. A., Gecz, J. & Hameister, H. Evolution of the human X—a smart and sexy chromosome that controls speciation and development. *Cytogenet. Genome Res.* **99,** 141–145 (2002).
75. Bourque, G. & Pevzner, P. A. Genome-scale evolution: reconstructing gene orders in the ancestral species. *Genome Res.* **12,** 26–36 (2002).
76. Murphy, W. J., Bourque, G., Tesler, G., Pevzner, P. & O'Brien, S. J. Reconstructing the genomic architecture of mammalian ancestors using multispecies comparative maps. *Hum. Genom.* **1,** 30–40 (2003).
77. Kirkness, E. F. *et al.* The dog genome: survey sequencing and comparative analysis. *Science* **301,** 1898–1903 (2003).
78. Murphy, W. J., Sun, S., Chen, Z. Q., Pecon-Slattery, J. & O'Brien, S. J. Extensive conservation of sex chromosome organization between cat and human revealed by parallel radiation hybrid mapping. *Genome Res.* **9,** 1223–1230 (1999).
79. Ventura, M., Archidiacono, N. & Rocchi, M. Centromere emergence in evolution. *Genome Res.* **11,** 595–599 (2001).
80. Yunis, J. J. & Prakash, O. The origin of man: a chromosomal pictorial legacy. *Science* **215,** 1525–1530 (1982).
81. Murphy, W. J., Fronicke, L., O'Brien, S. J. & Stanyon, R. The origin of human chromosome 1 and its homologs in placental mammals. *Genome Res.* **13,** 1880–1888 (2003).
82. Stanyon, R., Stone, G., Garcia, M. & Froenicke, L. Reciprocal chromosome painting shows that squirrels, unlike murid rodents, have a highly conserved genome organization. *Genomics* **82,** 245–249 (2003).
83. Bailey, J. A. *et al.* Recent segmental duplications in the human genome. *Science* **297,** 1003–1007 (2002).
84. Thomas, J. W. *et al.* Pericentromeric duplications in the laboratory mouse. *Genome Res.* **13,** 55–63 (2003).
85. Horvath, J. E. *et al.* Using a pericentromeric interspersed repeat to recapitulate the phylogeny and expansion of human centromeric segmental duplications. *Mol. Biol. Evol.* **20,** 1463–1479 (2003).
86. Guy, J. *et al.* Genomic sequence and transcriptional profile of the boundary between pericentromeric satellites and genes on human chromosome arm 10p. *Genome Res.* **13,** 159–172 (2003).
87. Tuzun, E., Bailey, J. A. & Eichler, E. E. Recent segmental duplications in the working draft assembly of the brown Norway rat. *Genome Res.* **14,** 493–506 (2004).
88. Pruitt, K. D. & Maglott, D. R. RefSeq and LocusLink: NCBI gene-centered resources. *Nucleic Acids Res.* **29,** 137–140 (2001).
89. Yang, S. *et al.* Patterns of insertions and their covariation with substitutions in the rat, mouse and human genomes. *Genome Res.* **14,** 517–527 (2004).
90. Roskin, K. M., Diekhans, M. & Haussler, D. in *Proc. 7th Annu. Int. Conf. Res. Comput. Mol. Biol. (RECOMB 2003)* (eds Vingron, M., Istrail, S., Pevzner, P. & Waterman, M.) doi:10.1145/640075.640109, 257–266 (ACM Press, New York, 2003).
91. Chiaromonte, F. *et al.* The share of human genomic DNA under selection estimated from human–mouse genomic alignments. *Cold Spring Harbor Symp. Quant. Biol.* (in the press).
92. Cooper, G. M. *et al.* Characterization of evolutionary rates and constraints in three mammalian genomes. *Genome Res.* **14,** 539–548 (2004).
93. Dermitzakis, E. T. *et al.* Numerous potentially functional but non-genic conserved sequences on human chromosome 21. *Nature* **420,** 578–582 (2002).
94. Dermitzakis, E. T. *et al.* Evolutionary discrimination of mammalian conserved non-genic sequences (CNGs). *Science* **302,** 1033–1035 (2003).
95. Nekrutenko, A. Rat–mouse comparisons to identify rodent-specific exons. *Genome Res.* (in the press).
96. Hardison, R. C. *et al.* Covariation in frequencies of substitution, deletion, transposition, and recombination during eutherian evolution. *Genome Res.* **13,** 13–26 (2003).
97. Thomas, J. W. *et al.* Comparative analyses of multi-species sequences from targeted genomic regions. *Nature* **424,** 788–793 (2003).
98. Cooper, G. M., Brudno, M., Green, E. D., Batzoglou, S. & Sidow, A. Quantitative estimates of sequence divergence for comparative analyses of mammalian genomes. *Genome Res.* **13,** 813–820 (2003).
99. Huckins, C. The spermatogonial stem cell population in adult rats. I. Their morphology, proliferation and maturation. *Anat. Rec.* **169,** 533–557 (1971).
100. Clermont, Y. Kinetics of spermatogenesis in mammals: seminiferous epithelium cycle and spermatogonial renewal. *Physiol. Rev.* **52,** 198–236 (1972).
101. Makova, K. D., Yang, S. & Chiaromonte, F. Insertions and deletions are male biased too: A whole-genome analysis in rodents. *Genome Res.* **14,** 567–573 (2004).
102. Sundstrom, H., Webster, M. T. & Ellegren, H. Is the rate of insertion and deletion mutation male biased? Molecular evolutionary analysis of avian and primate sex chromosome sequences. *Genetics* **164,** 259–268 (2003).
103. Chang, B. H. & Li, W. H. Estimating the intensity of male-driven evolution in rodents by using X-linked and Y-linked Ube 1 genes and pseudogenes. *J. Mol. Evol.* **40,** 70–77 (1995).
104. Chang, B. H., Shimmin, L. C., Shyue, S. K., Hewett-Emmett, D. & Li, W. H. Weak male-driven molecular evolution in rodents. *Proc. Natl Acad. Sci. USA* **91,** 827–831 (1994).
105. Bird, A. P. DNA methylation and the frequency of CpG in animal DNA. *Nucleic Acids Res.* **8,** 1499–1504 (1980).
106. Antequera, F. & Bird, A. Number of CpG islands and genes in human and mouse. *Proc. Natl Acad. Sci. USA* **90,** 11995–11999 (1993).
107. Jensen-Seaman, M. I. *et al.* Comparative recombination rates in the rat, mouse, and human genomes. *Genome Res.* **14,** 528–538 (2004).
108. Birdsell, J. A. Integrating genomics, bioinformatics, and classical genetics to study the effects of recombination on genome evolution. *Mol. Biol. Evol.* **19,** 1181–1197 (2002).
109. Montoya-Burgos, J. I., Boursot, P. & Galtier, N. Recombination explains isochores in mammalian genomes. *Trends Genet.* **19,** 128–130 (2003).
110. Bray, N. & Pachter, L. MAVID Constrained ancestral alignment of multiple sequence. *Genome Res.* **14,** 693–699 (2004).
111. Yap, V. B. & Pachter, L. Identification of evolutionary hotspots in the rodent genomes. *Genome Res.* **14,** 574–579 (2004).
112. Hubbard, T. *et al.* The Ensembl genome database project. *Nucleic Acids Res.* **30,** 38–41 (2002).
113. Vitt, U. *et al.* Identification of candidate disease genes by EST alignments, synteny and expression and verification of Ensembl genes on rat chromosome 1q43-54. *Genome Res.* **14,** 640–650 (2004).
114. Burge, C. & Karlin, S. Prediction of complete gene structures in human genomic DNA. *J. Mol. Biol.* **268,** 78–94 (1997).
115. Guigo, R., Knudsen, S., Drake, N. & Smith, T. Prediction of gene structure. *J. Mol. Biol.* **226,** 141–157 (1992).
116. Solovyev, V. V., Salamov, A. A. & Lawrence, C. B. Identification of human gene structure using linear discriminant functions and dynamic programming. *Proc. Int. Conf. Intell. Syst. Mol. Biol.* **3,** 367–375 (1995).
117. Parra, G. *et al.* Comparative gene prediction in human and mouse. *Genome Res.* **13,** 108–117 (2003).
118. Alexandersson, M., Cawley, S. & Pachter, L. SLAM—Cross-species gene finding with a generalized pair hidden Markov model. *Genome Res.* **13,** 496–502 (2003).
119. Flicek, P., Keibler, E., Hu, P., Korf, I. & Brent, M. R. Leveraging the mouse genome for gene prediction in human: from whole-genome shotgun reads to a global synteny map. *Genome Res.* **13,** 46–54 (2003).
120. Korf, I., Flicek, P., Duan, D. & Brent, M. R. Integrating genomic homology into gene structure prediction. *Bioinformatics* **17** (suppl. 1), S140–S148 (2001).
121. Wu, J. Q., Shteynberg, D., Arumugam, M., Gibbs, R. A. & Brent, M. R. Identification of rat genes by TWINSCAN gene prediction, RT–PCR, and direct sequencing. *Genome Res.* **14,** 655–671 (2004).
122. Dewey, C. *et al.* Accurate identification of novel human genes through simultaneous gene prediction in human, mouse and rat. *Genome Res.* **14,** 661–664 (2004).
123. Kent, W. J. BLAT—the BLAST-like alignment tool. *Genome Res.* **12,** 656–664 (2002).
124. Puente, X. S. & Lopez-Otin, C. A. A genomic analysis of rat proteases and protease inhibitors. *Genome Res.* **14,** 609–622 (2004).
125. Puente, X. S., Sanchez, L. M., Overall, C. M. & Lopez-Otin, C. Human and mouse proteases: a comparative genomic approach. *Nature Rev. Genet.* **4,** 544–558 (2003).
126. Hurst, L. D. The Ka/Ks ratio: diagnosing the form of sequence evolution. *Trends Genet.* **18,** 486–487 (2002).
127. Makalowski, W. & Boguski, M. S. Evolutionary parameters of the transcribed mammalian genome: an analysis of 2,820 orthologous rodent and human sequences. *Proc. Natl Acad. Sci. USA* **95,** 9407–9412 (1998).
128. Wolfe, K. H. & Sharp, P. M. Mammalian gene evolution: nucleotide sequence divergence between mouse and rat. *J. Mol. Evol.* **37,** 441–456 (1993).
129. Modrek, B. & Lee, C. J. Alternative splicing in the human, mouse and rat genomes is associated with an increased frequency of exon creation and/or loss. *Nature Genet.* **34,** 177–180 (2003).
130. Nekrutenko, A., Makova, K. D. & Li, W. H. The $K_A/K_S$ ratio test for assessing the protein-coding potential of genomic regions: an empirical and simulation study. *Genome Res.* **12,** 198–202 (2002).

131. Nekrutenko, A., Chung, W. Y. & Li, W. H. An evolutionary approach reveals a high protein-coding capacity of the human genome. *Trends Genet.* **19,** 306–310 (2003).
132. Taylor, M. S., Ponting, C. P. & Copley, R. R. Occurrence and consequences of coding sequence insertions and deletions in mammalian genomes. *Genome Res.* **14,** 555–566 (2004).
133. Green, H. & Wang, N. Codon reiteration and the evolution of proteins. *Proc. Natl Acad. Sci. USA* **91,** 4298–4302 (1994).
134. Levinson, G. & Gutman, G. A. Slipped-strand mispairing: a major mechanism for DNA sequence evolution. *Mol. Biol. Evol.* **4,** 203–221 (1987).
135. Alba, M. M. & Guigo, R. Comparative analysis of amino acid repeats in rodents and humans. *Genome Res.* **14,** 549–554 (2004).
136. Alba, M. M., Santibanez-Koref, M. F. & Hancock, J. M. Conservation of polyglutamine tract size between mice and humans depends on codon interruption. *Mol. Biol. Evol.* **16,** 1641–1644 (1999).
137. Burge, C. B., Padgett, R. A. & Sharp, P. A. Evolutionary fates and origins of U12-type introns. *Mol. Cell* **2,** 773–785 (1998).
138. Ohno, S. *Evolution by Gene Duplication* (Springer, Berlin, 1970).
139. Emes, R. D., Goodstadt, L., Winter, E. E. & Ponting, C. P. Comparison of the genomes of human and mouse lays the foundation of genome zoology. *Hum. Mol. Genet.* **12,** 701–709 (2003).
140. Lynch, M. & Conery, J. S. The evolutionary fate and consequences of duplicate genes. *Science* **290,** 1151–1155 (2000).
141. Prince, V. E. & Pickett, F. B. Splitting pairs: the diverging fates of duplicated genes. *Nature Rev. Genet.* **3,** 827–837 (2002).
142. Hughes, A. L. *Adaptive Evolution of Genes and Genomes* Ch. 7, 143–179 (Oxford Univ. Press, New York, 1999).
143. Tagle, D. A. *et al.* Embryonic epsilon and γ globin genes of a prosimian primate (*Galago crassicaudatus*). Nucleotide and amino acid sequences, developmental regulation and phylogenetic footprints. *J. Mol. Biol.* **203,** 439–455 (1988).
144. Altschul, S. F. & Lipman, D. J. Protein database searches for multiple alignments. *Proc. Natl Acad. Sci. USA* **87,** 5509–5513 (1990).
145. Gumucio, D. L. *et al.* Phylogenetic footprinting reveals a nuclear protein which binds to silencer sequences in the human γ and ε globin genes. *Mol. Cell. Biol.* **12,** 4919–4929 (1992).
146. Hardison, R. *et al.* Comparative analysis of the locus control region of the rabbit β-like gene cluster: HS3 increases transient expression of an embryonic ε-globin gene. *Nucleic Acids Res.* **21,** 1265–1272 (1993).
147. Boffelli, D. *et al.* Phylogenetic shadowing of primate sequences to find functional regions of the human genome. *Science* **299,** 1391–1394 (2003).
148. Elnitski, L. *et al.* Distinguishing regulatory DNA from neutral sites. *Genome Res.* **13,** 64–72 (2003).
149. Loots, G. G., Ovcharenko, I., Pachter, L., Dubchak, I. & Rubin, E. M. rVista for comparative sequence-based discovery of functional transcription factor binding sites. *Genome Res.* **12,** 832–839 (2002).
150. Pennacchio, L. A. & Rubin, E. M. Genomic strategies to identify mammalian regulatory sequences. *Nature Rev. Genet.* **2,** 100–109 (2001).
151. Margulies, E. H., Blanchette, M., Haussler, D. & Green, E. Identification and characterization of multi-species conserved sequences. *Genome Res.* **13,** 2507–2518 (2003).
152. Kolbe, D., *et al.* Regulatory potential scores from genome-wide 3-way alignments of human, mouse and rat. *Genome Res.* **14,** 700–707 (2004).
153. Wingender, E. *et al.* The TRANSFAC system on gene expression regulation. *Nucleic Acids Res.* **29,** 281–283 (2001).
154. Trinklein, N. D., Aldred, S. J., Saldanha, A. J. & Myers, R. M. Identification and functional analysis of human transcriptional promoters. *Genome Res.* **13,** 308–312 (2003).
155. Philipsen, S., Pruzina, S. & Grosveld, F. The minimal requirements for activity in transgenic mice of hypersensitive site 3 of the β globin locus control region. *EMBO J.* **12,** 1077–1085 (1993).
156. Reddy, P. M. & Shen, C. K. Protein–DNA interactions *in vivo* of an erythroid-specific, human β-globin locus enhancer. *Proc. Natl Acad. Sci. USA* **88,** 8676–8680 (1991).
157. Strauss, E. C. & Orkin, S. H. *In vivo* protein-DNA interactions at hypersensitive site 3 of the human β-globin locus control region. *Proc. Natl Acad. Sci. USA* **89,** 5809–5813 (1992).
158. Hillier, L. W. *et al.* The DNA sequence of human chromosome 7. *Nature* **424,** 157–164 (2003).
159. Torrents, D., Suyama, M. & Bork, P. A genome-wide survey of human pseudogenes. *Genome Res.* **13,** 2559–2567 (2003).
160. Zhang, Z., Harrison, P. & Gerstein, M. Identification and analysis of over 2000 ribosomal protein pseudogenes in the human genome. *Genome Res.* **12,** 1466–1482 (2002).
161. Mulder, N. J. *et al.* The InterPro Database 2003 brings increased coverage and new features. *Nucleic Acids Res.* **31,** 315–318 (2003).
162. Oh, B., Hwang, S. Y., Solter, D. & Knowles, B. B. Spindlin, a major maternal transcript expressed in the mouse during the transition from oocyte to embryo. *Development* **124,** 493–503 (1997).
163. Garcia-Meunier, P., Etienne-Julan, M., Fort, P., Piechaczyk, M. & Bonhomme, F. Concerted evolution in the GAPDH family of retrotransposed pseudogenes. *Mamm. Genome* **4,** 695–703 (1993).
164. Smit, A. F. Interspersed repeats and other mementos of transposable elements in mammalian genomes. *Curr. Opin. Genet. Dev.* **9,** 657–663 (1999).
165. Prak, E. T. & Kazazian, H. H. Jr Mobile elements and the human genome. *Nature Rev. Genet.* **1,** 134–144 (2000).
166. Ostertag, E. M. & Kazazian, H. H. Jr Biology of mammalian L1 retrotransposons. *Annu. Rev. Genet.* **35,** 501–538 (2001).
167. Weiner, A. M. SINEs and LINEs: the art of biting the hand that feeds you. *Curr. Opin. Cell Biol.* **14,** 343–350 (2002).
168. Martin, S. L. & Bushman, F. D. Nucleic acid chaperone activity of the ORF1 protein from the mouse LINE-1 retrotransposon. *Mol. Cell. Biol.* **21,** 467–475 (2001).
169. Hayward, B. E., Zavanelli, M. & Furano, A. V. Recombination creates novel L1 (LINE-1) elements in *Rattus norvegicus*. *Genetics* **146,** 641–654 (1997).
170. Dewannieux, M., Esnault, C. & Heidmann, T. LINE-mediated retrotransposition of marked Alu sequences. *Nature Genet.* **35,** 41–48 (2003).
171. Quentin, Y. A master sequence related to a free left Alu monomer (FLAM) at the origin of the B1 family in rodent genomes. *Nucleic Acids Res.* **22,** 2222–2227 (1994).
172. Cantrell, M. A. *et al.* An ancient retrovirus-like element contains hot spots for SINE insertion. *Genetics* **158,** 769–777 (2001).
173. Rothenburg, S., Eiben, M., Koch-Nolte, F. & Haag, F. Independent integration of rodent identifier (ID) elements into orthologous sites of some RT6 alleles of *Rattus norvegicus* and *Rattus rattus*. *J. Mol. Evol.* **55,** 251–259 (2002).
174. Roy-Engel, A. M. *et al.* Non-traditional Alu evolution and primate genomic diversity. *J. Mol. Biol.* **316,** 1033–1040 (2002).
175. Salem, A. H., Kilroy, G. E., Watkins, W. S., Jorde, L. B. & Batzer, M. A. Recently integrated Alu elements and human genomic diversity. *Mol. Biol. Evol.* **20,** 1349–1361 (2003).
176. Salem, A. H. *et al.* Alu elements and hominid phylogenetics. *Proc. Natl Acad. Sci. USA* **100,** 12787–127891 (2003).
177. Smit, A. F. Identification of a new, abundant superfamily of mammalian LTR-transposons. *Nucleic Acids Res.* **21,** 1863–1872 (1993).
178. Benit, L. *et al.* Cloning of a new murine endogenous retrovirus, MuERV-L, with strong similarity to the human HERV-L element and with a gag coding sequence closely related to the Fv1 restriction gene. *J. Virol.* **71,** 5652–5657 (1997).
179. Costas, J. Molecular characterization of the recent intragenomic spread of the murine endogenous retrovirus MuERV-L. *J. Mol. Evol.* **56,** 181–186 (2003).
180. Emes, R. D., Beatson, S. A., Ponting, C. P. & Goodstadt, L. Evolution and comparative genomics of odorant- and pheromone-associated genes in rodents. *Genome Res.* **14,** 591–602 (2004).
181. Young, J. M. *et al.* Different evolutionary processes shaped the mouse and human olfactory receptor gene families. *Hum. Mol. Genet.* **11,** 535–546 (2002).
182. Zhang, X. & Firestein, S. The olfactory receptor gene superfamily of the mouse. *Nature Neurosci.* **5,** 124–133 (2002).
183. Rouquier, S., Blancher, A. & Giorgi, D. The olfactory receptor gene repertoire in primates and mouse: evidence for reduction of the functional fraction in primates. *Proc. Natl Acad. Sci. USA* **97,** 2870–2874 (2000).
184. Clark, A. J., Hickman, J. & Bishop, J. A 45-kb DNA domain with two divergently orientated genes is the unit of organisation of the murine major urinary protein genes. *EMBO J.* **3,** 2055–2064 (1984).
185. Mural, R. J. *et al.* A comparison of whole-genome shotgun-derived mouse chromosome 16 and the human genome. *Science* **296,** 1661–1671 (2002).
186. Cavaggioni, A. & Mucignat-Caretta, C. Major urinary proteins, $\alpha_{2U}$-globulins and aphrodisin. *Biochim. Biophys. Acta* **1482,** 218–228 (2000).
187. Hurst, J. L. *et al.* Individual recognition in mice mediated by major urinary proteins. *Nature* **414,** 631–634 (2001).
188. Danielson, P. B. The cytochrome P450 superfamily: biochemistry, evolution and drug metabolism in humans. *Curr. Drug Metab.* **3,** 561–597 (2002).
189. Nelson, D. R. Cytochrome P450 and the individuality of species. *Arch. Biochem. Biophys.* **369,** 1–10 (1999).
190. Scarborough, P. E., Ma, J., Qu, W. & Zeldin, D. C. P450 subfamily CYP2J and their role in the bioactivation of arachidonic acid in extrahepatic tissues. *Drug Metab. Rev.* **31,** 205–234 (1999).
191. Willson, T. M. & Kliewer, S. A. PXR, CAR and drug metabolism. *Nature Rev. Drug Discov.* **1,** 259–266 (2002).
192. Gurates, B. *et al.* WT1 and DAX-1 inhibit aromatase P450 expression in human endometrial and endometriotic stromal cells. *J. Clin. Endocrinol. Metab.* **87,** 4369–4377 (2002).
193. Zhang, Z. *et al.* Genomic analysis of the nuclear receptor family: new insights into structure, regulation, and evolution from the rat genome. *Genome Res.* **14,** 580–590 (2004).
194. Lopez-Otin, C. & Overall, C. M. Protease degradomics: a new challenge for proteomics. *Nature Rev. Mol. Cell Biol.* **3,** 509–519 (2002).
195. Stenson, P. D. *et al.* Human Gene Mutation Database (HGMD): 2003 update. *Hum. Mutat.* **21,** 577–581 (2003).
196. Huang, H. *et al.* Evolutionary conservation of human disease gene orthologs in the rat and mouse genomes. *Genome Biol.* (submitted).
197. Duret, L. & Mouchiroud, D. Determinants of substitution rates in mammalian genes: expression pattern affects selection intensity but not mutation rate. *Mol. Biol. Evol.* **17,** 68–74 (2000).
198. Reddy, P. S. & Housman, D. E. The complex pathology of trinucleotide repeats. *Curr. Opin. Cell Biol.* **9,** 364–372 (1997).
199. The International HapMap Consortium. The International HapMap Project. *Nature* **426,** 789–796 (2003).
200. Wade, C. M. *et al.* The mosaic structure of variation in the laboratory mouse genome. *Nature* **420,** 574–578 (2002).
201. Zimdahl, H. *et al.* A SNP map of the rat genome generated from cDNA sequences. *Science* **303,** 807 (2004).
202. Mendell, J. T. & Dietz, H. C. When the message goes awry: disease-producing mutations that influence mRNA content and performance. *Cell* **107,** 411–414 (2001).
203. Venter, J. C. *et al.* The sequence of the human genome. *Science* **291,** 1304–1351 (2001).
204. Marra, M. *et al.* A map for sequence analysis of the *Arabidopsis thaliana* genome. *Nature Genet.* **22,** 265–270 (1999).
205. Marra, M. A. *et al.* High throughput fingerprint analysis of large-insert clones. *Genome Res.* **7,** 1072–1084 (1997).
206. The International Human Genome Mapping Consortium. A physical map of the human genome. *Nature* **409,** 934–941 (2001).
207. Schein, J. E. A. in *Bacterial Artificial Chromosomes: Methods and Protocols* (eds Zhao, S. & Stodolsky, M.) 143–156 (Humana, Totowa, New Jersey, 2004).
208. Soderlund, C. I. *et al.* FPC: a system for building contigs from restriction fingerprinted clones. *Comput. Appl. Biosci.* **13,** 523–535 (1997).
209. Soderlund, C. S. *et al.* Contigs built with fingerprints, markers, and FPC V4.7. *Genome Res.* **10,** 1772–1787 (2000).
210. Ness, S. R. *et al.* Assembly of fingerprint contigs: parallelized FPC. *Bioinformatics* **18,** 484–485 (2002).
211. Woon, P. Y. *et al.* Construction and characterization of a 10-fold genome equivalent rat P1-derived artificial chromosome library. *Genomics* **50,** 306–316 (1998).
212. Watanabe, T. K. *et al.* A radiation hybrid map of the rat genome containing 5,255 markers. *Nature Genet.* **22,** 27–36 (1999).

213. Schuler, G. D. Sequence mapping by electronic PCR. *Genome Res.* **7,** 541–550 (1997).
214. Benson, G. Tandem repeats finder: a program to analyze DNA sequences. *Nucleic Acids Res.* **27,** 573–580 (1999).
215. Blanchette, M. *et al.* Aligning multiple genomic sequences with the threaded blockset aligner. *Genome Res.* **14,** 708–715 (2004).
216. Brudno, M. *et al.* LAGAN and Multi-LAGAN: efficient tools for large-scale multiple alignment of genomic DNA. *Genome Res.* **13,** 721–731 (2003).
217. Brudno, M. *et al.* Automated whole-genome multiple alignment of rat, mouse, and human. *Genome Res.* **14,** 685–692 (2004).
218. Bailey, J. A., Yavor, A. M., Massa, H. F., Trask, B. J. & Eichler, E. E. Segmental duplications: organization and impact within the current human genome project assembly. *Genome Res.* **11,** 1005–1017 (2001).
219. Schwartz, S. *et al.* MultiPipMaker and supporting tools: Alignments and analysis of multiple genomic DNA sequences. *Nucleic Acids Res.* **31,** 3518–3524 (2003).
220. Altschul, S. F. *et al.* Gapped BLAST and PSI-BLAST: a new generation of protein database search programs. *Nucleic Acids Res.* **25,** 3389–3402 (1997).
221. Birney, E. & Durbin, R. Using GeneWise in the *Drosophila* annotation experiment. *Genome Res.* **10,** 547–548 (2000).
222. Yang, Z., Goldman, N. & Friday, A. Comparison of models for nucleotide substitution used in maximum-likelihood phylogenetic estimation. *Mol. Biol. Evol.* **11,** 316–324 (1994).
223. Chakrabarti, K. & Pachter, L. Visualization of multiple genome annotations and alignments with the K-BROWSER. *Genome Res.* **14,** 716–720 (2004).
224. Saitou, N. & Nei, M. The neighbor-joining method: a new method for reconstructing phylogenetic trees. *Mol. Biol. Evol.* **4,** 406–425 (1987).
225. Haldi, M. L. *et al.* Construction of a large-insert yeast artificial chromosome library of the rat genome. *Mamm. Genome* **8,** 284 (1997).

**Supplementary Information** accompanies the paper on **www.nature.com/nature**.

**Acknowledgements** Work at Baylor College of Medicine was supported by a grant from the NHGRI and NHLBI to R.A.G. Work at Genome Therapeutics was supported by grants from the NHGRI to D.S. A.S. acknowledges support from the NIGMS. M.B. acknowledges support from the NIH. N.H. was supported by the NGFN/BMBF (German Ministry for Research and Education). B.J.T. and J.M.Y. are supported by an NIH grant from the NIDCD. K.M.R. and G.M.C. are Howard Hughes Medical Institute Predoctoral Fellows. L.M.D'S., K.M. and K.J.K. are supported by training fellowships from the W. M. Keck Foundation to the Gulf Coast Consortia through the Keck Center for Computational and Structural Biology. Work at Case Western Reserve was supported in part by NIH grants to E.E.E. Work at IMIM was supported by a grant from Plan Nacional de I + D (Spain). M.M.A. acknowledges support from programme Ramón y Cajal and a grant from the Spanish Ministry of Science and Technology. Work at Universidad de Oviedo was supported by grants from the European Union, Obra Social Cajastur and Gobierno del Principado de Asturias. Work at Penn State University was supported by NHGRI grants. Work at the University of California Berkeley was supported by a grant from the NIH. Work at the Washington University School of Medicine Genome Sequencing Center and the British Columbia Cancer Agency Genome Sciences Centre was supported by an NIH grant. Work at UCSC and CHORI was supported by the NHGRI.

**Competing interests statement** The authors declare that they have no competing financial interests.

**Correspondence** and requests for materials should be addressed to R.A.G. (agibbs@bcm.tmc.edu). The genomic sequence is available under accession numbers AABR03000000 to AABR03137910 in the international sequence databases (GenBank, DDBJ and EMBL).

**Rat Genome Sequencing Project Consortium** **(Participants are arranged under area of contribution, and then by institution.)**

**DNA sequencing: Baylor College of Medicine** Richard A. Gibbs (Principal Investigator)[1], George M. Weinstock (Co-principal Investigator)[1], Michael L. Metzker[1], Donna M. Muzny[1], Erica J. Sodergren[1], Steven Scherer[1], Graham Scott[1], David Steffen[1], Kim C. Worley[1], Paula E. Burch[1], Geoffrey Okwuonu[1], Sandra Hines[1], Lora Lewis[1], Christine DeRamo[1], Oliver Delgado[1], Shannon Dugan-Rocha[1], George Miner[1], Margaret Morgan[1], Alicia Hawes[1], Rachel Gill[1]; **Celera** Robert A. Holt (Principal Investigator)[2,3], Mark D. Adams[3,4], Peter G. Amanatides[3,5], Holly Baden-Tillson[3,6], Mary Barnstead[3,7], Soo Chin[3], Cheryl A. Evans[3], Steve Ferriera[3,8], Carl Fosler[3], Anna Glodek[3,9], Zhiping Gu[3], Don Jennings[3], Cheryl L. Kraft[3,10], Trixie Nguyen[3], Cynthia M. Pfannkoch[3,6], Cynthia Sitter[3,11], Granger G. Sutton[3], J. Craig Venter[3,8], Trevor Woodage[3]; **Genome Therapeutics** Douglas Smith (Principal Investigator)[12,13], Hong-Mei Lee[12], Erik Gustafson[12,13], Patrick Cahill[12], Arnold Kana[12], Lynn Doucette-Stamm[12,13], Keith Weinstock[12], Kim Fechtel[12]; **University of Utah** Robert B. Weiss (Principal Investigator)[14], Diane M. Dunn[14]; **NISC Comparative Sequencing Program, NHGRI** Eric D. Green[15], Robert W. Blakesley[15], Gerard G. Bouffard[15]

**BAC library production: Children's Hospital Oakland Research Institute** Pieter J. de Jong (Principal Investigator)[16], Kazutoyo Osoegawa[16], Baoli Zhu[16]

**BAC fingerprinting: British Columbia Cancer Agency, Canada's Michael Smith Genome Sciences Centre** Marco Marra (Principal Investigator)[2], Jacqueline Schein (Principal Investigator)[2], Ian Bosdet[2], Chris Fjell[2], Steven Jones[2], Martin Krzywinski[2], Carrie Mathewson[2], Asim Siddiqui[2], Natasja Wye[2]; **Genome Sequencing Center, Washington University School of Medicine** John McPherson[1,17]

**BAC end sequencing: TIGR** Shaying Zhao (Principal Investigator)[18], Claire M. Fraser[18], Jyoti Shetty[18], Sofiya Shatsman[18], Keita Geer[18], Yixin Chen[18], Sofyia Abramzon[18], William C. Nierman[18]

**Sequence assembly: Baylor College of Medicine** Richard A. Gibbs (Principal Investigator)[1], George M. Weinstock (Principal Investigator)[1], Paul H. Havlak[1], Rui Chen[1], K. James Durbin[1], Amy Egan[1], Yanru Ren[1], Xing-Zhi Song[1], Bingshan Li[1], Yue Liu[1], Xiang Qin[1]

**Analysis and annotation: Affymetrix** Simon Cawley[19]; **Baylor College of Medicine** George M. Weinstock (Coordinator)[1], Kim C. Worley (Overall Coordinator)[1], A. J. Cooney[20], Richard A. Gibbs[1], Lisa M. D'Souza[1], Kirt Martin[1], Jia Qian Wu[1], Manuel L. Gonzalez-Garay[1], Andrew R. Jackson[1], Kenneth J. Kalafus[1,58], Michael P. McLeod[1], Aleksandar Milosavljevic[1], Davinder Virk[1], Andrei Volkov[1], David A. Wheeler[1], Zhengdong Zhang[1]; **Case Western Reserve University** Jeffrey A. Bailey[4], Evan E. Eichler[4], Eray Tuzun[4]; **EBI, Wellcome Trust Genome Campus** Ewan Birney[21], Emmanuel Mongin[21], Abel Ureta-Vidal[21], Cara Woodwark[21]; **EMBL, Heidelberg** Evgeny Zdobnov[22], Peer Bork[22,23], Mikita Suyama[22], David Torrents[22]; **Fraunhofer-Chalmers Research Centre for Industrial Mathematics, Gothenburg** Marina Alexandersson[24]; **Fred Hutchinson Cancer Research Center** Barbara J. Trask[25], Janet M. Young[25]; **Genome Therapeutics** Douglas Smith (Principal Investigator)[12,13], Hui Huang[12], Kim Fechtel[12], Huajun Wang[12], Heming Xing[12], Keith Weinstock[12]; **Incyte Corporation** Sue Daniels[26], Darryl Gietzen[26], Jeanette Schmidt[26], Kristian Stevens[26], Ursula Vitt[26], Jim Wingrove[26]; **Institut Municipal d'Investigacio Medica, Barcelona** Francisco Camara[27], M. Mar Albà[27], Josep F. Abril[27], Roderic Guigo[27]; **The Institute for Systems Biology** Arian Smit[28]; **Lawrence Berkeley National Laboratory** Inna Dubchak[29,30], Edward M. Rubin[29,30], Olivier Couronne[29,30], Alexander Poliakov[29]; **Max Delbrück Center for Molecular Medicine** Norbert Hübner[23], Detlev Ganten[23], Claudia Goesele[23,31], Oliver Hummel[23,31], Thomas Kreitler[23,31], Young-Ae Lee[23], Jan Monti[23], Herbert Schulz[23], Heike Zimdahl[23];

  

articles

**Max Planck Institute for Molecular Genetics, Berlin** Heinz Himmelbauer[31], Hans Lehrach[31]; **Medical College of Wisconsin** Howard J. Jacob (Principal Investigator)[32], Susan Bromberg[33], Jo Gullings-Handley[32], Michael I. Jensen-Seaman[32], Anne E. Kwitek[32], Jozef Lazar[32], Dean Pasko[33], Peter J. Tonellato[32], Simon Twigger[32]; **MRC Functional Genetics Unit, University of Oxford** Chris P. Ponting (Leader, Genes and Proteins Analysis Group)[34], Jose M. Duarte[34], Stephen Rice[34], Leo Goodstadt[34], Scott A. Beatson[34], Richard D. Emes[34], Eitan E. Winter[34], Caleb Webber[34]; **MWG-Biotech** Petra Brandt[35], Gerald Nyakatura[35]; **Pennsylvania State University** Margaret Adetobi[36], Francesca Chiaromonte[36], Laura Elnitski[36], Pallavi Eswara[36], Ross C. Hardison[36], Minmei Hou[36], Diana Kolbe[36], Kateryna Makova[36], Webb Miller[36], Anton Nekrutenko[36], Cathy Riemer[36], Scott Schwartz[36], James Taylor[36], Shan Yang[36], Yi Zhang[36]; **Roche Genetics and Roche Center for Medical Genomics** Klaus Lindpaintner[37]; **Sanger Institute** T. Dan Andrews[38], Mario Caccamo[38], Michele Clamp[38], Laura Clarke[38], Valerie Curwen[38], Richard Durbin[38], Eduardo Eyras[38], Stephen M. Searle[38]; **Stanford University** Gregory M. Cooper (Co-Leader, Evolutionary Analysis Group)[39], Serafim Batzoglou[40], Michael Brudno[40], Arend Sidow[39], Eric A. Stone[39]; **The Center for the Advancement of Genomics** J. Craig Venter[3,8]; **University of Arizona** Bret A. Payseur[41]; **Université de Montréal** Guillaume Bourque[42]; **Universidad de Oviedo** Carlos López-Otín[43], Xose S. Puente[43]; **University of California, Berkeley** Kushal Chakrabarti[44], Sourav Chatterji[44], Colin Dewey[44], Lior Pachter[45], Nicolas Bray[45], Von Bing Yap[45], Anat Caspi[46]; **University of California, San Diego** Glenn Tesler[47], Pavel A. Pevzner[48]; **University of California, Santa Cruz** David Haussler (Co-Leader, Evolutionary Analysis Group)[49], Krishna M. Roskin[50], Robert Baertsch[50], Hiram Clawson[50], Terrence S. Furey[50], Angie S. Hinrichs[50], Donna Karolchik[50], William J. Kent[50], Kate R. Rosenbloom[50], Heather Trumbower[50], Matt Weirauch[36,50]; **University of Wales College of Medicine** David N. Cooper[51], Peter D. Stenson[51]; **University of Western Ontario** Bin Ma[52]; **Washington University** Michael Brent[53], Manimozhiyan Arumugam[53], David Shteynberg[53]; **Wellcome Trust Centre for Human Genetics, University of Oxford** Richard R. Copley[54], Martin S. Taylor[54]; **The Wistar Institute** Harold Riethman[55], Uma Mudunuri[55]

**Scientific management:** Jane Peterson[56], Mark Guyer[56], Adam Felsenfeld[56], Susan Old[57], Stephen Mockrin[57] & Francis Collins[56]

*Affiliations for participants: 1, Human Genome Sequencing Center, Department of Molecular and Human Genetics, Baylor College of Medicine, MS BCM226, One Baylor Plaza, Houston, Texas 77030, USA ⟨http://www.hgsc.bcm.tmc.edu⟩; 2, British Columbia Cancer Agency, Canada's Michael Smith Genome Sciences Centre, 600 W 10th Avenue, Vancouver, British Columbia V5Z 4E6, Canada ⟨http://www.bcgsc.ca⟩; 3, Celera, 45 West Gude Drive, Rockville, Maryland 20850, USA; 4, Department of Genetics and the Center for Computational Genomics, Case Western Reserve University, School of Medicine, 10900 Euclid Avenue, Cleveland, Ohio 44106, USA; 5, DSM Pharmaceuticals Inc., 5900 NW Greenville Blvd, Greenville, North Carolina 27834, USA; 6, The Institute for Biological Energy Alternatives (IBEA), 1901 Research Blvd, Rockville, Maryland 20850, USA; 7, Intronn, Inc., 910 Clopper Road, South Building, Gaithersburg, Maryland 20878, USA; 8, The Center for the Advancement of Genomics (TCAG), 1901 Research Blvd, Suite 600, Rockville, Maryland 20850, USA; 9, Avalon Pharmaceuticals, 20358 SenecaMeadows Parkway, Germantown, Maryland 20876, USA; 10, Basic Immunology Branch, Division of Allergy, Immunology and Transplantation, National Institute of Allergy and Infectious Diseases (NIAID), NIH, DHHS, 6610 Rockledge Blvd, Room 3005, Bethesda, Maryland 20892-7612, USA; 11, DynPort Vaccine Company, LLC, 64 Thomas Jefferson Drive, Frederick, Maryland 21702, USA; 12, Genome Therapeutics Corporation, 100 Beaver Street, Waltham, Massachusetts 02453, USA; 13, Agencourt Bioscience Corporation, 100 Cummings Center, Beverly, Massachusetts 01915, USA; 14, Department of Human Genetics, University of Utah, Salt Lake City, Utah 84112, USA; 15, NIH Intramural Sequencing Center (NISC) and Genome Technology Branch, National Human Genome Research Institute (NHGRI), National Institutes of Health, Bethesda, Maryland 20892, USA; 16, BACPAC Resources, Children's Hospital Oakland Research Institute, 747 52nd Street, Oakland, California 94609, USA ⟨http://bacpac.chori.org⟩; 17, Genome Sequencing Centre, Washington University School of Medicine, 4444 Forest Park Blvd, St Louis, Missouri 63108, USA ⟨http://genome.wustl.edu⟩; 18, The Institute for Genomic Research, 9712 Medical Center Dr., Rockville, Maryland 20850, USA ⟨http://www.tigr.org⟩; 19, Affymetrix, 6550 Vallejo St, Suite 100, Emeryville, California 94608, USA; 20, Department of Cell Biology, Baylor College of Medicine, One Baylor Plaza, Houston, Texas 77030, USA; 21, EBI, Wellcome Trust Genome Campus, Hinxton, Cambridgeshire CB10 1SD, UK; 22, EMBL, Meyerhofstrasse 1, Heidelberg 69117, Germany; 23, Max Delbrück Center for Molecular Medicine (MDC), Experimental Genetics of Cardiovascular Disease, Robert-Rössle-Strasse 10, Berlin 13125, Germany ⟨http://www.mdc-berlin.de/ratgenome/⟩; 24, Fraunhofer-Chalmers Research Centre for Industrial Mathematics, Chalmers Science Park, S-412 88 Gothenburg, Sweden; 25, Division of Human Biology, Fred Hutchinson Cancer Research Center, 1100 Fairview Avenue N., C3-168, Seattle, Washington 98109, USA ⟨http://www.fhcrc.org/labs/trask/⟩; 26, Incyte Corporation, 3160 Porter Drive, Palo Alto, California 94304, USA ⟨http://www.incyte.com⟩; 27, Grup de Recerca en Informàtica Biomèdia, Institut Municipal d'Investigacio Medica, Universitat Pompeu Fabra, and Programa de Bioinfomatica i Genomica, Centre de Regulacio Genomica, C/ Dr. Aiguader 80, 08003 Barcelona, Catalonia, Spain; 28, Computational Biology Group, The Institute for Systems Biology, 1441 North 34th Street, Seattle, Washington 98103, USA; 29, Genomics Division, Lawrence Berkeley National Laboratory, 1 Cyclotron Rd., Berkeley, California 94720, USA ⟨http://www.lbl.gov⟩; 30, US Department of Energy Joint Genome Institute, 2800 Mitchell Drive, Walnut Creek, California 94598, USA ⟨http://jgi.doe.gov⟩; 31, Max Planck Institute for Molecular Genetics, Ihnestrasse 73, Berlin 14195, Germany; 32, Human and Molecular Genetics Center, Bioinformatics Research Center, and Department of Physiology, Medical College of Wisconsin, Milwaukee, Wisconsin 53226, USA; 33, Rat Genome Database, Bioinformatics Research Center, Medical College of Wisconsin, Milwaukee, Wisconsin 53226, USA; 34, MRC Functional Genetics Unit, University of Oxford, Department of Human Anatomy and Genetics, South Parks Road, Oxford OX1 3QX, UK; 35, MWG-Biotech, Anzinger Strasse 7a, Ebersberg 85560, Germany; 36, Center for Comparative Genomics and Bioinformatics, Huck Institutes of Life Sciences, Departments of Biology, Statistics, Biochemistry and Molecular Biology, Computer Science and Engineering, and Health Evaluation Sciences, The Pennsylvania State University, University Park, Pennsylvania 16802, USA; 37, Roche Genetics and Roche Center for Medical Genomics, F. Hoffmann-La Roche Ltd, 4070 Basel, Switzerland; 38, Sanger Institute, The Wellcome Trust Genome Campus, Hinxton, Cambridgeshire CB10 1SA, UK; 39, Departments of Pathology and Genetics, Stanford University, Stanford, California 94305, USA; 40, S256 James H. Clark Center, Department of Computer Science, Stanford University, Stanford, California 94305, USA; 41, Department of Ecology and Evolutionary Biology, University of Arizona, Tucson, Arizona 85721, USA; 42, Centre de Recherches Mathématiques, Université de Montréal, 2920 Chemin de la tour, Montréal, Quebec H3T 1J8, Canada ⟨http://www.crm.umontreal.ca⟩; 43, Departamento de Bioquimica y Biologia Molecular, Instituto Universitario de Oncologia, Universidad de Oviedo, 33006 Oviedo, Spain ⟨http://web.uniovi.es/degradome⟩; 44, Department of Electrical Engineering and Computer Science, University of California Berkeley, Berkeley, California 94720, USA; 45, Department of Mathematics, University of California Berkeley, Berkeley, California 94720, USA; 46, Bioengineering Graduate Group, University of California Berkeley, Berkeley, California 94720, USA; 47, University of California, San Diego, Department of Mathematics, 9500 Gilman Drive, San Diego, California 92093-0112, USA ⟨http://www-cse.ucsd.edu/groups/bioinformatics⟩; 48, University of California, San Diego, Department of Computer Science and Engineering, 9500 Gilman Drive, San Diego, California 92093-0114, USA ⟨http://www-cse.ucsd.edu/groups/bioinformatics⟩; 49, Howard Hughes Medical Institute, Center for Biomolecular Science & Engineering, Mailstop SOE, Baskin School of Engineering, University of California, Santa Cruz, 1156 High Street, Santa Cruz, California 95064, USA; 50, UCSC Genome Bioinformatics Group, Center for Biomolecular Science and Engineering, Mailstop SOE, Baskin School of Engineering, University of California, Santa Cruz, 1156 High Street, Santa Cruz, California 95064, USA; 51, Institute of Medical Genetics, University of Wales College of Medicine, Heath Park, Cardiff, CF14 4XN, UK; 52, Department of Computer Science, University of Western Ontario, London, Ontario N6A 5B7, Canada; 53, Laboratory for Computational Genomics, Campus Box 1045, Washington University, St Louis, Missouri 63130, USA ⟨http://genes.cse.wustl.edu⟩; 54, Wellcome Trust Centre for Human Genetics, University of Oxford, Roosevelt Drive, Oxford OX3 7BN, UK; 55, The Wistar Institute, 3601 Spruce Street, Philadelphia, Pennsyvania 19104, USA; 56, US National Institutes of Health, National Human Genome Research Institute, 31 Center Drive, Bethesda, Maryland 20892, USA; 57, US National Institutes of Health, National Heart, Lung, and Blood Institute, Bethesda, Maryland 20892, USA; 58, Program in Structural and Computational Biology and Molecular Biophysics, Baylor College of Medicine, One Baylor Plaza, Houston, Texas 77030, USA*

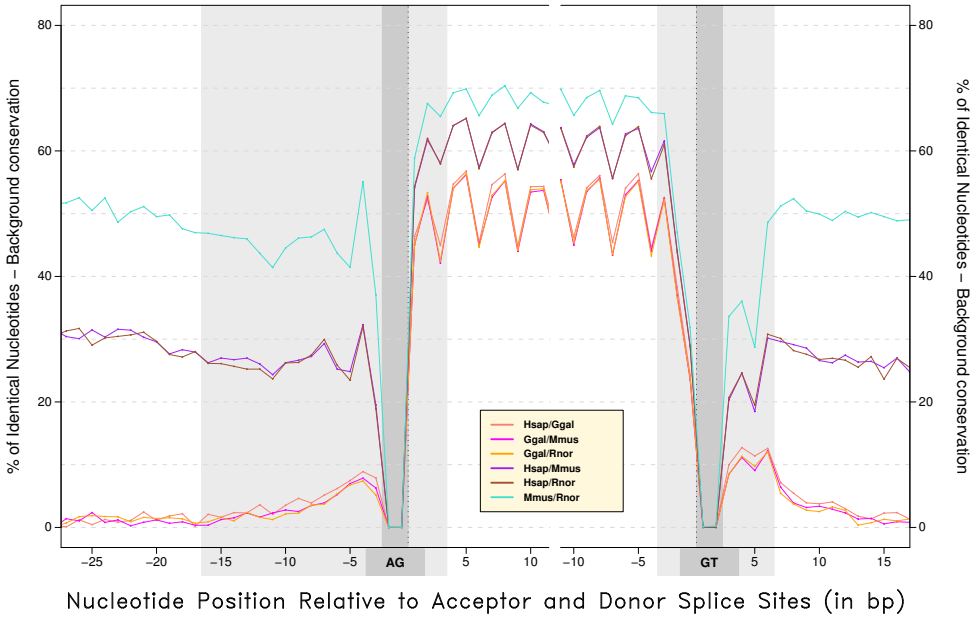


Figure 4.10: **Human/mouse/rat/chicken relative conservation over GT-AG splice site consensi.** The x-axis shows idealized base position from intron through exon to intron. The gray areas show the regions where expected conservation from the presence of splice site consensi was removed. Unlike inter-mammal comparisons, the chicken-mammal comparison shows a higher relative conservation rate at the splice sites than in the introns. Included as supplementary materials Figure 1 on Hillier *et al.* [2004].

## 4.3 The Comparative Analysis of Splice Sites in Vertebrates

### 4.3.1 Conservation of mammals and chicken orthologous splice sites

See section entitled "Evolutionary conservation of gene components" on page 142 (page 698 of Hillier *et al.* 2004).

Only the orthologous U12 introns of the four species were displayed in Figure 4.11. Further orthologous sets, including pair-wise and triads, are available at the supplementary materials web page (see page 213 on Web Glossary). It is worth to note that in the fourth example, the 16th intron of mouse gene *NM_007459* does not seem to be conforming to the U12 donor pattern. But it is not a case of conversion between U2 and U12 splice sites, just displacing the splice sites two nucleotides upstream we recover the U12 donor pattern and the overall alignment of the exonic regions improves.

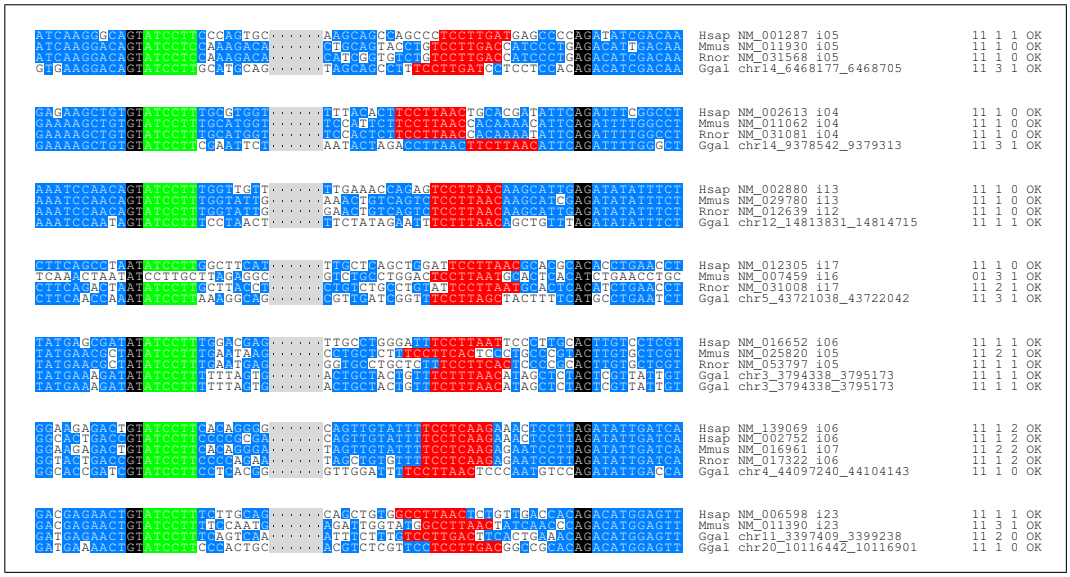


Figure 4.11: **Human, mouse, rat and chicken orthologous U12 intron sets.** Ungapped alignments of the donor (-10 to +16 around the 5′ splice sites) and the acceptor (-30 to +10 around the 3′ splice sites) sequences for all the orthologous U12 intron sets were drawn using `TeXshade` [Beitz, 2000]. Splice sites core signals are highlighted in a black box, the conserved U12 donor sequence (+3 to +8) is marked in green, sequence hits to the U12 branch point are colored in red, while conserved nucleotides at a given position are shown with a blue background.

### 4.3.2 Abril *et al*, *Genome Research*, 15(1):111–119, 2005

**PubMed Accession:**

http://www.ncbi.nlm.nih.gov/entrez/query.fcgi?cmd=Retrieve&db=PubMed&list_uids=15590946&dopt=Abstract

**Journal Abstract:**

http://www.genome.org/cgi/content/abstract/15/1/111

**Supplementary Materials:**

http://genome.imim.es/datasets/hmrg2004/

**Chicken Special/Letter**

# Comparison of splice sites in mammals and chicken

Josep F. Abril, Robert Castelo, and Roderic Guigó[1]

*Grup de Recerca en Informàtica Biomèdica, Institut Municipal d'Investigació Mèdica, Universitat Pompeu Fabra, and Programa de Bioinformàtica i Genòmica, Centre de Regulació Genòmica, C/ Dr. Aiguader 80, E-08003 Barcelona, Catalonia, Spain*

**We have carried out an initial analysis of the dynamics of the recent evolution of the splice-sites sequences on a large collection of human, rodent (mouse and rat), and chicken introns. Our results indicate that the sequences of splice sites are largely homogeneous within tetrapoda. We have also found that orthologous splice signals between human and rodents and within rodents are more conserved than unrelated splice sites, but the additional conservation can be explained mostly by background intron conservation. In contrast, additional conservation over background is detectable in orthologous mammalian and chicken splice sites. Our results also indicate that the U2 and UI2 intron classes seem to have evolved independently since the split of mammals and birds; we have not been able to find a convincing case of interconversion between these two classes in our collections of orthologous introns. Similarly, we have not found a single case of switching between AT-AC and GT-AG subtypes within UI2 introns, suggesting that this event has been a rare occurrence in recent evolutionary times. Switching between GT-AG and the noncanonical GC-AG U2 subtypes, on the contrary, does not appear to be unusual; in particular, T to C mutations appear to be relatively well tolerated in GT-AG introns with very strong donor sites.**

**[Supplemental material is available online at www.genome.org. The following individuals kindly provided reagents, samples, or unpublished information as indicated in the paper: P. Bork and I. Letunic.]**

Protein-coding genes are characteristically interrupted by introns in the genome of higher eukaryotic organisms. While intron function and origin has been debated at length (de Souza 2003; Fedorova and Fedorov 2003; Roy et al. 2003), recent comparative analyses show an abundance of conserved elements in intronic sequences (for instance, see Dermitzakis et al. 2002; Hare and Palumbi 2003). This strongly suggests that introns are rich in elements playing functional, probably regulatory, roles (Mattick 2001). Splicing of introns is found in all main branches of eukaryotes, that is, animals, plants, fungi, and protozoa, indicating an early origin of splicing within eukaryotes, or the existence, in the pre-eukaryotic world, of a precursor of splicing. Indeed, the two major molecular mechanisms by means of which splicing is produced, U2- and U12-dependent, seem to have evolved independently prior to the divergence of the animal and plant kingdoms (Burge et al. 1998; Zhu and Brendel 2003).

Within each of these two classes of splicing, sequence features involved in intron specification are essentially conserved across eukaryotes. In both classes, the sequence information needed to specify the 5′ and 3′ splice sites—hereafter also described as donor and acceptor sites respectively—is largely confined to their surrounding region (see Fig. 1). Conserved sequences in these regions interact with the splicing machinery to promote the assembly of the spliceosome and activate the biochemical pathway that leads to the production of the spliced mRNA (for review, see Burge et al. 1999). Despite the strong conservation, the sequence of splicing signals does not carry enough information to unequivocally specify introns in the large sequence of the pre-mRNA transcripts, occasionally hundreds of thousands of nucleotides long; and recent research suggests that signals other than those in the region of the splice sites play a role in the definition of the intron boundaries (for review, see Caceres and Kornblihtt 2002; Cartegni et al. 2002; Black 2003).

**[1]Corresponding author.**
**E-mail rguigo@imim.es; fax 34-93-221-32-37.**
Article and publication are at http://www.genome.org/cgi/doi/10.1101/gr.3108805. Article published online before print in December 2004.

Thus, in eukaryotic organisms, splicing introduces an additional level of decoding—prior to translation—on the sequence of the primary RNA transcript. There is a fundamental difference, however, between the genetic code—the mapping of nucleotide sequences (triplets) into 20 (or more) amino acids—and the splicing code—the mapping of nucleotide sequences into 3′ and 5′ intron boundaries. The genetic code is essentially deterministic; within a given species, a given triplet in the mRNA sequence results always in the same amino acid—the dual role in selenoproteins of the TGA triplet as stop and selenocysteine codon probably the most notable of all exceptions (for instance, see Kryukov et al. 2003). The splicing code, in contrast, is inherently stochastic; the probability of a splicing sequence in the primary transcript to participate in the definition of an intron boundary ranges from zero to one, and it is conditioned to very many different factors (which could be other sequences—maybe distant). The tissue-specific distribution of relative abundances of alternative splicing products (Xu et al. 2002; Yeo et al. 2004), for instance, reflects this nondeterministic nature of the splicing code.

The stochasticity of the splicing code offers opportunities for evolution that are absent in the highly deterministic genetic code. The availability of an increasing number of eukaryotic genomes makes it possible to investigate such an evolutionary process. Here, we report on findings obtained by comparing a large collection of orthologous introns (introns occurring at equivalent locations in orthologous genes) and their defining splice sites in human, mouse, rat, and chicken. Our results provide insights into the dynamics of the evolution of splice-site sequences during the most recent period of the history of life on earth.

## Results

In this section, we first report results concerning interconversion between the two major classes of introns, U2 and U12, and subtype switching within each class. Then, we report on the com-

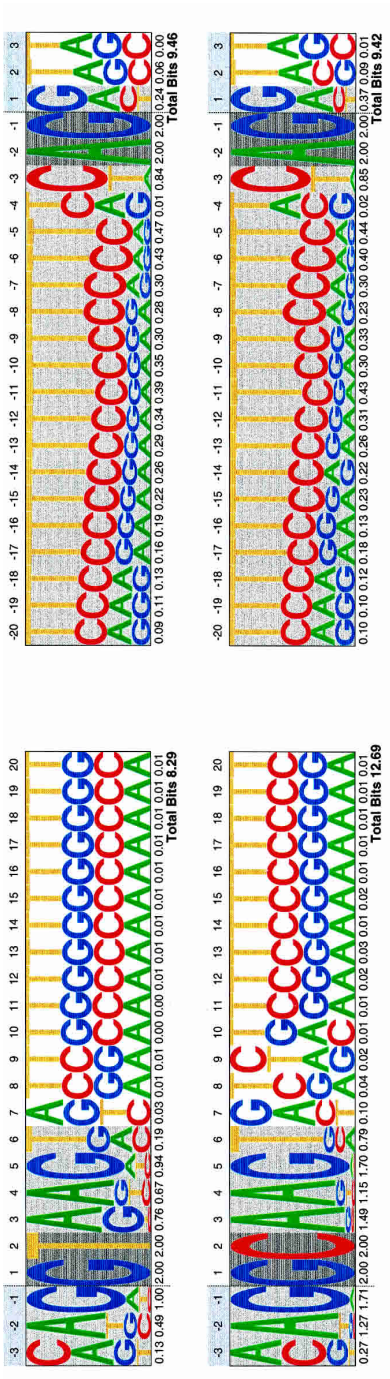


**Figure 1.** Donor and acceptor sites' pictograms. Pictograms of the donor (*left*) and the acceptor (*right*) site sequences for the U2 (*top*) and U12 (*bottom*) splice sites. The sequence plots for GT-AG and GC-AG U2 introns are given separately. The conserved sequence of the U12 branch point is also shown. From human, mouse, rat, and chicken RefSeq genes, a total number of 337,336, 2506, and 935 splice-site sequences from CDS introns from Ensembl were included in GT-AG, GC-AG, and U12 splice site sets, respectively, to produce the corresponding pictograms.

parison of splice-site sequences in human, rodents, and chicken. We have compared the overall sequence patterns of splice sites and investigated the level of sequence conservation between orthologous splice sites.

The analyses described here are very sensitive to the identification of true orthologous introns, as well as to the prediction of correct splice boundaries, particularly in the case of the non-canonical U12 introns. Because U12 introns constitute only a tiny fraction of all eukaryotic introns, computational gene prediction methods ignore them. Therefore, in absence of good cDNA coverage, computational gene catalogs are likely to heavily misrepresent them. Such is the case in the chicken genome. In an effort to conciliate the amount of data with reliability, we have resorted to different data sets to perform different types of analyses. Gene predictions from the RefSeq collection (Pruitt et al. 2003)—a collection of genes with good cDNA support—have been used for interspecific analysis of splice-site sequence patterns and for the identification and analysis of mammalian U12 introns. However, there are very few chicken genes in RefSeq. The larger—but strongly biased toward GT-AG canonical U2 introns—Ensembl collection (Birney et al. 2004; http://www.ensembl.org) has been used for interspecific comparison of splice-site patterns. A set of mammalian–avian curated orthologous introns—referred to as the HMRG set in this work (see Methods section)—has been used for the comparison of orthologous splice-site sequences. Table 1 describes the sizes of the data sets used in this study.

### Intron classes

Two distinct types of pre-mRNA introns are found in most higher eukaryotic organisms (Sharp and Burge 1997). They differ in the spliceosome complex that excise them during RNA processing. More than 99% of eukaryotic introns are spliced by the U2 spliceosome, while a minor class are spliced by the U12 spliceosome. U2 and U12 introns differ in the conserved sequences flanking their splice sites (see Fig. 1). Vertebrate U2 introns are characterized by the highly variable consensus [CA]AG/GT[AG]AGT at the donor (5′) site, (where [CA] means C or A, and / denotes the exon–intron boundary) and by a polypyrimidine-rich stretch between the acceptor site and a poorly conserved branch point. The branch point and the acceptor site are usually separated by 11–40 nucleotides, although cases are known where they can be over 100 nucleotides apart (Helfman and Ricci 1989; Smith and Nadal-Ginard 1989). U2 introns almost always exhibit the conserved GT and AG dinucleotides at the 5′ and 3′ intron boundaries, respectively. The only remarkable exception is the existence of U2 GC-AG introns, which appears with a frequency <1% (Burset et al. 2001).

U12 introns are characterized by a strong consensus/[AG]TATCCTT at the donor site, and TCCTT[AG]AC at the branch point. They also lack the polypyrimidine tract upstream of the acceptor site, characteristic of U2 introns. Also, in contrast to U2 introns, the distance between this acceptor site and the branch point is consistently short, between 10 and 20 nucleotides (Dietrich et al. 2001). Although initially discovered because of the unusual AT and AC dinucleotides at the 3′ and 5′ splice sites (Jackson 1991; Hall and Padgett 1994), it was later shown that U12 introns can exhibit a variety of terminal dinucleotides, the vast majority, however, are GT-AG or AT-AC (Dietrich et al. 1997; Sharp and Burge 1997; Levine and Durbin 2001; Zhu and Brendel 2003). Subtype switching within U12 introns, as well as conversion from U12 to U2 introns, has been documented (Burge and Karlin 1998), although amazing stability has been reported for U12 introns over very large evolutionary times (Zhu and Brendel 2003).

We have used the U12 donor site and branch point patterns above to identify U12 introns in the human and rodent RefSeq collections (see Methods). Table 2 lists the resulting frequencies of the different splice classes, and subtypes within each class. Numbers are consistent with those previously published (Burset et al. 2001; Levine and Durbin 2001). Identification of U12 introns was not attempted in chicken because of the small size of the RefSeq database for this organism. Figure 1 uses sequence pictograms to display the consensus for GT-AG U2 splice signals in mammals and chicken. It also displays the mammalian consensus for GC-AG U2 and U12 splice sites. In sequence pictograms (Schneider and Stephens 1990; Burge et al. 1999) the frequencies of the four nucleotides at each position along the signal are represented by the heights of their corresponding letters. The information content (intuitively, the deviation from random composition) is computed at each position, and summed up along the signal. The larger the information content, the more conserved the signal.

**Table 1.** Summary of initial data and filtered orthologs sets.

(A) Initial data sets

| | Ensembl[a] | | | UCSC genome browser[b] RefSeq[c] | | |
|---|---|---|---|---|---|---|
| Species | Version | Genes | Introns | Version | Genes | Introns |
| human[d] | v19.34a | 33,633 | 284,125 | HGv16/NCBI34 | 21,744 | 206,814 |
| mouse[e] | v19.30 | 30,665 | 218,163 | MGSCv4/NCBI32 | 17,988 | 139,258 |
| rat[f] | v19.3a | 28,545 | 192,459 | RGSCv3.1 | 4877 | 43,393 |
| chicken[g] | v22.1.1 | 28,491 | 252,226 | CGSCv2 | 1496 | 12,632 |

(B) Filtered orthologs

| | Sets | Genes | Introns | |
|---|---|---|---|---|
| Total | human | 6043 | 48,939 | (out of 51,876) |
| | mouse | 5680 | 45,543 | (out of 47,193) |
| | rat | 1847 | 13,929 | (out of 14,245) |
| Orthologs | human/mouse | 5550 | 44,119 | |
| | human/rat | 1737 | 13,259 | |
| | mouse/rat | 1416 | 9655 | |
| Triads | human/mouse/rat | 1283 | 8895 | |

(A) Initial data sets: the initial pool of genes/introns from which we filtered all the data sets for this work ([a]Birney et al. 2004; [b]Karolchik et al. 2003; [c]Pruitt et al. 2003; [d]Lander et al. 2001; [e]Waterston et al. 2002; [f]Rat Genome Sequencing Project Consortium 2004; [g]International Chicken Genome Sequencing Consortium 2004).
(B) Filtered orthologs: the number of RefSeq orthologous genes and introns derived from these data sets.

### Intron class conversion

Orthologous mapping revealed that in all cases, orthologous mouse–rat and human–rodent introns—from the RefSeq data set—were either both U12 or both U2. A few cases were initially classified as instances of intron conversion. After close inspection, however, we realized that all of these

**Table 2. Intron class and subclass frequencies in mammals**

| | | Human | Mouse | Rat |
|---|---|---|---|---|
| U2 | GT-AG | 48,212 (98.9%) | 44,817 (98.8%) | 13,707 (98.7%) |
| | GC-AG | 355 (0.7%) | 330 (0.7%) | 96 (0.7%) |
| | Other | 184 (0.4%) | 218 (0.5%) | 80 (0.6%) |
| | Total | 48,751 | 45,365 | 13,883 |
| U12 | GT-AG | 131 (69.7%) | 128 (71.9%) | 36 (78.3%) |
| | AT-AC | 51 (27.1%) | 47 (26.4%) | 9 (19.6%) |
| | Other | 6 (3.2%) | 3 (1.7%) | 1 (2.2%) |
| | Total | 188 | 178 | 46 |

cases could be explained either by misprediction of the intron boundaries or by splice sequence patterns slightly off consensus. (See Supplemental materials for the cross-species alignments at the intron boundaries of all predicted U12 introns). Remarkably, therefore, not one single convincing case of U12 to U2 conversion or vice-versa has occurred since the divergence of the human and rodent lineages. To investigate whether conservation of intron class extends beyond the mammalian lineage, we have mapped the 412 human, mouse, and rat U12 introns from Table 2, which correspond to 202 unique orthologs, into the chicken genome. The mapping was obtained by comparing, using exonerate (G. Slater, unpubl.), the two exons harboring the intron against the chicken genome sequence (see Methods). A total of 38 mammalian U12 introns were unequivocally mapped into the chicken genome. (See Supplemental material for cross-species alignments at the intron boundaries of the mammalian U12 introns mapped into the chicken genome). The 38 chicken introns had the typical donor-site sequence of U12 introns, and 36 had the typical U12 branch point. In the other two cases, sequences reminiscent of the U12 branch point could still be found, although departing clearly from the consensus. Since these two cases are both of the GT-AG U12 subtype, it is tempting to speculate that they may correspond to intermediates in the interconversion pathway between U12 and U2 introns. Against this hypothesis, however, is the fact that no strong polypyrimidine tract, suggestive of U2 function, can be found upstream of the acceptor site. With the exception of these two cases, the branchpoint sequence was extremely conserved between mammals and chicken, showing no more than two mismatches, but often being identical. The position of the branch point has also been conserved; with only one exception, the larger displacement observed was of 4 nucleotides. These results strongly argue that U2 and U12 introns have evolved independently, at least since the split of mammals and birds.

### Subtype switching

Although subtype switching between GT-AG and AT-AC U12 introns has been documented (Burge et al. 1998), we have not found any such case within rodents, between human and rodents, or between mammals and chicken in our set of U12 orthologous introns. It appears that this phenomenon occurs at a very slow rate over evolutionary time (see cross-species alignments of orthologous U12 introns in the Supplemental material).

Within U2 introns, on the contrary, switching between GC-AG and GT-AG subclasses, and vice-versa, is not unusual. Table 3A lists the pairwise frequency of subtype switching within U2 introns, and subtype distribution within orthologous mammalian triads. Because of the limited number of cases available in the RefSeq collection, we have ignored chicken genes in this analysis. A total of 190 of the 290 human (66%) and 289 mouse (66%) GC-AG introns are conserved in both species. Similar proportions are observed between human and rat. Within rodents, 60 of the 68 mouse (88%) and 67 rat (90%) GC-AG introns are conserved in both species. The availability of orthologous introns from three organisms allows the investigation of the dynamics of subtype switching within U2 introns (see Table 3B). We have divided GC-AG introns' orthologous triads into (1) "ancient"; the intron is GC-AG subtype in the three species, and thus it is likely to predate the split of human and rodents; (2) "modern"; the intron is GC-AG subtype in either human or rodents. Because of the lack of a reference out-group, however, we cannot distinguish here those ancient GC-AG introns that have reverted to GT-AG in one of the two lineages from those modern GC-AG introns that have arisen in one of the lineages; and (3) "recent"; the intron is of GC-AG subtype only in one of the rodent species. The most parsimonious hypothesis is that the switch to GC-AG has occurred after the split of mice and rats.

According to this classification, 47% (45) of the GC-AG introns are ancient, 36% (34) are modern, and 14% (13) are recent. Because human introns act as a reference out-group, we can establish (under the most parsimonious hypothesis) the direction of the GT/GC switch between mouse and rat orthologous introns. Although the numbers are too small to draw definitive conclusions, we observe more GT to GC than GC to GT substitutions (13 vs. 3). This is obviously mostly due to the overwhelmingly larger number of GT-AG than GC-AG introns, but indicates that switching from GT to GC in the donor site of U2 introns is not completely unfavorable. In this regard, it is interesting to note that GC-AG introns' exhibit a stronger and less variable do-

**Table 3. Observed cases of U2 subtype switching within mammals**

**(A) Orthologous pairs**

| | GT, GT | GC, GC | GC, GT | GT, GC |
|---|---|---|---|---|
| human/mouse | 38,922 | 190 | 100 | 99 |
| human/rat | 11,693 | 61 | 33 | 23 |
| mouse/rat | 8441 | 60 | 8 | 7 |

**(B) Orthologous triads**

| Human | Mouse | Rat | Occurrences |
|---|---|---|---|
| | "ancient" GT-AG | | |
| GT | GT | GT | 7784 |
| | "ancient" GC-AG | | |
| GC | GC | GC | 45 |
| | "moderate" GC-AG | | |
| GC | GT | GT | 23 |
| GT | GC | GC | 11 |
| | "recent" GC-AG | | |
| GT | GT | GC | 8 |
| GT | GC | GT | 5 |
| | "ancient" GC-AG, "recent" GC → GT | | |
| GC | GC | GT | 2 |
| GC | GT | GC | 1 |
| | | Total | 95 |

(A) Orthologous pairs: occurrence of donor site dinucleotide pairs at intron boundaries of orthologous intron pairs. For instance, we have found 65 instances in which the orthologous donor site is GC in human and GT in mouse.
(B) Orthologous triads: occurrence of donor site dinucleotides at intron boundaries in orthologous intron triads. For instance, we have found 23 cases in which the donor site is GC in human, but GT in both mouse and rat.

nor-site sequence than GT-AG introns (Fig. 1). Indeed, the information content of GC-AG donor sites is 12.4, while that of GT-AG donor sites is only 8.2. Probably, the substitution GT→GC, less favorable energetically, needs to be compensated by stronger complementarity in the rest of the site. Indeed, while GC-AG introns make up only 0.7% of all U2 introns (see Table 2), when considering only those U2 introns whose donor-site sequence is the perfect complement to the U1 snRNA 5′ end sequence ([AGC]AG/G[CT]AAGT), then, the percentage of GC-AG introns rises to 11.35% (317 of 2792).

### Comparison of splice site sequence patterns

We have investigated here whether the splice-site sequence patterns have changed appreciably since the mammalian and avian split. One way to investigate the variation is to visually compare pictograms or logos (Fig. 1) obtained from collections of sites from different species, derived from the Ensembl database. To facilitate this task, we have extended sequence pictograms into comparative pictograms. In these, the nucleotide distributions of the two species at each position are represented side by side, and the ratio of the nucleotide proportions indexes a range of colors from green to red, indicating nucleotide overrepresentation in one of the two species (see Methods and Supplemental material). Figure 2 shows the comparative pictograms for mouse and rat, human and mouse, and human and chicken. For reference, we have also computed them for human and zebrafish and human and fly. As it is possible to see, comparative pictograms suggest that splice sequence patterns are largely homogeneous within tetrapoda (the pictograms are mostly yellowish), but noticeably distinct from those of other vertebrate and invertebrate taxa. Statistical analysis in which we have explicitly computed the distances between splice-site sequence patterns, using a variety of methods, supports this interpretation (see Supplemental material).

### Sequence conservation of orthologous U2 splice sites

In this section, we investigate sequence conservation at orthologous splice sites. Here, we have used the HMRG set of curated mammalian–avian orthologous introns (Methods). In two ways, Figure 3 displays comparisons of orthologous splice sites, the percentage of sequence identity at each nucleotide position in the splice sites and at an intronic region 10 nucleotides long adjacent to the sites. Identity has been computed after aligning the orthologous splice-site sequences at the intron boundaries. Because these alignments are ungapped, the characteristic geometric decay of conservation within the intron observed for mouse–rat and for human–rodent comparisons is suggestive of significant sequence conservation between orthologous introns at this phylogenetic distance. In contrast, for mammalian and chicken comparisons, the ungapped alignment shows an almost abrupt decay right after the splice site—very similar to that observed when comparing unrelated sites.

To investigate what fraction of sequence conservation in splice sites is due to splicing function, we computed background sequence conservation between pairs of (randomly chosen) non-orthologous sites. As expected, background identity is ~25% outside of the splice signals. Within the splice signals, background conservation at each position roughly correlates with the information content at that position. Interestingly, at the acceptor site, it exhibits a bimodal shape—consistent with the polypyrimidine tract appearing at two different preferential locations. There is also a slow decay of background conservation upstream of the acceptor site—suggesting that the boundaries of this site are not precisely defined.

As shown in Figure 3, orthologous splice-site sequences are more conserved than expected solely from their role in splicing. Interestingly, this additional conservation is larger than that obtained at adjacent intronic sites for mammalian–chicken comparisons, but not for human–rodent and mouse–rat comparisons (Fig. 3, bottom). The abrupt decay of background conservation right after the donor site allows us to quantify this observation at these sites. This is less obvious in acceptor sites, because their boundaries are not as sharply defined. Indeed, we have computed the average sequence identity in the four rightmost intronic positions of the donor site (positions +3 to +6 in Fig. 1), and at four adjacent positions outside of the site (+7 to +10). The values of background conservation in these two regions are ~50% and 26%–27%, respectively, for all pairs of species. For mouse–rat orthologous comparisons, the values are 89% and 76%, respectively, for human–mouse, 78% and 53%, respectively, and for human–chicken, 62% and 31%, respectively. That is, conservation due to nonsaturation is smaller at the donor site than at adjacent positions ($89 - 50 = 39\%$ vs. $74 - 26 = 48\%$) for comparisons within rodents, similar for human–rodent comparisons (27% vs. 26%) and larger for human–chicken comparisons (12% vs. 4%). While it cannot be ruled out that this additional conservation reflects the existence of a small class of donor sites conserved beyond the generic consensus, a simpler explanation is that the reaching of saturation (understood here as the level of conservation at which orthologous sites are as conserved as unrelated sites, 27% identity at intronic sites, 50% at donor sites) is slower at sites under functional constraints. In the case of splicing, nucleotide substitutions at the splice sites may impair splice function. Thus, while the substitution process since the divergence of the mammalian and avian lineages has lead to almost complete saturation in proximal intronic sites (31% identity), donor sites (62% identity) are still far from saturation.

## Discussion

Thanks to the availability of genome sequences for a number of mammalian and one avian species, we have been able to inves

tigate the dynamics of the evolution of splice-site sequences in recent evolutionary times. Our results confirm that the splicing code is under evolution, albeit very slow. Indeed, while differences between overall splice-site sequence patterns correlate well with phylogenetic distance, they have remained largely homogeneous within tetrapoda, showing noticeable differences only at larger phylogenetic distances—such as those separating tetrapoda from fish.

Even though the splicing code appears to have remained quite constant within tetrapoda, our results also indicate that specific splice-site sequences may suffer significant changes during evolution and remain functional. Figure 3 displays the percentage of sequence identity at each nucleotide position across orthologous splice sites within rodents, between human and rodents, and within mammals and chicken. At all distances, orthologous splice-site sequences are more conserved than unrelated splice sites, but they have significantly diverged, showing an intermediate level of conservation between that of exon and intron sequences. The existence of additional sequences enhancing or repressing the recognition of the splice sites (for instance, see Caceres and Kornblihtt 2002; Cartegni et al. 2002; Black

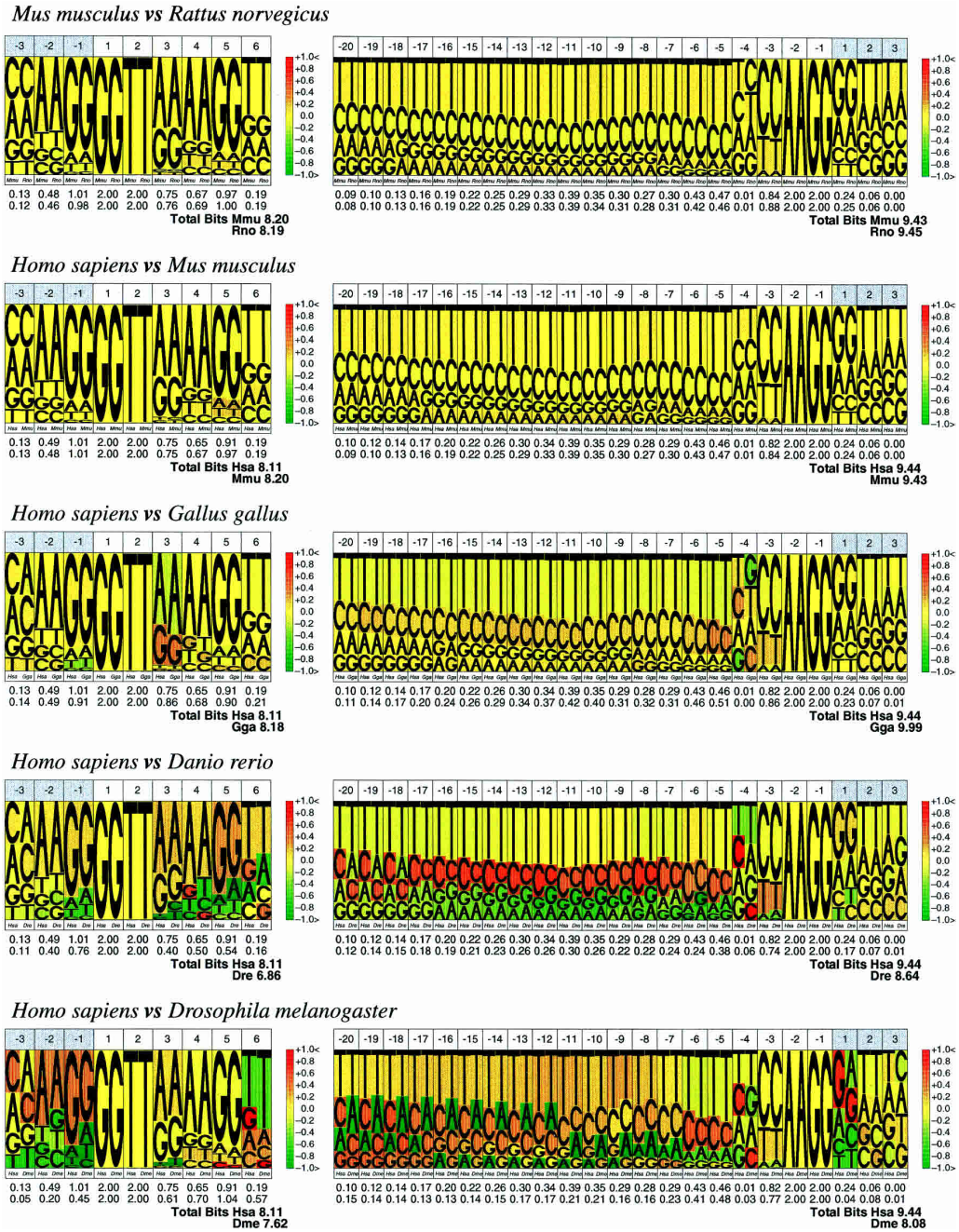


**Figure 2.** Comparative pictograms for donor and acceptor splice sites. Comparative pictograms of donor and acceptor sites for pairwise comparisons between species at different phylogenetic distances. At each position, the nucleotide distribution of the two species is displayed, the height of the letters corresponding to their relative frequency at the position. The color in the background of the letters indicates the underrepresentation (green) or overrepresentation (red) of a given nucleotide in the second species (*right*) with respect to the first (*left*).

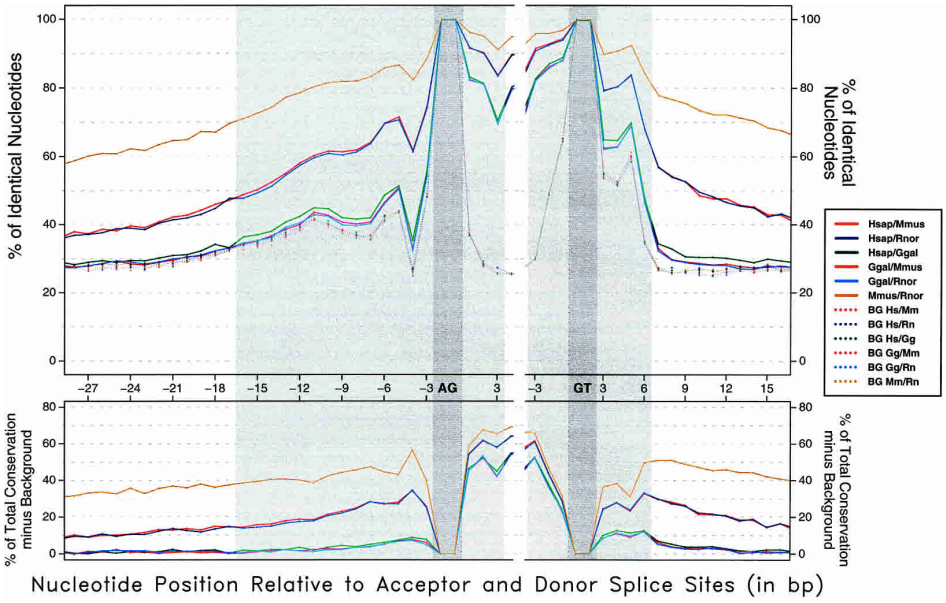


**Figure 3.** Sequence conservation level of orthologous GT-AG splice sites. Shaded gray areas correspond to the typical sequence span of splice-site signals. The average identity between the orthologous sequences is plotted across the splice signals (see Discussion). Background identity has been estimated from pairs of nonorthologous sites. (*Bottom*) The result of subtracting background conservation from total conservation.

2003) may partially explain the robustness of the exonic structure in front of changes in the splice-site sequences.

The greater conservation observed in mammalian chicken orthologous splice sites than in unrelated sites indicates that nucleotide substitution since the mammalian avian split has not yet reached saturation at these sites (estimated at ~50% identity at donor sites). At this phylogenetic distance, however, saturation has been reached at intronic sites, showing a level of conservation similar to that of unrelated sequences. This is the most likely explanation for the excess conservation over background observed in splice sites for comparisons between mammals and chicken, but absent in comparisons within mammals—where saturation has not been reached either at intronic sites.

In any case, the characteristic conservation of orthologous splice sites suggests that comparative prediction of splicing—through the modeling of the conservation in orthologous sites—could improve over methods based on the analysis of a single genome. Comparative prediction of splice sites could be particularly relevant to the prediction of alternative splicing—a problem still poorly solved—since it appears that a large fraction of alternative splicing events are conserved between related species, such as human and mouse (Thanaraj et al. 2003).

The availability of a large collection of orthologous intron sequences has also allowed us to investigate the evolutionary relationship between the minor U12 splicing class, and the major U2 class. Our results seem to indicate that U12 and U2 introns have evolved independently after the split of mammals and birds, since we have not been able to document a single convincing case of conversion between these two types of introns in our data sets. Certainly, because we have used a rather stringent criteria of U12 membership, it cannot be completely ruled out that such cases exist—maybe associated with dramatic changes in exonic structure, which our analysis cannot detect. On the other hand, although subtype switching between GT-AG and AT-AC U12 introns has been documented (Burge et al. 1998), we have not found any such case in our sets of U12 orthologous introns. In contrast, switching between the minor GC-AG and the major GT-AG subtypes within U2 introns is not unusual, and appears to be relatively well tolerated in introns with very strong donor sites. Comparison of orthologous introns has also allowed us to refine the sequences involved in the specification of the U12 introns (see Methods and Fig. 1). These sequences, while more conserved than signals involved in U2 intron specification, are more degenerate that previously thought.

Splicing remains an intriguing phenomenon. The results presented here, however, indicate that the increasing availability of sequences from genomes at different evolutionary distances will greatly contribute to the understanding of splicing, in particular, to understanding its history and its fundamental coding characteristics.

## Methods

All of the statistical analyses were performed with the R package (Ihaka and Gentleman 1996; http://www.r-project.org/) using ad hoc scripts for the preparation of exploratory data analysis plots.

### RefSeq genes and introns

Assembled chromosomal sequences and their associated annotations were downloaded from the UCSC Genome Browser (Kent et al. 2002; Karolchik et al. 2003; http://genome.cse.ucsc.edu/). The results described in this work were obtained on the assemblies listed in Table 1.

RefSeq genes interrupted with stop codons, or for which the amino acid sequence derived from the genomic coordinates had a difference of more than three amino acids in length or more than five gaps in the alignment when compared with the original amino acid sequence, were discarded. After this filtering step, 16,803 genes from the 21,744 annotated genes of the human HGv16 data set, 9734 genes from the 17,988 of the mouse MGSCv4, and 2783 genes from the 4877 of the rat RGSCv3.1 were retained.

### Orthologous mammalian RefSeq introns

#### *Gene sets*

The set of homologous gene pairs was downloaded from the NCBI's HomoloGene database (Zhang et al. 2000; http://www.ncbi.nlm.nih.gov/HomoloGene/). From 369,338 homolog pairs, there were 46,522 pairs corresponding to human–mouse, human–rat, or mouse–rat orthologous genes. Redundancy was removed in order to keep only unique putative ortholog pairs. Only those gene pairs in which the two members were in the final gene set resulting after the filtering process above were taken into account. Ternaries of human, mouse, and rat genes were built when possible. Otherwise, the gene pairs were considered.

This process yielded 1283 human–mouse–rat triads. In addition, 4267 human–mouse ortholog pairs, 454 human–rat pairs, and 133 mouse–rat pairs were obtained. These numbers correspond to 6043, 5680, and 1847 unique RefSeq genes for human, mouse, and rat, respectively. When performing pairwise comparisons, the corresponding genes in the triads were included in the set of pairs. Thus, the resulting extended pair-wise sets contained 5550 human–mouse, 1737 human–rat, and 1416 mouse–rat pairs. All data sets, as well as graphical displays of sequence comparisons of the orthologous sequences are available from http://genome.imim.es/datasets/hmrg2004/.

#### *Introns sets*

We devised a protocol to extract orthologous intron pairs and triads from the above set of orthologous genes. First, all of the pairs of consecutive exons for each gene were aligned with t_coffee (Notredame et al. 2000; http://igs-server.cnrs-mrs.fr/cnotred/Projectshomepage/tcoffeehomepage.html) using default parameters against all of the exonic pairs from the corresponding orthologous genes. This step ensured that we were working with the most accurate set of orthologous introns, despite changes in the exonic structure of orthologous genes (such as missing exons due to misannotations or gaps in the assemblies). Second, the exonic structure of the gene was projected onto the alignments. Third, from orthologous gene pairs or ternaries, only those exon pairs in which all intron positions occurred at conserved positions in the alignment and the intron phases were conserved and retained. Plots on which the exonic structures have been projected onto the alignments can be accessed at http://genome.imim.es/datasets/hmrg2004/.

### Orthologous HMRG introns

A set of human, mouse, rat, and chicken 1:1:1:1 confident orthologous introns was taken from International Chicken Genome Sequence Consortium (2004) (P. Bork and I. Letunic, pers. comm.). The set consisted of 1041 orthologous genes, totalizing 9110 orthologous introns. After mapping those genes into the annotations for the newer assemblies used in this analysis, 863 genes and 6524 introns remained in the four species orthologous set. The sequences 75 bp upstream and downstream of the signal core nucleotides (GT and AG for instance) were used in the orthologous splice-sites' sequence conservation analysis.

### Intron class

U12 introns were searched, relying on the conserved donor-site sequence and the acceptor-site branch point. Mammalian introns were initially considered to be U12 if (1) they matched the motif [AG]TATCCTT (where [AG] means A or G) from position +1 at the donor splice site; and (2) they matched the motif TCCT T[AG]A[CT] at the region from $-5$ to $-20$ upstream the acceptor splice site. When looking for the U12 branch point, up to two mismatches were allowed, and the hit was accepted if at least one adenine was found in position 6 or 7 of the motif—to avoid branch point hits without biological sense. Visual inspection of introns orthologous to U12 introns, but which initially failed to meet this criteria, suggested that this initial definition is too stringent. Therefore, we searched only for the presence of a strong branch point signal at the appropriate location in orthologous introns. After inspection of all of those cases in which the two orthologous introns contain such a signal, we found a few additional cases in which the donor-site sequences strongly resemble the characteristic U12 donor site sequence, but failed to match the consensus above. Indeed, we have found that only the nucleotides at positions +2 (T), +3 (A), +4 (T), and +5 (C) within the intron are absolutely conserved in U12 donor-site sequences (TATC). Position +6, thought to be an invariable C (Burge et al. 1999), may also be a T, and positions +7 and +8 can actually be occupied by any nucleotide. This more degenerate pattern was the one used to identify chicken U12 introns, where, at most, a gap (in addition to one mismatch) was also allowed to match the branch-point consensus. These results, which help to characterize the sequences that define U12 introns, illustrate the power of comparative genomics to refine our knowledge of the functional sequences encoded in eukaryotic genomes.

### Mapping of mammalian U12 introns into the chicken genome

DNA sequences of the exon-pairs delimiting each U12 intron were mapped into chicken genomic sequences using exonerate (http://www.ebi.ac.uk/guy/exonerate/). Only those alignments that preserved the mammalian splice site were taken into account. Introns obtained in that way were classified into U2/U12 classes following the same criteria as in the above section.

### Comparison of splice site sequence patterns

We have quantified the different use of nucleotides in splice sites by different species and represent it by comparative pictograms. A comparative pictogram is a graphical representation of the nucleotide proportions observed in two different sets of aligned sequences. In this article, these sets are splice sites of different species and the proportions are calculated for every position along the splice site. As in sequence pictograms, the sizes of nucleotides scale with their observed proportions, but here the nucleotides of the two sets are put side by side to ease their comparison. Moreover, the background occupied by each nucleotide is colored with the ratio of the proportions (the relative risk). Further details are given in the Supplemental material.

We have further analyzed the different nucleotide usage in splice sites of different species by two kinds of comparisons as follows: (1) by building confidence intervals for the relative risks and counting how many of them include a ratio value of 1 (i.e., no difference of nucleotide usage), and (2) by assessing the site species dependence, that is, the extent to what the occurrences of the observed splice sites depend, statistically speaking, on the

species to which they belong to. Further details are given in the Supplemental material also.

## Acknowledgments

We thank the International Chicken Genome Sequencing Consortium for providing the genomic sequences, as well as the Rat and Mouse Consortia from past collaborations. We are particularly grateful to Ivica Letunic and Peer Bork for providing the set of HMRG orthologous introns with which some of the analyses were performed. Juan Valcárcel, Genís Parra, Eduardo Eyras, Webb Miller, David Haussler, Robert Baertsch, Chris Ponting, Alberto Roverato, Kim Worley, and two anonymous referees are gratefully acknowledged for advice and helpful comments. We also thank Òscar González for keeping the database mirrors up to date. Special thanks to Jan-Jaap Wesselink and Charles Chapple for their suggestions when proofreading this document. J.F.A. is supported by a predoctoral fellowship from the "Fundació IMIM" (Spain). This research is supported by grant BIO2000-1358-C02-02 from "Plan Nacional de I+D" (Spain), and grant ASD from the European Commission.

## References

Birney, E., Andrews, T.D., Bevan, P., Caccamo, M., Chen, Y., Clarke, L., Coates, G., Cuff, J., Curwen, V., Cutts, T., et al. 2004. An overview of Ensembl. *Genome Res.* **14:** 925–928.

Black, D.L. 2003. Mechanisms of alternative pre-messenger RNA splicing. *Annu. Rev. Biochem.* **72:** 291–336.

Burge, C.B. and Karlin, S. 1998. Finding the genes in genomic DNA. *Curr. Opin. Struct. Biol.* **8:** 346–354.

Burge, C.B., Padgett, R.A., and Sharp, P.A. 1998. Evolutionary fates and origins of U12-type introns. *Mol. Cell* **2:** 773–785.

Burge, C.B., Tuschl, T., and Sharp, P.S. 1999. Splicing precursors to mRNAs by the spliceosomes. In *The RNA world* (eds. R.F. Gesteland et al.), pp. 525–560. Cold Spring Harbor Laboratory Press, Cold Spring Harbor, New York.

Burset, M., Seledtsov, I., and Solovyev, V. 2001. SpliceDB: Database of canonical and noncanonical mammalian splice sites. *Nucleic Acids Res.* **29:** 255–259.

Caceres, J.F. and Kornblihtt, A.R. 2002. Alternative splicing: Multiple control mechanisms and involvement in human disease. *Trends Genet.* **18:** 186–193.

Cartegni, L., Chew, S.L., and Krainer, A.R. 2002. Listening to silence and understanding nonsense: Exonic mutations that affect splicing. *Nat. Rev. Genet.* **3:** 285–298.

de Souza, S.J. 2003. The emergence of a synthetic theory of intron evolution. *Genetica* **118:** 117–121.

Dermitzakis, E.T., Reymond, A., Lyle, R., Scamuffa, N., Ucla, C., Deutsch, S., Stevenson, B.J., Flegel, V., Bucher, P., Jongeneel, C.V., et al. 2002. Numerous potentially functional but non-genic conserved sequences on human chromosome 21. *Nature* **420:** 578–582.

Dietrich, R.C., Incorvaia, R., and Padgett, R.A. 1997. Terminal intron dinucleotide sequences do not distinguish between U2- and U12-dependent introns. *Mol. Cell* **1:** 151–160.

Dietrich, R.C., Peris, M.J., Seyboldt, A.S., and Padgett, R.A. 2001. Role of the 3′ splice site in U12-dependent intron splicing. *Mol. Cell. Biol.* **21:** 1942–1952.

Fedorova, L. and Fedorov, A. 2003. Introns in gene evolution. *Genetica* **118:** 123–131.

Hall, S.L. and Padgett, R.A. 1994. Conserved sequences in a class of rare eukaryotic nuclear introns with non-consensus splice sites. *J. Mol. Biol.* **239:** 357–365.

Hare, M.P. and Palumbi, S.R. 2003. High intron sequence conservation across three mammalian orders suggests functional constraints. *Mol. Biol. Evol.* **20:** 969–978.

Helfman, D.M. and Ricci, W.M. 1989. Branch point selection in alternative splicing of tropomyosin pre-mRNAs. *Nucleic Acids Res.* **17:** 5633–5650.

Ihaka, R. and Gentleman, R. 1996. R: A language for data analysis and graphics. *J. Computat. Graph. Stat.* **5:** 299–314.

International Chicken Genome Sequencing Consortium. 2004. Sequence and comparative analysis of the chicken genome provide unique perspectives on vertebrate evolution. *Nature* (in press).

Jackson, I.J. 1991. A reappraisal of non-consensus mRNA splice sites. *Nucleic Acids Res.* **19:** 3795–3798.

Karolchik, D., Baertsch, R., Diekhans, M., Furey, T.S., Hinrichs, A., Lu, Y.T., Roskin, K.M., Schwartz, M., Sugnet, C.W., Thomas, D.J., et al. 2003. The UCSC genome browser database. *Nucleic Acids Res.* **31:** 51–54.

Kent, W.J., Sugnet, C.W., Furey, T.S., Roskin, K.M., Pringle, T.H., Zahler, A.M., and Haussler, D. 2002. The human genome browser at UCSC. *Genome Res.* **12:** 996–1006.

Kryukov, G., Castellano, S., Novoselov, S., Lobanov, A., Zehtab, O., Guigó;, R., and Gladyshev, V. 2003. Characterization of mammalian selenoproteomes. *Science* **300:** 1439–1443.

Lander, E.S., Linton, L.M., Birren, B., Nusbaum, C., Zody, M.C., Baldwin, J., Devon, K., Dewar, K., Doyle, M., FitzHugh, W., et al. 2001. Initial sequencing and analysis of the human genome. *Nature* **409:** 860–921.

Levine, A. and Durbin, R. 2001. A computational scan for U12-dependent introns in the human genome sequence. *Nucleic Acids Res.* **29:** 4006–4013.

Mattick, J.S. 2001. Non-coding RNAs: The architects of eukaryotic complexity. *EMBO Rep.* **2:** 986–991.

Notredame, C., Higgins, D.G., and Heringa, J. 2000. T-Coffee: A novel method for fast and accurate multiple sequence alignment. *J. Mol. Biol.* **302:** 205–217.

Pruitt, K.D., Tatusova, T., and Maglott, D.R. 2003. NCBI reference sequence project: Update and current status. *Nucleic Acids Res.* **31:** 34–37.

Rat Genome Sequencing Project Consortium. 2004. Genome sequence of the brown Norway rat yields insights into mammalian evolution. *Nature* **428:** 493–521.

Roy, S.W., Fedorov, A., and Gilbert, W. 2003. Large-scale comparison of intron positions in mammalian genes shows intron loss but no gain. *Proc. Natl. Acad. Sci.* **100:** 7158–7162.

Schneider, T. and Stephens, R. 1990. Sequence logos: A new way to display consensus sequences. *Nucleic Acids Res.* **18:** 6097–6100.

Sharp, P. and Burge, C. 1997. Classification of introns: U2-Type and U12-Type. *Cell* **91:** 875–879.

Smith, C.W. and Nadal-Ginard, B. 1989. Mutually exclusive splicing of α-tropomyosin exons enforced by an unusual lariat branch point location: Implications for constitutive splicing. *Cell* **56:** 749–758.

Thanaraj, T., Clark, F., and Muilu, J. 2003. Conservation of human alternative splice events in mouse. *Nucleic Acids Res.* **31:** 2544–2552.

Waterston, R.H., Lindblad-Toh, K., Birney, E., Rogers, J., Abril, J.F., Agarwal, P., Agarwala, R., Ainscough, R., Alexandersson, M., An, P., et al. 2002. Initial sequencing and comparative analysis of the mouse genome. *Nature* **420:** 520–562.

Xu, Q., Modrek, B., and Lee, C. 2002. Genome-wide detection of tissue-specific alternative splicing in the human transcriptome. *Nucleic Acids Res.* **30:** 3754–3766.

Yeo, G., Holste, D., Kreiman, G., and Burge, C. 2004. Variation in alternative splicing across human tissues. *Genome Biol.* **5:** R74.

Zhang, Z., Schwartz, S., Wagner, L., and Miller, W. 2000. A greedy algorithm for aligning DNA sequences. *J. Comput. Biol.* **7:** 203–214.

Zhu, W. and Brendel, V. 2003. Identification, characterization and molecular phylogeny of U12-dependent introns in the *Arabidopsis thaliana* genome. *Nucleic Acids Res.* **31:** 4561–4572.

## Web site references

http://genome.imim.es/datasets/hmrg2004/; further supplemental materials for this study.

http://genome.cse.ucsc.edu/; UCSC Genome Browser, from which the human, mouse, rat and chicken feature annotations and genome assemblies used in this study were downloaded.

http://www.ensembl.org/; Ensembl Genome Browser, from which a larger set of human, mouse, rat and chicken gene annotation sets were retrieved.

http://www.ncbi.nlm.nih.gov/HomoloGene/; NCBI's HomoloGene database, from where initial RefSeq orthologous pairs were obtained.

http://igs-server.cnrs-mrs.fr/cnotred/Projectshomepage/tcoffeehomepage.html; a multiple sequence alignment package.

http://www.ebi.ac.uk/guy/exonerate/; a generic tool for sequence comparison.

http://www.r-project.org/; the R project for statistical computing.

*Received August 4, 2004; accepted in revised form November 11, 2004.*

### 4.3.3 ICGSC, *Nature*, 432(7018):695–716, 2004

**PubMed Accession:**

http://www.ncbi.nlm.nih.gov/entrez/query.fcgi?cmd=Retrieve&db=PubMed&list_uids=15592404&dopt=Abstract

**Journal Abstract:**

http://www.nature.com/cgi-taf/DynaPage.taf?file=/nature/journal/v432/n7018/abs/nature03154_fs.html

**Supplementary Materials:**

See Section 4.3.2 and the following URL:
http://www.nature.com/nature/journal/v432/n7018/suppinfo/nature03154.html

articles

# Sequence and comparative analysis of the chicken genome provide unique perspectives on vertebrate evolution

**International Chicken Genome Sequencing Consortium***

**Lists of participants and affiliations appear at the end of the paper*

**We present here a draft genome sequence of the red jungle fowl, *Gallus gallus*. Because the chicken is a modern descendant of the dinosaurs and the first non-mammalian amniote to have its genome sequenced, the draft sequence of its genome—composed of approximately one billion base pairs of sequence and an estimated 20,000–23,000 genes—provides a new perspective on vertebrate genome evolution, while also improving the annotation of mammalian genomes. For example, the evolutionary distance between chicken and human provides high specificity in detecting functional elements, both non-coding and coding. Notably, many conserved non-coding sequences are far from genes and cannot be assigned to defined functional classes. In coding regions the evolutionary dynamics of protein domains and orthologous groups illustrate processes that distinguish the lineages leading to birds and mammals. The distinctive properties of avian microchromosomes, together with the inferred patterns of conserved synteny, provide additional insights into vertebrate chromosome architecture.**

Genome sequence comparison is a modern extension of the long-standing use of other species as models to illuminate aspects of human biology and medicine. Large-scale genome analyses also highlight the evolutionary dynamics of selective and mutational processes at different chronological scales[1–4]. We present here results obtained from an extensive analysis of a draft sequence of the chicken genome, which has evolved separately from mammalian genomes for ~310 million years (Myr)[4,5] (Fig. 1). This genome is the first to be sequenced at this particular evolutionary distance from humans, and, as shown previously[6–8], it provides an excellent signal-to-noise ratio for the detection of functional elements. Our analysis of the 6.6 × coverage draft sequence of the chicken genome resulted in the following main observations.

- The nearly threefold difference in size between the chicken and mammalian genomes reflects a substantial reduction in interspersed repeat content, pseudogenes and segmental duplications within the chicken genome.
- Chicken–human aligned segments tend to occur in long blocks of conserved synteny. We find a relatively low rate of chromosome translocations in both lineages from the last common ancestor, whereas intrachromosomal rearrangements (for example, inversions) are more common.
- Syntenic relationships for certain classes of non-coding RNA (ncRNA) genes differ from those of protein-coding genes. This observation implies a novel mode of evolution for some ncRNA genes.
- Expansion and contraction of multigene families seem to have been major factors in the independent evolution of mammals and birds.
- The sizes of chicken chromosomes, which span a range of nearly two orders of magnitude, correlate negatively with recombination rate, G+C and CpG content, and gene density but positively with repeat density.
- Synonymous substitution rates are elevated for genes in both chicken microchromosomes and in subtelomeric regions of macrochromosomes.
- There is a paucity of retroposed pseudogenes in the chicken genome, in contrast to mammalian genomes, greatly simplifying the classification of chicken gene content. This is explained by the

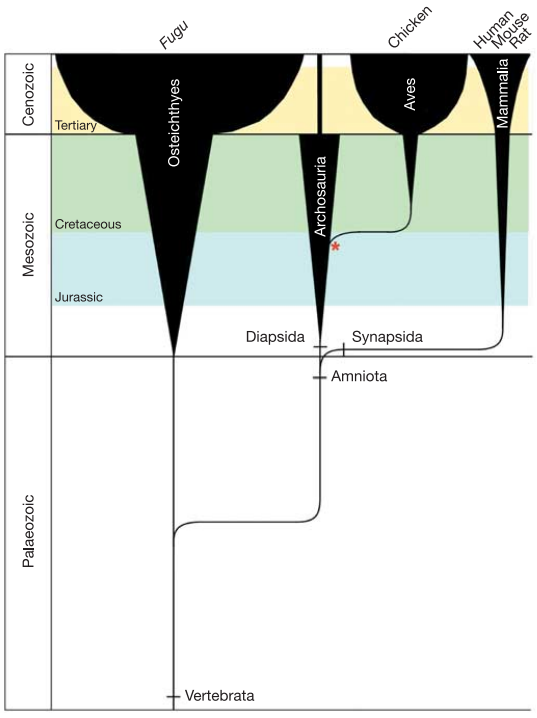


**Figure 1** Basal vertebrate evolution showing extant species whose genomes have been sequenced. The horizontal axis represents estimated relative species diversity. The Archosauria include the Aves, their Mesozoic dinosaur predecessors, and Crocodilia; the Lepidosauria (lizards, snakes and tuataras) are not indicated. Archaeopteryx (indicated by an asterisk) is considered to be the first known bird and lived approximately 150 Myr ago. See also ref. 159.

high specificity of the reverse transcriptase from the predominant interspersed repeat element in the chicken genome: the CR1 long interspersed nucleotide element (LINE).

- Unlike all other vertebrate genomes studied so far, no short interspersed nucleotide elements (SINEs) have been active in the chicken genome for the last ~50 Myr.
- Alignment of the chicken and human genomes identifies at least 70 megabases (Mb) of sequence that is highly likely to be functional in both species.
- Many of the chicken–human aligned, non-coding sequences occur far from genes, frequently in clusters that seem to be under selection for functions that are not yet understood.

## Perspectives on the domestic chicken

The chicken (*Gallus gallus*) is an important model organism that bridges the evolutionary gap between mammals and other vertebrates and serves as the main laboratory model for the ~9,600 extant avian species. The chicken also represents the first agricultural animal to have its genome sequenced. Modern birds (Ornithurae) evolved from therapod dinosaurs[9,10] in the middle of the Mesozoic era (Fig. 1). Chickens were domesticated in Asia at least by 5400 BC, perhaps as early as 8000 BC[11–13]. Darwin[14] suggested that the red jungle fowl was the nearest ancestor to the domestic chicken, a view later confirmed by mitochondrial DNA analysis[15].

Genetic analysis of the chicken dates back to the start of the twentieth century[16,17], and hundreds of well-characterized mutant stocks and inbred lines have been developed[18]. The chicken embryo has been an especially useful vertebrate system for developmental biologists[19] owing to experimental advantages of *in ovo* embryogenesis. Furthermore, the chicken has been used in seminal studies in virology, oncogenesis and immunology[20–22]. The chicken genetic linkage map, initiated early in the last century[23], now includes 2,172 genetic loci with a total length near 4,000 cM[24,25]. Most avian karyotypes contain chromosomes of markedly different lengths, termed the macro- and microchromosomes, and thus bird karyotypes are quite distinctive as compared with those of mammals[26]. The chicken karyotype ($2n = 78$) is made up of 38 autosomes and one pair of sex chromosomes, with the female as the heterogametic sex (ZW female, ZZ male).

## Sequencing and assembly

All sequencing libraries were prepared from DNA of a single female of the inbred line of red jungle fowl (UCD 001) to minimize heterozygosity and provide sequence for both the Z and W sex chromosomes, albeit at 50% of the autosomal coverage. The assembly was generated from ~6.6 × coverage in whole-genome shotgun reads, a combination of plasmid, fosmid and bacterial artificial chromosome (BAC)-end read pairs (Supplementary Table S1). The assembly (Table 1) was generated using PCAP[27], a parallel algorithm that exploits both read-pairing constraint information and base quality values (see Supplementary Information for a description of the methods).

A BAC-based physical map for the chicken was developed in parallel with the sequence assembly[28]. Along with the genetic map[25,29–31], this provides the main scaffolding for the assembly into larger ordered and oriented groupings ('ultracontigs') as well as the mechanism for chromosomal assignment (see Methods). After integrating data from the physical map with the assembly, several additional steps were taken to improve the initial assembly of chicken chromosome sequences. This included using expressed sequence tag (EST) and messenger RNA data to aid the ordering and orientation of sequence, and using map and sequence data to aid in localization of centromeres and telomeres (see Methods). The resulting assembly consists of 574 segments made up of 84 ultracontigs (ordered and oriented by their relationship to the physical map) and 490 'supercontigs' (ordered and oriented by read-pairing data, but not linked to the physical map) anchored to chicken chromosomes. Of the 1.05 gigabases (Gb) of assembled sequence, 933 Mb were localized to specific chromosomes, 907 Mb of which were ordered and oriented along those chromosomes.

Table 1 **Whole-genome assembly statistics**

| Genome feature | >1 kb number | N50 length (kb) | N50 number | Largest (kb) |
|---|---|---|---|---|
| Contigs | 98,612 | 36 | 7,486 | 442 |
| Supercontigs | 32,767 | 7,067 | 37 | 33,505 |

Statistics presented are for the whole-genome assembly before integration of physical mapping data. Contigs are contiguous sequences not interrupted by gaps, and supercontigs are ordered and oriented contigs including estimated gap sizes. The N50 statistic is defined as the largest length $L$ such that 50% of all nucleotides are contained in contigs of size at least $L$. A total of 10,743,700 reads were included in the final assembly. Only 4.39% of the total sequencing reads presented to the assembler were not used in the final assembly.

### Assessment of the coverage and quality of the genome assembly

We estimated the coverage of the assembly using both finished BACs and available mRNA sequences (Methods). In a set of 38 finished autosomal BAC sequences from the same red jungle fowl female (covering 6 Mb of sequence), 98% of finished bases could be aligned with the draft whole-genome shotgun assembly, with an overall substitution rate of 0.02% and no deletions or insertions. Similarly, of a set of 23,212 chicken mRNAs and 485,000 ESTs[32], 97% and 96% respectively are at least partially found in the assembly. Of these, 10% are only partially found or are fragmentary. This lack of contiguity contributes in part to the 5–10% of genes estimated to be absent from the Ensembl chicken gene set (see below). Representation of the (G+C)-rich extremes of the genome may be less complete. In one small region of incompletely sequenced BACs (3.6 Mb) orthologous to human chromosome 19 (HSA19) (I. Ovcharenko *et al.*, unpublished data), where the average G+C content was 52% (with some regions exceeding 60%), coverage fell to 82%. Furthermore, we examined a set of 400 genes that were represented in chicken mRNA or ESTs and had single orthologues in five diverse species (human, mouse, rat, *Takifugu rubripes* (*Fugu*) and *Drosophila*) but were predicted to be absent from, or at least partially truncated in, the chicken Ensembl gene set (see below). Over 70% were in fact partially found in the assembly. Of the 400, the largest fraction missing (21%) were HSA19 orthologues from a region known to be unusually rare in chicken clone libraries (L. Gordon *et al.*, unpublished data). The missing genes have a higher G+C content than average and many, including some HSA19 orthologues, are associated with intronic simple sequence repeats (see Methods).

Comparisons to 6 Mb of finished red jungle fowl BAC clone sequence revealed alignment with 311 chicken contigs from 62 supercontigs, which were used to assess possible ordering errors (see Methods). No orientation problems were detected, and only two order discordances (misordered sequence contigs within a supercontig) were discovered. This would extrapolate to a total of ~400 kilobases (kb) of misordered contigs in the current assembly. In addition, eight cases were found in which a contig was incorrectly inserted into a supercontig, equivalent to ~1 Mb of incorrect insertions in the full genome.

Recent duplications are especially difficult to place within whole genome assemblies. Relaxed assembly may collapse duplicated segments into one, and stringent assembly may break sequences into duplicates because of sequencing errors. In the chicken, 'all-versus-all' comparison shows that 11% (~123 Mb) of the genome sequence is in pairwise alignments larger than 1 kb with more than 90% sequence identity. The bulk (91% of the 11%), however, are highly similar (>98%) and might represent false duplication. In a direct test (see Methods), only 22% of duplications with near-perfect sequence identity (>98%) and 26% (32.3 out of 122.7 Mb) of the full set were confirmed.

Because the assembly process incorporated genetic markers (Supplementary Table S2), the genetic map does not provide

independent assessment. However, recent placement of 142 additional genetic markers, mapped after the assembly, suggests that less than 0.75% (~6 Mb) of the sequence has been assigned to a wrong chromosome. Thus, the assembly correctly places the vast majority of the chicken genome in long contiguous stretches. It is well ordered and oriented and faithfully represents older segmental duplications (at the cost of a modest false increase in the most recent duplications). The draft provides an excellent substrate for initial global analysis, recognizing that the elucidation of the full sequence will be critical to allow final, definitive conclusions.

## Gene content of the chicken genome

The genome sequence of an organism encodes both ncRNAs and proteins. Extensive analysis of the genome sequences of human[1], mouse[2] and rat[3] has provided our current best assessment of mammalian gene content and has illuminated much about the evolution of genes. The chicken genome provides new perspectives on both the structure and content of mammalian genes, as well as yielding insight into avian gene content and evolution of ncRNA genes.

### Non-coding RNA genes

A total of 571 ncRNA genes, from over 20 distinct gene families, were identified within the chicken genome assembly (Table 2) using bioinformatic approaches[33,34] (see Methods). Predicted ncRNA pseudogenes are greatly reduced in number relative to their human ncRNA counterparts. The chicken ncRNA predictions therefore represent a set that is mainly functional. If ncRNA genes maintain their placement with respect to neighbouring genes, chicken ncRNA gene locations could be used to identify which mammalian copies are likely to be functional and which are probable pseudogenes. However, few chicken and human ncRNA genes are paired in regions of conserved synteny (Table 2), relative to the high level of shared gene order observed for protein-coding genes (see below). Those classes of ncRNAs that are most often syntenic are microRNAs (miRNAs) and small nucleolar RNAs (snoRNAs), which are often found in the introns of protein-coding genes (or, rarely, of specialized 'host' genes[35]). Most ncRNA genes thus seem to have been translocated to distant genomic sites during vertebrate evolution, without accumulating large numbers of pseudogenes, as would be expected were this process to occur via retrotransposition. This is also in contrast to duplication of genes via unequal crossing over, which results in tandem copies. These insights will require considerably more analysis for a definitive resolution, but it seems that these ncRNAs may not use the same duplication and/or translocation mechanisms as protein-coding genes.

### Development of a protein-coding gene set

An evidence-based system (Ensembl[36]) and two comparative gene prediction methods (Twinscan[37] and SGP-2 (ref. 38)) together predicted a common set of 106,749 protein-coding exons, with 85,929 additional exons predicted by one or two methods (Supplementary Table S3). Particular attention was paid to the identification of selenoproteins, which are usually mispredicted in annotated genomes because of their usage of the TGA codon, usually a stop codon, to code for the amino acid selenocysteine (see Methods). Of the human genes predicted using chicken as the "informant", only 311 genes predicted by SGP-2 are absent from previously identified sets (namely, Vega[40], Ensembl[41], RefSeq[42], MGC[43] and H-Invitational[44]) and have homologous chicken predictions that possess orthologous intron positions. These data, and those of another study (E. Eyras *et al.*, unpublished data), suggest that most of the protein-coding genes conserved among vertebrates are represented in existing complementary DNA sets.

We tested the sensitivity and specificity of the chicken gene predictions. Sensitivity was assessed by comparing predicted exons to those of chicken cDNAs[32] representing long open reading frame (ORF)-containing protein-coding genes (Table 3). All three methods correctly predicted about 80% of cDNA-based exons with >80% coverage. An independent SAGE-based analysis (ref. 166, and M. B. Wahl *et al.*, unpublished data) provided a similar, although marginally lower, estimate. Specificity was assessed by testing random exon pairs from the prediction sets using polymerase chain reaction with reverse transcription (RT–PCR) (E. Eyras *et al.*, unpublished data, and ref. 44). Briefly, Ensembl predictions

Table 2 **Families of ncRNA genes in the chicken genome**

| RNA type | Number in chicken | Number in human | Chicken in synteny* | Conserved synteny† | Function |
|---|---|---|---|---|---|
| tRNA | 280 | 496‡ | 158 | 52 (33%) | Protein synthesis |
| 5S rRNA | 12 | 301 | 4 | 0 (0%) | Protein synthesis |
| 5.8S rRNA | 3 | 9 | 1 | 0 (0%) | Protein synthesis |
| 18S rRNA | 0 | 0‡ | – | – | Protein synthesis |
| 28S rRNA | 0 | 0‡ | – | – | Protein synthesis |
| U1 | 18 | 146 | | | Spliceosome |
| U2 | 6 | 88 | | | Spliceosome |
| U4 | 4 | 119 | | | Spliceosome |
| U5 | 9 | 36 | | | Spliceosome |
| U6 | 15 | 821 | 45 | 9 (20%) | Spliceosome |
| U4atac | 1§ | 1‡ | | | Minor spliceosome |
| U6atac | 4§ | 5‡ | | | Minor spliceosome |
| U11 | 1§ | 1‡ | | | Minor spliceosome |
| U12 | 1 | 2 | | | Minor spliceosome |
| miRNA | 121 | 191 | 87 | 77 (89%) | Translation repression |
| snoRNA | 83§ | 245‡ | 63 | 50 (79%) | rRNA/snRNA processing |
| RNase P | 1 | 1 | | | tRNA 5′-end processing |
| U7 | 1 | 184 | | | Histone mRNA 3′-end processing |
| SRP | 3 | 12 | | | Protein secretion |
| 7SK | 4 | 166 | 12 | 7 (58%) | Translational regulation (?) |
| Y | 2 | 739 | | | Ro RNP component |
| Telomerase RNA | 1 | 1 | | | Telomerase |
| BIC | 1 | 1 | – | – | Unknown |

ncRNA genes were predicted as described in the Methods, except where indicated. Some human gene counts include significant numbers of pseudogenes.
*The number of chicken predictions located in conserved blocks that have defined syntenic regions in human (grouped into classes).
†The proportion of chicken predictions that have a syntenic human prediction.
‡Human genome ncRNA predictions from T. Jones and S. R. Eddy (ftp://ftp.genetics.wustl.edu/pub/eddy/annotation/human-hg16/). This human set contains 7,196 ncRNAs, 6,124 of which are putative pseudogenes.
§Chicken ncRNA genes identified by homology.

Table 3 **Sensitivity of gene prediction**

| Feature | Ensembl | Twinscan | SGP-2 |
|---|---|---|---|
| Exact exon (%) | 61 | 53 | 60 |
| 80% coverage exon (%) | 85 | 77 | 85 |
| Total exons | 179,084 | 195,665 | 203,834 |

Sensitivity of gene predictions as measured by comparison to ORF-containing cDNAs. Numbers are the percentage of coding exons from the cDNA-based models found by the three prediction systems. The sensitivity numbers are quoted at two levels: exact exon prediction and >80% coverage of the cDNA exon.

have a false positive rate of ~4%. When an exon pair is predicted by any two of the three methods (predominantly joint Twinscan plus SGP-2 exons) ~50% are confirmed, suggesting that some genes are missing from the Ensembl set, but we cannot reliably distinguish these from a similarly large number of Twinscan plus SGP-2 false positives. Using our estimates of specificity and sensitivity, we predict a total of between 20,000 and 23,000 protein-coding genes in chicken, with 80–90% of these found in the present Ensembl set (see Methods). This estimate overlaps the lower bounds in the corresponding ranges for mammalian genomes determined by similar calculations (for example, see refs 2, 3, 45).

### Evolutionary conservation of gene components

Alignments of chicken and human orthologous protein-coding genes demonstrate the expected pattern of sequence conservation, with highest identity in protein-coding exons and minimal identity in introns (Fig. 2). These alignments allowed us to examine sequence conservation at different sites within genes.

Alignments of coding regions often did not extend to the previously annotated human protein start codons. Rather, we observed a fourfold increase in the frequency of methionine at the first position of the alignment (Fig. 3), suggesting that these internal ATG codons could be the true start sites for at least some of ~2,000 human genes. For these proteins, the overall distribution of amino acids upstream of the end of the alignment in human was markedly different from that downstream and was more consistent with a codon distribution derived from non-coding nucleotide sequence. Using this comparative signal and other features, such as the Kozak sequence[46], we can potentially improve the annotation of mammalian protein-coding start sites.

Sequence conservation around mammalian splice sites can be predicted by divergence at unselected (non-consensus) base pairs at the neutral rate, coupled with purifying selection on sites matching the splice site consensus[47]. Given the high level of neutral site divergence that has occurred between mammalian and chicken orthologous sequences (see neutral evolutionary rate, below), one would expect that orthologous mammalian–chicken splice sites should show a level of conservation no different from that of any unrelated pair of splice sites. However, in contrast to analogous comparisons within the mammalian lineage, there is a detectable signal in orthologous splice site comparisons beyond the consensus derived from comparing non-orthologous splice sites (Supplementary Fig. S1). This suggests that either some subtle classes of splice site sequences are conserved beyond the generic consensus that can only be observed at the bird–mammal evolutionary distance, or that there is a significant but weak conservation in mammalian introns that is not detectable in mammalian–bird alignments[48].

To explore the role of conserved non-coding sequence segments that are probably regulators of protein-coding genes, we examined the frequency of non-coding alignments of at least 100 base pairs (bp) in, respectively, the 5′ flanking region, 5′ untranslated region (UTR), at least one intron, 3′ UTR, or 3′ flanking region (see Methods) within human–chicken orthologue pairs in relation to gene function (as determined by gene ontology (GO) category, Table 4). Some GO categories (for example, development and transcriptional regulation) showed enrichment for conservation in all five regions, suggesting that conserved regulatory signals exist within all of these locations. However, other categories showed more specific patterns. As one example, introns of ion channel genes are particularly enriched for conserved sequences, in agreement with reports that such introns contain RNA-editing targets[49,50].

### Pseudogenes and retroposed copies in the chicken genome

Only 51 duplicates of protein-coding genes probably formed by retroposition (that is, exhibiting loss of introns)[51] were identified in the chicken genome, in contrast to the more than 15,000 cases observed in mammalian genomes[3,52]. In mammals, the ancient LINE1 (L1) transposable element is responsible for the origin of most if not all retroposed (pseudo) genes[53]. Although birds host their own LINE-like elements (chicken repeat 1 (CR1); see below)[54], the reverse transcriptase encoded by these elements is unlikely to copy polyadenylated mRNAs[55], probably explaining the paucity of processed pseudogenes in chicken. Within the set of 51 (Supplementary Table S4), 36 clearly represent pseudogenes, because their former coding regions are disabled by alterations (including frameshifts and premature stop codons) that preclude protein function. Among the remaining 15 elements, eight show strong evidence for selective constraint (Supplementary Table S4) and therefore may represent functional retroposed genes. We found no

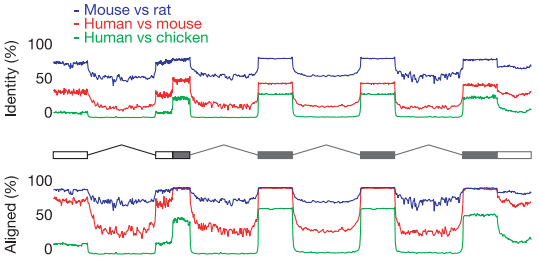


**Figure 2** An idealized protein-coding gene structure showing average percentage alignment and average percentage identity (including gaps and unaligned regions) over 10,000 orthologous gene structures in either human–chicken, human–mouse or mouse–rat alignments (as aligned by BLASTZ[156]). The reference structure was taken from human or mouse, and only those with cDNA-based definitions of the structure were used. The central figure shows an idealized gene structure, with the grey exons representing coding sequence and white boxes representing 3′ and 5′ untranslated regions.

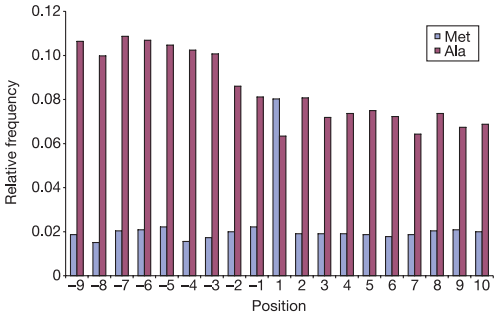


**Figure 3** Histogram of amino acid distributions centred on the start of human–chicken alignments where the alignment is >30 amino acids from the putative translation start in human and less than 100 amino acids in length, using the human protein sequence. Alanine is shown as an example of non-methionine amino acids: many amino acids show significant changes before compared with after the alignment.

Non-coding conservation is not uniformly distributed across the human genome. Fifty-seven segments of high non-coding conservation (average length 1.176 Mb and average CNF 13.1%, compared with a genome average of 1.7%; see Methods and Supplementary Table S7) were found to be gene poor (they cover 2.3% of the human genome but contain only 0.3% of the exons in RefSeq genes). They were also G+C poor (38.8% overall) and depleted for all classes of interspersed repeats, as are their chicken orthologues. They contain none of the 731 break points identified through an analysis of regions of conserved gene order between human and chicken with length exceeding 200 kb, and—from human–mouse neutral substitution rates estimated using interspersed repeats[126]—do not seem to have experienced particularly low mutation rates. The genes within or overlapping these 57 high-CNF segments, however, are significantly enriched for the GO categories associated with gene regulation (Fig. 17). Thus, the degree of non-coding sequence conservation is related to the biological function of the genes in the general genome neighbourhood. This enrichment is not merely a by-product of the gene-poor nature of these segments, because human gene-poor regions with low CNF are not enriched for the same GO categories[149].

The 57 high-CNF segments were found to contain 60.7% of 417 human–chicken ultraconserved elements (UCEs): sequences defined as being 200 bp or longer in orthologous chromosomal locations and 100% identical between the two species. Only 27.3% of these human–chicken UCEs overlap the 481 previously studied human–rodent UCEs[150], although all of them are found in the draft genomes of either mouse or rat, at 87–100% identity in the more conserved rodent. Human–chicken UCEs differ from human–rodent UCEs in containing far fewer exon-intersecting elements (7.9% versus 23%) and in showing only weak enrichment for proximity to genes whose products have a GO and InterPro classification associated with RNA splicing. The two UCE sets share a strong bias against harbouring human-verified single-nucleotide polymorphisms ($P < 10^{-40}$ compared to the genome-wide average in both cases). In both, the set of elements with no expression evidence (non-exonics in ref. 150) is found in or next to genes whose products are highly enriched for transcriptional regulation, DNA binding, homeodomains and developmental functions; many of these UCEs are found more than 100 kb away from the corresponding genes. Finally, in both sets, no UCEs except a handful of coding regions could be traced back through sequence similarity to *Ciona intestinalis*, *Caenorhabditis elegans* or *Drosophila melanogaster*. At the moment, little is understood about the functional significance of either the UCEs or the high-CNF segments that are far from genes.

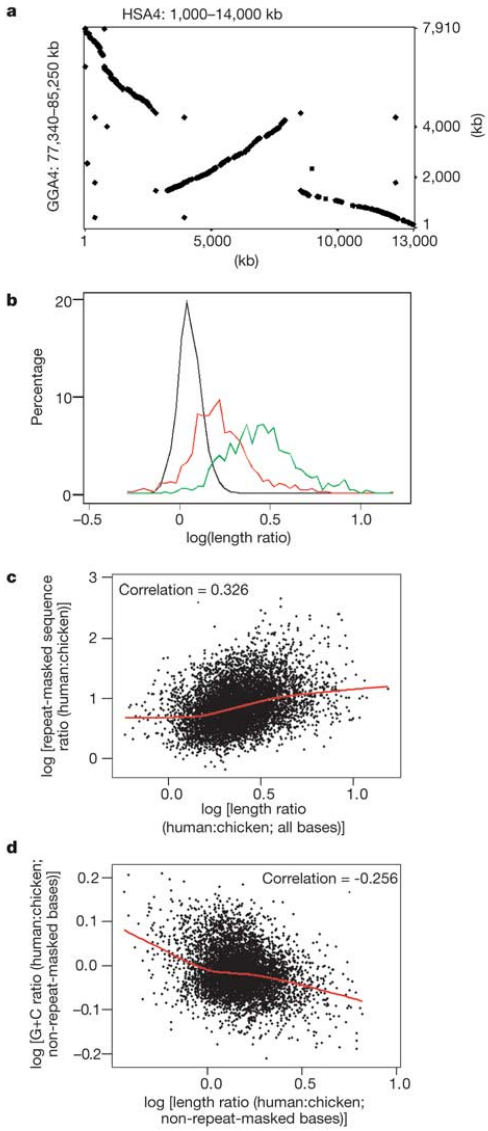


**Figure 15** Variation in the ratio of lengths of human and chicken DNA in aligned segments. **a**, Dot plot comparing orthologous regions of human and chicken, showing variable slope. **b**, Variation in log-transformed ratio of lengths of aligned segments, comparing human–chicken (green, all; non-repetitive, red) and human–mouse (black). **c**, Scatter plot of the log-transformed ratio of lengths of orthologous human and chicken segments versus ratio of repeat-masked sequence in the two species. **d**, Scatter plot of the log-transformed ratio of lengths versus ratio of G+C contents after removal of masked bases. Lowess smooths (locally weighted scatterplot smoothing) are superimposed (red curves; smoothing parameter 0.5). See Methods for details.

## Conclusion

The chicken genome represents an intermediate test case as a target

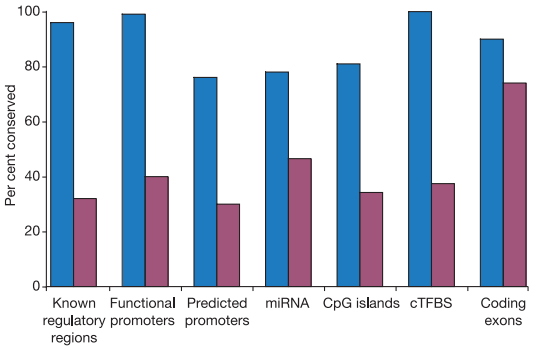


**Figure 16** All sets of functional elements in human–chicken alignments show reduced representation relative to human–mouse–rat alignments. We examined functional elements containing known regulatory regions[2,164], functional promoters and predicted promoters[165], miRNA[34], CpG islands, conserved transcription factor binding sites[3], and coding exons of known genes. The per cent of each category that aligns is shown for the human–mouse–rat alignments (HMR, blue) or human–chicken alignments (HC, red).

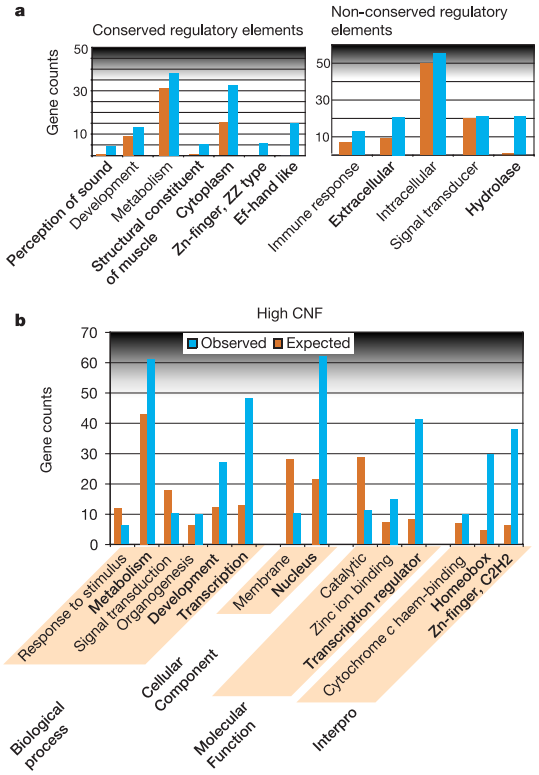


**Figure 17** Enrichment of particular GO categories in genes regulated by conserved or non-conserved *cis*-regulatory modules (**a**) and in high-CNF regions (**b**). The observed and expected gene counts are shown for GO categories with at least five genes from high-CNF segments. Significantly enriched categories are in bold; the largest significant *P*-value is 0.0022 and the others range from $10^{-10}$ to $10^{-25}$.

for genome sequence assembly and analysis. Although less than half the size of mammalian genomes, it is still much larger than those of *D. melanogaster*, *C. elegans* and even *T. rubripes*, and it lacks the dense linkage map platform that helped to assemble the first two. Unlike the rat and chimpanzee genomes, there was no closely related, high-quality genome sequence already available to provide a framework for assembly. Nevertheless, a relatively high-quality draft of the chicken genome has been achieved on the basis of only 6.6× whole-genome shotgun coverage, owing in part to the remarkably low level of recent transposon activity it has endured (Table 5).

The quality of this draft genome sequence makes it a key resource for comparative genomics. Natural selection and evolution provide us with many perspectives from which to view our own genome. Genomes of distant species resolve key processes that have been conserved over millennia, whereas those of our close relatives allow an analysis of rapidly changing sequence. In many respects, the chicken genome provides insights that were unavailable from previous sequences. For nearly every aspect of biology, it allows us to distinguish features of mammalian biology that are derived or ancient, and it reveals examples of mammalian innovation and adaptation.

The chicken is sufficiently distant that little unselected sequence has survived unchanged along the separate evolutionary paths to birds and mammals from their last common ancestor. Against this background, conserved non-coding sequences stand out clearly. Some of these represent known regulators (Fig. 16) and others use novel mechanisms yet to be identified. On the other hand, the counterparts of many functional mammalian sequence elements could not be identified in the chicken sequence. Either these represent mammalian innovations or else any commonality has been lost over the course of >310 Myr of separate mutation and fixation.

Chicken breeding, based on quantitative genetic methods, represents one of the most remarkable examples of directed evolution. Even after 50 yr of intensive selection, annual genetic progress in production traits remains undiminished[151]. An impressive list of chicken quantitative trait loci has already been identified[152], many with combined agricultural and medical relevance. The chicken genome sequence promotes both the development of more refined polymorphic maps (see the accompanying paper[153]) and the framework for discovering the functional polymorphisms underlying interesting quantitative traits, thus fully exploiting the genetic potential of the chicken.

The chicken genome is invaluable for shedding light on functional elements of the human genome and our unique evolutionary history. It also points the way forward to the great utility we can expect from the genome sequences of other carefully chosen species. The data presented here demonstrate both the unique value of the chicken as a model species and emphasize the incomplete nature of our collective understanding of complex organisms. This chicken genome sequence will both integrate and stimulate the expanding array of contributions from this versatile species. □

## Methods

### Domain matching and ranking

To identify known families of genes and domains we scanned respective proteomes for characteristic HMM profile signatures from Pfam[69] and SMART databases using HMMER (http://hmmer.wustl.edu/) software and applying corresponding family-specific cutoffs. The identified families were ranked by the number of matching genes requiring at least one matching transcript, and only counting repetitive matches once.

### Orthology detection

Orthologous relationships between genes of chicken, human, *Fugu* and others were inferred through systematic similarity searches at the level of the predicted proteins. We retained only the largest predicted ORF per locus, and compared those in an all-against-all fashion using the Smith–Waterman algorithm. We then formed orthologous groups using a variant of a strategy used earlier[137,154,155]. First, we grouped recently duplicated sequences within genomes into 'paralogous groups', to be treated as single sequences subsequently. For this, there was no fixed cutoff in similarity, but instead we started with a stringent similarity cutoff and relaxed it on each successive step, until all paralogous proteins were joined, thereby satisfying the following criteria: all members of a group had to be more similar to each other than to any other protein in any other genome; and all members of the group had to have hits that overlapped by at least 20 residues, to avoid 'domain walking'. After grouping paralogous proteins, we started to assign orthology between proteins by joining triangles of reciprocal best hits involving three different species (here, paralogous groups were represented by their best-matching member). Again, a stringent similarity cutoff was used first and relaxed on each successive step, and all proteins in a group were required to have hits overlapping by at least 20 residues. Finally, we joined any remaining nodes by allowing not only reciprocal triangles, but also reciprocal tuples.

### Detection of gene loss in mammals

The orthologous relations defined above were used to infer losses when a gene was found in chicken and in at least one earlier-branching animal, but not in any mammal. Of 122 candidate losses obtained in this manner, many were manually discounted after Blastp searches in mammalian genomes (thus hinting that several as-yet-unannotated genes in mammals remain to be predicted).

### Detection of orthologous introns

For each orthologous group we created a multiple alignment and mapped intron positions and protein features onto it. This procedure is incorporated into the SMART web server. To minimize errors due to erroneous alignments, introns flanking alignment gaps were discarded (less than 1% of all introns). To compensate for effects of intron sliding and to reduce further the impact of possible alignment errors, we allowed a window of 12 nucleotides in which we considered a position as conserved. Previous estimates indicated that the chance of independent intron insertion in such a window is <1%. To avoid biases due to incomplete gene predictions, we omitted 18,910 introns in regions that were missing from some of the predicted genes.

### Deriving tissue expression data

Chicken ESTs were mapped to the assembly, and to Ensembl genes (±1 kb), using BLAT and a 95% identity threshold, and were partitioned into ten (brain; fat and skin; bone and connective tissues; heart; kidney and adrenal tissues; immune; liver; female reproduction; alimentary; testis) distinct tissue types. Percentage amino acid sequence identities of 1:1 chicken–human orthologues were calculated as described previously (Fig. 6). Note that single genes may be assigned to multiple tissues.

### Whole-genome alignments

Human–chicken whole-genome alignments were obtained by using the program BLASTZ[156] to produce short (typically 100–1,000 bp) local alignments, and then assembling gap-free segments of those alignments into 'chains' in which aligned segments occur in the same order and orientation in both species[134]. These alignments—which were used to generate data for Figs 2, 15–17 and Table 4, and Supplementary Figs S1, S15 and Supplementary Tables S6 and S7—can be obtained from the U.C. Santa Cruz Browser (http://genome.ucsc.edu/). To compute the CNF of a human genomic interval, we limited consideration to non-repetitive bases that are not in a local alignment that intersects a protein-coding region, and determined the fraction of those bases that are within an alignment.

### Evolution of vertebrate genomes

The maps of conserved synteny (orthologous chromosomal segments with a conserved gene neighbourhood[133,134,137]) between chicken, human and mouse were produced using whole-genome DNA alignments post-processed into chains and nets[134] as well as looking for a conserved neighbourhood of orthologous genes as described previously[133,137]. We used gene-based synteny as input to MGR[157] and GRIMM[133,158] to look for parsimonious scenarios of rearrangements, starting from a set of 6,447 four-way orthologous genes pre-filtered for evidence of conserved pairwise synteny using SyntQL (E. Zdobnov, unpublished program) and applying GRIMM-Synteny[133] for more stringently defined 586 four-way human–mouse–rat–chicken synteny blocks.

Detailed descriptions of all methods are provided in the Supplementary Information.

Received 19 July; accepted 1 November 2004; doi:10.1038/nature03154.


1. The International Human Genome Sequencing Consortium. Initial sequencing and analysis of the human genome. *Nature* **409,** 860–921 (2001).
2. Mouse Genome Sequencing Consortium. Initial sequencing and comparative analysis of the mouse genome. *Nature* **420,** 520–562 (2002).
3. Rat Genome Sequencing Project Consortium. Genome sequence of the Brown Norway rat yields insights into mammalian evolution. *Nature* **428,** 493–521 (2004).
4. Hedges, S. B. The origin and evolution of model organisms. *Nature Rev. Genet.* **3,** 838–849 (2002).
5. Reisz, R. R. & Muller, J. Molecular timescales and the fossil record: a paleontological perspective. *Trends Genet.* **20,** 237–241 (2004).
6. Duret, L. & Bucher, P. Searching for regulatory elements in human noncoding sequences. *Curr. Opin. Struct. Biol.* **7,** 399–406 (1997).
7. Gottgens, B. *et al.* Analysis of vertebrate SCL loci identifies conserved enhancers. *Nature Biotechnol.* **18,** 181–186 (2000).
8. Thomas, J. W. *et al.* Comparative analyses of multi-species sequences from targeted genomic regions. *Nature* **424,** 788–793 (2003).
9. Ostrum, J. H. The origin of birds. *Annu. Rev. Earth Planet. Sci.* **3,** 55–77 (1975).
10. Sereno, P. C. The evolution of dinosaurs. *Science* **284,** 2137–2147 (1999).
11. Shinan, R. Several major achievements in early Neolithic China, ca. 5000 BC. *Kaogu–Archaeology* **1996,** 37–49 (1996); (trans. Cheung, W. K.) (ed. Gordon, B.) ⟨http://www.carleton.ca/~bgordon/Rice/papers/REN96.htm⟩.
12. Fitzpatrick, D. M. & Ahmed, K. Red roving fowl. *Down Earth* **9,** 28 (2000).
13. Crawford, R. D. (ed.) *Poultry Breeding and Genetics* (Elsevier, Amsterdam, 1995).
14. Darwin, C. *The Variation of Animals and Plants Under Domestication* (D. Appleton and Co., New York, 1896).
15. Fumihito, A. *et al.* One subspecies of the red jungle fowl (*Gallus gallus gallus*) suffices as the matriarchic ancestor of all domestic breeds. *Proc. Natl Acad. Sci. USA* **91,** 12505–12509 (1994).
16. Punnett, R. C. *Heredity in Poultry* (Macmillan, London, 1923).
17. Bateson, W. & Saunders, E. R. Experimental studies in the physiology of heredity. *Rep. Evol. Commun. R. Soc.* **1,** 1–160 (1902).
18. Pisenti, J. M. *et al.* Avian genetic resources at risk: An assessment and proposal for conservation of genetic stocks in the USA and Canada. *Avian Poultry Biol. Rev.* **12,** 1–102 (2001).
19. Brown, W. R., Hubbard, S. J., Tickle, C. & Wilson, S. A. The chicken as a model for large-scale analysis of vertebrate gene function. *Nature Rev. Genet.* **4,** 87–98 (2003).
20. Vogt, P. K. *Historical Introduction to the General Properties of Retroviruses* (eds Coffin, J. M., Hughes, S. H. & Varmus, H. E.) (Cold Spring Harbor Laboratory Press, Cold Spring Harbor, New York, 1997).
21. Stehelin, D., Varmus, H. E., Bishop, J. M. & Vogt, P. K. DNA related to the transforming gene(s) of avian sarcoma viruses is present in normal avian DNA. *Nature* **260,** 170–173 (1976).
22. Cooper, M. D., Raymond, D. A., Peterson, R. D., South, M. A. & Good, R. A. The functions of the thymus system and the bursa system in the chicken. *J. Exp. Med.* **123,** 75–102 (1966).
23. Hutt, F. B. *Genetics of the Fowl* (McGraw-Hill, New York, 1949).
24. Bitgood, J. J. & Somes, R. G. J. in *Genetic Maps* (ed. O'Brien, S.) 4333–4342 (Cold Spring Harbor Laboratory Press, Cold Spring Harbor, 1993).
25. Groenen, M. A. *et al.* A consensus linkage map of the chicken genome. *Genome Res.* **10,** 137–147 (2000).
26. Bloom, S. E., Delany, M. E. & Muscarella, D. E. *Constant and Variable Features of Avian Chromosomes* (eds Gibbins, A. & Etches, R. J.) (CRC Press, Boca Raton, Florida, 1993).
27. Huang, X., Wang, J., Aluru, S., Yang, S. P. & Hillier, L. PCAP: a whole-genome assembly program. *Genome Res.* **13,** 2164–2170 (2003).
28. Wallis, J. W. *et al.* A physical map of the chicken genome. *Nature* doi:10.1038/nature03030 (this issue).
29. Schmid, M. *et al.* First report on chicken genes and chromosomes 2000. *Cytogenet. Cell Genet.* **90,** 169–218 (2000).
30. Romanov, M. N., Price, J. A. & Dodgson, J. B. Integration of animal linkage and BAC contig maps using overgo hybridization. *Cytogenet. Genome Res.* **102,** 277–281 (2003).
31. Burt, D. W. *Comparative Genomics in Poultry Breeding and Biotechnology* (eds Muir, W. M. & Aggrey, S. E.) (CAB International, Wallingford, Oxon, 2003).
32. Hubbard, S. J. *et al.* Transcriptome analysis for the chicken based on 19,626 finished cDNA sequences and 485,337 Expressed Sequence Tags. *Genome Res.* (in the press).
33. Griffiths-Jones, S., Bateman, A., Marshall, M., Khanna, A. & Eddy, S. R. Rfam: an RNA family database. *Nucleic Acids Res.* **31,** 439–441 (2003).
34. Griffiths-Jones, S. The microRNA registry. *Nucleic Acids Res.* **32** (Database issue), D109–D111 (2004).
35. Hirose, T. & Steitz, J. A. Position within the host intron is critical for efficient processing of box C/D snoRNAs in mammalian cells. *Proc. Natl Acad. Sci. USA* **98,** 12914–12919 (2001).
36. Curwen, V. *et al.* The Ensembl automatic gene annotation system. *Genome Res.* **14,** 942–950 (2004).
37. Flicek, P., Keibler, E., Hu, P., Korf, I. & Brent, M. R. Leveraging the mouse genome for gene prediction in human: from whole-genome shotgun reads to a global synteny map. *Genome Res.* **13,** 46–54 (2003).
38. Parra, G. *et al.* Comparative gene prediction in human and mouse. *Genome Res.* **13,** 108–117 (2003).
39. Ashurst, J. L. & Collins, J. E. Gene annotation: prediction and testing. *Annu. Rev. Genomics Hum. Genet.* **4,** 69–88 (2003).
40. Birney, E. *et al.* An overview of Ensembl. *Genome Res.* **14,** 925–928 (2004).
41. Pruitt, K. D., Tatusova, T. & Maglott, D. R. NCBI Reference Sequence project: update and current status. *Nucleic Acids Res.* **31,** 34–37 (2003).
42. Strausberg, R. L. *et al.* Generation and initial analysis of more than 15,000 full-length human and mouse cDNA sequences. *Proc. Natl Acad. Sci. USA* **99,** 16899–16903 (2002).
43. Imanishi, T. *et al.* Integrative annotation of 21,037 human genes validated by full-length cDNA clones. *PLoS Biol.* **2,** E162 (2004).
44. Wu, J. Q., Shteynberg, D., Arumugam, M., Gibbs, R. A. & Brent, M. R. Identification of rat genes by TWINSCAN gene prediction, RT-PCR, and direct sequencing. *Genome Res.* **14,** 665–671 (2004).
45. Human Genome Sequencing Consortium. Finishing the euchromatic sequence of the human genome. *Nature* **431,** 931–945 (2004).
46. Kozak, M. How do eukaryotic ribosomes select initiation regions in messenger RNA? *Cell* **15,** 1109–1123 (1978).
47. Reymond, A. *et al.* Nineteen additional unpredicted transcripts from human chromosome 21. *Genomics* **79,** 824–832 (2002).
48. Abril, J. F., Castelo, R. & Guigo, R. Comparison of splice sites in mammals and chicken. *Genome Res.* (in the press).
49. Aruscavage, P. J. & Bass, B. L. A phylogenetic analysis reveals an unusual sequence conservation within introns involved in RNA editing. *RNA* **6,** 257–269 (2000).
50. Hoopengardner, B., Bhalla, T., Staber, C. & Reenan, R. Nervous system targets of RNA editing identified by comparative genomics. *Science* **301,** 832–836 (2003).
51. Long, M., Betran, E., Thornton, K. & Wang, W. The origin of new genes: glimpses from the young and old. *Nature Rev. Genet.* **4,** 865–875 (2003).
52. Torrents, D., Suyama, M., Zdobnov, E. & Bork, P. A genome-wide survey of human pseudogenes. *Genome Res.* **13,** 2559–2567 (2003).
53. Esnault, C., Maestre, J. & Heidmann, T. Human LINE retrotransposons generate processed pseudogenes. *Nature Genet.* **24,** 363–367 (2000).
54. Burch, J. B., Davis, D. L. & Haas, N. B. Chicken repeat 1 elements contain a pol-like open reading frame and belong to the non-long terminal repeat class of retrotransposons. *Proc. Natl Acad. Sci. USA* **90,** 8199–8203 (1993).
55. Haas, N. B. *et al.* Subfamilies of CR1 non-LTR retrotransposons have different 5′ UTR sequences but are otherwise conserved. *Gene* **265,** 175–183 (2001).
56. Olofsson, B. & Bernardi, G. The distribution of CR1, and Alu-like family of interspersed repeats, in the chicken genome. *Biochim. Biophys. Acta* **740,** 339–341 (1983).
57. Haas, N. B., Grabowski, J. M., Sivitz, A. B. & Burch, J. B. Chicken repeat 1 (CR1) elements, which define an ancient family of vertebrate non-LTR retrotransposons, contain two closely spaced open reading frames. *Gene* **197,** 305–309 (1997).
58. Adey, N. B., Tollefsbol, T. O., Sparks, A. B., Edgell, M. H. & Hutchison, C. A. III Molecular resurrection of an extinct ancestral promoter for mouse L1. *Proc. Natl Acad. Sci. USA* **91,** 1569–1573 (1994).
59. Smit, A. F., Toth, G., Riggs, A. D. & Jurka, J. Ancestral, mammalian-wide subfamilies of LINE-1 repetitive sequences. *J. Mol. Biol.* **246,** 401–417 (1995).
60. Ohshima, K., Hamada, M., Terai, Y. & Okada, N. The 3′ ends of tRNA-derived short interspersed repetitive elements are derived from the 3′ ends of long interspersed repetitive elements. *Mol. Cell. Biol.* **16,** 3756–3764 (1996).
61. Cordonnier, A., Casella, J. F. & Heidmann, T. Isolation of novel human endogenous retrovirus-like elements with foamy virus-related pol sequence. *J. Virol.* **69,** 5890–5897 (1995).
62. Smit, A. F. Identification of a new, abundant superfamily of mammalian LTR-transposons. *Nucleic Acids Res.* **21,** 1863–1872 (1993).
63. Smit, A. F. Interspersed repeats and other mementos of transposable elements in mammalian genomes. *Curr. Opin. Genet. Dev.* **9,** 657–663 (1999).
64. Duret, L. & Mouchiroud, D. Determinants of substitution rates in mammalian genes: expression pattern affects selection intensity but not mutation rate. *Mol. Biol. Evol.* **17,** 68–74 (2000).
65. Winter, E. E., Goodstadt, L. & Ponting, C. P. Elevated rates of protein secretion, evolution, and disease among tissue-specific genes. *Genome Res.* **14,** 54–61 (2004).
66. Zhang, L. & Li, W. H. Mammalian housekeeping genes evolve more slowly than tissue-specific genes. *Mol. Biol. Evol.* **21,** 236–239 (2004).
67. Aparicio, S. *et al.* Whole-genome shotgun assembly and analysis of the genome of *Fugu rubripes*. *Science* **297,** 1301–1310 (2002).
68. Mulder, N. J. *et al.* The InterPro Database, 2003 brings increased coverage and new features. *Nucleic Acids Res.* **31,** 315–318 (2003).
69. Bateman, A. *et al.* The Pfam protein families database. *Nucleic Acids Res.* **32** (Database issue), D138–D141 (2004).

articles


70. Letunic, I. *et al.* SMART 4.0: towards genomic data integration. *Nucleic Acids Res.* **32** (Database issue), D142–D144 (2004).
71. Fickenscher, H. & Pirzer, H. Interleukin-26. *Int. Immunopharmacol.* **4,** 609–613 (2004).
72. Copley, R. R., Goodstadt, L. & Ponting, C. Eukaryotic domain evolution inferred from genome comparisons. *Curr. Opin. Genet. Dev.* **13,** 623–628 (2003).
73. Kawasaki, K. & Weiss, K. M. Mineralized tissue and vertebrate evolution: the secretory calcium-binding phosphoprotein gene cluster. *Proc. Natl Acad. Sci. USA* **100,** 4060–4065 (2003).
74. Williams, A. J., Blacklow, S. C. & Collins, T. The zinc finger-associated SCAN box is a conserved oligomerization domain. *Mol. Cell. Biol.* **19,** 8526–8535 (1999).
75. Sander, T. L. *et al.* The SCAN domain defines a large family of zinc finger transcription factors. *Gene* **310,** 29–38 (2003).
76. Hughes, A. L. & Friedman, R. Differential loss of ancestral gene families as a source of genomic divergence in animals. *Proc. R. Soc. Lond. B* **271** (suppl. 3), S107–S109 (2004).
77. Krylov, D. M., Wolf, Y. I., Rogozin, I. B. & Koonin, E. V. Gene loss, protein sequence divergence, gene dispensability, expression level, and interactivity are correlated in eukaryotic evolution. *Genome Res.* **13,** 2229–2235 (2003).
78. Kang, W. & Reid, K. B. DMBT1, a regulator of mucosal homeostasis through the linking of mucosal defense and regeneration? *FEBS Lett.* **540,** 21–25 (2003).
79. Birney, E., Clamp, M. & Durbin, R. GeneWise and Genomewise. *Genome Res.* **14,** 988–995 (2004).
80. Shiina, T. *et al.* Genomic anatomy of a premier major histocompatibility complex paralogous region on chromosome 1q21-q22. *Genome Res.* **11,** 789–802 (2001).
81. Amadou, C. *et al.* Co-duplication of olfactory receptor and MHC class I genes in the mouse major histocompatibility complex. *Hum. Mol. Genet.* **12,** 3025–3040 (2003).
82. Malnic, B., Godfrey, P. A. & Buck, L. B. The human olfactory receptor gene family. *Proc. Natl Acad. Sci. USA* **101,** 2584–2589 (2004).
83. Alcock, J. *Animal Behaviour* (Sinauer Associates, Sunderland, Massachusetts, 1989).
84. Jones, R. B. & Roper, T. J. Olfaction in the domestic fowl: a critical review. *Physiol. Behav.* **62,** 1009–1018 (1997).
85. Mefford, H. C., Linardopoulou, E., Coil, D., van den Engh, G. & Trask, B. J. Comparative sequencing of a multicopy subtelomeric region containing olfactory receptor genes reveals multiple interactions between non-homologous chromosomes. *Hum. Mol. Genet.* **10,** 2363–2372 (2001).
86. Mefford, H. C. & Trask, B. J. The complex structure and dynamic evolution of human subtelomeres. *Nature Rev. Genet.* **3,** 91–102 (2002).
87. Rogers, M. A. *et al.* Characterization of a cluster of human high/ultrahigh sulfur keratin-associated protein genes embedded in the type I keratin gene domain on chromosome 17q12–21. *J. Biol. Chem.* **276,** 19440–19451 (2001).
88. Hesse, M., Zimek, A., Weber, K. & Magin, T. M. Comprehensive analysis of keratin gene clusters in humans and rodents. *Eur. J. Cell Biol.* **83,** 19–26 (2004).
89. Altmann, S. M., Mellon, M. T., Distel, D. L. & Kim, C. H. Molecular and functional analysis of an interferon gene from the zebrafish, *Danio rerio. J. Virol.* **77,** 1992–2002 (2003).
90. Hughes, A. L. & Roberts, R. M. Independent origin of IFN-α and IFN-β in birds and mammals. *J. Interferon Cytokine Res.* **20,** 737–739 (2000).
91. Smale, L., Lee, T. & Nunez, A. A. Mammalian diurnality: some facts and gaps. *J. Biol. Rhythms* **18,** 356–366 (2003).
92. Thoma, F. Light and dark in chromatin repair: repair of UV-induced DNA lesions by photolyase and nucleotide excision repair. *EMBO J.* **18,** 6585–6598 (1999).
93. Reverchon, S., Rouanet, C., Expert, D. & Nasser, W. Characterization of indigoidine biosynthetic genes in *Erwinia chrysanthemi* and role of this blue pigment in pathogenicity. *J. Bacteriol.* **184,** 654–665 (2002).
94. Shannon, M., Hamilton, A. T., Gordon, L., Branscomb, E. & Stubbs, L. Differential expansion of zinc-finger transcription factor loci in homologous human and mouse gene clusters. *Genome Res.* **13,** 1097–1110 (2003).
95. Zhao, G. Q. *et al.* The receptors for mammalian sweet and umami taste. *Cell* **115,** 255–266 (2003).
96. Bradbury, J. Taste perception: cracking the code. *PLoS Biol.* **2,** E64 (2004).
97. Bufe, B., Hofmann, T., Krautwurst, D., Raguse, J. D. & Meyerhof, W. The human TAS2R16 receptor mediates bitter taste in response to β-glucopyranosides. *Nature Genet.* **32,** 397–401 (2002).
98. Shi, P., Zhang, J., Yang, H. & Zhang, Y. P. Adaptive diversification of bitter taste receptor genes in mammalian evolution. *Mol. Biol. Evol.* **20,** 805–814 (2003).
99. Nordling, E., Persson, B. & Jornvall, H. Differential multiplicity of MDR alcohol dehydrogenases: enzyme genes in the human genome versus those in organisms initially studied. *Cell. Mol. Life Sci.* **59,** 1070–1075 (2002).
100. Hjelmqvist, L., Estonius, M. & Jornvall, H. The vertebrate alcohol dehydrogenase system: variable class II type form elucidates separate stages of enzymogenesis. *Proc. Natl Acad. Sci. USA* **92,** 10904–10908 (1995).
101. Tamir, H. & Ratner, S. Enzymes of arginine metabolism in chicks. *Arch. Biochem. Biophys.* **102,** 249–258 (1963).
102. McQueen, H. A. *et al.* CpG islands of chicken are concentrated on microchromosomes. *Nature Genet.* **12,** 321–324 (1996).
103. Andreozzi, L. *et al.* Compositional mapping of chicken chromosomes and identification of the gene-richest regions. *Chromosome Res.* **9,** 521–532 (2001).
104. Smith, J. *et al.* Differences in gene density on chicken macrochromosomes and microchromosomes. *Anim. Genet.* **31,** 96–103 (2000).
105. McQueen, H. A., Siriaco, G. & Bird, A. P. Chicken microchromosomes are hyperacetylated, early replicating, and gene rich. *Genome Res.* **8,** 621–630 (1998).
106. Grutzner, F. *et al.* Chicken microchromosomes are hypermethylated and can be identified by specific painting probes. *Cytogenet. Cell Genet.* **93,** 265–269 (2001).
107. Schmid, M., Enderle, E., Schindler, D. & Schempp, W. Chromosome banding and DNA replication patterns in bird karyotypes. *Cytogenet. Cell Genet.* **52,** 139–146 (1989).
108. Ponce de Leon, F. A., Li, Y. & Weng, Z. Early and late replicative chromosomal banding patterns of *Gallus domesticus. J. Hered.* **83,** 36–42 (1992).
109. Habermann, F. A. *et al.* Arrangements of macro- and microchromosomes in chicken cells. *Chromosome Res.* **9,** 569–584 (2001).
110. Holmquist, G. P. Evolution of chromosome bands: molecular ecology of noncoding DNA. *J. Mol. Evol.* **28,** 469–486 (1989).
111. Jensen-Seaman, M. I. *et al.* Comparative recombination rates in the rat, mouse, and human genomes. *Genome Res.* **14,** 528–538 (2004).
112. Meunier, J. & Duret, L. Recombination drives the evolution of GC-content in the human genome. *Mol. Biol. Evol.* **21,** 984–990 (2004).
113. Yang, S. *et al.* Patterns of insertions and their covariation with substitutions in the rat, mouse, and human genomes. *Genome Res.* **14,** 517–527 (2004).
114. Rodionov, A. V. Micro vs. macro: structural-functional organization of avian micro- and macrochromosomes. *Genetika* **32,** 597–608 (1996).
115. Marais, G. Biased gene conversion: implications for genome and sex evolution. *Trends Genet.* **19,** 330–338 (2003).
116. Eyre-Walker, A. & Hurst, L. D. The evolution of isochores. *Nature Rev. Genet.* **2,** 549–555 (2001).
117. Montoya-Burgos, J. I., Boursot, P. & Galtier, N. Recombination explains isochores in mammalian genomes. *Trends Genet.* **19,** 128–130 (2003).
118. Bird, A. P. DNA methylation and the frequency of CpG in animal DNA. *Nucleic Acids Res.* **8,** 1499–1504 (1980).
119. Gardiner-Garden, M. & Frommer, M. CpG islands in vertebrate genomes. *J. Mol. Biol.* **196,** 261–282 (1987).
120. Carvalho, A. B. & Clark, A. G. Intron size and natural selection. *Nature* **401,** 344 (1999).
121. Duret, L., Mouchiroud, D. & Gautier, C. Statistical analysis of vertebrate sequences reveals that long genes are scarce in GC-rich isochores. *J. Mol. Evol.* **40,** 308–317 (1995).
122. Hurst, L. D., Brunton, C. F. & Smith, N. G. Small introns tend to occur in GC-rich regions in some but not all vertebrates. *Trends Genet.* **15,** 437–439 (1999).
123. Versteeg, R. *et al.* The human transcriptome map reveals extremes in gene density, intron length, GC content, and repeat pattern for domains of highly and weakly expressed genes. *Genome Res.* **13,** 1998–2004 (2003).
124. Hill, W. G. & Robertson, A. The effect of linkage on limits to artificial selection. *Genet. Res.* **8,** 269–294 (1966).
125. Yang, Z. PAML: a program package for phylogenetic analysis by maximum likelihood. *Comput. Appl. Biosci.* **13,** 555–556 (1997).
126. Hardison, R. C. *et al.* Covariation in frequencies of substitution, deletion, transposition, and recombination during eutherian evolution. *Genome Res.* **13,** 13–26 (2003).
127. Axelsson, E., Webster, M. T., Smith, N. G. C., Burt, D. W. & Ellegren, H. Comparison of the chicken and turkey genomes reveals a higher rate of nucleotide divergence on microchromosomes than macrochromosomes. *Genome Res.* (in the press).
128. Wilkie, A. O. *et al.* Stable length polymorphism of up to 260 kb at the tip of the short arm of human chromosome 16. *Cell* **64,** 595–606 (1991).
129. Bailey, J. A. *et al.* Recent segmental duplications in the human genome. *Science* **297,** 1003–1007 (2002).
130. Bailey, J. A., Church, D. M., Ventura, M., Rocchi, M. & Eichler, E. E. Analysis of segmental duplications and genome assembly in the mouse. *Genome Res.* **14,** 789–801 (2004).
131. Tuzun, E., Bailey, J. A. & Eichler, E. E. Recent segmental duplications in the working draft assembly of the brown Norway rat. *Genome Res.* **14,** 493–506 (2004).
132. Cheung, J. *et al.* Recent segmental and gene duplications in the mouse genome. *Genome Biol.* **4,** R47 (2003).
133. Pevzner, P. & Tesler, G. Genome rearrangements in mammalian evolution: lessons from human and mouse genomes. *Genome Res.* **13,** 37–45 (2003).
134. Kent, W. J., Baertsch, R., Hinrichs, A., Miller, W. & Haussler, D. Evolution's cauldron: duplication, deletion, and rearrangement in the mouse and human genomes. *Proc. Natl Acad. Sci. USA* **100,** 11484–11489 (2003).
135. Bourque, G., Pevzner, P. A. & Tesler, G. Reconstructing the genomic architecture of ancestral mammals: lessons from human, mouse, and rat genomes. *Genome Res.* **14,** 507–516 (2004).
136. Murphy, W. J., Bourque, G., Tesler, G., Pevzner, P. A. & O'Brien, S. J. Reconstructing the genomic architecture of mammalian ancestors using multispecies comparative maps. *Human Genomics* **1,** 30–40 (2003).
137. Zdobnov, E. M. *et al.* Comparative genome and proteome analysis of *Anopheles gambiae* and *Drosophila melanogaster. Science* **298,** 149–159 (2002).
138. Jaillon, O. *et al.* Genome duplication in the teleost fish *Tetraodon nigroviridis* reveals the early vertebrate proto-karyotype. *Nature* **431,** 946–957 (2004).
139. Burt, D. W. *et al.* The dynamics of chromosome evolution in birds and mammals. *Nature* **402,** 411–413 (1999).
140. Murphy, W. J. *et al.* Resolution of the early placental mammal radiation using Bayesian phylogenetics. *Science* **294,** 2348–2351 (2001).
141. Bourque, G., Zdobnov, E. M., Bork, P., Pevzner, P. A. & Tesler, G. Comparative architectures of mammalian and chicken genomes reveal highly variable rates of genomic rearrangements across different lineages. *Genome Res.* (in the press).
142. Stanyon, R., Stone, G., Garcia, M. & Froenicke, L. Reciprocal chromosome painting shows that squirrels, unlike murid rodents, have a highly conserved genome organization. *Genomics* **82,** 245–249 (2003).
143. Gregory, T. R. Insertion-deletion biases and the evolution of genome size. *Gene* **324,** 15–34 (2004).
144. Smit, A. & Green, P. RepeatMasker ⟨http://ftp.genome.washington.edu/RM/RepeatMasker.html⟩ (1999).
145. Chiaromonte, F. *et al. The Genome of* Homo sapiens Vol. LXVIII (Cold Spring Harbor Press, Cold Spring Harbor, New York, 2003).
146. Dermitzakis, E. T. *et al.* Numerous potentially functional but non-genic conserved sequences on human chromosome 21. *Nature* **420,** 578–582 (2002).
147. Dunham, A. *et al.* The DNA sequence and analysis of human chromosome 13. *Nature* **428,** 522–528 (2004).
148. Grimwood, J. *et al.* The DNA sequence and biology of human chromosome 19. *Nature* **428,** 529–535 (2004).
149. Ovcharenko, I. *et al.* Evolution and functional classification of vertebrate gene deserts. *Genome Res.* (in the press).
150. Bejerano, G. *et al.* Ultraconserved elements in the human genome. *Science* **304,** 1321–1325 (2004).
151. Muir, W. M. & Aggrey, S. E. (eds) *Industrial Perspective on Problems and Issues Associated with Poultry Breeding* (CAB International, Wallingford, Oxon, 2003).

152. Andersson, L. & Georges, M. Domestic-animal genomics: deciphering the genetics of complex traits. *Nature Rev. Genet.* **5,** 202–212 (2004).
153. International Chicken Polymorphism Map Consortium. A genetic variation map for chicken with 2.8 million single-nucleotide polymorphisms. *Nature* doi:10.1038/nature03156 (this issue).
154. Koonin, E. V. A non-adaptationist perspective on evolution of genomic complexity or the continued dethroning of man. *Cell Cycle* **3,** 280–285 (2004).
155. von Mering, C. *et al.* STRING: a database of predicted functional associations between proteins. *Nucleic Acids Res.* **31,** 258–261 (2003).
156. Schwartz, S. *et al.* Human-mouse alignments with *Blastz*. *Genome Res.* **13,** 103–105 (2003).
157. Bourque, G. & Pevzner, P. A. Genome-scale evolution: reconstructing gene orders in the ancestral species. *Genome Res.* **12,** 26–36 (2002).
158. Tesler, G. GRIMM: genome rearrangements web server. *Bioinformatics* **18,** 492–493 (2002).
159. Benton, M. J. *Vertebrate Palaeontology* (Blackwell Science, Oxford, 2000).
160. Kapitonov, V. V. & Jurka, J. The esterase and PHD domains in CR1-like non-LTR retrotransposons. *Mol. Biol. Evol.* **20,** 38–46 (2003).
161. Vandergon, T. L. & Reitman, M. Evolution of chicken repeat 1 (CR1) elements: evidence for ancient subfamilies and multiple progenitors. *Mol. Biol. Evol.* **11,** 886–898 (1994).
162. Kedishvili, N. Y. *et al.* cDNA sequence and catalytic properties of a chick embryo alcohol dehydrogenase that oxidizes retinol and 3β,5α-hydroxysteroids. *J. Biol. Chem.* **272,** 7494–7500 (1997).
163. Estonius, M. *et al.* Avian alcohol dehydrogenase: the chicken liver enzyme. Primary structure, cDNA-cloning, and relationships to other alcohol dehydrogenases. *Eur. J. Biochem.* **194,** 593–602 (1990).
164. Elnitski, L. *et al.* Distinguishing regulatory DNA from neutral sites. *Genome Res.* **13,** 64–72 (2003).
165. Trinklein, N. D., Aldred, S. J., Saldanha, A. J. & Myers, R. M. Identification and functional analysis of human transcriptional promoters. *Genome Res.* **13,** 308–312 (2003).
166. Caldwell, R. B. *et al.* Full-length cDNAs from bursal lymphocytes to facilitate gene function analysis. *Genome Biol.* (in the press).


**Supplementary Information** accompanies the paper on **www.nature.com/nature**.

**Acknowledgements** The *Gallus gallus* sequence and map generation at Washington University School of Medicine's Genome Sequencing Center was supported by grants from the National Human Genome Research Institute (NHGRI). For work from other groups, we acknowledge the support of the Biotechnology and Biological Sciences Research Council, Center for Integrative Genomics Funds, Childcare and Lejeune Foundations, Chinese Academy of Sciences and Ministry of Science and Technology, Department of Energy, Desiree and Niels Yde Foundation, European Union, European Molecular Biology Laboratory, Fonds Quebeçois de la Recherche sur la Nature et les Technologies, Howard Hughes Medical Institute, National Institute for Diabetes and Digestive and Kidney Diseases, NHGRI, National Institutes of Health, National Natural Science Foundation of China, National Science Foundation, Novo Nordisk Foundation, Stowers Institute for Medical Research, Swedish Research Council, Swiss NCCR Frontiers in Genetics, Swiss National Science Foundation, USDA/CSREES National Research Initiative, USDA/CSREES National Animal Genome Research Program, Wallenberg Consortium North and the AgriFunGen program at the Swedish University of Agricultural Sciences, UK Medical Research Council, University of California Presidential Chair Fund, University of Pennsylvania Genomics Institute Award, University of Texas at Arlington, and the Wellcome Trust. Resources for exploring the sequence and annotation data are available on browser displays available at Ensembl (http://www.ensembl.org), UCSC (http://genome.ucsc.edu) and the NCBI (http://www.ncbi.nlm.nih.gov). We thank R. Waterston for advice regarding the manuscript.

**Competing interests statement** The authors declare that they have no competing financial interests.

**Correspondence** and requests for materials should be addressed to R.K.W. (rwilson@watson.wustl.edu). This *G. gallus* whole-genome shotgun project has been deposited at DDBJ/EMBL/GenBank under the project accession number AADN00000000. The version described in this paper is the first version, AADN01000000.

## International Chicken Genome Sequencing Consortium

**Overall coordination:** LaDeana W. Hillier[1], Webb Miller[2], Ewan Birney[3], Wesley Warren[1], Ross C. Hardison[2], Chris P. Ponting[4], Peer Bork[5,6], David W. Burt[7], Martien A. M. Groenen[8], Mary E. Delany[9], Jerry B. Dodgson[10]

**Genome fingerprint map, sequence and assembly:** Asif T. Chinwalla[1], Paul F. Cliften[1], Sandra W. Clifton[1], Kimberly D. Delehaunty[1], Catrina Fronick[1], Robert S. Fulton[1], Tina A. Graves[1], Colin Kremitzki[1], Dan Layman[1], Vincent Magrini[1], John D. McPherson[1], Tracie L. Miner, Patrick Minx[1], William E. Nash[1], Michael N. Nhan[1], Joanne O. Nelson[1], Lachlan G. Oddy[1], Craig S. Pohl[1], Jennifer Randall-Maher[1], Scott M. Smith[1], John W. Wallis[1], Shiaw-Pyng Yang[1]

**Mapping:** Michael N. Romanov[10], Catherine M. Rondelli[10], Bob Paton[7], Jacqueline Smith[7], David Morrice[7], Laura Daniels[9], Helen G. Tempest[11], Lindsay Robertson[11], Julio S. Masabanda[11], Darren K. Griffin[11], Alain Vignal[12], Valerie Fillon[12], Lina Jacobbson[13], Susanne Kerje[13], Leif Andersson[13], Richard P. M. Crooijmans[8], Jan Aerts[8], Jan J. van der Poel[8], Hans Ellegren[14]

**cDNA sequencing:** Randolph B. Caldwell[15], Simon J. Hubbard[16], Darren V. Grafham[17], Andrzej M. Kierzek[18], Stuart R. McLaren[17], Ian M. Overton[16], Hiroshi Arakawa[15], Kevin J. Beattie[19], Yuri Bezzubov[15], Paul E. Boardman[16], James K. Bonfield[17], Michael D. R. Croning[17], Robert M. Davies[17], Matthew D. Francis[17], Sean J. Humphray[17], Carol E. Scott[17], Ruth G. Taylor[17], Cheryll Tickle[19], William R. A. Brown[20], Jane Rogers[17], Jean-Marie Buerstedde[15], Stuart A. Wilson[21]

**Other sequencing and libraries:** Lisa Stubbs[22], Ivan Ovcharenko[22], Laurie Gordon[22], Susan Lucas[23], Marcia M. Miller[24], Hidetoshi Inoko[25], Takashi Shiina[25], Jim Kaufman[26], Jan Salomonsen[27], Karsten Skjoedt[28], Gane Ka-Shu Wong[29,30,31], Jun Wang[29,30], Bin Liu[29], Jian Wang[29,30], Jun Yu[29,30], Huanming Yang[29,30], Mikhail Nefedov[32], Maxim Koriabine[32], Pieter J. deJong[32]

**Analysis and annotation:** Leo Goodstadt[4], Caleb Webber[4], Nicholas J. Dickens[4], Ivica Letunic[6], Mikita Suyama[6], David Torrents[6], Christian von Mering[6], Evgeny M. Zdobnov[6], Kateryna Makova[2], Anton Nekrutenko[2], Laura Elnitski[2], Pallavi Eswara[2], David C. King[2], Shan Yang[2], Svitlana Tyekucheva[2], Anusha Radakrishnan[2], Robert S. Harris[2], Francesca Chiaromonte[2], James Taylor[2], Jianbin He[2], Monique Rijnkels[33], Sam Griffiths-Jones[17], Abel Ureta-Vidal[3], Michael M. Hoffman[3], Jessica Severin[3], Stephen M. J. Searle[17], Andy S. Law[7], David Speed[7], Dave Waddington[7], Ze Cheng[34], Eray Tuzun[34], Evan Eichler[34], Zhirong Bao[34], Paul Flicek[35], David D. Shteynberg[35], Michael R. Brent[35], Jacqueline M. Bye[17], Elizabeth J. Huckle[17], Sourav Chatterji[36], Colin Dewey[36], Lior Pachter[36], Andrei Kouranov[37], Zissimos Mourelatos[37], Artemis G. Hatzigeorgiou[37], Andrew H. Paterson[38], Robert Ivarie[38], Mikael Brandstrom[14], Erik Axelsson[14], Niclas Backstrom[14], Sofia Berlin[14], Matthew T. Webster[14], Olivier Pourquie[39], Alexandre Reymond[40], Catherine Ucla[40], Stylianos E. Antonarakis[40], Manyuan Long[41], J. J. Emerson[41], Esther Betrán[42], Isabelle Dupanloup[43], Henrik Kaessmann[43], Angie S. Hinrichs[44], Gill Bejerano[44], Terrence S. Furey[44], Rachel A. Harte[44], Brian Raney[44], Adam Siepel[13], W. James Kent[44], David Haussler[44,45], Eduardo Eyras[46], Robert Castelo[46], Josep F. Abril[46], Sergi Castellano[46], Francisco Camara[46], Genis Parra[46], Roderic Guigo[46], Guillaume Bourque[47], Glenn Tesler[48], Pavel A. Pevzner[49], Arian Smit[50]

**Project management:** Lucinda A. Fulton[1], Elaine R. Mardis[1] & Richard K. Wilson[1]

*Affiliations for participants: 1, Genome Sequencing Center, Washington University School of Medicine, Campus Box 8501, 4444 Forest Park Avenue, St Louis, Missouri 63108, USA; 2, Center for Comparative Genomics and Bioinformatics, Departments of Biology, Statistics, Biochemistry and Molecular Biology, Computer Science and Engineering, and Health Evaluation Sciences, The Pennsylvania State University, University Park, Pennsylvania 16802, USA; 3, EMBL-EBI, Wellcome Trust*

## articles

*Genome Campus, Hinxton, Cambridge CB10 1SD, UK; 4, MRC Functional Genetics Unit, University of Oxford, Department of Human Anatomy and Genetics, South Parks Road, Oxford OX1 3QX, UK; 5, Max-Delbrueck-Center for Molecular Medicine, 13025 Berlin, Robert-Roessle-Strasse 10, Germany; 6, EMBL, Meyerhofstrasse 1, 69012 Heidelberg, Germany; 7, Genomics and Genetics and Bioinformatics, Roslin Institute (Edinburgh), Midlothian EH25 9PS, UK; 8, Animal Breeding and Genetics Group, Wageningen University, Marijkeweg 40, 6709PG Wageningen, The Netherlands; 9, Department of Animal Science, 2131D Meyer Hall, One Shields Avenue, University of California, Davis, California 95616, USA; 10, Department of Microbiology and Molecular Genetics, Michigan State University, East Lansing, Michigan 48824, USA; 11, Cell and Chromosome Biology Group, Department of Biological Sciences, Brunel University, Uxbridge, Middlesex UB8 3PH, UK; 12, Laboratoire de Genetique Cellulaire, Centre INRA de Toulouse, BP 27 Auzeville, 31326 Castanet Tolosan, France; 13, Department of Medical Biochemistry and Microbiology, Uppsala University, Uppsala Biomedical Center, Box 597, SE-751 24 Uppsala, Sweden; 14, Department of Evolutionary Biology, Evolutionary Biology Centre, Uppsala University, Norbyvegen 18D, SE-752 36 Uppsala, Sweden; 15, Institut fuer Molekulare Strahlenbiologie, GSF–Forschungszentrum, Ingolstaedter Landstrasse 1, D-85764 Neuherberg, Germany; 16, Department of Biomolecular Sciences, UMIST, PO Box 88, Manchester, M60 1QD, UK; 17, The Sanger Institute, Wellcome Trust Genome Campus, Hinxton, Cambridgeshire CB10 1SA, UK; 18, Laboratory of Systems Biology, Institute of Biochemistry and Biophysics, Polish Academy of Sciences, Pawinskiego 5a, 02-106 Warszawa, Poland; 19, Division of Cell & Developmental Biology, School of Life Sciences, University of Dundee, Dundee DD15EH, UK; 20, Institute of Genetics, Nottingham University, Queen's Medical Centre, Nottingham NG7 2UH, UK; 21, Department of Molecular Biology and Biotechnology, University of Sheffield, Firth Court, Western Bank, Sheffield S10 2TN, UK; 22, EEBI Division and Genome Biology Division, Lawrence Livermore National Laboratory, Livermore, California 94550, USA; 23, DOE Joint Genome Institute, Walnut Creek, California 94598, USA; 24, Division of Molecular Biology, Beckman Research Institute, City of Hope National Medical Center, 1450 E. Duarte Road, Duarte, California 91010, USA; 25, Department of Molecular Life Science, Division of Basic Medical Science and Molecular Medicine, Tokai University School of Medicine, 143 Shimokasuya, Isehara 259-1143, Japan; 26, Institute for Animal Health, Compton, Berkshire RG20 7NN, UK; 27, The Royal Veterinary and Agricultural University, Department of Veterinary Pathobiology, Laboratory of Immunology, Stigboejlen 7, Frederiksberg, Copenhagen DK-1870, Denmark; 28, Department of Immunology and Medical Microbiology, University of Odense, Winslovparken 19, Odense, Copenhagen DK-5000, Denmark; 29, Beijing Institute of Genomics of Chinese Academy of Sciences, Beijing Genomics Institute, Beijing Proteomics Institute, Beijing 101300, China; 30, James D. Watson Institute of Genome Sciences of Zhejiang University, Hangzhou Genomics Institute, Key Laboratory of Bioinformatics of Zhejiang Province, Hangzhou 310007, China; 31, Genome Center, Department of Medicine, University of Washington, Seattle, Washington 98195, USA; 32, Children's Hospital Oakland Research Institute, 747 52nd Street, Oakland, California 94609, USA; 33, Children's Nutrition Research Center, Baylor College of Medicine, 1100 Bates Street, Houston, Texas 77030-2600, USA; 34, Genome Sciences, University of Washington School of Medicine, Seattle, Washington 98195, USA; 35, Laboratory for Computational Genomics, Campus Box 1045, Washington University, St Louis, Missouri 63130, USA; 36, Departments of Computer Science and Mathematics, U.C. Berkeley, Berkeley, California 94720-3840, USA; 37, Center for Bioinformatics, Departments of Genetics and Pathology, University of Pennsylvania, Medical School, Philadelphia, Pennsylvania 19104-6021, USA; 38, Plant Genome Mapping Laboratory and Department of Genetics, University of Georgia, Athens, Georgia 30602, USA; 39, Stowers Institute for Medical Research, 1000 East 50th Street, Kansas City, Missouri 64110, USA; 40, Department of Genetic Medicine and Development, University of Geneva Medical School, 1 rue Michel-Servet, 1211 Geneva, Switzerland; 41, Department of Ecology and Evolution, University of Chicago, Chicago, Illinois 60637, USA; 42, Department of Biology, University of Texas at Arlington, Arlington, Texas 76019, USA; 43, Center for Integrative Genomics, BEP, University of Lausanne, CH-1015 Lausanne, Switzerland; 44, UCSC Genome Bioinformatics Group, Center for Biomolecular Science & Engineering, Mailstop SOE, Baskin School of Engineering, University of California, Santa Cruz, 1156 High Street, Santa Cruz, California 95064, USA; 45, Howard Hughes Medical Institute, Center for Biomolecular Science & Engineering, Mailstop SOE, Baskin School of Engineering, University of California, Santa Cruz, 1156 High Street, Santa Cruz, California 95064, USA; 46, Grup de Recerca en Informatica Biomedica, Institut Municipal d'Investigacio Medica, Universitat Pompeu Fabra, and Programa de Bioinfomatica i Genomica, Centre de Regulacio Genomica, C/Dr. Aiguader 80, 08003 Barcelona, Catalonia, Spain; 47, Genome Institute of Singapore, 60 Biopolis Street, 02-01 Genome, 138672, Singapore; 48, University of California, San Diego, Department of Mathematics, 9500 Gilman Drive, La Jolla, California 92093-0112, USA; 49, University of California, San Diego, Department of Computer Science and Engineering, 9500 Gilman Drive, La Jolla, California 92093-0114, USA; 50, Computational Biology Group, The Institute for Systems Biology, 1441 North 34th Street, Seattle, Washington 98103, USA*

# Chapter 5

# Visualization Tools

If a picture is not worth a 1000 words,
to hell with it !
—Ad Reinhardt (note this is from the original Chinese quote
that "a picture is worth 10,000 words")

In this chapter the focus will shift towards the annotation and visualization process, describing those tools that permit to integrate data from different sources, including gene-prediction results, to present them to biologists in a comprehensive and comprehendible manner. These programs are intended to provide an overall view of our knowledge of a genomic region in a user-friendly interface, either static or interactive.

Before reporting our contribution to this field, we will place it in context with respect to other software. Therefore, a review of visualization tools provides the best frame to present our developments later. In the case of `gff2ps`, we have also participated in the cartography of the human, the fruit-fly and the mosquito genomes, and a special mention is deserved in the corresponding section.

## 5.1 A Review of Visualization Tools for Genomic Data

This section is not an in depth review, but an attempt to enumerate a broad spectrum of such software —ranging from the fully automated genome pipelines to the simple command-line programs—, and to highlight their application to comparative genome analyses. Programs are classified into three types: a) the database browsers, b) the annotation workbenches, that can be also used as browsers; and c) specific tools to visualize results from different sequence analysis, pointing the attention on those developed on top of alignment algorithms. We will not deal here with the libraries of code that contain programs or functions to plot data in any of the aforementioned classes, because they are of interest mostly to advanced users and computer specialists —for instance, `bioTk` [Searls, 1995], `bioWidgets` [Fischer *et al.*, 1999], the `Bioperl` Toolkit [Stajich *et al.*, 2002] or the Generic Model Organism Project (`GMOD`, see page 214, on Web Glossary).

### 5.1.1 Database browsers

A first entry point to the visualization of genomic analyses can be any of the web front-ends developed to publish genome annotations. For example, the ones offered by databases of species- specific genome projects, such as the *Saccharomyces cerevisiae* SGD [Christie *et al.*, 2004], the *Caenorhabditis elegans* WORMBASE [Harris *et al.*, 2004], the *Drosophila melanogaster* FLYBASE [The FlyBase Consortium, 2003], the mouse MGD [Bult *et al.*, 2004], the *Arabidopsis thaliana* TAIR [Rhee *et al.*, 2003], and so on. The expected evolution of these of interfaces was to summarize all the information under a unified graphical schema as the number of species being sequenced increased —as done in the `euGenes` [Gilbert, 2002], the Generic Genome Browser (`Gbrowse`, Stein *et al.* 2002) and the `GeneDB` [Hertz-Fowler *et al.*, 2004] systems.

The best example of such evolution is ACEDB [see page 213, on Web Glossary; Durbin and Thierry-Mieg, 1993; Eeckman and Durbin, 1995], a seminal genome database system developed since 1989 and originally tailored for the *C. elegans* genome project. The tools in it have been generalized and are now used in a variety of organism-specific databases as diverse as bacteria and eukaryotes [Walsh *et al.*, 1998]. Specialized displays for managing and publishing genomic data are available through its well-set-up graphical user interface. Two remarkable implementations are the `AceBrowser` [Stein and Thierry-Mieg, 1998] and `Jade` [Stein *et al.*, 1998] programs.

There has already been a worldwide effort to centralize all the information about sequenced genomes. The best examples are the three fully established whole-genome browsers: the NCBI MAP VIEWER [see page 215, on Web Glossary; Wheeler *et al.*, 2005], the UCSC GENOME BROWSER [see page 216, on Web Glossary; Karolchik *et al.*, 2004] and the ENSEMBL system at the Sanger Institute and the EBI [see page 213, on Web Glossary; Birney *et al.*, 2004a]. All three browsers present by default a set of "in-house" and/or contributed gene- finding predictions from different programs. This is an on-going effort and predictions are recomputed for each newly released assembly. However, only the UCSC and ENSEMBL systems distribute predictions fully-based on the comparative genomics approaches. In what follows, we briefly review these three main genome gates.

The NCBI MAP VIEWER shows ab initio gene models generated by `Gnomon` [NCBI, 2003], a heuristic tool able to find the maximal self-consistent set of transcript and protein alignments to genomic data. Other programs like, for instance, `GenomeScan` [Yeh *et al.*, 2001], use this information to parameterize the constraints for an underlying HMM-based gene prediction model. The browser is focused to display genome assemblies using sets of synchronized chromosomal maps, but also features tables of genetic loci in homologous segments of DNA between human and mouse —the so called Human-Mouse Homology Maps—, and has links to HOMOLOGENE, a database of curated and calculated gene homologues.

The ENSEMBL system can display simultaneously different sets of annotated features and predictions from several gene-prediction tools embedded in the ENSEMBL annotation pipeline (see for instance, Figures 1.4 and 5.1). An interesting feature of the ENSEMBL system is the inclusion of external data through a Distributed Annotation System (`DAS`, Dowell *et al.* 2001) server, which, on user demand, dynamically links third-party annotations to the genomic sequence under study. The `SGP2` [Parra *et al.*, 2003], `Twinscan` [Korf *et al.*, 2001], and `SLAM` [Alexandersson *et al.*, 2003] gene annotation tracks, for instance, can be easily included in the current view by switching on the corresponding check box in the '*DAS*

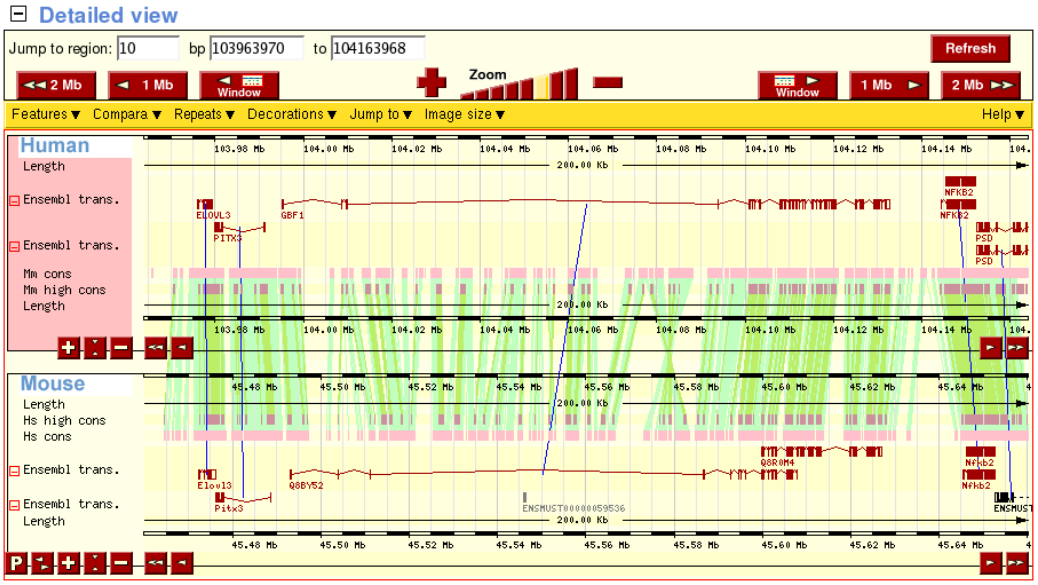


Figure 5.1: **Human *GBF1* loci genomic region and its counterpart in mouse.** Detailed view of the human/mouse homology block at the *GBF1* loci (human chromosome 10, between 103963970 bp and 104163968 bp) as shown by the **MultiContig View** page on ENSEMBL. Orthologous genes are connected by a blue line. Pink boxes represent the homologous regions between both species projected into each sequence. Those homology hits are connected by green shaded regions. Differences at sequence level, such as insertions/deletions and inversions, are easily spotted with that green shading.

*sources'* drop-down menu. A syntenic regions navigation tool is available at ENSEMBL (see upper right panel from Figure 1.4 and Clamp *et al.* 2003). It was initially developed for human-mouse comparisons but it has been extended to include further species comparisons, i.e. rat, chicken, fruit-fly and so on. An example of the MultiContig viewer is shown in Figure 5.1.

Finally, gene-predictions can also be retrieved from the UCSC browser by switching on the appropriate options in the drop-down menus from the navigation form. In addition, the UCSC GENOME BROWSER features a novel database named ZOO, on which analyses made over a set of homologous targeted genomic sequences from 12 species [Thomas *et al.*, 2003] are published. Furthermore, depending on which genome is being browsed, the annotated gene features can be combined with the results of a mixture of whole-genome precomputed alignments from `BLAT` [Kent, 2002], `BLASTZ` [Schwartz *et al.*, 2003b], `WABA` [Kent and Zahler, 2000], and/or `Exofish` ecores [Jaillon *et al.*, 2003].

Current genome browsers, however, lack the ability to clearly represent information across genomes. A multiple species genome browser system should be able to represent many-to-many genomic alignments as an alignment among genomes. Moreover, it is difficult for most systems to develop a representation that natively compares whole-genomes and not only targeted regions. In this regard, the `K-Browser` [Chakrabarti and Pachter, 2004] has been designed around two principles: genome symmetry —every genome con-

tains useful information, thus a browsing solution should not limit the ability to navigate within or across genomes—; and genome homology —related genomes have evolved from a common ancestor and these evolutionary relationships should be accurately reflected in both the representation and the visualization of information. The `K-Browser` takes as input a specific region in a specific genome and produces a set of images that succinctly represents the requested region and all orthologous regions. It can also provide the underlying multiple alignments.

### 5.1.2 Annotation workbenches

A myriad of sequence annotation workbenches have been developed during the last decade, but only a few have taken into account the comparative genomics perspective into their design. In this regard, it is worthwhile to cite `Alfresco` [Jareborg and Durbin, 2000], `genomeSCOUT` [Suter-Crazzolara and Kurapkat, 2000], `ERGO` [Overbeek *et al.*, 2003], `Theatre` [Edwards *et al.*, 2003], and `FamilyJewels` [Brown *et al.*, 2002]. Developed since the mid-nineties, these workbenches established the basis of modern annotation tools such as `Artemis` [Rutherford *et al.*, 2000] and `Apollo` [Lewis *et al.*, 2002]. The latter provides a human-mouse synteny panel that allows the user to compare and edit annotations for these two species. The `Artemis Comparison Tool` (`ACT`), based on the `Artemis` implementation, displays the results of a `BLASTN/TBLASTX` search along the sequence with the corresponding annotations. These tools are mainly employed by human curators for the reannotation labour necessary to improve the raw annotations from automated pipelines. In this regard, the `Otter` annotation system [Searle *et al.*, 2004] extends the ENSEMBL database schema to integrate manual annotations by exchanging data in `XML` format between machines and allowing multiuser annotation. Two annotation tools have `Otter` client support, `Apollo` and `Otter/Lace`. `Otter/Lace` is a `perl` wrapper round the `AceDB` annotation editor, and it is currently used by the Human and Vertebrate Annotation (HAVANA) group curators at the Sanger Center. A review of several annotation browsers from the end-user viewpoint can be found in Fortna and Gardiner [2001].

### 5.1.3 Tools for visualizing alignments

Despite the trend to move from the pair-wise sequence comparison tools (two species) to the comparison of multiple sequences (many species) [Miller, 2001], there is still a niche for pair-wise comparison tools. The main reason is that such one-to-one alignments provide an informative comparison, but with the lowest complexity of interpretation.

Pair-wise comparisons can be done in several ways. A `dot-plot` or comparison matrix simultaneously displays all the structures in common between two sequences [Fitch, 1966; Gibbs and McIntyre, 1970]. In this, the conserved, repeated or inverted repeated segments are clearly visualized. Accordingly, `dot-plot` like diagrams have been extensively used to define the conserved segments of large genomic sequences, and also to explore the repeat-rich regions [Waterston *et al.*, 2002]. These conserved segments can be further analyzed with, for instance, the `PiP`-like tools described below. Among the pair-wise tools, one can cite `DIAGON` [Staden, 1982], `LFASTA` [Pearson and Lipman, 1988], `Lav` [Schwartz *et al.*, 1991], `Blixem` [Sonnhammer and Durbin, 1994], `Dotter` [Sonnhammer and Durbin, 1995], `Laj` [Wilson *et al.*, 2001], `GenoPix2D` [Cannon *et al.*, 2003], or `NOPTALIGN` [Smoot *et al.*,

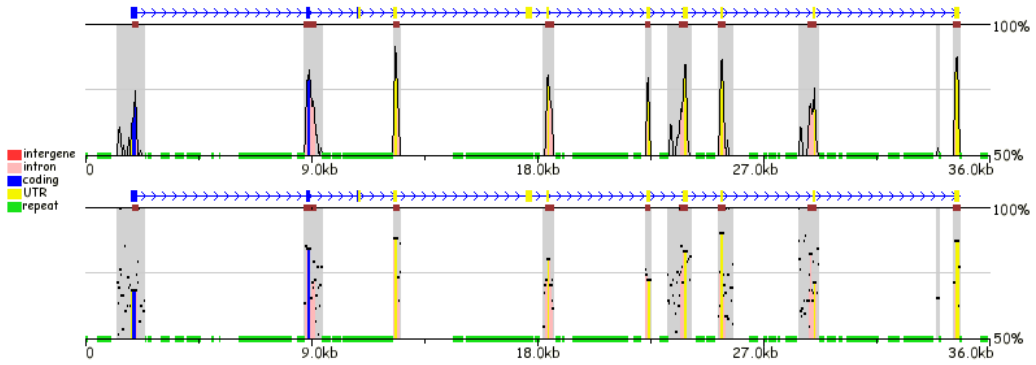


Figure 5.2: **A comparison of PiP-plots versus Smooth-plots.** Sequence between 95992 kb and 96028 kb from chromosome 8 was compared against its homologous mouse genomic sequence using the `zPicture` web server [Ovcharenko *et al.*, 2004a]. The same underlying alignment, computed with `BLASTZ` [Schwartz *et al.*, 2003b], is visualized as a pip-plot in the upper panel and as a smooth-plot in the bottom one, emulating the output from `PipMaker` [Schwartz *et al.*, 2000] and `VISTA` [Mayor *et al.*, 2000] respectively. Pip-plots display all the short ungapped alignments as black horizontal lines, while smooth-plots are constructed using, for each nucleotide, a 100 bp sliding window in which sequence identity is averaged. Boxes along the 100% identity baseline represent evolutionary conserved regions (ECRs), while those on the 50% baseline pinpoint the masked regions in which repetitive elements were found. *NM152416* gene structure (human hypothetical protein MGC40214) is depicted above the identity plots in both panels.

2004]. The `EMBOSS` suite [Olson, 2002; Rice *et al.*, 2000] provides several programs of this kind (`dottup`, `dotmatcher`, `dotpath` and `polydot`). The `gff2aplot` [Abril *et al.*, 2003] program falls within this software family. See Figure 5.8 on page 175 (Figure 1 on page 2478 of Abril *et al.* 2003), for examples of its output. Its major strength is to be independent of any alignment algorithm, as far as the input can be translated into the General Feature Format (`GFF`, see page 214, on Web Glossary). `TriCross` [Ray *et al.*, 2001], which extends the `dot-plot` concept to the simultaneous analysis of three sequences, renders the results in a three-dimensional Virtual Reality Modeling Language (VRML) representation.

Then again, those sequence comparisons can be represented in a more compact linear fashion. Several tools can be grouped here: `LAPS` (Local Alignment to POSTSCRIPT, Schwartz *et al.* 1991), `LalnView` [Duret *et al.*, 1996], and `GenomePixelizer` [Kozik *et al.*, 2002]. The latter has been applied to visualize inter- and intra-chromosomal segmental duplications in genomic sequences [Cheung *et al.*, 2003; Estivill *et al.*, 2002].

Another class of programs, so called `PiP`-like because they produce Percentage Identity Plots, were designed to represent data from underlying sequence alignment algorithms. Basically, they consist in a compact display of the results of aligning one sequence to one or more sequences, where the positions (in the first sequence) and the score of the alignment segments are plotted, along with icons for features in the first sequence. `MUMmer` [Delcher *et al.*, 1999; Kurtz *et al.*, 2004], `PipMaker` [Schwartz *et al.*, 2000], `Multi-PipMaker` [Schwartz *et al.*, 2003a], `VISTA` [Mayor *et al.*, 2000], `CGAT` [Lund *et al.*, 2000], and `SynPlot` [Göttgens *et al.*, 2001], are among these tools. They do not fit into the gene-prediction paradigm *sensu strictu*; in any case, they have proven their potential in finding and/or re-

fining protein-coding regions [Jang *et al.*, 1999; Pennacchio *et al.*, 2001; Reisman *et al.*, 2001; Tompa, 2001; Toyoda *et al.*, 2002; Wilson *et al.*, 2001], as well as the conserved non-coding sequences around them which may play a role in gene expression [Dubchak *et al.*, 2000; Gilligan *et al.*, 2002; Göttgens *et al.*, 2000, 2001; Hardison, 2000; Hardison *et al.*, 1997; Loots *et al.*, 2000; Oeltjen *et al.*, 1997; Ovcharenko and Loots, 2003b]. They even have been found useful in the analysis of the distribution of repetitive sequences [Chiaromonte *et al.*, 2001; Yuhki *et al.*, 2003]. See Figure 5.2 for an example of what can be done with these tools.

These programs have been reviewed in a number of occasions [Frazer *et al.*, 2003; Pennacchio and Rubin, 2001; Pennacchio, 2003; Pennacchio and Rubin, 2003; Thomas and Touchman, 2002; Ureta-Vidal *et al.*, 2003]. In Frazer *et al.* [2003], there is a good example of what can be achieved using those tools; it can be taken as a complete protocol describing how to retrieve the data sets, to prepare the sequences and complementary files, to compare them through the corresponding web browsers, and finally how to interpret their graphical outcomes. Two web servers have been deployed in an attempt to make those tools more interactive for the average user: the `ECR-Browser` (a navigation tool for Evolutionary Conserved Regions: Ovcharenko and Loots 2003a; Ovcharenko *et al.* 2004b) and `zPicture` (Ovcharenko *et al.* 2004a, and Figure 5.2). On the other hand, a comparison of the different alignment algorithm approaches behind some of those programs can be found in Ureta-Vidal *et al.* [2003]. `EnteriX` [Florea *et al.*, 2003] takes advantage of those principles to compare complete genomes of enteric bacteria. Nevertheless, the application of this algorithm to larger eukaryotic sequences, for instance to apply them in a whole-genome analysis, requires a large amount of computational resources. One drawback of these tools is that their input often needs to be defined within conserved genomic segments, for instance, regions of synteny between chromosomes, because sequence rearrangements can dramatically distort the corresponding alignments.

Some tools have been specifically devised for the analysis of regulatory regions, although they can use a similar approach that the one described above for programs such as `PipMaker` or `VISTA`. `ReguloGram` visualizes the density of co-occurring cis-element transcription factor binding sites measured within a 200 bp moving window through phylogenetically conserved regions. Within a high-scoring region, the relative arrangement of shared cis-elements within compositionally similar binding site clusters can be depicted then with `TraFacGram` [both, `ReguloGram` and `TraFacGram`, were described in Jegga *et al.* 2002]. `ConSite` [Lenhard *et al.*, 2003; Sandelin *et al.*, 2004] is a graphical web application that takes advantage of the phylogenetic footprinting to report putative transcription factor binding sites situated in conserved regions and located as pairs of sites in equivalent positions in alignments between two orthologous sequences.

Apart from raw sequence genomic comparisons, one might be interested in examining the gene distribution among two or more species. One of the first approaches to this was the `Oxford Grid` [Edwards, 1991]. Coordinates for successive chromosomes of two species were drawn along two axes as in a `dot-plot`, homologous loci were then depicted as dots. Pair-wise similarity scores have also been used to estimate closer neighbour relationships when analyzing many genomes as a whole. Those results have been commonly represented as pie charts or Venn diagrams [Blaxter *et al.*, 2002; Wood *et al.*, 2002], but this leads to an static view of the sequence relationships. A more dynamic view is the one offered by the `SimiTri` tool [Parkinson and Blaxter, 2003], in which the simultaneous display and analysis of the similarity relationships of the dataset of interest, in example the complete proteome of an organism, relative to three other databases can be achieved.

### 5.1.4 Tools for visualizing annotations

One of the first graphic programs devoted to determine the function of nucleic acid sequences was ANALYSEQ [Staden, 1984b], and its focus on finding coding-exons. In this context it is also worth mentioning, the RSVP package [Searls, 1993]—in which sequence analysis algorithms were encoded using the POSTSCRIPT language, and thus, could in principle be performed by the printer.

Although not necessarily comparative based, several gene-prediction tools display graphical output either through a web server or as a standalone software. This graphical output generally consists in colored shapes corresponding to coding exons or other functional elements along the genomic axis. This approach was notably pioneered in X-windows systems by GeneModeler [Fields and Soderlund, 1990] as an standalone platform, and by XGRAIL [Uberbacher and Mural, 1991] as a network-based client-server architecture. In all these cases, the visualization capabilities are strongly tied to a particular gene finding algorithm. More general and algorithm independent visualization tools have been also developed. This task has been facilitated by the general acceptance of GFF format, and its derivatives (see page 214 from Web Glossary), as a standard for genomic features annotations. gff2ps [Abril and Guigó, 2000], for instance, displays GFF files assuming that the file itself carries enough formatting information. Additional flexibility comes from the customization files defined by the user, and also because of the POSTSCRIPT output and the ability to handle multiple page formats. Examples of its output can be seen on Figure 5.4 on page 160 (Figure 1 on page 744 of Abril and Guigó 2000). Those people looking for an interactive and extensible visualization program, should take a look to the GUPPY system [Ueno *et al.*, 2003], implemented over the Lua scripting language [Ierusalimschy *et al.*, 1996]. Finally, it is worth to cite Sockeye [Montgomery *et al.*, 2004], a three-dimensional Java-based application that has been developed recently to compactly display comparative analyses.

Initial developments of circular maps were devoted to draw restriction maps over plasmid sequences, then were applied to represent bacterial circular chromosomes. However, linear maps are more appropriate for visualizing genomic features, and for comparative studies in particular —as Tufte [2001] claims, any distortion when plotting data that will lead to misinterpretation should be avoided. Among the tools developed to visualize genetic maps one can cite gRanch [Wada *et al.*, 1997], mapmerge [Nadkarni, 1998], mapplet [Jungfer and Rodriguez-Tome, 1998], FitMaps+ShowMap [Graziano and Arus, 2002], NCBI's MapViewer [Wheeler *et al.*, 2002], or cMap [Fang *et al.*, 2003]. Applications to produce circular or linear representations of genomic features were provided by several software packages; such as GCG [Devereux *et al.*, 1984], Staden [Staden *et al.*, 2000], SRS [Etzold and Argos, 1993], SEALS [Walker and Koonin, 1997], or EMBOSS [Olson, 2002; Rice *et al.*, 2000]. Further examples of this kind of tools are GenomePlot [Gibson and Smith, 2003], GenoMap [Sato and Ehira, 2003], and ZoomMap+MappetShow [Barillot *et al.*, 1999].

Finally, it is worth to mention a set of visualization tools that are useful in a more specific analysis context. For instance, graph-based display using exons as nodes produces more compact pictures of alternative splicing exonic structures. This approach has been implemented in SpliceNest [Coward *et al.*, 2002; Krause *et al.*, 2002], and SplicingGraphs [Heber *et al.*, 2002]. Software that analyses the repeats distribution and composition on genomic sequences often includes a graphical interface, in which repetitive regions are linked by using straight lines or arcs. In this category one can find MiroPEATS [Parsons,

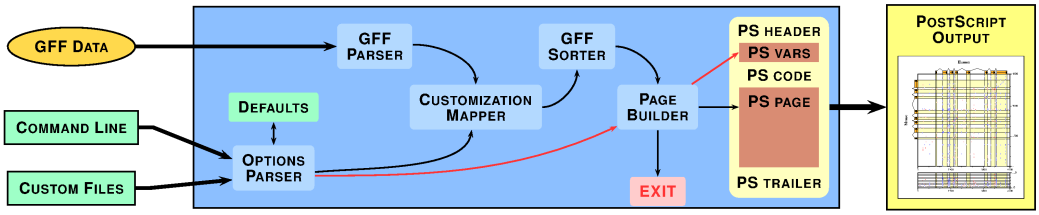


Figure 5.3: **Flow chart of internal main processes for `gff2ps` and `gff2aplot`.** Both tools were devised as standard `Unix` programs, they work as filters that process an input stream, in GFF, to produce an output stream, in POSTSCRIPT. Customization is provided by user-defined files or through command-line switches. Those settings are integrated with the input data to set a variables defining block and to bring forth the corresponding feature function calls in the page section of a POSTSCRIPT document. Such file is able to render the annotation plots thanks to specific POSTSCRIPT functions defined in its code section. The output document is self-contained, it has the data to plot and the commands to draw it.

1995], `REPUS` [Babenko *et al.*, 1999], `REPuter` [Kurtz and Schleiermacher, 1999], `Genome cryptographer` [Cleaver *et al.*, 2003], `Exact Match Annotator` [Healy *et al.*, 2003], `FORRepeats` [Lefebvre *et al.*, 2003], `GenomeComp` [Yang *et al.*, 2003], or `ADplot` [Taneda, 2004].

## 5.2 `gff2ps`: Visualizing Genomic Features

There are two major systems for representing graphic information on computers: raster and vector graphics. In raster graphics, an image is represented as a rectangular array of picture elements or pixels. Each pixel is represented either by its RGB color values or as an index into a list of colors. This series of pixels, also called a bitmap, is often stored in a compressed format. Since most display devices are also raster devices, displaying such a bitmap requires a viewer program to do little more than uncompress and transfer that bitmap to the screen. In a vector graphic system, an image is described as a series of geometric shapes. Rather than receiving a finished set of pixels, a vector viewing program, often also known as the interpreter, receives commands to draw shapes at specified sets of coordinates. In other words, it translates graphical objects into a virtual grid that is then projected in the corresponding raster device at a given fixed resolution. Although they are not as popular as raster graphics, vector graphics have one feature that makes them invaluable in many applications, they can be scaled without loss of image quality in the final rendering. This also means that once you generated an image you can zoom into any region of it to observe further details, which is done by the interpreter. To achieve the same with bitmaps requires to generate each zoom separately. This may not involve as much CPU time as needed by the vector graphics interpreter, but it is not efficient in storage space. Most of those arguments lead us to opt for a vector graphics programming language when developing most of our visualization tools, despite such systems do not have the same acceptance or support than a bitmap one. In any case, a vector graphic can be converted into a bitmap without loosing information while the other way around is not

always true.

Introduced in 1985, POSTSCRIPT is the name of a computer programming language developed originally by *Adobe Systems Incorporated* to communicate high-level graphic information to digital laser printers [Adobe S.I., 1999]. It is a flexible, compact, and powerful language both for expressing graphic images in a device-independent manner and for performing general programming tasks. The three most important aspects of the POSTSCRIPT programming language are that it is interpreted, that it is stack-based, and that it uses a unique data structure called a dictionary. The dictionary mechanism gives the POSTSCRIPT language a flexible, extensible base, and the fact that the language is interpreted and uses a stack model means that programs can be of arbitrary length and complexity. Since very little overhead is necessary to execute the programs, they can be interpreted directly from the input stream, which means that no memory restriction is placed on a POSTSCRIPT program other than memory allocated by the program itself [Reid, 1996]. Those programming features make the POSTSCRIPT language suitable for developing visualization tools in the genomic annotation field.

The combination of specific purpose POSTSCRIPT-generating scripts previously implemented by me, along with the establishment of annotation interchange formats by the genome annotation community, such as `GFF`, led to the definition of the initial `gff2ps` draft. `gff2ps` was initially conceived in 1999 as a general drawing tool to represent gene-finding annotations from different sources. The program assumes that the `GFF` input itself carries enough formatting information. Genomic annotations have a hierarchical structure inherent to the biological features represented by them. For instance, a sequence may contain several genes, which are made of one or more exons, which are delimited by different signals, such splice sites and initiation or stop codons. Such structure is encoded in the `GFF` records by settling a fixed feature attribute on each field, i.e. the initial and terminal coordinates, a score, the group belonging to, and so on (see an example of the `GFF` record structure on page 214 from Web Glossary). `gff2ps` internal flow chart is depicted in Figure 5.3. Two main code blocks define this program: the `gawk` input filter and the POSTSCRIPT drawing functions. The `gawk` code block is in charge of processing the `GFF` input records and the associated customization parameters, to produce specific POSTSCRIPT-function calls for that data. Then, it embeds that piece of code in the POSTSCRIPT document, which is by itself another code block.

Notable applications of `gff2ps` include the whole-genome annotation maps for several species —*Drosophila melanogaster* (Adams *et al*. 2000; see section 5.2.2 on page 161 and Figure 5.5), human (Venter *et al*. 2001; see section 5.2.3 on page 165 and Figure 5.6), the mouse chromosome 16 [Mural *et al*., 2002], *Anopheles gambiae* (Holt *et al*. 2002; see section 5.2.4 on page 169 and Figure 5.7), and *Blochmannia floridanus* [Gil *et al*., 2003]. Figure 3.8 on page 91 (Figure 2 on page 1142 of Guigó *et al*. [2003]) and bottom panel of Figure 5.10 are examples of using `gff2ps` in the comparative genomics context.

### 5.2.1 Abril and Guigó, *Bioinformatics*, 16(8):743–744, 2000

**PubMed Accession:**

http://www.ncbi.nlm.nih.gov/entrez/query.fcgi?cmd=Retrieve&db=PubMed&list_uids=11099262&dopt=Abstract

**Journal Abstract:**

http://bioinformatics.oupjournals.org/cgi/content/abstract/16/8/743

**Program Home Page:**

http://genome.imim.es/software/gfftools/GFF2PS.html

BIOINFORMATICS APPLICATIONS NOTE Vol. 16 no. 8 2000
Pages 743–744

# gff2ps: visualizing genomic annotations

*Josep F. Abril* and Roderic Guigó*

*Grup de Recerca en Informàtica Mèdica, Institut Municipal d'Investigació Mèdica (IMIM), Universitat Pompeu Fabra (UPF), C/ Dr. Aiguader, 80. 08003—Barcelona, Spain*

Received on December 15, 1999; revised on February 18, 2000; accepted on February 24, 2000

**Abstract**

***Summary:*** *gff2ps is a program for visualizing annotations of genomic sequences. The program takes the annotated features on a genomic sequence in GFF format as input, and produces a visual output in PostScript. While it can be used in a very simple way, it also allows for a great degree of customization through a number of options and/or customization files.*

***Availability:*** *gff2ps is freely available at http://www1.imim.es/~jabril/GFFTOOLS/GFF2PS.html*

***Contact:*** *jabril@imim.es*

***Supplementary information:*** *http://www1.imim.es/~jabril/GFFTOOLS/GFF2PS.html*

As genomic sequences accumulate, visualization tools are becoming essential for the analysis and interpretation of sequence data. Recently, a format has been proposed for specifying genes and other features associated with genomic sequences, the General Feature Format (GFF, proposed by Durbin and Haussler, http://www.sanger.ac.uk/Software/GFF/). In GFF each feature on the genomic sequence is described in a single-line record that essentially specifies the type and position of the feature on the genomic sequence. A grouping field allows to define sets of features within the GFF file. A number of tools have already been developed to deal with GFF files (see also at GFF URL). We have developed a tool, gff2ps, which allows for visualization of GFF files. gff2ps is a program written in GNU awk (http://www.gnu.org/software/gawk/gawk.html) and PostScript, running on UNIX platforms, that generates a PostScript file given a GFF file.

The page description language PostScript is recognized as the current *de facto* industry standard for high-quality printing. PostScript provides both a printer-independent and a computer-system-independent means to describe integrated text and graphics, which can be put out on a variety of printers, plotters and workstation screens. The generation of PostScript output is very common in sequence analysis tools. Notably, we can cite the RSVP package by Searls (1993).

*To whom correspondence should be addressed.

gff2ps plots the features from different sources specified on a GFF file in a number of parallel rows (the so-called tracks here) along the length of the output page(s) (see Figure 1 for examples). Actually these are 'virtual' pages (the so-called blocks here) allowing for several blocks to be included in a single physical page, or for splitting a single block in a number of physical pages. Features can be plotted in a variety of colors and shapes and those grouped together can be visually linked in a number of ways.

gff2ps allows for a substantial amount of customization through command line options, and configuration files. However, meaningful output in most cases, meaningful output can be obtained without the need of any customization, by simply calling gff2ps with the input GFF file. gff2ps assumes, by default, that the GFF file itself carries enough formatting information. The examples in the figure show the versatility of gff2ps. Additional examples can be found at the gff2ps web page, as well as a detailed User Manual.

One of the main advantages of gff2ps is its ability to manage many physical page formats, including user-defined ones. This allows, for instance, the generation of poster size genomic maps. As an example, we used gff2ps to display at the ISMB'99 meeting, the predictions submitted to the Genome Annotation Assessment Project (GASP1) (http://www.fruitfly.org/GASP1/). The GASP1 plot was generated on three B0 size posters from a GFF file of over 50 000 feature records. The program has also been used to obtain the poster figures of recent relevant papers in genomic research (Adams *et al.*, 2000; Reese, 2000).

**Acknowledgments**

We thank Moisès Burset and Genís Parra (IMIM) for their useful comments, Richard Bruskiewich (Sanger Center) for his helpful hints on the GFF format, also Elena Casacuberta and Amparo Monfort (CSIC) for motivating us to develop this tool. This work is supported by a grant from Plan Nacional de I+D, BIO98-0443-C02-01, and from a fellowship to J.A. from the Instituto de Salud Carlos III, 99/9345.

 

**J.F.Abril** and **R.Guigó**

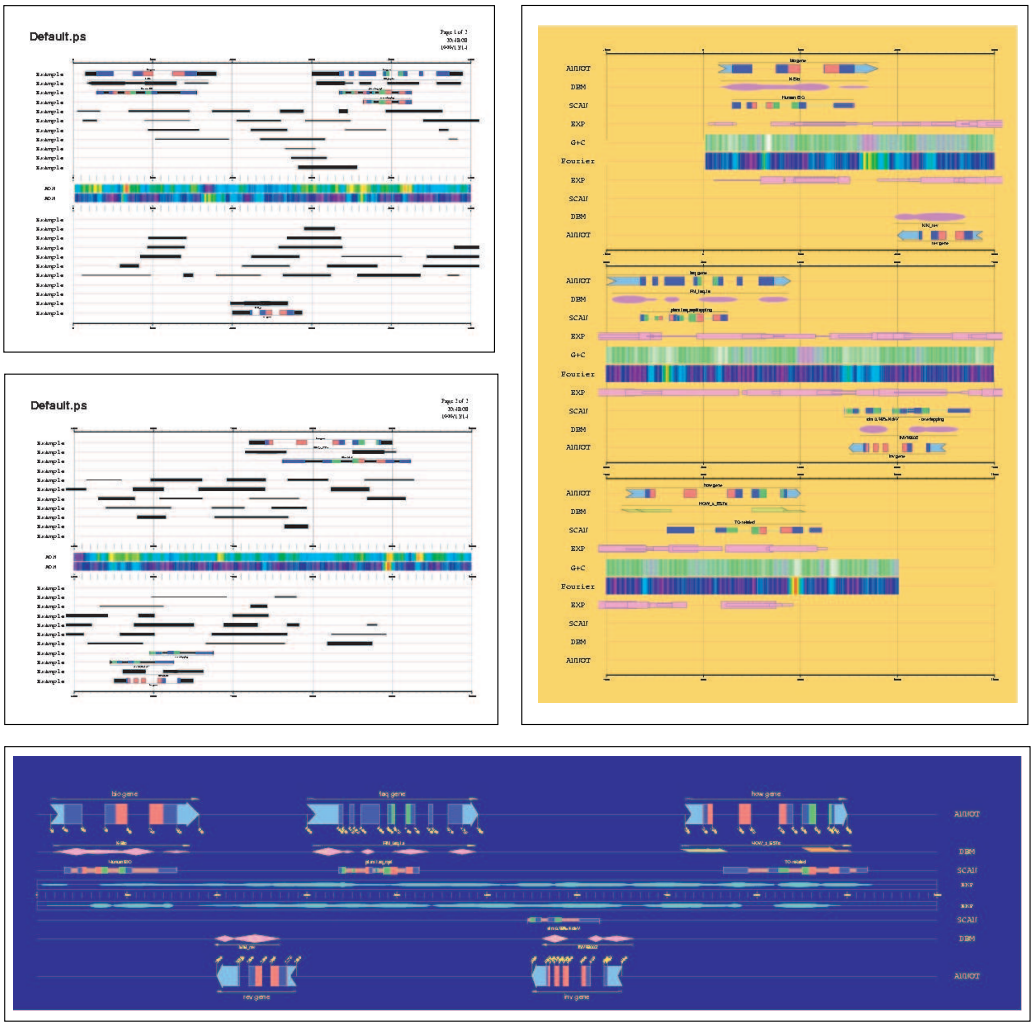


**Fig. 1.** Different views of the same input GFF file, using `gff2ps` with different configuration files and command-line options. The top two pages on the left were obtained using the default configuration (specifying only the number of pages, and output media size). By default, `gff2ps` makes a number of assumptions. Among others: (i) Features grouped from the GFF input file (ungrouped features are treated as a single element group) within the same source are plotted in the minimum number of tracks, guaranteeing that different groups do not overlap. (ii) The plot is fitted into a single block (assuming the length of the sequence to be the end of the most downstream feature), and the block is printed into a single physical page. (iii) Features for which the frame is specified are plotted using a two color code schema. The upstream half of the graphical element representing the frame of the feature and the downstream half the complement modulus 3 of its remainder. This is useful to check frame consistency between adjacent features (for instance, predicted exons). Two adjacent features are frame compatible when the color of the downstream half of the upstream feature matches the color of the upstream half of the downstream feature. (iv) If a score is provided for a feature, the feature is plotted with a height proportional to its score. (v) Obviously, all these default options can be overridden by the user. Notes: The real size color plots, the input GFF files, the configuration files and command line options used in each case, as well as additional examples can be found at: http://www1.imim.es/~jabril/GFFTOOLS/GFF2PS-Snapshots.html.

## References

Adams,M.D. and Abril,J.F. *et al.* (2000) The genome sequence of *Drosophila melanogaster*. *Science*, **287**(5461), 2185–2195.

Reese,M.G., Hartzell,G., Harris,N.L., Ohler,U., Abril,J.F. and Lewis,S.E. (2000) Genome annotation assessment in *Drosophila melanogaster*. *Genome Res.*, **10**, 483–501.

Searls,D.B. (1993) Doing sequence analysis with your printer. *Comput. Appl. Biosci.*, **9**(4), 421–426.

### 5.2.2 Adams *et al*, *Science*, 287(5461):2185–2195, 2000

**PubMed Accession:**

http://www.ncbi.nlm.nih.gov/entrez/query.fcgi?cmd=Retrieve&db=PubMed&list_uids=10731132&dopt=Abstract

**Journal Abstract:**

http://www.sciencemag.org/cgi/content/abstract/287/5461/2185

**Companion Poster:**

See Figure 5.5 and the following URLs:
http://www.sciencemag.org/feature/data/genomes/2000/drosophila.shl
http://genome.imim.es/references/genome_maps/2000_Science_v287_i5461_p2185_fig4_FlyGenome.ps.gz

THE *DROSOPHILA* GENOME
REVIEW

# The Genome Sequence of *Drosophila melanogaster*

Mark D. Adams,[1*] Susan E. Celniker,[2] Robert A. Holt,[1] Cheryl A. Evans,[1] Jeannine D. Gocayne,[1] Peter G. Amanatides,[1] Steven E. Scherer,[3] Peter W. Li,[1] Roger A. Hoskins,[2] Richard F. Galle,[2] Reed A. George,[2] Suzanna E. Lewis,[4] Stephen Richards,[2] Michael Ashburner,[5] Scott N. Henderson,[1] Granger G. Sutton,[1] Jennifer R. Wortman,[1] Mark D. Yandell,[1] Qing Zhang,[1] Lin X. Chen,[1] Rhonda C. Brandon,[1] Yu-Hui C. Rogers,[1] Robert G. Blazej,[2] Mark Champe,[2] Barret D. Pfeiffer,[2] Kenneth H. Wan,[2] Clare Doyle,[2] Evan G. Baxter,[2] Gregg Helt,[6] Catherine R. Nelson,[4] George L. Gabor Miklos,[7] Josep F. Abril,[8] Anna Agbayani,[2] Hui-Jin An,[1] Cynthia Andrews-Pfannkoch,[1] Danita Baldwin,[1] Richard M. Ballew,[1] Anand Basu,[1] James Baxendale,[1] Leyla Bayraktaroglu,[9] Ellen M. Beasley,[1] Karen Y. Beeson,[1] P. V. Benos,[10] Benjamin P. Berman,[2] Deepali Bhandari,[1] Slava Bolshakov,[11] Dana Borkova,[12] Michael R. Botchan,[13] John Bouck,[3] Peter Brokstein,[4] Phillipe Brottier,[14] Kenneth C. Burtis,[15] Dana A. Busam,[1] Heather Butler,[16] Edouard Cadieu,[17] Angela Center,[1] Ishwar Chandra,[1] J. Michael Cherry,[18] Simon Cawley,[19] Carl Dahlke,[1] Lionel B. Davenport,[1] Peter Davies,[1] Beatriz de Pablos,[20] Arthur Delcher,[1] Zuoming Deng,[1] Anne Deslattes Mays,[1] Ian Dew,[1] Suzanne M. Dietz,[1] Kristina Dodson,[1] Lisa E. Doup,[1] Michael Downes,[21] Shannon Dugan-Rocha,[3] Boris C. Dunkov,[22] Patrick Dunn,[1] Kenneth J. Durbin,[3] Carlos C. Evangelista,[1] Concepcion Ferraz,[23] Steven Ferriera,[1] Wolfgang Fleischmann,[5] Carl Fosler,[1] Andrei E. Gabrielian,[1] Neha S. Garg,[1] William M. Gelbart,[9] Ken Glasser,[1] Anna Glodek,[1] Fangcheng Gong,[1] J. Harley Gorrell,[3] Zhiping Gu,[1] Ping Guan,[1] Michael Harris,[1] Nomi L. Harris,[2] Damon Harvey,[4] Thomas J. Heiman,[1] Judith R. Hernandez,[3] Jarrett Houck,[1] Damon Hostin,[1] Kathryn A. Houston,[2] Timothy J. Howland,[1] Ming-Hui Wei,[1] Chinyere Ibegwam,[1] Mena Jalali,[1] Francis Kalush,[1] Gary H. Karpen,[21] Zhaoxi Ke,[1] James A. Kennison,[24] Karen A. Ketchum,[1] Bruce E. Kimmel,[2] Chinnappa D. Kodira,[1] Cheryl Kraft,[1] Saul Kravitz,[1] David Kulp,[6] Zhongwu Lai,[1] Paul Lasko,[25] Yiding Lei,[1] Alexander A. Levitsky,[1] Jiayin Li,[1] Zhenya Li,[1] Yong Liang,[1] Xiaoying Lin,[26] Xiangjun Liu,[1] Bettina Mattei,[1] Tina C. McIntosh,[1] Michael P. McLeod,[3] Duncan McPherson,[1] Gennady Merkulov,[1] Natalia V. Milshina,[1] Clark Mobarry,[1] Joe Morris,[6] Ali Moshrefi,[2] Stephen M. Mount,[27] Mee Moy,[1] Brian Murphy,[1] Lee Murphy,[28] Donna M. Muzny,[3] David L. Nelson,[3] David R. Nelson,[29] Keith A. Nelson,[1] Katherine Nixon,[2] Deborah R. Nusskern,[1] Joanne M. Pacleb,[2] Michael Palazzolo,[2] Gjange S. Pittman,[1] Sue Pan,[1] John Pollard,[1] Vinita Puri,[1] Martin G. Reese,[4] Knut Reinert,[1] Karin Remington,[1] Robert D. C. Saunders,[30] Frederick Scheeler,[1] Hua Shen,[3] Bixiang Christopher Shue,[1] Inga Sidén-Kiamos,[11] Michael Simpson,[1] Marian P. Skupski,[1] Tom Smith,[1] Eugene Spier,[1] Allan C. Spradling,[31] Mark Stapleton,[2] Renee Strong,[1] Eric Sun,[1] Robert Svirskas,[32] Cyndee Tector,[1] Russell Turner,[1] Eli Venter,[1] Aihui H. Wang,[1] Xin Wang,[1] Zhen-Yuan Wang,[1] David A. Wassarman,[33] George M. Weinstock,[3] Jean Weissenbach,[14] Sherita M. Williams,[1] Trevor Woodage,[1] Kim C. Worley,[3] David Wu,[1] Song Yang,[2] Q. Alison Yao,[1] Jane Ye,[1] Ru-Fang Yeh,[19] Jayshree S. Zaveri,[1] Ming Zhan,[1] Guangren Zhang,[1] Qi Zhao,[1] Liansheng Zheng,[1] Xiangqun H. Zheng,[1] Fei N. Zhong,[1] Wenyan Zhong,[1] Xiaojun Zhou,[3] Shiaoping Zhu,[1] Xiaohong Zhu,[1] Hamilton O. Smith,[1] Richard A. Gibbs,[3] Eugene W. Myers,[1] Gerald M. Rubin,[34] J. Craig Venter[1]

The fly *Drosophila melanogaster* is one of the most intensively studied organisms in biology and serves as a model system for the investigation of many developmental and cellular processes common to higher eukaryotes, including humans. We have determined the nucleotide sequence of nearly all of the ~120-megabase euchromatic portion of the *Drosophila* genome using a whole-genome shotgun sequencing strategy supported by extensive clone-based sequence and a high-quality bacterial artificial chromosome physical map. Efforts are under way to close the remaining gaps; however, the sequence is of sufficient accuracy and contiguity to be declared substantially complete and to support an initial analysis of genome structure and preliminary gene annotation and interpretation. The genome encodes ~13,600 genes, somewhat fewer than the smaller *Caenorhabditis elegans* genome, but with comparable functional diversity.

The annotated genome sequence of *Drosophila melanogaster*, together with its associated biology, will provide the foundation for a new era of sophisticated functional studies (*1*–*3*). Because of its historical importance, large research community, and powerful research tools, as well as its modest genome size, *Drosophila* was chosen as a test system to explore the applicability of whole-genome shotgun (WGS) sequencing for large and complex eukaryotic genomes (*4*). The groundwork for this project was laid over many years by the fly research community, which has molecularly characterized ~2500 genes; this work in turn has been supported by nearly a century of genetics (*5*). Since *Drosophila* was chosen in 1990 as one of the model organisms to be studied under the auspices of the federally funded Human Genome Project, genome projects in the United States, Europe, and Canada have produced a battery of genome-wide resources (Table 1). The Berkeley and European *Drosophila* Genome Projects (BDGP and EDGP) initiated genomic sequencing (Tables 1 to 3) and finished 29 Mb. The bacterial artificial chromosome (BAC) map and other genomic resources available for *Drosophila* serve both as an independent confirmation of the assembly of data from the shotgun strategy and as a set of resources for further biological analysis of the genome.

The *Drosophila* genome is ~180 Mb in size, a third of which is centric heterochromatin (Fig. 1). The 120 Mb of euchromatin is on two large autosomes and the X chromosome; the small fourth chromosome contains only ~1 Mb of euchromatin. The heterochromatin consists mainly of short, simple sequence elements repeated for many megabases, occasionally interrupted by inserted transposable elements, and tandem arrays of ribosomal RNA genes. It is known that there are small islands of unique sequence embedded within heterochromatin—for example, the mitogen-activated protein kinase gene *rolled* on chromosome 2, which is flanked on each side by at least 3 Mb of heterochromatin. Unlike the *C. elegans* genome, which can be completely cloned in yeast artificial chromosomes (YACs), the simple sequence repeats are not stable in YACs (*6*) or other large-insert cloning sys-

tems. This has led to a functional definition of the euchromatic genome as that portion of the genome that can be cloned stably in BACs. The euchromatic portion of the genome is the subject of both the federally funded *Drosophila* sequencing project and the work presented here. We began WGS sequencing of *Drosophila* less than 1 year ago, with two major goals: (i) to test the strategy on a large and complex eukaryotic genome as a prelude to sequencing the human genome, and (ii) to provide a complete, high-quality genomic sequence to the *Drosophila* research community so as to advance research in this important model organism.

WGS sequencing is an effective and efficient way to sequence the genomes of prokaryotes, which are generally between 0.5 and 6 Mb in size (*7*). In this strategy, all the DNA of an organism is sheared into segments a few thousand base pairs (bp) in length and cloned directly into a plasmid vector suitable for DNA sequencing. Sufficient DNA sequencing is performed so that each base pair is covered numerous times, in fragments of ~500 bp. After sequencing, the fragments are assembled in overlapping segments to reconstruct the complete genome sequence.

In addition to their much larger size, eukaryotic genomes often contain substantial amounts of repetitive sequence that have the potential to interfere with correct sequence assembly. Weber and Myers (*8*) presented a theoretical analysis of WGS sequencing in which they examined the impact of repetitive sequences, discussed experimental strategies to mitigate their effect on sequence assembly, and suggested that the WGS method could be applied effectively to large eukaryotic genomes. A key component of the strategy is obtaining sequence data from each end of the cloned DNA inserts; the juxtaposition of these end-sequences ("mate pairs") is a critical element in producing a correct assembly.

## Genomic Structure

WGS libraries were prepared with three different insert sizes of cloned DNA: 2 kb, 10 kb, and 130 kb. The 10-kb clones are large enough to span the most common repetitive sequence elements in *Drosophila*, the retrotransposons. End-sequence from the BACs provided long-range linking information that was used to confirm the overall structure of the assembly (*9*). More than 3 million sequence reads were obtained from whole-genome libraries (Fig. 2 and Table 2). Only ~2% of the sequence reads contained heterochromatic simple sequence repeats, indicating that the heterochromatic DNA is not stably cloned in the small-insert vectors used for the WGS libraries. A BAC-based physical map spanning >95% of the euchromatic portion of the genome was constructed by screening a BAC library with sequence-tagged site (STS) markers (*10*). More than 29 Mb of high-quality finished sequence has been completed from BAC, P1, and cosmid clones, and draft sequence data (~1.5× average coverage) were obtained from an additional 825 BAC and P1 clones spanning in total >90% of the genome (Table 3). The clone-based draft sequence served two purposes: It improved the likelihood of accurate assembly, and it allowed the identification of templates and primers for filling gaps that remain after assembly. An initial assembly was performed using the WGS data and BAC end-sequence [WGS-only assembly (*4*)]; subsequent assemblies included the clone-based draft sequence data (joint assembly). Figure 3 and Table 3 illustrate the status of the euchromatic sequence resulting from each of these assemblies and the current status following the directed gap closure completed to date. The sequence assembly process is described in detail in an accompanying paper (*11*).

Assembly resulted in a set of "scaffolds." Each scaffold is a set of contiguous sequences (contigs), ordered and oriented with respect to one another by mate-pairs such that the gaps between adjacent contigs are of known size and are spanned by clones with end-sequences flanking the gap. Gaps within scaffolds are called sequence gaps; gaps between scaffolds are called "physical gaps" because there are no clones identified spanning the gap. Two methods were used to map the scaffolds to chromosomes: (i) cross-referencing between STS markers present in the assembled sequence and the BAC-based STS content map, and (ii) cross-referencing between assembled sequence and shotgun sequence data obtained from individual tiling-path clones selected from the BAC physical map. The mapped scaffolds from the joint assembly, totaling 116.2 Mb after initial

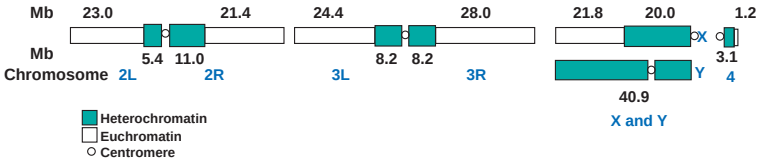


**Fig. 1.** Mitotic chromosomes of *D. melanogaster*, showing euchromatic regions, heterochromatic regions, and centromeres. Arms of the autosomes are designated 2L, 2R, 3L, 3R, and 4. The euchromatic length in megabases is derived from the sequence analysis. The heterochromatic lengths are estimated from direct measurements of mitotic chromosome lengths (*67*). The heterochromatic block of the X chromosome is polymorphic among stocks and varies from one-third to one-half of the length of the mitotic chromosome. The Y chromosome is nearly entirely heterochromatic.

[1]Celera Genomics, 45 West Gude Drive, Rockville, MD 20850, USA. [2]Berkeley *Drosophila* Genome Project (BDGP), Lawrence Berkeley National Laboratory, Berkeley, CA 94720, USA. [3]Human Genome Sequencing Center, Department of Molecular and Human Genetics, Baylor College of Medicine, Houston, TX 77030, USA. [4]BDGP, Department of Molecular and Cell Biology, University of California, Berkeley, CA 94720, USA. [5]European Molecular Biology Laboratory (EMBL)–European Bioinformatics Institute, Wellcome Trust Genome Campus, Hinxton, Cambridge CB10 1SD, UK. [6]Neomorphic Inc., 2612 Eighth Street, Berkeley, CA 94710, USA. [7]GenetixXpress Pty. Ltd., 78 Pacific Road, Palm Beach, Sydney, NSW 2108, Australia. [8]Department of Medical Informatics, IMIM–UPF C/Dr. Aiguader 80, 08003 Barcelona, Spain. [9]Department of Molecular and Cellular Biology, Harvard University, 16 Divinity Avenue, Cambridge, MA 02138, USA. [10]Department of Genetics, Box 8232, Washington University Medical School, 4566 Scott Avenue, St. Louis, MO 63110, USA. [11]Institute of Molecular Biology and Biotechnology, Forth, Heraklion, Greece. [12]European *Drosophila* Genome Project (EDGP), EMBL, Heidelberg, Germany. [13]Department of Molecular and Cell Biology, University of California, Berkeley, CA 94710, USA. [14]Genoscope, 2 rue Gaston Crémieux, 91000 Evry, France. [15]Section of Molecular and Cellular Biology, University of California, Davis, CA 95618, USA. [16]Department of Genetics, University of Cambridge, Cambridge CB2 3EH, UK. [17]EDGP, Rennes University Medical School, UPR 41 CNRS Recombinaisons Genetiques, Faculte de Medicine, 2 av. du Pr. Leon Bernard, 35043 Rennes Cedex, France. [18]Department of Genetics, Stanford University, Palo Alto, CA 94305, USA. [19]Department of Statistics, University of California, Berkeley, CA 94720, USA. [20]EDGP, Centro de Biología Molecular Severo Ochoa, CSIC, Universidad Autónoma de Madrid, 28049 Madrid, Spain. [21]MBVL, Salk Institute, 10010 North Torrey Pines Road, La Jolla, CA 92037, USA. [22]Department of Biochemistry and Center for Insect Science, University of Arizona, Tucson, AZ 85721, USA. [23]EDGP, Montpellier University Medical School, Institut de Genetique Humaine, CNRS (CRBM), 114 rue de la Cardonille, 34396 Montpellier Cedex 5, France. [24]Laboratory of Molecular Genetics, National Institute of Child Health and Human Development, National Institutes of Health (NIH), Bethesda, MD 20892, USA. [25]Department of Biology, McGill University, 1205 Avenue Docteur Penfield, Montreal, Quebec, Canada. [26]The Institute for Genomic Research, Rockville, MD 20850, USA. [27]Department of Cell Biology and Molecular Genetics, University of Maryland, College Park, MD 20742, USA. [28]EDGP, Sanger Centre, Wellcome Trust Genome Campus, Hinxton, Cambridge CB10 1SA, UK. [29]Department of Biochemistry, University of Tennessee, Memphis, TN 38163, USA. [30]EDGP, Department of Anatomy and Physiology, University of Dundee, Dundee DD1 4HN, UK, and Department of Biological Sciences, Open University, Milton Keynes MK7 6AA, UK. [31]HHMI/Embryology, Carnegie Institution of Washington, Baltimore, MD 21210, USA. [32]Motorola BioChip Systems, Tempe, AZ 85284, USA. [33]Cell Biology and Metabolism Branch, National Institute of Child Health and Human Development, NIH, Bethesda, MD 20892, USA. [34]Howard Hughes Medical Institute, BDGP, University of California, Berkeley, CA 94720, USA.

*To whom correspondence should be addressed.


Figure 5.5: **Coding Content of the *Drosophila* Genome.**

### 5.2.3 Venter *et al*, *Science*, 291(5507):1304–1351, 2001

**PubMed Accession:**

http://www.ncbi.nlm.nih.gov/entrez/query.fcgi?cmd=Retrieve&db=PubMed&list_uids=11181995&dopt=Abstract

**Journal Abstract:**

http://www.sciencemag.org/cgi/content/abstract/291/5507/1304

**Companion Poster:**

See Figure 5.6 and the following URLs:
http://www.sciencemag.org/cgi/content/full/291/5507/1304/DC2
http://genome.imim.es/references/genome_maps/2001_Science_v291_i5507_p1304_fig1_HumanGenome.ps.gz

THE HUMAN GENOME

# The Sequence of the Human Genome

J. Craig Venter,[1]* Mark D. Adams,[1] Eugene W. Myers,[1] Peter W. Li,[1] Richard J. Mural,[1] Granger G. Sutton,[1] Hamilton O. Smith,[1] Mark Yandell,[1] Cheryl A. Evans,[1] Robert A. Holt,[1] Jeannine D. Gocayne,[1] Peter Amanatides,[1] Richard M. Ballew,[1] Daniel H. Huson,[1] Jennifer Russo Wortman,[1] Qing Zhang,[1] Chinnappa D. Kodira,[1] Xiangqun H. Zheng,[1] Lin Chen,[1] Marian Skupski,[1] Gangadharan Subramanian,[1] Paul D. Thomas,[1] Jinghui Zhang,[1] George L. Gabor Miklos,[2] Catherine Nelson,[3] Samuel Broder,[1] Andrew G. Clark,[4] Joe Nadeau,[5] Victor A. McKusick,[6] Norton Zinder,[7] Arnold J. Levine,[7] Richard J. Roberts,[8] Mel Simon,[9] Carolyn Slayman,[10] Michael Hunkapiller,[11] Randall Bolanos,[1] Arthur Delcher,[1] Ian Dew,[1] Daniel Fasulo,[1] Michael Flanigan,[1] Liliana Florea,[1] Aaron Halpern,[1] Sridhar Hannenhalli,[1] Saul Kravitz,[1] Samuel Levy,[1] Clark Mobarry,[1] Knut Reinert,[1] Karin Remington,[1] Jane Abu-Threideh,[1] Ellen Beasley,[1] Kendra Biddick,[1] Vivien Bonazzi,[1] Rhonda Brandon,[1] Michele Cargill,[1] Ishwar Chandramouliswaran,[1] Rosane Charlab,[1] Kabir Chaturvedi,[1] Zuoming Deng,[1] Valentina Di Francesco,[1] Patrick Dunn,[1] Karen Eilbeck,[1] Carlos Evangelista,[1] Andrei E. Gabrielian,[1] Weiniu Gan,[1] Wangmao Ge,[1] Fangcheng Gong,[1] Zhiping Gu,[1] Ping Guan,[1] Thomas J. Heiman,[1] Maureen E. Higgins,[1] Rui-Ru Ji,[1] Zhaoxi Ke,[1] Karen A. Ketchum,[1] Zhongwu Lai,[1] Yiding Lei,[1] Zhenya Li,[1] Jiayin Li,[1] Yong Liang,[1] Xiaoying Lin,[1] Fu Lu,[1] Gennady V. Merkulov,[1] Natalia Milshina,[1] Helen M. Moore,[1] Ashwinikumar K Naik,[1] Vaibhav A. Narayan,[1] Beena Neelam,[1] Deborah Nusskern,[1] Douglas B. Rusch,[1] Steven Salzberg,[12] Wei Shao,[1] Bixiong Shue,[1] Jingtao Sun,[1] Zhen Yuan Wang,[1] Aihui Wang,[1] Xin Wang,[1] Jian Wang,[1] Ming-Hui Wei,[1] Ron Wides,[13] Chunlin Xiao,[1] Chunhua Yan,[1] Alison Yao,[1] Jane Ye,[1] Ming Zhan,[1] Weiqing Zhang,[1] Hongyu Zhang,[1] Qi Zhao,[1] Liansheng Zheng,[1] Fei Zhong,[1] Wenyan Zhong,[1] Shiaoping C. Zhu,[1] Shaying Zhao,[12] Dennis Gilbert,[1] Suzanna Baumhueter,[1] Gene Spier,[1] Christine Carter,[1] Anibal Cravchik,[1] Trevor Woodage,[1] Feroze Ali,[1] Huijin An,[1] Aderonke Awe,[1] Danita Baldwin,[1] Holly Baden,[1] Mary Barnstead,[1] Ian Barrow,[1] Karen Beeson,[1] Dana Busam,[1] Amy Carver,[1] Angela Center,[1] Ming Lai Cheng,[1] Liz Curry,[1] Steve Danaher,[1] Lionel Davenport,[1] Raymond Desilets,[1] Susanne Dietz,[1] Kristina Dodson,[1] Lisa Doup,[1] Steven Ferriera,[1] Neha Garg,[1] Andres Gluecksmann,[1] Brit Hart,[1] Jason Haynes,[1] Charles Haynes,[1] Cheryl Heiner,[1] Suzanne Hladun,[1] Damon Hostin,[1] Jarrett Houck,[1] Timothy Howland,[1] Chinyere Ibegwam,[1] Jeffery Johnson,[1] Francis Kalush,[1] Lesley Kline,[1] Shashi Koduru,[1] Amy Love,[1] Felecia Mann,[1] David May,[1] Steven McCawley,[1] Tina McIntosh,[1] Ivy McMullen,[1] Mee Moy,[1] Linda Moy,[1] Brian Murphy,[1] Keith Nelson,[1] Cynthia Pfannkoch,[1] Eric Pratts,[1] Vinita Puri,[1] Hina Qureshi,[1] Matthew Reardon,[1] Robert Rodriguez,[1] Yu-Hui Rogers,[1] Deanna Romblad,[1] Bob Ruhfel,[1] Richard Scott,[1] Cynthia Sitter,[1] Michelle Smallwood,[1] Erin Stewart,[1] Renee Strong,[1] Ellen Suh,[1] Reginald Thomas,[1] Ni Ni Tint,[1] Sukyee Tse,[1] Claire Vech,[1] Gary Wang,[1] Jeremy Wetter,[1] Sherita Williams,[1] Monica Williams,[1] Sandra Windsor,[1] Emily Winn-Deen,[1] Keriellen Wolfe,[1] Jayshree Zaveri,[1] Karena Zaveri,[1] Josep F. Abril,[14] Roderic Guigó,[14] Michael J. Campbell,[1] Kimmen V. Sjolander,[1] Brian Karlak,[1] Anish Kejariwal,[1] Huaiyu Mi,[1] Betty Lazareva,[1] Thomas Hatton,[1] Apurva Narechania,[1] Karen Diemer,[1] Anushya Muruganujan,[1] Nan Guo,[1] Shinji Sato,[1] Vineet Bafna,[1] Sorin Istrail,[1] Ross Lippert,[1] Russell Schwartz,[1] Brian Walenz,[1] Shibu Yooseph,[1] David Allen,[1] Anand Basu,[1] James Baxendale,[1] Louis Blick,[1] Marcelo Caminha,[1] John Carnes-Stine,[1] Parris Caulk,[1] Yen-Hui Chiang,[1] My Coyne,[1] Carl Dahlke,[1] Anne Deslattes Mays,[1] Maria Dombroski,[1] Michael Donnelly,[1] Dale Ely,[1] Shiva Esparham,[1] Carl Fosler,[1] Harold Gire,[1] Stephen Glanowski,[1] Kenneth Glasser,[1] Anna Glodek,[1] Mark Gorokhov,[1] Ken Graham,[1] Barry Gropman,[1] Michael Harris,[1] Jeremy Heil,[1] Scott Henderson,[1] Jeffrey Hoover,[1] Donald Jennings,[1] Catherine Jordan,[1] James Jordan,[1] John Kasha,[1] Leonid Kagan,[1] Cheryl Kraft,[1] Alexander Levitsky,[1] Mark Lewis,[1] Xiangjun Liu,[1] John Lopez,[1] Daniel Ma,[1] William Majoros,[1] Joe McDaniel,[1] Sean Murphy,[1] Matthew Newman,[1] Trung Nguyen,[1] Ngoc Nguyen,[1] Marc Nodell,[1] Sue Pan,[1] Jim Peck,[1] Marshall Peterson,[1] William Rowe,[1] Robert Sanders,[1] John Scott,[1] Michael Simpson,[1] Thomas Smith,[1] Arlan Sprague,[1] Timothy Stockwell,[1] Russell Turner,[1] Eli Venter,[1] Mei Wang,[1] Meiyuan Wen,[1] David Wu,[1] Mitchell Wu,[1] Ashley Xia,[1] Ali Zandieh,[1] Xiaohong Zhu[1]

## THE HUMAN GENOME

**A 2.91-billion base pair (bp) consensus sequence of the euchromatic portion of the human genome was generated by the whole-genome shotgun sequencing method. The 14.8-billion bp DNA sequence was generated over 9 months from 27,271,853 high-quality sequence reads (5.11-fold coverage of the genome) from both ends of plasmid clones made from the DNA of five individuals. Two assembly strategies—a whole-genome assembly and a regional chromosome assembly—were used, each combining sequence data from Celera and the publicly funded genome effort. The public data were shredded into 550-bp segments to create a 2.9-fold coverage of those genome regions that had been sequenced, without including biases inherent in the cloning and assembly procedure used by the publicly funded group. This brought the effective coverage in the assemblies to eightfold, reducing the number and size of gaps in the final assembly over what would be obtained with 5.11-fold coverage. The two assembly strategies yielded very similar results that largely agree with independent mapping data. The assemblies effectively cover the euchromatic regions of the human chromosomes. More than 90% of the genome is in scaffold assemblies of 100,000 bp or more, and 25% of the genome is in scaffolds of 10 million bp or larger. Analysis of the genome sequence revealed 26,588 protein-encoding transcripts for which there was strong corroborating evidence and an additional ~12,000 computationally derived genes with mouse matches or other weak supporting evidence. Although gene-dense clusters are obvious, almost half the genes are dispersed in low G+C sequence separated by large tracts of apparently noncoding sequence. Only 1.1% of the genome is spanned by exons, whereas 24% is in introns, with 75% of the genome being intergenic DNA. Duplications of segmental blocks, ranging in size up to chromosomal lengths, are abundant throughout the genome and reveal a complex evolutionary history. Comparative genomic analysis indicates vertebrate expansions of genes associated with neuronal function, with tissue-specific developmental regulation, and with the hemostasis and immune systems. DNA sequence comparisons between the consensus sequence and publicly funded genome data provided locations of 2.1 million single-nucleotide polymorphisms (SNPs). A random pair of human haploid genomes differed at a rate of 1 bp per 1250 on average, but there was marked heterogeneity in the level of polymorphism across the genome. Less than 1% of all SNPs resulted in variation in proteins, but the task of determining which SNPs have functional consequences remains an open challenge.**

Decoding of the DNA that constitutes the human genome has been widely anticipated for the contribution it will make toward understanding human evolution, the causation of disease, and the interplay between the environment and heredity in defining the human condition. A project with the goal of determining the complete nucleotide sequence of the human genome was first formally proposed in 1985 (*1*). In subsequent years, the idea met with mixed reactions in the scientific community (*2*). However, in 1990, the Human Genome Project (HGP) was officially initiated in the United States under the direction of the National Institutes of Health and the U.S. Department of Energy with a 15-year, $3 billion plan for completing the genome sequence. In 1998 we announced our intention to build a unique genome-sequencing facility, to determine the sequence of the human genome over a 3-year period. Here we report the penultimate milestone along the path toward that goal, a nearly complete sequence of the euchromatic portion of the human genome. The sequencing was performed by a whole-genome random shotgun method with subsequent assembly of the sequenced segments.

The modern history of DNA sequencing began in 1977, when Sanger reported his method for determining the order of nucleotides of DNA using chain-terminating nucleotide analogs (*3*). In the same year, the first human gene was isolated and sequenced (*4*). In 1986, Hood and co-workers (*5*) described an improvement in the Sanger sequencing method that included attaching fluorescent dyes to the nucleotides, which permitted them to be sequentially read by a computer. The first automated DNA sequencer, developed by Applied Biosystems in California in 1987, was shown to be successful when the sequences of two genes were obtained with this new technology (*6*). From early sequencing of human genomic regions (*7*), it became clear that cDNA sequences (which are reverse-transcribed from RNA) would be essential to annotate and validate gene predictions in the human genome. These studies were the basis in part for the development of the expressed sequence tag (EST) method of gene identification (*8*), which is a random selection, very high throughput sequencing approach to characterize cDNA libraries. The EST method led to the rapid discovery and mapping of human genes (*9*). The increasing numbers of human EST sequences necessitated the development of new computer algorithms to analyze large amounts of sequence data, and in 1993 at The Institute for Genomic Research (TIGR), an algorithm was developed that permitted assembly and analysis of hundreds of thousands of ESTs. This algorithm permitted characterization and annotation of human genes on the basis of 30,000 EST assemblies (*10*).

The complete 49-kbp bacteriophage lambda genome sequence was determined by a shotgun restriction digest method in 1982 (*11*). When considering methods for sequencing the smallpox virus genome in 1991 (*12*), a whole-genome shotgun sequencing method was discussed and subsequently rejected owing to the lack of appropriate software tools for genome assembly. However, in 1994, when a microbial genome-sequencing project was contemplated at TIGR, a whole-genome shotgun sequencing approach was considered possible with the TIGR EST assembly algorithm. In 1995, the 1.8-Mbp *Haemophilus influenzae* genome was completed by a whole-genome shotgun sequencing method (*13*). The experience with several subsequent genome-sequencing efforts established the broad applicability of this approach (*14*, *15*).

A key feature of the sequencing approach used for these megabase-size and larger genomes was the use of paired-end sequences (also called mate pairs), derived from subclone libraries with distinct insert sizes and cloning characteristics. Paired-end sequences are sequences 500 to 600 bp in length from both ends of double-stranded DNA clones of prescribed lengths. The success of using end sequences from long segments (18 to 20 kbp) of DNA cloned into bacteriophage lambda in assembly of the microbial genomes led to the suggestion (*16*) of an approach to simulta-

[1]Celera Genomics, 45 West Gude Drive, Rockville, MD 20850, USA. [2]GenetixXpress, 78 Pacific Road, Palm Beach, Sydney 2108, Australia. [3]Berkeley *Drosophila* Genome Project, University of California, Berkeley, CA 94720, USA. [4]Department of Biology, Penn State University, 208 Mueller Lab, University Park, PA 16802, USA. [5]Department of Genetics, Case Western Reserve University School of Medicine, BRB-630, 10900 Euclid Avenue, Cleveland, OH 44106, USA. [6]Johns Hopkins University School of Medicine, Johns Hopkins Hospital, 600 North Wolfe Street, Blalock 1007, Baltimore, MD 21287–4922, USA. [7]Rockefeller University, 1230 York Avenue, New York, NY 10021–6399, USA. [8]New England BioLabs, 32 Tozer Road, Beverly, MA 01915, USA. [9]Division of Biology, 147-75, California Institute of Technology, 1200 East California Boulevard, Pasadena, CA 91125, USA. [10]Yale University School of Medicine, 333 Cedar Street, P.O. Box 208000, New Haven, CT 06520–8000, USA. [11]Applied Biosystems, 850 Lincoln Centre Drive, Foster City, CA 94404, USA. [12]The Institute for Genomic Research, 9712 Medical Center Drive, Rockville, MD 20850, USA. [13]Faculty of Life Sciences, Bar-Ilan University, Ramat-Gan, 52900 Israel. [14]Grup de Recerca en Informàtica Mèdica, Institut Municipal d'Investigació Mèdica, Universitat Pompeu Fabra, 08003-Barcelona, Catalonia, Spain.

*To whom correspondence should be addressed. E-mail: humangenome@celera.com


Figure 5.6: **Annotation of the Celera Human Genome Assembly.**

### 5.2.4 Holt *et al*, *Science*, 298(5591):129–149, 2002

**PubMed Accession:**

http://www.ncbi.nlm.nih.gov/entrez/query.fcgi?cmd=Retrieve&db=PubMed&list_uids=12364791&dopt=Abstract

**Journal Abstract:**

http://www.sciencemag.org/cgi/content/abstract/298/5591/129

**Companion Poster:**

See Figure 5.7 and the following URLs:
http://www.sciencemag.org/cgi/content/full/298/5591/129/DC2
http://genome.imim.es/references/genome_maps/2002_Science_v298_i5591_p129_fig1_MosquitoGenome.ps.gz

RESEARCH ARTICLES

# The Genome Sequence of the Malaria Mosquito *Anopheles gambiae*

Robert A. Holt,[1]*† G. Mani Subramanian,[1] Aaron Halpern,[1] Granger G. Sutton,[1] Rosane Charlab,[1] Deborah R. Nusskern,[1] Patrick Wincker,[2] Andrew G. Clark,[3] José M. C. Ribeiro,[4] Ron Wides,[5] Steven L. Salzberg,[6] Brendan Loftus,[6] Mark Yandell,[1] William H. Majoros,[1,6] Douglas B. Rusch,[1] Zhongwu Lai,[1] Cheryl L. Kraft,[1] Josep F. Abril,[7] Veronique Anthouard,[2] Peter Arensburger,[8] Peter W. Atkinson,[8] Holly Baden,[1] Veronique de Berardinis,[2] Danita Baldwin,[1] Vladimir Benes,[9] Jim Biedler,[10] Claudia Blass,[9] Randall Bolanos,[1] Didier Boscus,[2] Mary Barnstead,[1] Shuang Cai,[1] Angela Center,[1] Kabir Chatuverdi,[1] George K. Christophides,[9] Mathew A. Chrystal,[11] Michele Clamp,[12] Anibal Cravchik,[1] Val Curwen,[12] Ali Dana,[11] Art Delcher,[1] Ian Dew,[1] Cheryl A. Evans,[1] Michael Flanigan,[1] Anne Grundschober-Freimoser,[13] Lisa Friedli,[8] Zhiping Gu,[1] Ping Guan,[1] Roderic Guigo,[7] Maureen E. Hillenmeyer,[11] Susanne L. Hladun,[1] James R. Hogan,[11] Young S. Hong,[11] Jeffrey Hoover,[1] Olivier Jaillon,[2] Zhaoxi Ke,[1,11] Chinnappa Kodira,[1] Elena Kokoza,[14] Anastasios Koutsos,[15,16] Ivica Letunic,[9] Alex Levitsky,[1] Yong Liang,[1] Jhy-Jhu Lin,[1,6] Neil F. Lobo,[11] John R. Lopez,[1] Joel A. Malek,[6]‡ Tina C. McIntosh,[1] Stephan Meister,[9] Jason Miller,[1] Clark Mobarry,[1] Emmanuel Mongin,[17] Sean D. Murphy,[1] David A. O'Brochta,[13] Cynthia Pfannkoch,[1] Rong Qi,[1] Megan A. Regier,[1] Karin Remington,[1] Hongguang Shao,[10] Maria V. Sharakhova,[11] Cynthia D. Sitter,[1] Jyoti Shetty,[6] Thomas J. Smith,[1] Renee Strong,[1] Jingtao Sun,[1] Dana Thomasova,[9] Lucas Q. Ton,[11] Pantelis Topalis,[15] Zhijian Tu,[10] Maria F. Unger,[11] Brian Walenz,[1] Aihui Wang,[1] Jian Wang,[1] Mei Wang,[1] Xuelan Wang,[11]§ Kerry J. Woodford,[1] Jennifer R. Wortman,[1,6] Martin Wu,[6] Alison Yao,[1] Evgeny M. Zdobnov,[9] Hongyu Zhang,[1] Qi Zhao,[1] Shaying Zhao,[6] Shiaoping C. Zhu,[1] Igor Zhimulev,[14] Mario Coluzzi,[18] Alessandra della Torre,[18] Charles W. Roth,[19] Christos Louis,[15,16] Francis Kalush,[1] Richard J. Mural,[1] Eugene W. Myers,[1] Mark D. Adams,[1] Hamilton O. Smith,[1] Samuel Broder,[1] Malcolm J. Gardner,[6] Claire M. Fraser,[6] Ewan Birney,[17] Peer Bork,[9] Paul T. Brey,[19] J. Craig Venter,[1,6] Jean Weissenbach,[2] Fotis C. Kafatos,[9] Frank H. Collins,[11]† Stephen L. Hoffman[1]‖

*Anopheles gambiae* is the principal vector of malaria, a disease that afflicts more than 500 million people and causes more than 1 million deaths each year. Tenfold shotgun sequence coverage was obtained from the PEST strain of *A. gambiae* and assembled into scaffolds that span 278 million base pairs. A total of 91% of the genome was organized in 303 scaffolds; the largest scaffold was 23.1 million base pairs. There was substantial genetic variation within this strain, and the apparent existence of two haplotypes of approximately equal frequency ("dual haplotypes") in a substantial fraction of the genome likely reflects the outbred nature of the PEST strain. The sequence produced a conservative inference of more than 400,000 single-nucleotide polymorphisms that showed a markedly bimodal density distribution. Analysis of the genome sequence revealed strong evidence for about 14,000 protein-encoding transcripts. Prominent expansions in specific families of proteins likely involved in cell adhesion and immunity were noted. An expressed sequence tag analysis of genes regulated by blood feeding provided insights into the physiological adaptations of a hematophagous insect.

The mosquito is both an elegant, exquisitely adapted organism and a scourge of humanity. The principal mosquito-borne human illnesses of malaria, filariasis, dengue, and yellow fever are at this time almost exclusively restricted to the tropics. Malaria, the most important parasitic disease in the world, is thought to be responsible for 500 million cases of illness and up to 2.7 million deaths annually, more than 90% of which occur in sub-Saharan Africa (*1*).

*Anopheles gambiae* is the major vector of *Plasmodium falciparum* in Africa and is one of the most efficient malaria vectors in the world. Its blood meals come almost exclusively from humans, its larvae develop in temporary bodies of water produced by human activities (e.g., agricultural irrigation or flooded human or domestic animal footprints), and adults rest primarily in human dwellings. During the 1950s and early 1960s, the World Health Organization ( WHO) malaria eradication campaign succeeded in eradicating malaria from Europe and sharply reduced its prevalence in many other parts of the world, primarily through programs that combined mosquito control with antimalarial drugs such as chloroquine. Sub-Saharan Af-

[1]Celera Genomics, 45 West Gude Drive, Rockville, MD 20850, USA. [2]Genoscope/Centre National de Sequencage and CNRS-UMR 8030, 2 rue Gaston Cremieux, 91057 Evry Cedex 06, France. [3]Molecular Biology and Genetics, Cornell University, Ithaca, NY 14853, USA. [4]Laboratory of Malaria and Vector Research, National Institute of Allergy and Infectious Diseases (NIAID), Building 4, Room 126, 4 Center Drive, MSC-0425, Bethesda, MD 20892, USA. [5]Faculty of Life Sciences, Bar-Ilan University, Ramat-Gan, Israel. [6]The Institute for Genomic Research (TIGR), 9712 Medical Center Drive, Rockville, MD 20850, USA. [7]Grup de Recerca en Informatica Biomedica, IMIM/UPF/CRG, Barcelona, Catalonia, Spain. [8]Department of Entomology, University of California, Riverside, CA 92521, USA. [9]European Molecular Biology Laboratory, Meyerhofstr. 1, 69117 Heidelberg, Germany. [10]Virginia Polytechnic Institute and State University, Blacksburg, VA 24061, USA. [11]Center for Tropical Disease Research and Training, University of Notre Dame, Galvin Life Sciences Building, Notre Dame, IN 46556, USA. [12]Wellcome Trust Sanger Institute, Wellcome Trust Genome Campus, Hinxton, Cambridge CB10 1SA, UK. [13]Center for Agricultural Biotechnology, University of Maryland Biotechnology Institute, College Park, MD 20742, USA. [14]Institute of Cytology and Genetics, Lavrentyeva ave 10, Novosibirsk 630090, Russia. [15]Institute of Molecular Biology and Biotechnology of the Foundation of Research and Technology–Hellas (IMBB-FORTH), Post Office Box 1527, GR-711 10 Heraklion, Crete, Greece, and University of Crete, GR-711 10 Heraklion, Crete, Greece. [16]Department of Biology, University of Crete, GR-711 10 Heraklion, Crete, Greece. [17]European Bioinformatics Institute, Wellcome Trust Genome Campus, Hinxton, Cambridge CB10 1SD, UK. [18]Dipartimento di Scienze di Sanità Pubblica, Sezione di Parassitologia, Università degli Studi di Roma "La Sapienza," P.le Aldo Moro 5, 00185 Roma, Italy. [19]Unité de Biochimie et Biologie Moléculaire des Insectes, Institut Pasteur, Paris 75724 Cedex 15, France.

*Present address: Canada's Michael Smith Genome Science Centre, British Columbia Cancer Agency, Room 3427, 600 West 10th Avenue, Vancouver, British Columbia V5Z 4E6, Canada.

‡Present address: Agencourt Bioscience Corporation, 100 Cummings Center, Suite 107J, Beverly, MA 01915, USA.

§Present address: Department of Pharmacology, Sun Yat-Sen Medical School, Sun Yat-Sen University #74, Zhongshan 2nd Road, Guangzhou (Canton), 510089, P. R. China.

‖Present address: Sanaria, 308 Argosy Drive, Gaithersburg, MD 20878, USA.

†To whom correspondence should be addressed. E-mail: robert.holt@celera.com, rholt@bcgsc.ca (R.A.H.), frank.h.collins.75@nd.edu (F.H.C.).

rica, for the most part, did not benefit from the malaria eradication program, but the widespread availability of chloroquine and other affordable antimalarial drugs no doubt helped to control malaria mortality and morbidity. Unfortunately, with the appearance of chloroquine-resistant malaria parasites and the development of resistance of mosquitoes to the insecticides used to control disease transmission, malaria in Africa is again on the rise. Even control programs based on insecticide-impregnated bed nets, now widely advocated by WHO, are threatened by the development of insecticide resistance in *A. gambiae* and other vectors. New malaria control techniques are urgently needed in sub-Saharan Africa, and to meet this challenge we must grasp both the ecological and molecular complexities of the mosquito. The International *Anopheles gambiae* Genome Project has been undertaken with the hope that the sequence presented here will serve as a valuable molecular entomology resource, leading ultimately to effective intervention in the transmission of malaria and perhaps other mosquito-borne diseases.

## Strain Selection

Populations of *A. gambiae sensu stricto* are highly structured into several morphologically indistinguishable forms. Paracentric inversions of the right arm of chromosome 2 define five different "cytotypes" or "chromosomal forms" (Mopti, Bamako, Bissau, Forest, and Savanna), and variation in the frequencies of these forms correlates with climatic conditions, vegetation zones, and human domestic environments (*2, 3*). An alternative classification system based on fixed differences in ribosomal DNA recognizes two "molecular forms" (M and S) (*4*). The S and M molecular forms were initially observed in the Savanna and Mopti chromosomal forms, respectively. However, analysis of *A. gambiae* populations from many areas of Africa has shown that the molecular and chromosomal forms do not always coincide. This can be explained if it is assumed that inversion arrangements are not directly involved in any reproductive isolating mechanism and therefore do not actually specify different taxonomic units. Indeed, laboratory crossing experiments have failed to show evidence of any premating or postmating reproductive isolation between chromosomal forms (*5*).

The *A. gambiae* PEST strain was chosen for this genome project because clones from two different PEST strain BAC (bacterial artificial chromosome) libraries had already been end-sequenced and mapped physically, in situ, to chromosomes. Further, all individuals in the colony have the standard chromosome arrangement without any of the paracentric inversion polymorphisms that are typical of both wild populations and most other colonies (*6*), and the colony has an X-linked pink eye mutation that can readily be used as an indicator of cross-colony contamination (*7*). The PEST strain was originally used in the early 1990s to measure the reservoir of mosquito-infective *Plasmodium* gametocytes in people from western Kenya. The PEST strain was produced by crossing a laboratory strain originating in Nigeria and containing the eye mutation with the offspring of field-collected *A. gambiae* from the Asembo Bay area of western Kenya, and then reselecting for the pink eye phenotype (*8*). Outbreeding was repeated three times, yielding a colony whose genetic composition is predominantly derived from the Savanna form of *A. gambiae* found in western Kenya. This colony, when tested, was fully susceptible to *P. falciparum* from western Kenya (*9*). The PEST strain is maintained at the Institut Pasteur (Paris), and *A. gambiae* strains with various biological features can be obtained from the Malaria Research and Reference Reagent Resource Center (www.malaria.mr4.org).

## Sequencing and Assembly

Plasmid and BAC DNA libraries were constructed with stringently size-selected PEST strain DNA. Two BAC libraries were constructed, one (ND-TAM) using DNA from whole adult male and female mosquitoes and the other (ND-1) using DNA from ovaries of PEST females collected about 24 hours after the blood meal (full development of a set of eggs requires ~48 hours). Plasmid libraries containing inserts of 2.5, 10, and 50 kb were constructed with DNA derived from either 330 male or 430 female mosquitoes. For each sex, several libraries of each insert size class were made, and these were sequenced such that there was approximately equal coverage from male and female mosquitoes in the final data set. DNA extraction, library construction, and DNA sequencing were undertaken by means of standard methods (*10–12*). Celera, the French National Sequencing Center (Genoscope), and TIGR contributed sequence data that collectively provided 10.2-fold sequence coverage and 103.6-fold clone coverage of the genome, assuming the indicated genome size of 278 million base pairs (Mbp) (tables S1 and S2). Electropherograms have been submitted to the National Center for Biotechnology Information trace repository (www.ncbi.nlm.nih.gov/Traces/trace.cgi) and are publicly available as a searchable data set.

The whole-genome data set was assembled with the Celera assembler (*8*), which has previously been used to assemble the *Drosophila*, human, and mouse genomes (*12–15*). The whole-genome assembly resulted in 8987 scaffolds spanning 278 Mbp of the *Anopheles* genome (table S2). The largest scaffold was 23.1 Mbp and the largest contig was 0.8 Mbp. Scaffolds are separated by interscaffold gaps that have no physical clones spanning them, although small scaffolds are expected to fit within interscaffold gaps. The sequence that is missing in the intrascaffold gaps is largely composed of (i) short regions that lacked coverage because of random sampling, and (ii) repeat sequences that could not be entirely filled using mate pairs [sequence reads from each end of a plasmid insert (*16*)]. Most intrascaffold gaps are spanned by 10-kbp clones that have been archived as frozen glycerol stocks. These clones have been submitted to the Malaria Research and Reference Reagent Resource

**Fig. 1 (foldout).** Annotation of the *Anopheles gambiae* genome sequence. The genome sequence is displayed on a nucleotide scale of about 200 kb/cm. Scaffold order along chromosomes was determined with the use of a physical map constructed by in situ hybridization of PEST strain BACs to salivary gland polytene chromosomes. Scaffold placement is shown in the track directly below the nucleotide scale. Individual scaffolds are identified by the last four digits of their GenBank accession number (e.g., scaffold AAAB01008987 is represented by 8987). For purposes of illustration, all scaffolds are separated by the average length of an interscaffold gap (317,904 bp, which is the total length of the unmapped scaffolds divided by the number of mapped scaffolds). Gaps between scaffolds are shaded gray in the scaffold track. The remainder of the figure is organized into three main groups of tracks: forward strand genes, sequence analysis, and reverse strand genes (from top to bottom, respectively). For each DNA strand (forward and reverse), each mapped gene is shown at genomic scale and is color-coded according to the automated annotation pipeline that predicted the gene (see Gene Authority panel on figure key). In addition, genes that are shorter than 10 kb and have two or fewer exons are shown in a separate track near the central sequence analysis section. All genes that are greater than 10 kb or have three or more exons are shown in an additional pair of tracks, expanded to a resolution close to 25 kb/cm. In these expanded tiers, exons are depicted as black boxes and introns are color-coded according to a set of Gene Ontology categories (GO, www.geneontology.org), as shown in the corresponding panel in the figure key. Three sequence analyses appear between the gene tracks: G+C content, sequence similarity to *Drosophila melanogaster*, and SNP density. The natural logarithm of the number of SNPs per 10 kb of sequence is used to color-code the SNP density analysis; G+C content is depicted by a nonlinear scale described in the figure key. Blocks of sequence with similarity to *D. melanogaster* genomic contigs are shown between the G+C and SNP tracks. Genes that have matching *A. gambiae* ESTs are shown directly flanking the central sequence analysis tracks, and are color-coded according to changes in EST density induced by a blood meal (see Post-Blood-Meal EST Density panel in figure key). This figure was generated with gff2ps (www1.imim.es/software/gfftools/GFF2PS.html), a genome annotation tool that converts General Feature Formatted records (www.sanger.ac.uk/Software/formats/GFF) to a Postscript output (*60*).

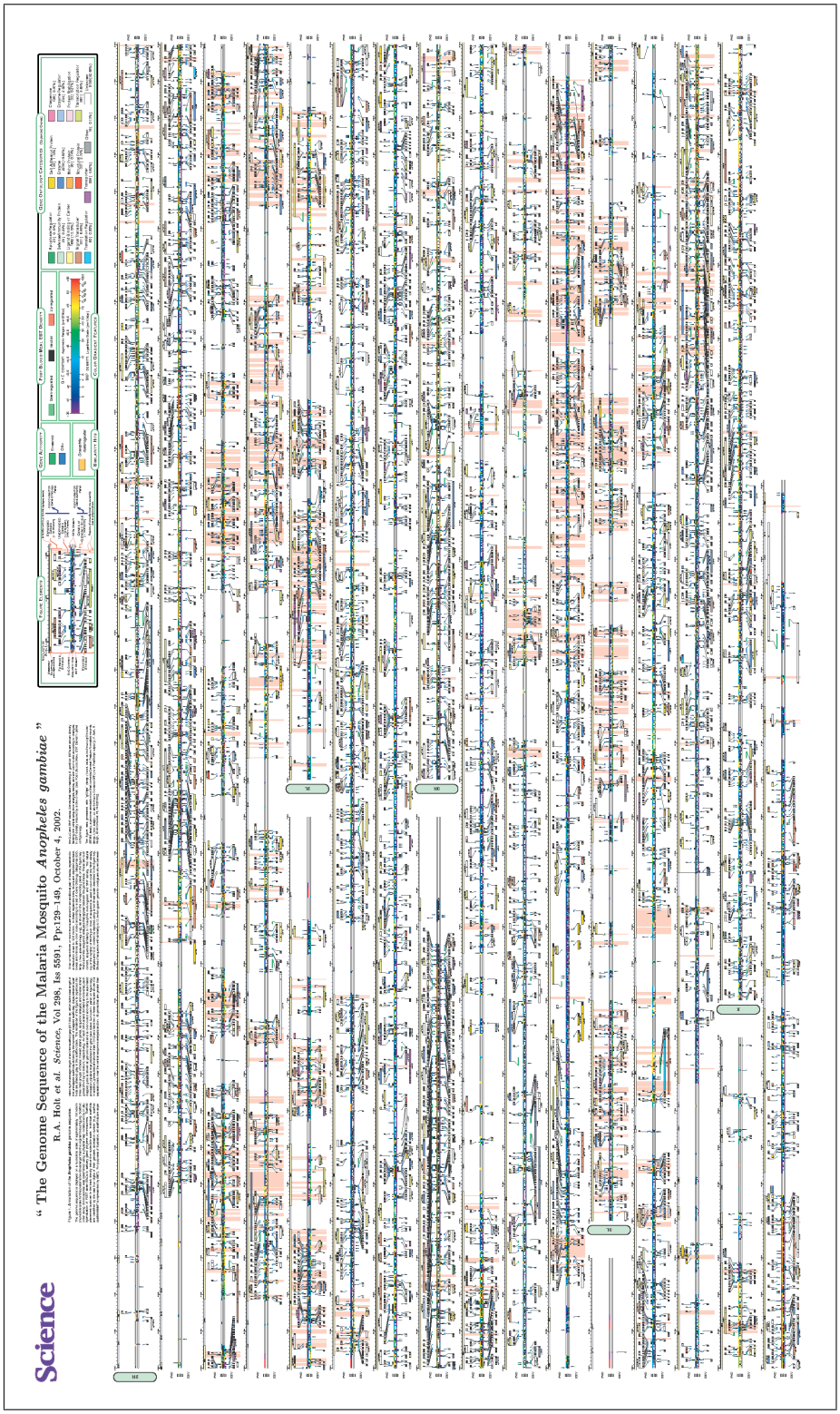


Figure 5.7: **Annotation of the *Anopheles gambiae* Genome Sequence.**

## 5.3 Software Developed for Comparative Analyses

### 5.3.1 `gff2aplot`: visualizing pairwise homology

`gff2aplot` was designed following the same principles as for `gff2ps`. Figure 5.3 illustrates the main internal processes flow chart for both tools. The problem to solve here was to integrate annotation information of two sequences being compared along with the pair-wise alignments obtained by other programs.

Due to the fact that each alignment software outputs alignments in their own format, it was decided to provide different filters to convert those alignment formats into a single interchange format. Such format was initially derived from `GFF` version 1, the so called `aplot` format. However, `GFF` version 2 provides enough flexibility to encode the alignment records into a more standardized way. Both alignment input formats, the `aplot` and the `GFF`v2, have been kept for backward compatibility in newer releases of `gff2aplot`. Use of an standardized input format permits to combine data from different alignment tools, or from different analyses made with the same tool—see for instance, right panel from Figure 5.8 on page 175 (Figure 1 on page 2478 of Abril *et al*. 2003)—, in order to compare them. An additional advantage of working with such filters to produce `GFF`-like records was the capability of visualizing that kind of data using `gff2ps` (as shown in Figure 5.10 lower panel).

Having that in mind, four programs have been implemented to date to complement `gff2aplot`, three `perl` scripts and another written in the `C` language. `parseblast` is a parser for the standard output from four of the BLAST program flavours available, say here `NCBI-Blast` [Altschul *et al*., 1990, 1997], `WU-Blast` [Gish, 1996–2004], `WebBlast` [Ferlanti *et al*., 1999] and `MegaBlast` [Zhang *et al*., 2000]. `blat2gff` converts `BLAT` [Kent, 2002] output into `GFF`, while `sim2gff` does the same for `SIM` [Huang and Miller, 1991] output. The `C` program, `ali2gff`, processes `SIM` or `Mummer` [Delcher *et al*., 1999] output to produce the `GFF` records for the alignment.

### 5.3.2 Abril *et al*, *Bioinformatics*, 19(18):2477–2479, 2003

**PubMed Accession:**

`http://www.ncbi.nlm.nih.gov/entrez/query.fcgi?cmd=Retrieve&db=PubMed&list_uids=14668236&dopt=Abstract`

**Journal Abstract:**

`http://bioinformatics.oupjournals.org/cgi/content/abstract/19/18/2477`

**Program Home Page:**

`http://genome.imim.es/software/gfftools/GFF2APLOT.html`

BIOINFORMATICS APPLICATIONS NOTE Vol. 19 no. 18 2003, pages 2477–2479
DOI: 10.1093/bioinformatics/btg334

# gff2aplot: Plotting sequence comparisons

Josep F. Abril[1,*], Roderic Guigó[1] and Thomas Wiehe[2,†]

[1]Grup de Recerca en Informàtica Biomèdica, Institut Municipal d'Investigació Mèdica (IMIM) Universitat Pompeu Fabra (UPF)—Centre de Regulació Genòmica (CRG), Passeig Marítim de la Barceloneta 37–49, 08003 Barcelona, Catalonia, Spain and [2]Freie Universität Berlin, Arnimallee 22, 14195 Berlin, Germany

Received on March 4, 2003; revised on June 11, 2003; accepted on June 20, 2003

**ABSTRACT**

**Summary:** gff2aplot is a program to visualize the alignment of two sequences together with their annotations. Input for the program consists of single or multiple files in GFF-format which specify the alignment coordinates and annotation features of both sequences. Output is in PostScript format of any size. The features to be displayed are highly customizable to meet user specific needs. The program serves to generate print-quality images for comparative genome sequence analysis.

**Availability:** gff2aplot is freely available under the GNU software licence and can be downloaded from the address specified below.

**Contact:** jabril@imim.es

**Supplementary information:** http://genome.imim.es/software/gfftools/GFF2APLOT.html

An often occurring task in comparative sequence analysis is to suggestively display a pairwise alignment, possibly together with domain annotations for one or both sequences. Some well-known programs are Dotter (Sonnhammer and Durbin, 1995), PipMaker (Schwartz *et al*., 2000), VISTA (Mayor *et al*., 2000) or Laj (Wilson *et al*., 2001). While the first tool is suited to interactively explore the site by site comparison of two sequences without annotations, the others produce a one-dimensional projection of a pairwise or a multiple alignment, along with the annotation features. In all these cases, however, the visualization tools are intrinsically tied to a specific underlying alignment algorithm. We have developed the program gff2aplot to generate two-dimensional annotated alignment plots in PostScript format. gff2aplot is not tied to a particular alignment algorithm, but rather can be used as a visualization filter after running some independent alignment tool. In this regard gff2aplot is related to Alfresco (Jareborg and Durbin, 2000), but while Alfresco is oriented towards highly interactive use and has limited printing capabilities, gff2aplot is intented for producing high quality printed images. The strategy used in gff2aplot is very similar to that employed in gff2ps (Abril and Guigó, 2000), a tool to visualize annotations of genomic sequences obtained from different sources. User may parse alignment segments from any of the current similarity search tools, and combine them if desired in the gff2aplot output. We provide several such filters from the gff2aplot website, to parse, for instance, NCBI-BLAST (Altschul *et al*., 1997), WU-BLAST (W. Gish, 1996–2003, http://blast.wustl.edu), SIM (Huang and Miller, 1991), MUMMER (Delcher *et al*., 1999) or BLAT (Kent, 2002). Integrating data will improve the information we obtain about pairs of genomic sequences. We distinguish records containing annotation features and those defining alignment segments. One or more ASCII input data files in GFF-format (see gff2aplot manual) can be processed in a single run. The image produced has a standard layout: it consists of two panels, placed above each other. The upper one displays the alignment of two sequences by means of a rectangular matrix. Sequence annotations are displayed along the top and left edges. The optional lower one contains vertical projections of the aligned fragments in the upper panel and displays their alignment scores or match percentages as in a PiPplot (see examples from Fig. 1). Sequence coordinate tags are shown on the lower and right edges of the panel frames. Projections of the annotated features can be shown under the alignment segments to highlight relationships between them. As in gff2ps, gff2aplot assumes that the input GFF records carry enough formatting information. Thus, in most cases, meaningful output can be obtained using the default settings. Nevertheless, gff2aplot allows for a high degree of customization. Almost any component of the plot can be configured, either through a very flexible customization file (several of such files can be processed for a single plot), or through command-line options (see gff2aplot manual). In particular, users can select any standard printing media size or define their own plot sizes.

gff2aplot is written in PERL and PostScript. It runs on UNIX or Linux platforms and it does not require any special compiler or additional software beyond the installation of Perl, version 5.5 or higher. The program generates a PostScript output file which can be viewed or printed with

*To whom correspondence should be addressed.
†Current Address: Universität zu Köln, Institut für Genetik, Weyertal 121, 50931 Köln, Germany.

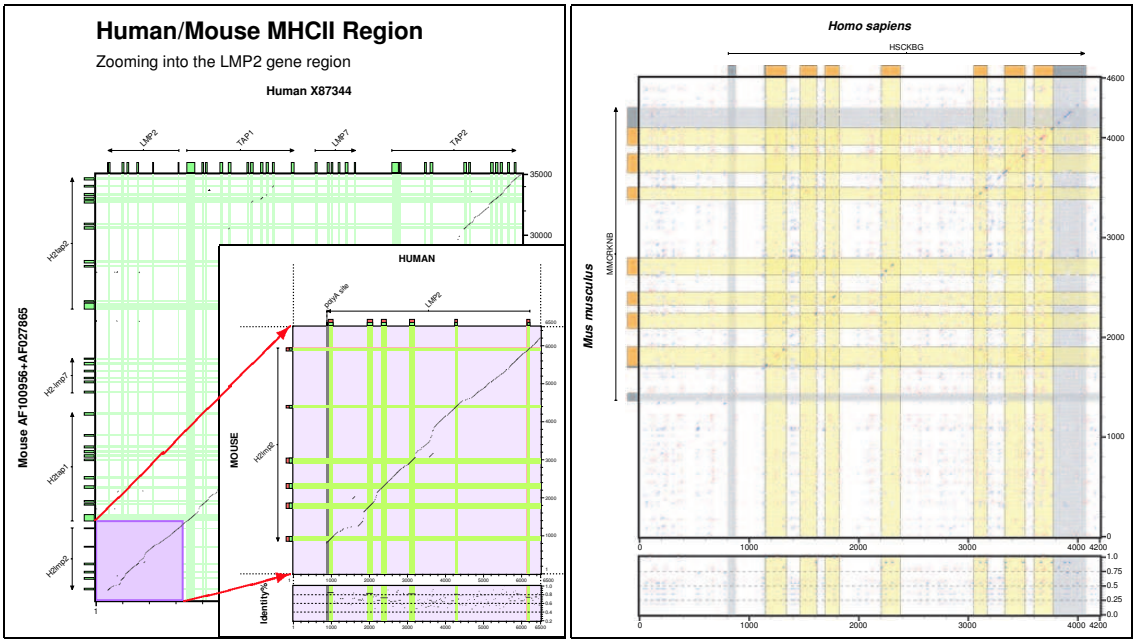


**Fig. 1.** (Left panel) Comparative analysis of a syntenic genomic region between human and mouse, extending across several genes (MHC II region, Accession Numbers shown on annotation axes main labels). Alignment was obtained using SIM (Huang and Miller, 1991). The pale violet box highlights the region being expanded in the bottom right plot, while red arrows show the corresponding areas on both figures. The region being expanded is the LMP2 human gene region and its counterpart in mouse. Green boxes and projections correspond to CDSs, as annotated in GenBank, while red boxes conform the predicted gene structure by program SGP-1 (Wiehe *et al*., 2001). (Right panel) All possible pairs of potential splice sites on human and mouse homologous sequences were analyzed against the corresponding gene structures, in this case for *creatine kinase B* gene (Accession Numbers X15334 and M74149, for human and mouse, respectively). `gff2aplot` combines here results from two different analysis, red bars correspond to putative donor sites and blue bars to acceptor site ones. All input and parameter files which were used to generate the examples in the figure are accessible from the `gff2aplot` website. Additional examples, as well as a detailed user manual, can also be found there.

any PostScript capable output device. Although PostScript lacks user-interactivity and hyper-link capability, for high-quality images the page description language PostScript has several advantages over bitmap graphics programs. Among these are the free scalability of all plots, the embed-ability of PostScript picture files into text documents (specially those written in LaTeX), the graphics device independence and the robustness with respect to handling large amounts of data. These properties have made `gff2ps` the tool of election to produce, among other applications, the gene content maps of the fly (Adams *et al*., 2000), human (Venter *et al*., 2001), and mosquito (Holt *et al*., 2002) genomes. Like `gff2ps`, the `gff2aplot` program described here is suitable as a filter for high-throughput analysis pipelines. The program has already been applied as a drawing tool for human/mouse comparisons in recent publications (e.g. Parra *et al*., 2003); development versions of `gff2aplot` have already been used in other papers (e.g. Reichwald *et al*., 2000; Wiehe *et al*., 2001). Although initially developed to display sequence similarity relationships, the simplicity and generality of the GFF standard may make `gff2aplot`, through its high customization capabilities, useful to display other matrix-like generic relationships between sequences, for example the splice sites analysis shown in the right panel of Figure 1.

## ACKNOWLEDGEMENTS

We would like to thank Matthias Platzer, Jena, for helpful comments while developing the program prototype, and the colleagues at the Genome BioInformatics Laboratory for their extensive testing of `gff2aplot`. J.F.A. is supported by a predoctoral fellowship from the 'Instituto de Salud Carlos III (Spain)', 99/9345. This work was also supported by a joint grant from the 'German Academic Exchange Service (DAAD)' to TW and the 'Ministerio de Educación y Ciencia (Spain)' to RG. Research at the Genome BioInformatics

Laboratory is supported by grant from 'Plan Nacional de I+D (Spain)' to RG, BIO2000-1358-C02-02.

## REFERENCES

Abril,J.F. and Guigó,R. (2000) gff2ps: Visualizing genomic annotations. *Bioinformatics*, **16**, 743–744.

Adams,M.D., Celniker,S.E., Holt,R.A., Evans,C.A., Gocayne,J.D., Amanatides,P.G., Scherer,S.E., Li,P.W., Hoskins,R.A., Galle,R.F. *et al*. (2000) The genome sequence of *Drosophila melanogaster*. *Science*, **287**, 2185–2195.

Altschul,S.F., Madden,T., Schaffer,A., Zhang,J., Zhang,Z., Miller,W. and Lipman.D. (1997) Gapped BLAST and PSI-BLAST: a new generation of protein database search programs. *Nucleic Acids Res.*, **25**, 3389–3402.

Delcher,A.L., Kasif,S., Fleischmann,R.D., Peterson,J., White,O. and Salzberg,S.L. (1999) Alignment of whole genomes. *Nucleic Acids Res.*, **27**, 2369–2376.

Holt,R.A., Subramanian,G.M., Halpern,A., Sutton,G.G., Charlab,R., Nusskern,D.R., Wincker,P., Clark,A.G., Ribeiro,J.M.C., Wides,R. *et al*. (2002). The genome sequence of the malaria mosquito *Anopheles gambiae*. *Science*, **298**, 129–149.

Huang,X. and Miller,W. (1991) A time-efficient, linear-space local similarity algorithm. *Adv. Appl. Math.*,**12**, 337–357.

Jareborg,N. and Durbin,R. (2000) Alfresco—A workbench for comparative genomic sequence analysis. *Genome Res.*, **10**, 1148–1157.

Kent,W.J. (2002) Blat—the blast-like alignment tool. *Genome Res.*, **12**, 656–664.

Mayor,C., Brudno,M., Schwartz,J.R., Poliakov,A., Rubin,E.M., Frazer,K.A., Pachter,L.S. and Dubchak,I. (2000) VISTA: Visualizing global DNA sequence alignments of arbitrary length. *Bioinformatics*, **16**, 1046–1047.

Parra,G., Agarwal,P., Abril,J.F., Wiehe,T., Fickett,J.W. and Guigó,R. (2003) Comparative gene prediction in human and mouse. *Genome Res.*, **13**, 108–117.

Reichwald,K., Thiesen,J., Wiehe,T., Weitzel,J., Strätling,W.H., Kioschis,P., Poustka,A., Rosenthal,A. and Platzer,M. (2000) Comparative sequence analysis of the MECP2-locus in human and mouse reveals new transcribed regions. *Mammalian Genome*, **11**, 182–190.

Schwartz,S., Zhang,Z., Frazer,K.A., Smit,A., Riemer,C., Bouck,J., Gibbs,R., Hardison,R. and Miller,W. (2000) PipMaker—A web server for aligning two genomic DNA sequences. *Genome Res.*, **10**, 577–586.

Sonnhammer,E.L. and Durbin,R. (1995) A dot-matrix program with dynamic threshold control suited for genomic DNA and protein sequence analysis. *Gene*, **167**, GC1–10.

Venter,C.J., Adams,M.D., Myers,E.W., Li,P.W., Mural,R.J., Sutton,G.G., Smith,H.O., Yandell,M., Evans,C.A., Holt,R.A. *et al*. (2001) The sequence of the human genome. *Science*, **291**, 1304–1351.

Wiehe,T., Gebauer-Jung,S., Mitchell-Olds,T. and Guigó,R. (2001) SGP-1: prediction and validation of homologous genes based on sequence alignments. *Genome Res.*, **11**, 1574–1583.

Wilson,M.D., Riemer,C., Martindale,D.W., Schnupf,P., Boright,A.P., Cheung,T.L., Hardy,D.M., Schwartz,S., Scherer,S.W., Tsui,L.-C., Miller,W. and Koop,B.F. (2001) Comparative analysis of the gene-dense *ACHE/TFR2* region on human chromosome 7q22 with the orthologous region on mouse chromosome 5. *Nucleic Acid Res.*, **29**, 1352–1365.

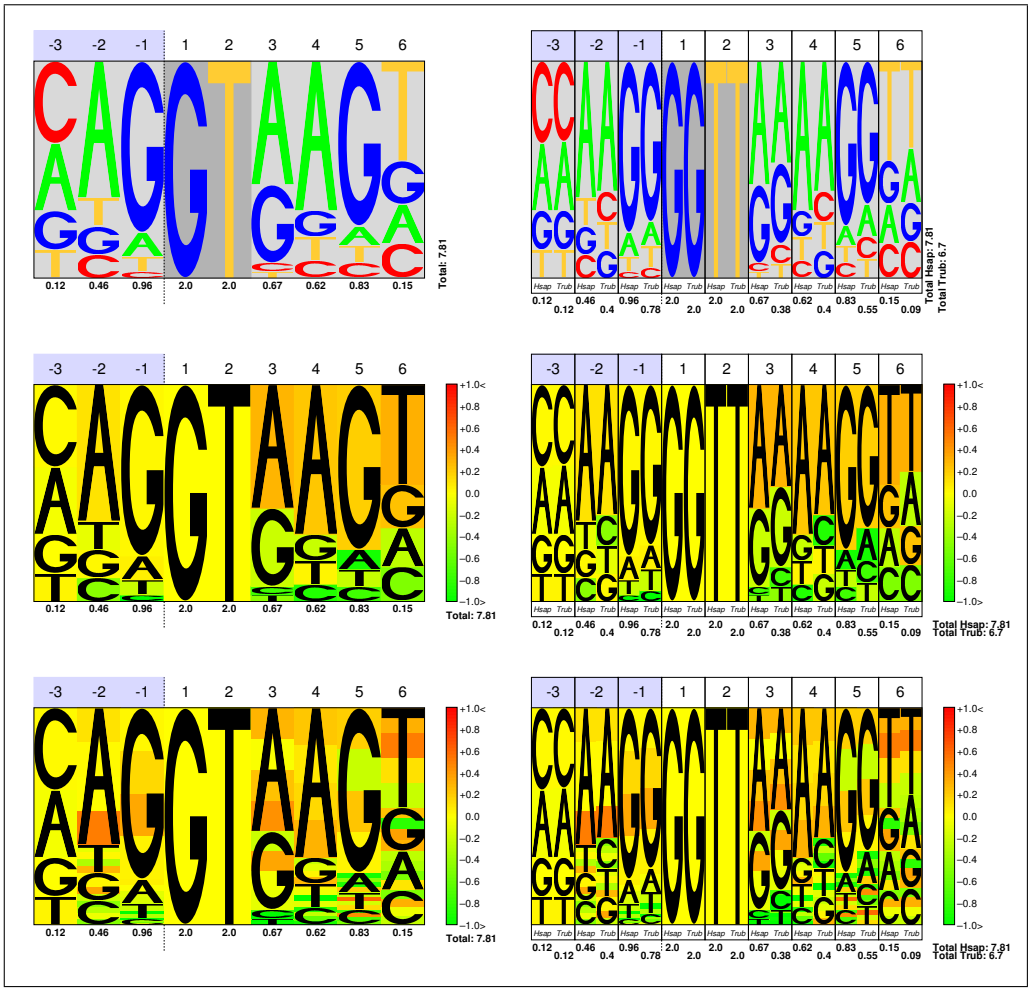

Figure 5.9: **Comparative pictograms.** We have initially developed `compi` to help in comparative analyses of splice sites. It can produce two kind of pictograms: the "standard" views, visualizing a pictogram for single species (left panels) and "comparative" views, currently set for pair-wise species matrices comparison (right panels). Depending on the input matrix, three different plots can be obtained, from top to bottom: the basic pictograms (with extra customizable layout), the Position-specific Scoring Matrices (PSMs) and the First-order Markov Models (FMMs) representations.

### 5.3.3 `compi`: Comparative pictograms

In sequence pictograms [Burge *et al.*, 1999]—which are analogous to sequence logos [Schneider and Stephens, 1990], the frequencies of the four nucleotides at each position along the signal—, the so called Position Weight Matrices [PWMs; Staden, 1984a, 1988; though the nowadays preferred term is Position-specific Scoring Matrices or PSMs] are represented by the heights of their corresponding letters. The information content (intu-

itively, the deviation from random composition) is computed at each position. It ranges from zero to two, with zero indicating random composition, and two indicating fixation of one nucleotide. The information content of the signal is the sum of the information content at each position. The larger the information content, the more conserved the signal (and, thus, more "informative": the smaller is the probability of finding it by chance). The relative entropy formula (also known as the Kullback-Leiber distance; Burge *et al*. 1999) is used to calculate the information content of the signal, as follows:

$$H_{signal} = \sum_{j=1}^{N} \sum_{i,j} P_{i,j} \log_2 \frac{P_{i,j}}{Q_i} \quad .$$

Where $N = length(signal)$, and $i \in \{A, C, G, T\}$. $P_{i,j}$ is the probability of finding nucleotide $i \in \{A, C, G, T\}$ in the $j^{th}$ nucleotide of the signal, and $Q_i$ is the probability of that nucleotide under the background distribution. By default, `compi` assumes the random distribution as background (so that, each $Q_i = \frac{1}{4}$), although other distributions can be provided by the user.

By inspecting the pictograms for two or more species, one tries to spot the different use, made by each of the species, of the nucleotides along the signal. This inspection, however, can become a difficult task for the following reasons. First, the differences in the size of each nucleotide can be difficult to observe as the two nucleotides are located in different pictures. Second, these differences are not quantified and thus we cannot assess with precision when a nucleotide is used more frequently in one of the species. Third, the assumption of marginal independence among the positions of the signal—implicit in PWMs—can hide relevant differences between species with regard to the dependencies between nearest neighbour positions along the splice signal.

We have tackled all three problems. First we have placed the nucleotides that occur in the same position, in the two species being compared, next to each other. Second we have calculated the ratio of the two relative frequencies (the odds) of each nucleotide in each position and represent the $\log_2$ of this ratio with a color code from green ($\log_2 \frac{1}{2} = -1$) to red ($\log_2 2 = 1$), where yellow is a ratio of 1 (0 in log-scale). The log-odds values of -1 and 1 work as saturation values and therefore, odds smaller than 0.5 or larger than 2 take green and red color, respectively. This color fills the rectangle defined by the nucleotide character and allows easy spotting of which nucleotides show a different occurrence between species. Third, we have extended the pictogram idea to represent first order dependencies between adjacent positions of the splice site—the so called First-order Markov Model (FMM). We have computed and represented the ratios of occurrence of each nucleotide with respect to the occurrence of every nucleotide in the previous positions. The representation has been implemented by splitting the rectangle defined by a nucleotide character in four equal rectangles, and filling out each of them with the color that corresponds to each of the ratios following a fixed order of A,C,G, and T. We shall refer to this representation as a *comparative pictogram* (`compi`). When rendering FMMs, the relative entropy at each position for each nucleotide is also weighted with respect to the occurrence of every nucleotide in the previous positions.

We split the task of producing the comparative pictograms in two, using separate `perl` scripts for each part. The first one computes nucleotide frequencies, ratios and First-order Markov dependencies from a set of sequences of fixed length. Then the matrices obtained

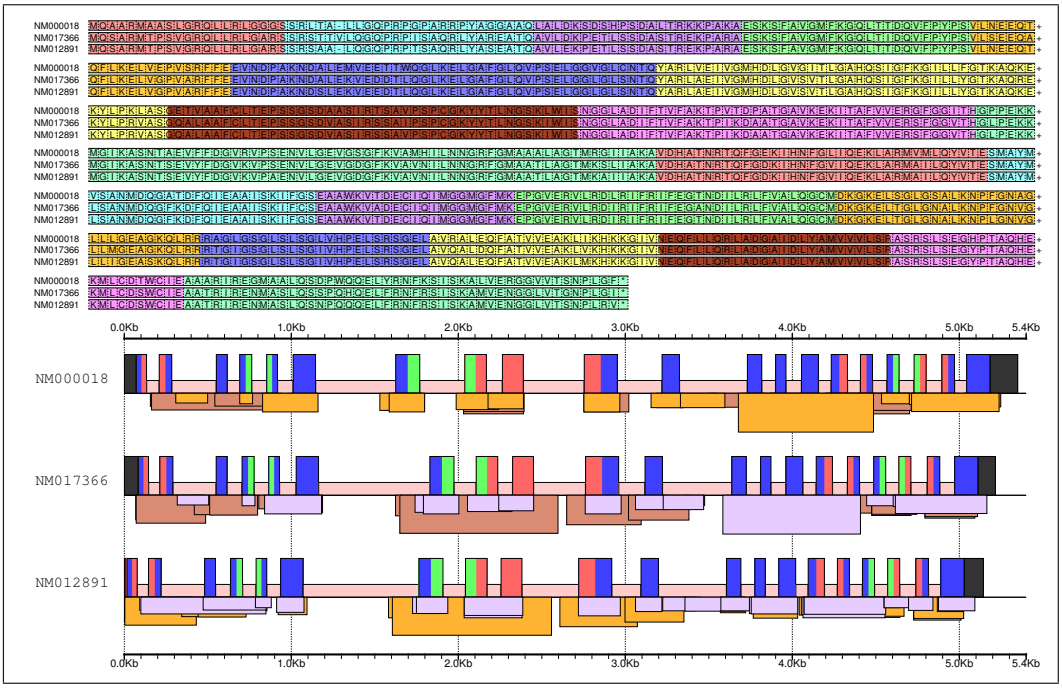


Figure 5.10: **Merging exonic structure with coding sequence alignments.** Comparing the exonic structure of a set of orthologous genes (REFSEQ codes *NM000018*, *NM017366*, and *NM012891* in human, mouse, and rat respectively). At the protein level (top), splice sites were mapped over the amino acid alignment, and consecutive underlying exons were represented by alternating light and dark grey boxes. At the genomic level (bottom), the exonic structures are depicted along with the filtered best hits calculated from pair-wise `WU-TBLASTX` [Gish, 1996–2004] of comparisons of each sequence against the other two. The height of the boxes under the sequence axes correlates with the alignment score. The lower panel was obtained by `gff2ps` [Abril and Guigó, 2000].

are processed by a second script which generates POSTSCRIPT code specifically developed for the corresponding graphical representation of the matrices. This script can produce six different outputs, three "standard" (visualizing a pictogram for single species) and three "comparative" views (currently set for pair-wise species matrices comparison), which are shown in Figure 5.9. Computing the matrices outside the graphical program gives more flexibility to the user, who can preprocess matrices from other software to fit the input format of our tool (see page 213, on Web Glossary). This tool has been used to produce the pairwise pictograms shown in Figure 4.13 on page 134 (Figure 2 on page 116 of Abril *et al.* 2005).

### 5.3.4 Other developments

Several graphical procedures have been developed other than those shown until now, although many of them either are not finished enough to release to the community, or are

quite specific for a given analysis to be really useful in another context. We are going to point out few of them in this section.

The need to combine the exonic structures along with sequence alignments at nucleotide or amino acid level, led to the development of the boxed alignments script for which an example is shown in Figure 5.10 upper panel. A more elaborated program developed in our group, named `exstral` (EXon STRucture over an ALignment, Castelo *et al.* 2004), produces a more quantitative output. However, its current text-based output lacks the integration achieved with the boxed alignments—for instance, to highlight subtle frame shifts in the exonic structure. The boxed alignments script generates a POSTSCRIPT plot. It will be interesting in the future to implement such kind of output into `exstral`.

As much important as writing procedures to analyze genomic data sets, is to choose an appropriate way to visualize the final results. The customization flexibility characteristic of `gff2ps` makes this tool useful to draw annotation features from different kind of analyses. Given a properly formatted input set of GFF records and taking the time to define an associated customization file or files, a researcher can obtain simple or complex representations of his annotations. It is then easy to apply those settings to a set of annotations for different sequences. Lower panel from Figure 5.10 shows an example of using `gff2ps` in a comparative genomics approach.

# Chapter 6

# Discussion

> So easy it seamed once found, which yet unfound
> most would have thought impossible
>
> —John Milton

A central goal of genome analysis is the identification of all human genes. This task remains challenging, but is greatly aided by the near-complete sequence of the human genome [International Human Genome Sequencing Consortium, IHGSC, 2004], together with other improved resources (such as expanded cDNA collections, genome sequence from other organisms and better computational methods). The inventory of the best-defined functional components in the human genome—the protein coding sequences—is still incomplete for a number of reasons, including the fragmented nature of eukaryotic genes. The human gene number estimates, though, are coming closer to the real number of genes, as can be seen in Figure 6.1. To this end, there are several ongoing projects focusing on the definition of the precise catalog of human genes. One of those projects is the Vertebrate Genome Annotation (VEGA) database, a central repository for high quality, frequently updated, manual annotations of vertebrate finished genome sequences [Ashurst *et al.*, 2005]. The comparative sequencing program at the NIH Intramural Sequencing Center (NISC) aims to sequence and to analyze targeted genomic regions in multiple vertebrates [Thomas *et al.*, 2003]. The initial target of this project was a genomic segment of about 1.8 Mb on human chromosome 7*q*31.3 containing the gene encoding the cystic fibrosis transmembrane conductance regulator (*CFTR*) and nine other genes. Sequence clones for the orthologous genomic segments in multiple other vertebrates were obtained in order to perform an exhaustive comparative analysis of that region. The American National Human Genome Research Institute (NHGRI) launched a public research consortium, the ENCyclopedia Of DNA Elements (ENCODE) project [ENCODE Project Consortium, 2004], in September 2003, to carry out a project to identify all functional elements in the human genome sequence. The project is currently in its pilot phase, the evaluation of the procedures that can be applied cost-effectively and at high-throughput to accurately and comprehensively characterize large sequences. A set of 44 discrete regions—ranging in size from 0.5 to 2 Mb, that together constitute ∼1% of the human genome (30 Mb)—was chosen to represent a range of genomic features.

The unexpectedly low number of genes identified in the human genome raises again the

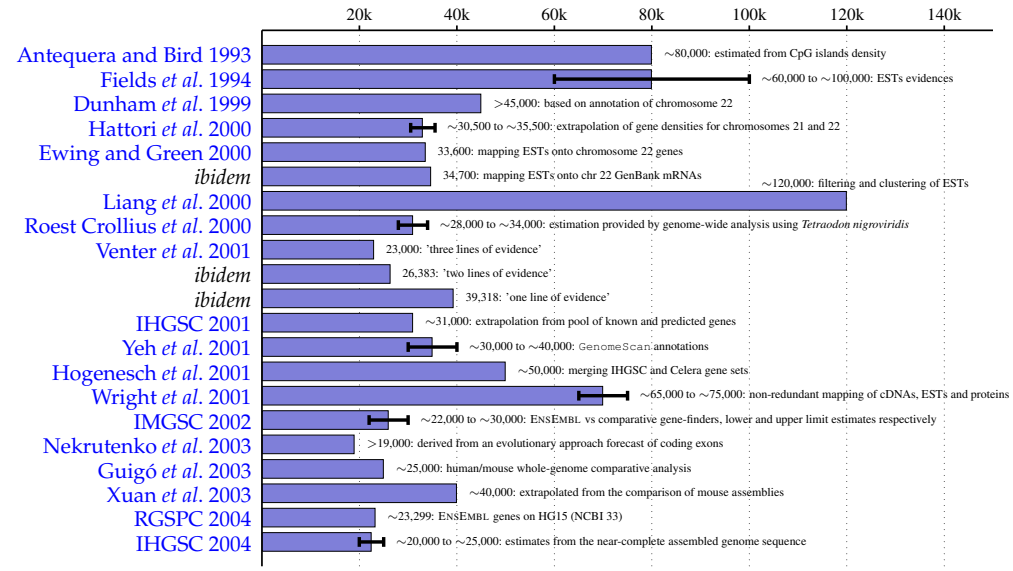


Figure 6.1: **Human gene number estimates in the genome era.** The figure depicts the number of human genes (blue bar) from various estimates, along with the references in which they were reported. It is worth to note that genes may produce more than one transcription unit or transcripts, which is not taken into account in this picture. Adapted from Harrison *et al.* [2002].

question of the source of an organism's complexity. One possible source is the greater structural complexity of the human genes, along with a higher level of regulation of those genes and the pathways in which they are involved. Another source are post-transcriptional modifications, more than 200 types are known and is predicted that three different modified proteins are produced for each human gene on average [Banks *et al.*, 2000]. Furthermore, alternative splicing of human genes might provide many more proteins per gene than in other organisms. Nevertheless, in Brett *et al.* [2002] they found similar levels of alternative splicing across species which argues against an overall increase in splicing as a source of increase in genome and organism complexity. Their data also suggested that a wide variety of gene products are further diversified by post-translational modifications. More recently, though, Pan *et al.* [2005] have provided evidence that at least 11% of human and mouse cassette alternative splicing events represent conserved exons that undergo species-specific alternative splicing. Such events have the potential to modulate frequently the structural and functional properties of proteins that are attributed to conserved domains. Therefore, they conclude that they could have an important role in the evolutionary differences between mammalian species. On the other hand, the recent identification of several types of ncRNAs, such as small nucleolar RNAs, microRNAs, guide RNAs and anti-sense RNAs, would significantly expand the complexity of the human genome [Storz, 2002]. Given the absence of a diagnostic open reading frame, a major question arises on how these genes can be identified. Novel evidences obtained by using high-density oligonucleotide arrays on different cell lines provide support for transcription outside well-characterized human exons [Kampa *et al.*, 2004]. Those transcribed regions, also known as transfrags, will provide a new view of the human transcriptome by mapping transcription to the genomic

sequences.

One of the major obstacles towards the completion of the catalog of human genes is our inability to assess the reliability of the large number of computational gene predictions that have yet to be verified experimentally. Results described in Parra *et al.* [2003] demonstrate that through the comparison of related genomes, human and mouse in that example, and using the available comparative gene-finding tools, the false-positive rate can be reduced significantly, resulting in an improved catalog of vertebrate genes. Indeed, the experimental verification of a subset of those predictions provided evidence for at least 1000 previously non-confirmed genes [Guigó *et al.*, 2003]. The availability of another vertebrate species whose evolutionary position lies between mammals and fish would be of great utility to complete the vertebrates gene catalog. The success of these studies, suggests a new paradigm in high throughput genome annotation, in which gene predictions serve as the hypothesis that drives experimental determination of intron-exon structures. Therefore, it is clear that with the accumulation of genomic data from other species and a better understanding of the mechanisms and the signals involved in the transfer of information from sequence to function, more accurate computational models will be available. Those models have to face not only the complexity inherent to the biological processes and their regulatory pathways, but also the complexity of the inter- and intra-specific variability due to evolutionary events that led to the actual genomes of individuals and populations.

Existing gene finding programs, although significantly advanced over those that were available a few years ago, still have several important limitations. Almost without exception, computational gene finders predict only the coding fraction of a single spliced form of non-overlapping, canonical protein-coding genes. Annotation pipelines are currently able to extend those annotations by incorporating other biological features of clear interest for the research community, including non-coding mRNAs, pseudogenes, regulatory elements and transcription start sites, anti-sense transcripts, but also other genome-scale data collections such as gene expression profiles, protein interaction and genetic variation. However, a better understanding of the molecular mechanisms involved in gene expression and the integration of this knowledge into the theoretical models underlying the gene prediction software, may lead to systems that will be accurate enough to render both experimental verification and manual curation largely unnecessary [Brent and Guigó, 2004]. As more animal genomes are sequenced, deeper sequence alignments will contribute further to the definition of signals such as regulatory elements. The application of comparative genomics to study gene regulation has focused largely on the identification of shared regulatory sequences to explain similar patterns of gene expression between species. By contrast, the differences in gene regulation between organisms, and the role of these differences in speciation, have only just begun to be examined [Pennacchio and Rubin, 2001].

As more evidence of the conservation of exonic structures between orthologous genes and the sequence features that define such exons are accumulated [Waterston *et al.*, 2002; Gibbs *et al.*, 2004; Hillier *et al.*, 2004; Abril *et al.*, 2005], the analysis of the extent of that conservation becomes relevant to the prediction of alternative splicing events. Further evidence suggests that a large fraction of alternative splicing events is conserved between related species, such as human and mouse [Thanaraj *et al.*, 2003]. The analysis of the conserved sequence features involved in splice site definition, as well as in the regulation of splicing, will shed light on the code that determines the final pool of eukaryotic genes products. Alternative splicing remains, however, as a poorly solved problem. On the other hand, a comparison of the structural and mechanistic features of the major-class and minor-

class, U2- and U12-types respectively, spliceosomes has provided many valuable insights into the essential catalytic elements of the splicing reaction. The rate-limiting excision of U12-type introns and their use in alternative expression of proteins *in vivo* indicates that they might be potential targets of gene regulation. Assessing gene expression patterns in transgenic organisms with U12 to U2 intron mutations should provide vital evidence and help to rationalize the continued presence of these rare introns in metazoan genomes [Patel and Steitz, 2003]. The existence of a second spliceosome raises the possibility that a third or fourth might be awaiting discovery. The degeneracy of the consensus sequences defining those signals would make yet another class of introns difficult to detect. Indeed, the GT-AG U12-type introns might well have been ignored for the initial focus on AT-AC introns.

Another promising research area involves the analysis of the polymorphisms that fall within the sequences defining splice sites or in the splicing regulatory sequences. Mutations in exonic or intronic regulatory elements that cause severe splicing defects might just be the tip of the iceberg. There might be also many genomic variants, including small indels and single nucleotide polymorphisms (SNPs), that cause partial splicing defects that are only pathogenic in specific tissues under the influence of a set of specific regulatory splicing factors. Similar to splicing, all those processes are rarely considered when assessing the clinical significance of genomic variants [Pagani and Baralle, 2004]. In this regard, we have gathered a database, to be explored in future analyses, which integrates gene structures for reference human genes [RefSeq; Pruitt *et al*. 2005], the conservation scores from phylo-HMM based multiple alignments (for human, chimpanzee, mouse, rat, and chicken, and downloaded from the UCSC Genome Browser; Karolchik *et al*. 2003) and a large collection of human SNPs from NCBI dbSNP [Sherry *et al*., 2001].

Visualization tools will continue to play a key role in the integration of the genomic annotation data sets, in order to extract biological meaning from that flood of information. Due to the intrinsic dynamic nature of the annotation data sets, database browsers have become standard tools at the laboratory to retrieve the latest updates on genomic annotations and to navigate through the many different databases available. All public genome browsers have their particular strengths: the UCSC Genome Browser exemplifies speed; NCBI Map Viewer is integrated into a larger site and is linked to the impressive range of databases that NCBI curates; `GBrowse` is a sophisticated toolkit designed to simplify building data browsers to display custom data; Ensembl provides flexibility and a broad range of data displays [Stalker *et al*., 2004]. Notwithstanding, command-line flexible visualization tools still have their niche, as it is the case for `gff2ps`, `gff2aplot`, `compi` and similar tools. Although raster graphics are more popular and are currently best supported by web browsers, we still advocate the use of vector graphics to visualize genomic annotations. Vector graphics have one feature that makes them invaluable for many applications: they can be scaled without loss of image quality. For a long time, PostScript has been the *de facto* standard of the graphics industry, and it has been well supported on `*nix` systems which provided not only interpreters, such as `ghostscript`, but also graphical interfaces for those interpreters, such as `ghostview`. With the advent of `XML` technologies, an emerging new graphics standard, the Scalable Vector Graphics format (`SVG`) will become the successor of PostScript, at least for distributing vector graphics on the Internet. However, PostScript is by itself a programming language. When self-contained documents are created, the data and the code to visualize such data share a single file, as happens for instance with `gff2ps` output.

In conclusion, finding all functional elements of genome sequences and using this information to improve the health of individuals and society, are the focus of the next phase of the Human Genome Project [Collins *et al.*, 2003]. Comparative analyses from multiple species at varying evolutionary distances are a powerful approach for identifying coding and functional non-coding sequences, as well as sequences that are unique for a given organism. Those techniques will continue to play a major role in the accurate annotation procedures required to understand the puzzling patchworks that are our genomes.

# Chapter 7

# Conclusions

> Errors, like straws, upon surface flow;
> he who would search for pearls must dive below...
> —John Dryden, "*All for love*"

In short, the research presented here has contributed to:

1. The development of a semi-automatic computational pipeline to perform whole genome analyses when comparing the human and mouse genomes. The main results are described hereunder:

   (a) The analyses included the production of gene predictions by `geneid`, an "*ab initio*" gene-finding software, and `SGP2`, initially a wrapper for `TBLASTX` and `geneid` to perform pair-wise comparative gene-finding.

   (b) Moreover, the evaluation of the predictions using a reference set of annotations and the visualization of the results, were among the steps of this pipeline.

   (c) The results from this pipeline, together with those provided by the people from the `Twinscan` project, were filtered by Genís Parra. Using an enrichment protocol based on the conservation of exonic structure between orthologous predictions between human and mouse, he supplied gene candidates for RT-PCR amplification to validate such predictions.

   (d) Several programs from this analysis pipeline have been adapted by Francisco Câmara. Currently, they are routinely used to predict genes on each new assembly version of several eukaryotic genomes. These species include human, mouse, rat, chicken, fruitfly, and the list keeps growing.

2. Describing the signals delimiting the boundaries between exons and introns. Taking advantage of the conservation of the exonic structures of orthologous genes in vertebrates, we have been able to tackle the comparative analysis of splice sites from orthologous introns. This research yielded the following results:

   (a) Human introns are on average larger than their respective orthologs in rodents. This can be explained by an increase in the repetitive sequences within those

introns in the human lineage or by a loss of such repeats in the rodents lineage. The analysis of the distribution of ancient repeats, predating the split between human and rodents, supports the latter.

(b) We provide insights into the dynamics of the evolution of splice site sequences within four vertebrate genomes: human, mouse, rat and chicken. Our results confirm that the splicing code is under evolution, albeit very slow, remaining largely homogeneous within tetrapoda and showing noticeable differences only at larger phylogenetic distances.

(c) The greater conservation observed in mammalian/chicken orthologous splice sites compared to unrelated sites indicates that nucleotide substitution since the mammalian/avian split has not yet reached saturation at these sites. Saturation has been reached at intronic sites, which show a conservation level similar to that of unrelated sequences.

(d) The characteristic conservation of orthologous splice sites suggests that comparative prediction of splicing could improve methods based on the analysis of a single genome. Comparative prediction of splice sites could be particularly relevant to the prediction of alternative splicing features, a problem far from being solved.

(e) Our results seem to indicate that U2 and U12 introns have evolved independently after the split of mammals and birds, since we have not been able to document a single convincing case of conversion between these two types of introns.

(f) Furthermore, comparison of orthologous introns has also allowed us to define better the sequences involved in the specification of U12 introns. These sequences, while more conserved than signals involved in U2 intron specification, are more degenerate than previously thought.

3. The implementation of visualization tools for annotations obtained by gene-finding tools on genomic sequences, such as `gff2ps`, and to summarize the outcomes of comparative analyses, such as `gff2aplot` and `compi`. The main results are listed below:

(a) `gff2ps` was devised to provide scalability and a flexible customization of the annotation feature attributes.

(b) We have applied `gff2ps` to the "cartography" of sequence features for whole genomes of human, the fruitfly and the malaria mosquito. In those cases we had to implement specific software to integrate the large annotation data sets from these genomes and to provide specific customization parameters.

(c) `gff2aplot` produces pair-wise alignment plots along with the annotation features of the sequences.

(d) `compi` extends pictograms to compare the nucleotide frequencies of sequence patterns side-by-side. We used this tool in our orthologous splice sites signal comparison.

(e) Several of the tools we have developed, including `gff2ps` and `gff2aplot`, have been made publicly available at our web site. They have been used with success by other groups to visualize the results of their own research.

# APPENDICES

There and back again...
—Bilbo Baggins, "*The Hobbit*"

# Curriculum Vitae

Josep F. Abril graduated on 1998 in Biology (Bachelor's degree) by **Universitat de Barcelona** (UB). He spent his last years as undergraduate collaborating with the laboratory of genome analysis at the **Grup de Recerca en Informàtica Biomèdica** (GRIB), under Dr. Roderic Guigó supervision. He obtained the Research competence and Advanced Studies Diploma ("*Diploma d'Estudis Avançats*", DEA) on 2002 by **Department of Experimental Sciences and Health** of **Universitat Pompeu Fabra** (UPF). From late 1998 till early 2005 he stayed as a *PhD* student, under supervision of Dr. Roderic Guigó within the GRIB.

Since 2000, he has been in charge of the **Genome Bioinformatics Lab** web site[1]. Among different software developments, it is worth to mention his contributions to visualization of genomic annotations, `gff2ps` and `gff2aplot`. `gff2ps` was used to visualize different whole genome maps, including those for human, the fruitfly and the malaria mosquito.

He has been teaching assistant for the practicals of the Bioinformatics course taught by the the **Genome Bioinformatics Laboratory** at **Universitat Pompeu Fabra**, between 2001 and 2005. Additionally, he has taught an introductory `perl` course for the **MSc on Bioinformatics for Health Sciences**, co-directed by **Universitat Pompeu Fabra** and **Universitat de Barcelona**, in 2004. He participated in the organization and presentation of the Bioinformatics stand for the "*Fira Viu la Ciència Contemporània*" (FVCC'03, a popular science fair) organized by the **Societat Catalana de Biologia**, in Barcelona in May 2003. He was also one of the organizers and lecturers of the workshops on "Computational Analysis of DNA Sequences" by **La Caixa**, held in Barcelona in November 2003 and 2004, and in Madrid in June 2004. He was invited speaker on the $4^{th}$ meeting of the **Sociedad Española de Genética** held in El Escorial on October 2003.

He is currently involved in the management of paper contributions to the **$4^{th}$ European Conference on Computational Biology** (ECCB'05[2]), to be held in Madrid, Spain (September 28–October 1, 2005). He is also participating in the organization of the **ENCODE Genome Annotation Assessment Project** (EGASP'05[3]) workshop, to be held at the **Wellcome Trust Sanger Institute** (May 6–7, 2005).

His main research interest focuses on the computational analysis of the exonic structure of eukaryotic genes, its definition, evolution and association with genetic disorders. Gene-finding and the visualization of genomic annotations are also within those interests.

---

[1] GBL @ GRIB[IMIM-UPF-CRG] at: `http://genome.imim.es/`

[2] ECCB'05 at: `http://www.eccb05.org/`

[3] EGASP'05 at: `http://genome.imim.es/gencode/workshop2005.html`

# List of Publications

## Articles


J.F. Abril, R. Castelo and R. Guigó.
"Comparison of splice sites in mammals and chicken."
*Genome Research*, 15(1):111–119, 2005.


International Chicken Genome Sequencing Consortium (including J.F. Abril).
"Sequence and comparative analysis of the chicken genome provide unique perspectives on vertebrate evolution."
*Nature*, 432(7018):695–716, 2004.


Rat Genome Sequencing Project Consortium (including J.F. Abril).
"Genome sequence of the brown Norway rat yields insights into mammalian evolution."
*Nature*, 428(6982):493–521, 2004.


J.F. Abril, R. Guigó and T. Wiehe.
"`gff2aplot`: Plotting sequence comparisons."
*Bioinformatics*, 19(18):2477–2479, 2003.


R. Guigó, E.T. Dermitzakis, P. Agarwal, C.P. Ponting, G. Parra, A. Reymond, J.F. Abril, E. Keibler, R. Lyle, C. Ucla, S.E. Antonarakis and M.R. Brent.
"Comparison of mouse and human genomes followed by experimental verification yields an estimated 1,019 additional genes."
*Proc. Nat. Acad. Sci.*, 100(3):1140–1145, 2003.


G. Parra, P. Agarwal, J.F. Abril, T. Wiehe, J.W. Fickett and R. Guigó.
"Comparative gene prediction in human and mouse."
*Genome Research*, 13(1):108–117, 2003.


Mouse Genome Sequencing Consortium (including J.F. Abril).
"Initial sequencing and comparative analysis of the mouse genome."
*Nature*, 420(6915):520–562, 2002


R.A. Holt *et al* (including J.F. Abril).
"The Genome Sequence of the Malaria Mosquito *Anopheles gambiae*."
*Science*, 298(5591):129–149, 2002.


G. Glökner, L. Eichinger, K. Szafranski, J.A. Pachebat, A.T. Bankier, P.H. Dear, R. Lehmann, C. Baumgart, G. Parra, J.F. Abril, R. Guigó, K. Kumpf, B. Tunggal, the *Dictyostelium* Genome Sequencing Consortium, E. Cox, M.A. Quail, M. Platzer, A. Rosenthal and A.A. Noegel.
"Sequence and Analysis of Chromosome 2 of *Dictyostelium discoideum*."
*Nature*, 418(6893):79–85, 2002.


J.C. Venter *et al* (including J.F. Abril).
"The Sequence of the Human Genome."
*Science*, 291(5507):1304–1351, 2001.


T. Thomson, J.J. Lozano, R. Carrió, F. Serras, N. Loukili, M. Valeri, B. Cormand, M.P. del Río, J.F. Abril, M. Burset, E. Sancho, J. Merino, A. Macaya, M. Corominas and R. Guigó.
"Fusion of the human gene for the polyubiquitination co-effector uev-1 with kua, a newly identified gene."
*Genome Research*, 10(11):1743–1756, 2000.


J.F. Abril and R. Guigó.
"`gff2ps`: visualizing genomic annotations."
*Bioinformatics*, 16(8):743–744, 2000.


R. Guigó, P. Agarwal, J.F. Abril, M. Burset and J.W. Fickett.
"An Assessment of Gene Prediction Accuracy in Large DNA Sequences."
*Genome Research*, 10(10):1631–1642, 2000.


M.G. Reese, G. Hartzell, N.L. Harris, U. Ohler, J.F. Abril and S.E. Lewis.
"Genome Annotation Assesment in *Drosophila melanogaster*."
*Genome Research*, 10(4):483–501, 2000.


M.D. Adams *et al* (including J.F. Abril).
"The Genome Sequence of *Drosophila melanogaster*."
*Science*, 287(5461):2185–2195, 2000.

## Book Chapters


J.F. Abril, S. Castellano and R. Guigó.
"Comparative gene prediction."
In M.D. Adams editor:
**Comparative Genomics: A Guide to the Analysis of Eukaryotic Genomes.**
Humana Press, 2004 (*in press*).


R. Guigó, M. Burset, P. Agarwal, J.F. Abril, R.F. Smith and J.W. Fickett.
"Sequence Similarity Based Gene Prediction."
In S. Suhai editor:
**Genomics and Proteomics: Functional and Computational Aspects.**
Plenum Publishing Corporation, 2000. ISBN: 0–306–46312–1.

## Posters

J. Lagarde, J.F. Abril, F. Denoeud, R. Guigó and the GENCODE Consortium.
"`ENr334`: Computational Gene Predictions, VEGA Annotations and GENCODE Experimental Validations."
CSHL - Genomics Workshop "Identification of Functional Elements in Mammalian Genomes", New York, USA (2004)

J.F. Abril, M. Albà, E. Blanco, M. Burset, F. Câmara, S. Castellano, R. Castelo, O. Gonzalez, G. Parra and R. Guigó.
"Understanding the Eukaryotic Genome Sequence."
Inaugural Symposium of the Center for Genomic Regulation, Barcelona, Spain (2002)

E. Blanco, G. Parra, S. Castellano, J.F. Abril, M. Burset, X. Fustero, X. Messeguer and R. Guigó.
"Gene Prediction in the Post-Genomic Era."
IX$^{th}$ ISMB, Copenhagen, Denmark (2001)

G. Glöckner, L. Eichinger, K. Szafranski, P. Dear, J. Pachebat, K. Kumpf, R. Lehmann, J.F. Abril, G. Parra, R. Guigó, B. Tunggal, E. Cox, M.A. Quail, M. Platzer, A. Rosenthal, A.A. Noegel and the *Dictyostelium* Genome Sequencing Consortium.
"Sequence and Analysis of Chromosome 2 from the Model Organism *Dictyostelium discoideum*."
CSHL - Genome Sequencing & Biology, New York, USA (2001)

J.F. Abril, E. Blanco, M. Burset, S. Castellano, X. Fustero, G. Parra and R. Guigó.
"Genome Informatics Research Laboratory: Main Research Topics."
I$^{st}$ Jornadas de Bioinformática, Cartagena, Spain (2000)

T. Wiehe, J.F. Abril, M. Burset, S. Gebauer-Jung and R. Guigó.
"Comparative Genomics: At the Crossroads of Evolutionary Biology and Genome Sequence Analysis."
VII$^{th}$ ESEB, Barcelona, Spain (1999)

T. Wiehe, J.F. Abril, M. Burset, S. Gebauer-Jung and R. Guigó.
"Gene Prediction and Validation Based on Homologous Genomic Sequences."
VII$^{th}$ ISMB, Heidelberg, Germany (1999)

J.F. Abril, T. Wiehe, M. Burset and R. Guigó.
"Tools to Visualize Genome Annotations."
III$^{rd}$ RECOMB, Lyon, France (1999)

M. Burset, J.F. Abril and R. Guigó.
"`GeneID-3`, from DNA Sequence to Protein Function."
V$^{th}$ ISMB, Halkidiki, Greece (1997)

# Contact Information

Find below, in alphabetical order, the contact information of some of the authors of the research presented here:


**Josep F. Abril Ferrando** — *PhD Researcher*
Genome Bioinformatics Research Lab
Research Group in Biomedical Informatics
Institut Municipal d'Investigació Mèdica
Dr. Aiguader, 80, 08003 Barcelona (Spain)
Phone: +34 93 224 0890 || Fax: +34 93 224 0875
E-mail: jabril *at* imim.es
Web: http://genome.imim.es/~jabril/

**Mark D. Adams** — *Associate Professor*
Department of Genetics
Case Western Reserve University
10900 Euclid Avenue, Cleveland, OH 44106 (USA)
Phone: +01 216 368 2791
E-mail: mda13 *at* cwru.edu
Web: http://genomics.case.edu/people_adams.html

**Pankaj Agarwal** — *Investigator*
Department of Bioinformatics
GlaxoSmithKline Pharmaceuticals R&D
709 Swedeland Road, UW2230, King of Prussia, PA 19406-0939 (USA)
E-mail: pankaj.agarwal *at* gsk.com

**Ewan Birney** — *Research Group Leader*
EMBL Outstation - Hinxton
European Bioinformatics Institute
Wellcome Trust Genome Campus
Hinxton, Cambridge, CB10 1SD (United Kingdom)
Phone: +44 (0)1223 494 420 || Fax: +44 (0)1223 494 468
E-mail: birney *at* ebi.ac.uk
Web: http://www.ebi.ac.uk/~birney/

**Robert Castelo Valdueza** — *Senior Researcher*
Genome Bioinformatics Research Lab

Research Group in Biomedical Informatics
Institut Municipal d'Investigació Mèdica
Dr. Aiguader, 80, 08003 Barcelona (Spain)
Phone: +34 93 224 0884 || Fax: +34 93 224 0875
E-mail: rcastelo *at* imim.es
Web: http://genome.imim.es/~rcastelo/

**Roderic Guigó i Serra** — *Research Group Leader*
Genome Bioinformatics Research Lab
Research Group in Biomedical Informatics
Institut Municipal d'Investigació Mèdica
Dr. Aiguader, 80, 08003 Barcelona (Spain)
Phone: +34 93 224 0877 || Fax: +34 93 224 0875
E-mail: rguigo *at* imim.es
Web: http://genome.imim.es/~rguigo/

**Robert Holt** — *Research Head*
Sequencing Group
Genome Sciences Centre
BC Cancer Research Centre
Suite 100, 570 West 7th Ave, Vancouver, BC, V5Z 4S6 (Canada)
Phone: +01 604 877 6276
Email: rholt *at* bcgsc.ca
Web: http://www.bcgsc.ca/about/faculty/person?pid=rholt

**Genís Parra Farré** — *PhD Researcher*
Genome Bioinformatics Research Lab
Research Group in Biomedical Informatics
Institut Municipal d'Investigació Mèdica
Dr. Aiguader, 80, 08003 Barcelona (Spain)
Phone: +34 93 224 0884 || Fax: +34 93 224 0875
E-mail: gparra *at* imim.es
Web: http://genome.imim.es/~gparra/

**Martin G. Reese** — *Investigator*
Omicia Inc.
5980 Horton Street, Suite 235, Emeryville, CA 94608 (USA)
Phone: +01 510 595 0800 || Fax: +01 510 588 4523
E-mail: mreese *at* omicia.com

**Thomas Wiehe** — *Research Group Leader*
Institut fuer Molekularbiologie und Biochemie
Freie Universität Berlin
Berlin Center for Genome Based Bioinformatics
Arnimallee 22, 14195 Berlin (Germany)
Phone: +49 30 8445 1504 || Fax: +49 30 8445 1504
E-mail: twiehe *at* zedat.fu-berlin.de
Web: http://www.bcbio.de/jrg_wiehe/

# Miscellanea

This thesis layout is largely derived from the LaTeX template created by Robert Castelo in 2002[1]. His templates were extended by Sergi Castellano and Genís Parra for their theses (see the corresponding references in page 254). The templates on which this document was built were derived from them. Here, some comments on it and the source code for download are provided.

## Technical comments

This book was typeset with GNU `emacs` 21.3.1 in LaTeX mode and converted to PDF with `pdflatex` 3.14159-1.10b (Web2C 7.4.5). All running on a linux box with Red Hat Fedora Core 2 and kernel 2.6.9-1.6. LaTeX is a document preparation system, powerful, robust and able to achieve professional results [Lamport, 1994]. However, the learning curve may be stiff. Therefore, a link to an initial template is given at the end of this chapter for your convenience.

The main document, `thesis.tex`, depends on several LaTeX files—including each chapter, the tables and few PostScript figures—, but it also depends on other files—such as style files, hacked LaTeX packages, several bitmaps and the PDF files for the attached papers—. Furthermore, `pdflatex` had to be run several times, together with BibTeX (to produce the bibliography chapter), `makeindex` (to build the index, the glossaries and the acronyms list), `thumbpdf` (to generate the main PDF document thumbnails), and few `perl` scripts. A `Makefile` was written to automatize the compilation process of the whole document. In fact, the `Makefile` was extended to produce four versions of the main document. The "*draft*" version does not include figures and the PDF files for the papers, and it displays crop marks and boxes around several elements (such as the area reserved for the pictures). The "*proofs*", where everything is included but crop marks and boxes are kept, and different hyperlink types use different colors. The "*pdf*" version is the electronic version in which all the hyperlinks are marked in blue color, crop marks are disabled. Finally, the "*press*" version is very similar to the "*pdf*" one, currently the only difference is that all the hyperlinks are black (to save some money when printing the hardcopy, of course). The `Makefile` also includes a rule to build the final book "*cover*", which recycles

[1] R. Castelo, April 2002.
"The Discrete Acyclic Digraph Markov Model in Data Mining"
Faculteit Wiskunde en Informatica, Universiteit Utrecht

the `abstract.tex` file and takes some customization from the same style file as the main `thesis.tex` file.

The compilation of a complete version of this document takes about 600 seconds—of course, the "*draft*" version takes much less—with an AMD Athlon 64 processor 3200+, with 512 KB of RAM. This is mainly due to the several steps required to ensure that every reference, index and so on, is in place. The basic build series of commands is the following: an initial `pdflatex`, a BIBTEX run to produce the bibliography, a second run of `pdflatex` to include it, three calls to `makeindex` (one for the Acronyms Glossary, another for the Web Glossary and the last for the standard Glossary of terms), a third run of `pdflatex` to include the glossaries, another call to `makeindex` (to generate the final index) and to `pdflatex`, then `makeindex` and `pdflatex` are run again, an extra run of `pdflatex` is followed by `thumbpdf`, and a final `pdflatex` to obtain the finished document. If any problem was found, like missing references, an extra round of `pdflatex`, BIBTEX and `pdflatex` is performed by the `Makefile`.

Here you can find the version of some of the programs refereed above: BIBTEX version 0.99c (Web2C 7.4.5), `thumbpdf` version 3.2 (2002/05/26), and `makeindex` version 2.14 (2002/10/02).

## LATEX Packages

As there are four versions of the document, the `ifthen` package was used to define version specific parameters, as well as to include different files. The package `geometry` facilitates the definition of the page layout. The current document original dimensions for both, the electronic and printed versions, are 170 mm width by 240 mm height. The "*cover*" requires `calc` to calculate automatically the total width for the page layout, which includes the front and the back covers and the spine width. The main document basic font size is the default value for the "`book`" document class, 10 pt.

The `crop` package is usefull to define the trimming marks for the "*draft*" and "*proofs*" versions of this document. It distinguishes between the logical page, the page sizes defined by the user, and the physical page, the page size for the hardcopy. The `layout` package is used in the "*draft*" version to show on the first page the LATEX variable settings controlling the page layout. Another useful package has been `nextpage`, which provides additional "`clear...page`" commands that ensure to get empty even pages at the end of chapters—and of course, to ensure that all chapters begin at odd pages—, even with automatically generated sections like the Bibliography and the Index.

The `babel` package provides a set of options that allow the user to choose the language(s) in which the document will be typeset, for instance language-specific hyphenation patterns. The default language was set to "`english`", while "`catalan`" and "`spanish`" were also loaded for using them for the corresponding translations of the ABSTRACT (see pages xxv and xxvii respectively).

When working with `pdflatex` there are three unvaluable packages: `pdfpages`, which makes it easy to embed external PDF documents, such as the attached publications (see for instance page 158); `thumbpdf`, it must be included in files for which a user wants to generate thumbnails (which are created by the `thumbpdf` program); and `hyperref`, which extends the functionality of all the LATEX cross-referencing commands to produce `special`

commands which a driver can turn into hypertext links. To protect URL characters we must load the `url` package, unless we have already provided `hyperref`. This package has its own version of the `url` macro, enhanced to provide clickable URLs.

To include POSTSCRIPT figures one needs `graphics` and/or `graphicx`, those packages are modified by **`pdflatex`** so that they are able to include bitmaps (PNGs, JPEGs, and so on) and PDF files into the document. `color` facilitates the specification of user-defined colors (such as the cover green shades). Figures generated with LaTeX can use any of the following packages: `pstricks`, `pstcol`, `multido`.

The bibliography was produced with BibTeX. The package `natbib` (NATural sciences BIBliography) provides both author-year and numerical citations; and it makes possible to define different citation styles. We have set the following options: "`square`", to put citations within square brackets; "`colon`", to separate multiple citations with colons; and "`authoryear`" to show author and year citations (instead of numerical citations). The style "`plainnat`" was then applied to format the bibliography.

`makeidx` provides the macros required to make a subject index. To show the capital letter section headings, few variables were redefined on an auxiliary file (`header.ist`). Three glossaries were generated for this document: the acronyms (see page 203), the web references (see page 213) and the glossary of terms (see page 207). The package `glossary` allowed us to customize the format of these three sections.

We also defined a style file named `mythesis.sty`. It loads the following font packages: `fontenc` (with "`T1`" option), to set extended font encoding (accents and so on); `textcomp`, to include some extra symbols, such as the Euro symbol for instance; `pifont`, for SYMBOL and ZAPF DINGBATS fonts; `mathpazo`, with which roman family and formulas are set to PALATINO; `avant`, with which sans-serif family is set to AVANT GARDE; and `courier`, to set typewriter family to COURIER. Accessory documents, such as LaTeX-generated figures, can use the following font packages: `times`, `t1enc`, and `helvet`.

Other packages that were loaded are: `fancyhdr`, to produce nice headings; `fancyvrb`, to extend the `verbatim` environment; `comment`, to hide parts of the original LaTeX files; `rotating`, to rotate boxes of text; and `multirow`, to get multirow cells within the `tabular` environment.

## Getting the template files

You are free to copy, modify and distribute the template files of this thesis, under the terms of the GNU Free Documentation License as published by the Free Software Foundation. Any script bundled in this distribution, including the `Makefile`, is under the terms of the GNU General Public License. The template for this document and all related files will be available from:

`http://genome.imim.es/~jabril/thesis/`

# Abbreviations

**3′ss** 3′ Splice Site (intronic, acceptor site)

**5′ss** 5′ Splice Site (intronic, donor site)

**aa** Amino Acids (protein sequence length unit)

**ACT** Artemis Comparison Tool

**ASD** Alternative Splicing Database

**BLAST** Basic Local Alignment Search Tool

**BLAT** BLAST-Like Alignment Tool

**bp** Base Pairs (nucleotide sequence length unit)

**CDS** CoDing Sequence (protein-coding)

**CTD** Carboxy-Terminal Domain (of RNApolII)

**DAS** Distributed Annotation System

**DNA** DeoxyriboNucleic Acid

**EBI** European Bioinformatics Institute

**ECR** Evolutionary Conserved Regions

**EHMM** Evolutionary Hidden Markov Model

**EJC** Exon-Junction Complex

**ENCODE** ENCyclopedia Of DNA Elements

**ESE** Exonic Splicing Enhancer

**ESS** Exonic Splicing Silencer

**FMM** First-order Markov Model

**FTP** File Transfer Protocol

**GASP** Genome Annotation Assessment Project
**GFF** General Feature Format
**GHMM** Generalized Hidden Markov Model
**GNU-GPL** GNU General Public License
**GPHMM** Generalized Pair HMM

**HAVANA** Human And Vertebrate Analysis aNd Annotation
**HMM** Hidden Markov Model

**ICGSC** International Chicken Genome Sequencing Consortium
**IHGSC** International Human Genome Sequencing Consortium
**IMGSC** International Mouse Genome Sequencing Consortium
**ISE** Intronic Splicing Enhancer
**ISS** Intronic Splicing Silencer

**mRNA** Messenger RNA
**mRNP** mRNA-protein Particle

**NCBI** National Center for Biotechnology Information
**ncRNA** Non-Coding RNA
**NIH** National Institutes of Health
**NISC** NIH Intramural Sequencing Center
**NMD** Nonsense-Mediated mRNA Decay

**ORF** Open Reading Frame

**PHMM** Pair Hidden Markov Model
**phylo-HMM** Phylogenetic Hidden Markov Model
**PiPs** Percentage Identity Plots
**PSM** Position-specific Scoring Matrix
**PTC** Premature Termination Codon
**PWM** Position Weight Matrix

**RGSPC** Rat Genome Sequencing Project Consortium
**RNA** RiboNucleic Acid
**rRNA** Ribosomal RNA

| Symbol | Meaning | Origin of designation |
|---|---|---|
| A | A | **A**denine |
| C | C | **C**ytosine |
| G | G | **G**uanine |
| T | T | **T**hymine |
| U | U | **U**racil |
| R | A or G | pu**R**ine |
| Y | C or T | p**Y**rimidine |
| M | A or C | a**M**ino |
| K | G or T | **K**etone |
| W | A or T | **W**eak interaction (2 H bonds) |
| S | C or G | **S**trong interaction (2 H bonds) |
| B | C or G or T | not-A, **B** follows A in the alphabet |
| D | A or G or T | not-C, **D** follows C |
| H | A or C or T | not-G, **H** follows G |
| V | A or C or G | not-T (not-U), **V** follows U |
| N | G or A or T or C | a**N**y (unspecified) |
| X | G or A or T or C | a**N**y (often meaning unknown) |

Table E.1: **Extended DNA / RNA alphabet.** It includes symbols coding for nucleotide ambiguity. Adapted from IUPAC-IUB for nucleotide nomenclature [Cornish-Bowden, 1985].

**SNP** Single Nucleotide Polymorphism

**snRNP** Small Nuclear RiboNucleoprotein Particle

**SVG** Scalable Vector Graphics

**tRNA** Transfer RNA

**U2AF** U2 Auxiliary Factor

**UCSC** University of California, Santa Cruz

**URL** Uniform Resource Locator

**UTR** UnTRanslated sequence

**VEGA** VErtebrate Genome Annotation

**VRML** Virtual Reality Modeling Language

**WABA** Wobble Aware Bulk Aligner

| Symbols | | Amino Acid | Codons |
|---|---|---|---|
| A | Ala | Alanine | **GCA** GCC **GCG** GCU |
| C | Cys | Cysteine | **UGC** UGU |
| D \| B | Asp | Aspartic acid | **GAC** GAU |
| E \| Z | Glu | Glutamic acid | **GAA** GAG |
| F | Phe | Phenylalanine | **UUC** UUU |
| G | Gly | Glycine | **GGA** GGC **GGG** GGU |
| H | His | Histidine | **CAC** CAU |
| I | Ile | Isoleucine | **AUA** AUC **AUU** |
| K | Lys | Lysine | **AAA** AAG |
| L | Leu | Leucine | **UUA** UUG **CUA** CUC **CUG** CUU |
| M | Met | Metionine | **AUG** |
| N \| B | Asn | Asparagine | **AAC** AAU |
| P | Pro | Proline | **CCA** CCC **CCG** CCU |
| Q \| Z | Gln | Glutamine | **CAA** CAG |
| R | Arg | Arginine | **AGA** AGG **CGA** CGC **CGG** CGU |
| S | Ser | Serine | **AGC** AGU **UCA** UCC **UCG** UCU |
| T | Thr | Threonine | **ACA** ACC **ACG** ACU |
| V | Val | Valine | **GUA** GUC **GUG** GUU |
| W | Trp | Tryptophan | **UGG** |
| Y | Tyr | Tyrosine | **UAC** UAU |
| X | Any | Unknown aa | **NNN** |
| * | (!) | Stop codon: ocre | **UAA** |
| * | (#) | Stop codon: amber | **UAG** |
| * | (@) | Stop codon: opal | **UGA** |
| U | Sec | Selenocysteine | **UGA** |

Table E.2: **The standard genetic code.** Synonymous codons are alternatively boldfaced to ease their distinction. Single letter notation follows IUPAC-IUB for amino acid symbols [IUPAC-IUB JCBN, 1984, 1993]. Termination codons are listed separately and their extended symbol codes are shown in brackets. This extended notation was devised in our laboratory to distinguish each stop codon on translated sequences; i.e., when analyzing those sequences to look for selenocysteine amino acid codon corresponding to UGA termination codon [Hatfield and Gladyshev, 2002].

# Glossary

### Acceptor Splice Site

The binding site of the spliceosome on the 3′ side of an intron and the 5′ side of an exon. This term is preferred over 3′ site because there can be multiple acceptor sites, in which case 3′ site is ambiguous. Also, one would have to refer to the 3′ site on the 5′ side of an exon, which is confusing. Mechanistically, an acceptor site defines the beginning of the exon, not the other way around.

### Algorithm

A systematic procedure for solving a problem in a finite number of steps, typically involving a repetition of operations. Once specified, an algorithm can be written in a computer language and run as a program. Named after an Iranian mathematician, Al-Khawarizmi.

### Alignment

The procedure of comparing two or more sequences by looking for a series of individual characters or character patterns that are in the same order in the sequences. There are two type of alignments: local, which attempts to align regions of sequences with the highest density of matches (one or more islands of subalignments are created in doing so); and global, which attempts to match as many characters as possible, from end to end, in the set of sequences.

### Annotation

The elucidation and description of biologically relevant features in the sequence is essential in order for genome data to be useful. The quality with which annotation is done will have direct impact on the value of the sequence. At a minimum, the data must be annotated to indicate the existence of gene coding regions and control regions. Further annotation activities that add value to a genome include finding simple and complex repeats, characterizing the organization of promoters and gene families, the distribution of G+C content, tying together evidence for functional motifs and homologs and so forth.

### Capping

The process by which eukaryotic mRNA is modified by the addition at the 5′ terminus of an m7G(5′)$ppp$(5′)N structure. Capping is essential for several important steps of gene expression, for instance, mRNA stabilization, splicing, mRNA export from the nucleus and initiation of translation.

### Consensus Sequence (consensus)

The simplest form of a consensus sequence is created by picking the most frequent base at some position in a set of aligned DNA, RNA or protein sequences. The process of creating a consensus destroys the frequency information and leads to many errors in interpreting sequences. It is one of the worst pitfalls in molecular biology. Suppose a position in a binding site had 75% A. The consensus would be A. Later, after having forgotten the origin of the consensus while trying to make a prediction, one would be wrong 25% of the time.

### Conserved

Derived from a common ancestor and retained in contemporary related species. Conserved features may or may not be under selection.

### Conserved Segments

Also known as **Conserved Linkages**, is a special case of the conserved synteny in which the order of multiple orthologous genes is the same in the compared species.

### Distributed Annotation System

The distributed annotation system [DAS, Dowell *et al*. 2001] is a client-server system in which a single client integrates information from multiple servers. It allows a single machine to gather up genome annotation information from multiple distant web sites, collate the information, and display it to the user in a single view. Little coordination is needed among the various information providers.

### Donor Splice Site

The binding site of the spliceosome on the 5′ side of an intron and the 3′ side of an exon. This term is preferred over 5′ site because there can be multiple donor sites, in which case 5′ site is ambiguous. Also, one would have to refer to the 5′ site on the 3′ side of an exon, which is confusing. Mechanistically, a donor site defines the end of the exon, not the other way around.

### Dot-Plot

A graphical representation of the regions of similarity between two sequences. The two sequences are placed on the axes of a rectangular matrix and (in the simplest forms of dotplot) wherever there is a similarity between the sequences a dot is placed on that matrix. A dot-plot gives an overview of all possible alignments between two sequences, where each diagonal corresponds to a possible (ungapped) alignment.

### Enhancer

Control element that elevates the levels of transcription from a promoter, independent of orientation or distance. Those intronic and exonic *cis*-acting elements stimulating splicing and that are important for correct splice-site identification.

### Eukaryote

Organisms with intracellular membranous organelles such as the nucleus and mitochondria.

### Exon

The segment of a pre-mRNA that contains protein-coding sequence and/or the 5′ or 3′ untranslated sequences, which must be spliced together with other exons to produce a mature mRNA.

### Exon-definition model

A model in which exon units, rather than intron units, are initially defined by pairings of spliceosomal components across exons.

### Gene

A functional unit of the genome. When not specifically stated, "gene" is usually considered a "protein-coding" gene, but many genes do not contain the instructions for proteins (see non-coding RNA).

### Genome

The complete genetic material for an organism. All the DNA contained in an organism or a cell, which includes both the chromosomes within the nucleus and the DNA in mitochondria.

### Genome Browser

A web-based or standalone software that serves as a front-end to navigate through a database of genomic annotations for one or more species. A genome browser stacks annotation tracks beneath genome coordinate positions, allowing rapid visual correlation of different types of information. The genome browser itself does not draw conclusions; rather, it collates all relevant information in one location, leaving the exploration and interpretation to the researcher.

### Hidden Markov models

Probability models that were first developed in the speech-recognition field and later applied to protein- and DNA-sequence pattern recognition. Hidden Markov models (HMMs) represent a system as a set of discrete states and as transitions between those states. Each transition has an associated probability. Markov models are hidden when one or more of the states cannot be observed directly. HMMs are valuable in bioinformatics because they allow a search or alignment algorithm to be built on firm probability bases, and it is straightforward to train the parameters (transition probabilities) with known data.

### Homologs

Features in species being compared that are similar because they are ancestrally related.

### Homology Blocks

Also defined as **Conserved Synteny**, occurs when the orthologs of genes that are on the same chromosome in one species are also on the same chromosome in the comparison species.

### Intron

An intervening non-coding sequence that interrupts two exons and that must be excised from pre-mRNA transcripts before translation.

### Intron Branch Point

The adenosine residue near the 3′ end of an intron the 2′ hydroxyl group of which becomes linked to the 5′ end of the intron during the first step of splicing.

### Intron-definition model

protect A model that proposes the initial pairwise interaction of spliceosomal components across introns, defining introns units that subsequently interact to promote spliceosome assembly and catalysis.

### Lariat

An RNA, the 5′ end of which is joined by a phospodiester linkage to the 2′ hydroxyl of an internal nucleotide, thereby creating a lasso-shaped molecule.

### Neural Networks

A collection of mathematical models that emulate some of the observed properties of biological nervous systems and draw on the analogies of adaptative biological learning. Many highly interconnected processing elements that are analogous to neurons, are tied together with weighted connections that are analogous to synapses. Once it is trained on known exon or intron sample sequences, it will be able to predict exons or introns in a query sequence automatically.

### Non-Coding RNA

Some RNAs, like tRNAs or rRNAs, do not contain information for protein sequences. The RNA molecule for those genes defines a function by itself and does not need to get translated into protein.

### Open Reading Frame

Each strand of DNA has three frames. Any subsequence that does not contain stop codons in a particular frame is an open reading frame.

### Orthologs

Homologous features that separated because of a speciation event, they derive from the same gene in the last common ancestor. See Jensen [2001] for more information on this item.

### Paralogs

Homologous features that separated because of duplication events.

### Phylogenetic Distances

Measures of the degree of separation between two organisms or their genomes, expressed in various terms such as the number of accumulated sequence changes, number of years or number of generations. The distances are often placed on phylogenetic trees, which show the deduced relationships among the organisms.

### Pip-Plot

Pip-plots display all the ungapped alignments between two sequences as black horizontal lines. The length of the line corresponds to the length of the alignment, while its height corresponds to the percent identity of the alignment. An example of a tool producing this output is `PipMaker` [Schwartz *et al.*, 2000].

### Prokaryote

Organisms that do not contain intracellular membranous organelles. All bacteria are prokaryotes.

### Promoter Element

A region of DNA extending 150-300 bp upstream from the transcription start site that contains binding sites for RNA polymerase and a number of proteins that regulate the rate of transcription of the adjacent gene. In RNA synthesis, promoters are a means to demarcate which genes should be used for messenger RNA creation—and, by extension, control which proteins the cell manufactures.

### Proteome

The complete set of all proteins produced by a particular organism. Many proteins undergo post-translational modifications that add or subtract features from a protein. Therefore, a particular mRNA might have many different protein isoforms.

### Pseudogene

A DNA sequence that was derived originally from a functional protein-coding gene that has lost its function, owing to the presence of one or more inactivating mutations.

### Regulatory Element

A *cis*-acting DNA sequence that is required for a gene to be transcribed, or to be transcribed in the proper cell type(s) and developmental stage(s). These sequences are recognized by different transcription factors which modulate the binding or the activity of the RNA polimerase. These sequences comprise promoter regions, enhancers and

### Sequence Pattern

A sequence pattern is defined by a set of aligned nucleotide or amino acid sequences (i.e. binding sites, splicing signals, and so on), or by a common protein structure. In contrast, consensus sequences, regular expressions, sequence logos and pictograms are only models of the patterns found experimentally or in nature. Models do not capture everything in nature. For example, there might be correlations between two different positions in a binding site. A more sophisticated model might capture these but still not capture three-way correlations. It is impossible to make the more detailed model if there is not enough data.

### Silencer

Control element that supresses gene expression independent of orientation or distance. Those intronic and exonic *cis*-acting elements repressing splicing and that are important for correct splice-site identification.

### Small Nuclear Ribonucleoprotein Particle

A particle that is found in the cell nucleus and consist of a tight complex between a short RNA molecule (up to 300 nucleotides) and one or more proteins. SnRNPs are involved in pre-mRNA processing and transfer RNA biogenesis.

### Smooth-Plot

Smooth-plots are constructed using, for each nucleotide, a 100 bp sliding window in which sequence identity between two sequences is averaged. Such a window centered at every nucleotide in the base sequence is used to calculate the number of matches inside of this window. Percent identity counts in a sliding window are utilized to calculate the height of the smooth conservation graph at each point. Basically, smooth-graph is a smooth average of the Pip-plot. Smooth-graphs present a simplified and clearer view in the conservation profile but loses information regarding gap distribution in the alignment. An example of a tool producing this output is `VISTA` [Mayor *et al.*, 2000].

### Spliceosome

A large complex that consist of five splicing small nuclear ribonucleoprotein particles as well as numerous protein factors. It mediates the excision of introns from pre-mRNA transcripts and ligates exon ends to produce mature mRNA.

### Synteny

The property of being on the same chromosome *sensu strictu* [Passarge *et al.*, 1999]. Nowadays is often used as synonymous of **Homology Blocks**, specially within the gene-finding terminology.

### Training Data Set

The known examples of an object (for example, an exon) that are used to train prediction algorithms, so that they learn the rules for predicting an object. They can be positive training sets (consisting of true objects, such as exons) or negative training sets (consisting of false objects, such as pseudogenes).

### Transcriptome

The complete set of transcripts for a particular genome. This term is often used to mean the mRNAs of protein coding genes and their alternatively spliced variants.

# WebSite References

### ACEDB genome database

ACEDB is a genome database designed specifically for handling bioinformatic data flexibly. It includes tools designed to manipulate genomic data, but is increasingly also used for non-biological data.

`http://www.acedb.org/`

### Analysis of mammalian and chicken splice sites

This web page summarizes the supplementary materials for Abril *et al*. [2005].

`http://genome.imim.es/datasets/hmrg2004/`

### Assessment of gene prediction accuracy in large DNA sequences

Given the absence of experimentally verified large genomic data sets, a semi-artificial test set comprising a number of short single-gene genomic sequences with randomly generated intergenic regions was built in order to analyze gene-prediction programs accuracy [Guigó *et al*., 2000].

`http://genome.imim.es/datasets/gpeval2000/`

### `compi` home page

`compi` is a `perl` script to produce *comparative pictograms*, a graphical representation of nucleotide frequencies at each position of a sequence motif or a pair-wise comparison between two sequence patterns. Latest version, as well as examples, of this program will be available from the URL below:

`http://genome.imim.es/software/compi/`

### ENSEMBL Genome Browser

ENSEMBL is a joint project between EMBL - EBI and the Sanger Institute to develop a software system which produces and maintains automatic annotation on metazoan genomes. The following URL corresponds to the project main page:

`http://www.ensembl.org/`

### Gene Predictions on Genomes

A repository of gene predictions on eukaryotic genomes. It contains the results from `geneid` and `SGP2` when applied on each novel genome assembly. Annotations for several species, including human, chimp, mouse, rat, chicken and the fruitfly, can be retrieved from:

`http://genome.imim.es/genepredictions/`

### `geneid` predictions submitted to GASP1

A set of training sequences (exons/introns) and the resulting parameters required to run `geneid` on *Drosophila melanogaster* genome.

`http://genome.imim.es/datasets/Dro_me/`

### General Feature Format (GFF)

Initially proposed at Sanger Center by Richard Durbin and David Haussler in 1997, it was proposed as a protocol for the transfer of annotation features information. It has undergone two major reviews, each one defining a new version (`GFF` v1, v2 and v3). It also inspired a derivated format known as Gene Transfer Format (GTF, `http://genes.cs.wustl.edu/GTF2.html`), which has additional structure that warrants a separate definition and format name. Main fields of the `GFF` format are:

```
seqname source feature start end score strand frame [attributes] [# comments]
```

Further information is available at:

`http://www.sanger.ac.uk/Software/formats/GFF/GFF_Spec.shtml`

### Generic Model Organism Project

The home page of a joint effort by the model organism system databases WORMBASE, FLYBASE, MGI, SGD, GRAMENE, RAT GENOME DATABASE, ECOCYC, and TAIR to develop reusable components suitable for creating new community databases of biology.

`http://www.gmod.org/`

### Genome Annotation Assessment Project (GASP1)

Community wide experiment to assess gene prediction on long eukaryotic genomic sequences: The Adh region (2.9Mb) in *Drosophila melanogaster*.

`http://www.fruitfly.org/GASP1/`

### `gff2aplot` home page

`gff2aplot` is a tool for generating pair-wise alignment-plots for genomic sequences in POSTSCRIPT [Abril *et al.*, 2003]. Latest version of this program can be retrieved from this URL, as well as examples and tutorials on how to use it.

`http://genome.imim.es/software/gfftools/GFF2APLOT.html`

### gff2ps home page

This is the home page for gff2ps, a program for visualizing annotations of genomic sequences [Abril and Guigó, 2000]. The program takes as input the annotated features on a genomic sequence in GFF format, and produces a visual output in POSTSCRIPT. It has been successfully used to generate the whole genome maps of different eukaryotic organisms, including human. Latest version of this program can be retrieved from this URL, as well as examples and tutorials on how to use it.

http://genome.imim.es/software/gfftools/GFF2PS.html

### Making the three panels poster for the ISMB99 GASP1 tutorial

The posters made for the GASP1 tutorial and shown at ISMB'99 meeting are an example of what can be done with the gff2ps visualization tool. There you will find three examples of what can be generated from the same data-set, applying a slightly modified customization file and few command-line options.

http://genome.imim.es/software/gfftools/GFF2PS-ADHposter.html

### Mouse genome supplementary materials

Description of the software and data presented in Guigó *et al.* [2003] and Waterston *et al.* [2002]. In that paper it was estimated that near a thousand novel human genes that do not overlap known proteins can be verified experimentally. The method is based in the comparison of human and mouse genomes to enhance the resulting gene-predictions, plus a filtering step from which a sample of mouse predictions were tested by RT-PCR amplification and direct sequencing.

http://genome.imim.es/datasets/mouse2002/

### NCBI MAP VIEWER

The NCBI MAP VIEWER provides special browsing capabilities for a subset of organisms in ENTREZ Genomes (http://www.ncbi.nlm.nih.gov/entrez/query.fcgi?db=Genome). Available organism genomes are listed on the NCBI MAP VIEWER Home Page. This browser allows the visitor to view and search an organism's complete genome, display chromosome maps, and zoom into progressively greater levels of detail, down to the sequence data for a region of interest.

http://www.ncbi.nlm.nih.gov/mapview/

### RepeatMasker

RepeatMasker is a program that screens DNA sequences for interspersed repeats and low complexity DNA sequences. The output of the program is a detailed annotation of the repeats that are present in the query sequence as well as a modified version of the query sequence in which all the annotated repeats have been masked (by default replaced by Ns).

http://www.repeatmasker.org/

### SGP2 home page

SGP2 is a program to predict genes by comparing anonymous genomic sequences from two different species. It combines TBLASTX, a sequence similarity search program, with geneid, an "*ab initio*" gene prediction program. The latest version of SGP2 is downloadable from this site. A web server has been developed recently by Genís Parra, and it is available at http://genome.imim.es/software/sgp2/sgp2.html

http://genome.imim.es/software/sgp2/

### SGP2 supplementary materials

Supplementary materials for the SGP2 paper [Parra *et al.*, 2003] are available from this section. SGP2 is a gene prediction program that combines "*ab initio*" gene prediction with TBLASTX searches between two genome sequences to provide both sensitive and specific gene predictions.

http://genome.imim.es/datasets/sgp2002/

### UCSC GENOME BROWSER

This site contains the reference sequence and working draft assemblies for a large collection of genomes. It also shows the *CFTR* (cystic fibrosis) region in 13 species and provides a portal to the ENCODE project. The UCSC GENOME BROWSER zooms and scrolls over chromosomes, showing the work of annotators worldwide.

http://genome.ucsc.edu/

# Bibliography


**J.F. Abril**, R. Castelo, and R. Guigó. Comparison of splice sites in mammals and chicken. *Genome Res*, 15(1):111–119, Jan 3 2005. *Published online before print in Dec 8, 2004.*

**J.F. Abril** and R. Guigó. `gff2ps`: visualizing genomic annotations. *Bioinformatics*, 16(8):743–4, Aug 2000.

**J.F. Abril**, R. Guigó, and T. Wiehe. `gff2aplot`: Plotting sequence comparisons. *Bioinformatics*, 19 (18):2477–2479, Dec 12 2003.

M.D. Adams, S.E. Celniker, R.A. Holt, C.A. Evans, J.D. Gocayne, P.G. Amanatides, S.E. Scherer, P.W. Li, R.A. Hoskins, R.F. Galle, R.A. George, S.E. Lewis, S. Richards, M. Ashburner, S.N. Henderson, and others (including **J.F. Abril**). The genome sequence of *Drosophila melanogaster*. *Science*, 287 (5461):2185–95, Mar 24 2000.

Adobe Systems Inc. *PostScript Language Reference Manual.* Addison-Wesley Publishing Company, Inc., third edition, March 1999. ISBN 0-201-37922-8.

M. Aebi, H. Hornig, and C. Weissmann. 5′ cleavage site in eukaryotic pre-mRNA splicing is determined by the overall 5′ splice region, not by the conserved 5′ `GU`. *Cell*, 50(2):237–46, Jul 17 1987.

M. Alexandersson, S. Cawley, and L. Pachter. `SLAM`: cross-species gene finding and alignment with a generalized pair hidden Markov model. *Genome Res*, 13(3):496–502, Mar 2003.

S.F. Altschul, W. Gish, W. Miller, E.W. Myers, and D.J. Lipman. Basic local alignment search tool. *J Mol Biol*, 215(3):403–10, Oct 5 1990.

S.F. Altschul, T.L. Madden, A.A. Schaffer, J. Zhang, Z. Zhang, W. Miller, and D.J. Lipman. Gapped `BLAST` and `PSI-BLAST`: a new generation of protein database search programs. *Nucleic Acids Res*, 25(17):3389–402, Sep 1 1997.

F. Antequera and A. Bird. Number of CpG islands and genes in human and mouse. *Proc Natl Acad Sci U S A*, 90(24):11995–9, Dec 15 1993.

J.L. Ashurst, C.K. Chen, J.G. Gilbert, K. Jekosch, S. Keenan, P. Meidl, S.M. Searle, J. Stalker, R. Storey, S. Trevanion, L. Wilming, and T. Hubbard. The VErtebrate Genome Annotation (VEGA) database. *Nucleic Acids Res*, 33 Database Issue:D459–65, Jan 1 2005.

V.N. Babenko, P.S. Kosarev, O.V. Vishnevsky, V.G. Levitsky, V.V. Basin, and A.S. Frolov. Investigating extended regulatory regions of genomic DNA sequences. *Bioinformatics*, 15(7-8):644–53, Jul-Aug 1999.

V. Bafna and D.H. Huson. "The conserved exon method for gene finding.". In *Proc Int Conf Intell Syst Mol Biol*, volume 8, pages 3–12, 2000.

R.E. Banks, M.J. Dunn, D.F. Hochstrasser, J.C. Sanchez, W. Blackstock, D.J. Pappin, and P.J. Selby. Proteomics: new perspectives, new biomedical opportunities. *Lancet*, 356(9243):1749–56, Nov 18 2000.

E. Barillot, S. Pook, F. Guyon, C. Cussat-Blanc, E. Viara, and G. Vaysseix. The HUGEMAP Database: interconnection and visualization of human genome maps. *Nucleic Acids Res*, 27(1):119–22, Jan 1 1999.

S. Batzoglou, L. Pachter, J.P. Mesirov, B. Berger, and E.S. Lander. Human and mouse gene structure: comparative analysis and application to exon prediction. *Genome Res*, 10(7):950–8, Jul 2000.

E. Beitz. `TEXshade`: shading and labeling of multiple sequence alignments using LaTeX 2$_\varepsilon$. *Bioinformatics*, 16(2):135–9, Feb 2000.

S.M. Berget, C. Moore, and P.A. Sharp. Spliced segments at the 5′ terminus of adenovirus 2 late mRNA. *Proc Natl Acad Sci U S A*, 74(8):3171–5, Aug 1977.

E. Birney, D. Andrews, P. Bevan, M. Caccamo, G. Cameron, Y. Chen, L. Clarke, G. Coates, T. Cox, J. Cuff, V. Curwen, T. Cutts, T. Down, R. Durbin, E. Eyras, et al. ENSEMBL 2004. *Nucleic Acids Res*, 32(1):D468–70, Jan 1 2004a.

E. Birney, M. Clamp, and R. Durbin. `GeneWise` and `Genomewise`. *Genome Res*, 14(5):988–95, May 2004b.

E. Birney and R. Durbin. `Dynamite`: a flexible code generating language for dynamic programming methods used in sequence comparison. *Proc Int Conf Intell Syst Mol Biol*, 5:56–64, 1997.

D.L. Black. Mechanisms of alternative pre-messenger RNA splicing. *Annu Rev Biochem*, 72:291–336, 2003.

F.R. Blattner and J.L. Schroeder. A computer package for DNA sequence analysis. *Nucleic Acids Res*, 12(1 Pt 2):615–7, Jan 11 1984.

M. Blaxter, J. Daub, D. Guiliano, J. Parkinson, and C. Whitton. The *Brugia malayi* genome project: expressed sequence tags and gene discovery. *Trans R Soc Trop Med Hyg*, 96(1):7–17, Jan-Feb 2002.

P. Blayo, P. Rouzé, and M.-F. Sagot. Orphan gene finding - An exon assembly approach. *Theoretical Computer Science*, 290(3):1407–1431, 2002.

D. Boffelli, J. McAuliffe, D. Ovcharenko, K.D. Lewis, I. Ovcharenko, L. Pachter, and E.M. Rubin. Phylogenetic shadowing of primate sequences to find functional regions of the human genome. *Science*, 299(5611):1391–4, Feb 28 2003.

M. Borodovsky and J. McIninch. `GeneMark`: Parallel gene recognition for both DNA strands. *Computer and Chemistry*, 17:123–134, 1993.

M.R. Brent and R. Guigó. Recent advances in gene structure prediction. *Curr Opin Struct Biol*, 14(3): 264–72, Jun 2004.

D. Brett, H. Pospisil, J. Valcarcel, J. Reich, and P. Bork. Alternative splicing and genome complexity. *Nat Genet*, 30(1):29–30, Jan 2002.

C.T. Brown, A.G. Rust, P.J. Clarke, Z. Pan, M.J. Schilstra, T. De Buysscher, G. Griffin, B.J. Wold, R.A. Cameron, E.H. Davidson, and H. Bolouri. New computational approaches for analysis of cis-regulatory networks. *Dev Biol*, 246(1):86–102, Jun 1 2002.

A.R. Buchman and P. Berg. Comparison of intron-dependent and intron-independent gene expression. *Mol Cell Biol*, 8(10):4395–405, Oct 1988.

C.J. Bult, J.A. Blake, J.E. Richardson, J.A. Kadin, J.T. Eppig, R.M. Baldarelli, K. Barsanti, M. Baya, J.S. Beal, W.J. Boddy, D.W. Bradt, D.L. Burkart, N.E. Butler, J. Campbell, R. Corey, et al. The Mouse Genome Database (MGD): integrating biology with the genome. *Nucleic Acids Res*, 32 Database issue: D476–81, Jan 1 2004.

C. Burge and S. Karlin. Prediction of complete gene structures in human genomic DNA. *J Mol Biol*, 268(1):78–94, Apr 25 1997.

C. B. Burge, T. Tuschl, and P. S. Sharp. *The RNA world*, volume 37 of *Cold Spring Harbor Monograph Series*, chapter "Splicing Precursors to mRNAs by the Spliceosomes.", pages 525–560. Cold Spring Harbor Laboratory Press, Cold Spring Harbor, New York, USA, 2nd edition, 1999. ISBN 0-87969-589-7.

C.B. Burge, R.A. Padgett, and P.A. Sharp. Evolutionary fates and origins of U12-type introns. *Mol Cell*, 2(6):773–85, Dec 1998.

M. Burset and R. Guigó. Evaluation of gene structure prediction programs. *Genomics*, 34(3):353–67, Jun 15 1996.

M. Burset, I.A. Seledtsov, and V.V. Solovyev. Analysis of canonical and non-canonical splice sites in mammalian genomes. *Nucleic Acids Res*, 28(21):4364–75, Nov 1 2000.

S.B. Cannon, A. Kozik, B. Chan, R. Michelmore, and N.D. Young. DiagHunter and GenoPix2D: programs for genomic comparisons, large-scale homology discovery and visualization. *Genome Biol*, 4(10):R68, 2003.

L. Cartegni, S.L. Chew, and A.R. Krainer. Listening to silence and understanding nonsense: exonic mutations that affect splicing. *Nat Rev Genet*, 3(4):285–98, Apr 2002.

R. Castelo, G. Parra, and R. Guigó. exstral: EXon STRucture over an ALignment. *unpublished* 2004.

M. Chagoyen, M.E. Kurul, P.A. De-Alarcon, J.M. Carazo, and A. Gupta. Designing and executing scientific workflows with a programmable integrator. *Bioinformatics*, 20(13):2092–100, Sep 1 2004.

K. Chakrabarti and L. Pachter. Visualization of multiple genome annotations and alignments with the K-BROWSER. *Genome Res*, 14(4):716–20, Apr 2004.

J. Cheung, X. Estivill, R. Khaja, J.R. MacDonald, K. Lau, L.C. Tsui, and S.W. Scherer. Genome-wide detection of segmental duplications and potential assembly errors in the human genome sequence. *Genome Biol*, 4(4):R25, 2003.

F. Chiaromonte, S. Yang, L. Elnitski, V.B. Yap, W. Miller, and R.C. Hardison. Association between divergence and interspersed repeats in mammalian noncoding genomic DNA. *Proc Natl Acad Sci U S A*, 98(25):14503–8, Dec 4 2001.

L.T. Chow, R.E. Gelinas, T.R. Broker, and R.J. Roberts. An amazing sequence arrangement at the 5′ ends of adenovirus 2 messenger RNA. *Cell*, 12(1):1–8, Sep 1977.

K.R. Christie, S. Weng, R. Balakrishnan, M.C. Costanzo, K. Dolinski, S.S. Dwight, S.R. Engel, B. Feierbach, D.G. Fisk, J.E. Hirschman, E.L. Hong, L. Issel-Tarver, R. Nash, A. Sethuraman, B. Starr, et al. *Saccharomyces* Genome Database (SGD) provides tools to identify and analyze sequences from *Saccharomyces cerevisiae* and related sequences from other organisms. *Nucleic Acids Res*, 32(1):D311–4, Jan 1 2004.

T.J. Chuang, W.C. Lin, H.C. Lee, C.W. Wang, K.L. Hsiao, Z.H. Wang, D. Shieh, S.C. Lin, and L.Y. Ch'ang. A complexity reduction algorithm for analysis and annotation of large genomic sequences. *Genome Res*, 13(2):313–22, Feb 2003.

M. Clamp, D. Andrews, D. Barker, P. Bevan, G. Cameron, Y. Chen, L. Clark, T. Cox, J. Cuff, V. Curwen, T. Down, R. Durbin, E. Eyras, J. Gilbert, M. Hammond, et al. ENSEMBL 2002: accommodating comparative genomics. *Nucleic Acids Res*, 31(1):38–42, Jan 1 2003.

J.E. Cleaver, C. Collins, J. Ellis, and S. Volik. Genome sequence and splice site analysis of low-fidelity DNA polymerases H and I involved in replication of damaged DNA. *Genomics*, 82(5):561–70, Nov 2003.

C.A. Collins and C. Guthrie. The question remains: is the spliceosome a ribozyme? *Nat Struct Biol*, 7 (10):850–4, Oct 2000.

F.S. Collins, E.D. Green, A.E. Guttmacher, and M.S. Guyer. A vision for the future of genomics research. *Nature*, 422(6934):835–47, Apr 24 2003.

J.W. Conaway, A. Shilatifard, A. Dvir, and R.C. Conaway. Control of elongation by RNA polymerase II. *Trends Biochem Sci*, 25(8):375–80, Aug 2000.

J. Corden and C. Ingles. *Transccriptional Regulation*, chapter "Carboxy-terminal domain of the largest subunit of eukaryotic RNA polymerase II", pages 81–108. Cold Spring Harbor Laboratory Press, Cold Spring Harbor, NY (USA), 1992.

A. Cornish-Bowden. Nomenclature for incompletely specified bases in nucleic acid sequences: recommendations 1984. *Nucleic Acids Res*, 13(9):3021–30, May 10 1985.

E. Coward, S.A. Haas, and M. Vingron. `SpliceNest`: visualizing gene structure and alternative splicing based on EST clusters. *Trends Genetics*, 18(1):53–55, 2002.

P. Cramer, C.G. Pesce, F.E. Baralle, and A.R. Kornblihtt. Functional association between promoter structure and transcript alternative splicing. *Proc Natl Acad Sci U S A*, 94(21):11456–60, Oct 14 1997.

V. Curwen, E. Eyras, T.D. Andrews, L. Clarke, E. Mongin, S.M. Searle, and M. Clamp. The ENSEMBL automatic gene annotation system. *Genome Res*, 14(5):942–50, May 2004.

B. Datta and A.M. Weiner. Genetic evidence for base pairing between U2 and U6 snRNA in mammalian mRNA splicing. *Nature*, 352(6338):821–4, Aug 29 1991.

M. de la Mata, C.R. Alonso, S. Kadener, J.P. Fededa, M. Blaustein, F. Pelisch, P. Cramer, D. Bentley, and A.R. Kornblihtt. A slow RNA polymerase II affects alternative splicing *in vivo*. *Mol Cell*, 12(2): 525–32, Aug 2003.

A.L. Delcher, S. Kasif, R.D. Fleischmann, J. Peterson, O. White, and S.L. Salzberg. Alignment of whole genomes. *Nucleic Acids Res*, 27(11):2369–76, Jun 1 1999.

E.T. Dermitzakis, A. Reymond, R. Lyle, N. Scamuffa, C. Ucla, S. Deutsch, B.J. Stevenson, V. Flegel, P. Bucher, C.V. Jongeneel, and S.E. Antonarakis. Numerous potentially functional but non-genic conserved sequences on human chromosome 21. *Nature*, 420(6915):578–82, Dec 5 2002.

J. Devereux, P. Haeberli, and O. Smithies. A comprehensive set of sequence analysis programs for the VAX. *Nucleic Acids Res*, 12(1 Pt 1):387–95, Jan 11 1984.

C. Dewey, J.Q. Wu, S. Cawley, M. Alexandersson, R. Gibbs, and L. Pachter. Accurate identification of novel human genes through simultaneous gene prediction in human, mouse, and rat. *Genome Res*, 14(4):661–4, Apr 2004.

R.C. Dietrich, R. Incorvaia, and R.A. Padgett. Terminal intron dinucleotide sequences do not distinguish between U2- and U12-dependent introns. *Mol Cell*, 1(1):151–60, Dec 1997.

S. Dong and D.B. Searls. Gene structure prediction by linguistic methods. *Genomics*, 23(3):540–51, Oct 1994.

R.D. Dowell, R.M. Jokerst, A. Day, S.R. Eddy, and L. Stein. The distributed annotation system. *BMC Bioinformatics*, 2(1):7, 2001.

I. Dubchak, M. Brudno, G.G. Loots, L. Pachter, C. Mayor, E.M. Rubin, and K.A. Frazer. Active conservation of noncoding sequences revealed by three-way species comparisons. *Genome Res*, 10(9): 1304–6, Sep 2000.

I. Dunham, N. Shimizu, B.A. Roe, S. Chissoe, A.R. Hunt, J.E. Collins, R. Bruskiewich, D.M. Beare, M. Clamp, L.J. Smink, R. Ainscough, J.P. Almeida, A. Babbage, C. Bagguley, J. Bailey, et al. The DNA sequence of human chromosome 22. *Nature*, 402(6761):489–95, Dec 2 1999.

R. Durbin, S. Eddy, A. Crogh, and G. Mitchison. *Biological Sequence Analysis: Probabilistic Models of Protein and Nucleic Acids*. Cambridge University Press, first edition, 1998. ISBN 0-521-62971-3.

R. Durbin and J. Thierry-Mieg. The ACEDB genome database. URL `http://www.acedb.org/`. *unpublished* 1993.

L. Duret, E. Gasteiger, and G. Perriere. `LALNVIEW`: a graphical viewer for pairwise sequence alignments. *Comput Appl Biosci*, 12(6):507–10, Dec 1996.

I. Ebersberger, D. Metzler, C. Schwarz, and S. Paabo. Genomewide comparison of DNA sequences between humans and chimpanzees. *Am J Hum Genet*, 70(6):1490–7, Jun 2002.

J.H. Edwards. The `Oxford Grid`. *Ann Hum Genet*, 55 ( Pt 1):17–31, Jan 1991.

Y.J. Edwards, T.J. Carver, T. Vavouri, M. Frith, M.J. Bishop, and G. Elgar. `Theatre`: A software tool for detailed comparative analysis and visualization of genomic sequence. *Nucleic Acids Res*, 31(13): 3510–7, Jul 1 2003.

F.H. Eeckman and R. Durbin. `ACeDB` and `macace`. *Methods Cell Biol*, 48:583–605, 1995.

ENCODE Project Consortium. The ENCODE (ENCyclopedia Of DNA Elements) Project. *Science*, 306 (5696):636–40, Oct 22 2004.

X. Estivill, J. Cheung, M.A. Pujana, K. Nakabayashi, S.W. Scherer, and L.C. Tsui. Chromosomal regions containing high-density and ambiguously mapped putative single nucleotide polymorphisms (SNPs) correlate with segmental duplications in the human genome. *Hum Mol Genet*, 11 (17):1987–95, Aug 15 2002.

T. Etzold and P. Argos. `SRS`—an indexing and retrieval tool for flat file data libraries. *Comput Appl Biosci*, 9(1):49–57, Feb 1993.

B. Ewing and P. Green. Analysis of expressed sequence tags indicates 35,000 human genes. *Nat Genet*, 25(2):232–4, Jun 2000.

Z. Fang, M. Polacco, S. Chen, S. Schroeder, D. Hancock, H. Sanchez, and E. Coe. `cMap`: the comparative genetic map viewer. *Bioinformatics*, 19(3):416–7, Feb 12 2003.

A. Fedorov, A.F. Merican, and W. Gilbert. Large-scale comparison of intron positions among animal, plant, and fungal genes. *Proc Natl Acad Sci U S A*, 99(25):16128–33, Dec 10 2002.

E.S. Ferlanti, J.F. Ryan, I. Makalowska, and A.D. Baxevanis. `WebBLAST` 2.0: an integrated solution for organizing and analyzing sequence data. *Bioinformatics*, 15(5):422–3, May 1999.

J.W. Fickett. Recognition of protein coding regions in DNA sequences. *Nucleic Acids Res*, 10(17): 5303–18, Sep 11 1982.

C. Fields, M.D. Adams, O. White, and J.C. Venter. How many genes in the human genome? *Nat Genet*, 7(3):345–6, Jul 1994.

C.A. Fields and C.A. Soderlund. `gm`: a practical tool for automating DNA sequence analysis. *Comput Appl Biosci*, 6(3):263–70, Jul 1990.

S. Fischer, J. Crabtree, B. Brunk, M. Gibson, and G.C. Overton. `bioWidgets`: data interaction components for genomics. *Bioinformatics*, 15(10):837–46, Oct 1999.

W.M. Fitch. An improved method of testing for evolutionary homology. *J Mol Biol*, 16(1):9–16, Mar 1966.

P. Flicek, E. Keibler, P. Hu, I. Korf, and M.R. Brent. Leveraging the mouse genome for gene prediction in human: from whole-genome shotgun reads to a global synteny map. *Genome Res*, 13(1):46–54, Jan 2003.

L. Florea, G. Hartzell, Z. Zhang, G.M. Rubin, and W. Miller. A computer program for aligning a cDNA sequence with a genomic DNA sequence. *Genome Res*, 8(9):967–74, Sep 1998.

L. Florea, M. McClelland, C. Riemer, S. Schwartz, and W. Miller. `EnteriX` 2003: Visualization tools for genome alignments of Enterobacteriaceae. *Nucleic Acids Res*, 31(13):3527–32, Jul 1 2003.

A. Fortna and K. Gardiner. Genomic sequence analysis tools: a user's guide. *Trends Genet*, 17(3): 158–64, Mar 2001.

K.A. Frazer, L. Elnitski, D.M. Church, I. Dubchak, and R.C. Hardison. Cross-species sequence comparisons: a review of methods and available resources. *Genome Res*, 13(1):1–12, Jan 2003.

X.D. Fu. Towards a splicing code. *Cell*, 119(6):736–8, Dec 17 2004.

M.S. Gelfand. Computer prediction of the exon-intron structure of mammalian pre-mRNAs. *Nucleic Acids Res*, 18(19):5865–9, Oct 11 1990.

M.S. Gelfand, A.A. Mironov, and P.A. Pevzner. Gene recognition via spliced sequence alignment. *Proc Natl Acad Sci U S A*, 93(17):9061–6, Aug 20 1996.

A.J. Gibbs and G.A. McIntyre. The `diagram`, a method for comparing sequences. Its use with amino acid and nucleotide sequences. *Eur J Biochem*, 16(1):1–11, Sep 1970.

R.A. Gibbs, G.M. Weinstock, M.L. Metzker, D.M. Muzny, E.J. Sodergren, S. Scherer, G. Scott, D. Steffen, K.C. Worley, P.E. Burch, G. Okwuonu, S. Hines, L. Lewis, C. DeRamo, O. Delgado, and others (Rat Genome Sequencing Project Consortium, RGSPC; including **J.F. Abril**). Genome sequence of the Brown Norway rat yields insights into mammalian evolution. *Nature*, 428(6982):493–521, Apr 1 2004.

R. Gibson and D.R. Smith. Genome visualization made fast and simple. *Bioinformatics*, 19(11):1449–50, Jul 22 2003.

R. Gil, F.J. Silva, E. Zientz, F. Delmotte, F. Gonzalez-Candelas, A. Latorre, C. Rausell, J. Kamerbeek, J. Gadau, B. Holldobler, R.C. van Ham, R. Gross, and A. Moya. The genome sequence of *Blochmannia floridanus*: comparative analysis of reduced genomes. *Proc Natl Acad Sci U S A*, 100(16):9388–93, Aug 5 2003.

D.G. Gilbert. `euGenes`: a eukaryote genome information system. *Nucleic Acids Res*, 30(1):145–8, Jan 1 2002.

P. Gilligan, S. Brenner, and B. Venkatesh. *Fugu* and human sequence comparison identifies novel human genes and conserved non-coding sequences. *Gene*, 294(1-2):35–44, Jul 10 2002.

W. Gish. Washington University BLAST. URL http://blast.wustl.edu. *unpublished* 1996–2004.

J.D. Glasner, P. Liss, 3.r.d. Plunkett G, A. Darling, T. Prasad, M. Rusch, A. Byrnes, M. Gilson, B. Biehl, F.R. Blattner, and N.T. Perna. ASAP, a systematic annotation package for community analysis of genomes. *Nucleic Acids Res*, 31(1):147–51, Jan 1 2003.

A.C. Goldstrohm, A.L. Greenleaf, and M.A. Garcia-Blanco. Co-transcriptional splicing of pre-messenger RNAs: considerations for the mechanism of alternative splicing. *Gene*, 277(1-2):31–47, Oct 17 2001.

N. Goodman. Biological data becomes computer literate: new advances in bioinformatics. *Curr Opin Biotechnol*, 13(1):68–71, Feb 2002.

B. Göttgens, L.M. Barton, J.G. Gilbert, A.J. Bench, M.J. Sanchez, S. Bahn, S. Mistry, D. Grafham, A. McMurray, M. Vaudin, E. Amaya, D.R. Bentley, A.R. Green, and A.M. Sinclair. Analysis of vertebrate *SCL* loci identifies conserved enhancers. *Nat Biotechnol*, 18(2):181–6, Feb 2000.

B. Göttgens, J.G. Gilbert, L.M. Barton, D. Grafham, J. Rogers, D.R. Bentley, and A.R. Green. Long-range comparison of human and mouse *SCL* loci: localized regions of sensitivity to restriction endonucleases correspond precisely with peaks of conserved noncoding sequences. *Genome Res*, 11(1):87–97, Jan 2001.

E. Graziano and P. Arus. FITMAPS and SHOWMAP: two programs for graphical comparison and plotting of genetic maps. *J Hered*, 93(3):225–7, May-Jun 2002.

A.L. Greenleaf. Positive patches and negative noodles: linking RNA processing to transcription? *Trends Biochem Sci*, 18(4):117–9, Apr 1993.

R. Guigo. Assembling genes from predicted exons in linear time with dynamic programming. *J Comput Biol*, 5(4):681–702, Winter 1998.

R. Guigó. *Genetic Databases.*, chapter "DNA Composition, Codon Usage and Exon Prediction.", pages 53–80. Academic Press, San Diego, California, USA, 1999. ISBN 0-12-101625-0.

R. Guigó, P. Agarwal, **J.F. Abril**, M. Burset, and J.W. Fickett. An assessment of gene prediction accuracy in large DNA sequences. *Genome Res*, 10(10):1631–42, Oct 2000.

R. Guigó, E.T. Dermitzakis, P. Agarwal, C.P. Ponting, G. Parra, A. Reymond, **J.F. Abril**, E. Keibler, R. Lyle, C. Ucla, S.E. Antonarakis, and M.R. Brent. Comparison of mouse and human genomes followed by experimental verification yields an estimated 1,019 additional genes. *Proc Natl Acad Sci U S A*, 100(3):1140–5, Feb 4 2003.

R. Guigó, S. Knudsen, N. Drake, and T. Smith. Prediction of gene structure. *J Mol Biol*, 226(1):141–57, Jul 5 1992.

R. Guigó and M.Q. Zhang. *Mammalian Genomics.*, chapter "Gene predictions and Annotations.", page (*in press*). CAB International, 2004. ISBN 0-851-99910-7.

C. Gybas and P. Jambeck. *Developing Bioinformatics Computer Skills.* O'Reilly & Associates, Inc., first edition, April 2003. ISBN 1-56592-664-1.

S.L. Hall and R.A. Padgett. Conserved sequences in a class of rare eukaryotic nuclear introns with non-consensus splice sites. *J Mol Biol*, 239(3):357–65, Jun 10 1994.

S.L. Hall and R.A. Padgett. Requirement of U12 snRNA for in vivo splicing of a minor class of eukaryotic nuclear pre-mRNA introns. *Science*, 271(5256):1716–8, Mar 22 1996.

R.C. Hardison. Conserved noncoding sequences are reliable guides to regulatory elements. *Trends Genet*, 16(9):369–72, Sep 2000.

R.C. Hardison, J. Oeltjen, and W. Miller. Long human-mouse sequence alignments reveal novel regulatory elements: a reason to sequence the mouse genome. *Genome Res*, 7(10):959–66, Oct 1997.

M.P. Hare and S.R. Palumbi. High intron sequence conservation across three mammalian orders suggests functional constraints. *Mol Biol Evol*, 20(6):969–78, Jun 2003.

T.W. Harris, N. Chen, F. Cunningham, M. Tello-Ruiz, I. Antoshechkin, C. Bastiani, T. Bieri, D. Blasiar, K. Bradnam, J. Chan, C.K. Chen, W.J. Chen, P. Davis, E. Kenny, R. Kishore, et al. WormBase: a multi-species resource for nematode biology and genomics. *Nucleic Acids Res*, 32(1):D411–7, Jan 1 2004.

P.M. Harrison, A. Kumar, N. Lang, M. Snyder, and M. Gerstein. A question of size: the eukaryotic proteome and the problems in defining it. *Nucleic Acids Res*, 30(5):1083–90, Mar 1 2002.

M.L. Hastings and A.R. Krainer. Pre-mRNA splicing in the new millennium. *Curr Opin Cell Biol*, 13 (3):302–9, Jun 2001.

D.L. Hatfield and V.N. Gladyshev. How selenium has altered our understanding of the genetic code. *Mol Cell Biol*, 22(11):3565–76, Jun 2002.

M. Hattori, A. Fujiyama, T.D. Taylor, H. Watanabe, T. Yada, H.S. Park, A. Toyoda, K. Ishii, Y. Totoki, D.K. Choi, Y. Groner, E. Soeda, M. Ohki, T. Takagi, Y. Sakaki, et al. The DNA sequence of human chromosome 21. *Nature*, 405(6784):311–9, May 18 2000.

T.P. Hausner, L.M. Giglio, and A.M. Weiner. Evidence for base-pairing between mammalian U2 and U6 small nuclear ribonucleoprotein particles. *Genes Dev*, 4(12A):2146–56, Dec 1990.

J. Healy, E.E. Thomas, J.T. Schwartz, and M. Wigler. Annotating large genomes with exact word matches. *Genome Res*, 13(10):2306–15, Oct 2003.

S. Heber, M. Alekseyev, S.H. Sze, H. Tang, and P.A. Pevzner. Splicing graphs and EST assembly problem. *Bioinformatics*, 18 Suppl 1:S181–8, Jul 2002.

J. Henderson, S. Salzberg, and K.H. Fasman. Finding genes in DNA with a Hidden Markov Model. *J Comput Biol*, 4(2):127–41, Summer 1997.

M.W. Hentze and A.E. Kulozik. A perfect message: RNA surveillance and nonsense-mediated decay. *Cell*, 96(3):307–10, Feb 5 1999.

C. Hertz-Fowler, C.S. Peacock, V. Wood, M. Aslett, A. Kerhornou, P. Mooney, A. Tivey, M. Berriman, N. Hall, K. Rutherford, J. Parkhill, A.C. Ivens, M.A. Rajandream, and B. Barrell. GeneDB: a resource for prokaryotic and eukaryotic organisms. *Nucleic Acids Res*, 32 Database issue:D339–43, Jan 1 2004.

L.W. Hillier, W. Miller, E. Birney, W. Warren, R.C. Hardison, C.P. Ponting, P. Bork, D.W. Burt, M.A. Groenen, M.E. Delany, J.B. Dodgson, G. Fingerprint Map Sequence, Assembly, A.T. Chinwalla, P.F. Cliften, S.W. Clifton, and others (International Chicken Genome Sequencing Consortium, ICGSC; including **J.F. Abril**). Sequence and comparative analysis of the chicken genome provide unique perspectives on vertebrate evolution. *Nature*, 432(7018):695–716, Dec 9 2004.

H. Le Hir, E. Izaurralde, L.E. Maquat, and M.J. Moore. The spliceosome deposits multiple proteins 20-24 nucleotides upstream of mRNA exon-exon junctions. *EMBO J*, 19(24):6860–9, Dec 15 2000.

J.B. Hogenesch, K.A. Ching, S. Batalov, A.I. Su, J.R. Walker, Y. Zhou, S.A. Kay, P.G. Schultz, and M.P. Cooke. A comparison of the CELERA and ENSEMBL predicted gene sets reveals little overlap in novel genes. *Cell*, 106(4):413–5, Aug 24 2001.

R.A. Holt, G.M. Subramanian, A. Halpern, G.G. Sutton, R. Charlab, D.R. Nusskern, P. Wincker, A.G. Clark, J.M. Ribeiro, R. Wides, S.L. Salzberg, B. Loftus, M. Yandell, W.H. Majoros, D.B. Rusch, and others (including **J.F. Abril**). The genome sequence of the malaria mosquito *Anopheles gambiae*. *Science*, 298(5591):129–49, Oct 4 2002.

S. Hoon, K.K. Ratnapu, J.M. Chia, B. Kumarasamy, X. Juguang, M. Clamp, A. Stabenau, S. Potter, L. Clarke, and E. Stupka. `Biopipe`: a flexible framework for protocol-based bioinformatics analysis. *Genome Res*, 13(8):1904–15, Aug 2003.

K.J. Howe, C.M. Kane, and J.r. Ares M. Perturbation of transcription elongation influences the fidelity of internal exon inclusion in *Saccharomyces cerevisiae*. *RNA*, 9(8):993–1006, Aug 2003.

X. Huang and W. Miller. A time-efficient, linear-space local similarity algorithm. *Adv. Appl. Math.*, 12:337–357, 1991.

A.K. Hudek, J. Cheung, A.P. Boright, and S.W. Scherer. `Genescript`: DNA sequence annotation pipeline. *Bioinformatics*, 19(9):1177–8, Jun 12 2003.

G.B. Hutchinson and M.R. Hayden. The prediction of exons through an analysis of spliceable open reading frames. *Nucleic Acids Res*, 20(13):3453–62, Jul 11 1992.

R. Ierusalimschy, L. H. de Figueiredo, and W. Celes Filho. Lua—an extensible extension language. *Softw. Pract. Exper.*, 26(6):635–652, 1996.

R. Incorvaia and R.A. Padgett. Base pairing with U6atac snRNA is required for 5′ splice site activation of U12-dependent introns *in vivo*. *RNA*, 4(6):709–18, Jun 1998.

International Human Genome Sequencing Consortium, IHGSC. Finishing the euchromatic sequence of the human genome. *Nature*, 431(7011):931–45, Oct 21 2004.

Y. Ishigaki, X. Li, G. Serin, and L.E. Maquat. Evidence for a pioneer round of mRNA translation: mRNAs subject to nonsense-mediated decay in mammalian cells are bound by *CBP80* and *CBP20*. *Cell*, 106(5):607–17, Sep 7 2001.

IUPAC-IUB JCBN. IUPAC-IUB Joint Commission on Biochemical Nomenclature (JCBN). Nomenclature and symbolism for amino acids and peptides. Recommendations 1983. *Biochem J*, 219(2): 345–73, Apr 15 1984.

IUPAC-IUB JCBN. IUPAC-IUB Joint Commission on Biochemical Nomenclature (JCBN). Nomenclature and symbolism for amino acids and peptides. Corrections to recommendations 1983. *Eur J Biochem*, 213(1):2, Apr 1 1993.

I.J. Jackson. A reappraisal of non-consensus mRNA splice sites. *Nucleic Acids Res*, 19(14):3795–8, Jul 25 1991.

O. Jaillon, C. Dossat, R. Eckenberg, K. Eiglmeier, B. Segurens, J.M. Aury, C.W. Roth, C. Scarpelli, P.T. Brey, J. Weissenbach, and P. Wincker. Assessing the *Drosophila melanogaster* and *Anopheles gambiae* genome annotations using genome-wide sequence comparisons. *Genome Res*, 13(7):1595–9, Jul 2003.

D.C. Jamison. Open bioinformatics. *Bioinformatics*, 19(6):679–80, Apr 12 2003.

W. Jang, A. Hua, S.V. Spilson, W. Miller, B.A. Roe, and M.H. Meisler. Comparative sequence of human and mouse BAC clones from the *mnd2* region of chromosome 2p13. *Genome Res*, 9(1):53–61, Jan 1999.

N. Jareborg and R. Durbin. Alfresco–a workbench for comparative genomic sequence analysis. *Genome Res*, 10(8):1148–57, Aug 2000.

A.G. Jegga, S.P. Sherwood, J.W. Carman, A.T. Pinski, J.L. Phillips, J.P. Pestian, and B.J. Aronow. Detection and visualization of compositionally similar cis-regulatory element clusters in orthologous and coordinately controlled genes. *Genome Res*, 12(9):1408–17, Sep 2002.

R.A. Jensen. Orthologs and paralogs - we need to get it right. *Genome Biol*, 2(8):INTERACTIONS1002, 2001.

K. Jungfer and P. Rodriguez-Tome. Mapplet: a CORBA-based genome map viewer. *Bioinformatics*, 14 (8):734–8, 1998.

D. Kampa, J. Cheng, P. Kapranov, M. Yamanaka, S. Brubaker, S. Cawley, J. Drenkow, A. Piccolboni, S. Bekiranov, G. Helt, H. Tammana, and T.R. Gingeras. Novel RNAs identified from an in-depth analysis of the transcriptome of human chromosomes 21 and 22. *Genome Res*, 14(3):331–42, Mar 2004.

D. Karolchik, R. Baertsch, M. Diekhans, T.S. Furey, A. Hinrichs, Y.T. Lu, K.M. Roskin, M. Schwartz, C.W. Sugnet, D.J. Thomas, R.J. Weber, D. Haussler, and W.J. Kent. The UCSC GENOME BROWSER Database. *Nucleic Acids Res*, 31(1):51–4, Jan 1 2003.

D. Karolchik, A.S. Hinrichs, T.S. Furey, K.M. Roskin, C.W. Sugnet, D. Haussler, and W.J. Kent. The UCSC TABLE BROWSER data retrieval tool. *Nucleic Acids Res*, 32(1):D493–6, Jan 1 2004.

L.P. Keegan, A. Gallo, and M.A. O'Connell. The many roles of an RNA editor. *Nat Rev Genet*, 2(11): 869–78, Nov 2001.

C. Keller, M. Corcoran, and R.J. Roberts. Computer programs for handling nucleic acid sequences. *Nucleic Acids Res*, 12(1 Pt 1):379–86, Jan 11 1984.

W.J. Kent. BLAT—the BLAST-like alignment tool. *Genome Res*, 12(4):656–64, Apr 2002.

W.J. Kent, C.W. Sugnet, T.S. Furey, K.M. Roskin, T.H. Pringle, A.M. Zahler, and D. Haussler. The human genome browser at UCSC. *Genome Res*, 12(6):996–1006, Jun 2002.

W.J. Kent and A.M. Zahler. Conservation, regulation, synteny, and introns in a large-scale *C. briggsae-C. elegans* genomic alignment. *Genome Res*, 10(8):1115–25, Aug 2000.

Paul Kitts. *The NCBI handbook [Internet]*, chapter Genome Assembly and Annotation Process. National Library of Medicine (US), National Center for Biotechnology Information, Bethesda (MD), October 2002. URL http://www.ncbi.nlm.nih.gov/books/bv.fcgi?rid=handbook.chapter.1440.

J. Kling. Ultrafast DNA sequencing. *Nat Biotechnol*, 21(12):1425–7, Dec 2003.

I. Kolossova and R.A. Padgett. U11 snRNA interacts in vivo with the 5′ splice site of U12-dependent (AU-AC) pre-mRNA introns. *RNA*, 3(3):227–33, Mar 1997.

M.M. Konarska and P.A. Sharp. Interactions between small nuclear ribonucleoprotein particles in formation of spliceosomes. *Cell*, 49(6):763–74, Jun 19 1987.

I. Korf, P. Flicek, D. Duan, and M.R. Brent. Integrating genomic homology into gene structure prediction. *Bioinformatics*, 17 Suppl 1:S140–8, 2001.

A. Kozik, E. Kochetkova, and R. Michelmore. `GenomePixelizer`—a visualization program for comparative genomics within and between species. *Bioinformatics*, 18(2):335–6, Feb 2002.

A. Krause, S.A. Haas, E. Coward, and M. Vingron. SYSTERS, GeneNest, SpliceNest: exploring sequence space from genome to protein. *Nucleic Acids Res*, 30(1):299–300, Jan 1 2002.

A. Krogh. Two methods for improving performance of an HMM and their application for gene finding. *Proc Int Conf Intell Syst Mol Biol*, 5:179–86, 1997.

D. Kulp, D. Haussler, M. G. Reese, and F. H. Eeckman. "A Generalized Hidden Markov Model for the Recognition of Human Genes in DNA.". In D. J. States, P. Agarwal, T. Gaasterland, L. Hunter, and R. Smith, editors, *Proc Int Conf Intell Syst Mol Biol*, volume 4, pages 134–142, Menlo Park, California, 1996. AAAI press.

S. Kurtz, A. Phillippy, A.L. Delcher, M. Smoot, M. Shumway, C. Antonescu, and S.L. Salzberg. Versatile and open software for comparing large genomes. *Genome Biol*, 5(2):R12, 2004.

S. Kurtz and C. Schleiermacher. `REPuter`: fast computation of maximal repeats in complete genomes. *Bioinformatics*, 15(5):426–7, May 1999.

A.I. Lamond, M.M. Konarska, P.J. Grabowski, and P.A. Sharp. Spliceosome assembly involves the binding and release of U4 small nuclear ribonucleoprotein. *Proc Natl Acad Sci U S A*, 85(2):411–5, Jan 1988.

L. Lamport. *LaTeX A Document Preparation System.* Addison Wesley, second edition, 1994.

E.S. Lander, L.M. Linton, B. Birren, C. Nusbaum, M.C. Zody, J. Baldwin, K. Devon, K. Dewar, M. Doyle, W. FitzHugh, R. Funke, D. Gage, K. Harris, A. Heaford, J. Howland, and others (International Human Genome Sequencing Consortium, IHGSC). Initial sequencing and analysis of the human genome. *Nature*, 409(6822):860–921, Feb 15 2001.

A. Lefebvre, T. Lecroq, H. Dauchel, and J. Alexandre. `FORRepeats`: detects repeats on entire chromosomes and between genomes. *Bioinformatics*, 19(3):319–26, Feb 12 2003.

B. Lenhard, A. Sandelin, L. Mendoza, P. Engstrom, N. Jareborg, and W.W. Wasserman. Identification of conserved regulatory elements by comparative genome analysis. *J Biol*, 2(2):13, 2003.

C. Letondal. A Web interface generator for molecular biology programs in Unix. *Bioinformatics*, 17(1): 73–82, Jan 2001.

S.E. Lewis, S.M. Searle, N. Harris, M. Gibson, V. Lyer, J. Richter, C. Wiel, L. Bayraktaroglir, E. Birney, M.A. Crosby, J.S. Kaminker, B.B. Matthews, S.E. Prochnik, C.D. Smithy, J.L. Tupy, et al. `Apollo`: a sequence annotation editor. *Genome Biol*, 3(12):RESEARCH0082, 2002.

F. Liang, I. Holt, G. Pertea, S. Karamycheva, S.L. Salzberg, and J. Quackenbush. Gene index analysis of the human genome estimates approximately 120,000 genes. *Nat Genet*, 25(2):239–40, Jun 2000.

H.X. Liu, M. Zhang, and A.R. Krainer. Identification of functional exonic splicing enhancer motifs recognized by individual SR proteins. *Genes Dev*, 12(13):1998–2012, Jul 1 1998.

G.G. Loots, R.M. Locksley, C.M. Blankespoor, Z.E. Wang, W. Miller, E.M. Rubin, and K.A. Frazer. Identification of a coordinate regulator of *interleukins* 4, 13, and 5 by cross-species sequence comparisons. *Science*, 288(5463):136–40, Apr 7 2000.

S. Lu and B.R. Cullen. Analysis of the stimulatory effect of splicing on mRNA production and utilization in mammalian cells. *RNA*, 9(5):618–30, May 2003.

A.V. Lukashin and M. Borodovsky. GeneMark.hmm: new solutions for gene finding. *Nucleic Acids Res*, 26(4):1107–15, Feb 15 1998.

J. Lund, F. Chen, A. Hua, B. Roe, M. Budarf, B.S. Emanuel, and R.H. Reeves. Comparative sequence analysis of 634 kb of the mouse chromosome 16 region of conserved synteny with the human velocardiofacial syndrome region on chromosome 22q11.2. *Genomics*, 63(3):374–83, Feb 1 2000.

H.R. Luo, G.A. Moreau, N. Levin, and M.J. Moore. The human *Prp8* protein is a component of both U2- and U12-dependent spliceosomes. *RNA*, 5(7):893–908, Jul 1999.

H.D. Madhani and C. Guthrie. A novel base-pairing interaction between U2 and U6 snRNAs suggests a mechanism for the catalytic activation of the spliceosome. *Cell*, 71(5):803–17, Nov 27 1992.

E.M. Makarov, O.V. Makarova, H. Urlaub, M. Gentzel, C.L. Will, M. Wilm, and R. Luhrmann. Small nuclear ribonucleoprotein remodeling during catalytic activation of the spliceosome. *Science*, 298 (5601):2205–8, Dec 13 2002.

L. E. Maquat. *Translational Control of Gene Expression*, volume 39 of *Cold Spring Harbor Monograph Series*, chapter "Nonsense-mediated RNA decay in mammalian cells: a splicing-dependent means to down-regulate the levels of mRNAs that premature terminate translation.", pages 849–868. Cold Spring Harbor Laboratory Press, Cold Spring Harbor, NY (USA), 2000. ISBN 0-87969-618-4.

L.E. Maquat. When cells stop making sense: effects of nonsense codons on RNA metabolism in vertebrate cells. *RNA*, 1(5):453–65, Jul 1995.

C. Mayor, M. Brudno, J.R. Schwartz, A. Poliakov, E.M. Rubin, K.A. Frazer, L.S. Pachter, and I. Dubchak. VISTA: visualizing global DNA sequence alignments of arbitrary length. *Bioinformatics*, 16(11):1046–7, Nov 2000.

T.S. McConnell, S.J. Cho, M.J. Frilander, and J.A. Steitz. Branchpoint selection in the splicing of U12-dependent introns *in vitro*. *RNA*, 8(5):579–86, May 2002.

S. McCracken, N. Fong, E. Rosonina, K. Yankulov, G. Brothers, D. Siderovski, A. Hessel, S. Foster, S. Shuman, and D.L. Bentley. 5'-Capping enzymes are targeted to pre-mRNA by binding to the phosphorylated carboxy-terminal domain of RNA polymerase II. *Genes Dev*, 11(24):3306–18, Dec 15 1997a.

S. McCracken, N. Fong, K. Yankulov, S. Ballantyne, G. Pan, J. Greenblatt, S.D. Patterson, M. Wickens, and D.L. Bentley. The C-terminal domain of RNA polymerase II couples mRNA processing to transcription. *Nature*, 385(6614):357–61, Jan 23 1997b.

I.M. Meyer and R. Durbin. Comparative *ab initio* prediction of gene structures using pair HMMs. *Bioinformatics*, 18(10):1309–18, Oct 2002.

I.M. Meyer and R. Durbin. Gene structure conservation aids similarity based gene prediction. *Nucleic Acids Res*, 32(2):776–83, 2004.

W. Miller. Comparison of genomic DNA sequences: solved and unsolved problems. *Bioinformatics*, 17(5):391–7, May 2001.

B. Modrek, A. Resch, C. Grasso, and C. Lee. Genome-wide detection of alternative splicing in expressed sequences of human genes. *Nucleic Acids Res*, 29(13):2850–9, Jul 1 2001.

S.B. Montgomery, T. Astakhova, M. Bilenky, E. Birney, T. Fu, M. Hassel, C. Melsopp, M. Rak, A.G. Robertson, M. Sleumer, A.S. Siddiqui, and S.J. Jones. Sockeye: a 3D environment for comparative genomics. *Genome Res*, 14(5):956–62, May 2004.

K.A. Montzka and J.A. Steitz. Additional low-abundance human small nuclear ribonucleoproteins: U11, U12, etc. *Proc Natl Acad Sci U S A*, 85(23):8885–9, Dec 1988.

R. Mott. `EST_GENOME`: a program to align spliced DNA sequences to unspliced genomic DNA. *Comput Appl Biosci*, 13(4):477–8, Aug 1997.

S.M. Mount. A catalogue of splice junction sequences. *Nucleic Acids Res*, 10(2):459–72, Jan 22 1982.

T. Mourier and D.C. Jeffares. Eukaryotic intron loss. *Science*, 300(5624):1393, May 30 2003.

C.J. Mungall, S. Misra, B.P. Berman, J. Carlson, E. Frise, N. Harris, B. Marshall, S. Shu, J.S. Kaminker, S.E. Prochnik, C.D. Smith, E. Smith, J.L. Tupy, C. Wiel, G.M. Rubin, et al. An integrated computational pipeline and database to support whole-genome sequence annotation. *Genome Biol*, 3(12): RESEARCH0081, 2002.

R.J. Mural, M.D. Adams, E.W. Myers, H.O. Smith, G.L. Miklos, R. Wides, A. Halpern, P.W. Li, G.G. Sutton, J. Nadeau, S.L. Salzberg, R.A. Holt, C.D. Kodira, F. Lu, L. Chen, et al. A comparison of whole-genome shotgun-derived mouse chromosome 16 and the human genome. *Science*, 296 (5573):1661–71, May 31 2002.

P. Nadkarni. `Mapmerge`: merge genomic maps. *Bioinformatics*, 14(4):310–6, 1998.

NCBI. `Gnomon`, predicting gene structures in genomic DNA. URL `http://www.ncbi.nlm.nih.gov/genome/guide/gnomon.html`. *unpublished* 2003.

A. Nekrutenko, W.Y. Chung, and W.H. Li. An evolutionary approach reveals a high protein-coding capacity of the human genome. *Trends Genet*, 19(6):306–10, Jun 2003.

A. Newman and C. Norman. Mutations in yeast U5 snRNA alter the specificity of 5′ splice-site cleavage. *Cell*, 65(1):115–23, Apr 5 1991.

A.J. Newman and C. Norman. U5 snRNA interacts with exon sequences at 5′ and 3′ splice sites. *Cell*, 68(4):743–54, Feb 21 1992.

A. Nott, S.H. Meislin, and M.J. Moore. A quantitative analysis of intron effects on mammalian gene expression. *RNA*, 9(5):607–17, May 2003.

J.C. Oeltjen, T.M. Malley, D.M. Muzny, W. Miller, R.A. Gibbs, and J.W. Belmont. Large-scale comparative sequence analysis of the human and murine Bruton's *tyrosine kinase* loci reveals conserved regulatory domains. *Genome Res*, 7(4):315–29, Apr 1997.

S.A. Olson. `EMBOSS` opens up sequence analysis. European Molecular Biology Open Software Suite. *Brief Bioinform*, 3(1):87–91, Mar 2002.

L.R. Otake, P. Scamborova, C. Hashimoto, and J.A. Steitz. The divergent U12-type spliceosome is required for pre-mRNA splicing and is essential for development in *Drosophila*. *Mol Cell*, 9(2): 439–46, Feb 2002.

I. Ovcharenko and G.G. Loots. Comparative genomic tools for exploring the human genome. *Cold Spring Harb Symp Quant Biol*, 68:283–91, 2003a.

I. Ovcharenko and G.G. Loots. Finding the Needle in the Haystack: Computational Strategies for Discovering Regulatory Sequences in Genomes. *Current Genomics*, 4(7):557–568, 2003b.

I. Ovcharenko, G.G. Loots, R.C. Hardison, W. Miller, and L. Stubbs. `zPicture`: dynamic alignment and visualization tool for analyzing conservation profiles. *Genome Res*, 14(3):472–7, Mar 2004a.

I. Ovcharenko, M.A. Nobrega, G.G. Loots, and L. Stubbs. ECR Browser: a tool for visualizing and accessing data from comparisons of multiple vertebrate genomes. *Nucleic Acids Res*, 32(Web Server issue):W280–6, Jul 1 2004b.

R. Overbeek, N. Larsen, T. Walunas, M. D'Souza, G. Pusch, J.r. Selkov E, K. Liolios, V. Joukov, D. Kaznadzey, I. Anderson, A. Bhattacharyya, H. Burd, W. Gardner, P. Hanke, V. Kapatral, et al. The ERGO genome analysis and discovery system. *Nucleic Acids Res*, 31(1):164–71, Jan 1 2003.

F. Pagani and F.E. Baralle. Genomic variants in exons and introns: identifying the splicing spoilers. *Nat Rev Genet*, 5(5):389–96, May 2004.

Q. Pan, M.A. Bakowski, Q. Morris, W. Zhang, B.J. Frey, T.R. Hughes, and B.J. Blencowe. Alternative splicing of conserved exons is frequently species-specific in human and mouse. *Trends Genet*, 21(2): 73–7, Feb 2005.

J. Parkinson and M. Blaxter. SimiTri—visualizing similarity relationships for groups of sequences. *Bioinformatics*, 19(3):390–5, Feb 12 2003.

G. Parra, P. Agarwal, **J.F. Abril**, T. Wiehe, J.W. Fickett, and R. Guigó. Comparative gene prediction in human and mouse. *Genome Res*, 13(1):108–17, Jan 2003.

J.D. Parsons. Miropeats: graphical DNA sequence comparisons. *Comput Appl Biosci*, 11(6):615–9, Dec 1995.

E. Passarge, B. Horsthemke, and R.A. Farber. Incorrect use of the term synteny. *Nat Genet*, 23(4):387, Dec 1999.

A.A. Patel and J.A. Steitz. Splicing double: insights from the second spliceosome. *Nat Rev Mol Cell Biol*, 4(12):960–70, Dec 2003.

W.R. Pearson and D.J. Lipman. Improved tools for biological sequence comparison. *Proc Natl Acad Sci U S A*, 85(8):2444–8, Apr 1988.

C.N.S. Pedersen and T. Scharl. "Comparative Methods for Gene Structure Prediction in Homologous Sequences.". In R. Guigó and D. Gusfield, editors, *"Algorithms in Bioinformatics": Proceedings of the Second International Workshop, WABI 2002*, volume 2452 of *Lecture Notes in Computer Science*, pages 220–234. Springer-Verlag, Berlin Heidelberg, 2002. ISBN 3-540-44211-1.

J.S. Pedersen and J. Hein. Gene finding with a hidden Markov model of genome structure and evolution. *Bioinformatics*, 19(2):219–27, Jan 22 2003.

L.A. Pennacchio. Insights from human/mouse genome comparisons. *Mamm Genome*, 14(7):429–36, Jul 2003.

L.A. Pennacchio, M. Olivier, J.A. Hubacek, J.C. Cohen, D.R. Cox, J.C. Fruchart, R.M. Krauss, and E.M. Rubin. An apolipoprotein influencing triglycerides in humans and mice revealed by comparative sequencing. *Science*, 294(5540):169–73, Oct 5 2001.

L.A. Pennacchio and E.M. Rubin. Genomic strategies to identify mammalian regulatory sequences. *Nat Rev Genet*, 2(2):100–9, Feb 2001.

L.A. Pennacchio and E.M. Rubin. Comparative genomic tools and databases: providing insights into the human genome. *J Clin Invest*, 111(8):1099–106, Apr 2003.

E. Pennisi. Bioinformatics. Gene counters struggle to get the right answer. *Science*, 301(5636):1040–1, Aug 22 2003.

S.C. Potter, L. Clarke, V. Curwen, S. Keenan, E. Mongin, S.M. Searle, A. Stabenau, R. Storey, and M. Clamp. The `Ensembl` analysis pipeline. *Genome Res*, 14(5):934–41, May 2004.

N.J. Proudfoot, A. Furger, and M.J. Dye. Integrating mRNA processing with transcription. *Cell*, 108 (4):501–12, Feb 22 2002.

K.D. Pruitt and D.R. Maglott. REFSEQ and LOCUSLINK: NCBI gene-centered resources. *Nucleic Acids Res*, 29(1):137–40, Jan 1 2001.

K.D. Pruitt, T. Tatusova, and D.R. Maglott. NCBI Reference Sequence (REFSEQ): a curated non-redundant sequence database of genomes, transcripts and proteins. *Nucleic Acids Res*, 33 Database Issue:D501–4, Jan 1 2005.

J. Pustell and F.C. Kafatos. A convenient and adaptable package of DNA sequence analysis programs for microcomputers. *Nucleic Acids Res*, 10(1):51–9, Jan 11 1982.

W.C. Ray, J.r. Munson RS, and C.J. Daniels. `Tricross`: using dot-plots in sequence-id space to detect uncataloged intergenic features. *Bioinformatics*, 17(12):1105–12, Dec 2001.

R. Reed. Initial splice-site recognition and pairing during pre-mRNA splicing. *Curr Opin Genet Dev*, 6(2):215–20, Apr 1996.

M.G. Reese, G. Hartzell, N.L. Harris, U. Ohler, **J.F. Abril**, and S.E. Lewis. Genome annotation assessment in *Drosophila melanogaster*. *Genome Res*, 10(4):483–501, Apr 2000.

V.L. Reichert, H. Le Hir, M.S. Jurica, and M.J. Moore. 5′ exon interactions within the human spliceosome establish a framework for exon junction complex structure and assembly. *Genes Dev*, 16(21): 2778–91, Nov 1 2002.

K. Reichwald, J. Thiesen, T. Wiehe, J. Weitzel, W.A. Poustka, A. Rosenthal, M. Platzer, W.H. Stratling, and P. Kioschis. Comparative sequence analysis of the *MECP2*-locus in human and mouse reveals new transcribed regions. *Mamm Genome*, 11(3):182–90, Mar 2000.

Glenn C. Reid. *PostScript Language Program Design*. Addison-Wesley Publishing Company, Inc., twelfth edition, March 1996. ISBN 0-201-14396-8.

D. Reisman, E. Eaton, D. McMillin, N.A. Doudican, and K. Boggs. Cloning and characterization of murine *p53* upstream sequences reveals additional positive transcriptional regulatory elements. *Gene*, 274(1-2):129–37, Aug 22 2001.

S.Y. Rhee, W. Beavis, T.Z. Berardini, G. Chen, D. Dixon, A. Doyle, M. Garcia-Hernandez, E. Huala, G. Lander, M. Montoya, N. Miller, L.A. Mueller, S. Mundodi, L. Reiser, J. Tacklind, et al. The *Arabidopsis* Information Resource (`TAIR`): a model organism database providing a centralized, curated gateway to *Arabidopsis* biology, research materials and community. *Nucleic Acids Res*, 31(1):224–8, Jan 1 2003.

P. Rice, I. Longden, and A. Bleasby. `EMBOSS`: the European Molecular Biology Open Software Suite. *Trends Genet*, 16(6):276–7, Jun 2000.

H. Roest Crollius, O. Jaillon, A. Bernot, C. Dasilva, L. Bouneau, C. Fischer, C. Fizames, P. Wincker, P. Brottier, F. Quetier, W. Saurin, and J. Weissenbach. Estimate of human gene number provided by genome-wide analysis using *Tetraodon nigroviridis* DNA sequence. *Nat Genet*, 25(2):235–8, Jun 2000.

S. Rogic, A.K. Mackworth, and F.B. Ouellette. Evaluation of gene-finding programs on mammalian sequences. *Genome Res*, 11(5):817–32, May 2001.

I.B. Rogozin and Y.I. Pavlov. Theoretical analysis of mutation hotspots and their DNA sequence context specificity. *Mutat Res*, 544(1):65–85, Sep 2003.

S.W. Roy. Recent evidence for the exon theory of genes. *Genetica*, 118(2-3):251–66, Jul 2003.

K. Rutherford, J. Parkhill, J. Crook, T. Horsnell, P. Rice, M.A. Rajandream, and B. Barrell. `Artemis`: sequence visualization and annotation. *Bioinformatics*, 16(10):944–5, Oct 2000.

W.S. Ryu and J.E. Mertz. Simian virus 40 late transcripts lacking excisable intervening sequences are defective in both stability in the nucleus and transport to the cytoplasm. *J Virol*, 63(10):4386–94, Oct 1989.

A.A. Salamov and V.V. Solovyev. *Ab initio* gene finding in *Drosophila* genomic DNA. *Genome Res*, 10 (4):516–22, Apr 2000.

S. Salzberg, A.L. Delcher, K.H. Fasman, and J. Henderson. A decision tree system for finding genes in DNA. *J Comput Biol*, 5(4):667–80, Winter 1998.

A. Sandelin, W.W. Wasserman, and B. Lenhard. `ConSite`: web-based prediction of regulatory elements using cross-species comparison. *Nucleic Acids Res*, 32(Web Server issue):W249–52, Jul 1 2004.

N. Sato and S. Ehira. `GenoMap`, a circular genome data viewer. *Bioinformatics*, 19(12):1583–4, Aug 12 2003.

T.D. Schaal and T. Maniatis. Multiple distinct splicing enhancers in the protein-coding sequences of a constitutively spliced pre-mRNA. *Mol Cell Biol*, 19(1):261–73, Jan 1999.

C. Schneider, C.L. Will, O.V. Makarova, E.M. Makarov, and R. Luhrmann. Human U4/U6.U5 and U4atac/U6atac.U5 tri-snRNPs exhibit similar protein compositions. *Mol Cell Biol*, 22(10):3219–29, May 2002.

T.D. Schneider and R.M. Stephens. Sequence logos: a new way to display consensus sequences. *Nucleic Acids Res*, 18(20):6097–100, Oct 25 1990.

S. Schwartz, L. Elnitski, M. Li, M. Weirauch, C. Riemer, A. Smit, E.D. Green, R.C. Hardison, and W. Miller. `MultiPipMaker` and supporting tools: Alignments and analysis of multiple genomic DNA sequences. *Nucleic Acids Res*, 31(13):3518–24, Jul 1 2003a.

S. Schwartz, W.J. Kent, A. Smit, Z. Zhang, R. Baertsch, R.C. Hardison, D. Haussler, and W. Miller. Human-mouse alignments with `BLASTZ`. *Genome Res*, 13(1):103–7, Jan 2003b.

S. Schwartz, W. Miller, C.M. Yang, and R.C. Hardison. Software tools for analyzing pairwise alignments of long sequences. *Nucleic Acids Res*, 19(17):4663–7, Sep 11 1991.

S. Schwartz, Z. Zhang, K.A. Frazer, A. Smit, C. Riemer, J. Bouck, R. Gibbs, R. Hardison, and W. Miller. `PipMaker`—a web server for aligning two genomic DNA sequences. *Genome Res*, 10(4):577–86, Apr 2000.

S.M. Searle, J. Gilbert, V. Iyer, and M. Clamp. The `otter` annotation system. *Genome Res*, 14(5): 963–70, May 2004.

D.B. Searls. Doing sequence analysis with your printer. *Comput Appl Biosci*, 9(4):421–6, Aug 1993.

D.B. Searls. `bioTk`: componentry for genome informatics graphical user interfaces. *Gene*, 163(2): GC1–16, Oct 3 1995.

P. Senapathy, M.B. Shapiro, and N.L. Harris. Splice junctions, branch point sites, and exons: sequence statistics, identification, and applications to genome project. *Methods Enzymol*, 183:252–78, 1990.

P.A. Sharp and C.B. Burge. Classification of introns: U2-type or U12-type. *Cell*, 91(7):875–9, Dec 26 1997.

J.C. Shepherd. Method to determine the reading frame of a protein from the purine/pyrimidine genome sequence and its possible evolutionary justification. *Proc Natl Acad Sci U S A*, 78(3):1596–600, Mar 1981.

S.T. Sherry, M.H. Ward, M. Kholodov, J. Baker, L. Phan, E.M. Smigielski, and K. Sirotkin. dbSNP: the NCBI database of genetic variation. *Nucleic Acids Res*, 29(1):308–11, Jan 1 2001.

A. Siepel and D. Haussler. Phylogenetic estimation of context-dependent substitution rates by maximum likelihood. *Mol Biol Evol*, 21(3):468–88, Mar 2004.

G.S. Slater and E. Birney. Automated generation of heuristics for biological sequence comparison. *BMC Bioinformatics*, 6(1):31, Feb 15 2005.

A.F.A. Smit, R. Hubley, and P. Green. `RepeatMasker`. URL http://www.repeatmasker.org/. *unpublished* 1996–2004.

M.W. Smith. Structure of vertebrate genes: a statistical analysis implicating selection. *J Mol Evol*, 27 (1):45–55, 1988.

M.E. Smoot, S.A. Guerlain, and W.R. Pearson. Visualization of near optimal sequence alignments. *Bioinformatics*, Jan 29 2004.

E.E. Snyder and G.D. Stormo. Identification of coding regions in genomic DNA sequences: an application of dynamic programming and neural networks. *Nucleic Acids Res*, 21(3):607–13, Feb 11 1993.

V.V. Solovyev, A.A. Salamov, and C.B. Lawrence. Predicting internal exons by oligonucleotide composition and discriminant analysis of spliceable open reading frames. *Nucleic Acids Res*, 22(24): 5156–63, Dec 11 1994.

E.L. Sonnhammer and R. Durbin. A workbench for large-scale sequence homology analysis. *Comput Appl Biosci*, 10(3):301–7, Jun 1994.

E.L. Sonnhammer and R. Durbin. A dot-matrix program with dynamic threshold control suited for genomic DNA and protein sequence analysis. *Gene*, 167(1-2):GC1–10, Dec 29 1995.

E.J. Sontheimer and J.A. Steitz. The U5 and U6 small nuclear RNAs as active site components of the spliceosome. *Science*, 262(5142):1989–96, Dec 24 1993.

R. Sorek and G. Ast. Intronic sequences flanking alternatively spliced exons are conserved between human and mouse. *Genome Res*, 13(7):1631–7, Jul 2003.

R. Staden. An interactive graphics program for comparing and aligning nucleic acid and amino acid sequences. *Nucleic Acids Res*, 10(9):2951–61, May 11 1982.

R. Staden. Computer methods to locate signals in nucleic acid sequences. *Nucleic Acids Res*, 12(1 Pt 2):505–19, Jan 11 1984a.

R. Staden. Graphic methods to determine the function of nucleic acid sequences. *Nucleic Acids Res*, 12(1 Pt 2):521–38, Jan 11 1984b.

R. Staden. The current status and portability of our sequence handling software. *Nucleic Acids Res*, 14(1):217–31, Jan 10 1986.

R. Staden. Methods to define and locate patterns of motifs in sequences. *Comput Appl Biosci*, 4(1): 53–60, Mar 1988.

R. Staden, K.F. Beal, and J.K. Bonfield. The `Staden` package, 1998. *Methods Mol Biol*, 132:115–30, 2000.

R. Staden and A.D. McLachlan. Codon preference and its use in identifying protein coding regions in long DNA sequences. *Nucleic Acids Res*, 10(1):141–56, Jan 11 1982.

J.E. Stajich, D. Block, K. Boulez, S.E. Brenner, S.A. Chervitz, C. Dagdigian, G. Fuellen, J.G. Gilbert, I. Korf, H. Lapp, H. Lehvaslaiho, C. Matsalla, C.J. Mungall, B.I. Osborne, M.R. Pocock, et al. The `Bioperl` toolkit: Perl modules for the life sciences. *Genome Res*, 12(10):1611–8, Oct 2002.

J. Stalker, B. Gibbins, P. Meidl, J. Smith, W. Spooner, H.R. Hotz, and A.V. Cox. The ENSEMBL Web site: mechanics of a genome browser. *Genome Res*, 14(5):951–5, May 2004.

M. Stanke and S. Waack. Gene prediction with a hidden Markov model and a new intron submodel. *Bioinformatics*, 19 Suppl 2:II215–II225, Oct 2003.

L. Stein. Genome annotation: from sequence to biology. *Nat Rev Genet*, 2(7):493–503, Jul 2001.

L.D. Stein, S. Cartinhour, D. Thierry-Mieg, and J. Thierry-Mieg. `JADE`: an approach for interconnecting bioinformatics databases. *Gene*, 209(1-2):GC39–GC43, Mar 16 1998.

L.D. Stein, C. Mungall, S. Shu, M. Caudy, M. Mangone, A. Day, E. Nickerson, J.E. Stajich, T.W. Harris, A. Arva, and S. Lewis. The `generic genome browser`: a building block for a model organism system database. *Genome Res*, 12(10):1599–610, Oct 2002.

L.D. Stein and J. Thierry-Mieg. Scriptable access to the *Caenorhabditis elegans* genome sequence and other `ACEDB` databases. *Genome Res*, 8(12):1308–15, Dec 1998.

R. Stevens, C. Goble, P. Baker, and A. Brass. A classification of tasks in bioinformatics. *Bioinformatics*, 17(2):180–8, Feb 2001.

A. Stoltzfus, J.r. Logsdon JM, J.D. Palmer, and W.F. Doolittle. Intron "sliding" and the diversity of intron positions. *Proc Natl Acad Sci U S A*, 94(20):10739–44, Sep 30 1997.

G. Storz. An expanding universe of noncoding RNAs. *Science*, 296(5571):1260–3, May 17 2002.

C. Suter-Crazzolara and G. Kurapkat. An infrastructure for comparative genomics to functionally characterize genes and proteins. *Genome Inform Ser Workshop Genome Inform*, 11:24–32, 2000.

A.V. Sverdlov, V.N. Babenko, I.B. Rogozin, and E.V. Koonin. Preferential loss and gain of introns in 3′ portions of genes suggests a reverse-transcription mechanism of intron insertion. *Gene*, 338(1): 85–91, Aug 18 2004.

A.V. Sverdlov, I.B. Rogozin, V.N. Babenko, and E.V. Koonin. Conservation versus parallel gains in intron evolution. *Nucleic Acids Res*, 33(6):1741–8, 2005.

A. Taneda. `ADplot`: detection and visualization of repetitive patterns in complete genomes. *Bioinformatics*, 20(5):701–8, Mar 22 2004.

W.Y. Tarn and J.A. Steitz. A novel spliceosome containing `U11`, `U12`, and `U5` snRNPs excises a minor class (`AT-AC`) intron *in vitro*. *Cell*, 84(5):801–11, Mar 8 1996.

T.A. Thanaraj, F. Clark, and J. Muilu. Conservation of human alternative splice events in mouse. *Nucleic Acids Res*, 31(10):2544–52, May 15 2003.

T.A. Thanaraj, S. Stamm, F. Clark, J.J. Riethoven, V. Le Texier, and J. Muilu. ASD: the Alternative Splicing Database. *Nucleic Acids Res*, 32 Database issue:D64–9, Jan 1 2004.

The `FlyBase` Consortium. The `FlyBase` database of the *Drosophila* genome projects and community literature. *Nucleic Acids Res*, 31(1):172–5, Jan 1 2003.

A. Thomas and M.H. Skolnick. A probabilistic model for detecting coding regions in DNA sequences. *IMA J Math Appl Med Biol*, 11(3):149–60, 1994.

J.W. Thomas and J.W. Touchman. Vertebrate genome sequencing: building a backbone for comparative genomics. *Trends Genet*, 18(2):104–8, Feb 2002.

J.W. Thomas, J.W. Touchman, R.W. Blakesley, G.G. Bouffard, S.M. Beckstrom-Sternberg, E.H. Margulies, M. Blanchette, A.C. Siepel, P.J. Thomas, J.C. McDowell, B. Maskeri, N.F. Hansen, M.S. Schwartz, R.J. Weber, W.J. Kent, et al. Comparative analyses of multi-species sequences from targeted genomic regions. *Nature*, 424(6950):788–93, Aug 14 2003.

J.D. Tisdall. *Mastering Perl for Bioinformatics.* O'Reilly & Associates, Inc., first edition, September 2003. ISBN 0-596-00307-2.

M. Tompa. Identifying functional elements by comparative DNA sequence analysis. *Genome Res*, 11 (7):1143–4, Jul 2001.

A. Toyoda, H. Noguchi, T.D. Taylor, T. Ito, M.T. Pletcher, Y. Sakaki, R.H. Reeves, and M. Hattori. Comparative genomic sequence analysis of the human chromosome 21 Down syndrome critical region. *Genome Res*, 12(9):1323–32, Sep 2002.

E.R. Tufte. *The Visual Display of Quantitative Information.* Graphics Press USA, second edition, January 2001. ISBN 0-961-39214-2.

E.C. Uberbacher and R.J. Mural. Locating protein-coding regions in human DNA sequences by a multiple sensor-neural network approach. *Proc Natl Acad Sci U S A*, 88(24):11261–5, Dec 15 1991.

Y. Ueno, M. Arita, T. Kumagai, and K. Asai. Processing sequence annotation data using the `Lua` programming language. *Genome Inform Ser Workshop Genome Inform*, 14:154–63, 2003.

A. Ureta-Vidal, L. Ettwiller, and E. Birney. Comparative genomics: genome-wide analysis in metazoan eukaryotes. *Nat Rev Genet*, 4(4):251–62, Apr 2003.

J. Usuka and V. Brendel. Gene structure prediction by spliced alignment of genomic DNA with protein sequences: increased accuracy by differential splice site scoring. *J Mol Biol*, 297(5):1075–85, Apr 14 2000.

J.C. Venter, M.D. Adams, E.W. Myers, P.W. Li, R.J. Mural, G.G. Sutton, H.O. Smith, M. Yandell, C.A. Evans, R.A. Holt, J.D. Gocayne, P. Amanatides, R.M. Ballew, D.H. Huson, J.R. Wortman, and others (including **J.F. Abril**). The sequence of the human genome. *Science*, 291(5507):1304–51, Feb 16 2001.

Y. Wada, K. Inoue, K. Ohga, and H. Yasue. Software tool for gene mapping: `gRanch`. *Comput Appl Biosci*, 13(3):323–4, Jun 1997.

D.R. Walker and E.V. Koonin. `SEALS`: a system for easy analysis of lots of sequences. *Proc Int Conf Intell Syst Mol Biol*, 5:333–9, 1997.

S. Walsh, M. Anderson, and S.W. Cartinhour. `ACEDB`: a database for genome information. *Methods Biochem Anal*, 39:299–318, 1998.

Z. Wang, M.E. Rolish, G. Yeo, V. Tung, M. Mawson, and C.B. Burge. Systematic identification and analysis of exonic splicing silencers. *Cell*, 119(6):831–45, Dec 17 2004.

D.A. Wassarman and J.A. Steitz. Interactions of small nuclear RNA's with precursor messenger RNA during *in vitro* splicing. *Science*, 257(5078):1918–25, Sep 25 1992.

R.H. Waterston, K. Lindblad-Toh, E. Birney, J. Rogers, **J.F. Abril**, P. Agarwal, R. Agarwala, R. Ainscough, M. Alexandersson, P. An, S.E. Antonarakis, J. Attwood, R. Baertsch, J. Bailey, K. Barlow, and others (International Mouse Genome Sequencing Consortium, IMGSC). Initial sequencing and comparative analysis of the mouse genome. *Nature*, 420(6915):520–62, Dec 5 2002.

S.J. Wheelan, D.M. Church, and J.M. Ostell. `Spidey`: a tool for mRNA-to-genomic alignments. *Genome Res*, 11(11):1952–7, Nov 2001.

D.L. Wheeler, T. Barrett, D.A. Benson, S.H. Bryant, K. Canese, D.M. Church, M. DiCuccio, R. Edgar, S. Federhen, W. Helmberg, D.L. Kenton, O. Khovayko, D.J. Lipman, T.L. Madden, D.R. Maglott, et al. Database resources of the National Center for Biotechnology Information. *Nucleic Acids Res*, 33 Database Issue:D39–45, Jan 1 2005.

D.L. Wheeler, D.M. Church, A.E. Lash, D.D. Leipe, T.L. Madden, J.U. Pontius, G.D. Schuler, L.M. Schriml, T.A. Tatusova, L. Wagner, and B.A. Rapp. Database resources of the National Center for Biotechnology Information: 2002 update. *Nucleic Acids Res*, 30(1):13–6, Jan 1 2002.

H.L. Wiegand, S. Lu, and B.R. Cullen. Exon junction complexes mediate the enhancing effect of splicing on mRNA expression. *Proc Natl Acad Sci U S A*, 100(20):11327–32, Sep 30 2003.

T. Wiehe, S. Gebauer-Jung, T. Mitchell-Olds, and R. Guigo. `SGP-1`: prediction and validation of homologous genes based on sequence alignments. *Genome Res*, 11(9):1574–83, Sep 2001.

T. Wiehe, R. Guigó, and W. Miller. Genome sequence comparisons: hurdles in the fast lane to functional genomics. *Brief Bioinform*, 1(4):381–8, Nov 2000.

C.L. Will, C. Schneider, A.M. MacMillan, N.F. Katopodis, G. Neubauer, M. Wilm, R. Luhrmann, and C.C. Query. A novel U2 and U11/U12 snRNP protein that associates with the pre-mRNA branch site. *EMBO J*, 20(16):4536–46, Aug 15 2001.

C.L. Will, C. Schneider, R. Reed, and R. Luhrmann. Identification of both shared and distinct proteins in the major and minor spliceosomes. *Science*, 284(5422):2003–5, Jun 18 1999.

M.D. Wilson, C. Riemer, D.W. Martindale, P. Schnupf, A.P. Boright, T.L. Cheung, D.M. Hardy, S. Schwartz, S.W. Scherer, L.C. Tsui, W. Miller, and B.F. Koop. Comparative analysis of the gene-dense *ACHE/TFR2* region on human chromosome 7q22 with the orthologous region on mouse chromosome 5. *Nucleic Acids Res*, 29(6):1352–65, Mar 15 2001.

V. Wood, R. Gwilliam, M.A. Rajandream, M. Lyne, R. Lyne, A. Stewart, J. Sgouros, N. Peat, J. Hayles, S. Baker, D. Basham, S. Bowman, K. Brooks, D. Brown, S. Brown, et al. The genome sequence of *Schizosaccharomyces pombe*. *Nature*, 415(6874):871–80, Feb 21 2002.

L. Woodley and J. Valcárcel. Regulation of alternative pre-mRNA splicing. *Briefings in Functional Genomics and Proteomics*, 1(3):266–77, Oct 2002.

F.A. Wright, W.J. Lemon, W.D. Zhao, R. Sears, D. Zhuo, J.P. Wang, H.Y. Yang, T. Baer, D. Stredney, J. Spitzner, A. Stutz, R. Krahe, and B. Yuan. A draft annotation and overview of the human genome. *Genome Biol*, 2(7):RESEARCH0025, 2001.

J.A. Wu and J.L. Manley. Base pairing between U2 and U6 snRNAs is necessary for splicing of a mammalian pre-mRNA. *Nature*, 352(6338):818–21, Aug 29 1991.

Q. Wu and A.R. Krainer. Splicing of a divergent subclass of AT-AC introns requires the major spliceosomal snRNAs. *RNA*, 3(6):586–601, Jun 1997.

J.R. Wyatt, E.J. Sontheimer, and J.A. Steitz. Site-specific cross-linking of mammalian U5 snRNP to the 5′ splice site before the first step of pre-mRNA splicing. *Genes Dev*, 6(12B):2542–53, Dec 1992.

Y. Xu, J.R. Einstein, R.J. Mural, M. Shah, and E.C. Uberbacher. An improved system for exon recognition and gene modeling in human DNA sequences. *Proc Int Conf Intell Syst Mol Biol*, 2:376–84, 1994a.

Y. Xu, R.J. Mural, and E.C. Uberbacher. Constructing gene models from accurately predicted exons: an application of dynamic programming. *Comput Appl Biosci*, 10(6):613–23, Dec 1994b.

Y. Xu, R.J. Mural, and E.C. Uberbacher. Inferring gene structures in genomic sequences using pattern recognition and expressed sequence tags. *Proc Int Conf Intell Syst Mol Biol*, 5:344–53, 1997.

Z. Xuan, J. Wang, and M.Q. Zhang. Computational comparison of two mouse draft genomes and the human golden path. *Genome Biol*, 4(1):R1, 2003.

J. Yang, J. Wang, Z.J. Yao, Q. Jin, Y. Shen, and R. Chen. GenomeComp: a visualization tool for microbial genome comparison. *J Microbiol Methods*, 54(3):423–6, Sep 2003.

K. Yankulov, J. Blau, T. Purton, S. Roberts, and D.L. Bentley. Transcriptional elongation by RNA polymerase II is stimulated by transactivators. *Cell*, 77(5):749–59, Jun 3 1994.

R.F. Yeh, L.P. Lim, and C.B. Burge. Computational inference of homologous gene structures in the human genome. *Genome Res*, 11(5):803–16, May 2001.

Y.T. Yu and J.A. Steitz. Site-specific crosslinking of mammalian U11 and U6atac to the 5′ splice site of an AT-AC intron. *Proc Natl Acad Sci U S A*, 94(12):6030–5, Jun 10 1997.

N. Yuhki, T. Beck, R.M. Stephens, Y. Nishigaki, K. Newmann, and S.J. O'Brien. Comparative genome organization of human, murine, and feline *MHC* class II region. *Genome Res*, 13(6A):1169–79, Jun 2003.

M.Q. Zhang. Identification of protein coding regions in the human genome by quadratic discriminant analysis. *Proc Natl Acad Sci U S A*, 94(2):565–8, Jan 21 1997.

M.Q. Zhang. Computational prediction of eukaryotic protein-coding genes. *Nat Rev Genet*, 3(9): 698–709, Sep 2002.

X.H. Zhang and L.A. Chasin. Computational definition of sequence motifs governing constitutive exon splicing. *Genes Dev*, 18(11):1241–50, Jun 1 2004.

Z. Zhang, S. Schwartz, L. Wagner, and W. Miller. A greedy algorithm for aligning DNA sequences. *J Comput Biol*, 7(1-2):203–14, Feb-Apr 2000.

D.A. Zorio and D.L. Bentley. The link between mRNA processing and transcription: communication works both ways. *Exp Cell Res*, 296(1):91–7, May 15 2004.

# Index

## T

# Notes

## Titles in the GBL Dissertation Series

**2002-01** M. Burset.
*Estudi computacional de l'especificació dels llocs d'splicing.*
[Computational analysis of the splice sites definition.]
Departament de Genètica, Universitat de Barcelona.

**2004-01** Sergi Castellano.
*Towards the characterization of the eukaryotic selenoproteome: a computational approach.*
Departament de Ciències Experimentals i de la Salut, Universitat Pompeu Fabra.

**2004-02** Genís Parra.
*Computational identification of genes: "ab initio" and comparative approaches.*
Departament de Ciències Experimentals i de la Salut, Universitat Pompeu Fabra.

**2005-01** Josep F. Abril.
*Comparative Analysis of Eukaryotic Gene Sequence Features.*
Departament de Ciències Experimentals i de la Salut, Universitat Pompeu Fabra.

Josep Francesc Abril Ferrando

# Comparative Analysis of Eukaryotic Gene Sequence Features

## Anàlisi Comparativa d'Elements de Seqüència dels Gens Eucariotes

The constantly increasing amount of available genome sequences, along with an increasing number of experimental techniques, will help to produce the complete catalog of cellular functions for different organisms, including humans. Such a catalog will define the base from which we will better understand how organisms work at the molecular level. At the same time it will shed light on which changes are associated with disease. Therefore, the raw sequence from genome sequencing projects is worthless without the complete analysis and further annotation of the genomic features that define those functions. This dissertation presents our contribution to three related aspects of gene annotation on eukaryotic genomes.

First, a comparison at sequence level of human and mouse genomes was performed by developing a semi-automatic analysis pipeline. The SGP2 gene-finding tool was developed from procedures used in this pipeline. The concept behind SGP2 is that similarity regions obtained by TBLASTX are used to increase the score of exons predicted by `geneid`, in order to produce a more accurate set of gene structures. SGP2 provides a specificity that is high enough for its predictions to be experimentally verified by RT-PCR. The RT-PCR validation of predicted splice junctions also serves as example of how combined computational and experimental approaches will yield the best results.

Then, we performed a descriptive analysis at sequence level of the splice site signals from a reliable set of orthologous genes for human, mouse, rat and chicken. We have explored the differences at nucleotide sequence level between U2 and U12 for the set of orthologous introns derived from those genes. We found that orthologous splice signals between human and rodents and within rodents are more conserved than unrelated splice sites. However, additional conservation can be explained mostly by background intron conservation. Additional conservation over background is detectable in orthologous mammalian and chicken splice sites. Our results also indicate that the U2 and U12 intron classes have evolved independently since the split of mammals and birds. We found neither convincing case of interconversion between these two classes in our sets of orthologous introns, nor any single case of switching between AT-AC and GT-AG subtypes within U12 introns. In contrast, switching between GT-AG and GC-AG U2 subtypes does not appear to be unusual.

Finally, we implemented visualization tools to integrate annotation features for gene-finding and comparative analyses. One of those tools, `gff2ps`, was used to draw the whole genome maps for human, fruitfly and mosquito. `gff2aplot` and the accompanying parsers facilitate the task of integrating sequence annotations with the output of homology-based tools, like BLAST. We have also adapted the concept of pictograms to the comparative analysis of orthologous splice sites, by developing `compi`.

**GBL Dissertation Series**
Universitat Pompeu Fabra

ISBN XX-XXX-XXXX-X